frontiers | Research Topics

Microbial ecological and biogeochemical processes in the soil-vadose zone-groundwater habitats, volume II

Edited by
Zifang Chi, Huai Li, Jiuling Li and Yi-Hao Luo

Published in
Frontiers in Microbiology

ISSN 1664-8714
ISBN 978-2-8325-5456-2
DOI 10.3389/978-2-8325-5456-2

About Frontiers

Frontiers is more than just an open access publisher of scholarly articles: it is a pioneering approach to the world of academia, radically improving the way scholarly research is managed. The grand vision of Frontiers is a world where all people have an equal opportunity to seek, share and generate knowledge. Frontiers provides immediate and permanent online open access to all its publications, but this alone is not enough to realize our grand goals.

Frontiers journal series

The Frontiers journal series is a multi-tier and interdisciplinary set of open-access, online journals, promising a paradigm shift from the current review, selection and dissemination processes in academic publishing. All Frontiers journals are driven by researchers for researchers; therefore, they constitute a service to the scholarly community. At the same time, the *Frontiers journal series* operates on a revolutionary invention, the tiered publishing system, initially addressing specific communities of scholars, and gradually climbing up to broader public understanding, thus serving the interests of the lay society, too.

Dedication to quality

Each Frontiers article is a landmark of the highest quality, thanks to genuinely collaborative interactions between authors and review editors, who include some of the world's best academicians. Research must be certified by peers before entering a stream of knowledge that may eventually reach the public - and shape society; therefore, Frontiers only applies the most rigorous and unbiased reviews. Frontiers revolutionizes research publishing by freely delivering the most outstanding research, evaluated with no bias from both the academic and social point of view. By applying the most advanced information technologies, Frontiers is catapulting scholarly publishing into a new generation.

What are Frontiers Research Topics?

Frontiers Research Topics are very popular trademarks of the *Frontiers journals series*: they are collections of at least ten articles, all centered on a particular subject. With their unique mix of varied contributions from Original Research to Review Articles, Frontiers Research Topics unify the most influential researchers, the latest key findings and historical advances in a hot research area.

Find out more on how to host your own Frontiers Research Topic or contribute to one as an author by contacting the Frontiers editorial office: frontiersin.org/about/contact

Microbial ecological and biogeochemical processes in the soil-vadose zone-groundwater habitats, volume II

Topic editors

Zifang Chi — Jilin University, China

Huai Li — Northeast Institute of Geography and Agroecology, Chinese Academy of Sciences (CAS), China

Jiuling Li — The University of Queensland, Australia

Yi-Hao Luo — Northeast Normal University, China

Citation

Chi, Z., Li, H., Li, J., Luo, Y.-H., eds. (2024). *Microbial ecological and biogeochemical processes in the soil-vadose zone-groundwater habitats, volume II*.

Lausanne: Frontiers Media SA. doi: 10.3389/978-2-8325-5456-2

Table of contents

frontiers | Frontiers in Microbiology

TYPE Editorial
PUBLISHED 09 September 2024
DOI 10.3389/fmicb.2024.1486331

OPEN ACCESS

EDITED AND REVIEWED BY
David Emerson,
Bigelow Laboratory For Ocean Sciences,
United States

*CORRESPONDENCE
Zifang Chi
✉ chizifang@jlu.edu.cn

RECEIVED 26 August 2024
ACCEPTED 30 August 2024
PUBLISHED 09 September 2024

CITATION
Li H, Chi Z, Li J and Luo Y (2024) Editorial: Microbial ecological and biogeochemical processes in the soil-vadose zone-groundwater habitats, volume II. *Front. Microbiol.* 15:1486331. doi: 10.3389/fmicb.2024.1486331

Editorial: Microbial ecological and biogeochemical processes in the soil-vadose zone-groundwater habitats, volume II

Huai Li[1], Zifang Chi[2]*, Jiuling Li[3] and Yihao Luo[4]

[1]State Key Laboratory of Black Soils Conservation and Utilization, Northeast Institute of Geography and Agroecology, Chinese Academy of Sciences, Changchun, China, [2]Key Lab of Groundwater Resources and Environment, Ministry of Education, Jilin University, Changchun, China, [3]Australian Centre for Water and Environmental Biotechnology, The University of Queensland, Brisbane, QLD, Australia, [4]Swette Center for Environmental Biotechnology, Biodesign Institute at Arizona State University, Tempe, AZ, United States

KEYWORDS

soil, vadose zone, groundwater, habitats, microbial ecological and biogeochemical processes

Editorial on the Research Topic
Microbial ecological and biogeochemical processes in the soil-vadose zone-groundwater habitats, volume II

Microorganisms regulate biogeochemical cycles and serve various functions within the soil, vadose zone, and groundwater habitats (Chi et al., 2022; Li et al., 2023). Microbial communities are highly sensitive to environmental changes and can respond rapidly to such alternations (Liang et al., 2023). The composition and functionality of microorganisms across different habitats are influenced by both biotic and abiotic factors, which in turn affect biochemical processes and overall ecosystem functions (Li et al., 2019, 2022). Natural wetlands, landfills, composts, vadose zones, and saturated aquifers are examples of the habitats typically found within soil, vadose zone, and groundwater. This topic aims to compile recent research on microbial ecological processes within the soil-vadose zone-groundwater continuum and to highlight the potential for achieving sustainable processes. There is significant interest in understanding these interconnected habitats, particularly regarding microbial pathways involved in material cycling, pollution control, and carbon neutrality. Thirteen articles included in this Research Topic have undergone rigorous peer review and have been selected for their contributions to these areas of study.

Ding et al. investigated the impact of key microorganisms on water quality stability within river-lake systems during periods of hydrological regulation. Their findings revealed that lake areas exhibited better water quality compared to both inflow and inflow areas, although no significant differences were observed in sediment composition. The study identified *Pseudomonas*, *Acinetobacter*, and *Microbacterium* as crucial in removal of nitrate and phosphates. However, an increase in flow velocity and nutrient load was found to negatively affect the abundance of these key microorganisms.

Li, Zhu et al. conducted short-term field soil incubation study using samples from the Svalbard glacier meltwater river at varying temperatures (2°C, 10°C, 20°C). The study found that CH_4 emissions in soil warming did not increase in the first several days, but site specificity was more important. However, emissions initially increased before gradually decreasing as the warming period extended. These results are significant for assessing GHG emission fluxes under global warming.

Xu et al. isolated a bacterium named NS-6 from sandstone oil in the Ordos Basin. This strain demonstrated exceptional urease production and calcium carbonates ($CaCO_3$) precipitation capabilities. Additionally, it was found to possess a serial of genes involved in urea catabolism and $CaCO_3$ deposition.

Yuan et al. discovered that phosphorus (P) components significantly influence bacterial and archaeal β-diversity in sediments. In Hongfeng Lake, β-diversity was influenced by metal oxide-bound inorganic P and sediment total P, whereas in Aha Lake, it's affected by reductant-soluble total P or calcium-bound inorganic P. Inorganic P had greater effects on bacterial β-diversity, while organic P more affected archaeal diversity.

Wang et al. investigated the effects of various fertilization treatments on soil antibiotic resistance genes (ARGs) and found that organic fertilizers led to a higher number and abundance of ARGs. In contrast, the changes in ARGs associated with chemical fertilizers were primarily due to the colonization of native microorganisms, and conventional fertilizers were in between. This finding offers valuable insights into the dynamics of ARGs under long-term application of different fertilizers.

Li H. et al. investigated the effects of different depths of groundwater irrigation on soil microorganisms in paddy wetlands. Their study revealed that microorganisms in shallow groundwater irrigation was highly sensitive to environmental changes, and Fe-anammox, nitrification, and methane oxidation were favorable under deep groundwater irrigation. The findings offer new ideas for controlling non-point source pollution and reducing greenhouse gas emissions in paddy wetlands.

Zhang L. et al. studied the seasonal variation of nitrogen-cycling genes in the sediment of Baiyangdian and identified dissimilatory nitrate reduction, assimilatory nitrate reduction, and denitrification were dominant nitrogen-cycling processes. Nitrification-related genes had high abundance in spring, while high denitrification-related genes in fall were observed. Dissolved organic carbon, water temperature, and antibiotics were significantly correlated with nitrogen-cycling processes.

Zhang R. et al. evaluated the impact of water management on soil physicochemical properties and enzyme activities in greenhouse grape cultivation. They found that while water stress had a minimal effect on soil physical–chemical properties, it significantly reduced the accumulation of soil microbial biomass carbon (MBC) content throughout the grape growing season and reduced soil microbial biomass nitrogen (MBN) content in later growth. Mild and moderate water stress conditions were also found to inhibit the activities of urease, catalase, and sucrase activities.

Du et al. developed a water quality index (WQI) model to evaluate the water quality on Hainan Island using data from 2015 to 2020. The results indicated a moderate overall water quality, with 86.36% of monitoring stations classified as having good quality, while 13.53% were categorized as poor or very poor. Poor quality was primarily observed in major cities and aquaculture areas, with worst conditions in March, October, and November. Key pollution sources included urbanization, agriculture, and industry.

Li, Hong et al. investigated the effects of *Pythium ultimum* on the migration and biodegradation of bacteria Diaphorobacter sp. LW2 in soils of different particle sizes. They found that the hyphae of *Pythium ultimum* facilitated the growth and migration of LW2, enabling it to move along or against the direction of hyphae growth. Pythium ultimum enhanced the migration and survival of LW2 in soil, improving the bioremediation of polluted soil.

Song et al. reviewed the critical role of freshwater wetland biodiversity in maintaining habitat functional stability. They examined the environmental drivers affecting habitat function stability, explored the effects of plant and microbial diversity on habitat function stability, revealed the impacts and mechanisms of habitat changes on biodiversity, and further proposed an outlook for research in freshwater wetland research.

Ali et al. studied the effectiveness of three novel modified surface flow constructed wetlands (CW1: Brick rubble, lignite, and *Lemna minor* L.; CW2: Brick rubble and lignite; CW3: *Lemna minor* L.) in treating sugar factory wastewater. The results suggested that CW1 exhibited high Chao1, Shannon, and Simpson indices. The denitrifying bacterial class Rhodobacteriaceae was found to be the most abundant in CW1. This finding supported that CW1 enhances the performance of water filtration in constructed wetlands.

Xing et al. analyzed vegetation changes and their drivers in the Changbai Mountain alpine tundra. The results revealed a decline in typical alpine plants and an increase in herbaceous plants. Species richness and diversity showed an upward trend across various elevations, with a notable shift toward herbaceous dominance. The study found that soil nutrients, rather than climate, were the primary drivers of short-term vegetation changes.

We think that all accepted articles in this Research Topic will provide new knowledge on microbial processes in soil-vadose zone-groundwater habitats.

Author contributions

HL: Writing – original draft. ZC: Conceptualization, Project administration, Writing – review & editing. JL: Writing – review & editing. YL: Writing – review & editing.

Funding

The author(s) declare financial support was received for the research, authorship, and/or publication of this article. This work was supported by the National Key R&D Program of China (NOs. 2023YFC3207704 and 2022YFF1300901), the National Natural Science Foundation of China (NOs. 42477025 and 42077353), and the Natural Science Foundation of Jilin Province (NOs. 20230101369JC and 20230101100JC).

Acknowledgments

Our topic editor's team thanks all the authors, reviewers, and editorial staff of Frontiers in Microbiology distinguished contributions to our Research Topic.

Conflict of interest

The authors declare that the research was conducted in the absence of any commercial or financial relationships that could be construed as a potential conflict of interest.

Publisher's note

References

Chi, Z., Zhu, Y., and Yin, Y. (2022). Insight into SO_4(-II)-dependent anaerobic methane oxidation in landfill: dual-substrates dynamics model, microbial community, function and metabolic pathway. *Waste Manage.* 141, 115–124. doi: 10.1016/j.wasman.2022.01.032

Li, H., Chi, Z., Li, J., and Luo, Y. (2023). Microbial ecological and biogeochemical processes in the soil-vadose zone-groundwater habitats. *Front. Microbiol.* 14:1238103. doi: 10.3389/fmicb.2023.1238103

Li, H., Chi, Z., Li, J., Wu, H., and Yan, B. (2019). Bacterial community structure and function in soils from tidal freshwater wetlands in a Chinese delta: potential impacts of salinity and nutrient. *Sci. Total Environ.* 696:134029. doi: 10.1016/j.scitotenv.2019.134029

Li, H., Liang, S., Chi, Z., Wu, H., and Yan, B. (2022). Unveiling microbial community and function involved in anammox in paddy vadose under groundwater irrigation. *Sci. Total Environ.* 849:157876. doi: 10.1016/j.scitotenv.2022.157876

Liang, S., Li, H., Wu, H., Yan, B., and Song, A. (2023). Microorganisms in coastal wetland sediments: a review on microbial community structure, functional gene, and environmental potential. *Front. Microbiol.* 14:1163896. doi: 10.3389/fmicb.2023.1163896

frontiers | Frontiers in Microbiology

TYPE Original Research
PUBLISHED 11 October 2023
DOI 10.3389/fmicb.2023.1279751

OPEN ACCESS

EDITED BY
Zifang Chi,
Jilin University, China

REVIEWED BY
Manoj Kumar Solanki,
University of Silesia in Katowice, Poland
Shangqi Xu,
Anhui Normal University, China

*CORRESPONDENCE
Runyu Zhang
✉ zhangrunyu@vip.gyig.ac.cn

RECEIVED 25 August 2023
ACCEPTED 27 September 2023
PUBLISHED 11 October 2023

CITATION
Yuan H, Zhang R, Li Q, Han Q, Lu Q and Wu J (2023) Unveiling the ecological significance of phosphorus fractions in shaping bacterial and archaeal beta diversity in mesotrophic lakes.
Front. Microbiol. 14:1279751.
doi: 10.3389/fmicb.2023.1279751

Unveiling the ecological significance of phosphorus fractions in shaping bacterial and archaeal beta diversity in mesotrophic lakes

Haijun Yuan[1,2], Runyu Zhang[1]*, Qiuxing Li[1,3], Qiao Han[1,2], Qiping Lu[1,2] and Jing Wu[1,2]

[1]State Key Laboratory of Environmental Geochemistry, Institute of Geochemistry, Chinese Academy of Sciences, Guiyang, China, [2]University of Chinese Academy of Sciences, Beijing, China, [3]College of Earth Science, Chengdu University of Technology, Chengdu, China

Both community variation and phosphorus (P) fractions have been extensively studied in aquatic ecosystems, but how P fractions affect the mechanism underlying microbial beta diversity remains elusive, especially in sediment cores. Here, we obtained two sediment cores to examine bacterial and archaeal beta diversity from mesotrophic lakes Hongfeng Lake and Aha Lake, having historically experienced severe eutrophication. Utilizing the Baselga's framework, we partitioned bacterial and archaeal total beta diversity into two components: species turnover and nestedness, and then examined their sediment-depth patterns and the effects of P fractions on them. We found that total beta diversity, species turnover or nestedness consistently increased with deeper sediment layers regarding bacteria and archaea. Notably, there were parallel patterns between bacteria and archaea for total beta diversity and species turnover, which is largely underlain by equivalent processes such as environmental selection. For both microbial taxa, total beta diversity and species turnover were primarily constrained by metal oxide-bound inorganic P (NaOH-Pi) and sediment total phosphorus (STP) in Hongfeng Lake, while largely affected by reductant-soluble total P or calcium-bound inorganic P in Aha Lake. Moreover, NaOH-Pi and STP could influence bacterial total beta diversity by driving species nestedness in Hongfeng Lake. The joint effects of organic P (Po), inorganic P (Pi) and total P fractions indicated that P fractions are important to bacterial and archaeal beta diversity. Compared to Po fractions, Pi fractions had greater pure effects on bacterial beta diversity. Intriguingly, for total beta diversity and species turnover, archaea rather than bacteria are well-explained by Po fractions in both lakes, implying that the archaeal community may be involved in Po mineralization. Overall, our study reveals the importance of P fractions to the mechanism underlying bacterial and archaeal beta diversity in sediments, and provides theoretical underpinnings for controlling P sources in biodiversity conservation.

KEYWORDS

bacteria, archaea, beta diversity, turnover, nestedness, phosphorus fractions, mesotrophic lakes

Introduction

Biodiversity has potentially dramatic effects on aquatic (Zhang et al., 2021; Wang et al., 2021a) or terrestrial (Delgado-Baquerizo et al., 2020; Zhao et al., 2022) ecosystem functioning and stability. Prior studies have documented that ecosystems containing more species exhibit higher levels of ecosystem functions (Xun et al., 2019). Especially in naturally assembled communities, high biodiversity shows a strong positive effect on multiple ecosystem functions such as biomass production and trophic interactions (van der Plas, 2019). More importantly, the ongoing biodiversity loss is dramatically weakening the functioning of ecosystems. As such, diversity-triggered deterministic assembly processes are critical to understanding the degradation or enhancement in ecosystem functioning (Moroenyane et al., 2016; Xun et al., 2019). In recent decades, untangling the underlying mechanisms of biodiversity or biogeographic patterns has been considered as a central topic in ecology and microbial ecology (Zhou and Ning, 2017; Wang W. et al., 2020). There is increasing evidence that microbial alpha diversity has a crucial role in ecosystem function or services, but less attention has been paid to beta diversity (i.e., community variation between biological composition) (Xun et al., 2019). Beta diversity bridges the gap between local (alpha) and regional (gamma) diversity and is often applied to quantify the variation of species compositions between different ecological communities (Whittaker, 1960). Particularly, beta diversity interacts with alpha-diversity gradients, both resulting from community assembly via local or regional environmental filters (Soininen et al., 2018). Moreover, beta diversity, in contrast to alpha diversity, can better capture spatial or temporal dynamics of biodiversity patterns. Considering beta diversity in landscape-scale conservation (also known as ecosystem approach, can bring huge benefits to biodiversity and economy at large landscape scales) efforts will greatly contribute to improving ecosystem function, particularly in abiotically heterogeneous landscapes (van der Plas et al., 2023). In aquatic or terrestrial ecosystems, microbes, as key factors driving biogeochemical cycling processes, have a critical role in ecosystem functioning and services and are fundamental in maintaining ecosystem stability (Singh et al., 2010; Wu et al., 2019). Meanwhile, such element cycles release large amounts of reactive nitrogen (N), phosphorus (P) and heavy metals, leading to dramatic growth of aquatic plants and phytoplankton that consume excessive nutrients dissolved oxygen and light intensity. Accordingly, aquatic ecosystems and biodiversity therein are substantially threatened by environmental stressors like eutrophication or chemical pollution (Xiong et al., 2020). Given that such relationship among biodiversity and ecosystem functioning is scale-dependent (van der Plas et al., 2023), examining microbial beta diversity along environmental gradients, such as sediment depth (Yuan et al., 2021), is essential for understanding the variations in ecosystem functioning and stability.

It has long been the core of community ecology for unraveling the driving mechanisms of ecological communities, reflecting that beta diversity plays a pivotal role in community assemblage (i.e., the mechanisms underlying biodiversity organization) (Mori et al., 2018). More recently, from micro- to macro-organisms, beta diversity has been extensively partitioned into components turnover and nestedness to examine the ecological processes that shape community structures (Marta et al., 2021). Based on Sørensen dissimilarity index, Baselga (2010) proposed a framework to decompose beta diversity into turnover (i.e., species replacement) and nestedness, which provides valuable insights into biodiversity effects. The former reflects the replacement between species without changing species richness, whereas the latter indicates the richness differences caused by non-random species gain and loss (Baselga, 2010). Partitioning beta diversity may yield additional insights into biodiversity effects such as selection and complementarity effects (Mori et al., 2018), which identify the possible contributions of the turnover or nestedness components, thereby revealing whether community variation result from species replacement and species gain or loss. Compared to traditional beta diversity index like Bray–Curtis dissimilarity, partitioning beta diversity can provide a valuable fresh perspective to address the underlying causes of community variation in response to environmental changes (Viana et al., 2016; García-Navas et al., 2022). Specifically, phosphorus, as a limiting nutrient, acts as environmental filtering to constrain biological succession (Zheng et al., 2021) and can also drive community variation by influencing species turnover or nestedness. For example, species turnover dominates bacterial total beta diversity in freshwater ecosystems, but is largely constrained by water total P, substantially altering the water-depth pattern of bacterial community variation (Wu et al., 2020; Yuan et al., 2022). Therefore, partitioning beta diversity may help disentangle the ecological mechanisms governing microbial community variation under P limitation.

Currently, phosphorus is recognized as a primary limiting nutrient element in both aquatic and terrestrial ecosystem productivity (Cramer, 2010) and poses a considerable threat to biodiversity conservation (Ceulemans et al., 2014). A growing body of evidence suggests that phosphate (PO_4^{3-}) or total phosphorus can essentially alter the structure of bacterial, archaeal and fungal communities in aquatic ecosystems (Zhang et al., 2021; Guo et al., 2022). However, the underlying mechanisms of microbial beta diversity under the influence of P fractions are, hitherto, underexplored, especially in sediment cores. According to the Psenner fractionation method (Psenner et al., 1988), P fractions are primarily classified into five categories: loosely adsorbed P (NH_4Cl-P), reductant-soluble P (BD-P), metal oxide-bound P (NaOH-P), calcium-bound P (HCl-P) and residual P (Res-P). Such P fractions can effectively distinguish the phosphorus sources buried in sediments and thereby disentangle the release mechanism of endogenous P in lakes or reservoirs (Zhu et al., 2013). Typically, such potentially mobile phosphorus can be well-applied to evaluate the mechanism underlying endogenous P released from sediments in lake ecosystems (Rydin, 2000). More recently, such relationship between P fractions and microbes is widely concerned in terrestrial ecosystems (Yang et al., 2023), but it is still largely missing in aquatic ecosystems. For example, microbial population have a crucial role in forming or releasing soil labile phosphorus across Tibetan alpine grasslands (Li et al., 2022), while P fractions can also influence the abundance of *Actinomycetes* by governing the enrichment of soil organic matter (Bian et al., 2022). Especially in rhizosphere soils, calcium-bound P can effectively inhibit the increase of microbial composition and biomass P (Teng et al., 2018). Conversely, in aquatic ecosystems, both mobile P and calcium-bound P are positively correlated with bacterial phyla such as *Firmicutes* and *Proteobacteria* (Yin et al., 2022). Notably, BD-P and NaOH-P are available and released easily from sediments, largely accelerating the eutrophication processes of water bodies and promoting the growth of phytoplankton (Cavalcante et al., 2018). Previous studies have

mostly focused on the importance of total phosphorus to microbial communities, largely neglecting the contribution of specific components contained in total phosphorus. Dividing total phosphorus into various forms (i.e., specific P components) of P is an effective method to study the compositions and properties of sediment P (Yin et al., 2022). Intriguingly, these sediment P fractions are closely related to the endogenous release mechanism of lake eutrophication (Zhu et al., 2013). Additionally, partitioning beta diversity into species turnover and nestedness can well reveal the succession mechanism underlying microbial communities (Marta et al., 2021). Correspondingly, based on the effects of phosphorus components on microbial beta diversity, it is not difficult to infer whether lake eutrophication poses a threat to microbial communities. As such, coupling P fractions with beta diversity partition may provide a better way to unravel the driving mechanisms underlying microbial community variation.

Here, we obtained two sediment cores from Hongfeng Lake and Aha Lake, both of which are located in the Yunnan-Guizhou Plateau, Southwest China. Bacterial and archaeal communities were then quantified with the sequencing data of the *16S rRNA* gene. According to Baselga's framework, we partitioned total beta diversity into turnover and nestedness, and then explored their sediment-depth patterns regarding bacteria and archaea. Further, we conducted in-depth analyses to uncover the relationships between beta diversity and P fractions. We primarily focused on three objectives: (1) to elucidate the mechanisms underlying bacterial or archaeal beta diversity along sediment depth and determine how turnover and nestedness essentially contribute to total beta diversity, (2) to reveal such cross-taxon relationship between bacteria and archaea in terms of beta diversity components, and (3) to identify the importance of each P fraction to microbial beta diversity and further evaluate how organic, inorganic and total P fractions drive bacterial and archaeal beta diversity.

Materials and methods

Study area and field sampling

The studied lakes, Hongfeng Lake and Aha Lake, have high internal P loading in sediments and are located in the karst region of the Yunnan-Guizhou Plateau, Southwest China. Hongfeng Lake, also known as Hongfeng Reservoir, has a surface area of 57.2 km^2 with a maximum water depth of 45 m and holds 601 million m^3 of lake water (Wang et al., 2016a). Hongfeng Lake is a typical P-limited artificial lake, showing a total P concentration of 0.03–0.10 mg L^{-1} and a TN/TP ratio of ~30 (Zhu et al., 2013). The total P content in sediments ranges from 766 to 4,306 mg kg^{-1}, with an average of 1815 mg kg^{-1} (Wang et al., 2015). In 1978, Hongfeng Lake began to serve as a fish farm for economic benefit (Chen et al., 2019), which largely promoted the transition of its trophic status from oligotrophic to eutrophic (Yu et al., 2022). In particular, due to large amounts of P released from fish food and excrement, Hongfeng Lake experienced severe eutrophication and algal blooms in the mid-late 1990s. Notably, algal blooms occur frequently in Hongfeng Lake even though external phosphorus loading is well controlled in recent decades (Ma et al., 2022), presumably owing to the internal phosphorus loading released from sediments.

Aha Lake, constructed or initially impounded in 1960, is a typical artificial lake and situated in the suburb of Guiyang City, the capital of Guizhou Province (Chen et al., 2015). Aha Lake shows a total watershed area of 190 km^2 and a capacity of 542 million m^3 and is mainly recharged by five tributaries such as the Youyu, Baiyan, Caichong, Lannigou and Sha Rivers (Ni et al., 2021). Notably, it covers a surface area of 4.5 km^2 and has a maximum water depth of 26 m (Chen et al., 2015). Aha Lake is a P-limited and deep plateau lake (Liu et al., 2019), with total P concentrations ranging from 0.022 to 0.205 mg L^{-1} and an average of 0.046 mg L^{-1} (Wang et al., 2021b). Owing to the aggravation of anoxia in the hypolimnion, large amounts of pollutants like phosphorus have been released from the sediments (Lan et al., 2017). Such phosphorus can broadly induce algal blooms and thereby endanger the water quality of this lake (Han et al., 2018).

As artificial karst lakes, both Hongfeng and Aha Lakes have frequently experienced severe eutrophication, thereby providing an ideal setting to study P fractions in sediments. Based on the profile change of sediment P, sediment core can effectively reflect the historical activities and human disturbance of a lake. Given that suspended particles form sediment profiles through sedimentation, large amounts of water P are buried in the sediments. Meanwhile, microbes ingest the nutrients such as phosphorus from the sediment to sustain growth. Using a gravitational sampler and a polyethylene tube, we obtained two sediment cores (i.e., HF1 and AH7, Figure 1) of 62 and 60 cm lengths from Hongfeng and Aha Lakes, respectively. With water depths of 15 and 22 m, HF1 and AH7 were collected in April and June 2022, respectively. The two cores were divided into 2 cm-long sediment samples *in situ*. Each sample was thoroughly stirred and homogenized, and then placed in two 20 mL sterile bottles. To avoid cross-contamination, one sterilized spoon is used for each sample when stirring. Notably, such samples must be transferred to laboratory at −20°C within an hour. For the 61 obtained samples, one bottle was stored at −80°C for biological analysis, and the other was freeze-dried and then stored at −20°C for physicochemical analysis.

Phosphorus fractions

The P fractions were measured by Psenner's sequential extraction scheme as modified by Hupfer et al. (1995). This scheme has been widely used in the field of lakes to study the P fractions in sediments and provides a theoretical basis for evaluating the endogenous release of P cycling. It generally divides sediment P into five fractions, that is, loosely adsorbed P (NH_4Cl-P), reductant-soluble P (BD-P), metal oxide-bound P (NaOH-P), calcium-bound P (HCl-P) and residual P (Res-P). BD-P refers to iron-bound P and NaOH-P indicates aluminum-bound P. It should be noted that the whole procedure was conducted with 0.20 g freeze-dried sediment for each sample. Briefly, such sediment was sequentially extracted with 1 M NH_4Cl for 0.5 h, 0.11 M $NaHCO_3/Na_2S_2O_4$ for 1 h, 1 M NaOH for 16 h and 0.5 M HCl for 16 h on a thermostatic shaker (220 r min^{-1}). After which, all the extracts were centrifuged at 4000 r min^{-1} for 15 min. Notably, these extracts must be filtered through a 0.45 μm polyethersulfone (PES) membrane (Jinteng, China) and then transferred to a 25 mL colorimetric tube. More importantly, when such extract with NaOH or HCl was diluted to 22 mL, its pH must be adjusted to neutral before determining the content of P fraction. Furthermore, these final residues were collected, burned at 500°C for 2 h and then shaken with

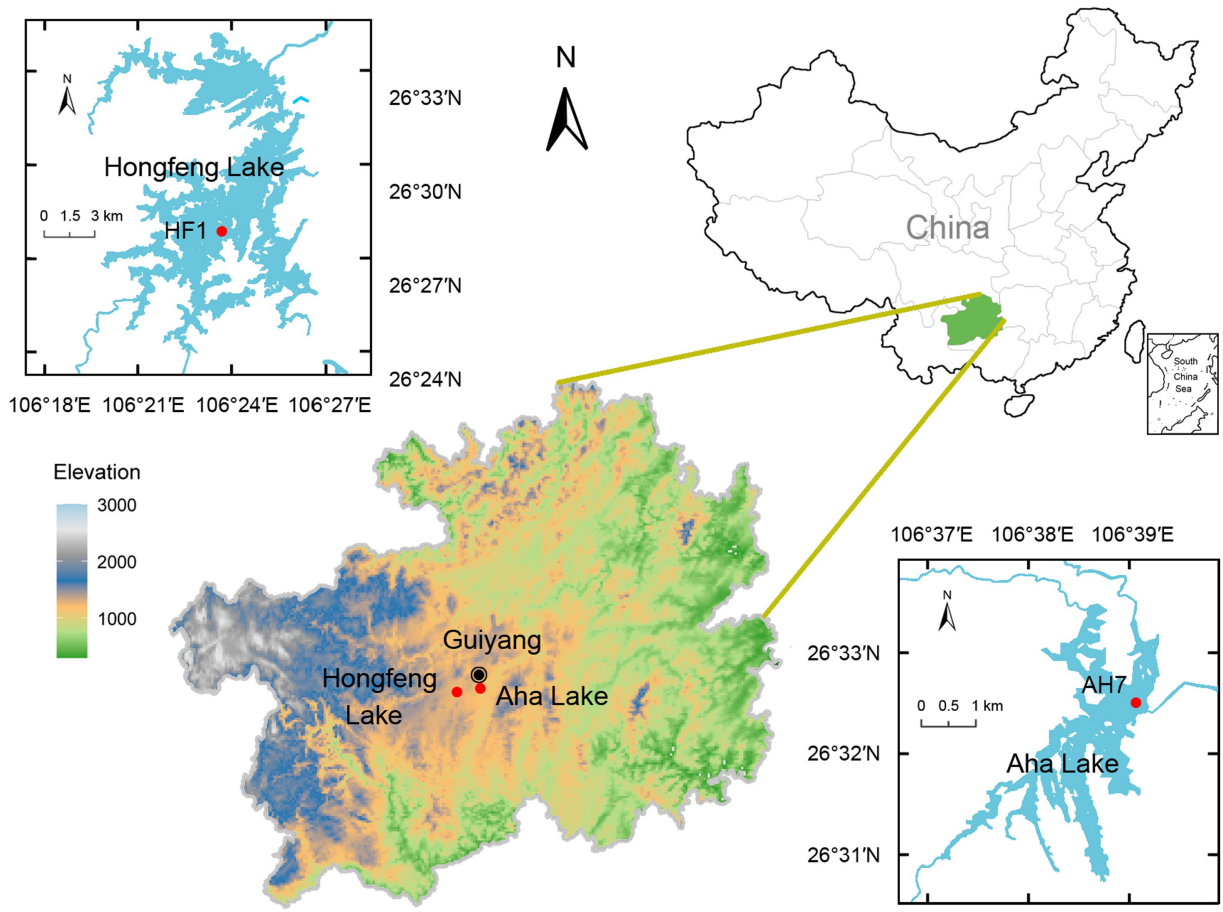

FIGURE 1
Study area and sampling location.

1 M HCl for 16 h to obtain the supernatant after centrifugation and filtration. Subsequently, the amount of PO_4^{3-} was quantified with the molybdate blue method (Murphy and Riley, 1962).

Such P fractions contain three forms: organic (Po), inorganic (Pi) and total P (TP). Based on the extraction procedure above, we directly determined the loosely adsorbed Pi (NH_4Cl-Pi), reductant-soluble Pi (BD-Pi), metal oxide-bound Pi (NaOH-Pi), calcium-bound Pi (HCl-Pi) and residual TP (Res-TP). Meanwhile, each extract was digested with 50 g L^{-1} $K_2S_2O_8$ at 120°C for 0.5 h to obtain their corresponding TP, that is, NH_4Cl-TP, BD-TP, NaOH-TP and HCl-TP. Then, organic P fractions NH_4Cl-Po, BD-Po, NaOH-Po and HCl-Po were calculated according to the difference between TP and Pi. Similarly, we obtained sediment total phosphorus (STP) based on the sum of the above total P fractions.

DNA sequencing and community analyses

Total DNA from 0.30 g sediment sample was extracted in triplicate with the MagaBio Soil/Feces Genomic DNA Purification Kit (Bioer, Hangzhou, China) based on the manufacturer's protocol. The DNA purity or concentrations were determined by spectrophotometry (NanoDrop One, United States). Then, the three DNA samples are thoroughly mixed before the polymerase chain reaction (PCR). To amplify the V4 regions of the bacterial and archaeal *16S rRNA* gene, we selected the universal primer pairs 515F (5′-GTGYCAGCMGCCGCGGTAA-3′) and 806R (5′-GGACTACNVGGGTWTCTAAT-3′) to perform the PCR (Apprill et al., 2015; Parada et al., 2016). The reaction conditions were as follows: 94°C for 5 min, followed by 30 cycles of 94°C for 30 s, 52°C for 30 s and 72°C for 30 s, all followed by a final elongation at 72°C for 10 min and termination of the reaction at 4°C. These PCR products were mixed at an equal density ratio and then purified with E.Z.N.A. Gel Extraction Kit (Omega, United States). Sequencing was conducted on the Illumina Nova6000 platform (Illumina Inc., CA, United States) to generate 250 bp paired-end reads.

For the raw data, the barcode sequence was separated and then removed from both ends of the sequence through the R-script written by Liu et al. (2021). According to the primer sequence, the reverse sequence was transposed to the forward direction. Such sequences were then processed with a pipeline combining USEARCH 11.0 and QIIME2. The high-quality reads were screened with the default values in USEARCH, and then binned into amplicon sequence variants (ASVs) after denoising by unoise3 (Edgar and Flyvbjerg, 2015). The taxonomic identification of ASVs for the sequences was assigned using the Ribosomal Database Project (RDP; http://rdp.cme.msu.edu/) classifier algorithm with a confidence threshold of 97%, and the feature table was generated for community analysis. The above

analyses were generally assisted by Liu's script (Liu et al., 2021). Based on the frequency of the minimum reads, bacterial and archaeal communities were rarefied at 49,000 and 100 sequences for Hongfeng Lake and 100,000 and 400 sequences for Aha Lake, respectively. These sequencing data have been deposited in the NCBI Sequence Read Achieve (SRA) under accession number PRJNA885467.

Statistical analyses

We first calculated the Sørensen dissimilarity index to indicate total beta diversity and decomposed it into species turnover and nestedness using package "betapart" in R (Baselga and Orme, 2012). According to Baselga's framework, species turnover and nestedness were employed with Simpson and nestedness coefficients, respectively. The sediment depth distances between the samples were then computed using the Euclidean distance. Subsequently, we examined the sediment-depth patterns for bacterial and archaeal beta diversity in both lakes. Such relationships were modeled with linear or quadratic models, and the significance was estimated by Mantel test (9,999 permutations). Moreover, for these P fractions, we also investigated the variation of organic, inorganic and total P fractions along sediment depth in both lakes.

Second, to investigate the influence of sediment P forms on microbial community compositions, we performed Spearman correlation analysis for the relative abundance of the top 30 bacterial genera or top 7 archaeal genera and P fractions. Such relationships were then clustered using an unweighted pair group method with arithmetic mean (UPGMA) on Euclidean distances. Furthermore, the Mantel test (Mantel, 1967) was conducted for bacteria and archaea to reveal the relationships between beta diversity and each P fraction. In addition, we also applied the Mantel test to examine such associations among bacteria and archaea in terms of beta diversity components, and conducted linear regressions to visualize their trends.

Third, to exclude the strong collinearity between all P fractions, we applied the varclus procedure of the Hmisc R package to detect the redundancy of the variables (Wang X.-B. et al., 2017). Notably, only one variable was preserved when a high correlation (Spearman $\rho^2 > 0.8$) was observed between these P fractions. Hence, as shown in Supplementary Figure S5, we removed NH_4Cl-Po, HCl-TP, NaOH-TP and BD-Pi from the datasets of Hongfeng and Aha Lakes. And then, using the MRM() function of the ecodist R package (Goslee and Urban, 2007), we performed multiple regression on distance matrices (MRM) (Lichstein, 2007) to quantify such association among beta diversity components and all P fractions. For such P fractions, the influence of multicollinearity must be excluded before applying MRM.

Finally, we conducted variation partitioning analysis (VPA) (Anderson and Cribble, 1998) to identify the relative explanatory power of organic, inorganic and total P fractions and their interaction on variation in total beta diversity and its components. For the two microbial taxonomic groups, forward selection (9,999 permutations) against such biological characteristic data was performed to select the significant variables before running VPA. All of the above analyses were implemented in R V4.2.1 with packages vegan V2.5-5 (Oksanen et al., 2013), betapart V1.5.1 (Baselga et al., 2018), ecodist V2.0.1 (Goslee and Urban, 2007) and Hmisc (Harrell, 2019).

Results

Vertical variation of bacterial or archaeal beta diversity and P fractions

Relationship among sediment depth and beta diversity was generally significant for bacteria or archaea in both lakes, as determined by *F*-test (Figure 2). For total beta diversity, bacteria or archaea had a significant upward trend toward deeper sediment layers. Compared to bacteria (HF: slope = 0.0009, AH: slope = 0.0009), archaea showed faster variation for total beta diversity in Hongfeng and Aha Lakes, with slopes of 0.0038 and 0.0021, respectively (Figures 2A,D and Supplementary Table S1). Similarly, archaea changed faster for species turnover than bacteria in Hongfeng Lake, with slopes of 0.0039 and 0.0008, respectively (Figure 2B and Supplementary Table S1). Significant sediment-depth pattern of species turnover was also observed in Aha Lake, but the rates of bacterial and archaeal changes were similar, with slopes of 0.0011 and 0.0012, respectively (Figure 2E and Supplementary Table S1). For species nestedness (differences in species richness), bacteria showed a significant positive relationship with sediment depth in Hongfeng Lake (Figure 2C), while archaea had an increasing ($p < 0.05$) depth-related pattern in Aha Lake (Figure 2F). Additionally, for alpha diversity, bacteria and archaea generally showed significant ($p < 0.05$) U-shaped or hump-shaped patterns along sediment-depth in both lakes (Supplementary Figure S6). In Hongfeng Lake, bacterial richness increased first and then decreased with sediment depth, while archaeal richness increased exponentially (Supplementary Figures S6A,D). For richness, evenness and Simpson diversity, whilst bacteria had significant ($p < 0.05$) depth-related patterns, there was little variation in Hongfeng Lake (Supplementary Figures S6A–C). Moreover, for evenness and Simpson diversity, bacteria decreased rapidly along sediment depth, while archaea increased slowly (Supplementary Figures S6B,C,E,F). Positive correlations among bacteria and archaea in terms of total beta diversity and its components were significantly assessed using Mantel test. For total beta diversity, bacteria and archaea showed the strongest cross-taxon congruence (Hongfeng: Mantel $r = 0.57$, $p < 0.001$; Aha: Mantel $r = 0.75$, $p < 0.001$, Figures 3A,D). Additionally, for species turnover, bacteria were significantly positively correlated with archaea (Hongfeng: Mantel $r = 0.49$, $p < 0.001$; Aha: Mantel $r = 0.49$, $p < 0.001$, Figures 3B,E). Notably, for species nestedness, bacteria had a high significant positive correlation (Mantel $r = 0.49$, $p < 0.001$) with archaea in Aha Lake, while weak association (Mantel $r = 0.07$, $p > 0.05$) in Hongfeng Lake (Figures 3C,F).

Generally, the content profiles of P fractions indicated that each P form had a decreasing trend toward deep sediments (Supplementary Figure S1). For total P fractions, BD-TP was relatively stable and declined from 264.79 $\mu g\,g^{-1}$ at 0–2 cm to 110.19 $\mu g\,g^{-1}$ at 60–62 cm depth in Hongfeng Lake, while it decreased sharply with sediment depth in 24–26 cm layers in Aha Lake (Supplementary Figures S1B,F). In addition, such decreasing trend was observed for NH_4Cl-TP in Hongfeng and Aha Lakes, with ranges of 3.44–27.53 and 1.59–35.14 $\mu g\,g^{-1}$, respectively (Supplementary Figures S1A,E). For Pi fractions, NaOH-Pi first increased greatly with depth in the 0–26 cm layers and then declined rapidly at depths greater than 46 cm in Hongfeng Lake, whereas it was relatively low (ranged at 138.15–838.55 $\mu g\,g^{-1}$) in the 12–32 cm layers

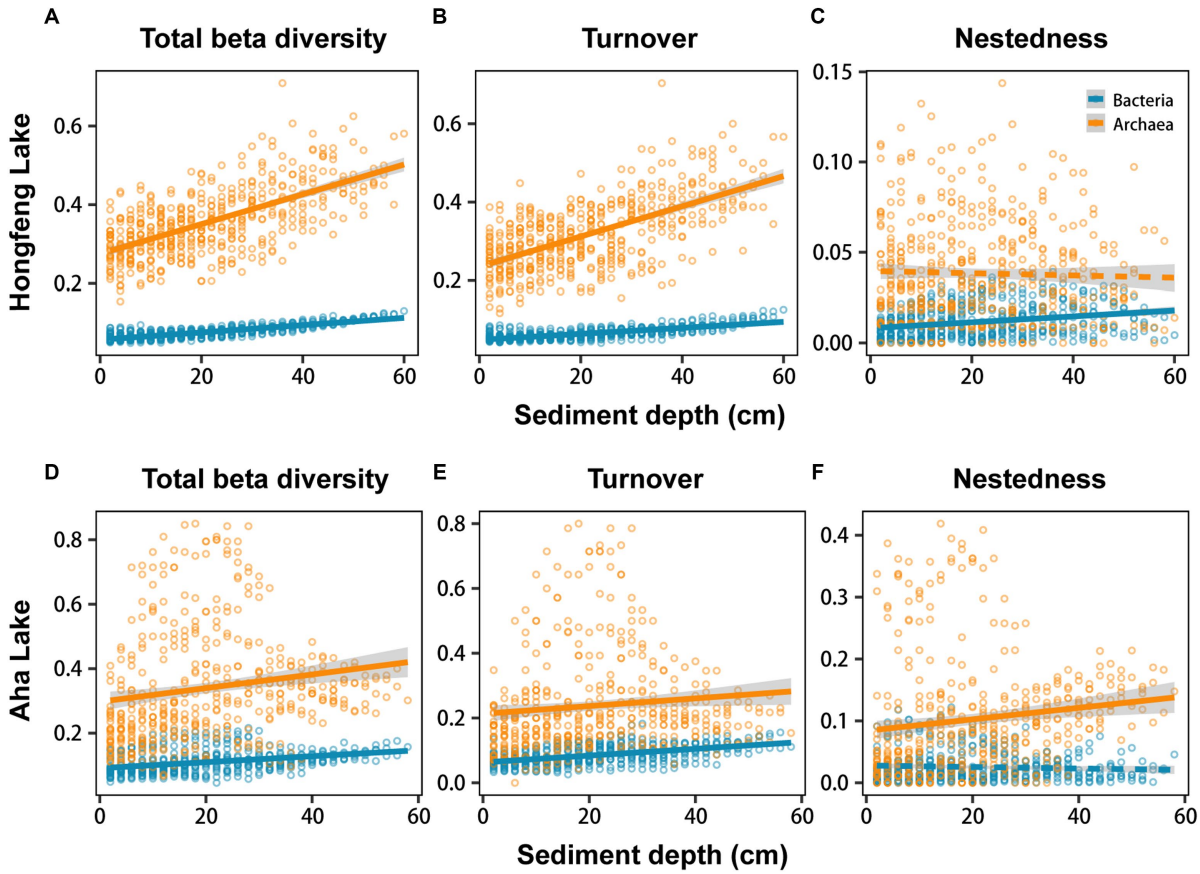

FIGURE 2
Sediment-depth patterns of bacterial and archaeal beta diversity in Hongfeng Lake **(A–C)** and Aha Lake **(D–F)**. The solid line indicates a significant relationship. More details for these models can be observed in Supplementary Table S1.

and had a general increasing trend in Aha Lake (Supplementary Figures S1C,G). Conversely, HCl-Pi declined rapidly with increasing sediment in Hongfeng Lake, and first declined greatly and then increased slightly in Aha Lake (Supplementary Figures S1D,H). For Po fractions, BD-Po showed a decreasing trend and declined from 124.35 $\mu g\,g^{-1}$ at 0–2 cm to 8.37 $\mu g\,g^{-1}$ at a 52–54 cm depth in Hongfeng Lake, while it changed slightly below 10 cm depth and then decreased sharply at depths greater than 12 cm in Aha Lake (Supplementary Figures S1B,F). Additionally, for NH_4Cl-P, BD-P, NaOH-P and HCl-P, the difference in organic (i.e., NH_4Cl-Po, BD-Po, NaOH-Po and HCl-Po), inorganic (NH_4Cl-Pi, BD-Pi, NaOH-Pi and HCl-Pi) and total P (NH_4Cl-TP, BD-TP, NaOH-TP and HCl-TP) forms was significantly ($p < 0.05$) observed between the two lakes (Supplementary Figure S2).

Linkages of microbial compositions and beta diversity with P fractions

Based on the Spearman correlation, strong association between bacterial or archaeal composition and P fractions was observed in both lakes (Figure 4; Supplementary Figure S3). For bacterial compositions, the total or inorganic P fractions such as NH_4Cl-TP, NH_4Cl-Pi, HCl-TP, and HCl-Pi had strong ($p < 0.05$) positive correlations with the dominant genera such as *Lentimicrobium* and *Saccharicrinis*, and significant ($p < 0.05$) negative correlations with other dominant genera like *Dethiosulfatarculus* and *Archangium* in both lakes (Figure 4). Additionally, organic P fractions such as BD-Po, NaOH-Po and NH_4Cl-Po were strongly correlated with such dominant genera while HCl-Po showed weak correlations in Hongfeng Lake (Figure 4A). Similarly, there was a weak and nonsignificant relationship between HCl-Po and bacterial genera in Aha Lake (Figure 4B). Generally, compared to organic P fractions, the total or inorganic P fractions had stronger correlations with bacterial compositions in Aha Lake (Figure 4B). For archaeal compositions, *Methanothermobacter* and *Methanosalsum* are the dominant genera governing the variation of communities along a sediment depth gradient. As a mesophilic Fe(III)-reducing microorganisms, *Methanothermobacter* can couple oxidation of organic matters (e.g., Po) with the reduction of structural iron. *Methanosalsum* commonly inhabit the hypersaline alkaline lakes, and are the obligately anaerobic high salt-tolerant and alkaliphilic euryarchaea. *Methanosalsum* can regulate or provide an alkaline environment to promote the combination of Fe, Al, and Ca ions with phosphate to form insoluble P fractions. In Hongfeng Lake, the total or inorganic P fractions such as BD-TP, BD-Pi, NH_4Cl-TP, NH_4Cl-Pi, HCl-TP and HCl-Pi were positively correlated with *Methanothermobacter* and *Methanosalsum*, while negatively correlated with *Thermofilum* and *Thermogladius*

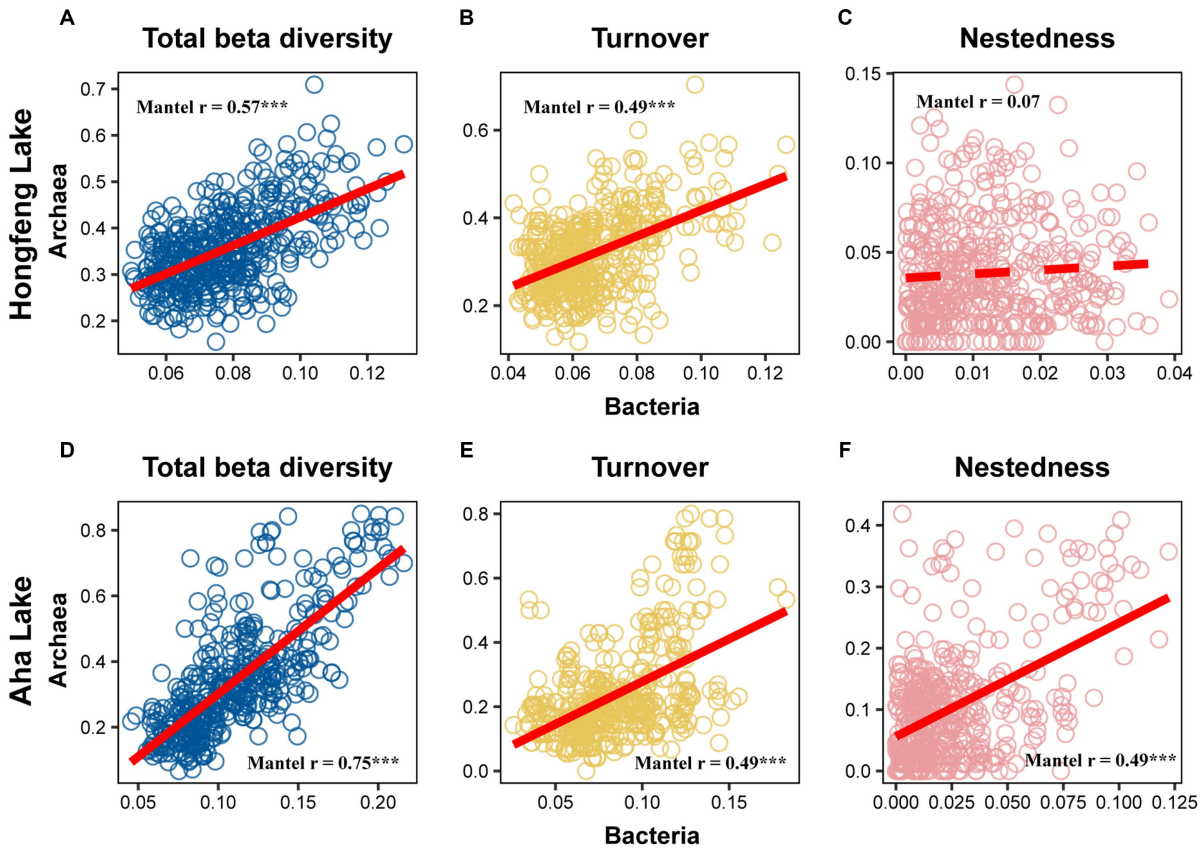

FIGURE 3
Correlation between bacterial and archaeal beta diversity in Hongfeng Lake **(A–C)** and Aha Lake **(D–F)**. The solid line indicates significant relationship. *$p \leq 0.05$; **$p < 0.01$; ***$p < 0.001$.

(Supplementary Figure S3A). Moreover, BD-Po and NaOH-Po had strong correlations with the top 7 genera in Hongfeng Lake, whereas HCl-Po and NH_4Cl-Po showed weak correlations (Supplementary Figure S3A). In Aha Lake, *Methanothermobacter* was positively correlated with total or inorganic P fractions, including HCl-TP, BD-TP, NH_4Cl-TP, HCl-Pi, BD-Pi and NH_4Cl-Pi, and negatively correlated with NaOH-TP and NaOH-Pi (Supplementary Figure S3B). Conversely, *Methanosalsum* showed negative correlations with HCl-TP, BD-TP, NH_4Cl-TP, HCl-Pi, BD-Pi, and NH_4Cl-Pi, whereas it was positively correlated with NaOH-TP and NaOH-Pi (Supplementary Figure S3B).

Furthermore, for both microbial taxa, Mantel test indicated that total beta diversity and its components also had strong correlations with P fractions (Supplementary Figure S4). For bacteria, total beta diversity or turnover were positively correlated with NH_4Cl-Pi (Mantel $r = 0.43$ and 0.32) and BD-Po (Mantel $r = 0.42$ and 0.35) in Hongfeng Lake, and with NH_4Cl-Pi (Mantel $r = 0.46$ and 0.50), BD-TP (Mantel $r = 0.42$ and 0.55) and HCl-Pi (Mantel $r = 0.51$ and 0.46) in Aha Lake (Supplementary Figure S4). Note that the nestedness component had strong correlations with BD-TP (Mantel $r = 0.47$) and BD-Pi (Mantel $r = 0.52$) in Hongfeng Lake (Supplementary Figure S4). For archaea, the total beta diversity or turnover showed significant positive correlations with NH_4Cl-Pi (Mantel $r = 0.44$ and 0.38), BD-TP (Mantel $r = 0.38$ and 0.40), HCl-Pi (Mantel $r = 0.36$ and 0.40) and Res-TP (Mantel $r = 0.40$ and 0.44) in Hongfeng Lake, and with BD-TP (Mantel $r = 0.44$ and 0.53), NaOH-Pi (Mantel $r = 0.47$ and 0.46) and HCl-Pi (Mantel $r = 0.49$ and 0.48) in Aha Lake (Supplementary Figure S4). Collectively, for bacteria and archaea, both total beta diversity and species turnover are strongly correlated with P fractions.

Effects of P fractions on bacterial and archaeal beta diversity

Based on the MRM (multiple regression on distance matrices) analyses, the importance of each P fraction to beta diversity varied across microbial taxa (Figure 5). For bacteria, compared to Aha Lake, NaOH-Pi and sediment total P contributed the relatively larger linear coefficient (i.e., effect size) to explain total beta diversity (linear coefficient = 0.47 and −0.62), species turnover (linear coefficient = 0.72 and −1.00) and nestedness (linear coefficient = −0.37 and 0.57, Figure 5) in Hongfeng Lake. Conversely, there was nonsignificant independent influence among total beta diversity and such P fractions in Aha Lake. Moreover, BD-TP was the most important driver of species turnover and nestedness in Aha Lake, with linear coefficients of 0.45 and −0.49, respectively (Figure 5). For archaea, BD-TP, NaOH-Pi and sediment total P showed high relative importance in explaining the total beta diversity (linear coefficient = 0.54, 0.39 and −0.72) and turnover component (linear coefficient = 0.58, 0.42 and −0.75) in Hongfeng Lake (Figure 5). Inconsistently, archaeal total beta diversity was primarily affected by HCl-Pi (linear coefficient = 0.34, $p < 0.05$) in Aha Lake, while only BD-TP (linear coefficient = 0.33,

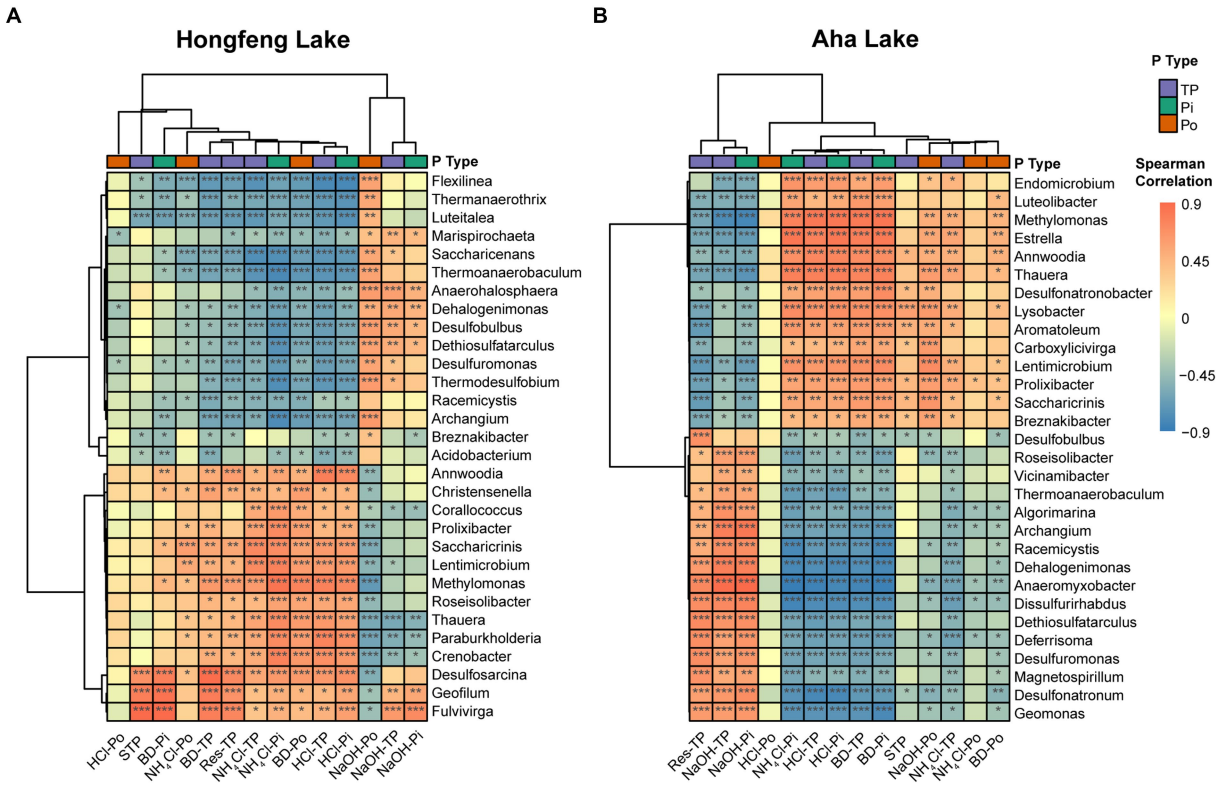

FIGURE 4
Cluster analysis of bacterial communities and P fractions at the genus level in Hongfeng Lake **(A)** and Aha Lake **(B)**. The heatmaps show the Spearman correlationship between the relative abundance of the top 30 genera and P fractions. Red denotes a positive relationship and blue indicates a negative correlation. ***$p < 0.001$, **$p < 0.01$, *$p < 0.05$.

$p < 0.05$) constrained the turnover component. Notably, for archaea, P fractions had no independent influence on species nestedness in both lakes ($p > 0.05$, Figure 5).

In the VPAs, for bacteria or archaea, total beta diversity ($R^2 = 0.12$ and 0.11, respectively) and turnover component ($R^2 = 0.15$ and 0.15, respectively) were mostly explained by the joint effects of the-Po fractions, Pi fractions and TP fractions in Hongfeng Lake (Figure 6A); however, in Aha Lake, the Pi fractions and TP fractions jointly accounted for 16% and 25% of variations in the total beta diversity, while 20% and 47% of variation in the turnover component (Figure 6B). Similarly, for bacteria, the joint effects of the Pi fractions and TP fractions explained 40% of the variation in the nestedness component in Hongfeng Lake (Figure 6A). For beta diversity components, compared to Po fractions, the Pi fractions showed a greater pure effect on bacteria, while the pure effect of Po fractions on archaea was stronger than that on bacteria (Figure 6).

Discussion

Unraveling the mechanisms underlying spatial and temporal variations in biodiversity has long been a central goal in ecology (Peters et al., 2019; Zhao et al., 2019). It has long been recognized that species turnover (i.e., species replacement) and nestedness (i.e., differences in species richness) partitioned by total beta diversity can underpin the processes shaping community structures (Zhang et al., 2020; Marta et al., 2021). For microbial succession, previous studies have mostly focused on how phosphate (i.e., PO_4^{3-}) or total P affects community variation. Much less is known, however, about the importance of P fractions to beta diversity components. To our knowledge, this study represents the first attempt to investigate how P fractions affect microbial total beta diversity and their components. We examined the variations in bacterial and archaeal beta diversity and their components along sediment depth, and further identified the relative importance of organic, inorganic and total P fractions to beta diversity. We found that (1) both bacteria and archaea had significant depth-related patterns in total beta diversity, turnover or nestedness, (2) there was taxonomic dependency among bacteria and archaea for beta diversity patterns along sediment depth, (3) the importance of each P fraction (i.e., NH_4Cl-Pi, BD-Pi, NaOH-Pi, HCl-Pi, NH_4Cl-Po, BD-Po, NaOH-Po, HCl-Po, NH_4Cl-TP, BD-TP, NaOH-TP, HCl-TP and Res-TP) to total beta diversity or species turnover varied with microbial taxonomic groups, and (4) Pi fractions have higher explanation than Po fractions for bacterial beta diversity, while archaeal total beta diversity or turnover component are well explained by Po fractions.

Species turnover is the most important component contributing to total beta diversity and has been examined extensively in aquatic ecosystems (Lima et al., 2020). In this study, the total beta diversity or species turnover of bacteria and archaea increased consistently along sediment depth (Figures 2A,B,D,E), largely consolidating the predominance of species turnover. Such patterns exhibited a similar trend toward deep sediments, which aligns with the general pattern of

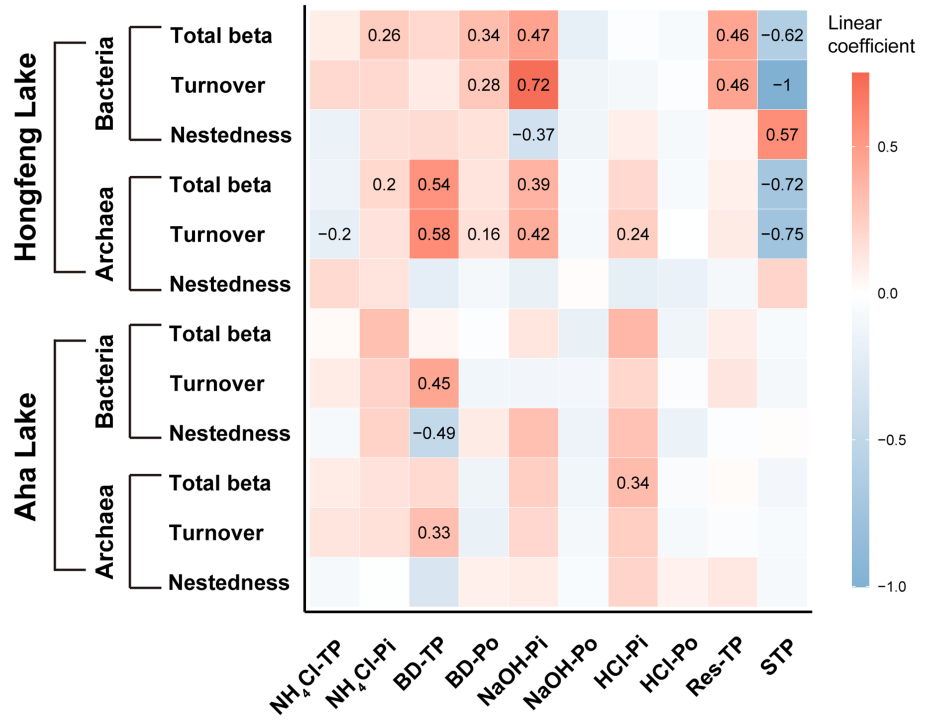

FIGURE 5
Effects of phosphorus fractions on bacterial and archaeal beta diversity. The P fractions include organic, inorganic and total P fractions. Significant relationships are visualized with squares showing numerical value. Color and value indicate the linear coefficient.

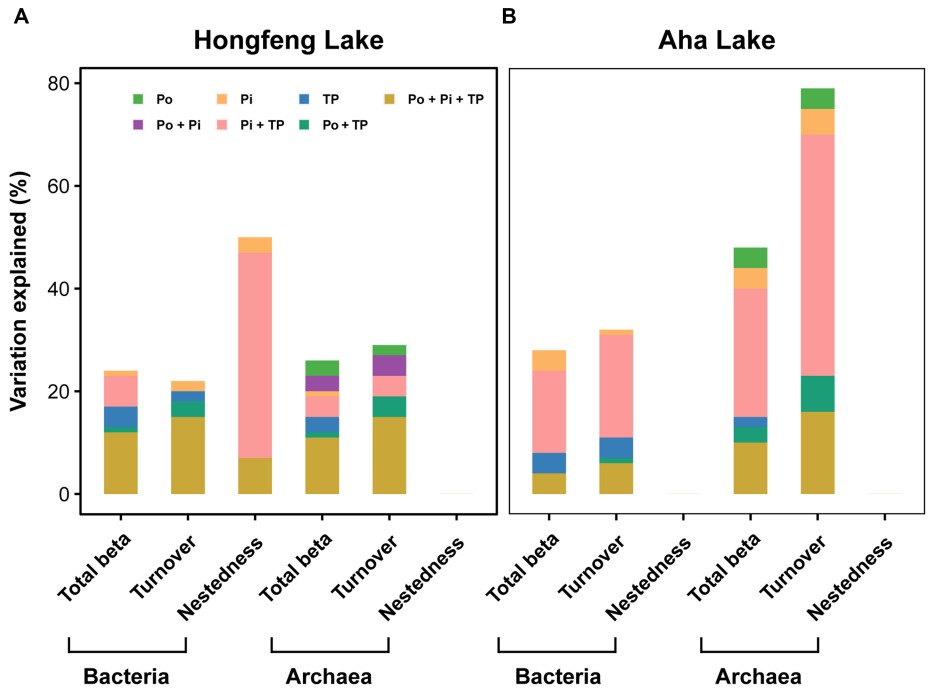

FIGURE 6
Relative importance of organic, inorganic and total P fractions in explaining variation of bacterial and archaeal beta diversity in Hongfeng Lake **(A)** and Aha Lake **(B)**. Variation partition analysis was performed to reveal the pure and joint effects of organic (Po), inorganic (Pi) and total P (TP) fractions on bacterial and archaeal beta diversity. The selected variables are shown in Supplementary Table S2. Statistical significance was evaluated using the Monte Carlo permutation test (9,999, $p < 0.01$).

species composition (Rooney and Azeria, 2015), where cross-taxon congruence (i.e., parallel diversity patterns among different taxa) happens if different biological groups are spatially covary in alpha or beta diversity. As expected, bacteria showed significant positive correlation (i.e., indicating parallel patterns between bacteria and archaea regarding total beta diversity and turnover) with archaea in terms of total beta diversity and turnover (Figures 3A,B,D,E), which is consistent with Yuan et al. (2022) and further underpins the taxonomical dependency between bacteria and archaea. More interestingly, such congruence indicates parallel patterns between both microbial taxa, which may be affected by similar processes like environmental selection (Shade et al., 2018). As previously reported (Specziár et al., 2018), the mechanisms responsible for species turnover are primarily triggered by environmental filtering, species competition or historical events (e.g., dispersal limitation). The intensity of selection may thus be related to environmental heterogeneity of sediment P fractions (Supplementary Figures S2, S4), which is supported by several studies addressing the importance of environmental selection on microbial communities (Yuan et al., 2021).

For bacteria or archaea, total beta diversity is generally predominated by species turnover and nestedness (Figure 2), but the species turnover explains a greater proportion of beta diversity than nestedness (Supplementary Table S1). Namely, turnover component contributes largely to total beta diversity, whereas nestedness component plays a smaller role, which is in line with previous studies on pond communities (Hill et al., 2017) and marine benthos (Bevilacqua and Terlizzi, 2020). In pond habitats, for macroinvertebrate, total beta diversity almost entirely reflects patterns of species turnover rather than nestedness. Likewise, for marine benthos, the compositional beta diversity is mainly due to species turnover, with a negligible contribution of nestedness. Species nestedness (i.e., differences in species richness caused by species gains or losses) exerts a weak influence on total beta diversity but can allow us to explicitly link species gains or losses to the mechanisms underlying compositional changes (Marta et al., 2021). For the nestedness component, our findings revealed a significant increasing depth-related pattern for bacteria in Hongfeng Lake and for archaea in Aha Lake (Figures 2C,F). The reasons for the different patterns of bacteria and archaea between the two lakes are manifold, among which is that nestedness differences stem mainly from species thinning or other ecological processes like human disturbance (Legendre, 2014). It is worth noting that species thinning may be related to intraspecific competition (i.e., a competition between individuals from the same species). Generally, competition occurs when the environmental capability supplying resources fails to meet the biological requirement, causing the organisms to interfere with each other. Intraspecific competition largely constrains the growth of organisms in populations, thereby resulting in species gain or loss (i.e., species nestedness). More specifically, intraspecific competition can lead to self-thinning, in which less-capable individuals die while more-competitive individuals survive (Begon et al., 1990). Our findings reflected that intraspecific competition affects the nestedness component through species thinning and thereby govern community composition, which is supported by strong associations between the top 30 bacterial genera or top 7 archaeal genera and P fractions (Figure 4; Supplementary Figure S3). For instance, *Geofilum* and *Fulvivirga* show significant positive correlations with BD-Pi, BD-TP, NH_4Cl-TP, NH_4Cl-Pi, BD-Po, HCl-TP, HCl-Pi, NaOH-TP and NaOH-Pi in Hongfeng Lake, implying that the two microbes may compete within the species for the same nutrients. Although bacteria had no significant depth-related pattern for nestedness in Aha Lake, it is not difficult to comprehend that intraspecific competition occurs within bacterial communities living in the P-limited habitat (Figure 4B).

Beta diversity is substantially governed by species pool (i.e., the set of potential species coexisting in a target community in a certain region) and could be constrained by local environmental factors. Previous studies have shown that environmental selection is the main ecological process in driving the biogeographic patterns of biodiversity (Wang J. et al., 2017). In our study, the decreasing trend of P fractions along sediment depth was generally found in NH_4Cl-P, BD-P, NaOH-P or HCl-P (Supplementary Figure S1) and there existed significant differences between the two lakes regarding such P fractions (Supplementary Figure S2), indicating strong environmental heterogeneity between Hongfeng and Aha Lakes. Environmental heterogeneity can effectively determine the ecological processes in controlling microbial community variation in freshwater ecosystems (Huber et al., 2020). In particular, strong heterogeneous selection (i.e., selection by environmental heterogeneity), limiting the biological growth to produce community variation (i.e., beta diversity), can filter species from the species pool to increase or promote beta diversity (Zhang et al., 2020). For bacteria or archaea, we observed that total beta diversity and turnover showed strong correlations with P fractions such as NH_4Cl-Pi and BD-Po in Hongfeng Lake, and with P fractions like BD-TP and HCl-Pi in Aha Lake (Supplementary Figure S4), largely confirming that P fractions have profound effects on biodiversity in P-limited lakes. Further, the result of the MRM analyses suggested that, environmental distance of P fractions such as NaOH-Pi, BD-TP and HCl-Pi can individually affect total beta diversity or species turnover regarding both microbial taxa (Figure 5), confirming that environmental selection has a dominant influence on the mechanisms underlying variation in bacterial or archaeal communities. As such, the depth-decay patterns of bacterial and archaeal beta diversity may be mainly attributed to the environmental selection.

Environmental factors can directly drive the variation in total beta diversity and also alter it by affecting species turnover and nestedness, thereby exerting a profound influence on the maintenance of biodiversity in aquatic or terrestrial ecosystems (Martiny et al., 2011). Thus, our findings further revealed the pure and joint effects of the organic, inorganic and total P fractions on bacterial and archaeal beta diversity. Generally, such P fractions had high explanations for bacterial or archaeal beta diversity in Hongfeng and Aha Lakes. Especially, the joint effects of inorganic and total P fractions could explain a great proportion of total beta diversity or its components (Figure 6). These results, together with those reported in previous studies (Watson et al., 2018; Pu et al., 2020; Yin et al., 2022), collectively indicate a close link between microbial community variation and P fractions, which is interesting but rarely reported in aquatic ecosystems. Moreover, for the pure effect, we found that the Pi fractions had a higher explanation than Po fractions for bacterial beta diversity (Figure 6). As an essential component of nucleic acids, lipids or storage energy molecules, Pi can substantially influence the shaping of microbial community structure and ecological patterns or processes (Zheng et al., 2021). As such, this finding largely stresses the importance of Pi in shaping bacterial community structures,

which is concordant with previous findings on aquatic bacteria (Yuan et al., 2022) or phytoplankton (Guo et al., 2022). For example, in less eutrophic lowland streams, changes in soluble reactive phosphorus (i.e., Pi) between sites are the key driver homogenizing the total β-diversity of phytoplankton (Frau et al., 2023). Admittedly, Pi is an indispensable nutrient triggering the growth of aquatic microorganisms and has been widely reported in previous literature (Carvalho et al., 2011). More intriguingly, for total beta diversity or species turnover, we found that Po fractions had a higher explanation for archaea than bacteria (Figure 6), presumably owing to the anaerobic biodegradation of *Euryarchaeota*. Recent studies have suggested that sediment aeration can increase the content of reductant-soluble phosphorus fractions (Fe/Al-P) and promote the mineralization of organic phosphorus to the labile form (Dieter et al., 2015). In fact, due to the lack of oxygen content, bacterial communities are gradually dominated by anaerobic reductive bacteria toward deep sediments (Fonseca et al., 2022). In our study, *Euryarchaeota* is the dominant phylum of the archaeal community and contains large amounts of anaerobic methane oxidizing archaea such as *Methanothermobacter* and *Methanosalsum*. More intriguingly, *Methanothermobacter* was significantly ($p < 0.05$) negatively correlated with NaOH-Po in Hongfeng Lake, while *Methanosalsum* had significant ($p < 0.05$) negative correlation with NaOH-Po and BD-Po in Aha Lake (Supplementary Figure S3), indicating obvious differences in the Po mineralizing archaea between the two lakes. Such oxidizing archaea can completely mineralize organic matters like Po fractions to inorganic form under anaerobic conditions, wherein inorganic P can be well absorbed by archaea to promote their body growth (Baker et al., 2020). Furthermore, for bacteria and archaea, such effects including pure and joint effects, also indicated that P fractions could influence total beta diversity by driving its turnover component, reflecting the predominance of species turnover by environmental or spatial filters. Taken together, these findings emphasize the importance of P fractions to variations in bacterial and archaeal communities and have important implications (e.g., maintaining biodiversity by regulating nutrients like P based on the properties of P fractions) for how we protect biological diversity in aquatic ecosystems.

Nevertheless, there are two caveats to the interpretation of our studies. First, for bacteria or archaea, species nestedness may be governed by other ecological processes in Aha Lake. As previously reported (Rapacciuolo et al., 2019), strong Mantel correlation between bacteria and archaea regarding nestedness component, indicates that their parallel patterns may be driven by similar processes in Aha Lake (Figure 3F). Surprisingly, P fractions show a low explanation (i.e., P sources were abundant in sediments without limiting species gain and loss) for species nestedness in Aha Lake (Figures 5, 6), implying that their depth-related patterns may not be determined by the selection of P fractions, but may be influenced by species interaction or other environmental factors. Consistently, recent studies have suggested that species nestedness shows complex nonlinear relationships with extirpation and colonization (Lu et al., 2019), which largely determines whether beta diversity increases or decreases (Tatsumi et al., 2020). Therefore, for such unique species nestedness, extirpation and colonization considered in future theoretical works may better explain such biogeographic patterns in community variation. Note that both species turnover or nestedness and extirpation or colonization, can largely reveal the underlying mechanisms of bacterial and archaeal succession, thereby enhancing our understanding of the distribution of microbial communities and providing direct evidence for studying the function and stability of lake ecosystems.

Second, this study primarily focused on the environmental selection imposed by P fractions for microbial community variation, without considering the influence of stochastic ecological processes. It is broadly recognized that community assembly is simultaneously governed by deterministic (e.g., species-environment associations and habitat filtering) and stochastic (e.g., ecological drift and dispersal limitation) processes (Wang et al., 2013). Ecologically, deterministic selection by specific environmental variables is generally pivotal, although in some cases, stochastic or neutral processes may dominate (Stegen et al., 2012). For instance, in the Shenzhen River-Bay system, South China, environmental selection such as salinity and water temperature are pronounced for governing bacterial and archaeal community composition and assembly processes (Wang Y. et al., 2020). Likewise, such major role of deterministic processes has also been observed in soils (Moroenyane et al., 2016) and rivers (Vilmi et al., 2020). Similarly, phosphorus fractions contain large amounts of organic or inorganic P, providing essential nutrients for microbial growth (Zheng et al., 2021). Such nutrients can alter even biodiversity and its relationship with temperature in large-scale field experiments (Wang et al., 2016b). Thus, as an environmental filtering, P fractions can deterministically govern bacterial and archaeal community variation. Especially in mesotrophic lakes, controlling endogenous phosphorus release through community response of sediment microbes can effectively improve lake water quality, thereby strengthening lake conservation and management. Briefly, our study points to general rules controlling the relative contribution of species turnover and nestedness regarding bacteria and archaea, and we also encourage further works to complement such results by considering more ecological processes like deterministic and stochastic processes.

Conclusion

In summary, our findings elucidated the underlying mechanisms of bacterial or archaeal communities along sediment depth and provided ecological insights into how eutrophication poses a threat to microbial diversity. This study for the first time revealed the importance of P fractions to the mechanism underlying microbial total beta diversity in aquatic ecosystems. For bacteria and archaea, we found significant increasing depth-related patterns in total beta diversity, species turnover or nestedness. Intriguingly, bacteria showed significant parallel patterns with archaea regarding total beta diversity and species turnover, which is largely supported by similar processes like environmental selection. For both microbial taxa, total beta diversity and species turnover were primarily constrained by NaOH-Pi and STP in Hongfeng Lake, while largely affected by BD-TP or HCl-Pi in Aha Lake. Moreover, NaOH-Pi and sediment total phosphorus can influence bacterial total beta diversity by driving species nestedness in Hongfeng Lake. The joint effects of Po fractions, Pi fractions and TP fractions indicated that the P fractions are important for bacterial and archaeal beta diversity. Compared to Po fractions, Pi fractions have greater pure effects on bacterial beta diversity. Meanwhile, Po fractions show a higher explanation for archaeal beta diversity than bacteria. To date, both partitioning beta diversity and P fractions are pervasive topics in ecology or environmental science, but they are rarely coupled to reveal the biological effects in the P cycle or the effects of the P source on biodiversity conservation. In fact, sediment microbes and

P fractions determine whether the trophic state of the lake will transition from mesotrophic to eutrophication, and have crucial roles in the biogeochemical process of lake P cycling. Further studies should be encouraged to investigate the associations between P fractions and more taxonomic groups like fungi and algae in aquatic ecosystems with different trophic states (e.g., eutrophic and oligotrophic).

Data availability statement

The datasets presented in this study can be found in online repositories. The names of the repository/repositories and accession number(s) can be found in the article/Supplementary material.

Author contributions

HY: Conceptualization, Data curation, Formal analysis, Investigation, Methodology, Software, Validation, Visualization, Writing – original draft, Writing – review & editing. RZ: Conceptualization, Data curation, Funding acquisition, Investigation, Project administration, Resources, Supervision, Validation, Writing – review & editing. QLi: Conceptualization, Formal analysis, Investigation, Methodology, Software, Supervision, Validation, Visualization, Writing – review & editing. QH: Formal analysis, Investigation, Methodology, Project administration, Software, Writing – review & editing. QLu: Investigation, Project administration, Supervision, Validation, Writing – review & editing. JW: Data curation, Investigation, Supervision, Writing – review & editing.

Funding

The author(s) declare financial support was received for the research, authorship, and/or publication of this article. This work was supported by the National Natural Science Foundation of China (42177244 and U1612442), the State Key Laboratory of Environmental Geochemistry (SKLEG2021203) and Guizhou Provincial 2021 Science and Technology Subsidies (No. GZ2021SIG).

Acknowledgments

The authors appreciate Jianjun Wang for valuable suggestions on our preliminary draft and thank Guangdong Magigene Biotechnology Co., Ltd. (Guangzhou, China) for help with the data analysis of high throughput sequencing.

Conflict of interest

The authors declare that the research was conducted in the absence of any commercial or financial relationships that could be construed as a potential conflict of interest.

Publisher's note

Supplementary material

The Supplementary material for this article can be found online at: https://www.frontiersin.org/articles/10.3389/fmicb.2023.1279751/full#supplementary-material

References

Anderson, M. J., and Cribble, N. A. (1998). Partitioning the variation among spatial, temporal and environmental components in a multivariate data set. *Aust. J. Ecol.* 23, 158–167. doi: 10.1111/j.1442-9993.1998.tb00713.x

Apprill, A., McNally, S. P., Parsons, R. J., and Weber, L. (2015). Minor revision to V4 region SSU rRNA 806R gene primer greatly increases detection of SAR11 bacterioplankton. *Aquat. Microb. Ecol.* 75, 129–137. doi: 10.3354/ame01753

Baker, B. J., de Anda, V., Seitz, K. W., Dombrowski, N., Santoro, A. E., and Lloyd, K. G. (2020). Diversity, ecology and evolution of Archaea. *Nat. Microbiol.* 5, 887–900. doi: 10.1038/s41564-020-0715-z

Baselga, A. (2010). Partitioning the turnover and nestedness components of beta diversity. *Glob. Ecol. Biogeogr.* 19, 134–143. doi: 10.1111/j.1466-8238.2009.00490.x

Baselga, A., and Orme, C. D. L. (2012). Betapart: an R package for the study of beta diversity. *Methods Ecol. Evol.* 3, 808–812. doi: 10.1111/j.2041-210X.2012.00224.x

Baselga, A., Orme, D., Villeger, S., De Bortoli, J., Leprieur, F., Baselga, M. A. (2018). Package 'betapart'. *Partitioning beta diversity into turnover and nestedness components, version, 1.*

Begon, M., Harper, J. L., and Townsend, C. R. (1990). *Ecology: Individuals, populations and communities*, *2*. London: Blackwell Science Publishing.

Bevilacqua, S., and Terlizzi, A. (2020). Nestedness and turnover unveil inverse spatial patterns of compositional and functional β-diversity at varying depth in marine benthos. *Divers. Distrib.* 26, 743–757. doi: 10.1111/ddi.13025

Bian, T., Zheng, S., Li, X., Wang, S., Zhang, X., Wang, Z., et al. (2022). The variation of soil phosphorus fractions and microbial community composition under consecutive cucumber cropping in a greenhouse. *Horticulturae* 8:320. doi: 10.3390/horticulturae8040320

Carvalho, L., Miller, C. A., Scott, E. M., Codd, G. A., Davies, P. S., and Tyler, A. N. (2011). Cyanobacterial blooms: statistical models describing risk factors for national-scale lake assessment and lake management. *Sci. Total Environ.* 409, 5353–5358. doi: 10.1016/j.scitotenv.2011.09.030

Cavalcante, H., Araújo, F., Noyma, N. P., and Becker, V. (2018). Phosphorus fractionation in sediments of tropical semiarid reservoirs. *Sci. Total Environ.* 619-620, 1022–1029. doi: 10.1016/j.scitotenv.2017.11.204

Ceulemans, T., Stevens, C. J., Duchateau, L., Jacquemyn, H., Gowing, D. J. G., Merckx, R., et al. (2014). Soil phosphorus constrains biodiversity across European grasslands. *Glob. Chang. Biol.* 20, 3814–3822. doi: 10.1111/gcb.12650

Chen, J., Yang, H., Zhang, D. D., Xu, D., Luo, J., and Wang, J. (2015). A particular river-whiting phenomenon caused by discharge of hypolimnetic water from a stratified reservoir. *PLoS One* 10:e0137860. doi: 10.1371/journal.pone.0137860

Chen, J., Zeng, Y., Yu, J., Wang, J., Yang, H., and Lu, Y. (2019). Preferential regeneration of P relative to C in a freshwater lake. *Chemosphere* 222, 15–21. doi: 10.1016/j.chemosphere.2019.01.088

Cramer, M. D. (2010). Phosphate as a limiting resource: introduction. *Plant Soil* 334, 1–10. doi: 10.1007/s11104-010-0497-9

Delgado-Baquerizo, M., Reich, P. B., Trivedi, C., Eldridge, D. J., Abades, S., Alfaro, F. D., et al. (2020). Multiple elements of soil biodiversity drive ecosystem functions across biomes. *Nat. Ecol. Evol.* 4, 210–220. doi: 10.1038/s41559-019-1084-y

Dieter, D., Herzog, C., and Hupfer, M. (2015). Effects of drying on phosphorus uptake in re-flooded lake sediments. *Environ. Sci. Pollut. Res.* 22, 17065–17081. doi: 10.1007/s11356-015-4904-x

Edgar, R. C., and Flyvbjerg, H. (2015). Error filtering, pair assembly and error correction for next-generation sequencing reads. *Bioinformatics* 31, 3476–3482. doi: 10.1093/bioinformatics/btv401

Fonseca, A., Espinoza, C., Nielsen, L. P., Marshall, I. P. G., and Gallardo, V. A. (2022). Bacterial community of sediments under the eastern boundary current system shows high microdiversity and a latitudinal spatial pattern. *Front. Microbiol.* 13:1016418. doi: 10.3389/fmicb.2022.1016418

Frau, D., Pineda, A., Mayora, G., and Gutierrez, M. F. (2023). Eutrophication as a homogenizer process of phytoplankton β-diversity in lowland streams. *Limnologica* 99:126058. doi: 10.1016/j.limno.2023.126058

García-Navas, V., Martínez-Núñez, C., Tarifa, R., Molina-Pardo, J. L., Valera, F., Salido, T., et al. (2022). Partitioning beta diversity to untangle mechanisms underlying the assembly of bird communities in Mediterranean olive groves. *Divers. Distrib.* 28, 112–127. doi: 10.1111/ddi.13445

Goslee, S., and Urban, D. (2007). Ecodist: dissimilarity-based functions for ecological analysis. *Package 'ecodist'*. R Package Version 1.

Guo, C., Zhu, M., Xu, H., Zhang, Y., Qin, B., Zhu, G., et al. (2022). Spatiotemporal dependency of resource use efficiency on phytoplankton diversity in Lake Taihu. *Limnol. Oceanogr.* 67, 830–842. doi: 10.1002/lno.12038

Han, M., Li, Q., Chen, H., Xiao, J., and Jiang, F. (2018). Spatial and temporal variations in cyanobacteria and microcystins in Aha reservoir, Southwest China. *J. Oceanol. Limnol.* 36, 1126–1131. doi: 10.1007/s00343-018-7178-6

Harrell, F. (2019). *Package 'Hmisc'*. R Package Version 4.3-0

Hill, M. J., Heino, J., Thornhill, I., Ryves, D. B., and Wood, P. J. (2017). Effects of dispersal mode on the environmental and spatial correlates of nestedness and species turnover in pond communities. *Oikos* 126, 1575–1585. doi: 10.1111/oik.04266

Huber, P., Metz, S., Unrein, F., Mayora, G., Sarmento, H., and Devercelli, M. (2020). Environmental heterogeneity determines the ecological processes that govern bacterial metacommunity assembly in a floodplain river system. *ISME J.* 14, 2951–2966. doi: 10.1038/s41396-020-0723-2

Hupfer, M., Gächter, R., and Giovanoli, R. (1995). Transformation of phosphorus species in settling seston and during early sediment diagenesis. *Aquat. Sci.* 57, 305–324. doi: 10.1007/BF00878395

Lan, C., Chen, J., Wang, J., Guo, J., Yu, J., Yu, P., et al. (2017). Application of circular bubble plume diffusers to restore water quality in a sub-deep reservoir. *Int. J. Environ. Res. Public Health* 14:1298. doi: 10.3390/ijerph14111298

Legendre, P. (2014). Interpreting the replacement and richness difference components of beta diversity. *Glob. Ecol. Biogeogr.* 23, 1324–1334. doi: 10.1111/geb.12207

Li, Z., Zhang, D., Peng, Y., Qin, S., Wang, L., Hou, E., et al. (2022). Divergent drivers of various topsoil phosphorus fractions across Tibetan alpine grasslands. *J. Geophys. Res. Biogeosci.* 127:e2022JG006795. doi: 10.1029/2022JG006795

Lichstein, J. W. (2007). Multiple regression on distance matrices: a multivariate spatial analysis tool. *Plant Ecol.* 188, 117–131. doi: 10.1007/s11258-006-9126-3

Lima, M., Schneck, F., Haig They, N., Oliveira Crossetti, L., Bohnenberger, J. E., McMahon, K. D., et al. (2020). Turnover is replaced by nestedness with increasing geographical distance in bacterial communities of coastal shallow lakes. *Mar. Freshw. Res.* 71, 1086–1098. doi: 10.1071/MF19110

Liu, Y.-X., Qin, Y., Chen, T., Lu, M., Qian, X., Guo, X., et al. (2021). A practical guide to amplicon and metagenomic analysis of microbiome data. *Protein Cell* 12, 315–330. doi: 10.1007/s13238-020-00724-8

Liu, Y., Wang, J., Chen, J., Zhang, R., Ji, Y., and Jin, Z. (2019). Pretreatment method for the analysis of phosphate oxygen isotope ($\delta^{18}O_p$) of different phosphorus fractions in freshwater sediments. *Sci. Total Environ.* 685, 229–238. doi: 10.1016/j.scitotenv.2019.05.238

Lu, M., Vasseur, D., and Jetz, W. (2019). Beta diversity patterns derived from island biogeography theory. *Am. Nat.* 194, E52–E65. doi: 10.1086/704181

Ma, Y., Li, Q., Pan, S., Liu, C., Han, M., and Brancelj, A. (2022). Niche and interspecific associations of *Pseudoanabaena limnetica*—exploring the influencing factors of its succession stage. *Ecol. Indic.* 138:108806. doi: 10.1016/j.ecolind.2022.108806

Mantel, N. (1967). The detection of disease clustering and a generalized regression approach. *Cancer Res.* 27, 209–220.

Marta, S., Brunetti, M., Manenti, R., Provenzale, A., and Ficetola, G. F. (2021). Climate and land-use changes drive biodiversity turnover in arthropod assemblages over 150 years. *Nat. Ecol. Evol.* 5, 1291–1300. doi: 10.1038/s41559-021-01513-0

Martiny, J. B. H., Eisen, J. A., Penn, K., Allison, S. D., and Horner-Devine, M. C. (2011). Drivers of bacterial β-diversity depend on spatial scale. *Proc. Natl. Acad. Sci. U. S. A.* 108, 7850–7854. doi: 10.1073/pnas.1016308108

Mori, A. S., Isbell, F., and Seidl, R. (2018). β-diversity, community assembly, and ecosystem functioning. *Trends Ecol. Evol.* 33, 549–564. doi: 10.1016/j.tree.2018.04.012

Moroenyane, I., Chimphango, S. B. M., Wang, J., Kim, H. K., and Adams, J. M. (2016). Deterministic assembly processes govern bacterial community structure in the fynbos, South Africa. *Microb. Ecol.* 72, 313–323. doi: 10.1007/s00248-016-0761-5

Murphy, J., and Riley, J. P. (1962). A modified single solution method for the determination of phosphate in natural waters. *Anal. Chim. Acta* 27, 31–36. doi: 10.1016/S0003-2670(00)88444-5

Ni, M., Ge, Q., Li, S., Wang, Z., and Wu, Y. (2021). Trophic state index linked to partial pressure of aquatic carbon dioxide in a typical karst plateau lake. *Ecol. Indic.* 120:106912. doi: 10.1016/j.ecolind.2020.106912

Oksanen, J., Simpson, G. L., Blanchet, F. G., Kindt, R., Legendre, P., Minchin, P. R., et al. (2013). *Vegan: community ecology package*. R Package Version 2.3-10 CRAN.

Parada, A. E., Needham, D. M., and Fuhrman, J. A. (2016). Every base matters: assessing small subunit rRNA primers for marine microbiomes with mock communities, time series and global field samples. *Environ. Microbiol.* 18, 1403–1414. doi: 10.1111/1462-2920.13023

Peters, M. K., Hemp, A., Appelhans, T., Becker, J. N., Behler, C., Classen, A., et al. (2019). Climate-land-use interactions shape tropical mountain biodiversity and ecosystem functions. *Nature* 568, 88–92. doi: 10.1038/s41586-019-1048-z

Psenner, R., Bostrom, B., Dinka, M., Pettersson, K., Pucsko, R., and Sager, M. (1988). Fractionation of phosphorus in suspended matter and sediments. *Arch. Hydrobiol. Beihefte Ergebnisse Limnol.* 30, 98–109.

Pu, J., Ni, Z., and Wang, S. (2020). Characteristics of bioavailable phosphorus in sediment and potential environmental risks in Poyang Lake: the largest freshwater lake in China. *Ecol. Indic.* 115:106409. doi: 10.1016/j.ecolind.2020.106409

Rapacciuolo, G., Beman, J. M., Schiebelhut, L. M., and Dawson, M. N. (2019). Microbes and macro-invertebrates show parallel β-diversity but contrasting α-diversity patterns in a marine natural experiment. *Proc. R. Soc. Lond. B* 286:20190999. doi: 10.1098/rspb.2019.0999

Rooney, R. C., and Azeria, E. T. (2015). The strength of cross-taxon congruence in species composition varies with the size of regional species pools and the intensity of human disturbance. *J. Biogeogr.* 42, 439–451. doi: 10.1111/jbi.12400

Rydin, E. (2000). Potentially mobile phosphorus in Lake Erken sediment. *Water Res.* 34, 2037–2042. doi: 10.1016/S0043-1354(99)00375-9

Shade, A., Dunn, R. R., Blowes, S. A., Keil, P., Bohannan, B. J. M., Herrmann, M., et al. (2018). Macroecology to unite all life, large and small. *Trends Ecol. Evol.* 33, 731–744. doi: 10.1016/j.tree.2018.08.005

Singh, B. K., Bardgett, R. D., Smith, P., and Reay, D. S. (2010). Microorganisms and climate change: terrestrial feedbacks and mitigation options. *Nat. Rev. Microbiol.* 8, 779–790. doi: 10.1038/nrmicro2439

Soininen, J., Heino, J., and Wang, J. (2018). A meta-analysis of nestedness and turnover components of beta diversity across organisms and ecosystems. *Glob. Ecol. Biogeogr.* 27, 96–109. doi: 10.1111/geb.12660

Specziár, A., Árva, D., Tóth, M., Móra, A., Schmera, D., Várbíró, G., et al. (2018). Environmental and spatial drivers of beta diversity components of chironomid metacommunities in contrasting freshwater systems. *Hydrobiologia* 819, 123–143. doi: 10.1007/s10750-018-3632-x

Stegen, J. C., Lin, X., Konopka, A. E., and Fredrickson, J. K. (2012). Stochastic and deterministic assembly processes in subsurface microbial communities. *ISME J.* 6, 1653–1664. doi: 10.1038/ismej.2012.22

Tatsumi, S., Strengbom, J., Čugunovs, M., and Kouki, J. (2020). Partitioning the colonization and extinction components of beta diversity across disturbance gradients. *Ecology* 101:e03183. doi: 10.1002/ecy.3183

Teng, Z., Zhu, Y., Li, M., and Whelan, M. J. (2018). Microbial community composition and activity controls phosphorus transformation in rhizosphere soils of the Yeyahu Wetland in Beijing, China. *Sci. Total Environ.* 628–629, 1266–1277. doi: 10.1016/j.scitotenv.2018.02.115

van der Plas, F. (2019). Biodiversity and ecosystem functioning in naturally assembled communities. *Biol. Rev.* 94, 1220–1245. doi: 10.1111/brv.12499

van der Plas, F., Hennecke, J., Chase, J. M., van Ruijven, J., and Barry, K. E. (2023). Universal beta-diversity-functioning relationships are neither observed nor expected. *Trends Ecol. Evol.* 38, 532–544. doi: 10.1016/j.tree.2023.01.008

Viana, D. S., Figuerola, J., Schwenk, K., Manca, M., Hobaek, A., Mjelde, M., et al. (2016). Assembly mechanisms determining high species turnover in aquatic communities over regional and continental scales. *Ecography* 39, 281–288. doi: 10.1111/ecog.01231

Vilmi, A., Zhao, W., Picazo, F., Li, M., Heino, J., Soininen, J., et al. (2020). Ecological processes underlying community assembly of aquatic bacteria and macroinvertebrates under contrasting climates on the Tibetan Plateau. *Sci. Total Environ.* 702:134974. doi: 10.1016/j.scitotenv.2019.134974

Wang, J., Chen, J., Chen, Q., Jin, Z., and Zeng, H. (2021b). Biogeochemical cycling of phosphorus in deep-water reservoirs [in Chinese]. *J. Quat. Sci.* 41, 1192–1205. doi: 10.11928/j.issn.1001-7410.2021.04.25

Wang, J., Chen, J., Christopher, D., Haiquan, Y., and Zhihui, D. (2015). Spatial distribution, fractions, and potential release of sediment phosphorus in the Hongfeng Reservoir, Southwest China. *Lake Reserv. Manag.* 31, 214–224. doi: 10.1080/10402381.2015.1062835

Wang, J., Chen, J., Ding, S., Guo, J., Christopher, D., Dai, Z., et al. (2016a). Effects of seasonal hypoxia on the release of phosphorus from sediments in deep-water ecosystem:

a case study in Hongfeng reservoir, Southwest China. *Environ. Pollut.* 219, 858–865. doi: 10.1016/j.envpol.2016.08.013

Wang, W., Feng, C., Liu, F., and Li, J. (2020). Biodiversity conservation in China: a review of recent studies and practices. *Environ. Sci. Ecotechnol.* 2:100025. doi: 10.1016/j.ese.2020.100025

Wang, X.-B., Lü, X.-T., Yao, J., Wang, Z. W., Deng, Y., Cheng, W. X., et al. (2017). Habitat-specific patterns and drivers of bacterial β-diversity in China's drylands. *ISME J.* 11, 1345–1358. doi: 10.1038/ismej.2017.11

Wang, J., Pan, F., Soininen, J., Heino, J., and Shen, J. (2016b). Nutrient enrichment modifies temperature-biodiversity relationships in large-scale field experiments. *Nat. Commun.* 7:13960. doi: 10.1038/ncomms13960

Wang, Y., Pan, J., Yang, J., Zhou, Z., Pan, Y., and Li, M. (2020). Patterns and processes of free-living and particle-associated bacterioplankton and archaeaplankton communities in a subtropical river-bay system in South China. *Limnol. Oceanogr.* 65, S161–S179. doi: 10.1002/lno.11314

Wang, J., Shen, J., Wu, Y., Tu, C., Soininen, J., Stegen, J. C., et al. (2013). Phylogenetic beta diversity in bacterial assemblages across ecosystems: deterministic versus stochastic processes. *ISME J.* 7, 1310–1321. doi: 10.1038/ismej.2013.30

Wang, J., Soininen, J., and Heino, J. (2021a). Ecological indicators for aquatic biodiversity, ecosystem functions, human activities and climate change. *Ecol. Indic.* 132:108250. doi: 10.1016/j.ecolind.2021.108250

Wang, J., Zhang, T., Li, L., Li, J., Feng, Y., and Lu, Q. (2017). The patterns and drivers of bacterial and fungal β-diversity in a typical dryland ecosystem of Northwest China. *Front. Microbiol.* 8:2126. doi: 10.3389/fmicb.2017.02126

Watson, S. J., Cade-Menun, B. J., Needoba, J. A., and Peterson, T. D. (2018). Phosphorus forms in sediments of a river-dominated estuary. *Front. Mar. Sci.* 5:302. doi: 10.3389/fmars.2018.00302

Whittaker, R. H. (1960). Vegetation of the Siskiyou Mountains, Oregon and California. *Ecol. Monogr.* 30, 279–338. doi: 10.2307/1943563

Wu, K., Zhao, W., Li, M., Picazo, F., Soininen, J., Shen, J., et al. (2020). Taxonomic dependency of beta diversity components in benthic communities of bacteria, diatoms and chironomids along a water-depth gradient. *Sci. Total Environ.* 741:140462. doi: 10.1016/j.scitotenv.2020.140462

Wu, K., Zhao, W., Wang, Q., Yang, X., Zhu, L., Shen, J., et al. (2019). The relative abundance of benthic bacterial Phyla along a water-depth gradient in a plateau Lake: physical, chemical, and biotic drivers. *Front. Microbiol.* 10:1521. doi: 10.3389/fmicb.2019.01521

Xiong, W., Huang, X., Chen, Y., Fu, R., Du, X., Chen, X., et al. (2020). Zooplankton biodiversity monitoring in polluted freshwater ecosystems: a technical review. *Environ. Sci. Ecotechnol.* 1:100008. doi: 10.1016/j.ese.2019.100008

Xun, W., Li, W., Xiong, W., Ren, Y., Liu, Y., Miao, Y., et al. (2019). Diversity-triggered deterministic bacterial assembly constrains community functions. *Nat. Commun.* 10:3833. doi: 10.1038/s41467-019-11787-5

Yang, J., Shi, J., Jiang, L., Zhang, S., Wei, F., Guo, Z., et al. (2023). Co-occurrence network in core microorganisms driving the transformation of phosphorous fractionations during phosphorus recovery product used as soil fertilizer. *Sci. Total Environ.* 871:162081. doi: 10.1016/j.scitotenv.2023.162081

Yin, H., Zhang, M., Yin, P., and Li, J. (2022). Characterization of internal phosphorus loading in the sediment of a large eutrophic Lake (Lake Taihu, China). *Water Res.* 225:119125. doi: 10.1016/j.watres.2022.119125

Yu, J., Zeng, Y., Chen, J., Liao, P., Yang, H., and Yin, C. (2022). Organic phosphorus regeneration enhanced since eutrophication occurred in the sub-deep reservoir. *Environ. Pollut.* 306:119350. doi: 10.1016/j.envpol.2022.119350

Yuan, H., Meng, F., Yamamoto, M., Liu, X., Dong, H., Shen, J., et al. (2021). Linking historical vegetation to bacterial succession under the contrasting climates of the Tibetan Plateau. *Ecol. Indic.* 126:107625. doi: 10.1016/j.ecolind.2021.107625

Yuan, H., Zhang, W., Yin, H., Zhang, R., and Wang, J. (2022). Taxonomic dependency of beta diversity for bacteria, archaea and fungi in a semi-arid lake. *Front. Microbiol.* 13:998496. doi: 10.3389/fmicb.2022.998496

Zhang, W., Chen, R., Meng, F., Yuan, H., Geng, M., Cheng, L., et al. (2021). Ecosystem functioning is linked to microbial evenness and community composition along depth gradient in a semiarid lake. *Ecol. Indic.* 132:108314. doi: 10.1016/j.ecolind.2021.108314

Zhang, X., Liu, S., Wang, J., Huang, Y., Freedman, Z., Fu, S., et al. (2020). Local community assembly mechanisms shape soil bacterial β diversity patterns along a latitudinal gradient. *Nat. Commun.* 11:5428. doi: 10.1038/s41467-020-19228-4

Zhao, W., Hu, A., Ni, Z., Wang, Q., Zhang, E., Yang, X., et al. (2019). Biodiversity patterns across taxonomic groups along a lake water-depth gradient: effects of abiotic and biotic drivers. *Sci. Total Environ.* 686, 1262–1271. doi: 10.1016/j.scitotenv.2019.05.381

Zhao, L., Wang, S., Shen, R., Gong, Y., Wang, C., Hong, P., et al. (2022). Biodiversity stabilizes plant communities through statistical-averaging effects rather than compensatory dynamics. *Nat. Commun.* 13:7804. doi: 10.1038/s41467-022-35514-9

Zheng, L., Wang, X., Ding, A., Yuan, D., Tan, Q., Xing, Y., et al. (2021). Ecological insights into community interactions, assembly processes and function in the denitrifying phosphorus removal activated sludge driven by phosphorus sources. *Front. Microbiol.* 12:779369. doi: 10.3389/fmicb.2021.779369

Zhou, J., and Ning, D. (2017). Stochastic community assembly: does it matter in microbial ecology? *Microbiol. Mol. Biol. Rev.* 81, e00002–e00017. doi: 10.1128/mmbr.00002-17

Zhu, Y., Zhang, R., Wu, F., Qu, X., Xie, F., and Fu, Z. (2013). Phosphorus fractions and bioavailability in relation to particle size characteristics in sediments from Lake Hongfeng, Southwest China. *Environ. Earth Sci.* 68, 1041–1052. doi: 10.1007/s12665-012-1806-9

frontiers | Frontiers in Microbiology

TYPE Original Research
PUBLISHED 13 October 2023
DOI 10.3389/fmicb.2023.1258659

OPEN ACCESS

EDITED BY
Yizhi Sheng,
China University of Geosciences, China

REVIEWED BY
Alain Isabwe,
University of Michigan, United States
Jianwei Zhao,
Huazhong Agricultural University, China

*CORRESPONDENCE
Wei Yang
✉ yangwei@bnu.edu.cn

RECEIVED 24 July 2023
ACCEPTED 12 September 2023
PUBLISHED 13 October 2023

CITATION
Ding J, Yang W, Liu X, Zhao Q, Dong W, Zhang C, Liu H and Zhao Y (2023) Unraveling the rate-limiting step in microorganisms' mediation of denitrification and phosphorus absorption/transport processes in a highly regulated river-lake system.
Front. Microbiol. 14:1258659.
doi: 10.3389/fmicb.2023.1258659

Unraveling the rate-limiting step in microorganisms' mediation of denitrification and phosphorus absorption/transport processes in a highly regulated river-lake system

Jiewei Ding[1], Wei Yang[1]*, Xinyu Liu[1], Qingqing Zhao[2], Weiping Dong[1], Chuqi Zhang[1], Haifei Liu[1] and Yanwei Zhao[1]

[1]State Key Laboratory of Water Environment Simulation, School of Environment, Beijing Normal University, Beijing, China, [2]Shandong Provincial Key Laboratory of Applied Microbiology, Ecology Institute, Qilu University of Technology (Shandong Academy of Sciences), Ji'nan, China

River–lake ecosystems are indispensable hubs for water transfers and flow regulation engineering, which have frequent and complex artificial hydrological regulation processes, and the water quality is often unstable. Microorganisms usually affect these systems by driving the nutrient cycling process. Thus, understanding the key biochemical rate-limiting steps under highly regulated conditions was critical for the water quality stability of river–lake ecosystems. This study investigated how the key microorganisms and genes involving nitrogen and phosphorus cycling contributed to the stability of water by combining 16S rRNA and metagenomic sequencing using the Dongping river–lake system as the case study. The results showed that nitrogen and phosphorus concentrations were significantly lower in lake zones than in river inflow and outflow zones ($p < 0.05$). *Pseudomonas*, *Acinetobacter*, and *Microbacterium* were the key microorganisms associated with nitrate and phosphate removal. These microorganisms contributed to key genes that promote denitrification (*nirB*/*narG*/*narH*/*nasA*) and phosphorus absorption and transport (*pstA*/*pstB*/*pstC*/*pstS*). Partial least squares path modeling (PLS-PM) revealed that environmental factors (especially flow velocity and COD concentration) have a significant negative effect on the key microbial abundance ($p < 0.001$). Our study provides theoretical support for the effective management and protection of water transfer and the regulation function of the river–lake system.

KEYWORDS

river-lake ecosystems, nutrient cycling process, biochemical rate-limiting steps, key microorganisms, key genes

1. Introduction

As the most widely distributed ancient community on Earth, microorganisms are characterized by rich species diversity, sensitive responses to environmental cues, and diverse functions (Banerjee et al., 2018). The degradation of pollutants by microorganisms and the biotransformation of nutrients in freshwater systems often drive the system's material circulation and energy flows, thereby contributing to the system's health and stability (Reid et al., 2019; Wu et al., 2021). Microorganisms control geochemical processes in interbasin

water transfer and play an irreplaceable role in indicating water quality (Chung et al., 2020; Zhang et al., 2021). Restoring and maintaining a good water microecosystem can promote the improvement of water self-purification capacity, which is conducive to the restoration and improvement of the water ecological environment (Deng et al., 2023). The complex biogeochemical nutrient cycles usually involve multiple steps (Lammel et al., 2015; Zheng et al., 2018; Sankar et al., 2019), in which the functional genes serve as an important medium for the function of microorganisms and can be an important basis for evaluating the functional potential of microbial communities (Djemiel et al., 2022). Wang et al. (2020a) found that in groundwater contaminated with As, *Proteobacteria* can contribute to the expression of As efflux genes *arsB* and *acr3* to enable microorganisms to display detoxification strategies to pump As out of cells and improve water quality. Wan et al. (2023) have confirmed that in the freshwater system that accepts the addition of foreign organic matter, core microorganisms (e.g., *Rhizobia*) can promote changes in primary productivity by altering the abundance of N_2-fixation genes, resulting in a healthier and more sustainable freshwater system. In addition, a recent study found that microorganisms can regulate endogenous phosphorus release pollution in natural water bodies through functional genes (*ppk*) that contribute to phosphorus transformation (Zhuo et al., 2023). Hence, understanding the microbial community's composition and functional genes is essential to maintaining the water quality and stability of freshwater ecosystems.

River–lake systems contribute greatly to flood control and storage, water conservation, species conservation, and biodiversity maintenance (Huang et al., 2021; Fernanda et al., 2022). However, the hydrological conditions in river–lake systems were complex, and especially during the period of regulation, flow shocks often led to unstable water quality states (Yang et al., 2017). It is imperative to maintain the water quality and stability of river–lake systems. Many studies have shown that the concentrations of nitrogen and phosphorus are the limiting factors for the water quality stability in river–lake systems (Wang et al., 2020b; Yu et al., 2023). Furthermore, nitrogen and phosphorus are the basic nutrients in the energy flow and material cycle of aquatic ecosystems, and too much or too little would disrupt the ecosystem balance (Zhang et al., 2017; Liang et al., 2021).

Previous studies have found that changes in hydrological conditions (rapid flow, etc.) were critical to shaping the dynamics of freshwater ecosystems (Wiens, 2002; McCluney et al., 2014). Hydrological changes have also been shown to be a major driver for the assembly process of freshwater microbial community aggregation processes and community structure (Pablo Nino-Garcia et al., 2016). Isabwe et al. (2018) also confirmed that the aggregation process of bacterial communities was affected by different hydrological conditions. In the dry season with a low flow rate, the aggregation pattern of bacterial communities was a deterministic process, while in the rainy season with a high flow rate, the bacterial communities were controlled by both stochastic and deterministic processes. In addition, Zhang et al. (2022) found that changes in surface hydrological conditions can lead to differences in microbial community structure and dominant groups, such as the increase of *Actinobacteria* due to low water volume, thus affecting the metabolic activity of microbial communities. Complex hydrological conditions can also affect the composition and potential functional trends of microbial communities (Cheng et al., 2019). Arnon et al. (2007) found that the high flow rate conditions can promote the transfer of chemical substances between water and sediment, provide nutrients for microorganisms, and promote the denitrification process. While the study of Hui et al. (2021) showed that the specific low flow velocity conditions in the flow intersection area would enrich the microorganisms that converted with nitrogen, and these microorganisms could provide *nap* and *narG* genes to effectively promote nitrate removal. Additionally, lakes and rivers have different environmental characteristics, such as organic matter content and pH, which affect the status of certain microbial communities that perform specific functions and consequently affect the stability of water quality (Ren et al., 2017; Tang C. et al., 2020; Crevecoeur et al., 2023). These studies have explored the contribution of microorganisms to the stability of water quality in rivers and lakes and the influence of environmental factors on microbial communities. However, there are still limitations. The key rate-limiting steps for water quality stability in the microbial-driven biochemical cycle are not clear, the ideal microbial communities and genes to improve water quality stability are still unrevealed, and how to promote the formation of these microbial communities and genes through artificial regulation is still not conclusive. These defects are undoubtedly unfavorable to the guidance of water transfer and regulation projects in river–lake systems.

In this study, we surveyed four zones with different hydrological conditions in the Dongping river–lake system. As an important hub of the South-to-North Water Diversion Project, Dongping Lake not only serves the function of water resource regulation but also provides potential drinking water for Beijing and Tianjin. Hence, it is imperative to ensure the water quality stability of the river–lake systems during the regulation period. Our study aimed to (1) identify the differences in physical and chemical properties in different zones of the river–lake system; (2) explore the spatial changes of microbial communities in different zones of the river–lake system; (3) investigate the key biochemical rate-limiting steps of the nitrogen and phosphorus cycles; (4) identify the contribution of key microorganisms and genes to the rate-limiting steps; and (5) determine the environmental variables affecting key microorganisms and genes. Our study will provide suggestions for the coordination of regulation and water quality stability from the perspective of microorganisms and support the long-term sustainable development of river–lake systems.

2. Materials and methods

2.1. Study area and sample collection

Dongping Lake is an important hub of the world's largest artificial water conservancy project, China's South-to-North Water Diversion Project. It receives its primary inflow from the Dawen River in the east and discharges water to the Yellow River through the two manmade Chenshankou and Qinghemen sluice gates in

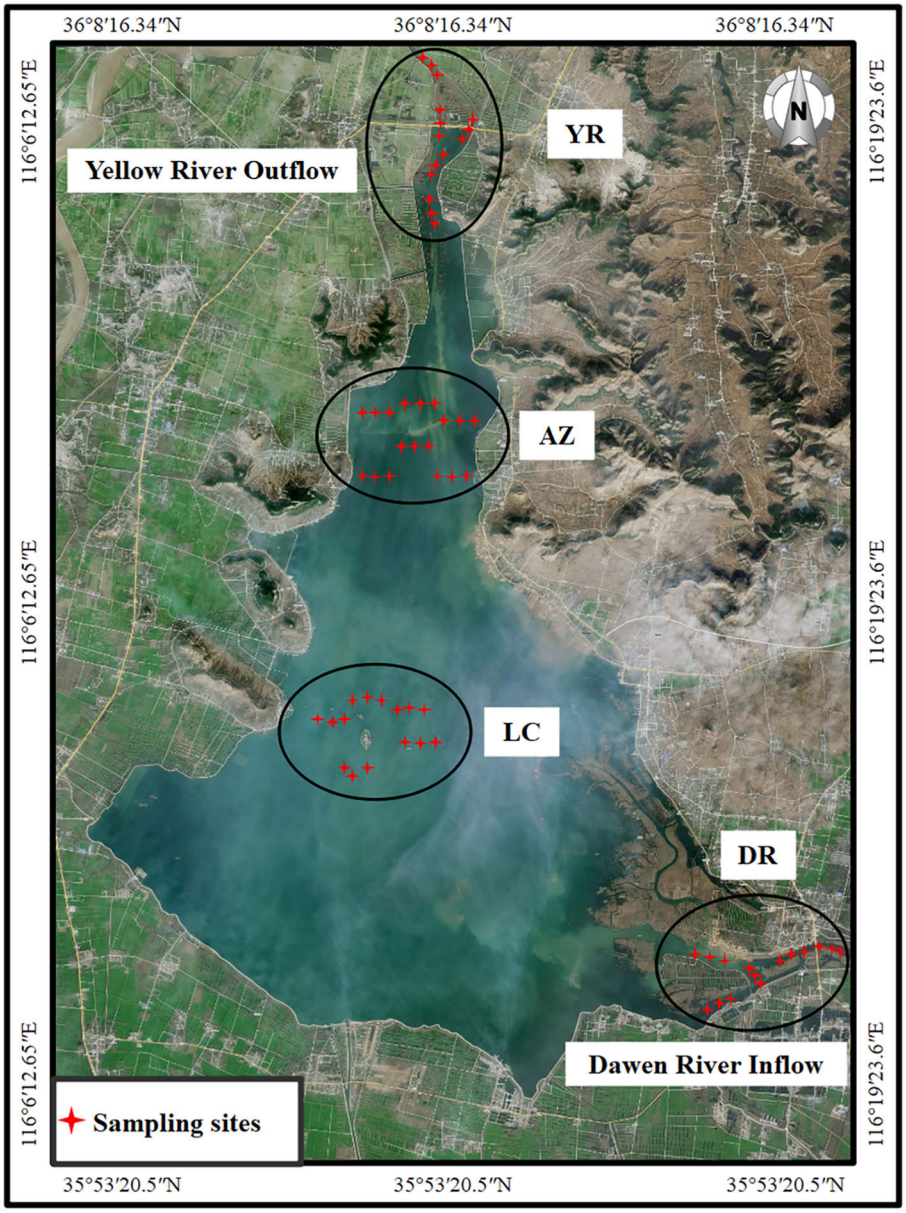

FIGURE 1
Location map of sampling sites. DR, Dawen River inflow zone; LC, lake center zone; AZ, aquaculture zone; YR, Yellow River outflow zone.

the north (Figure 1), with a high frequency of regulation (e.g., flow releases and storage). It is a typical river–lake transition area with complex hydrological conditions and drastic changes in water quality (Chen et al., 2014). Especially when the flood was discharged by these artificial gate dams, the huge impact of water flow led to an unstable sedimentary environment and fluctuating water quality.

Based on the strategic position and functional zoning, we divided this lake–river system into four zones: the Dawen River inflow zone (the main inflow river of the lake, DR), the lake center zone (natural ecological protection center area, LC), the aquaculture zone (there are artificial release and naturally raised fish, AZ), and the Yellow River outflow zone (transferring water storage through the sluice gate and providing drinking water source area, YR). The samples were collected in July 2022, during which Dongping Lake is in the artificial flood discharge and regulation period. At each sampling site, we collected five water samples and five sediment samples with triplicate samplings. We collected 1.0-L water samples at a depth of 0.5 m in polyethylene bottles and collected sediment source samples to a depth of 5 cm with a Peterson mud sampler (TC-600BD, Qingdao, China). Samples used to determine physical and chemical properties were immediately sent to a laboratory for testing. Water samples for microbial determination were immediately filtered, and the filter membranes were securely placed at −80°C. Sediment samples were securely placed at −80°C for <48 h until we could extract microbial determination.

2.2. Measurement of physicochemical parameters

We measured the water temperature (T), dissolved oxygen (DO), pH, specific conductance of the water (SPC), and the oxidation–reduction potential (ORP) at the study sites using a HACH HQ30d portable measuring instrument (HACH, Loveland, CO, USA). We measured the flow velocity (V) using a Doppler current meter (SF-6526J-21, Beijing, China). We measured the water's transparency (SD) using a Secchi disk *in situ*. For the chemical properties, we measured the chemical oxygen demand (COD), total nitrogen (TN), ammonia nitrogen (NH_4^+-N), nitrate nitrogen (NO_3^--N), nitrite nitrogen (NO_2^--N), total phosphorus (TP), and phosphate (PO_4^{3-}) values according to the standard methods defined by China's Ministry of Ecology and Environment (Supplementary Table S1). We measured all environmental parameters three times to mitigate random measurement errors, and we used the average value to represent each sample in our subsequent analyses. All environmental parameters that required laboratory testing were measured within 48 h.

2.3. Microbial sequencing and analysis

Microbial bacterial 16s rRNA and metagenomic sequencing were conducted in our study. The 16s rRNA data were used for microbial community structure-related analysis, while metagenomic data were used for microbial gene abundance and key biochemical step analysis. The relevant sequencing processes and analysis methods are shown in the Supplementary Text description of the microbial 16S rRNA and metagenomic sequencing. Our sequencing data has been uploaded to the National Center for Biotechnology Information (NCBL) database. The accession number is SRP457080.

2.4. Statistical analyses

The data were analyzed using the SPSS software, version 22.0 (https://www.ibm.com/spss). We used a one-way analysis of variance (ANOVA) with location as the level to test for significant differences. Where the ANOVA results were significant, we used least-significant difference (LSD) tests to identify pairs of values that differed significantly, with significance defined as $p < 0.05$. The independent sample *t*-tests were used for significant differences in topological values for the empirical and random networks (for specific analysis, see Supplementary Text description of the data analysis tools and methods).

3. Results

3.1. Physical and chemical properties

In the water column (Table 1), the nutrient concentrations of nitrogen (TN, NH_4^+-N, and NO_3^--N) and phosphorus (TP and PO_4^{3-}), which were major pollutants in the water environment (Dong et al., 2021), showed the order of YR > DR > AZ > LC. In particular, the values of NH_4^+-N, NO_3^--N, TP, PO_4^{3-} in the YR and DR zones were significantly higher than those of AZ and LC ($p < 0.05$). The concentration of COD also showed significant differences ($p < 0.05$), with the highest concentration in YR (19.0 ± 3.16), followed by DR (17.8 ± 1.17), AZ (16.0 ± 1.40), and LC (15.0 ± 2.00). In addition, although the flow velocity values did not show significant differences in different zones, they also showed a higher trend in the YR and DR. These results showed that the water quality in the lake zone was significantly better than that in the zones where rivers flow in and out (especially in the zones with artificially constructed gates and dams) during the regulation period of the river–lake system. In sediments, the concentration of nitrogen and phosphorus varies in different zones, but the difference was not significant. The COD content (0.58 ± 0.10 mg/g) was highest in the YR, by 0.02, 0.08, and 0.26 mg/g compared with the other zones, but the difference was only significant for the DR.

It was worth noting that the TN was strongly and significantly correlated with NO_3^--N concentration ($R = 0.72$, $p < 0.01$), as well as TP and PO_4^{3-} concentration ($R = 0.86$, $p < 0.01$) (Supplementary Figure S1). Therefore, the regulation of nitrate and phosphate concentrations was the key to maintaining the steady state of water quality during regulation in this study, and microbial-mediated pathways related to nitrate and phosphate should also be a major focus of this study.

3.2. Microbial community structure and composition

Hierarchical clustering and PCoA results showed that all samples in our study can be well classified and clustered into three categories: zones where rivers flow in and out (DRW and YRW), lakes (LCW and AZW), and sediments (DRS, LCS, AZS, and YRS) (Figure 2A; Supplementary Figure S2). In this study, these three categories were defined as river–water, lake–water, and sediment. ANOSIM results showed significant differences ($R = 0.669$, $p = 0.0001$) among these three groups (Supplementary Figure S3), which implied the clustering was reasonable and reliable (Shang et al., 2023). Based on this result, the composition and structure of the microbial community were analyzed (Figure 2B). Their values are shown in Supplementary Table S2.

At the phylum level, there were significant differences in the relative abundance of the dominant microorganisms in the river, lake, and sediment ($p < 0.05$). The relative abundance of *Proteobacteria* (47.9 ± 5.4%, mean ± SD; 40.9 ± 5.1%), *Actinobacteriota* (16.6 ± 3.3%; 20.2 ± 3.3%), and *Firmicutes* (8.3 ± 3.3%; 18.2 ± 3.3%) in rivers and lakes was significantly higher than that in sediments ($p < 0.05$), with percentages of 1.5 and 1.3, 3.6 and 4.4, and 1.5 and 3.3 times those in the sediment, respectively. In the sediment, the relative abundances of *Chloroflexi* (12.0 ± 3.3%), *Desulfobacterota* (6.3 ± 0.8%), and *Acidobacteriota* (7.1 ± 2.3%) were significantly higher than those in rivers and lakes ($p < 0.05$), with abundances of 9.7 and 11.2%, 5.3 and 5.9%, and 4.5 and 6.7%, respectively.

At the genus level, *hgcI_clade*, *Pseudomonas*, *Comamonadaceae*, *Acinetobacter*, *Hydrogenophaga*, and

10.3389/fmicb.2023.1258659

TABLE 1 Analysis of the physical and chemical properties of water and sediment in the study area.

Samples	Indicators	Location			
		DR	LC	AZ	YR
Water	*SD* (cm)	44.800 ± 2.79^{b}	81.200 ± 12.54^{a}	62.200 ± 14.60^{b}	44.800 ± 3.66^{b}
	T (°C)	27.540 ± 0.27^{c}	28.380 ± 0.07^{b}	27.100 ± 0.06^{c}	30.640 ± 0.82^{a}
	DO (mg/L)	5.206 ± 0.69^{b}	5.588 ± 0.39^{b}	7.838 ± 1.07^{a}	5.088 ± 0.64^{b}
	SPC (us/cm^{-1})	722.800 ± 10.13^{b}	$1{,}006.000 \pm 100.94^{a}$	$1{,}066.200 \pm 66.41^{a}$	999.600 ± 29.23^{a}
	ORP (mV)	134.780 ± 2.78^{a}	127.600 ± 9.73^{a}	112.080 ± 5.75^{b}	128.060 ± 8.00^{a}
	pH	8.566 ± 0.23^{a}	8.534 ± 0.13^{a}	8.752 ± 0.16^{a}	8.524 ± 0.07^{a}
	V (m/s)	0.338 ± 0.06^{a}	0.280 ± 0.05^{a}	0.294 ± 0.05^{a}	0.364 ± 0.09^{a}
	D (m)	2.060 ± 0.56^{a}	1.580 ± 0.36^{ab}	1.860 ± 0.31^{a}	1.070 ± 0.20^{b}
	COD (mg/L)	17.800 ± 1.17^{ab}	15.000 ± 2.00^{b}	16.000 ± 1.40^{ab}	19.000 ± 3.16^{a}
	TN (mg/L)	1.924 ± 0.49^{a}	1.810 ± 0.45^{a}	1.908 ± 0.50^{a}	2.224 ± 0.47^{a}
	NH_4^+-N (mg/L)	0.146 ± 0.09^{a}	0.079 ± 0.06^{a}	0.110 ± 0.02^{a}	0.366 ± 0.04^{a}
	NO_3^--N (mg/L)	0.229 ± 0.04^{a}	0.1080 ± 0.05^{b}	0.120 ± 0.07^{b}	0.350 ± 0.04^{a}
	NO_2^--N (mg/L)	0.030 ± 0.02^{a}	0.0180 ± 0.01^{a}	0.025 ± 0.02^{a}	0.017 ± 0.01^{a}
	TP (mg/L)	0.124 ± 0.04^{a}	0.096 ± 0.05^{b}	0.088 ± 0.04^{b}	0.172 ± 0.06^{a}
	PO_4^{3-} (mg/L)	0.068 ± 0.04^{a}	0.056 ± 0.03^{b}	0.042 ± 0.02^{b}	0.082 ± 0.05^{a}
Sediment	*COD* (mg/g)	0.322 ± 0.08^{b}	0.500 ± 0.12^{a}	0.564 ± 0.11^{a}	0.584 ± 0.10^{a}
	TN (mg/g)	1.444 ± 0.19^{a}	1.310 ± 0.26^{a}	1.204 ± 0.13^{a}	0.848 ± 0.09^{a}
	NH_4^+-N (mg/g)	0.424 ± 0.06^{a}	0.409 ± 0.09^{ab}	0.331 ± 0.02^{ab}	0.207 ± 0.03^{c}
	NO_3^--N (mg/g)	0.172 ± 0.05^{a}	0.161 ± 0.06^{a}	0.162 ± 0.05^{a}	0.193 ± 0.02^{a}
	NO_2^--N (mg/g)	0.036 ± 0.01^{a}	0.037 ± 0.01^{a}	0.040 ± 0.01^{a}	0.039 ± 0.01^{a}
	TP (mg/g)	0.284 ± 0.09^{a}	0.276 ± 0.04^{a}	0.330 ± 0.05^{a}	0.268 ± 0.06^{a}
	PO_4^{3-} (mg/g)	0.208 ± 0.06^{a}	0.206 ± 0.03^{a}	0.198 ± 0.02^{a}	0.192 ± 0.02^{a}

Values are mean ± SD. Different letters (a, b, and c) represent significant differences ($p < 0.05$) among sampling sites.

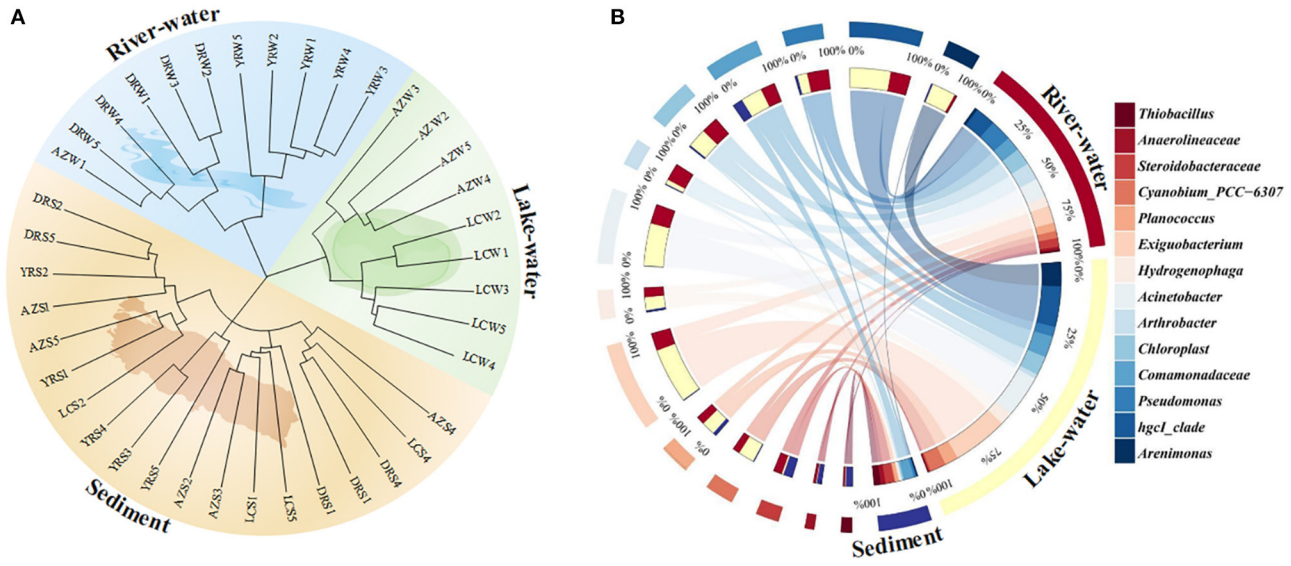

FIGURE 2
Microbial community structure and composition in the Dongping river-lake system. **(A)** microbial community hierarchical clustering; **(B)** dominant microorganisms at the genus levels in river water, lake water, and sediment. W and S stand for water column and sediment, respectively. Genera that could not be defined were traced back to the family and order level.

10.3389/fmicb.2023.1258659

Exiguobacterium had a higher relative abundance in river water and lake water, but their abundances in the sediment were <1%. However, *Thiobacillus*, *Anaerolineaceae*, and *Steroidobacteraceae* had a high abundance (>2.0%) in the sediment but were rarely detected in the river and lake. The abundance of *Arenimonas* was significantly higher in the lake water (5.3 ± 1.3%) ($p < 0.05$), 4.7 and 5.0% more than in the river water and sediment, respectively. The *Pseudomonas* abundance was significantly greater in the lake water (4.7 ± 1.3%), followed by the river water (2.2 ± 0.6%) and sediment (0.5 ± 0.1%) ($p < 0.05$). The relative abundance of *Comamonadaceae* in the river water (4.7 ± 2.2%) was slightly higher than in the other zones ($p < 0.05$). The *Acinetobacter* relative abundance was 9.3 ± 2.7% in the lake water, which was 5 and 9.3% higher than in the river water and the sediment zone, respectively ($p < 0.05$). In addition, the relative abundance of *Exiguobacterium* in the lake-water zone reached 12.1 ± 3.6%, which was significantly higher than in the river water (3.9 ± 0.8%) and sediment (0.1 ± 0.0%) ($p < 0.05$).

Table 2 summarizes the characteristics of microbial molecular ecological networks. The microbial molecular ecological network constructed by our research was scientific and reasonable (see Supplementary Text description of the topological characteristics of the molecular ecological network). All ecological networks were dominated by positive correlations, with values ranging from 75.4 to 83.2% (Figure 3; Supplementary Table S3). It is worth noting that there was a significant difference among the results of average path length ($p < 0.05$), and the order was as follows: lake water (8.392) > river water (6.432) > sediment (6.077). The modularity of microbial communities showed significant differences ($p < 0.05$), and the order was lake water (0.728) > river water (0.726) > sediment (0.635). The keystone taxa can be used as indicators of the microbial community (Banerjee et al., 2018), and the keystone taxa were identified in this study (Supplementary Table S4; Figure 3).

3.3. Nitrogen and phosphorus metabolic pathways driven by key microbial communities and genes

The specific functions of microbial communities (such as nitrogen and phosphorus conversion) were closely related to metabolic pathways (Xiong et al., 2023). The results showed that the KO pathway (Supplementary Figures S4, S5) involved in the nitrogen and phosphorus cycle was highly expressed in lake water. Microbial functional genes were crucial for the transformation of nutrients (Li et al., 2022) to identify the genes that play key roles in the pathway of this river–lake system, we analyzed the expression levels of genes related to nitrogen and phosphorus pathways (Supplementary Figure S6) and the contribution of key genes (Figure 4). The results showed that the *nirB* (3.6%), *narG* (5.5%), narH (2.5%), and *nasA* (2.8%) genes related to the nitrate cycle and the *ppk* (6.5%), *pstA* (4.3%), *pstB* (4.2%), *pstC* (4.4%), and *pstS* (6.4%) genes related to the phosphate cycle were highly expressed in all samples (Supplementary Figure S6), and most (nitrate: *nirB*/*narG*/*narH*/*nasA*; phosphorus: *pstA*/*pstB*/*pstC*/*pstS*) were expressed significantly higher in the lake water than in

TABLE 2 Topological properties of the empirical networks and their associated random networks in the different zones: River-water, Lake-water and Sediment zones.

Zones	Empirical network								Random network			
	Nodes	Links	Average connective degree	Average path length	Average clustering coefficient	Modularity	R^2	Small-world coefficient	Average path length (SD)	Average clustering coefficient (SD)	Modularity (SD)
River-water	375	1,819	9.701	6.432*	0.584**	0.726*	0.791	3.384	2.944 (0.025)	0.079 (0.006)	0.259 (0.004)
Lake-water	369	1,725	9.350	8.392*	0.585**	0.728*	0.663	46.644	5.353 (0.067)	0.008 (0.004)	0.626 (0.007)
Sediment	296	1,153	7.791	6.077*	0.528**	0.635*	0.922	5.352	3.080 (0.032)	0.050 (0.005)	0.303 (0.005)

Values are means, with the SD in brackets. *$p < 0.05$, **$p < 0.01$.

the river water and sediment (Figure 4). These genes are closely related to nitrate reduction, phosphate absorption, and transport (Yu et al., 2018; Li et al., 2023; Liu et al., 2023). On this basis, the main microorganisms contributing these genes with high expression in lakes were identified in this study through the combination of species annotation and gene abundance calculation (Supplementary Figure S7; the detailed descriptions are shown in the Supplementary Text description of the analysis of key microorganisms contributing nitrogen and phosphorus genes). The results showed that *Pseudomonas*, *Acinetobacter*, *Nocardioides*, *Microbacterium*, *Agromyces*, and *Aeromonas* had a relatively high contribution of genes involved in the nitrate-phosphate cycle, especially in lake water. These microorganisms were defined as the key microorganisms that we should focus on in our study.

3.4. The influencing factors of nitrate and phosphate concentration

The results showed that there was a significant positive correlation between the abundance of key microbial abundance and the genes promoting nitrogen reduction (0.836, $p < 0.001$) and phosphorus absorption and transport (0.873, $p < 0.001$, Figure 5). The effect of key gene abundance on nitrogen (-0.898, $p < 0.001$) and phosphorus (-0.242, $p < 0.001$) concentration showed a highly significant negative trend. The environmental factors showed strong positive effects on the concentrations of nitrogen (0.697) and phosphorus (0.333), and the effect on nitrogen was significant ($p < 0.05$). There was a significant negative effect (-0.648, $p < 0.001$) of environmental factors on the abundance of key microbial species. In the environmental factors, the factor load of V (0.727) and COD concentration (0.839) was obviously high and significant ($p < 0.001$), and showed strong significant positive correlations with the concentrations of nitrate and phosphate and negative correlations with key microbial abundance (Supplementary Table S5), respectively.

4. Discussion

This study revealed the key rate-limiting steps of microbial-mediated nitrogen and phosphorus cycling in a highly regulated river–lake system. Our original goals were confirmed. Specifically, we found that the concentration of nitrogen and phosphorus in lake water was significantly lower than that in river water; that is, the water quality was more stable. In addition, the stability of the microbial community and the abundance of key microorganisms associated with nitrogen and phosphorus conversion were higher in lake water. Key microorganisms and genes-driven denitrification and phosphorus absorption/transport processes become key biochemical rate-limiting steps. COD concentration and flow velocity were the most important environmental variables that affect key microorganisms and genes.

4.1. Effects of physicochemical characteristics on microbial communities in different zones

Our study has revealed that flow velocity and COD concentration in river water were obviously higher than in lake water. In the Dongping river–lake system, the water surface in the lake zone was wide and the flow velocity was relatively slow (Liu et al., 2022), while in the inflow area, the water surface was narrow and the flow velocity was fast (Liu et al., 2016). During the regulation period, there was often a huge water impact, which undoubtedly increased the flow velocity in the outflow area (Zhang et al., 2012). The Dawen River mainly passes through rural areas, and organic matter in soil, farm compost, and decaying plants will enter the river with rainwater and irrigation water, resulting in a high COD concentration (Lv et al., 2018). In addition, some of the pollutants generated by human activities were discharged into the river and accumulated at the gates. When the flood was discharged, the gates were opened, and the pollutants were released along with the flow (Piirsoo et al., 2018; Watkins et al., 2019). This may also lead to higher COD concentration in the outflow zones.

We found that high flow velocity in river water zones has negative effects on the stability of microbial communities. In lake water zones with relatively low flow velocity, the microbial network has the longest path length, which suggests that when the environment is disturbed (e.g., through water inflows or releases), the response rate is the slowest for microorganisms in the lake zone, and the impact of environmental disturbance will not spread quickly to the whole microbial molecular ecological network (Jeanbille et al., 2016). The modularity of the microbial community in the lake water was the highest, which was similar to the study of Khu et al. (2023), who found that the low flow velocity conditions were more conducive to microbial growth and formed a higher degree of modularity. The high degree of modularity indicated that the function of the microbial community was more complex, and the microbial community has a strong ability to resist environmental stress (Feng et al., 2017). In addition, the numerous positive correlations in lake water represented that microorganisms were more inclined toward cooperative relationships, which promoted the stability of microbial communities (Layeghifard et al., 2017). The influence of higher flow velocity and COD concentration on the abundance of key microorganisms was negative in our study. When the water flow velocity increased, the desorption force generated by flow shear reduced the adsorption of microorganisms to suspended matter in the water, inhibiting the formation of biofilm (Tian et al., 2017). High COD concentration indicated that the water accepts more organic pollutants, and the biodegradation of these organic substances will consume DO (Liu et al., 2021). Most of the key microorganisms found in our study were aerobic denitrifying bacteria and phosphorus-accumulating organisms (PAOs), which need DO for their own reproduction (Zhao et al., 2022; Shen et al., 2023), so high COD concentration will inhibit the abundance of these key microorganisms.

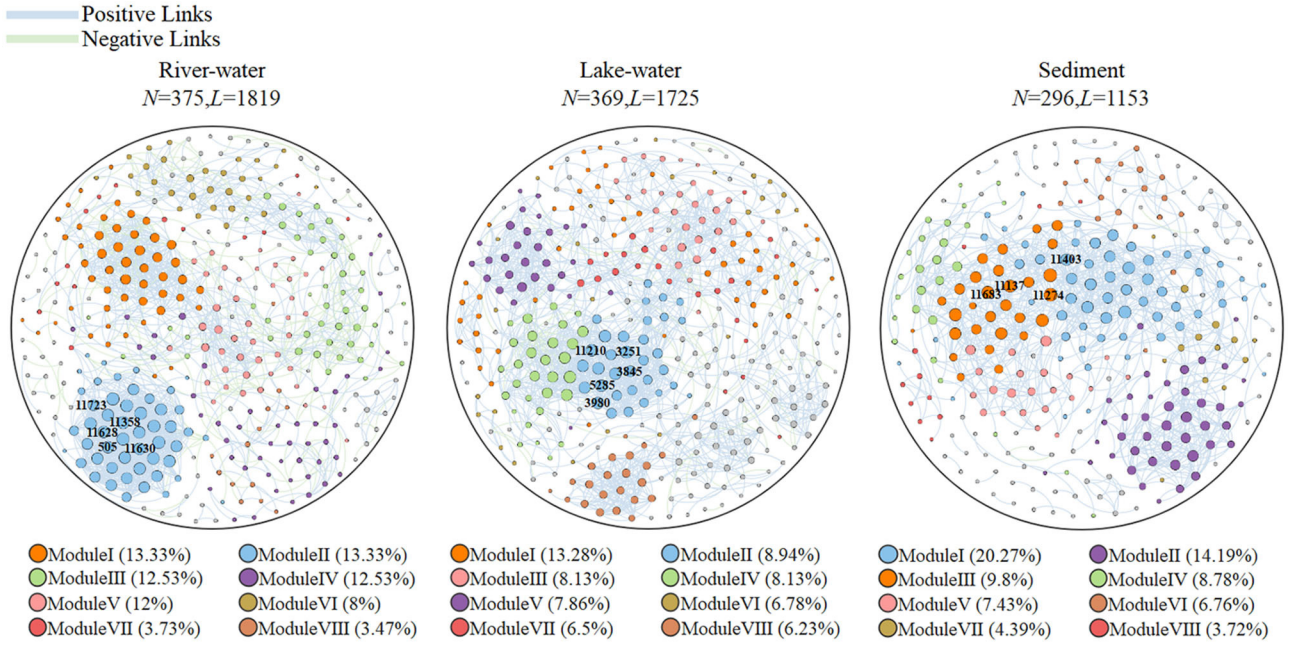

FIGURE 3
Topological networks of the river water, lake water, and sediment. *N* is the number of network nodes; *L* is the number of network edges. The blue edges represent positive connections, and the green edges represent negative connections. Modules I to VIII represent different aggregation modules. The microorganisms labeled with operational taxonomy unit (OTU) numbers are the keystone taxa.

4.2. The rate-limiting steps in microorganism-mediated nitrogen and phosphorus cycles

We found that total nitrogen and total phosphorus concentrations depend on NO_3^--N and PO_4^{3-} concentrations in the water column. Therefore, we conclude that controlling NO_3^--N and PO_4^{3-} concentrations was the key to maintaining water quality stability during water regulation. Previous studies have also confirmed our findings about nitrate nitrogen and phosphate, which are often used as key indicators in water quality monitoring to judge the deterioration of water quality for subsequent control (Rashid and Romshoo, 2013; Bhurtun et al., 2019). Hence, microorganism-mediated steps that can affect nitrate and phosphate conversion become the focus of this study, which may also be a key step in water quality stability during water regulation.

We found that *Pseudomonas*, *Acinetobacter*, and *Microbacterium* were dominant and keystone taxa in the lake-water (Figures 2, 3) zones. The dominant microorganisms with high biomass can affect some broad community processes, and rare keystone taxa are more visible in narrower processes; they are the drivers of microbial community structure and function, such as a particular one in the nitrogen and phosphorus cycles (Banerjee et al., 2018). In addition, we found that *Pseudomonas* mainly contributes *nirB*, *narG*, and *narH* genes, while *Acinetobacter* can contribute *nirB*, *pstB*, *pstC*, and *pstS* genes. *Microbacterium* contributed the *nasA*, *pstA*, and *pstB* genes. For the nitrogen cycle, *nirB* is the gene corresponding to the nitrite assimilation reductase, *narG*/*narH* corresponds to denitrification, and *nasA* corresponds to nitrate assimilation reduction (Wang et al., 2018). For the phosphorus cycle, *pstA*, *pstB*, *pstC*, and *pstS* were the corresponding genes for phosphate absorption and transport, and these were the key to the function of PAOs (Singleton et al., 2021). In addition, previous studies have confirmed our findings: *Pseudomoas* was confirmed to be aerobic denitrifying bacteria (Shen et al., 2023), and the presence of *Pseudomonas* and *Acinetobacter* can accelerate the rate of nitrate reduction in sewage (Hu et al., 2022; Xiao et al., 2023). *Pseudomonas* and *Acinetobacter* are typical PAOs, that can realize excessive phosphate absorption through the aerobic phosphorus absorption process (He et al., 2020). *Microbacterium* was found to be denitrifying bacteria (Tang et al., 2023) and have good phosphorus removal potential (Wang et al., 2016). Hence, these microorganisms contribute significantly to the lower nitrogen and phosphorus concentrations in the lake zone. Hence, these dominant and keystone taxa may dominate the denitrification, phosphate absorption, and transport pathways to become key rate-limiting steps for water quality stabilization in this river–lake system.

4.3. Analysis of key factors affecting nitrogen and phosphorus concentration and water quality improvement strategies

We found that the inhibition of key genes on nitrogen and phosphorus concentrations was significant. This also showed that the key genes defined in this study can indeed promote the processes of denitrification and phosphorus absorption and

10.3389/fmicb.2023.1258659

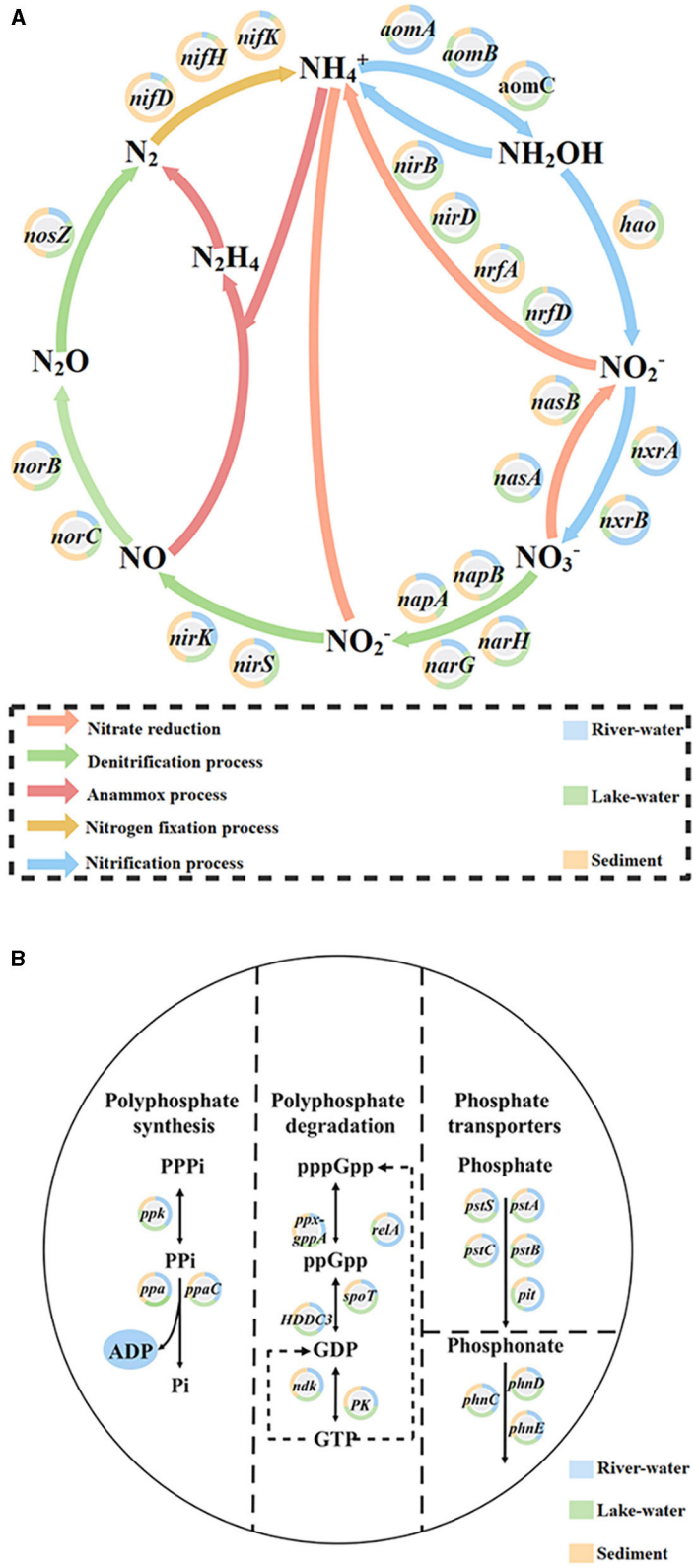

FIGURE 4
The proportion of **(A)** nitrogen and **(B)** phosphorus cycling-related genes expressed in river water, lake water, and sediment in each pathway.

10.3389/fmicb.2023.1258659

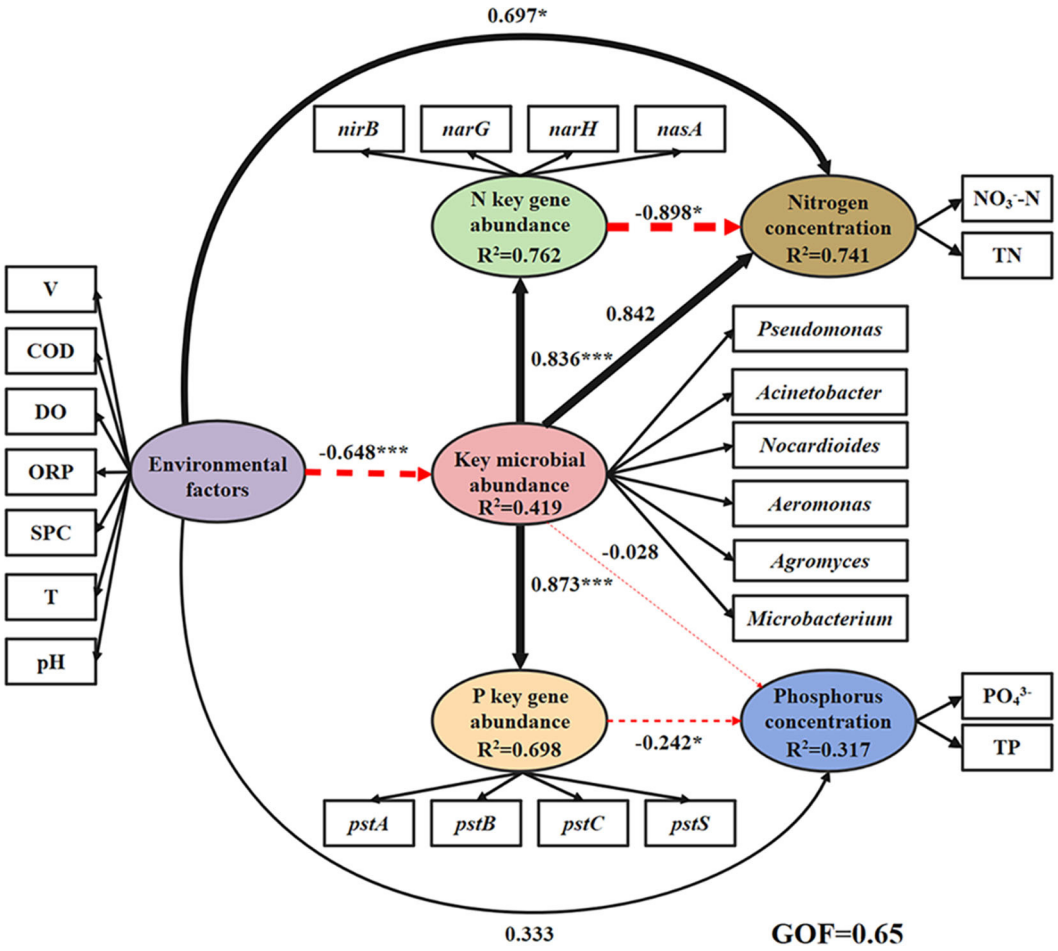

FIGURE 5
The relationship and influence of environmental factors, key microbial abundance, nitrogen/phosphorus cycling gene abundance, and nitrogen/phosphorus concentrations are shown by partial least squares path modeling (PLS-PM) in the water. GOF, Goodness-of-Fit (0.67 indicates a good fit). The black line represents the positive correlation, the red line represents the negative correlation, and the thickness of the line represents the size of the path coefficient (value range 0–1). *$p < 0.05$, ***$p < 0.001$.

transport. In addition, the increase in the abundance of key microorganisms was significantly beneficial to the abundance of nitrogen and phosphorus genes. These further confirmed the importance of microorganism-mediated denitrification, phosphorus absorption, and transport pathways for water quality stability. However, we found that high flow velocity and COD concentration may not be conducive to the stability of water quality during the regulation period. Hydrological disturbance, especially the increase in flow velocity, will cause the exchange of sediments and water in shallow lakes (Tang X. et al., 2020; Luo et al., 2022), resulting in the release of nitrogen and phosphorus from the sediments, which further increases the concentration of pollutants in the water phase (Huang et al., 2015; Peng et al., 2021). The higher COD concentration may be unfavorable to the propagation of aerobic denitrifying microorganisms and PAOs (as mentioned in Section 4.1), resulting in higher nitrogen and phosphorus concentrations in water.

In summary, in this study, maintaining the abundance of key microorganisms (especially the dominant and keystone taxa) and controlling the regulation flow as well as the concentration of pollutants accepted by the water body were crucial to maintaining the stability of water quality during hydrological regulation. Based on this, important strategies were proposed to protect water quality in this study (Figure 6A). On the scale of hydrological regulation, we suggest adopting the mode of cross-peak flood regulation to reduce the kinetic energy of flow to a certain extent and weaken the exchange between water and sediment. In terms of the water quality supervision scale of the accepted water bodies, we suggest increasing the monitoring of the incoming water quality of the Dawen River, removing the sewage behavior along the river, and regularly cleaning up the plant spoilage litter in the river to reduce the organic matter content. On the scale of the microbial community, we propose to add key microbial complex agents containing *Pseudomonas*, *Acinetobacter*, and *Microbacterium* in the inflow and outflow zones during the regulation period. Through the above strategies, the ideal microbial community gene function model was finally achieved (Figure 6B). It can promote nitrogen and phosphorus removal to maintain water quality stability.

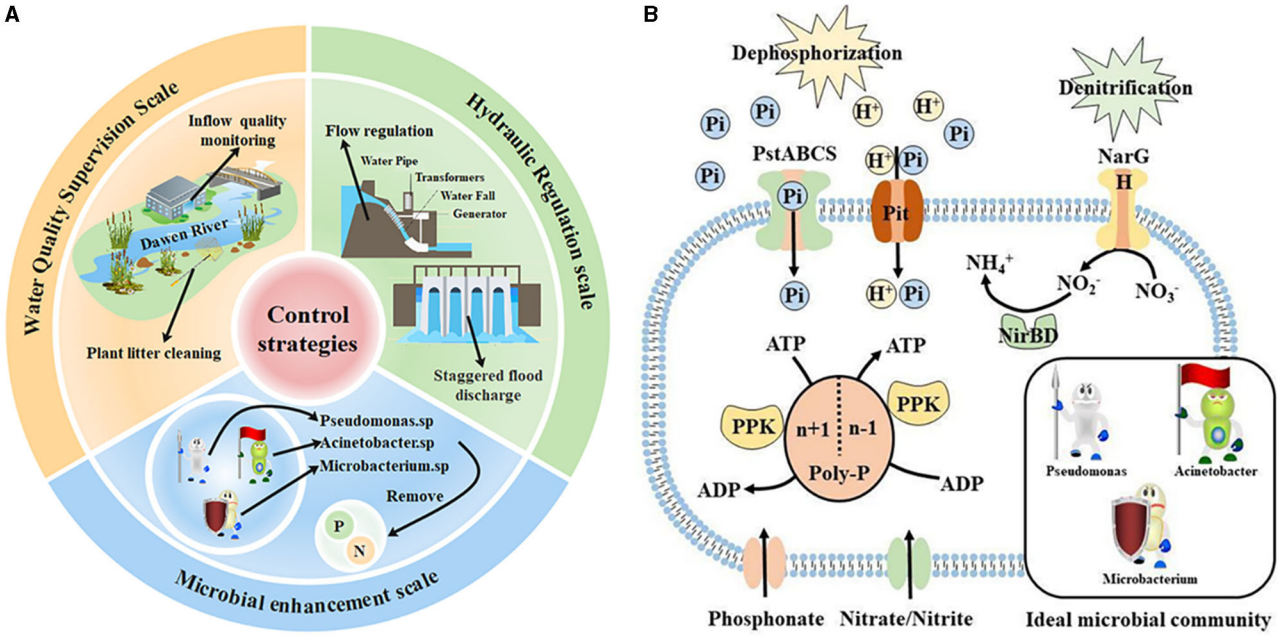

FIGURE 6
(A) Water quality stability improvement strategies and **(B)** ideal microbial community gene function model.

5. Conclusion

In this study, we have revealed the important influence of microorganisms on water quality stability in a highly regulated river–lake system using the Dongping river–lake system as the case study. The lake zones showed better water quality compared with the discharge and inflow zones. In sediments, there was no significant difference in nitrogen and phosphorus concentrations. Denitrification and phosphorus absorption and transport mediated by key microorganisms were key rate-limiting steps for water quality stability. *Pseudomonas*, *Acinetobacter*, and *Microbacterium* have the most important effects on denitrification, phosphorus absorption, and transport steps. The increase in flow velocity and nutrient load was unfavorable to key microbial abundance. This study will help us ensure the quality and health of water during the process of water transfers and flow regulation engineering.

Data availability statement

The original microbial sequencing data presented in the study are publicly available. This data has been uploaded to the National Center for Biotechnology Information (NCBI) database under the accession number PRJNA1009027 (https://www.ncbi.nlm.nih.gov/bioproject/PRJNA1009027). The original contributions presented in the study are included in the article/Supplementary material. Further inquiries can be directed to the corresponding authors.

Author contributions

JD: Data curation, Methodology, Writing—original draft. WY: Funding acquisition, Supervision, Writing—review and editing. XL: Data curation, Investigation, Writing—review and editing. QZ: Data curation, Writing—review and editing. WD: Data curation, Writing—review and editing. CZ: Data curation, Writing—review and editing. HL: Writing—review and editing. YZ: Writing—review and editing.

Funding

The author(s) declare financial support was received for the research, authorship, and/or publication of this article. This work was supported by the Major Scientific and Technological Innovation Projects in Shandong Province (2021CXGC011201), the National Natural Science Foundation of China (No. 552 52079006), and the Joint study on ecological protection and high-quality development in the Yellow River basin (2022-YRUC-01-0202).

Conflict of interest

The authors declare that the research was conducted in the absence of any commercial or financial relationships that could be construed as a potential conflict of interest.

Publisher's note

All claims expressed in this article are solely those of the authors and do not necessarily represent those of

their affiliated organizations, or those of the publisher, the editors and the reviewers. Any product that may be evaluated in this article, or claim that may be made by its manufacturer, is not guaranteed or endorsed by the publisher.

Supplementary material

The Supplementary Material for this article can be found online at: https://www.frontiersin.org/articles/10.3389/fmicb.2023.1258659/full#supplementary-material

References

Arnon, S., Packman, A. I., Peterson, C. G., and Gray, K. A. (2007). Effects of overlying velocity on periphyton structure and denitrification. *J. Geophys. Res. Biogeosci.* 112, G01002. doi: 10.1029/2006JG000235

Banerjee, S., Schlaeppi, K., and van der Heijden, M. G. A. (2018). Keystone taxa as drivers of microbiome structure and functioning. *Nat. Rev. Microbiol.* 16, 567–576. doi: 10.1038/s41579-018-0024-1

Bhurtun, P., Lesven, L., Ruckebusch, C., Halkett, C., Cornard, and, J.-P., and Billon, G. (2019). Understanding the impact of the changes in weather conditions on surface water quality. *Sci. Total Environ.* 652, 289–299. doi: 10.1016/j.scitotenv.2018.10.246

Chen, Y., Chen, S., Yu, S., Zhang, Z., Yang, L., and Yao, M. (2014). Distribution and speciation of phosphorus in sediments of Dongping Lake, North China. *Environ. Sci. Eur.* 72, 3173–3182. doi: 10.1007/s12665-014-3223-8

Cheng, H., Cheng, L., Wang, L., Zhu, T., Cai, W., Hua, Z., et al. (2019). Changes of bacterial communities in response to prolonged hydrodynamic disturbances in the eutrophic water-sediment systems. *Int. J. Environ. Res. Public Health.* 16, 3868. doi: 10.3390/ijerph16203868

Chung, T., Weller, D. L., and Kovac, J. (2020). The Composition of microbial communities in six streams, and its association with environmental conditions, and foodbornepathogen isolation. *Front. Microbiol.* 11, 1757. doi: 10.3389/fmicb.2020.01757

Crevecoeur, S., Edge, T. A., Watson, L. C., Watson, S. B., Greer, C. W., Ciborowski, J. J. H., et al. (2023). Spatio-temporal connectivity of the aquatic microbiome associated with cyanobacterial blooms along a Great Lake riverine-lacustrine continuum. *Front. Microbiol.* 14, 1073753. doi: 10.3389/fmicb.2023.1073753

Deng, Y., Fu, S., Xu, M., Liu, H., Jiang, L., Liu, X., et al. (2023). Purification and water resource circulation utilization of Cd-containing wastewater during microbial remediation of Cd-polluted soil. *Environ. Res.* 219, 115036. doi: 10.1016/j.envres.2022.115036

Djemiel, C., Maron, P.-A., Terrat, S., Dequiedt, S., Cottin, A., and Ranjard, L. (2022). Inferring microbiota functions from taxonomic genes: a review. *GigaScience.* 11, giab090. doi: 10.1093/gigascience/giab090

Dong, B., Qin, T., Wang, Y., Zhao, Y., Liu, S., Feng, J., et al. (2021). Spatiotemporal variation of nitrogen and phosphorus and its main influencing factors in Huangshui River basin. *Environ. Monit. Assess.* 193, 292. doi: 10.1007/s10661-021-09067-1

Feng, K., Zhang, Z., Cai, W., Liu, W., Xu, M., Yin, H., et al. (2017). Biodiversity and species competition regulate the resilience of microbial biofilm community. *Mol. Ecol.* 26, 6170–6182. doi: 10.1111/mec.14356

Fernanda, P. A., Liu, S., Yuan, T., Ramalingam, B., Lu, J., and Sekar, R. (2022). Diversity and abundance of antibiotic resistance genes and their relationship with nutrients and land use of the inflow rivers of Taihu Lake. *Front. Microbiol.* 13, 1009297. doi: 10.3389/fmicb.2022.1009297

He, Q., Wang, H., Chen, L., Gao, S., Zhang, W., Song, J., et al. (2020). Elevated salinity deteriorated enhanced biological phosphorus removal in an aerobic granular sludge sequencing batch reactor performing simultaneous nitrification, denitrification and phosphorus removal. *J. Hazard. Mater.* 390, 121782. doi: 10.1016/j.jhazmat.2019.121782

Hu, Y., Liu, T., Chen, N., and Feng, C. (2022). Changes in microbial community diversity, composition, and functions upon nitrate and Cr(VI) contaminated groundwater. *Chemosphere.* 288, 132476. doi: 10.1016/j.chemosphere.2021.132476

Huang, F., Ochoa, C. G., Guo, L., Wu, Y., and Qian, B. (2021). Investigating variation characteristics and driving forces of lake water level complexity in a complex river-lake system. *Stoch. Environ. Res. Risk Assess.* 35, 1003–1017. doi: 10.1007/s00477-020-01907-9

Huang, J., Xu, Q., Xi, B., Wang, X., Li, W., Gao, G., et al. (2015). Impacts of hydrodynamic disturbance on sediment resuspension, phosphorus and phosphatase release, and cyanobacterial growth in Lake Tai. *Environ. Earth Sci.* 74, 3945–3954. doi: 10.1007/s12665-015-4083-6

Hui, C., Li, Y., Zhang, W., Yang, G., Wang, H., Gao, Y., et al. (2021). Coupling genomics and hydraulic information to predict the nitrogen dynamics in a channel confluence. *Environ. Sci. Technol.* 55, 4616–4628. doi: 10.1021/acs.est.0c04018

Isabwe, A., Yang, J. R., Wang, Y., Liu, L., Chen, H., and Yang, J. (2018). Community assembly processes underlying phytoplankton and bacterioplankton across a hydrologic change in a human-impacted river. *Sci. Total Environ.* 630, 658–667. doi: 10.1016/j.scitotenv.2018.02.210

Jeanbille, M., Gury, J., Duran, R., Tronczynski, J., Agogue, H., Ben Said, O., et al. (2016). Response of core microbial consortia to chronic hydrocarbon contaminations in coastal sediment habitats. *Front. Microbiol.* 7, 01637. doi: 10.3389/fmicb.2016.01637

Khu, S. T., Changchun, X., and Wang, T. (2023). Effects of flow velocity on biofilm composition and microbial molecular ecological network in reclaimed water distribution systems. *Chemosphere.* 341, 140010. doi: 10.1016/j.chemosphere.2023.140010

Lammel, D. R., Feigl, B. J., Cerri, C. C., and Nuesslein, K. (2015). Specific microbial gene abundances and soil parameters contribute to C, N, and greenhouse gas process rates after land use change in Southern Amazonian Soils. *Front. Microbiol.* 6, 1057. doi: 10.3389/fmicb.2015.01057

Layeghifard, M., Hwang, D. M., and Guttman, D. S. (2017). Disentangling interactions in the microbiome: a network perspective. *Trends Microbiol.* 25, 217–228. doi: 10.1016/j.tim.2016.11.008

Li, J., Liu, H., Liu, Z., Zhang, X., Blake, R. E., Huang, Z., et al. (2023). Transformation mechanism of methylphosphonate to methane by *Burkholderia* sp: Insight from multi-labeled water isotope probing and transcriptomic. *Environ. Res.* 218, 114970. doi: 10.1016/j.envres.2022.114970

Li, Y., Dong, R., Guo, J., Wang, L., and Zhao, J. (2022). Effects of Mn^{2+} and humic acid on microbial community structures, functional genes for nitrogen and phosphorus removal, and heavy metal resistance genes in wastewater treatment. *J. Environ. Manage.* 313, 115028. doi: 10.1016/j.jenvman.2022.115028

Liang, J., Yi, Y., Li, X., Yuan, Y., Yang, S., Li, X., et al. (2021). Detecting changes in water level caused by climate, land cover and dam construction in interconnected river-lake systems. *Sci. Total Environ.* 788, 147692. doi: 10.1016/j.scitotenv.2021.147692

Liu, F., Wang, Z., Wu, B., Bjerg, J. T., Hu, W., Guo, X., et al. (2021). Cable bacteria extend the impacts of elevated dissolved oxygen into anoxic sediments. *ISME J.* 15, 1551–1563. doi: 10.1038/s41396-020-00869-8

Liu, J., Li, F. Y., Liu, J., Wang, S., Liu, H., Ding, Y., et al. (2023). Grazing promotes soil phosphorus cycling by enhancing soil microbial functional genes for phosphorus transformation in plant rhizosphere in a semi-arid natural grassland. *Geoderma.* 430, 116303. doi: 10.1016/j.geoderma.2022.116303

Liu, T., Cao, Q., Zhang, J., Yang, L., Zhang, Z., and Deng, H. (2022). Enzyme activity and greenhouse gas emission flux and its influencing factors in Dongping Lake (in Chinese). *Yellow River.* 44, 106–111. doi: 10.3969/i.issn.1000-1379.2022.02.021

Liu, X., Yao, X., Dong, J., Liu, Y., and Zhang, J. (2016). Fluorescence features of chromophoric dissolved organic matter in Dongping Lake and their environmental significance (in Chinese). *J. Ecol. Rural. Environ.* 32, 933–939. doi: 10.11934/j.issn.1673-4831.2016.06.010

Luo, W., Lu, J., Zhu, S., Yue, Y., and Xiao, L. (2022). Investigation of the impact of hydrodynamic conditions on sediment resuspension in shallow lakes. *Int. J. Digit Earth.* 15, 1676–1691. doi: 10.1080/17538947.2022.2131007

Lv, W., Yao, X., and Zhang, B. (2018). Correlations between fluorescence characteristics of chromophoric dissolved organic matter and nutrients in Dawen River and Dongping Lake (in Chinese). *Ecol. Environ.* 27, 565–572. doi: 10.16258/j.cnki.1674-5906.2018.03.022

McCluney, K. E., Poff, N. L., Palmer, M. A., Thorp, J. H., Poole, G. C., Williams, B. S., et al. (2014). Riverine macrosystems ecology: sensitivity, resistance, and resilience of whole river basins with human alterations. *Front. Ecol. Environ.* 12, 48–58. doi: 10.1890/120367

Pablo Nino-Garcia, J., Ruiz-Gonzalez, C., and del Giorgio, P. A. (2016). Interactions between hydrology and water chemistry shape bacterioplankton biogeography across boreal freshwater networks. *ISME J.* 10, 1755–1766. doi: 10.1038/ismej.2015.226

Peng, C., Huang, Y., Yan, X., Jiang, L., Wu, X., Zhang, W., et al. (2021). Effect of overlying water pH, temperature, and hydraulic disturbance on heavy metal and nutrient release from drinking water reservoir sediments. *Water Environ. Res.* 93, 2135–2148. doi: 10.1002/wer.1587

Piirsoo, K., Laas, A., Meinson, P., Noges, P., Pall, P., Viik, M., et al. (2018). Changes in particulate organic matter passing through a large shallow lowland lake. *Proc. Estonian Acad. Sci.* 67, 93–105. doi: 10.3176/proc.2018.1.05

Rashid, I., and Romshoo, S. A. (2013). Impact of anthropogenic activities on water quality of Lidder River in Kashmir Himalayas. *Environ. Monit. Assess.* 185, 4705–4719. doi: 10.1007/s10661-012-2898-0

Reid, A. J., Carlson, A. K., Creed, I. F., Eliason, E. J., Gell, P. A., Johnson, P. T. J., et al. (2019). Emerging threats and persistent conservation challenges for freshwater biodiversity. *Biol. Rev.* 94, 849–873. doi: 10.1111/brv.12480

Ren, Z., Wang, F., Qu, X., Elser, J. J., Liu, Y., and Chu, L. (2017). Taxonomic and functional differences between microbial communities in Qinghai Lake and its input streams. *Front. Microbiol.* 8, 2319. doi: 10.3389/fmicb.2017.02319

Sankar, M. S., Dash, P., Singh, S., Lu, Y., Mercer, A. E., and Chen, S. (2019). Effect of photo-biodegradation and biodegradation on the biogeochemical cycling of dissolved organic matter across diverse surface water bodies. *J. Environ. Sci.* 77, 130–147. doi: 10.1016/j.jes.2018.06.021

Shang, J., Zhang, W., Li, Y., Zheng, J., Ma, X., Wang, L., et al. (2023). How nutrient loading leads to alternative stable states in microbially mediated N-cycle pathways: A new insight into bioavailable nitrogen removal in urban rivers. *Water Res.* 236, 119938. doi: 10.1016/j.watres.2023.119938

Shen, T., Jiang, J., Li, N., and Luo, X. (2023). Aerobic denitrifiers and the application in remediation of micro-polluted water source (in Chinese). *Acta Microbiol. Sin.* 63, 465–482. doi: 10.13343/j.cnki.wsxb.20220410

Singleton, C. M., Petriglieri, F., Kristensen, J. M., Kirkegaard, R. H., Michaelsen, T. Y., Andersen, M. H., et al. (2021). Connecting structure to function with the recovery of over 1000 high-quality metagenome-assembled genomes from activated sludge using long-read sequencing. *Nat. Commun.* 12, 2009. doi: 10.1038/s41467-021-22203-2

Tang, C., Li, Y., He, C., and Acharya, K. (2020). Dynamic behavior of sediment resuspension and nutrients release in the shallow and wind-exposed Meiliang Bay of Lake Taihu. *Sci. Total Environ.* 708, 135131. doi: 10.1016/j.scitotenv.2019.135131

Tang, X., Xie, G., Shao, K., Hu, Y., Cai, J., Bai, C., et al. (2020). Contrast diversity patterns and processes of microbial community assembly in a river-lake continuum across a catchment scale in northwestern China. *Environ. Microbiol.* 15, 13. doi: 10.1186/s40793-020-00360-z

Tang, Y., Li, T., Xu, Y., Ren, H., and Huang, H. (2023). Effects of electrical stimulation on purification of secondary effluent containing chlorophenols by denitrification biofilter. *Environ. Res.* 216, 114535. doi: 10.1016/j.envres.2022.114535

Tian, Z., Qian, F., Yang, Y., Wen, Y., and Yaqing, S. (2017). Hydrodynamic effects on characteristics of biofilm formation and quorum sensing system. *Water Purif. Technol.* 36, 26–32. doi: 10.15890/j.cnki.jsjs.2017.11.005

Wan, L., Cao, L., Song, C., Cao, X., and Zhou, Y. (2023). Metagenomic insights into feasibility of agricultural wastes on optimizing water quality and natural bait by regulating microbial loop. *Environ. Res.* 217, 114941. doi: 10.1016/j.envres.2022.114941

Wang, L., Yin, Z., and Jing, C. (2020a). Metagenomic insights into microbial arsenic metabolism in shallow groundwater of Datong basin, China. *Chemosphere.* 245, 125603. doi: 10.1016/j.chemosphere.2019.125603

Wang, T., Pan, J., and Liu, X. (2016). Study on screening of phosphate-accumulating organisms and analysis of phosphorus removal characteristics. *Water Resour. Prot.* 32, 63–66. doi: 10.3880/j.issn.1004-6933.2016.05.013

Wang, Z., Lin, J., Zhang, Y., Wang, H., Qian, C., Chen, Y., et al. (2020b). Water quality limits of nitrogen and phosphorus in the inflow rivers of Poyang Lake. *Res. Environ. Sci.* 33, 1163–1169. doi: 10.13198j.issn.1001-6929.2020.03.45

Wang, Z., Wang, S., Liu, Y., Feng, K., and Deng, Y. (2018). The applications of metagenomics in the detection of environmental microbes involving in nitrogen cycle (in Chinese). *Biotechnol. Bull.* 34, 1–14. doi: 10.13560/j.cnki.biotech.bull.1985.2018-0024

Watkins, L., McGrattan, S., Sullivan, P. J., and Walter, M. T. (2019). The effect of dams on river transport of microplastic pollution. *Sci. Total Environ.* 664, 834–840. doi: 10.1016/j.scitotenv.2019.02.028

Wiens, J. A. (2002). Riverine landscapes: taking landscape ecology into the water. *Freshw. Biol.* 47, 501–515. doi: 10.1046/j.1365-2427.2002.00887.x

Wu, H., Hao, B., Cai, Y., Liu, G., and Xing, W. (2021). Effects of submerged vegetation on sediment nitrogen-cycling bacterial communities in Honghu Lake (China). *Sci. Total Environ.* 755, 142541. doi: 10.1016/j.scitotenv.2020.142541

Xiao, X., Guo, H., Ma, F., Zhang, J., Ma, X., and You, S. (2023). New insights into mycelial pellets for aerobic sludge granulation in membrane bioreactor: Bio-functional interactions among metazoans, microbial communities and protein expression. *Water Res.* 228, 119361. doi: 10.1016/j.watres.2022.119361

Xiong, W., Wang, S., Jin, Y., Wu, Z., Liu, D., and Su, H. (2023). Insights into nitrogen and phosphorus metabolic mechanisms of algal-bacterial aerobic granular sludge via metagenomics: Performance, microbial community and functional genes. *Bioresour. Technol.* 369, 128442. doi: 10.1016/j.biortech.2022.128442

Yang, Y., Gao, B., Hao, H., Zhou, H., and Lu, J. (2017). Nitrogen and phosphorus in sediments in China: A national-scale assessment and review. *Sci. Total Environ.* 576, 840–849. doi: 10.1016/j.scitotenv.2016.10.136

Yu, H., He, Z., Wang, A., Xie, J., Wu, L., Van Nostrand, J. D., et al. (2018). Divergent responses of forest soil microbial communities under elevated CO_2 in different depths of upper soil layers. *Appl. Environ. Microbiol.* 84, e01694–e01617. doi: 10.1128/AEM.01694-17

Yu, S., Du, X., Lei, Q., Wang, X., Wu, S., and Liu, H. (2023). Long-term variations of water quality and nutrient load inputs in a large shallow lake of Yellow River Basin: Implications for lake water quality improvements. *Sci. Total Environ.* 900, 165776. doi: 10.1016/j.scitotenv.2023.165776

Zhang, L., Yin, W., Wang, C., Zhang, A., Zhang, H., Zhang, T., et al. (2021). Untangling microbiota diversity and assembly patterns in the world's largest water diversion canal. *Water Res.* 204, 117617. doi: 10.1016/j.watres.2021.117617

Zhang, W. Q., Jin, X., Liu, D., Lang, C., and Shan, B. Q. (2017). Temporal and spatial variation of nitrogen and phosphorus and eutrophication assessment for a typical arid river-Fuyang River in northern China. *J. Environ. Sci.* 55, 41–48. doi: 10.1016/j.jes.2016.07.004

Zhang, Y., Naafs, B. D. A., Huang, X., Song, Q., Xue, J., Wang, R., et al. (2022). Variations in wetland hydrology drive rapid changes in the microbial community, carbon metabolic activity, and greenhouse gas fluxes. *Geochim. Cosmochim. Acta.* 317, 269–285. doi: 10.1016/j.gca.2021.11.014

Zhang, Y., Xia, J., Shao, Q., and Zhang, X. (2012). Experimental and simulation studies on the impact of sluice regulation on water quantity and quality processes. *J. Hydrol. Eng.* 17, 467–477. doi: 10.1061/(ASCE)HE.1943-5584.0000463

Zhao, W., Bi, X., Peng, Y., and Bai, M. (2022). Research advances of the phosphorus-accumulating organisms of *Candidatus* Accumulibacter, *Dechloromonas* and *Tetrasphaera*: Metabolic mechanisms, applications and influencing factors. *Chemosphere.* 307, 135675. doi: 10.1016/j.chemosphere.2022.135675

Zheng, B., Zhu, Y., Sardans, J., Penuelas, J., and Su, J. (2018). QMEC: a tool for high-throughput quantitative assessment of microbial functional potential in C, N, P, and S biogeochemical cycling. *Sci. China Life Sci.* 61, 1451–1462. doi: 10.1007/s11427-018-9364-7

Zhuo, T., Wan, Q., Chai, B., Lei, X., He, L., and Chen, B. (2023). Microbial pathways in the coupling of iron, sulfur, and phosphorus cycles at the sediment-water interface of a river system: An in situ study involving the DGT technique. *Sci. Total Environ.* 863, 160855. doi: 10.1016/j.scitotenv.2022.160855

frontiers | Frontiers in Microbiology

TYPE Original Research
PUBLISHED 20 October 2023
DOI 10.3389/fmicb.2023.1291599

OPEN ACCESS

EDITED BY
Huai Li,
Chinese Academy of Sciences (CAS), China

REVIEWED BY
Chenwei Zheng,
Arizona State University, United States
Ke Zhao,
Jilin Jianzhu University, China
Gefu Zhu,
Renmin University of China, China

*CORRESPONDENCE
Zhuoran Wang
✉ zrwang20@mails.jlu.edu.cn

RECEIVED 09 September 2023
ACCEPTED 09 October 2023
PUBLISHED 20 October 2023

CITATION
Wang Z, Zhang N, Li C and Shao L (2023) Diversity of antibiotic resistance genes in soils with four different fertilization treatments. *Front. Microbiol.* 14:1291599. doi: 10.3389/fmicb.2023.1291599

Diversity of antibiotic resistance genes in soils with four different fertilization treatments

Zhuoran Wang[1,2,3]*, Na Zhang[4], Chunming Li[4] and Liang Shao[4]

[1]Key Laboratory of Groundwater Resources and Environment of Ministry of Education, College of New Energy and Environment, Jilin University, Changchun, China, [2]Jilin Provincial Key Laboratory of Water Resources and Environment, College of New Energy and Environment, Jilin University, Changchun, China, [3]National and Local Joint Engineering Laboratory for Petrochemical Contaminated Site Control and Remediation Technology, Jilin University, Changchun, China, [4]Jilin Bishuiyuan Water Science and Technology Ltd., Co., Changchun, Jilin, China

Although the enrichment of resistance genes in soil has been explored in recent years, there are still some key questions to be addressed regarding the variation of ARG composition in soil with different fertilization treatments, such as the core ARGs in soil after different fertilization treatments, the correlation between ARGs and bacterial taxa, etc. For soils after different fertilization treatments, the distribution and combination of ARG in three typical fertilization methods (organic fertilizer alone, chemical fertilizer alone, and conventional fertilizer) and non-fertilized soils were investigated in this study using high-throughput fluorescence quantitative PCR (HT-qPCR) technique. The application of organic fertilizers significantly increased the abundance and quantity of ARGs and their subtypes in the soil compared to the non-fertilized soil, where sul1 was the ARGs specific to organic fertilizers alone and in higher abundance. The conventional fertilizer application also showed significant enrichment of ARGs, which indicated that manure addition often had a more decisive effect on ARGs in soil than chemical fertilizers, and three bacteria, *Pseudonocardia*, *Irregularibacter*, and *Castllaniella*, were the key bacteria affecting ARG changes in soil after fertilization. In addition, nutrient factors and heavy metals also affect the distribution of ARGs in soil and are positively correlated. This paper reveals the possible reasons for the increase in the number of total soil ARGs and their relative abundance under different fertilization treatments, which has positive implications for controlling the transmission of ARGs through the soil-human pathway.

KEYWORDS

soil properties, antibiotic resistance genes, bacterial community, fertilization, horizontal gene transfer

1. Introduction

Antibiotics were first discovered in the 1920s and are widely used to fight bacterial diseases because of their killing or immunosuppressive effects on pathogens (Sarmah et al., 2006; Olesen et al., 2018). Antibiotics are used not only to treat various infectious diseases, but also to ensure medical safety. However, the long-term use of antibiotics can make a large number of disease-causing bacteria resistant to antibiotics, which poses a serious threat to human public health safety, and because the large-scale unregulated use of antibiotics generates important selection pressure for drug-resistant bacteria, making the bacteria in the environment resistant or even multi-drug resistant, causing a series of environmental problems (Zhou et al., 2013; Zhi et al., 2019). It was reported that livestock accounted for 52% of the 196,000 tons of antibiotics used in China, with non-medical use accounting for 70% of all veterinary use (Liu et al., 2022). Due

to the slow absorption and low degradation rate of antibiotics in animals, only 10% can be absorbed and utilized, and most of the antibiotics used in excess will be excreted in their original form or metabolites through urine or feces, and then enter the water, soil and air, causing environmental pollution (Karci and Balcioglu, 2009; Zhang et al., 2015). The sources of ARGs include both intrinsic resistance and exogenous inputs (Boxall et al., 2006). Among them, an important source of ARGs production in soil is exogenous input. The main use of antibiotics as drugs to treat infections caused by pathogens is to protect human health and promote the healthy development of animal husbandry (Lillenberg et al., 2010), but excessive use is not only not absorbed and utilized by humans and farm animals, but also excreted out of the body with manure and eventually into the environment. Antibiotics in the environment can put stronger selection pressure on indigenous microorganisms, leading to the development of antibiotic resistance (Karkman et al., 2019; Xu et al., 2022).

Antibiotic resistance genes (ARGs) are genetic elements carried by microorganisms that cause them to develop resistance to target antibiotics (Fu et al., 2022). They are persistent and are the source of bacterial drug resistance. After the death of microbial strains carrying ARGs, the DNA carrying ARGs is released into the environment and persists for a long time under the protection of deoxyribonuclease (DNAse). Eventually, this exposed DNA in the environment can be transferred into other microbial strains at the genetic level (Hill and Top, 1998). ARGs are difficult to disappear once they are produced, and even if antibiotic selective pressure disappears, ARGs will still persist in microbial populations (Crecchio et al., 2005). While soil is considered as a huge reservoir of ARGs in the natural environment, human activities such as irrigation with reclaimed water and manure application have greatly increased the antibiotic resistance of soil (Salyers and Amábile-Cuevas, 1997; Mustafa and Scholz, 2011), but soil antibiotic residues accumulate day by day due to irrigation with antibiotic-containing wastewater and continuous input of livestock manure as organic fertilizer to farmland (Yang et al., 2017). During vegetable cultivation, large amounts of animal manure are also applied to improve soil fertility and yield. Numerous studies have shown that manure application not only inputs exogenous ARGs to the soil, but also promotes the proliferation of indigenous drug-resistant bacteria, thus causing enrichment of ARGs in the soil (Pruden et al., 2006; Gao et al., 2018; Apreja et al., 2022). The application of livestock manure and organic fertilizers is not only the most important way for antibiotics to enter the soil, but also an important source of ARGs contamination in the soil environment (Xiong et al., 2018). Application of organic manure to agricultural soils did lead to a significant increase in the level of microbial antibiotic resistance in the soil (Heuer et al., 2011a). Marti conducted various microscopic and field experiments on agricultural soils to which pig manure, chicken manure, and cow manure were applied and found that the application of all three manures resulted in a significant increase in the abundance of ARGs in the soil (Marti et al., 2013). Schmitt found that tetracycline ARGs (*tetT*, *tetW*, *tetZ*) were commonly present in swine manure and soil, while *tetY*, *tetS*, *tetC*, *tetQ*, *tetH* were also introduced into the soil by manure application (Schmitt et al., 2006). Tang studied rice fields with long-term application of organic fertilizers in the past decades and found that long-term application of organic fertilizers significantly increased the abundance of ARGs in farm soils (Tang et al., 2015). Heuer found that application of manure containing sulfa drugs significantly increased the abundance of sul2 (Heuer et al., 2011b). Ross and Topp's study also showed that application of cow manure increased the resistance of ARGs in bacteria (Ross and Topp, 2015). Wu detected high levels of tetracycline-based ARGs in soil near pig farms (Wu et al., 2010). All of the above findings suggest that the application of livestock manure and organic fertilizers is not only the most important way for antibiotics to enter the soil, but also an important source of ARGs contamination in the soil environment.

In this study, we set up an inorganic fertilizer group, an organic fertilizer group and an additional conventional fertilizer group (organic fertilizer mixed with inorganic fertilizer) to compare with the control group. High-throughput fluorescence quantitative PCR (HT-qPCR) was used to analyze ARGs in different treatment groups to assess the similarities and differences of total and core ARGs in different treatment groups, and also to determine the bacterial communities and physicochemical properties affecting the composition of ARGs in soil. This result will help to reduce the enrichment of ARGs during fertilization and has positive implications for explaining the mechanism.

2. Materials and methods

2.1. Experimental design

In this study, samples were collected from a vegetable base in Daxing District, Beijing (N39。66′, E116。57′), and a greenhouse with an area of 488 m^2 (61 m × 8 m) was selected for a long-term locational trial of eggplant-sweet pepper rotation. The greenhouse was started in spring 2009 with four different fertilizer treatments as: no fertilizer (CK), chemical fertilizer alone (IF), organic fertilizer alone (OF), and conventional fertilizer (MF) (organic fertilizer mixed with chemical fertilizer).

Organic fertilizer is produced by a large commercial organic fertilizer factory in Beijing, the main raw materials are chicken manure and edible bacteria bran, which are powdered substances made by high temperature aerobic fermentation. Three plots were set up for each treatment, for a total of 12 plots. A 50 cm deep partition was set up between each treatment, separated by plastic film to avoid interference between different treatments (Rambaut et al., 2022). The greenhouse grows two crops of vegetables per year, with the eggplant season running from February to July and the bell pepper season running from August to January. One fertilization treatment was applied before each vegetable crop, setting the control group as no fertilizer (CK), the fertilizer alone group (IF) with 0.04 kg/m^2 of urea, 0.05 kg/m^2 of diammonium phosphate and 0.03 kg/m^2 of potassium sulfate, the organic fertilizer alone group (OF) with 2.38 kg/m^2 (commercial organic fertilizer), and the conventional fertilizer group (MF) with a compound fertilizer (N, P and K content of 20, 10 and 15%, respectively) 0.06 kg/m^2 and commercial organic fertilizer 1.20 kg/m^2 in the conventional fertilizer group (MF). The application rates of N, P, K fertilizer were converted from plant uptake amount considering the fertilizer utilization ratio (Cui et al., 2022; Edouard et al., 2022; Li et al., 2022).

2.2. Sample collection

The collection of soil samples for this experiment was conducted in October 2019. A 5-point mixed sampling method was used to take the top soil (0–20 cm) of each plot, four different treatments, and three

samples were collected from each treatment, for a total of 12 soil samples.

2.3. DNA extraction and high-throughput sequencing of bacterial 16S rRNA genes

2.3.1. Soil sample DNA extraction

DNA extraction of soil samples was performed using the kit Fast DNA SPIN Kit for Soil (USA). The instructions were followed. After DNA extraction, the concentration of DNA extracted is measured and a portion of it is used for 16SrRNA sequencing and the rest for PCR quantification and other applications, and stored at −20°C for a long time until use.

2.3.2. High-throughput fluorescent quantitative PCR technology (HT-qPCR)

ARGs were quantified using the Wafergen Smart Chip Real-Time Quantitative PCR System (Wafergen Inc. USA). 384 primer pairs were set (Looft et al., 2012; Chen et al., 2015; Gou et al., 2018), including 348 ARGs, 32 transposase genes, one 16S rRNA gene, and three integrase genes (int1, intl2, and intl3). These 348 primers for ARGs cover almost all known subtypes of ARGs. The primer premix is sprayed on the same chip as the sample premix for subsequent amplification analysis. The thermal cycling process is: 10 min at 95°C, followed by 40 cycles at 95°C for 30 s and 60°C for 30 s. The relative copy number of ARGs can be calculated by the formula (Su et al., 2015) (1).

$$\text{Relative copy number of genes} = 10^{\left[(26 - \text{Ct}) / (10/3)\right]} \quad (1)$$

(Note: Ct value is the number of cycles required for the fluorescence signal of the test gene to reach a set threshold).

2.4. Statistical analysis

EXCEL 2013 was used to organize the data, Origin Pro 8.5 was used to draw bar graphs, the pheatmap package in R language was used to draw heat maps, the vegan package was used for redundancy analysis (RDA), and the TukeyHSD method was used for statistical analysis and PcoA principal coordinate analysis. Mantel test and typical correlation analysis (RDA) were used to explain the relationships between heavy metals (As, Hg, Cu, Cr, Pb, Cd, Zn), nutrient factors (organic matter, effective phosphorus, fast-acting potassium, total nitrogen), pH and ARGs. $p < 0.05$ indicates significant differences at 95% confidence interval. Network plots were drawn using Gephi software.

3. Results and discussion

3.1. Diversity of ARGs in soils

3.1.1. Component analysis of ARGs in soils

The number of ARGs subtypes in soils applied with different types of fertilizers was examined, and a total of 37–76 ARGs subtypes were detected in the soils of four different fertilization treatments (Figure 1). They belong to Aminoglycoside, *β*-Lactamase, Chloramphenicol, MLSB, Multidrug, Clycopeptide, Sulfonamide, Tetracycline, Fluoroquinolone, and Others. The highest number of ARGs was 76 in organic fertilized soils, followed by 52 in conventionally fertilized soils, 37 in chemical fertilized soils alone, and the lowest number of ARGs was 36 in non-fertilized soils (Figure 2). There were 16 core ARGs (ARGs common to soils with different fertilization treatments) for no fertilizer, chemical fertilizer alone, organic fertilizer alone and conventionally fertilized soils, with β-lactams accounting for the largest number, 37.5% of the total purpose, and multiresistant and sulfonamides the least, both at 6.25%. There were 9 subtypes of ARGs specific to the no-fertilizer treatment, the largest number being aminoglycosides (*aac*, *aac(6′)-Ib(aacA4)-01*, *aadA5-01*, *aph*), 5 fertilizers alone, with the same number accounted for by different types, and 24 organic fertilizers alone, with the largest number being macrolides (*erm(36)*, *ermB*, *ermF lnuA-01*, *lnuB-01*, *lnuB-02*), followed by tetracyclines (*tet(32)*, *tetM-01*, *tetM-02*, *tetPB-03*, *tetX*) with aminoglycosides (aminoglycosides *aacA*, *aadA-1-01*, *aadD*, *aph(2′)-Id-02*, *str*), and 7 conventional fertilizers. The most multidrug-resistant classes (*ceoA*, *marR-01*, *mexE*). The total number of ARGs in the soil with organic fertilizer alone was approximately twice as high as that in the soil without fertilizer and the specific ARGs subtypes were much higher than those in the other three treatment groups, indicating that organic fertilizer alone increased the diversity of soil ARGs. In addition, for soils with mono-applied organic fertilizers, Aminoglycoside and MLSB ARGs were the most abundant, followed by Multidrug, which were largely consistent with the most numerous subtypes of endemic ARGs in mono-applied organic fertilizers. And it has been reported in the literature that long-term application of chicken manure significantly enriched the ARG associated with *β*-lactams and tetracyclines in the soil, which is consistent with the results obtained from the application of organic fertilizer alone in this study, where there was a significant increase in the number of *β*-lactam and tetracycline-based resistance genes in the OF group (Chen et al., 2016). Interestingly, the total count of ARGs in non-fertilized soil

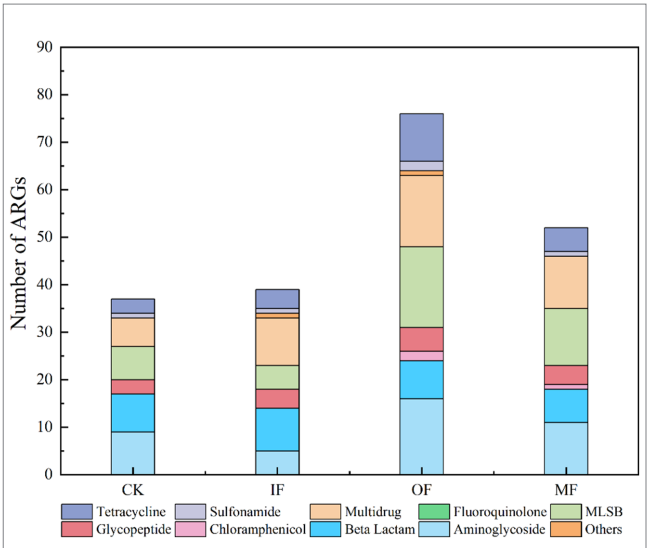

FIGURE 1
The number of ARGs in the soil amended with different fertilizers.

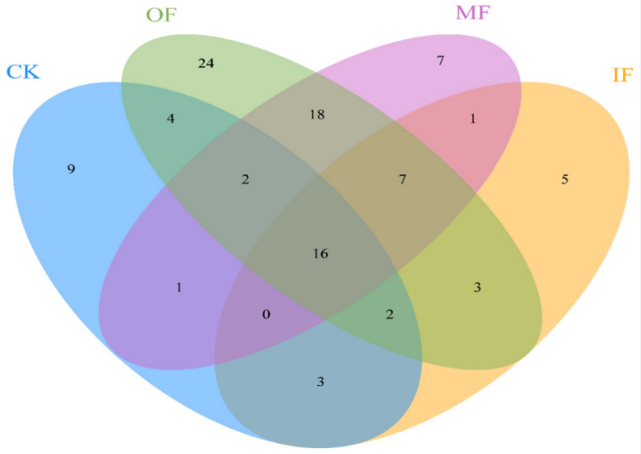

FIGURE 2
Venn plots of soils treated with different fertilizers.

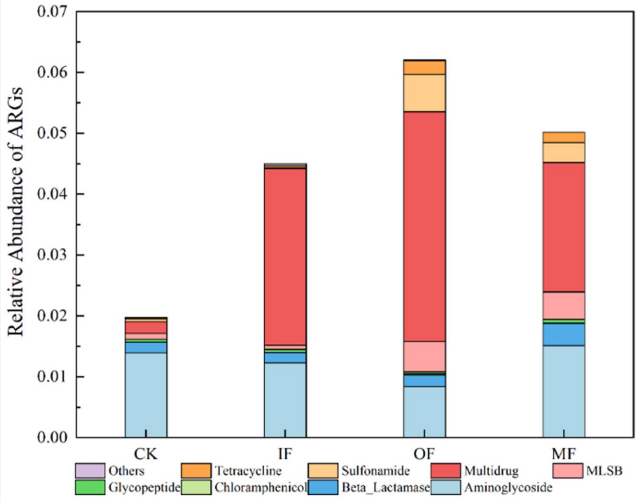

FIGURE 3
Relative abundance of ARGs in the soil amended with different fertilizers.

varied by merely one ARG subtype in comparison to that of the fertilized soil alone, which also augmented the diversity of ARGs, albeit to a vastly lesser extent compared to the soil treated with organic fertilizer alone. This minimal increase could be ascribed to the alterations in the population of natural antibiotic-resistant bacteria in the soil post fertilizer application. There was a significant increase in the variety of ARGs in the conventional fertilizer application compared to the no fertilizer and single fertilizer application groups, although organic fertilizers were also added but still compared to single fertilizer application.

3.1.2. Abundance analysis of ARGs in soils

Figure 3 represents the relative abundance of ARGs in soils with different fertilization treatments. The results from the figure show that the relative abundance of total ARGs in soils with no fertilizer, chemical fertilizer alone, organic fertilizer alone, and conventional fertilizer were 0.01978, 0.04498, 0.06203, and 0.05016, respectively, with OF > MF > IF> CK. This finding is similar to the previously reported values of ARGs abundance in soils applied with chemical and organic fertilizers. The total relative abundance of ARGs was significantly higher in the organic fertilized soil than in the non-fertilized, chemical fertilized alone and conventional fertilized soils. The relative abundance of ARGs of multiple resistance classes was significantly higher than that of other resistance genotypes in soils without fertilizer, with chemical fertilizer alone and with organic fertilizer alone. It has been reported that microorganisms carrying multi-drug resistant genes may be resistant to a variety of antibiotics and have the potential to develop into "superbugs" which, if not controlled, can increase the lethality of human infections. In addition to multidrug-resistant classes, aminoglycosides, sulfonamides and macrolide ARGs also had high abundance in soils with single organic fertilizer application, and the relative abundance of multidrug-resistant classes accounted for 60% of the total relative abundance, and the highest relative abundance of aminoglycosides ARGs was found in soils without fertilizer application. It was also observed that fertilizer application alone had little effect on the total abundance of soil ARGs and the abundance of different types of ARGs, but the application of organic fertilizer significantly increased the abundance of macrolide and sulfonamide ARGs. Wang also found that the application of organic fertilizers significantly increased the relative abundance and the number of ARGs detected (Wang et al., 2020), and the application of chemical fertilizers had less effect on the relative abundance of ARGs than that of organic fertilizers due to the fact that when ARBs in manure were introduced into the soil, the ARGs they carried could also be transferred horizontally to the soil, whereas when inorganic fertilizers were applied only the native ARG-carrying microorganisms in the soil were proliferated. The utilization of animal feces as organic fertilizer through composting is a common practice. Following the composting process, a notable augmentation in the abundance of *Bacillus* spp. is often observed in the soil. It has been established that *Bacillus* spp. serve as host bacteria for resistance genes associated with tetracyclines, sulfonamides, and β-lactams, among others. In synthesis, the remarkable increase in the abundance of ARGs post organic fertilizer application can be ascribed to the substantial influx of *Bacillus* spp. into the soil via composting. The ARGs have the potential to be transferred horizontally to other media, thereby leading to a significant augmentation in both the abundance and diversity of ARGs within the soil. As a host for a myriad of ARGs, *Bacillus* spp. consequently lead to a significant rise in ARG abundance in the groups treated with organic fertilizer (Qi et al., 2023). The abundance of multi-drug resistant ARGs in soils with organic fertilizer application increased one-fold compared with that in conventionally fertilized soils and 12-fold compared with that in non-fertilized soils, indicating that the application of organic fertilizer seriously affected the abundance of ARGs. In view of the resistance of multi-drug resistant ARGs and their potential hazards, we need to treat them in some way before organic fertilizer application to mitigate their effects on the abundance of ARGs. For example, He added biochar to the

application of manure to make the antibiotic resistance genes in agricultural soils gradually dissipate (He et al., 2021).

3.1.3. Distribution characteristics of ARGs in soils

To investigate the differences in the characteristics of ARGs in vegetable soils under different fertilization practices, PCoA was performed on the abundance data of ARGs (Figure 4). PCoA1 and PCoA2 explained 77.16 and 16.24% of the variation in the composition of ARGs, respectively. The results of the principal coordinate analysis showed that three fertilization methods, chemical fertilizer alone, organic fertilizer alone and conventional fertilizer, significantly changed the distribution characteristics of soil ARGs (PERMANOVA for treatments: $R^2 = 0.9735$, $p = 0.001$, Adonis analysis), IF, OF, MF all significantly changed the composition of ARGs in the soil compared to the control. This result further supports the difference in the composition of ARGs in soils with different fertilization treatments.

Figure 5 show heat maps of the relative abundance of ARGs subtypes in soils with different fertilization treatments. The results show that the application of organic fertilizer caused a significant increase in the abundance of most ARGs subtypes in the soil compared to the control soil without fertilizer application. And the application of organic fertilizer significantly increased the abundance of ARGs isoforms such as *mepA*, *qacEdeltal-01*, *acrA-04*, etc. in the soil for multiple resistance classes of resistance genes. There were 24 ARGs specific to the soil with organic fertilizer alone, indicating that the application of organic fertilizer could increase the variety of ARGs in the soil; sul1 (sulfonamides) was the ARGs specific to the soil with organic fertilizer alone, and the relative abundance was high.

The abundance of *vanRA-01* (glycopeptides) was significantly increased in the soil with single fertilizer treatment compared to the soil without fertilizer, and the difference between the shared ARGs in the soil without fertilizer and the soil with single fertilizer was not significant. *oprJ* (multiresistant) was detected only in the soil with single fertilizer and the soil with single organic fertilizer, and its relative abundance was high. *mexF* (multiresistant) subtype had higher abundance in the soil with three different fertilizer applications except for the soil without fertilizer. The high abundance of *mexF* (multidrug-resistant) subtypes in all three fertilized soils, except the non-fertilized soils, indicated that fertilizer application increased the variety of ARGs in the soil. Conventional fertilization had higher relative abundance of *fox5* (β-lactams) and *sul2* (sulfonamides) compared to the other three fertilization treatment conditions. The figure also shows that *aac(6)-Ib(aka aacA4)-03* (an aminoglycoside resistance gene) had higher abundance in all treatments, indicating that they have some stability in the soil and should be a key concern.

In addition, *sul2*, a sulfonamide resistance gene, was detected in soils treated with either chemical fertilizer alone, organic fertilizer alone, conventional fertilizer application, and no fertilizer application, and the gene copy number was as high as about 1.44×10^{-3} per gram of soil, while sul1 (sulfonamide), a specific ARGs, was detected in soils treated with organic fertilizer alone, and the gene copy number per gram of soil up to 4.72×10^{-3}, indicating that the application of organic fertilizer changed the type of ARGs in the soil. One study found that *sul2*, a sulfonamide resistance gene, was also detected in 100% of black soil farm soils with organic fertilizer application, which is consistent with the findings of this paper (Yang et al., 2016). Related studies showed that the abundance of sulfonamide ARGs in soil increased significantly after fertilizer application. β-lactams, multi-drug resistant, macrolides, and tetracyclines ARGs were detected to varying degrees, and the detection rates were all different, indicating that the application of organic and chemical fertilizers in vegetable soils had a significant effect on these types of ARGs, increasing the subtypes and abundance of ARGs (Schmitt et al., 2006). This result is consistent with the findings of Zhang in vegetable field soils (Zhang et al., 2022). Wu Nan detected the presence of five dominant tetracycline resistance genes *tetB/P*, *tetM*, *tetO*, *tetT*, and *tetW* in soil near a pig farm in Beijing, with the highest level of *tet(W)* 2.16×108 copies·g^{-1} (dry soil), which was $2.89 \pm 0.54 \times 106$ copies·g^{-1} (dry soil) was about two orders of magnitude higher (Wu et al., 2009). It indicates that either organic fertilizers, chemical fertilizers or mixed application treatments will increase the level of ARGs in the soil. Once the horizontal shift of ARGs in soil occurs, it will definitely have serious impact on the safety of agricultural products and human safety (Riahi et al., 2022).

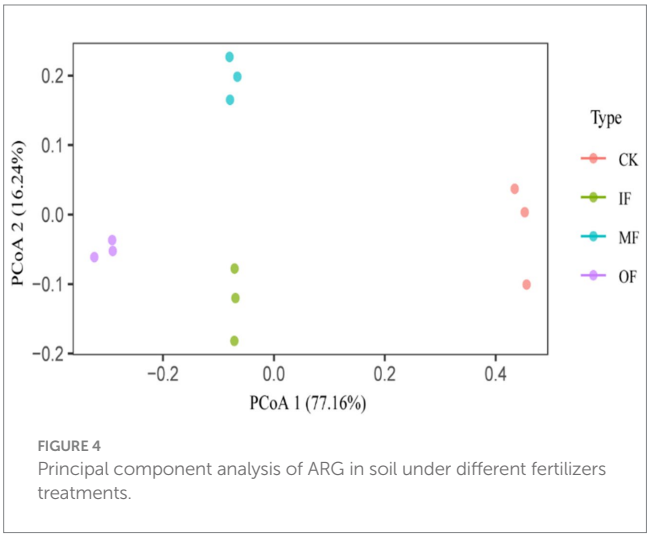

FIGURE 4
Principal component analysis of ARG in soil under different fertilizers treatments.

3.1.4. Correlation analysis of ARGs and physicochemical properties in soils

To assess the correlation between soil ARGs and physicochemical factors, Mantel tests were conducted to determine the abundance of ARGs in vegetable soils with heavy metals, organic matter (OM), total nitrogen (TN), effective phosphorus (AP), and fast-acting potassium (AK) contents as well as pH in four different fertilization treatments. The results showed (Table 1) that heavy metals Cu, Zn, Cd, and As were significantly and positively correlated with ARGs ($p < 0.01$); organic matter, total nitrogen, effective phosphorus, and fast-acting potassium were also significantly and positively correlated with ARGs ($p < 0.01$).

RDA was used to further assess the contribution of individual variables to the changes in ARGs, and the results are shown in Figure 6. The results in the figure show that there are 11 environmental factors scattered in four quadrants and mostly clustered in the first and fourth quadrants. The eigenvalues of the 1st and 2nd sorting axes were

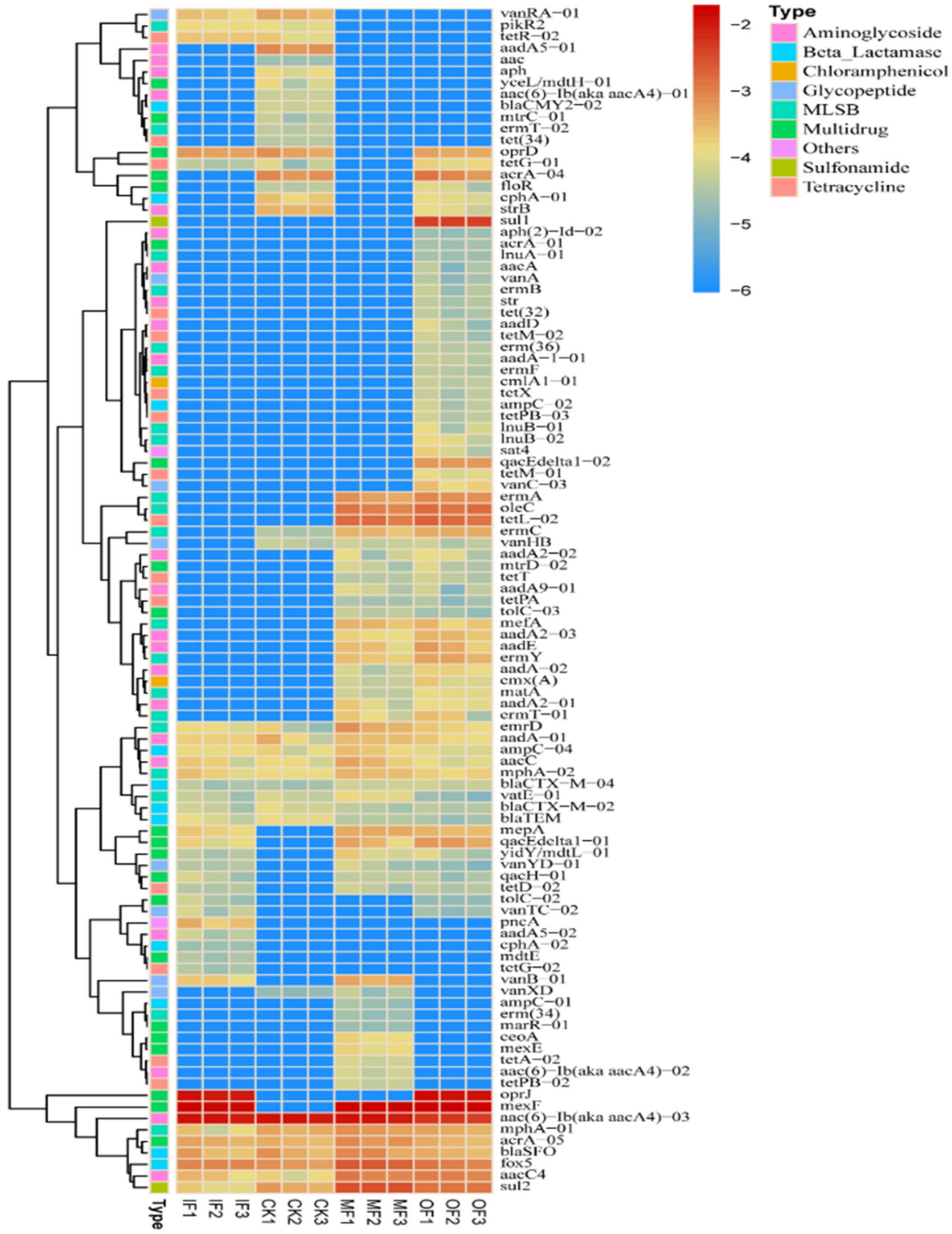

FIGURE 5
Heat map of ARGs subtypes in soils under different fertilizers treatments.

62.25 and 22.68%, respectively, which could explain 84.93% of the total variance value of the ARGs variance. Redundancy analysis showed that ARGs in organic fertilized soils were significantly and positively correlated with Pb, Cu, Zn, Cd, total N, organic matter, and effective phosphorus; while pH was significantly and positively correlated with ARGs in control soils, and As, Hg, and Cr were significantly and positively correlated with ARGs in chemical fertilizer alone and conventionally fertilized soils. The utilization of Cu and Zn in soil leads to a rise in the abundance of ARGs, due to the co-selection effect of heavy metals, where the host bacteria of ARGs proliferate alongside heavy metals in the soil, thereby intensifying the horizontal gene transfer of ARGs. Soil physicochemical properties such as pH also play a pivotal role; under alkaline soil conditions, the abundance of ARGs exhibits a positive correlation with pH as it can enhance the activity of other organic matter. Total nitrogen and organic matter, serving as organic substances, supply nutrients to the soil, promoting the proliferation of relevant microbial communities, and thus exacerbating the dissemination of ARGs (Shi et al., 2023).

It can also be seen from the figure that the distribution of ARGs of fertilizer-applied soils clustered with conventionally fertilized soils

TABLE 1 Mantel test reveals the relationship between ARGs and physicochemical properties.

Factors	Statistic (r)	Sig. (P)
Cu	0.644	0.0037*
Zn	0.867	0.0007*
Pb	−0.044	0.5696
Cd	0.763	0.0011*
Cr	0.084	0.2421
As	−0.146	0.0048*
Hg	0.065	0.2777
pH	0.281	0.0565
TN	0.653	0.0013*
OM	0.770	0.0002*
AP	0.926	0.0002*
AK	0.926	0.0004*

TN, total nitrogen; OM, organic matter; AP, active phosphorus; AK, fast-acting potassium; *significant correlation ($p < 0.01$).

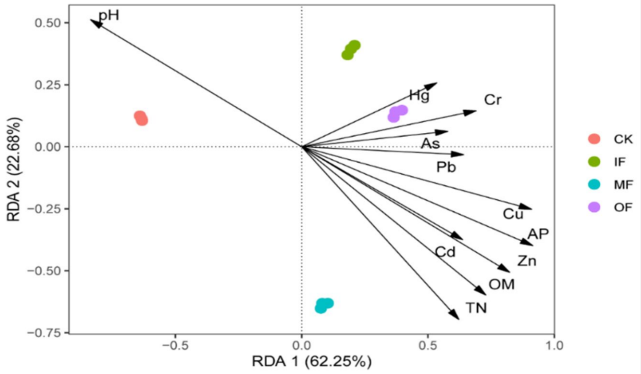

FIGURE 6
Redundancy analysis of soil ARGs and physical and chemical properties.

in the first quadrant, while the ARGs of no fertilizer and organic fertilizer alone were scattered in the second and fourth quadrants, indicating that the application of organic fertilizer significantly changed the distribution characteristics of soil ARGs. In Dong's study total and effective amounts of Cu and Zn were significantly correlated with *qepA* and *qnrS*. Heavy metals can persist in the environment for a long period of time and increase the abundance of ARGs under sustained selective pressure, and previous studies have also demonstrated that replacing chemical fertilizers with organic fertilizers induces the accumulation of Cd, Pb, Cu, and Zn in the soil, suggesting that fertilizer treatments can influence the abundance of resistance genes associated with them by affecting the accumulation of heavy metals in the soil (Dong et al., 2022; Liu et al., 2023). He studied paddy soils from seven different areas in Sichuan Province and also found a significant positive correlation between total nitrogen and ARGs (He et al., 2020). Other studies have shown that heavy metals and organic matter can promote the persistence and diffusion ability of ARGs in the environment. Therefore, heavy metals and nutrient factors are closely related to ARGs in vegetable soils.

3.2. Co-occurrence analysis of ARGs and bacterial communities in soils

The symbiotic relationship between ARGs and bacterial families was investigated using Pearson's based network analysis and the results are shown in Figure 7 and Qi et al. (2022). Two nodes are connected to indicate the co-occurrence of bacteria and ARGs, and the graph consists of 43 nodes and 40 edges. These nodes contain three bacterial and 40 ARGs subtypes, and the ARGs cover eight classes of resistance gene types. *Pseudonocardia* has 9 lines of association with ARGs ($p < 0.001$), including multiresistant classes, macrolides, β-lactams, aminoglycosamides, tetracyclines, and the most subtypes of aminoglycoside ARGs, with 4. *Irregularibacter* has seven linkages with ARGs ($p < 0.001$), including tetracyclines, macrolides, multiresistant classes, aminoglycosides and β-lactams, the most numerous of which are the multiresistant classes with three subtypes of ARGs and the other classes with one subtype of ARGs each. *Castllaniella* has 24 linkages to ARGs ($p < 0.001$), which include sulfonamides, chloramphenicol, glycopeptides, and others in addition to macrolides, aminoglycosides, tetracyclines, β-lactams, multiresistance, and tetracyclines, and have 1, 1, 2, and 1 subtype of ARGs, respectively. The above results indicate that all three bacteria (*Pseudonocardia*, *Irregularibacter*, and *Castllaniella*) were significantly correlated with ARGs, which is consistent with the previously reported findings that some ARGs were significantly correlated with multiple bacterial taxa (Looft et al., 2012; Su et al., 2015). Correlation analysis revealed that the bacterial genera *Pseudonocardia*, *Irregularibacter*, and *Castellaniella* could potentially serve as host bacteria facilitating the transfer of ARGs. *Pseudonocardia*, commonly found in soil, plants, and various environmental settings, may promote the horizontal gene transfer of a multitude of ARGs (Ejtahed et al., 2020). *Castellaniella*, known to prevail under antibiotic stress, could be a potential reservoir of antibiotic-resistant bacteria, thereby facilitating the horizontal transfer of ARGs within the environment.

4. Conclusion

In summary, changes in fertilization practices affect the composition of ARGs in soil, increasing their subtypes as well as abundance. According to our results, although organic fertilizers were also added to the conventional fertilizer application, the increase in the number of ARGs and their abundance was much less than that of the organic fertilizer application alone, while compared to the chemical fertilizer application alone, there was a significant increase in ARGs in the conventionally fertilized soil due to the addition of organic fertilizers. We suggest that the application of organic fertilizers leads to higher number and abundance of ARGs in the soil, and the main reason may be that the ARGs carried in organic fertilizers spread to the soil, while the alteration of ARGs from chemical fertilizer application comes only from the colonization of native microorganisms, and conventional fertilizers are in between. Soil factors TN, OM, AP, AK and heavy metals Cu, Zn, Cd and As contributed more to the variation of ARGs in soil than other factors. These findings provide a more comprehensive insight into the changes of ARGs in soil ecology under long-term application of different types of fertilizers.

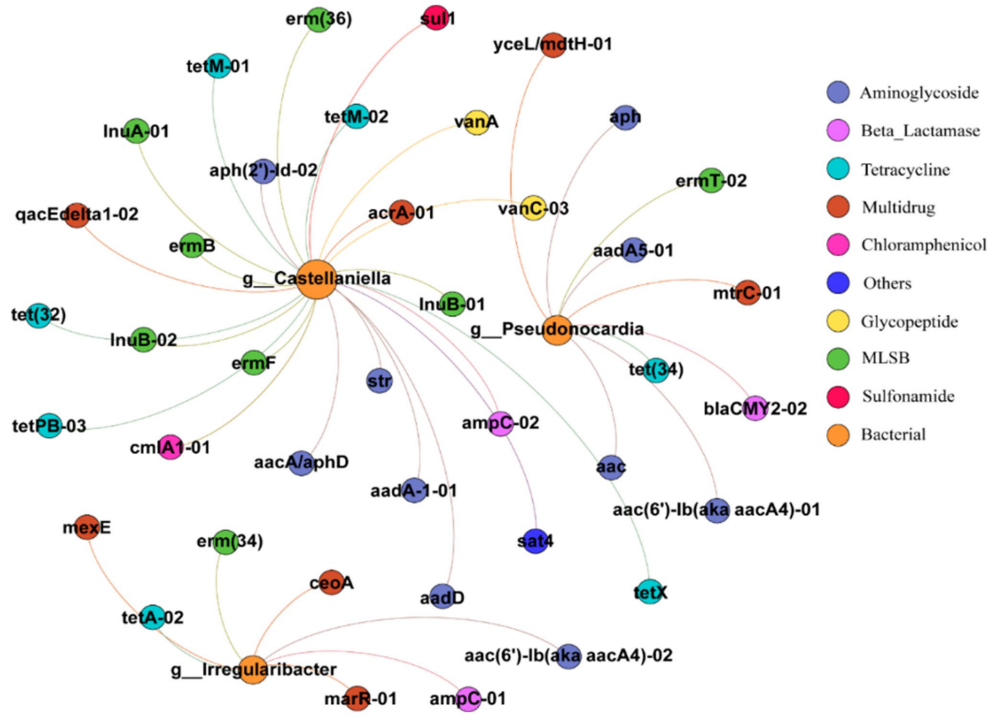

FIGURE 7
Network diagram of ARGs and bacterial community in soil (circle size represents the total abundance of ARGs and bacteria, node size is weighted according to the number of connections, and one node represents one ARG and bacteria).

Data availability statement

The original contributions presented in the study are included in the article/supplementary material, further inquiries can be directed to the corresponding author.

Author contributions

ZW: Conceptualization, Formal analysis, Investigation, Visualization, Writing – review & editing, Writing – original draft. NZ: Resources, Validation, Writing – review & editing. CL: Formal analysis, Writing – review & editing. LS: Investigation, Writing – review & editing.

Funding

The author(s) declare that no financial support was received for the research, authorship, and/or publication of this article.

Conflict of interest

NZ, CL, and LS were employed by Jilin Bishuiyuan Water Science and Technology Ltd., Co.

The remaining author declares that the research was conducted in the absence of any commercial or financial relationships that could be construed as a potential conflict of interest.

Publisher's note

All claims expressed in this article are solely those of the authors and do not necessarily represent those of their affiliated organizations, or those of the publisher, the editors and the reviewers. Any product that may be evaluated in this article, or claim that may be made by its manufacturer, is not guaranteed or endorsed by the publisher.

References

Apreja, M., Sharma, A., Balda, S., Kataria, K., Capalash, N., and Sharma, P. (2022). Antibiotic residues in environment: antimicrobial resistance development, ecological risks, and bioremediation. *Environ. Sci. Pollut. Res.* 29, 3355–3371. doi: 10.1007/s11356-021-17374-w

Boxall, A. B. A., Johnson, P., Smith, E. J., Sinclair, C. J., Stutt, E., and Levy, L. S. (2006). Uptake of veterinary medicines from soils into plants. *J. Agric. Food Chem.* 54, 2288–2297. doi: 10.1021/jf053041t

Chen, Q. L., An, X. L., Li, H., Su, J. Q., Ma, Y. B., and Zhu, Y. G. (2016). Long-term field application of sewage sludge increases the abundance of antibiotic resistance genes in soil. *Environ. Int.* 92-93, 1–10. doi: 10.1016/j.envint.2016.03.026

Chen, Z. Y., Zhang, Y. J., Gao, Y. Z., Boyd, S. A., Zhu, D. Q., and Li, H. (2015). Influence of dissolved organic matter on tetracycline bioavailability to an antibiotic-resistant bacterium. *Environ. Sci. Technol.* 49, 10903–10910. doi: 10.1021/acs.est.5b02158

Crecchio, C., Ruggiero, P., Curci, M., Colombo, C., Palumbo, G., and Stotzky, G. (2005). Binding of DNA from *Bacillus subtilis* on montmorillonite-humic acids-aluminum or iron hydroxypolymers: effects on transformation and protection against DNase. *Soil Sci. Soc. Am. J.* 69, 834–841. doi: 10.2136/sssaj2004.0166

Cui, E., Fan, X., Hu, C., Neal, A. L., Cui, B., Liu, C., et al. (2022). Reduction effect of individual N, P, K fertilization on antibiotic resistance genes in reclaimed water irrigated soil. *Ecotoxicol. Environ. Saf.* 231:113185. doi: 10.1016/j.ecoenv.2022.113185

Dong, Z., Wang, J., Wang, L., Zhu, L., Wang, J., Zhao, X., et al. (2022). Distribution of quinolone and macrolide resistance genes and their co-occurrence with heavy metal resistance genes in vegetable soils with long-term application of manure. *Environ. Geochem. Health* 44, 3343–3358. doi: 10.1007/s10653-021-01102-x

Edouard, L. R., Emmanuel, T., and Jonathan, V. (2022). *Trade-off between short and long-term effects of mineral, organic or mixed mineral-organic fertilisation on grass yield of tropical permanent grassland[JJ*. Euro. J. Agro. 141.

Ejtahed, H. S., Angoorani, P., Soroush, A. R., Hasani-Ranjbar, S, Siadat, S. D., and Larijani, B. (2020). Gut microbiota-derived metabolites in obesity: a systematic review. *Biosci. Microbiota. Food Health.* 39, 65–76. doi: 10.12938/bmfh.2019-026

Fu, S. Z., Wang, Q. Y., Wang, R., Zhang, Y. X., Lan, R. T., He, F. L., et al. (2022). Horizontal transfer of antibiotic resistance genes within the bacterial communities in aquacultural environment. *Sci. Total Environ.* 820:153286. doi: 10.1016/j.scitotenv.2022.153286

Gao, M., Qiu, T. L., Sun, Y. M., and Wang, X. M. (2018). The abundance and diversity of antibiotic resistance genes in the atmospheric environment of composting plants. *Environ. Int.* 116, 229–238. doi: 10.1016/j.envint.2018.04.028

Gou, M., Hu, H. W., Zhang, Y. J., Wang, J. T., Hayden, H., Tang, Y. Q., et al. (2018). Aerobic composting reduces antibiotic resistance genes in cattle manure and the resistome dissemination in agricultural soils. *Sci. Total Environ.* 612, 1300–1310. doi: 10.1016/j.scitotenv.2017.09.028

He, Y., Dong, Z. J., and Yan, L. (2020). Diversity of antibiotic resistance genes in paddy soils in Sichuan Province, China. *J. Agric. Environ. Sci.* 39, 1249–1258. doi: 10.11654/jaes.2019-1355

He, L. Y., He, L. K., Gao, F. Z., Wu, D. L., Zou, H. Y., Bai, H., et al. (2021). Dissipation of antibiotic resistance genes in manure-amended agricultural soil. *Sci. Total Environ.* 787:147582. doi: 10.1016/j.scitotenv.2021.147582

Heuer, H., Schmitt, H., and Smalla, K. (2011a). Antibiotic resistance gene spread due to manure application on agricultural fields. *Curr. Opin. Microbiol.* 14, 236–243. doi: 10.1016/j.mib.2011.04.009

Heuer, H., Solehati, Q., Zimmerling, U., Kleineidam, K., Schloter, M., Muller, T., et al. (2011b). Accumulation of sulfonamide resistance genes in arable soils due to repeated application of manure containing sulfadiazine. *Appl. Environ. Microbiol.* 77, 2527–2530. doi: 10.1128/aem.02577-10

Hill, K. E., and Top, E. M. (1998). Gene transfer in soil systems using microcosms. *FEMS Microbiol. Ecol.* 25, 319–329. doi: 10.1111/j.1574-6941.1998.tb00483.x

Karci, A., and Balcioglu, I. A. (2009). Investigation of the tetracycline, sulfonamide, and fluoroquinolone antimicrobial compounds in animal manure and agricultural soils in Turkey. *Sci. Total Environ.* 407, 4652–4664. doi: 10.1016/j.scitotenv.2009.04.047

Karkman, A., Parnanen, K., and Larsson, D. G. J. (2019). Fecal pollution can explain antibiotic resistance gene abundances in anthropogenically impacted environments. *Nat. Commun.* 10:80. doi: 10.1038/s41467-018-07992-3

Li, H., Zheng, X., Tan, L., Shao, Z., Cao, H., and Xu, Y. (2022). The vertical migration of antibiotic-resistant genes and pathogens in soil and vegetables after the application of different fertilizers. *Environ. Res.* 203:111884. doi: 10.1016/j.envres.2021.111884

Lillenberg, M., Litvin, S. V., Nei, L., Roasto, M., and Sepp, K. (2010). Enrofloxacin and ciprofloxacin uptake by plants from soil. *Agron. Res.* 8, 807–814.

Liu, Z., Bai, Y., Gao, J., and Li, J. (2023). Driving factors on accumulation of cadmium, lead, copper, zinc in agricultural soil and products of the North China plain. *Sci. Rep.* 13:7429. doi: 10.1038/s41598-023-34688-6

Liu, C. B., Li, B. L., Liu, M., and Mao, S. (2022). Demand, status, and prospect of antibiotics detection in the environment. *Sens. Actuators B: Chem.* 369:132383. doi: 10.1016/j.snb.2022.132383

Looft, T., Johnson, T. A., Allen, H. K., Bayles, D. O., Alt, D. P., Stedtfeld, R. D., et al. (2012). In-feed antibiotic effects on the swine intestinal microbiome. *Proc. Natl. Acad. Sci. U. S. A.* 109, 1691–1696. doi: 10.1073/pnas.1120238109

Marti, R., Scott, A., Tien, Y.-C., Murray, R., Sabourin, L., Zhang, Y., et al. (2013). Impact of manure fertilization on the abundance of antibiotic-resistant bacteria and frequency of detection of antibiotic resistance genes in soil and on vegetables at harvest. *Appl. Environ. Microbiol.* 79, 5701–5709. doi: 10.1128/aem.01682-13

Mustafa, A., and Scholz, M. (2011). Characterization of microbial communities transforming and removing nitrogen in wetlands. *Wetlands* 31, 583–592. doi: 10.1007/s13157-011-0175-6

Olesen, S. W., Barnett, M. L., MacFadden, D. R., Brownstein, J. S., Hernandez-Diaz, S., Lipsitch, M., et al. (2018). The distribution of antibiotic use and its association with antibiotic resistance. *eLife* 7:e39435. doi: 10.7554/eLife.39435

Pruden, A., Pei, R. T., Storteboom, H., and Carlson, K. H. (2006). Antibiotic resistance genes as emerging contaminants: studies in northern Colorado. *Environ. Sci. Technol.* 40, 7445–7450. doi: 10.1021/es060413l

Qi, Z., Jin, S., Guo, X., Tong, H., Ren, N., and You, S. (2023). Distribution and transmission of β-lactamase resistance genes in meal-to-milk chain on dairy farm. *Environ. Pollut.* 15:121831. doi: 10.1016/j.envpol.2023.121831

Qi, Z., Le, Z., Han, F., Qi, Y., and Liu, R. (2022). β-lactamase genes transmission influenced by tetracycline, sulfonamide and β-lactams antibiotics contamination in the on-site farm soil. *Ecotoxicol. Environ. Saf.* 241:113753. doi: 10.1016/j.ecoenv.2022.113753

Rambaut, L. A. E., Tillard, E., Vayssières, J., Lecomte, P., and Salgado, P. (2022). Trade-off between short and long-term effects of mineral, organic or mixed mineral-organic fertilisation on grass yield of tropical permanent grassland. *Eur. J. Agron.* 141:126635. doi: 10.1016/j.eja.2022.126635

Riahi, H. S., Heidarieh, P., and Fatahi-Bafghi, M. (2022). Genus Pseudonocardia: what we know about its biological properties, abilities and current application in biotechnology. *J. Appl. Microbiol.* 132, 890–906. doi: 10.1111/jam.15271

Ross, J., and Topp, E. (2015). Abundance of antibiotic resistance genes in bacteriophage following soil fertilization with dairy manure or municipal biosolids, and evidence for potential transduction. *Appl. Environ. Microbiol.* 81, 7905–7913. doi: 10.1128/aem.02363-15

Salyers, A. A., and Amábile-Cuevas, C. F. (1997). Why are antibiotic resistance genes so resistant to elimination? *Antimicrob. Agents Chemother.* 41, 2321–2325. doi: 10.1128/AAC.41.11.2321

Sarmah, A. K., Meyer, M. T., and Boxall, A. B. A. (2006). A global perspective on the use, sales, exposure pathways, occurrence, fate and effects of veterinary antibiotics (VAs) in the environment. *Chemosphere* 65, 725–759. doi: 10.1016/j.chemosphere.2006.03.026

Schmitt, H., Stoob, K., Hamscher, G., Smit, E., and Seinen, W. (2006). Tetracyclines and tetracycline resistance in agricultural soils: microcosm and field studies. *Microb. Ecol.* 51, 267–276. doi: 10.1007/s00248-006-9035-y

Shi, H., Hu, X., Zhang, J., Li, W., Xu, J., Hu, B., et al. (2023). Soil minerals and organic matters affect ARGs transformation by changing the morphology of plasmid and bacterial responses. *J. Hazard. Mater.* 457:131727. doi: 10.1016/j.jhazmat.2023.131727

Su, J. Q., Wei, B., Ou-Yang, W. Y., Huang, F. Y., Zhao, Y., Xu, H. J., et al. (2015). Antibiotic resistome and its association with bacterial communities during sewage sludge composting. *Environ. Sci. Technol.* 49, 7356–7363. doi: 10.1021/acs.est.5b01012

Tang, X. J., Lou, C. L., Wang, S. X., Lu, Y. H., Liu, M., Hashmi, M. Z., et al. (2015). Effects of long-term manure applications on the occurrence of antibiotics and antibiotic resistance genes (ARGs) in paddy soils: evidence from four field experiments in south of China. *Soil Biol. Biochem.* 90, 179–187. doi: 10.1016/j.soilbio.2015.07.027

Wang, F. H., Han, W. X., Chen, S. M., Dong, W. X., Qiao, M., Hu, C. S., et al. (2020). Fifteen-year application of manure and chemical fertilizers differently impacts soil ARGs and microbial community structure. *Front. Microbiol.* 11:62. doi: 10.3389/fmicb.2020.00062

Wu, N., Qiao, M., Zhang, B., Cheng, W. D., and Zhu, Y. G. (2010). Abundance and diversity of tetracycline resistance genes in soils adjacent to representative swine feedlots in China. *Environ. Sci. Technol.* 44, 6933–6939. doi: 10.1021/es1007802

Wu, N., Qiao, M., and Zhu, Y. (2009). Detection and quantification of five tetracycline resistance genes in pig farm soils. *Ecotoxicology* 4, 705–710. doi: 10.1016/S0378-1097(00)00347-5

Xiong, W. G., Wang, M., Dai, J. J., Sun, Y. X., and Zeng, Z. L. (2018). Application of manure containing tetracyclines slowed down the dissipation of tet resistance genes and caused changes in the composition of soil bacteria. *Ecotoxicol. Environ. Saf.* 147, 455–460. doi: 10.1016/j.ecoenv.2017.08.061

Xu, L. S., Wang, W. Z., and Xu, W. H. (2022). Effects of tetracycline antibiotics in chicken manure on soil microbes and antibiotic resistance genes (ARGs). *Environ. Geochem. Health* 44, 273–284. doi: 10.1007/s10653-021-01004-y

Yang, Y. Y., Xu, C., Cao, X. H., Lin, H., and Wang, J. (2017). Antibiotic resistance genes in surface water of eutrophic urban lakes are related to heavy metals, antibiotics, lake morphology and anthropic impact. *Ecotoxicology* 26, 831–840. doi: 10.1007/s10646-017-1814-3

Yang, Q., Zhang, H., Guo, Y., and Tian, T. (2016). Influence of chicken manure fertilization on antibiotic-resistant Bacteria in soil and the endophytic Bacteria of Pakchoi. *Int. J. Environ. Res. Public Health* 13:662. doi: 10.3390/ijerph13070662

Zhang, Q. Q., Ying, G. G., Pan, C. G., Liu, Y. S., and Zhao, J. L. (2015). Comprehensive evaluation of antibiotics emission and fate in the river basins of China: source analysis, multimedia modeling, and linkage to bacterial resistance. *Environ. Sci. Technol.* 49, 6772–6782. doi: 10.1021/acs.est.5b00729

Zhang, Y., Zhou, J., Wu, J., Hua, Q. W., and Bao, C. X. (2022). Distribution and transfer of antibiotic resistance genes in different soil-plant systems. *Environ. Sci. Pollut. Res.* 29, 59159–59172. doi: 10.1007/s11356-021-17465-8

Zhi, D., Yang, D. X., Zheng, Y. X., Yang, Y., He, Y. Z., Luo, L., et al. (2019). Current progress in the adsorption, transport and biodegradation of antibiotics in soil. *J. Environ. Manag.* 251:109598. doi: 10.1016/j.jenvman.2019.109598

Zhou, L. J., Ying, G. G., Liu, S., Zhang, R. Q., Lai, H. J., Chen, Z. F., et al. (2013). Excretion masses and environmental occurrence of antibiotics in typical swine and dairy cattle farms in China. *Sci. Total Environ.* 444, 183–195. doi: 10.1016/j.scitotenv.2012.11.087

frontiers | Frontiers in Microbiology

TYPE Original Research
PUBLISHED 01 November 2023
DOI 10.3389/fmicb.2023.1277709

OPEN ACCESS

EDITED BY
Zifang Chi,
Jilin University, China

REVIEWED BY
Hana Stiborova,
University of Chemistry and Technology in Prague, Czechia
Chunqiao Xiao,
Wuhan Institute of Technology, China
Hui Zhao,
Shandong University of Science and Technology, China

*CORRESPONDENCE
Yanling Ma
✉ mayanling@nwu.edu.cn

RECEIVED 15 August 2023
ACCEPTED 17 October 2023
PUBLISHED 01 November 2023

CITATION
Xu R, Zhang S, Ma Z, Rao Q and Ma Y (2023) Characterization and genome analysis of *Neobacillus mesonae* NS-6, a ureolysis-driven strain inducing calcium carbonate precipitation. *Front. Microbiol.* 14:1277709. doi: 10.3389/fmicb.2023.1277709

Characterization and genome analysis of *Neobacillus mesonae* NS-6, a ureolysis-driven strain inducing calcium carbonate precipitation

Rui Xu[1], Shuqi Zhang[1], Zhiwei Ma[1], Qingyan Rao[1] and Yanling Ma[2]*

[1]College of Life Science, Northwest University, Xi'an, Shaanxi, China, [2]Shaanxi Provincial Key Laboratory of Biotechnology, Key Laboratory of Resources Biology and Biotechnology in Western China, Ministry of Education, College of Life Science, Northwest University, Xi'an, Shaanxi, China

In this study, a highly promising bacterium was isolated from sandstone oil in the Ordos Basin, named strain NS-6 which exhibited exceptional urease production ability and demonstrated superior efficiency in inducing the deposition of calcium carbonate ($CaCO_3$). Through morphological and physiochemical characteristics analysis, as well as 16S rRNA sequencing, strain NS-6 was identified as *Neobacillus mesonae*. The activity of urease and the formation of $CaCO_3$ increased over time, reaching a maximum of 7.9 mmol/L/min and 184 mg (4.60 mg/mL) respectively at 32 h of incubation. Scanning Electron Microscopy (SEM) revealed $CaCO_3$ crystals ranging in size from 5 to 6 μm, and Energy Dispersive X-ray (EDX) analysis verified the presence of calcium, carbon, and oxygen within the crystals. X-ray Diffraction (XRD) analysis further confirmed the composition of these $CaCO_3$ crystals as calcite and vaterite. Furthermore, the maximum deposition of $CaCO_3$ by strain NS-6 was achieved using response surface methodology (RSM), amounting to 193.8 mg (4.845 mg/mL) when the concentration of calcium ions was 0.5 mmol/L supplemented with 0.9 mmol/L of urea at pH 8.0. Genome-wide analysis revealed that strain NS-6 possesses a chromosome of 5,736,360 base pairs, containing 5,442 predicted genes, including 3,966 predicted functional genes and 1,476 functionally unknown genes. Genes like *ure*A, *ure*B, and *ure*C related to urea catabolism were identified by gene annotation, indicating that strain NS-6 is a typical urease-producing bacterium and possesses a serial of genes involved in metabolic pathways that mediated the deposition of $CaCO_3$ at genetic level.

KEYWORDS

***Neobacillus mesonae*, urease activity, calcium carbonate, biomineralization, whole-genome sequencing, response surface methodology**

1. Introduction

Microbially induced calcium carbonate precipitation (MICP) encompasses a range of processes that find significant applications in the fields of geotechnical and environmental engineering (Xu and Wang, 2023). Various studies have demonstrated that certain naturally occurring microbes are capable of rapidly producing thick mineral crystals with desirable gelling characteristics through their own metabolic activities, given appropriate living conditions,

nutrition, and other external factors (Bhutange et al., 2020). Notably, the processes referred to MICP provide stringent control over the composition, structure, size and morphology of biominerals. So far, research on the application value of MICP has maintained a booming trend that includes the utilization of MICP for bio-concrete materials, reinforcement of rocks and soil, restoration of cultural artifacts, plugging of geological formations to enhance oil recovery and facilitate geologic CO_2 sequestration, aimed with the advantages of environmental protection and ecological sustainability (Krajewska, 2018; Ortega et al., 2020; Al et al., 2022).

Various biological pathways have been proposed for MICP with extensive research conducted in recent years to understand the mechanisms and biochemical reactions involved (Zhang et al., 2023). Among these pathways, the most widely utilized method of MICP is based on the hydrolysis of urea by urease-producing bacteria. This approach offers several advantages, including rapid reaction rates, easy control of the process, high conversion efficiency, and more (Liu J. et al., 2021). Biologically induced mineralization occurs when urease-producing bacteria produce calcium carbonate ($CaCO_3$), resulting in the gradual coating of bacterial cells as the number of $CaCO_3$ crystals increases. This coating makes it difficult for the cells to transport and utilize nutrients required for metabolic activities, leading to their eventual death in solution (Kappaun et al., 2018; Naz et al., 2020). The type, size, and morphology of the mineralization products vary depending on the specific bacterial strains used under the same culture conditions. Therefore, the selection of appropriate ureolytic bacteria plays a crucial role in the success of solidification. In the past decade, various ureolytic bacterial species, including *Sporosarcina pasteurii*, *Citrobacter*, and *Enterobacter*, have been reported in MICP research (Kappaun et al., 2018; Keykha et al., 2019; Naz et al., 2020; Song et al., 2022). These literatures highlight how both bacterial species and abiotic factors can influence the mode and characteristics of $CaCO_3$ formation, especially pH variations can lead to the precipitation of various $CaCO_3$ forms. Alkaline conditions ($pH > 8$) promote the development of calcic carbonate, while acidic conditions ($pH < 7$) are more likely to yield calcite. Temperature also exerts influence over crystal shape and arrangement, wherein the deposition process is frequently expedited at higher temperatures, although lower temperatures can result in the formation of smaller crystals. High concentrations of calcium ions generally lead to increased $CaCO_3$ deposition, and they can also give rise to crystals with distinct morphologies. Additionally, various strains of urease-producing bacteria may exert different effects on the morphology of $CaCO_3$ crystals. Nutrient concentrations in the growth medium, like carbon and nitrogen and phosphorus sources, can impact bacterial growth and metabolism, consequently influencing the morphology of $CaCO_3$ crystals. The effectiveness and availability of nucleation sites can further modify the morphology of $CaCO_3$ crystals. The presence of the right nucleation site can induce growth in a specific direction, resulting in crystals with unique morphologies. Some bacterial strains may exhibit a tendency to produce large crystals, while others may yield small, uniformly shaped crystals. Most of the previous work to optimize MICP has focused on optimizing treatment conditions while considering the microbes as formulation ingredients, however, various properties of bacteria still need to be further explored accompanied by the molecular mechanisms underpinning MICP and the interplay between the abiotic factors. Thus, researchers should diligently search for new bacterial species to achieve efficient MICP, and the selection of an appropriate optimization scheme is crucial for enhancing large scale engineering practices of MICP technology.

The present study aimed to isolate and identify a strain named NS-6 that exhibited urease activity, and the morphological characteristics of $CaCO_3$ and the influence of abiotic factors on $CaCO_3$ formation by the isolated strain were investigated. The objectives of this research were as follows: (i) characterizing the NS-6 strain with high urease capability, (ii) conducting a preliminary assessment of $CaCO_3$ formation, (iii) optimizing factors using the response surface method (RSM), and (iv) annotating the molecular mechanism through genome-wide sequencing and identification. These findings will provide valuable insights into the mechanisms and formation of carbonate minerals using a newly biological resource, thereby enabling wider industrial applications of MICP.

2. Materials and methods

2.1. Chemicals and culture media

A urea agar base plate was prepared for isolation and identification of urease-producing bacteria, consisting of 1.0 g/L peptone, 5.0 g/L NaCl, 2.0 g/L KH_2PO_4, 0.2% phenol red, 2.0 g/L urea, and 0.1 g/L glucose. Luria-Bertani (LB) broth was used for presentation and pre-culture, comprising 10.0 g/L tryptone, 5.0 g/L yeast extract, and 5.0 g/L NaCl. The mineral salt medium (MSM) contained $(NH_4)_2SO_4$ at a concentration of 1.0 g/L, KH_2PO_4 at 7.0 g/L, K_2HPO_4 at 3.0 g/L, $MgSO_4 \bullet 7\ H_2O$ at 3.0 g/L, and NaCl at 0.5 g/L (pH 7.0–7.2). For the calcium deposition tests, a mixture of 1,000 mL yeast powder (20.0 g/L), ammonium sulfate (10.0 g/L), and distilled water (pH 8.0) was used, following the NH4-YE culture medium advised by ATCC (Zhao et al., 2019). All culture media were adjusted to pH 7.0 and sterilized at 121°C for 20 min, except for urea and glucose that were filtered through a sterile 0.45 um membrane before being added to the urea agar base plate. All organic solvents and other reagents used in this study were of analytical grade.

2.2. Isolation and identification of urease producing bacterial strain

The ureolytic bacteria were isolated using the dilution plate and direct streak techniques. In detail, 10 mL of sandstone oil was added to 90 mL of MSM and cultured for 7 d at 30°C with 180 rpm shaking to enrich the bacteria. Then, 1 mL of the gradient-diluted enrichment solution from the MSM culture was coated onto a urea agar base plate and incubated for 24–48 h at 30°C. Colonies that exhibited the ability to hydrolyze urea and change the color of the agar base plate from orange to pink were selected for purification. A pure culture, named strain NS-6, was identified as having high levels of urease activity (Van et al., 2010; Gupta et al., 2022; Leeprasert et al., 2022). A negative control was prepared using *E. coli* DH5α, a known non-ureolytic bacterium. Strain NS-6 was then identified through morphological and biochemical characteristics, as well as 16S rRNA sequencing. Gram staining, nitrate reduction testing, and determination of other enzyme activities such as oxidase and catalase follow Bergey's Manual of Determinative Bacteriology (Liu X. G. et al., 2021). The 16S rRNA gene sequence of strain NS-6 was amplified, the amplification of DNA

fragments was carried out using the primer pairs including forward primer (CAGAGTTTGATCCTGGCT) and reverse primer (AGGAGGTGATCCAGCCGCA). The PCR amplification program consisted of an initial pre-denaturation step at 94°C for 5 min, followed by 35 cycles of denaturation at 94°C for 30 s, annealing at 55°C for 30 s, and extension at 72°C for 60 s, The final extension was performed at 72°C for 10 min. and compared to other sequences in GenBank through the Basic Local Alignment Search Tool (BLAST) to construct a phylogenetic tree using the neighbor-joining method in MEGA 7 software (Yoo et al., 2021; Uyar and Avcı, 2023). The NS-6 strain was stored at −80°C in 30% glycerol (Xu et al., 2022).

2.3. Urease activity and $CaCO_3$ formation

Urease activity can be determined by measuring the change in conductivity per unit time. One unit of urease activity is defined as the amount of enzyme that hydrolyzes 1 μmol of urea per mL per minute, as determined by the method described by Yi et al. (2021) In brief, strain NS-6 was inoculated into NB-urea broth (0.3% nutrient broth and 2% urea, pH 8.0) at 30°C, and time-dependent urease activity was measured as follows. A mixture of 13.5 mL of 1.6 mmol/L urea solution and 1.5 mL of bacterial solution was prepared and incubated at 37°C for 5 min. During the cultivation process, the conductivity of the mixture (in mS/cm) was measured using a conductivity meter (DDS-307, Digital Conductivity Meter, China). Each treatment was repeated at least three times.

To investigate and quantify the formation of $CaCO_3$ by strain NS-6, 3.0 mL of stationary phase bacterial cells (1% v/v) were inoculated into 300 mL liquid NH4-YE medium supplemented with 2% urea and 25 mM $CaCl_2$. The mixture was incubated at 30°C and 200 rpm for 48 h. After incubation, 30 mL of the culture was sampled every 8 h. The samples were centrifuged at 5,000 rpm for 3 min to remove the supernatant, and the resulting precipitated $CaCO_3$ was collected. The collected precipitates were then filtered and washed with absolute ethanol and deionized water to eliminate any residual cells and culture components. Subsequently, the precipitates were dried for 24 h at 80°C in a vacuum drying oven and weighed. To further analyze the $CaCO_3$, it was washed with HCl solution, dried again, and weighed. The quantity of $CaCO_3$ was determined by calculating the mass difference between the two dryings. The dried $CaCO_3$ samples were preserved for future studies.

2.4. Micro-morphological characterization of $CaCO_3$ crystals

A field emission scanning electron microscope (SEM, FEI Quanta 450, America) was employed to observe the micro-morphology of the mineralized products using an accelerating voltage of 1.5 kV. Concurrently, the sample surface was coated with a conductive gold film to facilitate electron flow and prevent bright spots in the captured images caused by electron aggregation, as the sample is non-conductive. Fourier-transform infrared spectroscopy (Nicolet iS50 FT-IR, Thermo Fisher, United States) was utilized to characterize the functional groups present in the mineralized products. The measured wavenumber range was from 4,000 cm^{-1} to 500 cm^{-1} at 25°C (Mohan et al., 2018). Additionally, X-ray diffraction analysis (XRD, Smartlab 9kw, Japan) was performed to determine the characteristic X-ray diffraction peaks of the mineralized products. The phase composition and crystal form of the X-ray diffraction peaks were analyzed using Jade 6 software. The scanning range was set at 5–75°, with a scanning step size of 0.02°. Thermogravimetry and differential scanning calorimetry (TG-DSC, TA Q600, America) were employed to investigate the simultaneous thermal analysis of the precipitates under a nitrogen atmosphere, with a heating rate of 20°C/min within the temperature range of 30°C to 950°C (Yi et al., 2021). All measurements were performed in triplicate.

2.5. Optimization of $CaCO_3$ production by response surface method

The response surface method (RSM) was utilized to optimize the critical variables and their interactions in the formation of $CaCO_3$ by strain NS-6. The independent variables, pH, urea concentration, and calcium ion concentration, were selected based on the results of the single-factor experiment (Supplementary Figure S1). Following the Box–Behnken central experimental design principle, a three-factor, three-level response surface analysis was conducted using a single-factor experimental design approach, with the optimal value as the central point and values above and below as the response surface experimental design levels (Wu et al., 2023). The experimental design, consisting of 17 treatments and 3 variables, was generated using Design-Expert V 10.0 software (Supplementary Tables S1, S2), with three replicates at the midpoint. By utilizing equation (1), a quadratic polynomial regression equation between the factor levels and response was derived.

$$Y_i = b_0 + \sum b_i X_i + \sum b_{ij} X_i X_j + b_{ii} X^2{}_i \quad (1)$$

In this study, Y_i was used to represent the predicted response, while X_i and X_j were variables. The constant b_0 was denoted as a constant term, b_i referred to a linear coefficient, b_{ij} indicated an interaction coefficient, and b_{ii} represented a quadratic coefficient. Analysis of variance (ANOVA) was conducted to assess the statistical significance. The experiments were performed in 50 mL centrifuge tubes with transparent polypropylene material and a pointed bottom. The quantity of $CaCO_3$ was determined using the gravimetric method. The calculation formula used was as follows:

$$\text{Quantity of } CaCO_3 = M_1 - M_2 \quad (2)$$

In this context, "M_1" represents the amount of $CaCO_3$ generated by strain NS-6, while "M_2" stands for the quantity resulting from the abiotic treatments.

2.6. Complete genome sequencing of strain NS-6

High-quality genomic DNA from strain NS-6 was extracted using the Bacterial Genome Extraction kit (Tiangen, Beijing), following the manufacturer's instructions. Subsequently, the obtained DNA was sent to Shanghai Meiji Bioinformatics Technology Co., Ltd. for whole-genome sequencing, with the aim of understanding the genetic-level molecular

mechanisms underlying $CaCO_3$ formation. Before being assembled into a contig using the hierarchical genome assembly technique (HGAP) version 2.2 of Canu, all clean reads underwent filtration and quality control based on the method described by Koren et al. (2017). CDS prediction, tRNA prediction, and rRNA prediction were performed using Glimmer, tRNA-scan-SE, and Barrnap, respectively, as described by Delcher et al. (2007). The predicted CDSs were annotated using sequence alignment techniques against the NR, Swiss-Prot, Pfam, GO, COG, and

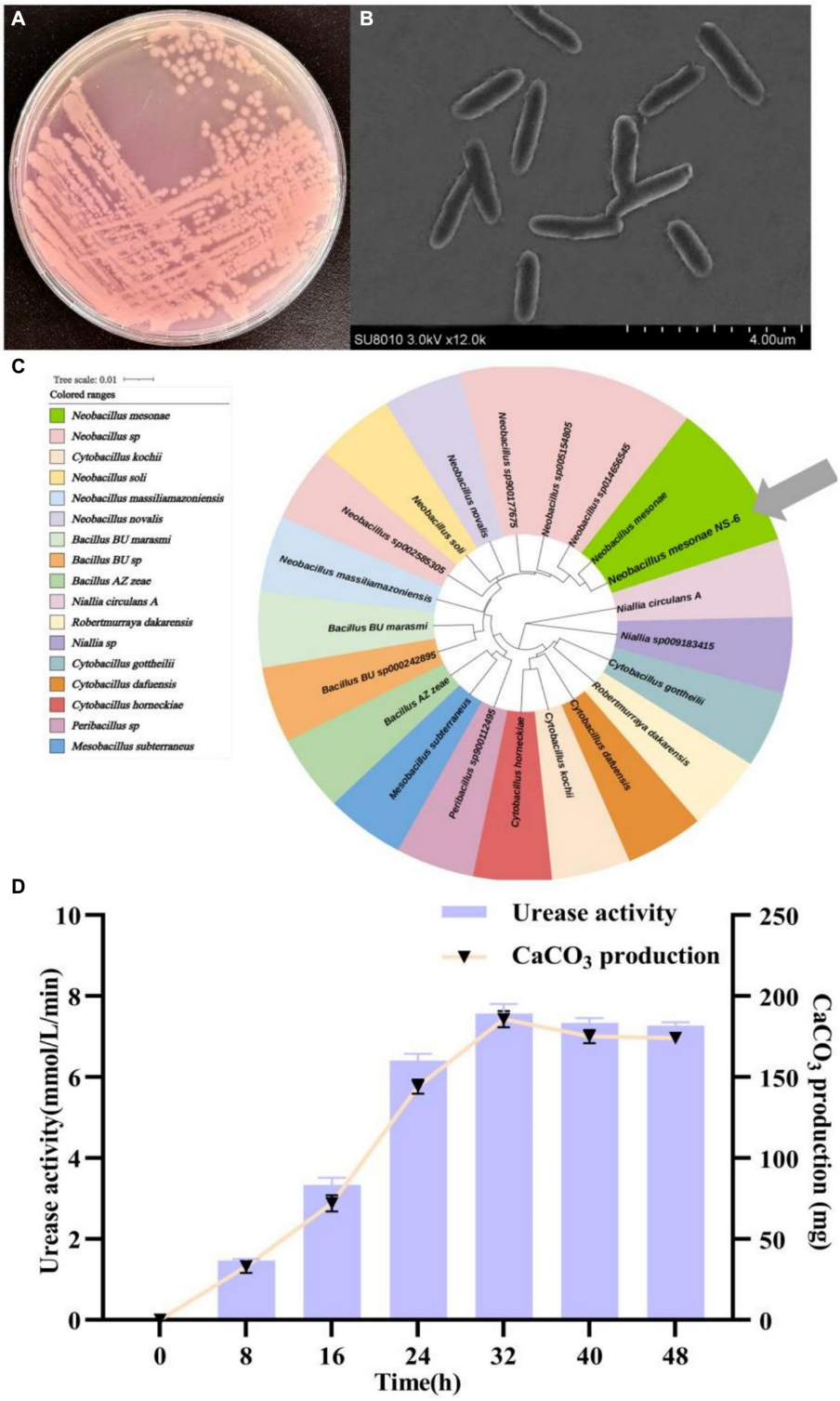

FIGURE 1
Morphology and identification of strain NS-6. **(A)** Typical colonies of strain NS-6 inoculated on a urea agar base plate, **(B)** Scanning electron microscope image of strain NS-6, **(C)** Phylogenetic tree constructed by adjacency method between strain NS-6 and 16S rRNA gene of related bacteria in MEGA 7.0 software, **(D)** Urease activity and calcium carbonate ($CaCO_3$) production of strain NS-6 at 48 h of cultivation.

KEGG databases. Quick alignment of each set of query proteins with the databases allowed retrieval of gene annotations for the top matches (e-value $<10^{-5}$). To analyze the genome of strain NS-6, the IslandViewer4 online website (Bertelli et al., 2022) was utilized, employing the IslandPick, IslandPath-DIMOB, and SIGI-HMM methods.

3. Results

3.1. Identification and characteristics of strain NS-6

Numerous bacterial strains exhibiting morphological variations were observed to undergo a color change from orange to pink when inoculated on a urea agar base plate. Among these strains, a particular strain, designated NS-6, displayed a deep pink color due to its high urease activity. This strain was subsequently screened and identified. Following incubation on a urea agar base plate at 30°C for 48 h, individual colonies of the NS-6 strain exhibited a spherical shape with conical protrusions and ragged edges. Microscopic analysis revealed that the cell size was approximately 2.0 μm in diameter and rod-shaped (Figures 1A,B). The NS-6 strain exhibited positive activity in oxidase, catalase, nitrate reduction, and sugar fermentation tests shown in Table 1. Phylogenetic analysis further indicated that strain NS-6 shared a 99.8% homology with *Neobacillus mesonae* GCF-001636315.1 (Figure 1C). Additionally, Figure 1D demonstrated the changes in urease activity and $CaCO_3$ formation over time for strain NS-6, which increased steadily and reached maximum values of 7.9 mmol/L and 184 mg (4.60 mg/mL) at 32 h of cultivation. Moreover, the deposition of $CaCO_3$ was found to be quantitatively enhanced under conditions involving a calcium chloride concentration of 0.4–0.6 mmol/L, urea concentration of 0.8–1.0 mmol/L, temperature of 30°C, and pH range of 7–9, as depicted in Supplementary Figure S1. Those findings aligned with the optimal temperature and pH values reported in the earlier research works for the other urease-producing bacteria, and strain NS-6 exhibited significantly high urease activity at 32 h of cultivation compared to previously reported urease-producing bacteria (Qian et al., 2021; Song et al., 2022; Diez-Marulanda and Brandao, 2023).

TABLE 1 Physiological and biochemical characteristics of strain NS-6.

Characteristics	Strain NS-6	Characteristics	Strain NS-6
Colony color	Milky white	Citrate experiment	–
Cellular morphology	Long-rod	Lipid hydrolysis	–
Temperature for growth	20–45°C	Oxidase	+
pH for growth	6–9	Hydrogen peroxidase	+
NaCl for growth	0–100 g/L	Protease	+
Motility	+	Contact enzyme	+
Indole production	–	β-Galactosidase	+
Hemolysis	–	Lecithinase	–
Denitrification	+	Glucose	+
Gram stain	+	Maltose	+
Nitrate reduction	+	Lactose	+
Starch	–	Mannose	–
Gelatin hydrolysis	–	V-P test	–

3.2. Formation and structural characterization of $CaCO_3$ crystals

The formation of precipitated $CaCO_3$ by strain NS-6 was investigated using NH4-YE culture medium, along with a negative control. The results showed that the $CaCO_3$ precipitation by NS-6 exhibited irregular spherical compact large particles with a dense filling (Figure 2A). EDS analysis revealed the presence of Na, Cl, and

TABLE 2 Strain NS-6 induced calcium carbonate (CaCO3) precipitation fitting quadratic polynomial model analysis of variance (ANOVA).

Source	Sum of squares	*df*	Mean square	*F*-value	*p*-value	
Model	8382.23	9	931.36	490.19	<0.0001	Significant
A-pH	312.5	1	312.5	164.47	<0.0001	
B-Urea concentration	18	1	18	9.47	0.0179	
C-Calcium ion concentration	2,178	1	2,178	1146.32	<0.0001	
AB	36	1	36	18.95	0.0033	
AC	441	1	441	232.11	<0.0001	
BC	1	1	1	0.5263	0.4917	
A^2	4352.09	1	4352.09	2290.58	<0.0001	
B^2	186.2	1	186.2	98	<0.0001	
C^2	523.46	1	523.46	275.51	<0.0001	
Residual	13.3	7	1.9			
Lack of Fit	2.5	3	0.8333	0.3086	0.8192	Not significant
Pure Error	10.8	4	2.7			
Cor Total	8395.53	16				

other elements in addition to C, Ca, and O in the $CaCO_3$ precipitate, indicating the presence of $CaCO_3$ crystals (Figure 2B). XRD spectra confirmed the results of FESEM imaging, showing that the $CaCO_3$ precipitation with the addition of strain NS-6 mainly consisted of calcite and vaterite (Figure 2C). Simultaneously, an analysis of calcite and spherulite content using XRD was conducted, and calculated their respective yield proportions by measuring the peak areas and masses of the respective minerals in the samples and underwent rigorous statistical analysis to ensure precision. The results revealed that calcite accounted for 31.7% in the sample, while spherulite constituted of 68.3%. Furthermore, the FT-IR spectra of the precipitated $CaCO_3$ showed characteristic diffraction peaks at 710 cm^{-1} and 872 cm^{-1}, which corresponded to the characteristic diffraction peaks of calcite. The characteristic diffraction peaks at 1,070 cm^{-1} and 868 cm^{-1} mainly corresponded to the spherulite characteristic diffraction peaks. Notably, the characteristic diffraction peak at 1650 cm^{-1} indicated the

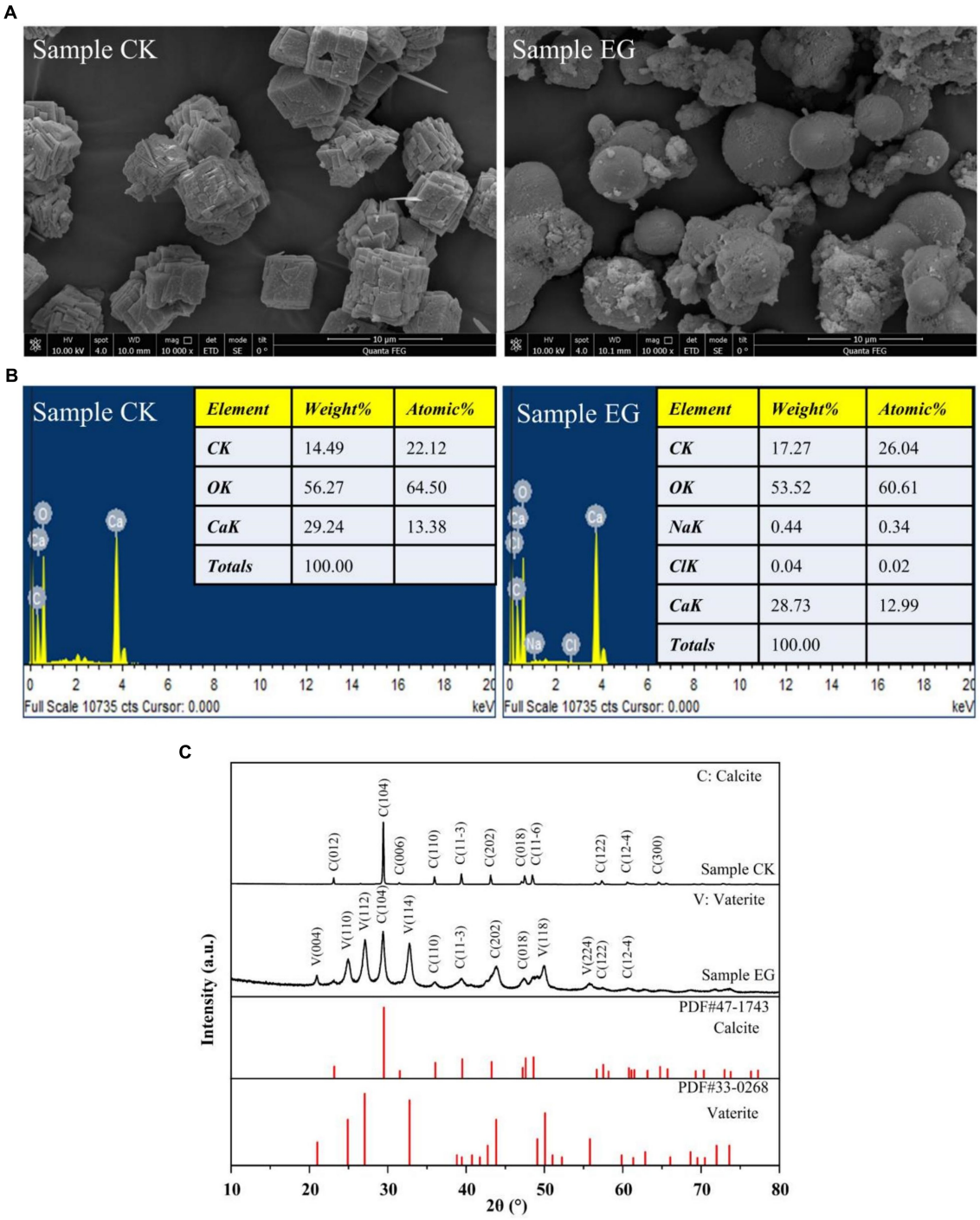

FIGURE 2
FESEM images **(A)**, EDS spectrum **(B)**, and XRD pattern of precipitated $CaCO_3$ **(C)**. Sample CK was in the presence of *E. coli*, and sample EG was in the presence of strain NS-6.

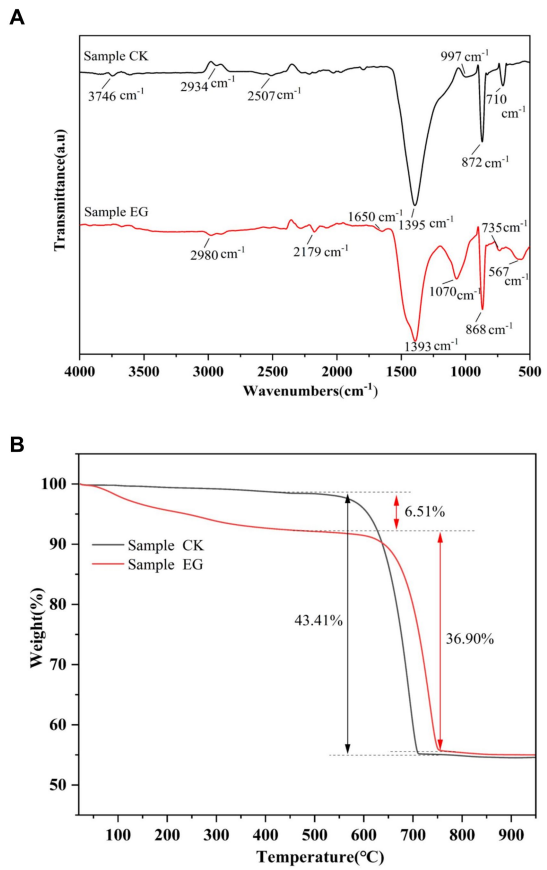

FIGURE 3
FT-IR spectra of precipitated $CaCO_3$ **(A)**, and TG-DSC curves of precipitated $CaCO_3$ **(B)**. Sample CK represented in the presence of *E. coli*, and sample EG represented in the presence of strain NS-6.

TABLE 3 General characteristics of NS-6 genome.

Feature	Chromosome
Genome size (bp)	5,736,360
GC content (%)	40.32%
Total genes	5,442
rRNA genes	41
tRNA genes	110
Other ncRNA	119
Genes with predicted function	3,966
Genes with unknown function	1,476
Genomic Islands	13
CDSs assigned to COGs	4,518
GenBank accession no.	CP128196.1

presence of a symmetric stretching of the carboxyl group (-COO-) in the protein secreted by strain NS-6 compared to the pure water system forming $CaCO_3$ (Figure 3A). Thermogravimetric analysis revealed that the thermogravimetric curve of $CaCO_3$ formed in the pure water system had a weight loss phase, with a total weight loss of 43.41% in the temperature range of 500–780°C, mainly due to the decomposition of $CaCO_3$. On the other hand, the $CaCO_3$ precipitated by strain NS-6 showed two weight loss stages on the TG curve (Figure 3B). The first

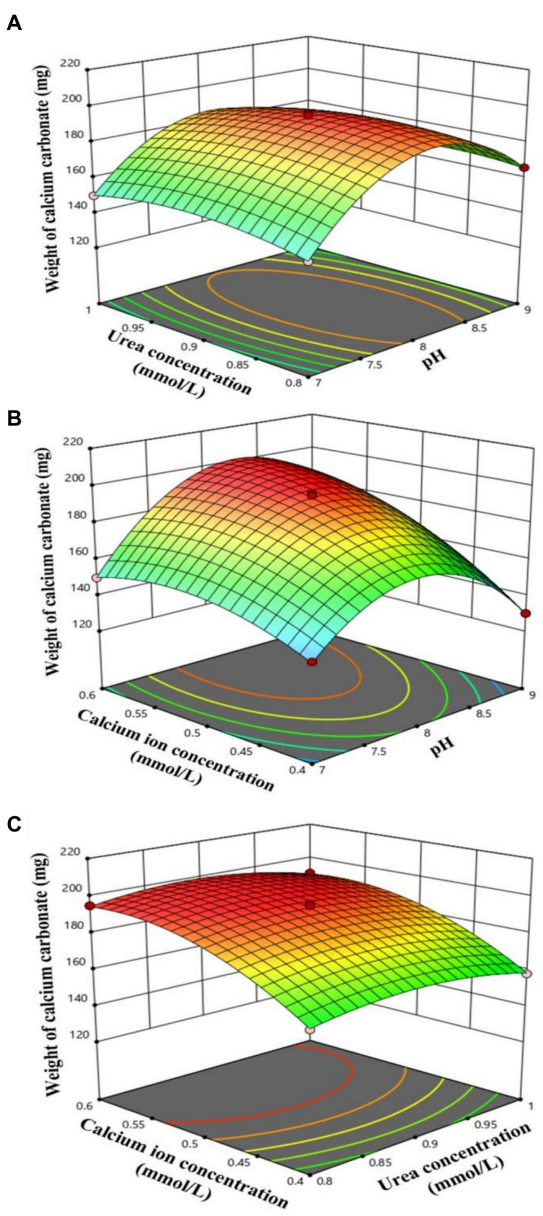

FIGURE 4
Response surface plots of the interaction effects of pH **(A)**, urea concentration **(B)** and calcium ion concentration **(C)** on the induction of $CaCO_3$ precipitation by strain NS-6. **(A)** Interaction between pH and urea concentration, **(B)** Interaction between pH and calcium ion concentration, **(C)** Interaction between urea concentration and calcium ion concentration.

weight loss phase occurred between 50 and 500°C, with a weight loss of 6.51%, attributed to the combustion and decomposition of bacterially secreted proteins adsorbed on the precipitated $CaCO_3$. The second weight loss phase of 36.90% occurred in the range of 500–780°C, which was attributed to the decomposition of $CaCO_3$.

3.3. Optimization of conditions induced $CaCO_3$ precipitation

In this study, a Box–Behnken design based on response surface methodology (RSM) was employed to identify the key factors and

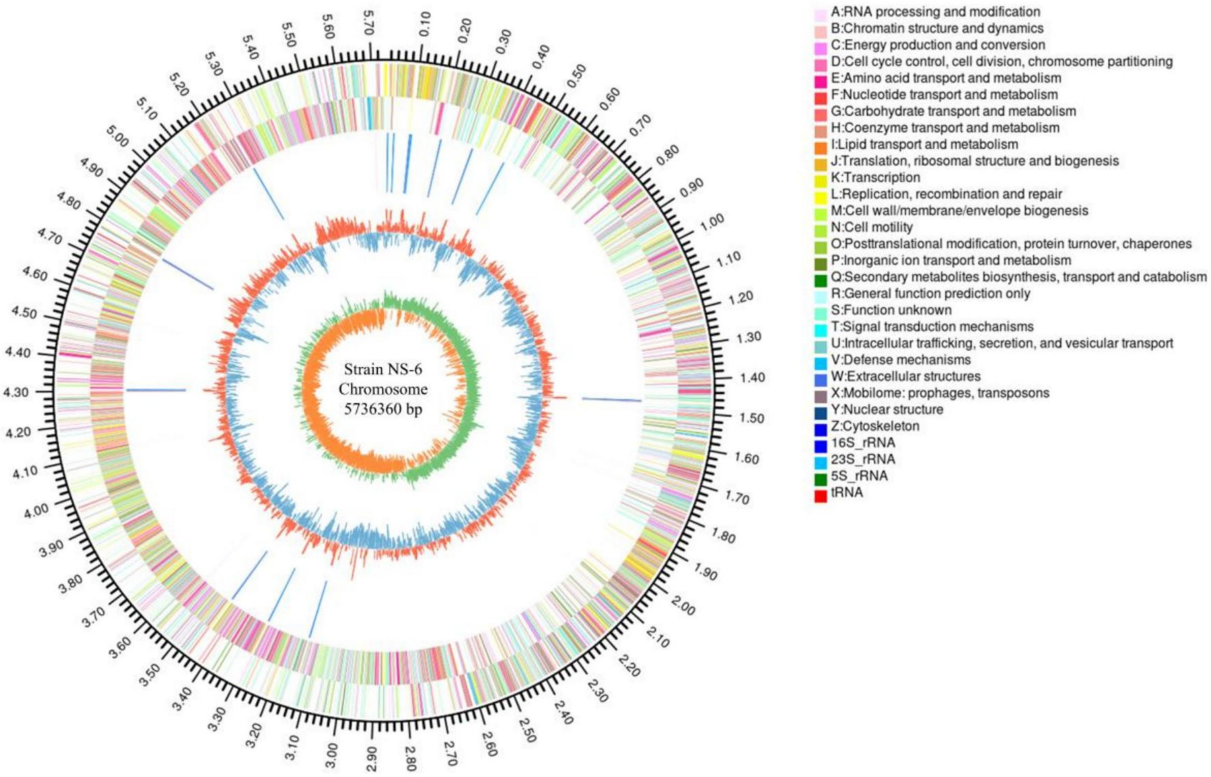

FIGURE 5
Graphical map of circular chromosome of the NS-6 strain.

TABLE 4 Partial genes involved in urea catabolism.

Locus tag	KO ID	Gene Name	Size (bp)	Gene Description	Predicted Function
Gene3392	K01430	*ureA*	303 bp	Urease subunit gamma [EC:3.5.1.5]	Small subunit of $(ureABC)_3$
Gene4915	K01430	*ureA*	303 bp	Urease subunit gamma [EC:3.5.1.5]	Small subunit of $(ureABC)_3$
Gene3391	K01429	*ureB*	330 bp	Urease subunit beta [EC:3.5.1.5]	Small subunit of $(ureABC)_3$
Gene4914	K01429	*ureB*	324 bp	Urease subunit beta [EC:3.5.1.5]	Small subunit of $(ureABC)_3$
Gene3390	K01428	*ureC*	1713 bp	Urease subunit alpha [EC:3.5.1.5]	Large catalytic subunit of $(ureABC)_3$
Gene4915	K01428	*ureC*	1713 bp	Urease subunit alpha [EC:3.5.1.5]	Large catalytic subunit of $(ureABC)_3$
Gene3386	K03190	*ureD*	825 bp	Urease accessory protein	Urease accessory protein for Ni
Gene4909	K03190	*ureD*	825 bp	Urease accessory protein	Urease accessory protein for Ni
Gene3389	K03187	*ureE*	456 bp	Urease accessory protein	Urease enzyme active site formation
Gene4912	K03187	*ureE*	456 bp	Urease accessory protein	Urease enzyme active site formation
Gene3388	K03188	*ureF*	699 bp	Urease accessory protein	Urease accessory protein for Ni
Gene4911	K03188	*ureF*	687 bp	Urease accessory protein	Urease accessory protein for Ni
Gene3387	K03189	*ureG*	612 bp	Urease accessory protein	Urease accessory protein u*reG* parfois + *ureH*
Gene4910	K03189	*ureG*	612 bp	Urease accessory protein	Urease accessory protein u*reG* parfois + *ureH*
Gene1990	K01999	*livK*	1,188 bp	ABC transporter substrate-binding protein	ABC high affinity urea uptake system substrate-binding *livK*
Gene2721	K21405	*acoR*	2,514 bp	transporter substrate-binding protein	High affinity urea uptake system substrate-binding *acoR*
Gene3183	K01998	*livM*	1,026 bp	Branched-chain amino acid ABC transporter permease	Branched-chain amino acid transport ATP-binding protein *livM*

(Continued)

TABLE 4 (Continued)

Locus tag	KO ID	Gene Name	Size (bp)	Gene Description	Predicted Function
Gene3184	K01997	*livH*	867 bp	Branched-chain amino acid ABC transporter permease	ABC high affinity urea uptake system permease *LivH*
Gene4888	K01996	*livF*	717 bp	ABC transporter ATP-binding protein	Branched-chain amino acid transport ATP-binding protein *livF*
Gene5433	K01995	*livG*	780 bp	ABC transporter ATP-binding protein	ABC high affinity urea uptake system ATPase *livG*

their interactions that influence the induction of $CaCO_3$ precipitation by strain NS-6. The results revealed that the pH (A), urea concentration (B), and calcium ion concentration (C) were the critical factors responsible for inducing $CaCO_3$ precipitation, with a range of 130 mg to 196 mg. The corresponding precipitation rate ranged from 3.25 mg/mL to 4.90 mg/mL (shown in Supplementary Table S2). To model the quantity of $CaCO_3$ precipitation induced by strain NS-6, a quadratic binomial regression equation (3) was fitted.

$$\begin{aligned}\text{Yiled of } CaCO_3\,(\text{mg}) &= +193.8 + 6.25\times A - 1.5\times B \\ &+16.5\times C - 3\times A\times B + 10.5\times A\times C - 0.5 \\ &\times B\times C - 32.15\times A^2 - 6.65\times B^2 - 11.15\times C^2 \end{aligned} \quad (3)$$

The ANOVA analysis of the quadratic polynomial model was presented in Table 2. The results show that the fitted terms were not statistically significant ($p = 0.8192 > 0.05$). However, the model had a high R^2 value of 0.9984 and $R^2_{Adj} = 0.9964$, indicating that the quadratic model accurately represents the relationship between the response and variables. Moreover, the results suggest that factors like pH (A) and calcium ion concentration (C), as well as the interaction term A × C and squared terms A^2, B^2, and C^2, had significant effects on the formation rate of precipitation ($p < 0.05$) (Karimifard and Alavi, 2019). To further enhance our understanding of the results, a three-dimensional response surface was generated (Figure 4), which illustrates the impact of pH (A), urea concentration (B), and calcium ion concentration (C) on the quantity of $CaCO_3$ precipitation while keeping other independent variables constant. From the 3D plot, it can be concluded that the variation in the surface due to pH (A) × calcium ion concentration (C) is greater than that due to pH (A) × urea concentration (B) and urea concentration (B) × calcium ion concentration (C) within the selected range of factors. The model predicts that a maximum amount of 193.8 mg (4.845 mg/mL) of $CaCO_3$ precipitation can be achieved at pH 8.0, urea concentration of 0.9 mmol/L, and calcium ion concentration of 0.5 mmol/L. The reliability of the polynomial model equation is assessed through the R^2 value, and its statistical significance is evaluated using the *F*-value. The *value of p*s of the model coefficients test the significance of the linear and squared effects of the influencing factors and their interaction effects.

3.4. Genome-wide sequencing and gene annotation

Aiming to better understand the genetic characteristics of strain NS-6, a genome-wide analysis was performed to reveal functional genes involved in the mineralization process. The genome of strain NS-6 consisted of a single chromosome spanning 5,736,360 base pairs (bp) with an average GC content of 40.32 mol% (Figure 5). Additionally, the genome contained 41 rRNAs and 110 tRNAs, and 13 genomic islands (GIs) were identified in strain NS-6 (Table 3 and Supplementary Figure S2). In terms of coding genes, there were a total of 2,676, 4,518, and 2,914 genes annotated for KEGG, COG, and GO databases, respectively (Figure 6). Notably, the genome analysis of strain NS-6 revealed the presence of urease-producing genes, namely *ure*A, *ure*B, and *ure*C, which encoded the γ subunit, β subunit, and α subunit of urease respectively, as well as genes encoded the urease accessory proteins UreD, UreE, UreF, and UreG (Table 4). This indicates that strain NS-6 is a typical urease-producing bacterium with a trimeric structure composed of two identical monomers, representative of urease enzymes, which was in agreement with earlier research works (Kappaun et al., 2018; Moro et al., 2022). These data through comprehensive whole-genome sequencing and functional annotation pave the way for future rational design of synthetic precipitator strains optimized for specific applications. The genome sequence of strain NS-6 has been submitted to the GeneBank database under accession number CP128196.1.

4. Discussion

Urea hydrolysis, facilitated by urease-producing bacteria (UPB), is crucial for MICP. Among UPB, *Bacillus pasteurelli* and *Pseudomonas aeruginosa* have garnered significant attention from researchers across various disciplines (Qian et al., 2018). However, it is worth noting that different strains of bacteria can induce varied mineralization products even when subjected to the same culture conditions (Jiang et al., 2020; Ali et al., 2023). As a ureolytic agent, the process involves the use of urease-producing bacteria, and the most commonly utilized bacteria in this regard are arguably *Sporosarcina pasteurii*, and others (Kappaun et al., 2018; Pakbaz et al., 2018; Keykha et al., 2019; Naz et al., 2020; Yu et al., 2021; Song et al., 2022). Herein, *Neobacillus mesonae* strain NS-6 that possessed urease-producing capabilities and exhibited tolerance to alkaline environments, might potentially serve as a novel bacterial species for facilitating MICP. The spherical shape of $CaCO_3$ crystals corresponded to vaterite, and the rhombohedral shape corresponded to calcite by strain NS-6, different from calcite mainly formed by other reported bacteria (Qian et al., 2021). Additionally, the expanded perlite particles exhibited numerous cavities, as observed through FESEM and XRD analysis. These cavities could potentially provide sufficient free oxygen for bacteria within the concrete, as well as offer attachment spaces for fixed bacteria to carry out their metabolic activities. Those results were coincident with some earlier research works, confirming that the specific morphology of formed crystals is

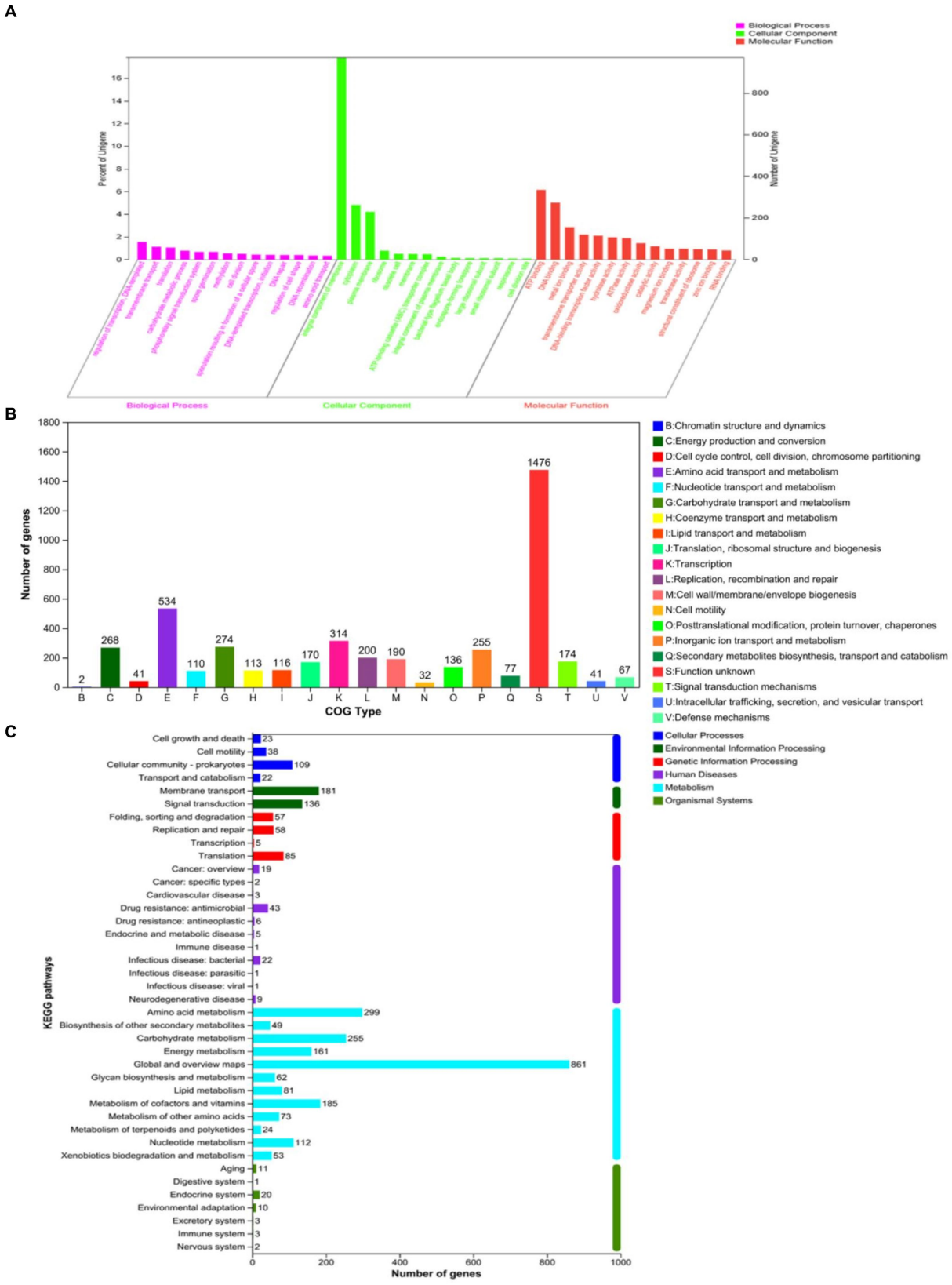

FIGURE 6
Number of genes associated with general functional categories, including **(A)** GO annotation map, **(B)** COG annotation map, and **(C)** KEGG annotation map of strain NS-6.

influenced by differences in bacterial genera (Zheng et al., 2019, 2020; Wang Z. J. et al., 2022).

Even more to the point, the MICP process could be studied systematically by examining the optimal conditions for the growth and metabolism of common MICP-assisting bacteria (Liu et al., 2023). The parameters that have an effect on the course of $CaCO_3$ precipitation and its efficiency, other than the type and concentration of bacteria/urease, primarily include the concentration of urea and calcium ions, as well as environmental factors such as temperature and pH value (Tang et al., 2020). RSM is a widely used optimization tool in the scientific community for studying the parameters that influence the process of MICP. By employing an appropriate experimental design, the number of required experiments can be reduced, allowing for the prediction of optimal performance conditions (Kumar and Kumar, 2021; Wang et al., 2021; Wang R. S. et al., 2022). To establish the relationship between the parameters and the quantity of $CaCO_3$ precipitation, the variation of factor levels was tested using RSM. The squared and interaction terms were found to have significant effects on the response values. The *F*-values in the current study indicate that, within the selected test range, the ranking of the three factors in terms of their influence on the quantity of $CaCO_3$ precipitation was calcium ion concentration > pH > urea concentration. This suggests that the optimal calcium ion concentration for $CaCO_3$ formation is particularly crucial for the practical application of strain NS-6. These findings were consistent with previous studies that have shown the significant influence of calcium salt type on microbially-induced $CaCO_3$ formation (Peng et al., 2022; Lv et al., 2023). It followed from the above that potential correlations between the variations in different factors were found during the experiments of the single influencing factor of MICP. Thus, not only the properties of the bacteria themselves, but also the environment and nutrients they were provided with had to be carefully considered when engineering bacteria for MICP and designing technological applications.

In addition to the optimal conditions for the formation of $CaCO_3$ precipitation, the presence of genes involved in urea catabolism was identified in the whole genome of strain NS-6. All these results revealed that strain NS-6 contained all the genes involved in urea metabolism, and the fermentation *in vitro* also showed that this isolate had ureolytic activity, which were similar to the other urease-producing bacteria (Jin et al., 2017). Particularly, higher habitat pH correlated with higher copy numbers of *ure*C in environmental bacteria, according to previous research (Keykha et al., 2019). The same trend occurs with this isolate studied here, where duplication occurs in the isolate exposed to alkaline condition. With the acquisition of sequencing information, the isolated newly ureolytic strain NS-6 is preferred model to explore the relative importance of the metabolic pathways, regulatory mechanisms for urease production and its potential applications in industry and agriculture.

In conclusion, the present study has clearly shown that strain-specific precipitation of calcium carbonates from a newly isolate NS-6 occur during its optimum deposition condition and genome sequencing, and, based on the type of polymorph precipitated, this technology can be applied for various purposes.

Data availability statement

The original contributions presented in the study are included in the article/Supplementary materials, further inquiries can be directed to the corresponding author.

Author contributions

RX: Data curation, Methodology, Resources, Software, Validation, Visualization, Writing – original draft. SZ: Formal analysis, Investigation, Methodology, Software, Data curation, Writing – original draft. ZM: Formal analysis, Methodology, Software, Visualization, Writing – original draft. QR: Data curation, Formal analysis, Investigation, Methodology, Software, Validation, Writing – original draft. YM: Conceptualization, Funding acquisition, Methodology, Project administration, Supervision, Validation, Writing – review & editing.

Funding

The author(s) declare financial support was received for the research, authorship, and/or publication of this article. The authors would like to acknowledge the support received from the National Natural Science Foundation of China (grant number 31000069) and the Key Project on Social Development of Science and Technology in Shaanxi Province (grant number 2017ZDXM-SF-105).

Conflict of interest

The authors declare that the research was conducted in the absence of any commercial or financial relationships that could be construed as a potential conflict of interest.

Publisher's note

Supplementary material

The Supplementary material for this article can be found online at: https://www.frontiersin.org/articles/10.3389/fmicb.2023.1277709/full#supplementary-material

References

Al, H. F., Belhaj, H., and Al, D. M. (2022). CO_2 sequestration overview in geological formations: trapping mechanisms matrix assessment. *Energies* 15:7805. doi: 10.3390/en15207805

Ali, M. F., Mukhtar, H., and Dufossé, L. (2023). Microbial calcite inducti-on: a magic that fortifies and heals concrete. *Environ. Sci. Technol.* 20, 1113–1134. doi: 10.1007/s13762-022-03941-2

Bertelli, C., Gray, K. L., Woods, N., Lim, A. C., Tilley, K. E., Winsor, G. L., et al. (2022). Enabling genomic island prediction and comparison in multiple genomes to investigate bacterial evolution and outbreaks. *Microb. Genom.* 8:000818. doi: 10.1099/mgen.0.000818

Bhutange, S. P., Latkar, M. V., and Chakrabarti, T. (2020). Studies on efficacy of biocementation of cement mortar using soil extract. *Clean. Product.* 274:122687. doi: 10.1016/j.jclepro.2020.122687

Delcher, A. L., Bratke, K. A., Powers, E. C., and Salzberg, S. L. (2007). Identifying bacterial genes and endosymbiont DNA with glimmer. *Bioinformatics* 23, 673–679. doi: 10.1093/bioinformatics/btm009

Diez-Marulanda, J. C., and Brandao, P. F. B. (2023). Isolation of urease-producing bacteria from cocoa farms soils in Santander, Colombia, for cadmium remediation. *3 Biotech* 13:98. doi: 10.1007/s13205-023-03495-1

Gupta, S., Thapliyal, P., Shah, V., and Daverey, A. (2022). Optimization of bio-calcification process for a newly isolated urease producing bacterial strain Advenelle sp. AV1. *Geomicrobiol J.* 39, 242–248. doi: 10.1080/01490451.2021.1980920

Jiang, L. H., Liu, X. D., Yin, H. Q., Liang, Y. L., Liu, H. W., Miao, B., et al. (2020). The utilization of biomineralization technique based on microbial induced phosphate precipitation in remediation of potentially toxic ions contaminated soil: a mini review. *Ecotoxicol. Environ. Saf.* 191:110009. doi: 10.1016/j.ecoenv.2019.110009

Jin, D., Zhao, S. G., Zheng, N., Bu, D. P., Beckers, Y., and Denman, S. E. (2017). Differences in Ureolytic bacterial composition between the rumen Digesta and Rumen Wall based on ureC gene classification. *Front. Microbiol.* 8:385. doi: 10.3389/fmicb.2017.00385

Kappaun, K., Piovesan, A. R., Carlini, C. R., and Ligabue-Braun, R. (2018). Ureases: historical aspects, catalytic, and non-catalytic properties - a review. *Adv. Res..* 13, 3–17. doi: 10.1016/j.jare.2018.05.010

Karimifard, S., and Alavi, M. M. R. (2019). Corrigendum to "application of response surface methodology in physicochemical removal of dyes from wastewater: a critical review". *Sci. Total Environ.* 650:696. doi: 10.1016/j.scitotenv.2018.08.435

Keykha, H. A., Asadi, A., Huat, B. B. K., and Kawasaki, S. (2019). Microbial induced calcite precipitation by Sporosarcina pasteurii and *Sporosarcina aquimarina*. *Environ. Geotechn.* 6, 562–566. doi: 10.1680/jenge.16.00009

Koren, S., Walenz, B. P., Berlin, K., Miller, J. R., Bergman, N. H., and Phillippy, A. M. (2017). Canu: scalable and accurate long-read assembly via adaptive k-mer weighting and repeat separation. *Genome Res.* 27, 722–736. doi: 10.1101/gr.215087.116

Krajewska, B. (2018). Urease-aided calcium carbonate mineralization for engineering applications: a review. *Adv. Res.* 13, 59–67. doi: 10.1016/j.jare.2017.10.009

Kumar, P., and Kumar, N. (2021). Process optimization for production of biodiesel from orange peel oil using response surface methodology. *Energy Sourc. Recov. Utiliz. Environ. Eff.* 43, 727–737. doi: 10.1080/15567036.2019.1631909

Leeprasert, L., Chonudomkul, D., and Boonmak, C. (2022). Biocalcifying potential of Ureolytic Bacteria isolated from soil for biocementation and material crack repair. *Microorganisms* 10, 963. doi: 10.3390/microorganisms10050963

Liu, Y., Ali, A., Su, J. F., Li, K., Hu, R. Z., and Wang, Z. (2023). Microbial-induced calcium carbonate precipitation: influencing factors, nucleation pathways, and application in waste water remediation. *Sci. Total Environ.* 860:160439. doi: 10.1016/j.scitotenv.2022.160439

Liu, J., Li, G., and Li, X. A. (2021). Geotechnical engineering properties of soils solidified by Microbially induced $CaCO_3$ precipitation (MICP). *Adv. Civil Eng.* 2021, 1–21. doi: 10.1155/2021/6683930

Liu, X. G., Qi, G. B., Wu, M., Pan, Y. T., and Liu, B. (2021). Universal fluorescence light-up gram-staining technique for living bacterial differentiation. *Chem. Mater.* 33, 9213–9220. doi: 10.1021/acs.chemmater.1c02817

Lv, C., Tang, C. S., Zhang, J. Z., Pan, X. H., and Liu, H. (2023). Effects of calcium sources and magnesium ions on the mechanical behavior of MICP-treated calcareous sand: experimental evidence and precipitated crystal insights. *Acta Geotech.* 18, 2703–2717. doi: 10.1007/s11440-022-01748-6

Mohan, N., Palangadan, R., Fernandez, F. B., and Varma, H. (2018). Preparation of hydroxyapatite porous scaffold from a 'coral-like' synthetic inorganic precursor for use as a bone substitute and a drug delivery vehicle. *Biomat. Adv.* 92, 329–337. doi: 10.1016/j.msec.2018.06.064

Moro, C. F., Nogueira, F. C. S., Almeida, C. G. M., Real-Guerra, R., Dalberto, P. F., Bizarro, C. V., et al. (2022). One enzyme, many faces: urease is also canatoxin. *J. Biomol. Struct. Dyn.* 12, 1–12. doi: 10.1080/07391102.2022.2158938

Naz, F., Kanwal, Latif, M., Salar, U., Khan, K. M., Al-Rashida, M., et al. (2020). 4-Oxycoumarinyl linked acetohydrazide Schiff bases as potent urease inhibitors. *Bioorg. Chem.* 105:104365. doi: 10.1016/j.bioorg.2020.104365

Ortega, V. E., Gudino, G. M., and Palma, C. A. (2020). Microbiologically induced carbonate precipitation in the restoration and conservation of cultural heritage materials. *Molecules* 25, 5499. doi: 10.3390/molec-ules25235499

Pakbaz, M. S., Behzadipour, H., and Ghezelbash, G. R. (2018). Evaluation of shear strength parameters of Sandy soils upon microbial treatment. *Geomicrobiol J.* 35, 721–726. doi: 10.1080/01490451.2018.1455766

Peng, J., Cao, T. C., He, J., Dai, D., and Tian, Y. M. (2022). Improvement of coral sand with MICP using various calcium sources in sea water environment. *Front. Phys.* 10:825409. doi: 10.3389/fphy.2022.825409

Qian, C. X., Ren, X. W., Rui, Y. F., and Wang, K. (2021). Characteristics of bio-CaCO3 from microbial bio-mineralization with different bacteria species. *Biochem. Eng. J.* 176:108180. doi: 10.1016/j.bej.2021.108180

Qian, C. X., Yu, X. N., and Wang, X. (2018). Potential uses and cementing mechanism of bio-carbonate cement and bio-phosphate cement. *AIP Adv.* 8, 095224. doi: 10.1063/1.5040730

Song, M. Z., Ju, T. Y., Meng, Y., Han, S. Y., Lin, L., and Jiang, J. G. (2022). A review on the applications of microbially induced calcium carbonate precipitation in solid waste treatment and soil remediation. *Chemosphere* 290:133229. doi: 10.1016/j.chemosphere.2021.133229

Tang, C. S., Yin, L. Y., Jiang, N. J., Zhu, C., Zeng, H., Li, H., et al. (2020). Factors affecting the performance of microbial-induced carbonate precipitation (MICP) treated soil: a review. *Environ. Earth Sci.* 79:94. doi: 10.1007/s12665-020-8840-9

Uyar, E., and Avcı, T. (2023). Screening and molecular identification of biosurfactant/bioemulsifier producing bacteria from crude oil contaminated soils samples. *Biologia* 78, 2179–2193. doi: 10.1007/s11756-023-01330-9

Van, P. L. A., Harkers, M. P., van Zwieten, G. A., van der Zon, W. H., and van der Star, W. R. L. (2010). Quantifying biomediated ground improvement by ureolysis: large-scale biogrout experiment[J]. *Geotech. Geoenviron. Eng.* 136, 1721–1728. doi: 10.1061/(asce)gt.1943-5606.0000382

Wang, Z., Li, J., Wu, W. J., Zhang, D. J., and Yu, N. (2021). Multitemperature parameter optimization for fused deposition modeling based on response surface methodology. *AIP Adv.* 11, 055315. doi: 10.1063/5.0049357

Wang, R. S., Sun, C., Xiu, S. C., Liang, D. M., and Li, B. (2022). Study of machiningparameters in reciprocating magnetorheological polishing process based on response surface methodology. *Indus. Lubric. Tribol.* 74, 1007–1014. doi: 10.1108/ILT-04-2022-0141

Wang, Z. J., Zhang, J. X., Li, M., Guo, S. J., Zhang, J. Q., and Zhu, G. L. (2022). Experimental study of microorganism-induced calcium carbonate precipitation to solidify coal gangue as backfill materials: mechanical properties and microstructure. *Environ. Sci. Pollut. Res.* 29, 45774–45782. doi: 10.1007/s11356-022-18975-9

Wu, F., Li, S. P., He, Y. L., Song, M. T., Ma, F. L., Teng, X., et al. (2023). Optimized design and performance of pre-cutting vibrating sugarcane sett metering device. *Sugar Tech.* 25, 210–222. doi: 10.1007/s12355-022-01168-6

Xu, F. L., and Wang, D. X. (2023). Review on soil solidification and heavy metal stabilization by microbial-induced carbonate precipitation (MICP) technology. *Geomicrobiol J.* 40, 503–518. doi: 10.1080/01490451.2023.2208113

Xu, Y. Y., Wei, F. D., Xu, R., Cheng, T., and Ma, Y. L. (2022). Characterization and genomic analysis of a nitrate reducing bacterium from shale oil in the Ordos Basin and the associated biosurfactant production. *Environ. Chem. Eng.* 10:108776. doi: 10.1016/j.jece.2022.108776

Yi, H. H., Zheng, T. W., Jia, Z. R., Su, T., and Wang, C. G. (2021). Study on the influencing factors and mechanism of calcium carbonate precipitateon induced by urease bacteria. *Cryst. Growth* 564:126113. doi: 10.1016/j.jcrysgro.2021.126113

Yoo, A., Lin, M. S., and Mustapha, A. (2021). Zinc oxide and silver nanoparticle effects on intestinal Bacteria. *Materials* 14, 2489. doi: 10.3390/ma14102489

Yu, X. N., He, Z. H., and Li, X. Y. (2021). Bio-cement-modified construction materials and their performances. *Environ. Sci. Pollut. Res.* 29, 11219–11231. doi: 10.1007/s11356-021-16401-0

Zhang, K., Tang, C. S., Jiang, N. J., Pan, X. H., Liu, B., Wang, Y. J., et al. (2023). Microbial-induced carbonate precipitation (MICP) technology: a review on the fundamentals and engineering applications. *Environ. Earth Sci.* 82:229. doi: 10.1007/s12665-023-10899-y

Zhao, Y., Xiao, Z. Y., Lv, J., Shen, W. Q., and Xu, R. C. (2019). A novel approach to enhance the urease activity of Sporosarcina pasteurii and its application on microbial-induced calcium carbonate precipitation for sand. *Geomicrobiol J.* 36, 819–825. doi: 10.1080/01490451.2019.1631911

Zheng, T. W., Yi, H. H., Zhang, S. Y., and Wang, C. G. (2020). Preparation and formation mechanism of calcium carbonate hollow microspheres. *Crys. Growth* 549:125870. doi: 10.1016/j.jcrysgro.2020.125870

Zheng, T. W., Zhang, X., and Yi, H. H. (2019). Spherical vaterite microspheres of calcium carbonate synthesized with poly (acrylic acid) and sodium dodecyl benzene sulfonate. *Crys. Growth* 528:125275. doi: 10.1016/j.jcrysgro.2019.125275

frontiers | Frontiers in Microbiology

TYPE Original Research
PUBLISHED 24 November 2023
DOI 10.3389/fmicb.2023.1276065

OPEN ACCESS

EDITED BY
Zifang Chi,
Jilin University, China

REVIEWED BY
Jiuling Li,
The University of Queensland, Australia
Sai Xu,
Nanjing University of Science and Technology, China

*CORRESPONDENCE
Zhuo-Yi Zhu
✉ zhu.zhuoyi@sjtu.edu.cn

RECEIVED 11 August 2023
ACCEPTED 19 October 2023
PUBLISHED 24 November 2023

CITATION
Li J, Zhu Z-Y, Yang Z, Li W, Lv Y and Zhang Y (2023) Soil microorganisms and methane emissions in response to short-term warming field incubation in Svalbard. *Front. Microbiol.* 14:1276065. doi: 10.3389/fmicb.2023.1276065

Soil microorganisms and methane emissions in response to short-term warming field incubation in Svalbard

Jiakang Li[1,2], Zhuo-Yi Zhu[1,3]*, Zhifeng Yang[4], Weiyi Li[5], Yongxin Lv[1,2] and Yu Zhang[1]

[1]Shanghai Key Laboratory of Polar Life and Environment Sciences, School of Oceanography, Shanghai Jiao Tong University, Shanghai, China, [2]School of Environmental Science and Engineering, Shanghai Jiao Tong University, Shanghai, China, [3]MNR Key Laboratory for Polar Science, Polar Research Institute of China, Shanghai, China, [4]Department of Microbiology and Plant Biology, University of Oklahoma, Norman, OK, United States, [5]School of Life Sciences and Biotechnology, Shanghai Jiao Tong University, Shanghai, China

Introduction: Global warming is caused by greenhouse gases (GHGs). It has been found that the release of methane (CH_4) from Arctic permafrost, soil, ocean, and sediment is closely related to microbial composition and soil factors resulting from warming over several months or years. However, it is unclear for how long continuous warming due to global warming affects the microbial composition and GHG release from soils along Arctic glacial meltwater rivers.

Methods: In this study, the soil upstream of the glacial meltwater river (GR) and the estuary (GR-0) in Svalbard, with strong soil heterogeneity, was subjected to short-term field incubation at 2°C (*in situ* temperature), 10°C, and 20°C. The incubation was carried out under anoxic conditions and lasted for few days. Bacterial composition and CH_4 production potential were determined based on high-throughput sequencing and physiochemical property measurements.

Results: Our results showed no significant differences in bacterial 16S rRNA gene copy number, bacterial composition, and methanogenic potential, as measured by mcrA gene copy number and CH4 concentration, during a 7- and 13-day warming field incubation with increasing temperatures, respectively. The CH_4 concentration at the GR site was higher than that at the GR-0 site, while the *mcrA* gene was lower at the GR site than that at the GR-0 site.

Discussion: Based on the warming field incubation, our results indicate that short-term warming, which is measured in days, affects soil microbial composition and CH_4 concentration less than the spatial scale, highlighting the importance of warming time in influencing CH_4 release from soil. In summary, our research implied that microbial composition and CH_4 emissions in soil warming do not increase in the first several days, but site specificity is more important. However, emissions will gradually increase first and then decrease as warming time increases over the long term. These results are important for understanding and exploring the GHG emission fluxes of high-latitude ecosystems under global warming.

KEYWORDS

Arctic soil, warming, field incubation, microorganisms, methane

1 Introduction

Arctic terrestrial ecosystems currently store the largest amounts of carbon in the high-latitude regions of the Earth. Over the last 30 years, the temperature levels of these regions have risen twice as fast as the global average, at 0.6°C per decade (Cohen et al., 2014; Schuur et al., 2015). It is a robust phenomenon known as Arctic amplification (Fengmin et al., 2019). The soil microorganisms play an important role in converting carbon compounds into organic or inorganic compounds, and their metabolic rate increases due to warming. When microbes break down organic carbon, they release greenhouse gases (GHGs) such as carbon dioxide (CO_2), nitrous oxide (N_2O), and methane (CH_4), leading to global climate change (Mehmood et al., 2020; Marushchak et al., 2021). In the past 800,000 years, the levels of atmospheric CO2, N2O, and CH4 have increased significantly. The current levels of these gases are 390.5 parts per million (ppm) for CO_2, 390.5 parts per billion (ppb) for N_2O, and 1,803.2 ppb for CH_4, and these levels are, respectively, 40, 20, and 150% higher than they were before the industrial era (Tian et al., 2016; Mehmood et al., 2020). CH_4, the second most important GHG after CO_2, accounts for at least 20% of the anthropogenic radiative forcing of warming agents since the preindustrial era. Moreover, the greenhouse effect of CH_4 is 28 times that of CO_2 in 100 years (Tian et al., 2016; Ganesan et al., 2019; Hui et al., 2020). In the Arctic region, CH_4 emissions range from 15 to 50 Tg/yr, as estimated by biogeochemistry models and atmospheric inversions between 2000 and 2017 (Saunois et al., 2016, 2020). Due to Arctic amplification, global climate change will lead to Arctic soil warming and CH_4 emissions. However, the duration of the impact of warming on the CH_4 release from the soil, causing climate change, is yet undiscovered.

Microbial metabolic processes have long been the key drivers and responders to climate change (Singh et al., 2010). According to research findings, different soil microorganisms produce GHGs through different metabolic pathways related to microbial composition, providing an improved understanding of GHG emissions. For example, most soil microorganisms contribute greatly to CO_2 emissions through decomposition and heterotrophic respiration (Watts et al., 2021). Similar to CO_2 emissions, biotic CH_4 emissions are controlled by soil microbial methanogenesis and CH_4 oxidation from the soil, lake, and other terrestrial places, especially Arctic soil (Nazaries et al., 2013; Tveit et al., 2013; Hamdan and Wickland, 2016; Knoblauch et al., 2018; Galera et al., 2023). Microbial methanogenesis is a process carried out by a group of anaerobic methanogenic archaea (Song et al., 2021). While the other microorganisms can catabolize CH_4, thus easing the release of CH_4 into the atmosphere, microbial methanogenesis contributes greatly to global CH_4 emissions, and understanding its response to warming time is fundamental to predicting the feedback between potent GHGs and climate change (Lee et al., 2012; Chen et al., 2020). Moreover, the microbial composition was expected to change under long-term warming measured by years (Deslippe et al., 2012; Pold et al., 2021; Zosso et al., 2021; Rijkers et al., 2022; Zhou et al., 2023). Meanwhile, biotic CH_4 emissions are also caused by warming through long-term microbial fermentation (Altshuler et al., 2019; Hui et al., 2020; Zhang et al., 2021). However, climate change is a process that accumulates over time; therefore, the duration of its impact on the environment is unknown. All global climate processes are based on and originate from short-term climate changes. Short-term processes start all long-term processes, and the feedback of short-term processes is more rapid and direct. Long-term processes are the net effect of accumulation and comprehensive influence of many short-term processes. Nevertheless, an analysis of microbial composition and CH_4 emissions due to short-term warming, measured in days, will help us understand the effects of warming on releasing greenhouse gases from the soil.

In addition to temperature and microbial control, soil characteristics, such as moisture, oxygen concentration, and vegetation types (substrates), are recognized as important drivers of the CH_4 emission fluxes (Nazaries et al., 2013; Voigt et al., 2019; Song et al., 2021). Warming can affect carbon emissions by altering the concentration of nutrients and the rate of decomposition of organic matter (Pareek, 2017). Simultaneously, soil moisture is closely related to the aerobic/anoxic boundary and may also vary with the evapotranspiration stimulated by warming, which eventually affects aerobic respiration and anaerobic methanogenesis (Zhang et al., 2023b). Consequently, wetter areas caused by future climate conditions will have higher moisture content, creating anaerobic conditions that increase CH_4 production and, at the same time, reduce CH_4 consumption by reducing O_2 production (Singh et al., 2010; Lawrence et al., 2015). Treat et al. (2014) found that, in terms of active-layer thickness, CO_2 and CH_4 emissions from peat depth ranged from 77% greater than to not significantly different from permafrost depths. This variation depends on the peat type and peat decomposition stage rather than the thermal state, as determined through an incubation experiment. However, few studies have examined the impact of these environmental factors on GHG emissions, particularly CH_4 emissions over warming periods in the Arctic.

Current studies about GHG emissions under Arctic soil warming focus on GHG release from soil affected by environmental factors (Elberling et al., 2008; Tian et al., 2016) and novel microbial communities (Wartiainen et al., 2003, 2006), which have been researched in the western Canadian Arctic (Barbier et al., 2012; Martineau et al., 2014). Few studies were carried out in Svalbard, except for the Ny-Alesund region (Tveit et al., 2015; Newsham et al., 2022). As mentioned previously, CH_4 emissions are affected by vegetation type, soil substrates, and moisture. Correspondingly, the soil of the Svalbard Glacier basin has great heterogeneity (Son and Lee, 2022). For example, corresponding to the Ny-Alesund tundra landform, the Barentsburg region has higher vegetation coverage and longer glacial meltwater rivers (nearly 10 km) than the Ny-Alesund Bay River (about 3 km). Temperatures in Svalbard's topsoil can reach more than 10°C and even approach 20°C in summer (Cappelletti et al., 2022; Magnani et al., 2022). Therefore, short-term warming experiments can provide a foundation for studying the effects of warming on the microbial composition and GHG release from the soil in Barentsburg.

Based on the background, warming and anoxic field experiments in this study were carried out with the glacial meltwater river soil around Barentsburg for 7 and 13 days. The short-term warming was explored from the changes in the bacterial 16S rRNA gene copy number and composition, abundance of

CH_4-producing genes, and CH_4 concentration in the soil, which affects bacterial diversity and CH_4 emissions. From the perspective of incubation experiments, this study revealed the relationship between short-term warming and CH_4 release from the soil near the upstream and estuary of the glacial meltwater river in Barentsburg.

2 Materials and methods

2.1 Soil samples and incubation experiments

We collected samples from the two sites near Barentsburg during July and August of 2018. One sample was collected from the soil (GR, 15°5′23.100"E, 77°58′39.173"N) upstream of the glacial meltwater river, while the other was taken from the soil (GR-0, 14°20′24.601"E, 78°1′29.143"N) at the estuary of the glacier meltwater river (Figure 1A) at 2°C. While in the field, we placed approximately 46 g of soil into 20 mL brown serum bottles (223762, Wheaton, USA) with a stopper and incubated them at three temperatures (2°C, 10°C, and 20°C). Bottles were filled to full, leaving no space with oxygen. After incubation, sacrificial sampling was taken on 0, 1, 3, 5, 7, and 13 days. The sample ID was named (GR/GR-0)-X-Y, where X represents the number of incubation days while Y represents the incubation temperature levels. Temperature readings were recorded at the *in situ* temperature of 2°C on days 1–3, 10°C on days 4–6, and 20°C on days 7–9. Approximately 8 g of the soil was stored in a Nasco Whirl-Pak sample bag (B01062WA, Nasco, USA) for measuring environmental parameters, and approximately 32 g of the soil was added into a 50 mL centrifuge tube with 20 mL RNA later (AM7021, Invitrogen, USA) for determining the composition of the microorganism community at 20°C. However, 3 mL of 2 mol/L NaOH was added to a 20-mL serum bottle along with 5 g soil for determining CH_4 concentration and stored at 4°C (Figure 1B).

2.2 Bacterial community analyses

The genomic DNA of six initial samples and 81 incubation samples stored in RNAlater at −20°C was extracted from approximately 0.5 g fresh, homogenized soil using the FastDNA® SPIN Kit for Soil (116560200, MP Biomedicals, USA). Before following the manufacturer's instructions, all the samples were washed with 1×PBS twice and centrifuged at 12,000×g for 5 min. The DNA concentration was then measured using a NanoDrop 2000 spectrometer (Thermo Fisher Scientific, USA). The V4 region of the bacterial 16S rRNA gene was amplified using the primers 533F (5′-TGCCAGCAGCCGCGGTAA-3′) and Bact 806R (5′-GGACTACHVGGGTWTCTAAT-3′) (Klindworth et al., 2012; Zhang et al., 2020) with an 8-bp unique barcode at the forward primer. The PCR procedure was performed in 50 μL reactions, which were repeated three times for increased accuracy. The thermal cycling conditions for the bacterial 16S *rRNA* gene involved an initial denaturation at 94°C for 5 min, followed by 25 cycles of denaturation at 94°C for 30 s, annealing at 58°C for 40 s, and extension at 72°C for 30 s with a final extension at 72°C for 10 min. The PCR products were gel-purified using an EZNA Gel Extraction Kit (Omega Bio-Tek, Inc., USA). The sequencing of purified DNA on the Illumina MiSeq platform was performed by the Personalbio Biotechnology company in Shanghai, China.

The analysis used the pipeline QIIME2 (version 2022.2) (Bolyen et al., 2019). First, the partial region was extracted using the corresponding primer set from the sequences in the SILVA (version 138) database and was used to train a classifier using the "feature-classifier" plugin. Then, all the datasets were grouped by the primer. After trimming of the corresponding primer, the sequencing quality of the raw reads was manually assessed to determine the appropriate truncated position for filtering low-quality regions. Paired-end reads were merged and dereplicated using the "dada2" plugin. Unassigned or eukaryotic ASVs were removed and the remaining ASVs were classified using the trained classifier.

2.3 Prepared templates for qPCR standard curves

The 16S *rRNA* gene copy number of bacteria was quantified by real-time quantitative polymerase chain reaction (qPCR) using bac341f (5′-CCTACGGGWGGCWGCA-3′) and prokaryotic 519r (5′-TTACCGCGGCKGCTG-3′) (Jorgensen et al., 2012). Abundances of the methyl Coenzyme M reductase subunit A (*mcrA*) gene in these river sediments were estimated by qPCR. The DNA fragments encoding the *mcrA* gene were amplified using PCR with the universal primers mlas-mod-F (5′-GGYGG TGTMGGDTTCACMCARTA-3′) and mcrA-rev-R (5′-CGTTCA TBGCGTAGTTVGGRTAGT-3′) (Angel et al., 2012). The program used in this procedure involved heating the sample at a temperature of 98°C for 3 min, followed by 40 heating cycles for 15 s at 98°C, 20 s at 58°C, and 30 s of extension at 72°C. Finally, a final elongation step was performed at 72°C for 10 min. The PCR products were purified using a gel extraction kit (DP219-02, TIANGEN, China). The purified PCR products (10 μL) mixed with 2×Taq PCR Mix (B639295, Sangon Biotech, China) in equal amounts at 72°C for 30 min were added to the end of the sequence. Then, 4 μL of the sequence solution was mixed with 5 μL of solution I and 1 μL pMD18-T vector provided by the pMD 18-T Vector Cloning Kit (6601, TAKARA, Japan). In total, 10 μL of the mixture was incubated at 16°C for 30 min. Then, a vial of DH5α competent cells (CD201-02, Trans, China) was thawed on ice. A 10-μL reaction mixture was added to 50 μL of DH5α competent cells and incubated on ice for 30 min after gentle mixing. The sample was heat shocked for 45 s at 42°C and then chilled on ice for 2 min. Then, 1 mL of Lysogeny broth (LB, tryptone 10 g/L, yeast extract 5 g/L, NaCl 10 g/L) medium was added from the competent cells kit to the transfected cells, followed by sample incubation at 37°C with shaking speed of 200×RPM for 1 h. Then, the samples were centrifuged at 1,500×g for 5 min, and 800 μL of the supernatant was removed from the tube. The cells were resuspended in the rest of the medium and then spread onto the solid LB medium with 100 μg/mL of ampicillin. The plate was incubated at 37°C overnight in an inverted position. Single colonies were selected for PCR with primers. The plasmid was extracted by DiaSpin plasmid DNA mini kit (B110091, Sangon Biotech, China).

10.3389/fmicb.2023.1276065

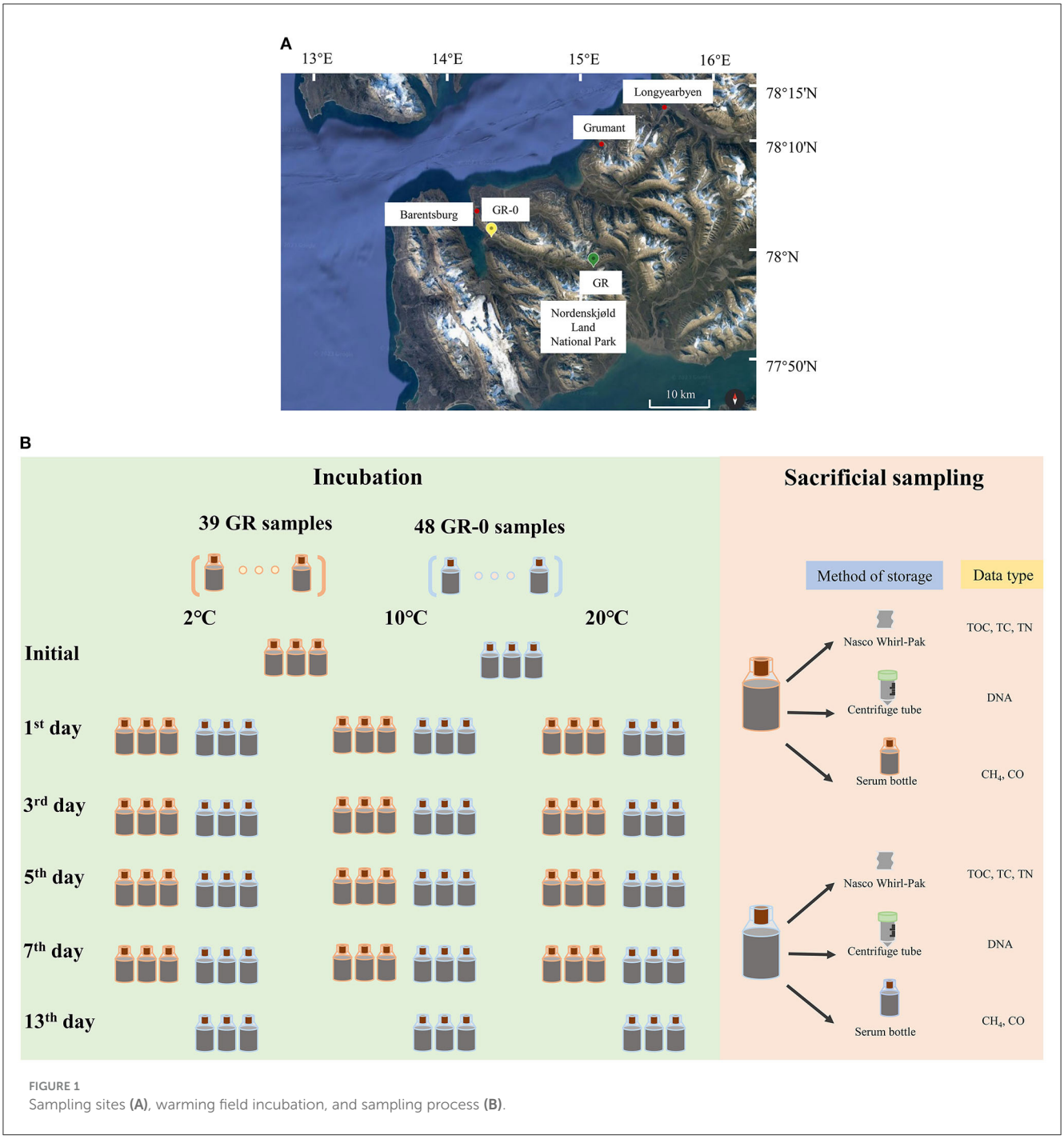

FIGURE 1
Sampling sites **(A)**, warming field incubation, and sampling process **(B)**.

The concentration of the plasmid extract was measured using a NanoDrop 2000 spectrometer (NanoDrop 2000/2000C, Thermo Fisher Scientific, USA).

2.4 Gene quantification performed by qPCR

This template used in qPCR for 16S rRNA and *mcrA* gene quantification is the incubation samples. Each reaction contained 20 μL 2×PowerUp™ SYBR Master Mix (A25742, Applied Biosystems, USA), 2 μL of template DNA, and 1 μL of each forward and reverse primer. The standard curve consisted of a diluted known amount of purified PCR product obtained from plasmid DNA using the bacterial 16S rRNA gene-specific primers bac341f/519r between 10^3 and 10^9 copies/μL. The amplification efficiency was between 90–110%, and the R^2 of the standard curve was above 0.90. The thermal cycle program was for 2 min at 50°C and 3 min at 98°C, followed by 40 cycles for 15 s at 98°C, 30 s at 55°C, and 30 s at 72°C. The standard curve consisted of a known amount of diluted purified PCR product obtained from plasmid DNA using the *mcrA* gene-specific primers mlas-mod-F/mcrA-rev-R between 10^2 and 10^7 copies/μL. The thermal cycling conditions

were followed by heating at 50°C for 2 min, 98°C for 3 min, followed by 40 cycles of heating at 98°C for 30 s, 58°C for 40 s, and 72°C for 30 s. Three replicates were performed for each sample, and the statistical analysis was performed using Student's *t*-test.

2.5 Environmental parameter determination

The soil was first freeze-dried, ground, and sieved. After removing the inorganic carbon from the soil using HCl and re-drying the samples, the organic carbon content (total carbon and total organic carbon) was measured using an element analyzer (Vario EL *III*, Elementar, Germany). The procedure for measuring the total nitrogen content was similar but lacked the reaction with acid. Based on repeated determinations, the detection limits for carbon and nitrogen were 8 μg, with a precision better than 6%. The soil samples used in the above parameters were stored at −20°C. The CH_4 and CO concentrations in the 20 mL serum bottle headspace were measured on a gas chromatograph with a flame ionization detector (GC-FID, GC-14B, Shimadzu, Japan) (Treat et al., 2014). For gas estimation, each gas sample (1 mL) was manually injected using an airtight syringe (81356, Hamilton, Switzerland). The CH_4 and CO concentrations in the sample were calculated by external calibration using a certified gas mixture with 50% CH_4 and 50% CO. The CH_4 and CO gas peaks were identified based on the retention time of standard CH_4 and CO gases. The response factor obtained was used to calculate the CH_4 and CO percentages in the incubation samples.

3 Results

3.1 Bacterial 16S rRNA gene copy numbers and diversity composition

The copy numbers of the bacterial 16S rRNA gene fragments in each DNA fraction were quantified by qPCR. The amplification efficiency ranged between 90 and 110%. At the GR site where the soil was incubated at 2°C (*in situ* temperature. Figure 2A), the average bacterial 16S rRNA gene copy numbers increased from 5.06 × 10^7 copies/g to 9.73 × 10^8 copies/g on Day 7. It increased from 5.06 × 10^7 copies/g to 1.17 × 10^9 copies/g on the 5th day at 10°C and from 5.06 × 10^7 copies/g to 1.97 × 10^9 copies/g on Day 5 at 20°C. The bacterial 16S rRNA gene copy numbers peaked on the 5th day at 10°C and 20°C, compared to those incubated at 2°C. At the GR-0 site where the soil was incubated at 2°C (Figure 2B), the average bacterial 16S *rRNA* gene copy numbers increased from 5.37 × 10^8 copies/g to 4.78 × 10^9 copies/g on Day 7. It increased from 5.37 × 10^8 copies/g to 4.01 × 10^9 copies/g on Day 7 at 10°C and to 2.93 × 10^9 copies/g on Day 7 at 20°C. However, the average bacterial 16S rRNA gene copy numbers increased at 2°C, 10°C, and 20°C with an increase in incubation time. In summary, the shift in bacterial 16S rRNA gene copy numbers of 39 GR and 48 GR-0 soil samples had no obvious difference with an increase in incubation temperatures: As the value of the Student's *t*-test is higher than 0.05, there was no significant difference.

Bacterial community composition was determined for each of the 87 incubation soil samples based on the 16S rRNA gene. The results show that the proportion of high-quality sequences is between 94.56 and 98.86%. The amplicon sequence variants (ASVs) belonging to different phyla have been found in 87 incubation samples at two different sites, totaling up to 1,011,481. The taxa at the GR site were dominated by six bacterial phyla: Actinobacteria (22–61%), Proteobacteria (11–50%), Firmicutes (8–18%), Bacteroidota (3–17%), Desulfobacterota (5–10%), and Acidobacteriota (2–6%) followed by Gemmatimonadota and Chloroflexi (Supplementary Figure 1A). Actinobacteria, one of the most widely distributed phyla among soil bacteria, are well known for their ability to degrade plant residues (cellulose) (Bao et al., 2019, 2021). However, at the GR-0 site, the dominant phyla were Proteobacteria (27–65%), Actinobacteriota (8–21%), Bacteroidota (4–15%), Desulfobacterota (2–7%), Gemmatimonadota (2–5%), and Firmicutes (1–20%), followed by Acidobacteriota and Nitrospirota (Supplementary Figure 1B). Those bacterial species have been reported as dominant groups in the other Svalbard regions (Son and Lee, 2022; Tian et al., 2022). At the family level (Figure 3), the bacterial community composition of the two sites did not show any significant difference with the increase in temperature and incubation time. The Shannon diversity metrics were invariable between samples ranging from 5 to 8 (GR) and 8 to 10 (GR-0). No statistically significant difference was found between the different sample types. Based on the differences at the phylum level, the two sites show differences at the family level. At the GR site, *Intrasporangiaceae*, *Gallionellaceae*, *Sulfuricellaceae*, and *Desulfitobacteriaceae* were the dominant groups (Figure 3A). Meanwhile, at the GR-0 site, *Comamonadaceae*, *Intrasporangiaceae*, *Nitrosomonadaceae*, and *Gemmatimonadaceae* were the main groups (Figure 3B).

3.2 CH_4 production potential

To determine the abundance of methanogenic archaea, we quantified the functional gene *mcrA*, which encodes methylcoenzyme M reductase and is a key enzyme in methanogenesis (Inagaki et al., 2004). Among the incubation samples at the GR site, the average copy number of *mcrA* genes reached the maximum on the 5th day at 10°C and 20°C, reaching 3.1 × 10^5 copies/g and 3.7 × 10^5 copies/g, respectively, except for 2°C, where they did not reach the maximum before decreasing. While, at 2°C, the average copy number of *mcrA* genes decreased from 1.2 × 10^5 copies/g on the first day to 1.4 × 10^4 copies/g on Day 7 (Figure 4A). However, the concentration of CH_4 in the soil showed an increasing trend during the incubation process at all three warming temperatures. Under 2°C, the average net increase of CH_4 for 2 days (from the third- to the fifth-day incubation) was 1.3 μmol/L. Under 10°C, the average net increase of CH_4 for 2 days was 3.9 μmol/L. At 20°C, the average net increase of CH_4 was 2.4 μmol/L for 2 days (Figure 4C). Compared to GR site incubation samples, the copy number of *mcrA* genes at the GR-0 site changed irregularly (Figure 4B). In addition, the concentration of CH_4 at the GR-0 site was an order of magnitude lower than that at the GR site, and there was no substantial variation in CH_4 concentration (Figure 4D).

10.3389/fmicb.2023.1276065

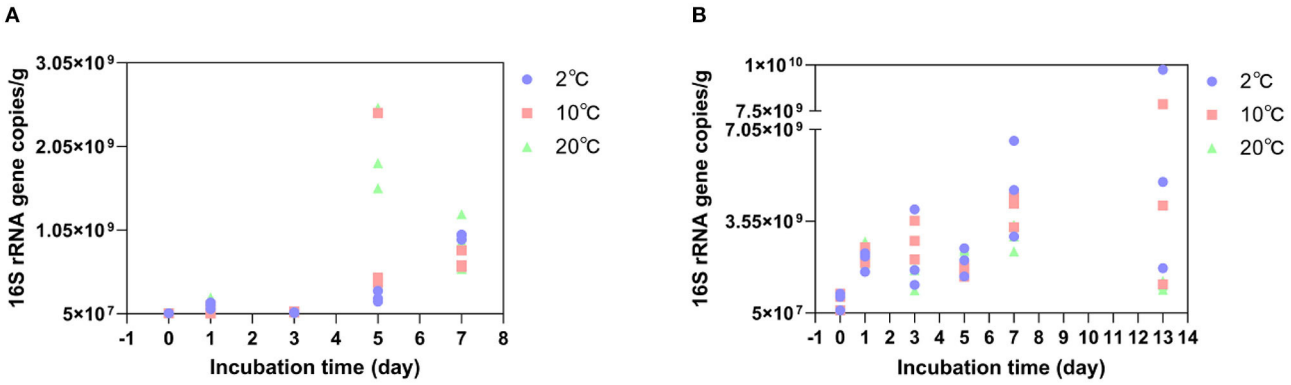

FIGURE 2
Bacterial 16S rRNA gene copy numbers change at different temperatures. **(A)** is the GR site, and **(B)** is the GR-0 site.

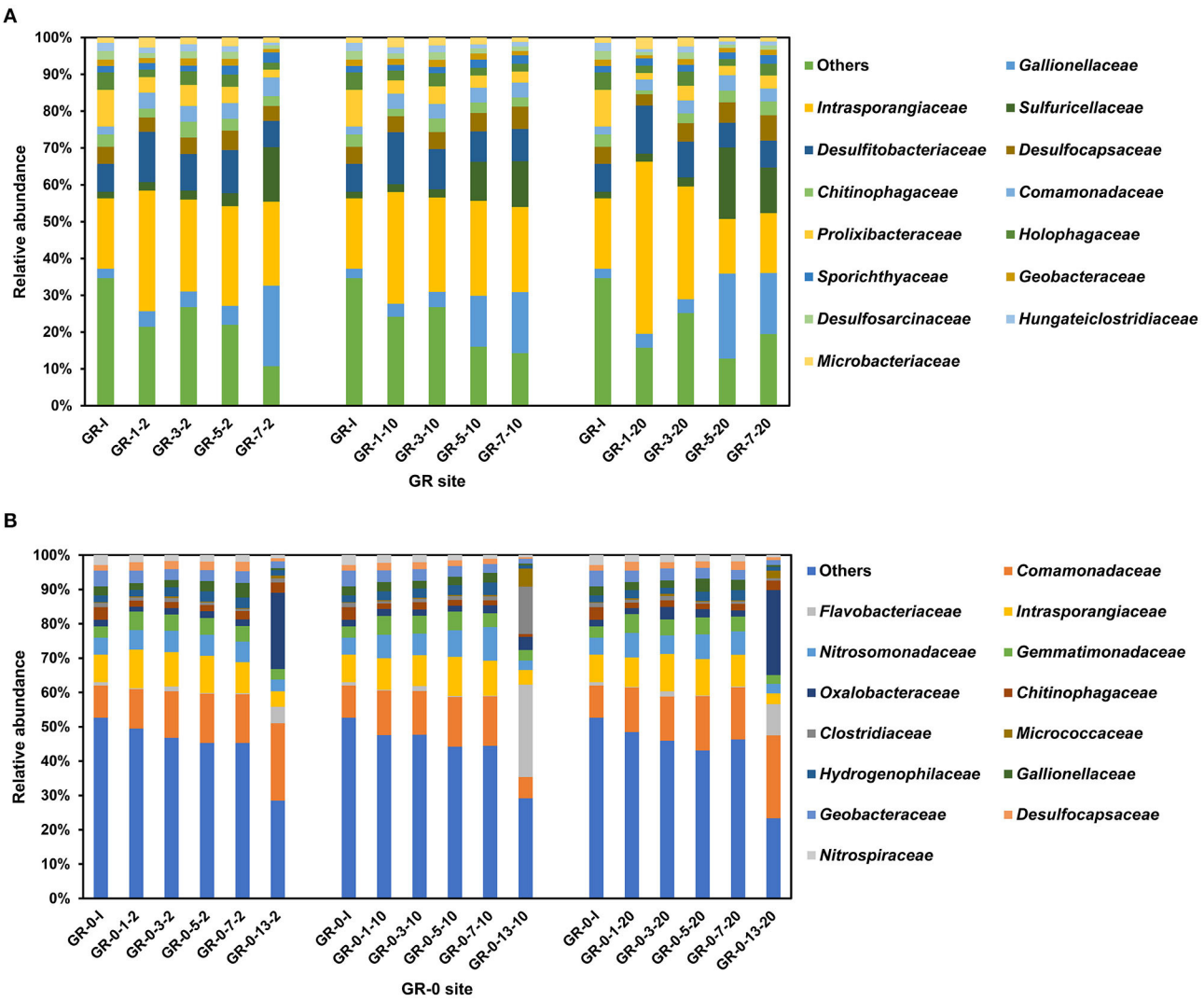

FIGURE 3
Relative abundance of bacterial community based on 16S rRNA gene at the family level. **(A)** is the GR site, and **(B)** is the GR-0 site. The first number is incubation day, and the third is incubation temperature. "I" means initial samples.

10.3389/fmicb.2023.1276065

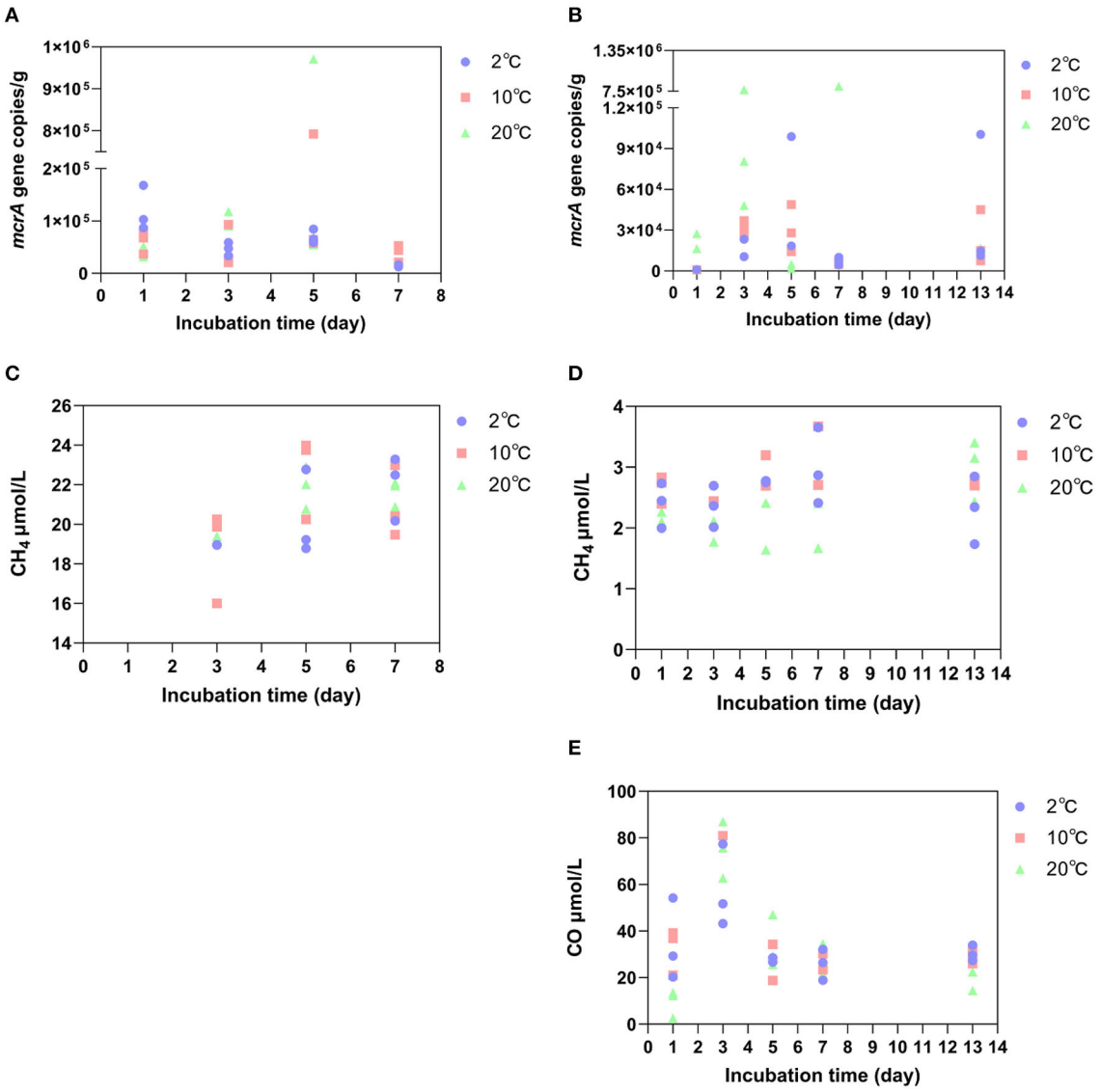

FIGURE 4
The abundance of the *mcrA* gene at the GR site **(A)** and GR-0 site **(B)**, as well as the concentration of CH_4 at the GR site **(C)** and GR-0 site **(D)**. The concentration of CO at the GR-0 site **(E)**.

3.3 Variations in temperature and soil environmental variables

When determining the gas content during the incubation period, we detected not only CH_4 gas but also carbon monoxide (CO) in incubated samples. However, it only exists at the GR-0 site. At all three different incubation temperatures, the concentration of CO was higher in the early stage of incubation (i.e., the first 3 days) and reached its maximum on the third day (Figure 4E), which was 57.4 μmol/L at 2°C, 90 μmol/L at 10°C, and 75.2 μmol/L at 20°C.

The environmental variables of the three incubation temperatures are shown in Table 1. As shown by the results, the contents of total organic carbon (TOC), total carbon (TC), and total nitrogen (TN) showed no obvious differences in the short-term warming field experiments of the GR and GR-0 soil samples. The content of TOC is between 0.8 and 1.4%, the content of TC is between 1.0 and 1.1%, and the content of TN is approximately 0.1%. In addition, the C/N ratio (TOC/TN) among incubation soil samples was <15, ranging from 7.7 to 14.2. At the GR site, the C/N ratio gradually increased to 14.2 under 20°C conditions. However, at the GR-0 site, the C/N ratio increased in the first 7 days at all three incubation temperatures and then decreased from Day 7 to Day 13. The mental test showed that soil CO ($0.2 <$ Mental's r < 0.4, Mental's $p < 0.05$), CH_4 ($0.2 <$ Mental's r < 0.4, Mental's $p < 0.01$), and TN ($0.2 <$ Mental's r < 0.4, Mental's $p < 0.05$) were the major factors affecting soil microbial composition (Supplementary Figure 2).

10.3389/fmicb.2023.1276065

TABLE 1 The average environmental value of the soil incubated at different temperatures.

Site ID	Incubation time (days)	Incubation temperature											
		2°C				10°C				20°C			
		TOC (%)	TC (%)	TN (%)	C/N ratio	TOC (%)	TC (%)	TN (%)	C/N ratio	TOC (%)	TC (%)	TN (%)	C/N ratio
GR	0	-	-	-	-	-	-	-	-	-	-	-	-
	1	1.1	1.0	0.1	10.5	0.9	1.0	0.1	8.7	0.8	1.0	0.1	7.9
	3	1.1	1.0	0.1	10.5	1.1	1.0	0.1	11.4	0.9	1.0	0.1	9.3
	5	1.2	1.0	0.1	11.3	1.1	1.0	0.1	10.9	1.2	1.0	0.1	11.3
	7	0.8	1.0	0.1	7.8	0.8	1.0	0.1	7.8	1.4	1.0	0.1	14.2
GR-0	0	0.8	1.0	0.1	8.8	0.8	1.0	0.1	8.8	0.8	1.0	0.1	8.8
	1	-	-	-	-	-	-	-	-	-	-	-	-
	3	-	-	-	-	-	-	-	-	-	-	-	-
	5	0.8	1.0	0.1	8.4	0.9	1.0	0.1	10.0	0.8	1.0	0.1	9.0
	7	1.3	1.0	0.1	14.0	1.0	1.0	0.1	11.0	1.1	1.0	0.1	11.2
	13	0.7	1.0	0.1	7.9	0.8	1.1	0.1	8.8	1.0	1.1	0.1	10.4

"-" means no data.

4 Discussion

4.1 Effects of short-term warming on microbial composition in Arctic soils

There were no changes in microbial composition during short-term soil warming, measured in days, under climate change (Figure 3). Previously, using 454 pyrosequencing of 16S rRNA genes, it was found that warming (+0.5 to 2°C) with open-top chambers for 3 years had altered the soil bacterial communities at two locations in the maritime Antarctic and one in the cool southern temperate zone, with consistent increases observed across all three locations in Alphaproteobacteria-to-Acidobacteria ratios (Yergeau et al., 2012). A study on long-term warming observed that slow-growing bacteria (K-selected), such as Gram-positive Actinobacteria, increased in dominance with warming at Toolik Lake in Alaska. This suggests that the increased dominance of these recalcitrant C-recyclers suggests a reduction in the availability of labile substrates with warming (Deslippe et al., 2012). However, a meta-analysis of field studies indicates that day, diurnal, and night warming had no effect on overall bacterial abundance, and no significant between-group heterogeneity was found for various measurement methods (Chen et al., 2015). Our results showed that no matter how the temperature changed, the microbial biomass (16S rRNA gene copy number) increased during the first 7- and 13-day incubation at 2°C, 10°C, and 20°C (Figure 2). Increases in microbial biomass and activity may have happened in a short-term climate change. However, the limitation of mineral nutrients such as nitrogen may constrain this response in the long term. Such mineral limitation will affect the dominance of oligotrophic and copiotrophic microorganisms in a given ecosystem, which in turn may influence GHG fluxes (Singh et al., 2010; Romero-Olivares et al., 2017).

We clustered and analyzed the bacterial community composition through complete linkage, using the largest numerical distance between two datasets as the distance between two groups for pairwise comparison to obtain data similarity between groups. The closer the distance, the shorter the branch distance of the cluster. Our results show samples of the same incubation time clustered on a branch (Supplementary Figure 3), and the microbial composition of the two sites (GR and GR-0) differed (Figure 3). However, the bacterial community composition showed no difference during warming incubation for 7 and 13 days, with no changes in the dominant species or the relative abundance of each community (Figure 3). The influence of incubation time and location along the river on the microbial community was greater than that of incubation temperatures. Since microorganisms adapt to grow in a specific temperature range, when the temperature fluctuates within its growth range, the microbial composition will not change obviously for the short term (Rijkers et al., 2022). However, due to a series of influences, such as vegetation type, soil water content, and soil depth, the microbial composition at different sampling sites showed obvious differences after long-term domestication (Son and Lee, 2022). These findings also agree with results from other Arctic tundra climate change experiments showing a strong response of soil microbial communities to

vegetation types and spatial scale (Campbell et al., 2010; Malard et al., 2021).

Meanwhile, at the upper stream of the glacial meltwater river, Actinobacteriota is the dominant group. The average number of CAZyme enzyme genes encoded in the genome of Actinomycetes is higher, and plant-derived organic matter can be used in soils with declining soil fertility (Bao et al., 2021). This result is consistent with the utilization of terrigenous organic matter by the bacteria in the upper stream of the river. The dominant group in the glacial meltwater river's estuary is Gammaproteobacteria, belonging to Proteobacteria. The class Gammaproteobacteria is known as one of the denitrifier groups, and many species of this class are cold-adapted. It thus might be an important group to determine the capacity of Arctic rivers to remove excess nitrogen (Franco et al., 2017; Uchida et al., 2018; Qian-Qian et al., 2021). More importantly, long-term warming rather than short-term induced changes in the composition of soil microbial communities can cause sustained changes in microbial activity, resulting in soil carbon emissions.

4.2 Effects of short-term warming on CH_4 release from Arctic soils

CH_4 emissions caused by warming on microbial metabolisms may be a long-term process measured by months or years rather than several days. A meta-analysis of field studies shows that soil microbial respiration causes carbon losses by 1–5 years of warming incubation. In comparison, it suggests that soil carbon losses decrease after long-term warming, especially after 10 years (Romero-Olivares et al., 2017). In addition, studies have documented changes in the CH_4 concentration of the Lagoon Pingo surface areas from April 2016 to October 2017, with the CH_4 concentration of 906.3 μmol/L in April 2016 and 601.9 μmol/L in March 2017. However, from 6 August 2017 to 24 August 2017, CH_4 concentrations were 338.1 μmol/L and 383.1 μmol/L, respectively. It can be concluded that the CH_4 emissions do not change much in the short term (Hodson et al., 2019). It is consistent with our results that CH_4 concentration at two different sites did not change with the increase of temperature (2°C, 10°C, and 20°C) and time (7 and 13 days) during incubation (Figures 4C, D). Moreover, Alaskan tundra soils at a depth of 45–55 cm were subjected to experimental *in situ* warming by nearly 1.1°C above ambient temperature, which corresponded with a 3-fold increase in the abundance of a single archaeal clade of the *Methanosarcinales* order and accompanied a comprehensive increase in the relative abundances of methanogenesis genes after 2-month incubation (Johnston et al., 2019). A whole-soil-profile 3-year warming experiment suggests that short-term warming does not alter microbial carbon use efficiency in either surface or deep soils (Zhang et al., 2023a). In our research, methanogenic gene abundance (*mcrA* gene copy numbers) in our short-term incubation did not increase with the anoxic warming experiment (Figures 4A, B). Nevertheless, a large amount of CO was detected at the GR-0 site (Figure 4E), which may be a product of microbial fermentation or incomplete oxidation under oxygen restriction (Terry et al., 2004; Diender et al., 2015). CO, as a chemically active gas, although its direct greenhouse effect is negligible, directly oxidizes the hydroxyl radicals in the atmosphere, becoming the main sink for hydroxyl radicals and hence being beneficial for the accumulation of CH_4 in the atmosphere (Borsdorff et al., 2019).

The effect of time on warming-induced carbon losses is described as follows: the results of our 13-day warming field experiment showed that warming did not affect the CH_4 concentration and methanogenic gene abundance. In the first few weeks of temperature rise, microbial metabolisms in response to environmental changes take time to accumulate (Voolstra and Ziegler, 2020), and the amount of change in its products must also accumulate. It concluded that warming-induced changes in the microbial community in the Arctic soils over a few weeks to months would amplify the instantaneous increase in the rates of CO_2 production and thus enhance carbon losses (Hartley et al., 2008). However, declines in the response of microbial respiration to warming in long-term experiments (>5 years) suggest that microbial activity acclimates to temperature, greatly reducing the potential for enhanced carbon losses (Hartley et al., 2008). Therefore, we suggested that CH_4 emissions in the process of soil warming have no increase in the short term, and with the increase in warming time, emissions will gradually increase in the long term. On the other hand, when microorganisms adapt to warming, CH_4 emissions will gradually decrease.

4.3 The factors affecting CH_4 production in the Arctic

Many factors, such as oxygen, moisture, vegetation type, seasonal change, and temperature, affect the product of CH_4 in the Arctic. Finally, CH_4 production is closely related to microorganisms in the Arctic soil, one of the most important areas of CH_4 emissions. Some studies suggest that warming surface soil may increase CO_2 emissions, while CH_4 production is more prevalent in deeper soils (Knoblauch et al., 2021; Galera et al., 2023). As mentioned above, when considering net emissions of CH_4 in soil with the anaerobic methanogenic archaea as the source and the trophic methanogenic oxidizing bacteria as the sink, the net CH_4 production value in the soil only occurs when the two cancel out. The study indicated that CH_4 flux was more strongly influenced by long-term gradients in soil moisture and vegetation than plant biomass, species composition, or nutrient availability (Torn and Chapin, 1993). This view is consistent with our experimental results: the difference in CH_4 concentration between the GR and GR-0 sites is an order of magnitude (Figures 4C, D), which may be caused by soil moisture. One of the primary reasons for the microhabitat differences within the soil is the soil water content, where methanotrophs require oxygen and methanogens are anaerobic (Freitag et al., 2010; Galera et al., 2023).

To sum up, regardless of the influence of environmental factors, warming might take time to accumulate to affect Arctic soil microbial respiration, the main metabolic activity in Arctic soil (Nazaries et al., 2013; Tveit et al., 2013; Hamdan and Wickland, 2016; Knoblauch et al., 2018; Galera et al., 2023). It was altering GHG emission fluxes (Figure 5; accumulation period). It takes several months, even years, for GHG produced by microorganisms to be released from the soil into the atmosphere, so there is a

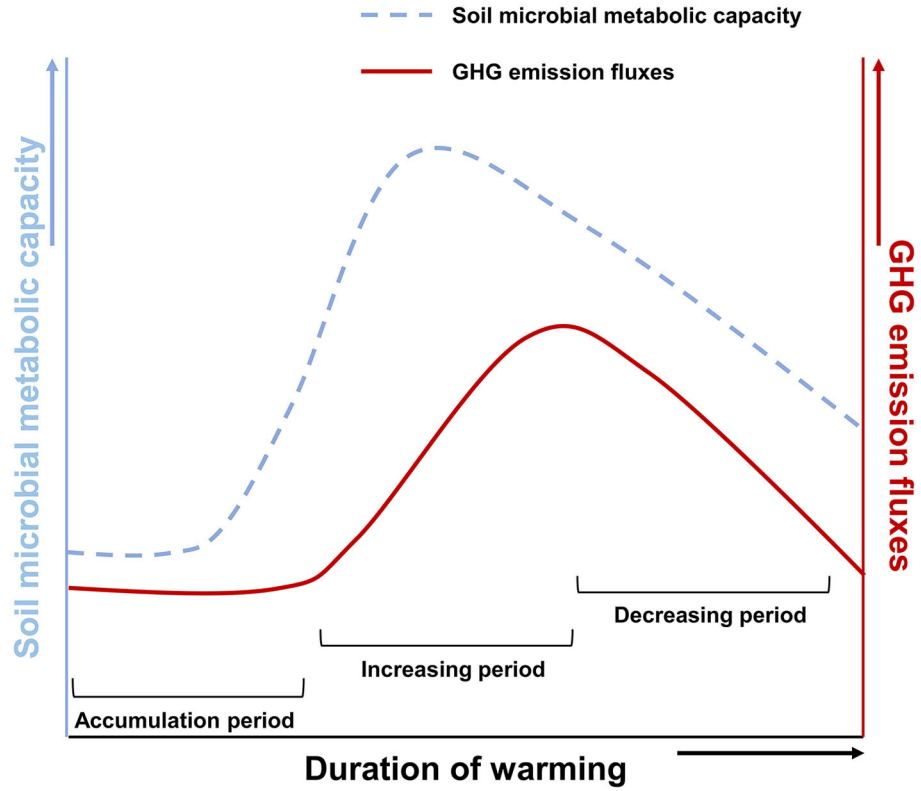

FIGURE 5
A schematic diagram of warming-induced soil microorganism respiration and GHG emission fluxes. The dotted line indicates microbial metabolic capacity. Solid lines show GHG emission fluxes.

lag. Besides, the effect of time on it is not a continuous positive correlation (Figure 5; increasing period). As time passes, this effect shows a trend of increasing and gradually weakening (Figure 5; decreasing period).

5 Conclusion and future perspectives

In summary, the warming field experiment was conducted by anaerobic incubating surface soil samples at two sites in the upper reaches and estuaries of the Barentsburg glacial meltwater river for 7 and 13 days. The results showed that the microbial composition at 10°C and 20°C was not different from that at 2°C. There was also no difference in soil microbial methanogenic gene abundance and CH_4 concentration after incubation. Therefore, we conclude that the acceleration of microbial respiration caused by warming will increase the CH_4 flux over at least 2 weeks. It is interesting that the GR-0 river bank site released more CO compared to the GR site, which did not emit any CO. The effects of global warming on microbial metabolisms and soil CH_4 emission fluxes could be studied through longer-term and continuous incubation experiments or observation. The above conclusions provide reference data for assessing CH_4 emission fluxes in the Arctic region and ideas for future research on the impact of warming on CH_4 emissions.

Data availability statement

The datasets presented in this study can be found in online repositories. The names of the repository/repositories and accession number(s) can be found in the article/Supplementary material.

Author contributions

JL: Conceptualization, Data curation, Formal analysis, Funding acquisition, Investigation, Methodology, Project administration, Resources, Software, Supervision, Validation, Visualization, Writing – original draft, Writing – review & editing. Z-YZ: Conceptualization, Data curation, Formal analysis, Funding acquisition, Investigation, Methodology, Project administration, Resources, Supervision, Validation, Visualization, Writing – review & editing. ZY: Data curation, Formal analysis, Investigation, Methodology, Resources, Writing – review & editing. WL: Methodology, Software, Visualization, Writing – review & editing. YL: Software, Writing – review & editing. YZ: Conceptualization, Funding acquisition, Validation, Writing – review & editing.

Funding

The author(s) declare financial support was received for the research, authorship, and/or publication of this article. This study was funded by the Shanghai Pilot Program for Basic Research of Shanghai Jiao Tong University (Grant No. 21TQ1400201), Shanghai Frontiers Science Center of Polar Science, the National Natural Science Foundation of China (Grant No. 41676188), and the Oceanic Interdisciplinary Program of Shanghai Jiao Tong University (Grant No. SL2022ZD207).

Acknowledgments

We thank the reviewers and the editor for their suggestions and comments, which improved the original manuscript constructively.

Conflict of interest

The authors declare that the research was conducted in the absence of any commercial or financial relationships that could be construed as a potential conflict of interest.

The author(s) declared that they were an editorial board member of Frontiers, at the time of submission. This had no impact on the peer review process and the final decision.

Publisher's note

All claims expressed in this article are solely those of the authors and do not necessarily represent those of their affiliated organizations, or those of the publisher, the editors and the reviewers. Any product that may be evaluated in this article, or claim that may be made by its manufacturer, is not guaranteed or endorsed by the publisher.

Supplementary material

The Supplementary Material for this article can be found online at: https://www.frontiersin.org/articles/10.3389/fmicb.2023.1276065/full#supplementary-material

References

Altshuler, I., Hamel, J., Turney, S., Magnuson, E., Lévesque, R., Greer, C. W., et al. (2019). Species interactions and distinct microbial communities in high Arctic permafrost affected cryosols are associated with the CH_4 and CO_2 gas fluxes. *Environ. Microbiol.* 21, 3711–3727. doi: 10.1111/1462-2920.14715

Angel, R., Claus, P., and Conrad, R. (2012). Methanogenic archaea are globally ubiquitous in aerated soils and become active under wet anoxic conditions. *ISME J.* 6, 847–862. doi: 10.1038/ismej.2011.141

Bao, Y., Dolfing, J., Guo, Z., Chen, R., Wu, M., Li, Z., et al. (2021). Important ecophysiological roles of non-dominant *Actinobacteria* in plant residue decomposition, especially in less fertile soils. *Microbiome* 9, 84. doi: 10.1186/s40168-021-01032-x

Bao, Y., Dolfing, J., Wang, B., Chen, R., Huang, M., Li, Z., et al. (2019). Bacterial communities involved directly or indirectly in the anaerobic degradation of cellulose. *Biol. Fertil. Soils* 55, 201–211. doi: 10.1007/s00374-019-01342-1

Barbier, B. A., Dziduch, I., Liebner, S., Ganzert, L., Lantuit, H., Pollard, W., et al. (2012). Methane-cycling communities in a permafrost-affected soil on Herschel Island, Western Canadian Arctic: active layer profiling of *mcrA* and *pmoA* genes. *FEMS Microbiol. Ecol.* 82, 287–302. doi: 10.1111/j.1574-6941.2012.01332.x

Bolyen, E., Rideout, J. R., Dillon, M. R., Bokulich, N. A., Abnet, C. C., Al-Ghalith, G. A., et al. (2019). Reproducible, interactive, scalable and extensible microbiome data science using QIIME 2. *Nat. Biotechnol.* 37, 852–857. doi: 10.1038/s41587-019-0209-9

Borsdorff, T., aan de Brugh, J., Pandey, S., Hasekamp, O., Aben, I., Houweling, S., et al. (2019). Carbon monoxide air pollution on sub-city scales and along arterial roads detected by the Tropospheric Monitoring Instrument. *Atmosphere Chem. Phys.* 19, 3579–3588. doi: 10.5194/acp-19-3579-2019

Campbell, B. J., Polson, S. W., Hanson, T. E., Mack, M. C., and Schuur, E. A. G. (2010). The effect of nutrient deposition on bacterial communities in Arctic tundra soil. *Environ. Microbiol.* 12, 1842–1854. doi: 10.1111/j.1462-2920.2010.02189.x

Cappelletti, D., Petroselli, C., Mateos, D., Herreras, M., Ferrero, L., Losi, N., et al. (2022). Vertical profiles of black carbon and nanoparticles pollutants measured by a tethered balloon in Longyearbyen (Svalbard islands). *Atmosph. Environ.* 290, 119373. doi: 10.1016/j.atmosenv.2022.119373

Chen, H., Zhu, T., Li, B., Fang, C., and Nie, M. (2020). The thermal response of soil microbial methanogenesis decreases in magnitude with changing temperature. *Nat. Commun.* 11, 5733. doi: 10.1038/s41467-020-19549-4

Chen, J., Luo, Y., Xia, J., Jiang, L., Zhou, X., Lu, M., et al. (2015). Stronger warming effects on microbial abundances in colder regions. *Scient. Rep.* 5, 18032. doi: 10.1038/srep18032

Cohen, J., Screen, J. A., Furtado, J. C., Barlow, M., Whittleston, D., Coumou, D., et al. (2014). Recent Arctic amplification and extreme mid-latitude weather. *Nat. Geosci.* 7, 627–637. doi: 10.1038/ngeo2234

Deslippe, J. R., Hartmann, M., Simard, S. W., and Mohn, W. W. (2012). Long-term warming alters the composition of Arctic soil microbial communities. *FEMS Microbiol. Ecol.* 82, 303–315. doi: 10.1111/j.1574-6941.2012.01350.x

Diender, M., Stams, A. J. M., and Sousa, D. Z. (2015). Pathways and bioenergetics of anaerobic carbon monoxide fermentation. *Front. Microbiol.* 6, 1275. doi: 10.3389/fmicb.2015.01275

Elberling, B., Nordstrøm, C., Grøndahl, L., Søgaard, H., Friborg, T., Christensen, T. R., et al. (2008). "High-Arctic soil CO_2 and CH_4 production controlled by temperature, water, freezing and snow," in *Advances in Ecological Research* (Academic Press), 441–472. doi: 10.1016/S0065-2504(07)00019-0

Fengmin, W., Wenkai, L., and Wei, L. (2019). Causes of arctic amplification: a review. *Adv. Earth Sci.* 34, 232–242. doi: 10.11867/j.issn.1001-8166.2019.03.0232

Franco, D. C., Signori, C. N., Duarte, R. T. D., Nakayama, C. R., Campos, L. S., and Pellizari, V. H. (2017). High prevalence of gammaproteobacteria in the sediments of admiralty bay and north bransfield basin, northwestern antarctic peninsula. *Front. Microbiol.* 8, 153. doi: 10.3389/fmicb.2017.00153

Freitag, T. E., Toet, S., Ineson, P., and Prosser, J. I. (2010). Links between methane flux and transcriptional activities of methanogens and methane oxidizers in a blanket peat bog. *FEMS Microbiol. Ecol.* 73, 157–165. doi: 10.1111/j.1574-6941.2010.00871.x

Galera, L., d., A., Eckhardt, T., Beer, C., Pfeiffer, E.-M., and Knoblauch, C. (2023). Ratio of *in situ* CO_2 to CH_4 production and its environmental controls in polygonal tundra soils of Samoylov Island, Northeastern Siberia. *J. Geophys. Res.* 128, e2022JG006956. doi: 10.1029/2022JG006956

Ganesan, A. L., Schwietzke, S., Poulter, B., Arnold, T., Lan, X., Rigby, M., et al. (2019). Advancing scientific understanding of the global methane budget in support of the Paris agreement. *Global Biogeochem. Cycles* 33, 1475–1512. doi: 10.1029/2018GB006065

Hamdan, L. J., and Wickland, K. P. (2016). Methane emissions from oceans, coasts, and freshwater habitats: new perspectives and feedbacks on climate. *Limnol. Oceanogr.* 61, S3–S12. doi: 10.1002/lno.10449

Hartley, I. P., Hopkins, D. W., Garnett, M. H., Sommerkorn, M., and Wookey, P. A. (2008). Soil microbial respiration in arctic soil does not acclimate to temperature. *Ecol. Lett.* 11, 1092–1100. doi: 10.1111/j.1461-0248.2008.01223.x

Hodson, A. J., Nowak, A., Redeker, K. R., Holmlund, E. S., Christiansen, H. H., and Turchyn, A. V. (2019). Seasonal dynamics of methane and carbon dioxide

evasion from an open system pingo: lagoon pingo, svalbard. *Front. Earth Sci.* 7, 30. doi: 10.3389/feart.2019.00030

Hui, D., Deng, Q., Tian, H., and Luo, Y. (2020). "Global Climate Change and Greenhouse Gases Emissions in Terrestrial Ecosystems," in *Handbook of Climate Change Mitigation and Adaptation,* eds. M. Lackner, B. Sajjadi and W.-Y. Chen. (New York, NY: Springer New York), 1–54. doi: 10.1007/978-1-4614-6431-0_13-3

Inagaki, F., Tsunogai, U., Suzuki, M., Kosaka, A., Machiyama, H., Takai, K., et al. (2004). Characterization of C_1-metabolizing prokaryotic communities in methane seep habitats at the kuroshima knoll, southern ryukyu Arc, by analyzing *pmoA*, *mmoX*, *mxaF*, *mcrA*, and 16S rRNA genes. *Appl. Environ. Microbiol.* 70, 7445–7455. doi: 10.1128/AEM.70.12.7445-7455.2004

Johnston, E. R., Hatt, J. K., He, Z., Wu, L., Guo, X., Luo, Y., et al. (2019). Responses of tundra soil microbial communities to half a decade of experimental warming at two critical depths. *Proc. Nat. Acad. Sci.* 116, 15096–15105. doi: 10.1073/pnas.1901307116

Jorgensen, S. L., Hannisdal, B., Lanzén, A., Baumberger, T., Flesland, K., Fonseca, R., et al. (2012). Correlating microbial community profiles with geochemical data in highly stratified sediments from the Arctic Mid-Ocean Ridge. *Proc. Nat. Acad. Sci.* 109, E2846–E2855. doi: 10.1073/pnas.1207574109

Klindworth, A., Pruesse, E., Schweer, T., Peplies, J., Quast, C., Horn, M., et al. (2012). Evaluation of general 16S ribosomal RNA gene PCR primers for classical and next-generation sequencing-based diversity studies. *Nucleic Acids Res.* 41, e1. doi: 10.1093/nar/gks808

Knoblauch, C., Beer, C., Liebner, S., Grigoriev, M. N., and Pfeiffer, E.-M. (2018). Methane production as key to the greenhouse gas budget of thawing permafrost. *Nat. Clim. Change* 8, 309–312. doi: 10.1038/s41558-018-0095-z

Knoblauch, C., Beer, C., Schuett, A., Sauerland, L., Liebner, S., Steinhof, A., et al. (2021). Carbon dioxide and methane release following abrupt thaw of pleistocene permafrost deposits in Arctic Siberia. *J. Geophys. Res.* 126, e2021JG006543. doi: 10.1029/2021JG006543

Lawrence, D. M., Koven, C. D., Swenson, S. C., Riley, W. J., and Slater, A. G. (2015). Permafrost thaw and resulting soil moisture changes regulate projected high-latitude CO_2 and CH_4 emissions. *Environ. Res. Lett.* 10, 094011. doi: 10.1088/1748-9326/10/9/094011

Lee, H., Schuur, E. A. G., Inglett, K. S., Lavoie, M., and Chanton, J. P. (2012). The rate of permafrost carbon release under aerobic and anaerobic conditions and its potential effects on climate. *Global Change Biol.* 18, 515–527. doi: 10.1111/j.1365-2486.2011.02519.x

Magnani, M., Baneschi, I., Giamberini, M., Raco, B., and Provenzale, A. (2022). Microscale drivers of summer CO_2 fluxes in the Svalbard High Arctic tundra. *Scient. Rep.* 12, 763. doi: 10.1038/s41598-021-04728-0

Malard, L. A., Anwar, M. Z., Jacobsen, C. S., and Pearce, D. A. (2021). Influence of spatial scale on structure of soil bacterial communities across an arctic landscape. *Appl. Environ. Microbiol.* 87, e02220. doi: 10.1128/AEM.02220-20

Martineau, C., Pan, Y., Bodrossy, L., Yergeau, E., Whyte, L. G., and Greer, C. W. (2014). Atmospheric methane oxidizers are present and active in Canadian high Arctic soils. *FEMS Microbiol. Ecol.* 89, 257–269. doi: 10.1111/1574-6941.12287

Marushchak, M. E., Kerttula, J., Diáková, K., Faguet, A., Gil, J., Grosse, G., et al. (2021). Thawing Yedoma permafrost is a neglected nitrous oxide source. *Nat. Commun.* 12, 7107. doi: 10.1038/s41467-021-27386-2

Mehmood, I., Bari, A., Irshad, S., Khalid, F., Liaqat, S., Anjum, H., et al. (2020). "Carbon Cycle in Response to Global Warming," in *Environment, Climate, Plant and Vegetation Growth,* eds. S. Fahad, M. Hasanuzzaman, M. Alam, H. Ullah, M. Saeed, I. Ali Khan and M. Adnan (Cham: Springer International Publishing), 1–15. doi: 10.1007/978-3-030-49732-3_1

Nazaries, L., Murrell, J. C., Millard, P., Baggs, L., and Singh, B. K. (2013). Methane, microbes and models: fundamental understanding of the soil methane cycle for future predictions. *Environ. Microbiol.* 15, 2395–2417. doi: 10.1111/1462-2920.12149

Newsham, K. K., Danielsen, B. K., Biersma, E. M., Elberling, B., Hillyard, G., Kumari, P., et al. (2022). Rapid response to experimental warming of a microbial community inhabiting high arctic patterned ground soil. *Biology* 11, 1819. doi: 10.3390/biology11121819

Pareek, N. (2017). Climate change impact on soils: adaptation and mitigation. *MOJ Ecol. Environ. Sci.* 2, 136–139. doi: 10.15406/mojes.2017.02.00026

Pold, G., Schimel, J. P., and Sistla, S. A. (2021). Soil bacterial communities vary more by season than with over two decades of experimental warming in Arctic tussock tundra. *Elementa* 9, 00116. doi: 10.1525/elementa.2021.00116

Qian-Qian, Z., Sheng-Long, J., Ke-Mao, L., Zhen-Bing, W., Hong-Tao, G., Jin-Wen, H., et al. (2021). Community structure of bacterioplankton and its relationship with environmental factors in the upper reaches of the Heihe River in Qinghai Plateau. *Environ. Microbiol.* 23, 1210–1221. doi: 10.1111/1462-2920.15358

Rijkers, R., Rousk, J., Aerts, R., Sigurdsson, B. D., and Weedon, J. T. (2022). Optimal growth temperature of Arctic soil bacterial communities increases under experimental warming. *Global Change Biol.* 28, 6050–6064. doi: 10.1111/gcb.16342

Romero-Olivares, A. L., Allison, S. D., and Treseder, K. K. (2017). Soil microbes and their response to experimental warming over time: a meta-analysis of field studies. *Soil Biol. Biochem.* 107, 32–40. doi: 10.1016/j.soilbio.2016.12.026

Saunois, M., Bousquet, P., Poulter, B., Peregon, A., Ciais, P., Canadell, J. G., et al. (2016). The global methane budget 2000–2012. *Earth Syst. Sci. Data* 8, 697–751. doi: 10.5194/essd-8-697-2016

Saunois, M., Stavert, A. R., Poulter, B., Bousquet, P., Canadell, J. G., Jackson, R. B., et al. (2020). The Global Methane Budget 2000–2017. *Earth Syst. Sci. Data* 12, 1561–1623. doi: 10.5194/essd-12-1561-2020

Schuur, E. A. G., McGuire, A. D., Schädel, C., Grosse, G., Harden, J. W., Hayes, D. J., et al. (2015). Climate change and the permafrost carbon feedback. *Nature* 520, 171–179. doi: 10.1038/nature14338

Singh, B. K., Bardgett, R. D., Smith, P., and Reay, D. S. (2010). Microorganisms and climate change: terrestrial feedbacks and mitigation options. *Nat. Rev. Microbiol.* 8, 779–790. doi: 10.1038/nrmicro2439

Son, D., and Lee, E. J. (2022). Soil microbial communities associated with three arctic plants in different local environments in Ny-Ålesund, Svalbard. *J. Microbiol. Biotechnol.* 32, 1275–1283. doi: 10.4014/jmb.2208.08009

Song, Y., Chen, L., Kang, L., Yang, G., Qin, S., Zhang, Q., et al. (2021). Methanogenic community, CH_4 production potential and its determinants in the active layer and permafrost deposits on the tibetan plateau. *Environ. Sci. Technol.* 55, 11412–11423. doi: 10.1021/acs.est.0c07267

Terry, V. C., Lars Olof, B., Yuri, C., Terry, C., Torben, R. C., Brian, H., et al. (2004). Effects on the function of Arctic ecosystems in the short-and long-term perspectives. *AMBIO* 33, 448–458. doi: 10.1579/0044-7447-33.7.448

Tian, C., Lv, Y., Yang, Z., Zhang, R., Zhu, Z., Ma, H., et al. (2022). Microbial community structure and metabolic potential at the initial stage of soil development of the glacial Forefields in Svalbard. *Microb. Ecol.* 86, 933–946. doi: 10.1007/s00248-022-02116-3

Tian, H., Lu, C., Ciais, P., Michalak, A. M., Canadell, J. G., Saikawa, E., et al. (2016). The terrestrial biosphere as a net source of greenhouse gases to the atmosphere. *Nature* 531, 225–228. doi: 10.1038/nature16946

Torn, M. S., and Chapin, F. S. (1993). Environmental and biotic controls over methane flux from Arctic tundra. *Chemosphere* 26, 357–368. doi: 10.1016/0045-6535(93)90431-4

Treat, C. C., Wollheim, W. M., Varner, R. K., Grandy, A. S., Talbot, J., and Frolking, S. (2014). Temperature and peat type control CO_2 and CH_4 production in Alaskan permafrost peats. *Global Change Biol.* 20, 2674–2686. doi: 10.1111/gcb.12572

Tveit, A., Schwacke, R., Svenning, M. M., and Urich, T. (2013). Organic carbon transformations in high-Arctic peat soils: key functions and microorganisms. *The ISME J.* 7, 299–311. doi: 10.1038/ismej.2012.99

Tveit, A. T., Urich, T., Frenzel, P., and Svenning, M. M. (2015). Metabolic and trophic interactions modulate methane production by Arctic peat microbiota in response to warming. *Proc. Nat. Acad. Sci.* 112, E2507–E2516. doi: 10.1073/pnas.1420797112

Uchida, Y., Mogi, H., Hamamoto, T., Nagane, M., Toda, M., Shimotsuma, M., et al. (2018). Changes in denitrification potentials and riverbank soil bacterial structures along Shibetsu River, Japan. *Appl. Environ. Soil Sci.* 2018, 2530946. doi: 10.1155/2018/2530946

Voigt, C., Marushchak, M. E., Mastepanov, M., Lamprecht, R. E., Christensen, T. R., Dorodnikov, M., et al. (2019). Ecosystem carbon response of an Arctic peatland to simulated permafrost thaw. *Global Change Biol.* 25, 1746–1764. doi: 10.1111/gcb.14574

Voolstra, C. R., and Ziegler, M. (2020). Adapting with microbial help: microbiome flexibility facilitates rapid responses to environmental change. *BioEssays* 42, 2000004. doi: 10.1002/bies.202000004

Wartiainen, I., Hestnes, A. G., McDonald, I. R., and Svenning, M. M. (2006). *Methylobacter tundripaludum* sp. nov., a methane-oxidizing bacterium from Arctic wetland soil on the Svalbard islands, Norway (78° N). *Int. J. System. Evolut. Microbiol.* 56, 109–113. doi: 10.1099/ijs.0.63728-0

Wartiainen, I., Hestnes, A. G., and Svenning, M. M. (2003). Methanotrophic diversity in high arctic wetlands on the islands of Svalbard (Norway)-denaturing gradient gel electrophoresis analysis of soil DNA and enrichment cultures. *Canad. J. Microbiol.* 49, 602–612. doi: 10.1139/w03-080

Watts, J. D., Natali, S. M., Minions, C., Risk, D., Arndt, K., Zona, D., et al. (2021). Soil respiration strongly offsets carbon uptake in Alaska and Northwest Canada. *Environ. Res. Lett.* 16, 084051. doi: 10.1088/1748-9326/ac1222

Yergeau, E., Bokhorst, S., Kang, S., Zhou, J., Greer, C. W., Aerts, R., et al. (2012). Shifts in soil microorganisms in response to warming are consistent across a range of Antarctic environments. *ISME J.* 6, 692–702. doi: 10.1038/ismej.2011.124

Zhang, F., Zhang, H., Pei, S., Zhan, L., and Ye, W. (2021). Effects of Arctic warming on microbes and methane in different land types in svalbard. *Water* 13, 3296. doi: 10.3390/w13223296

Zhang, K., Delgado-Baquerizo, M., Zhu, Y.-G., and Chu, H. (2020). Space is more important than season when shaping soil microbial communities at a large spatial scale. *mSystems* 5, 719. doi: 10.1128/mSystems.00783-19

Zhang, Q., Qin, W., Feng, J., Li, X., Zhang, Z., He, J.-S., et al. (2023a). Whole-soil-profile warming does not change microbial carbon use efficiency in surface and deep soils. *Proc. Nat. Acad. Sci.* 120, e2302190120. doi: 10.1073/pnas.2302190120

Zhang, Y., Song, C., Wang, X., Chen, N., Ma, G., Zhang, H., et al. (2023b). How climate warming and plant diversity affect carbon greenhouse gas emissions from boreal peatlands: Evidence from a mesocosm study. *J. Cleaner Prod.* 404, 136905. doi: 10.1016/j.jclepro.2023.136905

Zhou, X., Chen, X., Qi, X., Zeng, Y., Guo, X., Zhuang, G., et al. (2023). Soil bacterial communities associated with multi-nutrient cycling under long-term warming in the alpine meadow. *Front. Microbiol.* 14, 1136187. doi: 10.3389/fmicb.2023.1136187

Zosso, C. U., Ofiti, N. O. E., Soong, J. L., Solly, E. F., Torn, M. S., Huguet, A., et al. (2021). Whole-soil warming decreases abundance and modifies the community structure of microorganisms in the subsoil but not in surface soil. *Soil* 7, 477–494. doi: 10.5194/soil-7-477-2021

frontiers | Frontiers in Microbiology

TYPE Perspective
PUBLISHED 05 February 2024
DOI 10.3389/fmicb.2024.1363775

OPEN ACCESS

EDITED BY
Huai Li,
Chinese Academy of Sciences (CAS), China

REVIEWED BY
Fang-Li Luo,
Beijing Forestry University, China
Guan Bo,
Ludong University, China

*CORRESPONDENCE
Junhong Bai
junhongbai@163.com

RECEIVED 31 December 2023
ACCEPTED 22 January 2024
PUBLISHED 05 February 2024

CITATION
Zhang L, Bai J, Zhai Y, Zhang K, Wang Y, Tang R, Xiao R and Jorquera MA (2024) Seasonal changes in N-cycling functional genes in sediments and their influencing factors in a typical eutrophic shallow lake, China.
Front. Microbiol. 15:1363775.
doi: 10.3389/fmicb.2024.1363775

Seasonal changes in N-cycling functional genes in sediments and their influencing factors in a typical eutrophic shallow lake, China

Ling Zhang[1,2], Junhong Bai[1]*, Yujia Zhai[1], Kegang Zhang[3], Yaqi Wang[1], Ruoxuan Tang[1], Rong Xiao[4] and Milko A. Jorquera[5]

[1]School of Environment, Beijing Normal University, Beijing, China, [2]School of Chemistry and Chemical Engineering, Qinghai Normal University, Xining, China, [3]Department of Environmental Engineering and Science, North China Electric Power University, Baoding, China, [4]College of Environment & Safety Engineering, Fuzhou University, Fuzhou, China, [5]Laboratorio de Ecología Microbiana Aplicada (EMALAB), Departamento de Ciencias Químicas y Recursos Naturales, Universidad de La Frontera, Temuco, Chile

N-cycling processes mediated by microorganisms are directly linked to the eutrophication of lakes and ecosystem health. Exploring the variation and influencing factors of N-cycling-related genes is of great significance for controlling the eutrophication of lakes. However, seasonal dynamics of genomic information encoding nitrogen (N) cycling in sediments of eutrophic lakes have not yet been clearly addressed. We collected sediments in the Baiyangdian (BYD) Lake in four seasons to explore the dynamic variation of N-cycling functional genes based on a shotgun metagenome sequencing approach and to reveal their key influencing factors. Our results showed that dissimilatory nitrate reduction (DNRA), assimilatory nitrate reduction (ANRA), and denitrification were the dominant N-cycling processes, and the abundance of *nirS* and *amoC* were higher than other functional genes by at least one order of magnitude. Functional genes, such as *nirS*, *nirK* and *amoC*, generally showed a consistent decreasing trend from the warming season (i.e., spring, summer, fall) to the cold season (i.e., winter). Furthermore, a significantly higher abundance of nitrification functional genes (e.g., *amoB, amoC and hao*) in spring and denitrification functional genes (e.g., *nirS, norC and nosZ*) in fall were observed. N-cycling processes in four seasons were influenced by different dominant environmental factors. Generally, dissolved organic carbon (DOC) or sediment organic matter (SOM), water temperature (T) and antibiotics (e.g., Norfloxacin and ofloxacin) were significantly correlated with N-cycling processes. The findings imply that sediment organic carbon and antibiotics may be potentially key factors influencing N-cycling processes in lake ecosystems, which will provide a reference for nitrogen management in eutrophic lakes.

KEYWORDS

sediments, N-cycling, functional genes, seasonal changes, shallow lake

1 Introduction

Nitrogen input caused by human activities can greatly affect the processes of the N-cycling of lake ecosystems, leading to the eutrophication of water bodies (Basu et al., 2022; Jiang et al., 2023). It has been proved microorganisms, especially N-cycling functional genes are the key driver of the nitrogen transformation processes in the lakes (Isobe and Ohte, 2014). Therefore, N-cycling functional genes have been given more and more concerns for nitrogen removal of the eutrophic lakes.

N-cycling plays an important role in maintaining the ecological balance of lakes (Isobe and Ohte, 2014). Nitrogen in lakes exists in the form of inorganic nitrogen and organic nitrogen, which is absorbed and assimilated by algae, macrophytes (Wu et al., 2021), benthic animals and other organisms (Wu Y. et al., 2022), and can be converted into biological organic nitrogen (Pajares et al., 2017). After these organisms die, they release a large amount of organic nitrogen and inorganic nitrogen to water and sediments (Li et al., 2012; Wu et al., 2021). In eutrophic lakes, the microbial decomposition of a large number of dead aquatic organisms settling to the bottom of the lakes can cause a lower concentration of dissolved oxygen (Wu et al., 2021), which will lead to the production of ammonia, sulfide and other substances (Hu et al., 2023), having a negative impact on the lake ecosystem health (Wang M. et al., 2023; Wang X. et al., 2023).

The N-cycling processes in sediments mainly involve in nitrogen fixation, nitrification, denitrification, assimilatory nitrate reduction (ANRA), dissimilatory nitrate reduction (DNRA) and anammox (Hu et al., 2023), among which nitrification and denitrification are the most important nitrogen transformation processes. These processes induced by microorganisms can oxidize ammonia nitrogen into nitrate nitrogen, and reduce the bound nitrogen into N_2O or N_2 back to the atmosphere (Broman et al., 2021). Each pathway of the N-cycling process is completed by the enzyme encoded by the corresponding functional gene using the corresponding substrate catalysis (Broman et al., 2021). However, the abundance and diversity of N-cycling functional genes in lake ecosystems are greatly different due to different water quality (such as water temperature, and nitrogen to phosphorus ratio) (Basu et al., 2022), hydrological conditions (such as lake water exchange cycle) (Stoliker et al., 2016; Li et al., 2021) and seasons (Baumann et al., 2022). Therefore, it is of great significance to explore the changes of N-cycling functional genes in lakes and their influencing factors in different seasons.

Baiyangdian (BYD) Lake (38°43′ ~ 39°02′N, 115°38′ ~ 116°07′E) is the typical eutrophic wetland in North China and has a relatively important geographic position. The BYD Lake water is eutrophicated, accounting for 26.7% of areas "mildly eutrophicated," accounting for 53.3% of areas "moderately eutrophicated," and accounting for 20.0% of areas "severely eutrophicated" (Liu et al., 2020; Yao et al., 2023). However, serious eutrophication dominated by seasonal nitrogen and phosphorus pollution occurred due to intense agricultural activities and rural domestic sewage discharge in BYD Lake (Zhao et al., 2011; Cai et al., 2021). Because of the strong exchange between water and surface sediments in shallow lakes, eutrophication might affect the nitrogen cycle in sediments (Shi et al., 2022). The primary objectives of this work were: (1) the key functional genes related to N-cycling have seasonal variability in sediments in the BYD Lake; and (2) some environmental factors can play a key role in regulating the N-cycling process.

2 Seasonal variation of N-cycling functional genes

In the current study, a total of 36 sediment samples were collected in four seasons such as spring, summer, fall and winter during 2020–2021 (Supplementary Figure S1). We aimed to identify the major N-cycling gene families and their key environmental factors. A shotgun metagenome sequencing approach was applied to survey 6 important N-cycling processes and related functional genes (Supplementary Text S1): 1) nitrogen fixation (e.g., *nifH, nifD, nifK, vnfG,* and *vnfH*) (Jiang et al., 2022; Li et al., 2022); 2) nitrification (e.g., *amoA, amoB, amoC,* and *hao*) (Wang et al., 2022; Liao et al., 2023); 3) denitrification (e.g., *nirB, nirS, norC, narI and nirK,* and *nosZ*) (Waldrop et al., 2023); 4) DNRA (e.g., *napA, napB, narG, narH, narI, nrfH, nrtA, nirB, nirD, and nrfA*) (Jiang et al., 2023; Waldrop et al., 2023); 5) ANRA (e.g., *nasA, nasD, nirA,* and *nasE*) (Hu et al., 2023; Li et al., 2023); and 6) anammox (e.g., *nirK* and *nirS*) (Tu et al., 2017; Wang M. et al., 2023; Wang X. et al., 2023).

All the studied genes of N-cycling (including nitrification, denitrification, nitrogen fixation, DNRA, ANRA, and anammox) were present in the sediments of BYD Lake, although their abundance varied largely among four sampling seasons (Figure 1 and Supplementary Figures S2–S5). According to the results, the functional genes abundance of each N-cycling process followed the order DNRA > ANRA > denitrification > nitrogen fixation > nitrification > anammox (Figure 1A). In general, the abundances of functional genes involved in DNRA, ANRA and denitrification processes were higher than those of other related N-cycling processes, indicating that the sediments in BYD Lake had higher potential of NDRA, ADRA and denitrification. Interestingly, the functional genes of these three N-cycle processes exhibited higher abundance in fall than in other seasons (Figure 1A).

Overall, Figures 1B,C illustrated the seasonal variation of nitrification genes (e.g., *amoA, amoB, amoC, and hao*) and denitrification genes (e.g., *nirk, nirS, norC,* and *nosZ*) processes. Among the nitrification and denitrification genes, the abundance of *nirS* (from 0.47 to 1.96 $\log_{10}$ gene copies) and *amoC* (from 0.14 to 1.95 $\log_{10}$ gene copies) exceeded the abundance of other functional genes by at least one order of magnitude (Figures 1B,C). Meanwhile, the abundances of such functional genes as *nirS, nirK* and *amoC* genes generally showed a consistent decreasing trend from spring, summer, and fall to winter, while, the abundances of *nosZ* demonstrated an increasing trend, which ranged from 0.31 to 1.68 $\log_{10}$ gene copies.

A significantly higher abundance of nitrification gene (*amoB*) in spring (1.083 ± 0.10 $\log_{10}$ gene copies, $p < 0.01$) and fall (0.746 ± 0.19 $\log_{10}$ gene copies, $p < 0.05$) samples were observed than those in winter (0.42 ± 0.12 $\log_{10}$ gene copies) (Figure 1B). As for denitrification, the abundance of *nirK* had significantly higher values in spring (0.63 ± 0.43 $\log_{10}$ gene copies) than that in fall (0.37 ± 0.28 $\log_{10}$ gene copies) ($p < 0.01$, Figure 1C). On the contrary, the abundances of denitrification genes such as *nosZ* (1.15 ± 0.35 $\log_{10}$ gene copies, $p < 0.01$) and *norC* (1.32 ± 0.38 $\log_{10}$ gene copies, $p < 0.05$) in fall were significantly higher than those in spring (Figure 1C).

10.3389/fmicb.2024.1363775

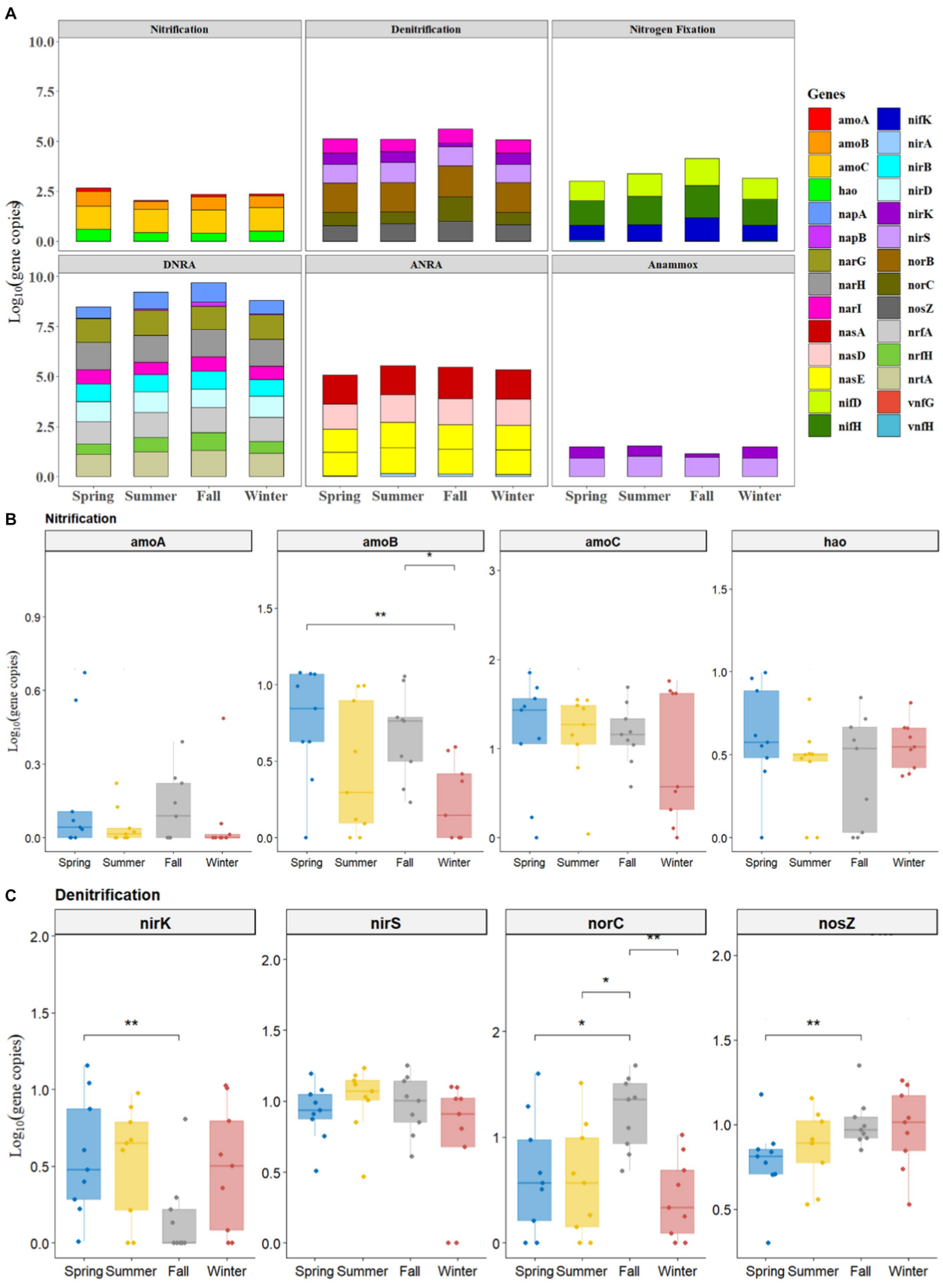

FIGURE 1
Seasonal profiles of all functional genes of nitrogen metabolism with 6 pathways **(A)** and nitrification genes **(B)** and denitrification genes **(C)**.

Moreover, significantly higher abundance of nitrogen fixation functional genes (e.g., *nifD, nifH*, and *nifK*) (Supplementary Figure S2), DNRA gene (*napB*, Supplementary Figure S3), ANRA gene (*nasA*, Supplementary Figure S4) in fall were observed than those observed in spring ($p < 0.05$). However, no significant differences were observed in functional genes involved in anammox among spring, summer, fall and winter ($p > 0.05$, Supplementary Figure S5).

3 Environmental factors influencing N-cycling functional genes in sediments

The relationships between selected environmental factors and abundances of studied N-cycling functional genes in sediments of BYD lakes are illustrated in Figure 2. In spring, the denitrification pathway was highly correlated with norfloxacin (NOR), NH_4_N and T ($r \geq 4$, $p = 0.01$–0.05, Figure 2). In contrast, the nitrification pathway had a significant correlation with sulfapyridine (SPD) ($r \geq 4$, $p < 0.01$, Figure 2). Pearson correlation analysis results showed that both denitrification functional genes *nirS* ($r = -0.7$) and *nosZ* ($r = 0.7$) were significantly correlated with tetracycline (TC) and oxytetracycline (OTC) ($p < 0.05$, Supplementary Figure S6), while both *nirS* ($r = -0.8$) and *norB* ($r = 0.9$) were significantly correlated with pH ($p < 0.05$). Generally, the *norC* abundance exhibited a significant correlation with antibiotics (NOR, $r = -0.8$; Ofloxacin, OFL, $r = 0.7$; roxithromycin, ROM, $r = 0.7$) ($p < 0.05$, Supplementary Figure S6) and some physical–chemical properties (NH_4_N, $r = -0.7$; DOC, $r = -0.8$; EC, $r = 0.8$; SOM, $r = -0.7$; T, $r = 0.8$) ($p < 0.05$, Supplementary Figure S6). There were statistically significant positive correlations between nitrification gene *hao* and antibiotics (SDZ, $r = 1$; OFL, $r = 0.7$, ROM, $r = 0.9$) ($p < 0.05$, Supplementary Figure S6), as well as EC ($r = 0.8$, $p < 0.05$). Besides, the nitrification gene *amoB* was significantly correlated with the pH ($r = 0.8$, $p < 0.05$, Supplementary Figure S6).

In summer, the denitrification pathway was significantly correlated with OFL ($r \geq 4$, $p < 0.01$, Figure 2), pH ($r \geq 4$, $p = 0.01$–0.05, Figure 2), SOM ($r \geq 4$, $p = 0.01$–0.05, Figure 2), T ($r \geq 4$, $p = 0.01$–0.05, Figure 2), respectively. In contrast, the nitrification pathway only showed significant correlations with NO_3_N ($r \geq 4$, $p = 0.01$–0.05, Figure 2). Furthermore, the correlation analysis results also showed that OFL, SOM, pH, and T have significant correlations with such denitrification genes as *nirK*, *norC and narl* ($p < 0.05$, Supplementary Figure S6).

In fall, the Mantel test results showed that denitrification pathway was correlated with NO_3_N ($r \geq 4$, $p = 0.01$–0.05, Figure 2), DOC ($r \geq 4$, $p < 0.01$, Figure 2), SOM ($r \geq 4$, $p < 0.01$, Figure 2), and WC ($r \geq 4$, $p < 0.01$, Figure 2), respectively. WC had a significant correlation with such denitrification genes as *nirS* ($r = -0.7$), *norC* ($r = -0.9$), *narl* ($r = 0.7$), and *nosZ* ($r = -0.8$) and nitrification gene *hao* ($r = -0.7$) ($p < 0.05$, Supplementary Figure S6). Additionally, DOC ($r = 0.7$) and SOM ($r = -0.9$) exhibited a significant correlation with *norC* and *hao* ($p < 0.05$, Supplementary Figure S6). Significant correlations were observed between denitrification gene *nirS* and NOR ($r = -0.9$, $p < 0.01$), OFL ($r = -0.8$, $p < 0.01$), TC ($r = -0.7$, $p < 0.05$), total antibiotics (SUM) ($r = -0.8$, $p < 0.05$). In contrast, in winter, the denitrification pathway was significantly correlated with EC and H ($r \geq 4$, $p = 0.01$–0.05, Figure 2). The denitrification gene *norC* and EC ($r = -0.7$, $p < 0.05$), *nosZ* and NO_3_N ($r = 0.7$, $p < 0.05$), nitrification gene *amoC* and CIP ($r = -0.7$, $p < 0.05$) showed a significant correlation (Supplementary Figure S6). Overall, no significant correlation was observed between the nitrification pathway and environmental factors in fall and winter ($p > 0.05$, Figure 2). What's more, the DNRA, ANRA, and anammox pathways were correlated with DOC or SOM ($p < 0.05$), and the nitrogen fixation pathway was correlated with NOR ($p < 0.05$).

4 Discussion

It is well known that many N-cycling processes are mediated by N-related microorganisms (Isobe and Ohte, 2014). The nitrification and denitrification functional gene abundance could be an indicator of nitrification and denitrification activities, which has been demonstrated by previous studies reporting a positive correlation between them (Jiang et al., 2022). Moreover, the synergistic effect is manifested in a positive correlation of their gene abundance because nitrification can provide sufficient nitrate for denitrification (Jiang et al., 2023). In the current study, a strong correlation was also observed between the abundance of functional genes associated with denitrification (e.g., *nirK, nirS,* and *norB*) and nitrification (e.g., *amoA, amoB* and *hao*) pathway in spring, fall and winter ($p < 0.05$). In summer, the supply of nitrate is limited due to higher temperatures and excessive consumption of oxygen by algae and aquatic plants (Zhou et al., 2021), which may be the reason why we did not observe the correlation between functional genes related to nitrification and denitrification processes in summer.

The different responses of the N cycling process to external stresses might be driven by the remodeling of the microbial community, which could be strongly affected by changes in physical–chemical properties (Tan et al., 2022). A previous study has shown that denitrification and DNRA rates were mainly regulated by the abundance of their functional genes (e.g., *nirS, nirK* and *nrfA*), followed by environmental factors (e.g., sediment organic carbon) (Jiang et al., 2023). Marshall et al. (2021) also reported a decrease in anammox functional gene abundance in conjunction with the decreasing organic carbon content. Similarly, in the current study, we also found that most of the N-cycling pathways (including denitrification, DNRA, ANRA, and anammox) were significantly correlated with SOM or DOC due to the influence of plant growth and litter in BYD Lake, the contents of SOM and DOC in sediment are higher in summer and fallMoreover, N-cycling functional genes including *norC, nirK, narI,* and hao showed a significant correlation with DOC ($p < 0.05$). This could be explained by the fact that organic carbon input can stimulate microbial N-cycling as organic carbon acts as an electron donor for various N-reduction pathways in organotrophic N-reducing reactions, such as denitrification (Baumann et al., 2022). Previous studies have also reported that higher available carbon (DOC) can promote denitrification (Stewart et al., 2013; Morse et al., 2014) due to N-cycling microorganisms can utilize organic carbon for mixed nutrient growth (Jiang et al., 2023). This further illustrates that the denitrification process in the BYD sediment is the dominant process.

Furthermore, our result showed that T (°C) significantly correlated with the denitrification pathway ($r \geq 4$, $p = 0.01$–0.05, Figure 2) in summer and fall. This also confirms that the nitrogen cycle process is a microbial-dominated process and is therefore more

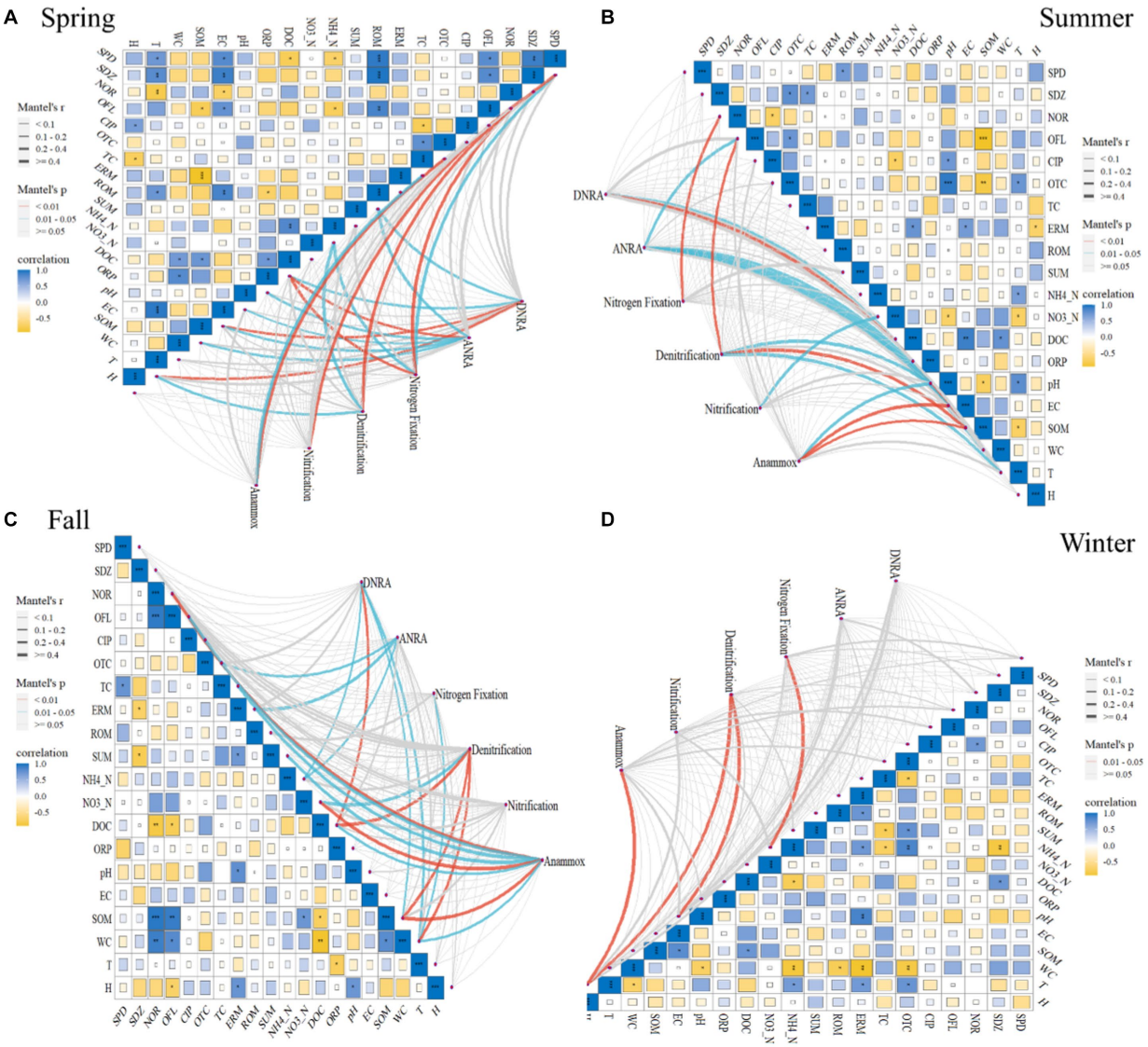

FIGURE 2
Relationships between functional genes and selected environmental factors, as revealed by the Mantel test in the Spring **(A)**, Summer **(B)**, Fall **(C)** and Winter **(D)**. The edge width is proportional to Mantel's *p* value, and the edge color indicates statistical significance. Pairwise correlations of edaphic variables were evaluated by Pearson's correlation and visualized by a heatmap with a color gradient (correlation coefficients from -1 to 1 correspond to colors from yellow to navy blue, respectively).

sensitive to temperature. Specifically, a significant correlation was observed between T and *nirK* (r = −0.7), *norC* (r = 0.9), *narI* (r = −0.7) ($p < 0.05$, Supplementary Figure S6). Studies have shown that the abundance of genes related to ANRN and denitrification pathways decreases with increasing temperature (Yang et al., 2023). Pajares et al. (2017) also found that *nirK* is negatively related to T, furthermore, the elevated temperature will increase denitrification rates (Dai et al., 2020). This highlights the importance of temperature as one of the main factors influencing the functional genes related to N-cycling in lakes (Yuan et al., 2023). Therefore, the impact of seasonal changes on N-cycling triggering the retention and emission of nitrogen in the lake should be paid more attention by the management department.

Previous studies have also reported that antibiotic pollution could alter the N-cycling process (Wu J. et al., 2022). For example, sulfadiazine inhibits functional genes related to denitrification and anaerobic ammonium oxidation in sediments (Wang M. et al., 2023; Wang X. et al., 2023). As well as, nitrifier-denitrification rates were inhibited by sulfamethoxazole (Chen et al., 2022). Remarkably, in the current study, N-cycling pathways significantly correlated with antibiotics. For instance, denitrification exhibited a significant correlation with NOR in spring ($r \geq 4$, $p = 0.01$–0.05, Figure 2), and OFL in summer ($r \geq 4$, $p = 0.01$–0.05, Figure 2). Nitrification was significantly correlated with SPD ($r \geq 4$, $p = 0.01$–0.05, Figure 2). Anammox had a significant correlation with TC in spring and fall, and NOR in fall ($r \geq 4$, $p = 0.01$–0.05, Figure 2). Our previous study (Zhang et al., 2023) found that NOR and OFL was the main antibiotics in BYD lake sediments, indicating that more attention should be paid to the effect of antibiotics on the N-cycling in the future. Consequently, more concerns should be given to antibiotics pollution in N-cycling studies in eutrophic water bodies.

Given this perspective, DOC or SOM, T and antibiotics (e.g., norfloxacin and ofloxacin) were significantly correlated with N-cycling

processes and they might be potentially key factors influencing the seasonal N-cycling processes in lake ecosystems.

Data availability statement

The original contributions presented in the study are included in the article/Supplementary material, further inquiries can be directed to the corresponding author.

Author contributions

LZ: Investigation, Visualization, Writing – original draft, Writing – review & editing. JB: Conceptualization, Data curation, Funding acquisition, Methodology, Writing – review & editing. YZ: Writing – review & editing. KZ: Writing – review & editing. YW: Writing – review & editing. RT: Writing – review & editing. RX: Writing – review & editing. MJ: Writing – review & editing.

Funding

The author(s) declare financial support was received for the research, authorship, and/or publication of this article. This study was financially supported by Projects of International Cooperation and Exchanges NSFC-ANID Fund (number 51961125201 in China and code NSFC190012 in Chile).

Conflict of interest

The authors declare that the research was conducted in the absence of any commercial or financial relationships that could be construed as a potential conflict of interest.

Publisher's note

All claims expressed in this article are solely those of the authors and do not necessarily represent those of their affiliated organizations, or those of the publisher, the editors and the reviewers. Any product that may be evaluated in this article, or claim that may be made by its manufacturer, is not guaranteed or endorsed by the publisher.

Supplementary material

The Supplementary material for this article can be found online at: https://www.frontiersin.org/articles/10.3389/fmicb.2024.1363775/full#supplementary-material

References

Basu, N. B., Van Meter, K. J., Byrnes, D. K., Van Cappellen, P., Brouwer, R., Jacobsen, B. H., et al. (2022). Managing nitrogen legacies to accelerate water quality improvement. *Nat. Geosci.* 15, 97–105. doi: 10.1038/s41561-021-00889-9

Baumann, K., Thoma, R., Callbeck, C. M., Niederdorfer, R., Schubert, C. J., Muller, B., et al. (2022). Microbial nitrogen transformation potential in sediments of two Contrasting Lakes is spatially structured but seasonally stable. *mSphere* 7:e101321:e0101321. doi: 10.1128/msphere.01013-21

Broman, E., Zilius, M., Samuiloviene, A., Vybernaite-Lubiene, I., Politi, T., Klawonn, I., et al. (2021). Active DNRA and denitrification in oxic hypereutrophic waters. *Water Res.* 194:116954. doi: 10.1016/j.watres.2021.116954

Cai, Y., Liang, J., Zhang, P., Wang, Q., Wu, Y., Ding, Y., et al. (2021). Review on strategies of close-to-natural wetland restoration and a brief case plan for a typical wetland in northern China. *Chemosphere* 285:131534. doi: 10.1016/j.chemosphere.2021.131534

Chen, C., Li, Y., Yin, G., Hou, L., Liu, M., Jiang, Y., et al. (2022). Antibiotics sulfamethoxazole alter nitrous oxide production and pathways in estuarine sediments: evidenced by the N15-O18 isotopes tracing. *J. Hazard. Mater.* 437:129281. doi: 10.1016/j.jhazmat.2022.129281

Dai, Z., Yu, M., Chen, H., Zhao, H., Huang, Y., Su, W., et al. (2020). Elevated temperature shifts soil N cycling from microbial immobilization to enhanced mineralization, nitrification and denitrification across global terrestrial ecosystems. *Glob. Chang. Biol.* 26, 5267–5276. doi: 10.1111/gcb.15211

Hu, X., Gu, H., Sun, X., Wang, Y., Liu, J., Yu, Z., et al. (2023). Distinct influence of conventional and biodegradable microplastics on microbe-driving nitrogen cycling processes in soils and plastispheres as evaluated by metagenomic analysis. *J. Hazard. Mater.* 451:131097. doi: 10.1016/j.jhazmat.2023.131097

Isobe, K., and Ohte, N. (2014). Ecological perspectives on microbes involved in N-cycling. *Microbes Environ.* 29, 4–16. doi: 10.1264/jsme2.me13159

Jiang, X., Liu, C., Cai, J., Hu, Y., Shao, K., Tang, X., et al. (2023). Relationships between environmental factors and N-cycling microbes reveal the indirect effect of further eutrophication on denitrification and DNRA in shallow lakes. *Water Res.* 245:120572. doi: 10.1016/j.watres.2023.120572

Jiang, T., Zhang, W., and Liang, Y. (2022). Uptake of individual and mixed per-and polyfluoroalkyl substances (PFAS) by soybean and their effects on functional genes related to nitrification, denitrification, and nitrogen fixation. *Sci. Total Environ.* 838:156640. doi: 10.1016/j.scitotenv.2022.156640

Li, X., Cui, B., Yang, Q., Tian, H., Lan, Y., Wang, T., et al. (2012). Detritus quality controls macrophyte decomposition under different nutrient concentrations in a eutrophic shallow lake, North China. *Plos One.* 7:e42042. doi: 10.1371/journal.pone.0042042

Li, S., Gang, D., Zhao, S., Qi, W., and Liu, H. (2021). Response of ammonia oxidation activities to water-level fluctuations in riparian zones in a column experiment. *Chemosphere* 269:128702. doi: 10.1016/j.chemosphere.2020.128702

Li, H., Miller, T., Lu, J., and Goel, R. (2022). Nitrogen fixation contribution to nitrogen cycling during cyanobacterial blooms in Utah Lake. *Chemosphere* 302:134784. doi: 10.1016/j.chemosphere.2022.134784

Li, Y., Wang, C., Wu, J., Zhang, Y., Li, Q., Liu, S., et al. (2023). The effects of localized plant–soil–microbe interactions on soil nitrogen cycle in maize rhizosphere soil under long-term fertilizers. *Agronomy* 13:2114. doi: 10.3390/agronomy13082114

Liao, J., Dou, Y., Yang, X., and An, S. (2023). Soil microbial community and their functional genes during grassland restoration. *J. Environ. Manag.* 325:116488. doi: 10.1016/j.jenvman.2022.116488

Liu, X., Bin, S., Yu, T., Meng, J., and Zhou, Y. (2020). Spatio-temporal variations in the characteristics of water eutrophication and sediment pollution in Baiyangdian Lake (in Chinese). *Environ. Sci.* 40, 2127–2136. doi: 10.13227/j.hjkx.201909263

Marshall, A. J., Longmore, A., Phillips, L., Tang, C., Hayden, H. L., Heidelberg, K. B., et al. (2021). Nitrogen cycling in coastal sediment microbial communities with seasonally variable benthic nutrient fluxes. *Aquat. Microb. Ecol.* 86, 1–19. doi: 10.3354/ame01954

Morse, J. L., Werner, S. F., Gillin, C. P., Goodale, C. L., Bailey, S. W., McGuire, K. J., et al. (2014). Searching for biogeochemical hot spots in three dimensions: soil C and N cycling in hydropedologic settings in a northern hardwood forest. *J. Geophys. Res. Biogeo.* 119, 1596–1607. doi: 10.1002/2013JG002589

Pajares, S., Merino Ibarra, M., Macek, M., and Alcocer, J. (2017). Vertical and seasonal distribution of picoplankton and functional nitrogen genes in a high-altitude warm-monomictic tropical lake. *Freshwater Biol.* 62, 1180–1193. doi: 10.1111/fwb.12935

Shi, W., Zhu, L., Van Dam, B., Smyth, A. R., Deng, J., Zhou, J., et al. (2022). Wind induced algal migration manipulates sediment denitrification N-loss patterns in shallow Taihu Lake, China. *Water Res.* 209:117887. doi: 10.1016/j.watres.2021.117887

Stewart, K. J., Brummell, M. E., Coxson, D. S., and Siciliano, S. D. (2013). How is nitrogen fixation in the high arctic linked to greenhouse gas emissions? *Plant Soil* 362, 215–229. doi: 10.1007/s11104-012-1282-8

Stoliker, D. L., Repert, D. A., Smith, R. L., Song, B., LeBlanc, D. R., McCobb, T. D., et al. (2016). Hydrologic controls on nitrogen cycling processes and functional gene

abundance in sediments of a groundwater flow-through Lake. *Environ. Sci. Technol.* 50, 3649–3657. doi: 10.1021/acs.est.5b06155

Tan, Y., Wang, Y., Chen, Z., Yang, M., Ning, Y., Zheng, C., et al. (2022). Long-term artificial drainage altered the product stoichiometry of denitrification in alpine peatland soil of Qinghai-Tibet plateau. *Geoderma* 428:116206. doi: 10.1016/j.geoderma.2022.116206

Tu, Q., He, Z., Wu, L., Xue, K., Xie, G., Chain, P., et al. (2017). Metagenomic reconstruction of nitrogen cycling pathways in a CO2-enriched grassland ecosystem. *Soil Biol. Biochem.* 106, 99–108. doi: 10.1016/j.soilbio.2016.12.017

Waldrop, M. P., Chabot, C. L., Liebner, S., Holm, S., Snyder, M. W., Dillon, M., et al. (2023). Permafrost microbial communities and functional genes are structured by latitudinal and soil geochemical gradients. *ISME J.* 17, 1224–1235. doi: 10.1038/s41396-023-01429-6

Wang, F., Liang, X., Ding, F., Ren, L., Liang, M., An, T., et al. (2022). The active functional microbes contribute differently to soil nitrification and denitrification potential under long-term fertilizer regimes in north-East China. *Front. Microbiol.* 13:1021080. doi: 10.3389/fmicb.2022.1021080

Wang, X., Wang, P., Wang, C., Chen, J., Hu, B., Yuan, Q., et al. (2023). Cascade damming impacts on microbial mediated nitrogen cycling in rivers. *Sci. Total Environ.* 903:166533. doi: 10.1016/j.scitotenv.2023.166533

Wang, M., Yu, Y., Ren, Y., Wang, J., and Chen, H. (2023). Effect of antibiotic and/or heavy metal on nitrogen cycle of sediment-water interface in aquaculture system: implications from sea cucumber culture. *Environ. Pollut.* 325:121453. doi: 10.1016/j.envpol.2023.121453

Wu, H., Hao, B., Cai, Y., Liu, G., and Xing, W. (2021). Effects of submerged vegetation on sediment nitrogen-cycling bacterial communities in Honghu Lake (China). *Sci. Total Environ.* 755:142541. doi: 10.1016/j.scitotenv.2020.142541

Wu, Y., Xu, L., Wang, Z., Cheng, J., Lu, J., You, H., et al. (2022). Microbially mediated Fe-N coupled cycling at different hydrological regimes in riparian wetland. *Sci. Total Environ.* 851:158237. doi: 10.1016/j.scitotenv.2022.158237

Wu, J., Zhang, Y., Huang, M., Zou, Z., Guo, S., Wang, J., et al. (2022). Sulfonamide antibiotics alter gaseous nitrogen emissions in the soil-plant system: a mesocosm experiment and meta-analysis. *Sci. Total Environ.* 828:154230. doi: 10.1016/j.scitotenv.2022.154230

Yang, J., Yu, Q., Su, W., Wang, S., Wang, X., Han, Q., et al. (2023). Metagenomics reveals elevated temperature causes nitrogen accumulation mainly by inhibiting nitrate reduction process in polluted water. *Sci. Total Environ.* 882:163631. doi: 10.1016/j.scitotenv.2023.163631

Yao, X., Wang, Z., Liu, W., Zhang, Y., Wang, T., and Li, Y. (2023). Pollution in river tributaries restricts the water quality of ecological water replenishment in the Baiyangdian watershed, China. *Environ. Sci. Pollut. Res. Int.* 30, 51556–51570. doi: 10.1007/s11356-023-25957-y

Yuan, H., Cai, Y., Wang, H., Liu, E., and Zeng, Q. (2023). Impact of seasonal change on dissimilatory nitrate reduction to ammonium (DNRA) triggering the retention of nitrogen in lake. *J. Environ. Manag.* 341:118050. doi: 10.1016/j.jenvman.2023.118050

Zhang, L., Bai, J., Zhang, K., Wang, Y., Xiao, R., Campos, M., et al. (2023). Occurrence, bioaccumulation and ecological risks of antibiotics in the water-plant-sediment systems in different functional areas of the largest shallow lake in North China: impacts of river input and historical agricultural activities. *Sci. Total Environ.* 857:159260. doi: 10.1016/j.scitotenv.2022.159260

Zhao, Y., Xia, X. H., Yang, Z. F., and Xia, N. (2011). Temporal and spatial variations of nutrients in Baiyangdian Lake, North China. *J. Environ. Inf.* 17, 102–108. doi: 10.3808/jei.201100192

Zhou, Y., Xu, X., Song, K., Yeerken, S., Deng, M., Li, L., et al. (2021). Nonlinear pattern and algal dual-impact in N2O emission with increasing trophic levels in shallow lakes. *Water Res.* 203:117489. doi: 10.1016/j.watres.2021.117489

frontiers | Frontiers in Microbiology

TYPE Original Research
PUBLISHED 21 February 2024
DOI 10.3389/fmicb.2024.1354279

OPEN ACCESS

EDITED BY
Yizhi Sheng,
China University of Geosciences, China

REVIEWED BY
Jia Meng,
Harbin Institute of Technology, China
Ren-Cun Jin,
Hangzhou Normal University, China
Chongjun Chen,
Suzhou University of Science and Technology, China

*CORRESPONDENCE
Zifang Chi
✉ chizifang@jlu.edu.cn

RECEIVED 12 December 2023
ACCEPTED 05 February 2024
PUBLISHED 21 February 2024

CITATION
Li H, Song A, Qiu L, Liang S and Chi Z (2024) Deep groundwater irrigation altered microbial community and increased anammox and methane oxidation in paddy wetlands of Sanjiang Plain, China.
Front. Microbiol. 15:1354279.
doi: 10.3389/fmicb.2024.1354279

Deep groundwater irrigation altered microbial community and increased anammox and methane oxidation in paddy wetlands of Sanjiang Plain, China

Huai Li[1], Aiwen Song[1,2], Ling Qiu[3], Shen Liang[1,2] and Zifang Chi[4]*

[1]State Key Laboratory of Black Soils Conservation and Utilization, Northeast Institute of Geography and Agroecology, Chinese Academy of Sciences, Changchun, China, [2]University of Chinese Academy of Sciences, Beijing, China, [3]Second Hospital of Jilin University, Changchun, China, [4]Key Lab of Groundwater Resources and Environment, Ministry of Education, Jilin University, Changchun, China

The over-utilizing of nitrogen fertilizers in paddy wetlands potentially threatens to the surrounding waterbody, and a deep understanding of the community and function of microorganisms is crucial for paddy non-point source pollution control. In this study, top soil samples (0–15 cm) of paddy wetlands under groundwater's irrigation at different depths (H1: 6.8 m, H2: 13.7 m, H3: 14.8 m, H4: 15.6 m, H5: 17.0 m, and H6: 17.8 m) were collected to investigate microbial community and function differences and their interrelation with soil properties. Results suggested some soil factor differences for groundwater's irrigation at different depths. Deep-groundwater's irrigation (H2-H6) was beneficial to the accumulation of various electron acceptors. Nitrifying-bacteria *Ellin6067* had high abundance under deep groundwater irrigation, which was consistent with its diverse metabolic capacity. Meanwhile, denitrifying bacteria had diverse distribution patterns. Iron-reducing bacteria *Geobacter* was abundant in H1, and *Anaeromyxobacter* was abundant under deep groundwater irrigation; both species could participate in Fe-anammox. Furthermore, *Geobacter* could perform dissimilatory nitrate reduction to ammonia using divalent iron and provide substrate supply for anammox. *Intrasporangium* and *norank_f_Gemmatimonadacea* had good chromium- and vanadium-reducting potentials and could promote the occurrence of anammox. Low abundances of methanotrophs *Methylocystis* and *norank_f_Methyloligellaceae* were associated with the relatively anoxic environment of paddy wetlands, and the presence of aerobic methane oxidation was favorable for *in-situ* methane abatement. Moisture, pH, and TP had crucial effects on microbial community under phylum- and genus-levels. Microorganisms under shallow groundwater irrigation were highly sensitive to environmental changes, and Fe-anammox, nitrification, and methane oxidation were favorable under deep groundwater irrigation. This study highlights the importance of comprehensively revealing the microbial community and function of paddy wetlands under groundwater's irrigation and reveals the underlying function of indigenous microorganisms in agricultural non-point pollution control and greenhouse gas abatement.

KEYWORDS

paddy wetlands, soil indigenous microorganisms, groundwater's irrigation, microbial community, microbial function

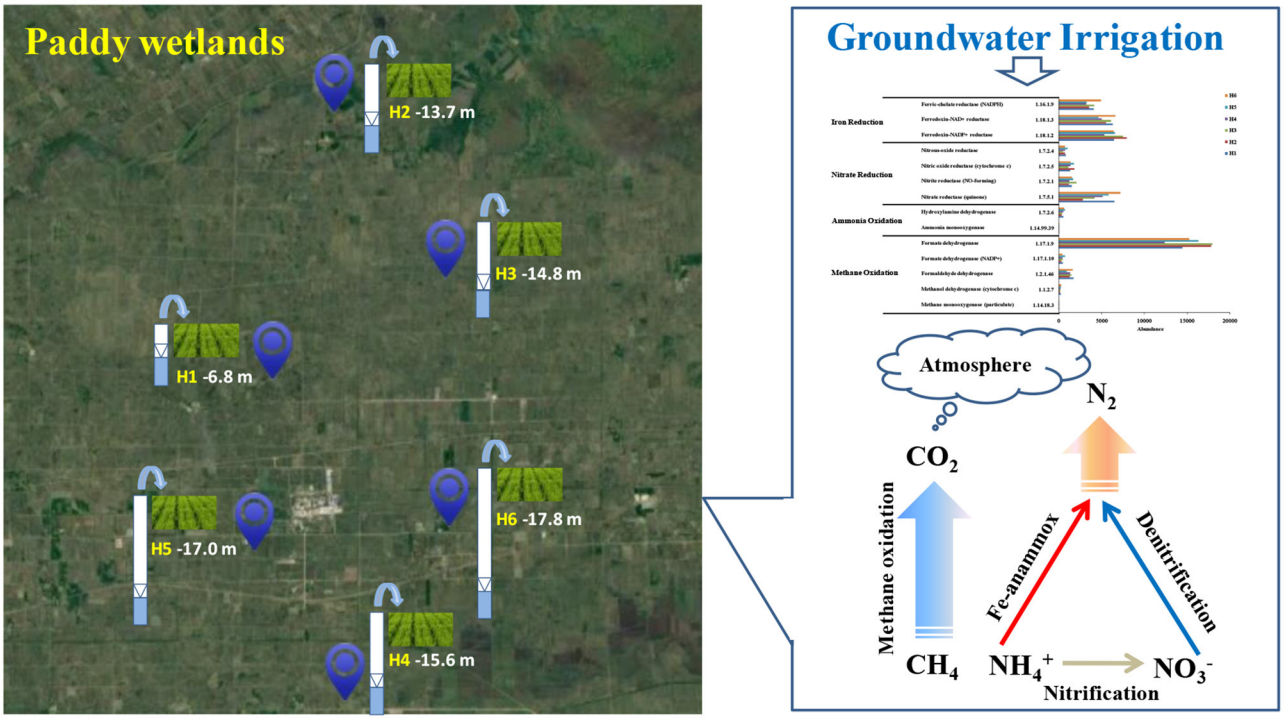

GRAPHICAL ABSTRACT

Highlights

- Deep groundwater irrigation favors the accumulation of multi-electron acceptors
- *Geobacter* and *Anaeromyxobacter* could participate in Fe-anammox
- *Methylocystis* and *norank_f_Methyloligellaceae* involve *in-situ* abatement of methane
- Moisture, pH, and TP play important roles in shaping microbial community
- Deep groundwater irrigation promotes Fe-anammox, nitrification, and methane oxidation

1 Introduction

Paddy wetlands, in which the constructed wetlands were coupled with water and fertilizer, had typical wetland ecosystems and vegetation characteristics and could provide unique habitats for microorganisms to ensure global food security (Ding et al., 2021). However, the excessive nitrogen-fertilizers application under large-scale irrigation could cause serious soil degradation and surrounding-water pollution, posing a major risk to human's health (Sun et al., 2021). In addition, paddy wetlands were one of the major sources of methane emission (Sun et al., 2019). Soil microorganisms regulated wetland biogeochemical cycles (Torsvik and Øvreås, 2002). Microbial species had various functions, such as denitrification and methane oxidation (Li et al., 2014; Chi et al., 2021a). Some biotic or abiotic factors could control microbial community composition and function, and microorganisms were sensitive and could respond rapidly to environmental changes (Guo et al., 2019; Pérez Castro et al., 2019). Therefore, revealing the community and function of microorganisms in paddy wetlands was crucial for maintaining their ecological stability and material management.

As efficient agronomic measures, fertilization and irrigation could affect microbial community and diversity in paddy wetlands (Wang et al., 2021). Environmental changes obviously altered microbial communities and activities, thereby affecting biogeochemical processes. Long-term fertilization could alter soil physicochemical properties, thereby affecting microbial communities (Guo et al., 2020). Hou et al. (2022) found that the long-term application of pig manure could promote the enrichment of complex organic-degrading bacteria and improve soil enzyme activity. Inorganic fertilizers could increase microbial diversity and change microbial community composition in paddy wetlands (Huang et al., 2019). The type of fertilizer had minimal influence on microbial community under long-term fertilization (Liu et al., 2022). Furthermore, irrigation could ensure rice growth and affect microbial community. Jiang et al. (2021) showed that irrigation combined with biochar could alleviate greenhouse gas emissions and alter microbial community. Irrigation modes had some effects on microbial community of paddy wetlands (Jin et al., 2020). Reclaimed water irrigation could improve soil microbial activity and fertility to a certain extent (Wei et al., 2017). Although some studies investigated microbial community of paddy wetlands under fertilization and irrigation, the effects of groundwater's irrigation at different depths on microbial community and diversity in paddy wetlands remain unknown.

Recent studies were involved in the function and metabolic potential of microorganisms (Chi et al., 2021d). Li et al. (2019) revealed the responses of nitrogen-metabolized pathways and relevant function genes to coastal environmental variations. Exogenous pollution input could alter microbial community, thus changing their metabolic function (Chi et al., 2021b). The genes encoding exogenous metabolism and nitrate-reducting were significantly enriched on coastal sediments (Su et al., 2018). The Sanjiang Plain was regarded as a representative of large-scale paddy development, and paddy wetlands was mainly irrigated using groundwater with various electron acceptors (Cao et al., 2016; Chong et al., 2020; Meng et al., 2021; Chen et al., 2024). However, research on the community and function of microorganisms in paddy wetlands under groundwater's irrigation was still lacking.

Microorganisms in paddy wetlands had vital effects on the nitrogen cycle, but a large knowledge gap existed regarding the influence of groundwater irrigation. We hypothesized that groundwater irrigation had significant effects on microbial communities and functions of paddy wetlands, and that the input of exogenous electron acceptors could improve soil material transformation. To test this hypothesis, we analyzed soil genetic data from paddy wetlands under groundwater irrigation using high-throughput sequencing. The aims in this study were as follows: (1) to reveal the microbial community composition and difference in paddy wetlands under groundwater's irrigation at different depths, (2) to elucidate the responses in the metabolic-pathways and related-enzyme genes of microorganisms, and (3) to explore the dominant enablers involving in microbial community and functional variation in paddy wetlands. This study can offer valuable academic references for non-point source pollution control and greenhouse gas reduction of paddy wetlands.

2 Materials and methods

2.1 Sampling area description

The research area was situated on Honghe Farm of Sanjiang Plain in the Heilongjiang Province, China, which belonged to the temperate- and continental-monsoon climate. The mean temperature and rainfall per year were 1.6°C−1.9°C and 565–600 mm, respectively. Precipitation was concentrated from June to August. Furthermore, the growing period of rice was from May to September, and the type of the soil was paddy soil. Urea was the main fertilizer with an average fertilization rate of 180 kg N/hm^2. The paddy wetlands in this area were mainly assarted from swamps and dry land in the last few decades, which were under groundwater's irrigation. Therefore, paddy wetlands under groundwater's irrigation at different depths, such as H1 (−6.8 m), H2 (−13.7 m), H3 (−14.8 m), H4 (−15.6 m), H5 (−17.0 m), and H6 (−17.8 m), were selected to investigate the underlying influence of groundwater's irrigation on microbial community and function of paddy wetlands (Figure 1). Here, we defined shallow- and deep-groundwater as less and more than 10 m at depth.

2.2 Soil collecting and analysis

Top soil samples (0–15 cm) in paddy wetlands were collected in triplicgot and mixed into a composite sample at sampling sites H1 (47°37′39″-N; 133°29′11″-E), H2 (47°43′15″-N; 133°31′6″-E), H3 (47°39′47″-N; 133°34′35″-E), H4 (47°30′55″-N; 133°31′27″-E), H5 (47°34′4″-N; 133°28′37″-E), and H6 (47°34′35″-N; 133°34′41″-E) in May 2021. Six soil samples were obtained and named H1, H2, H3, H4, H5, and H6. All soil samples were placed in plastic bags and then sent to the nearby laboratory on ice packs. A part was air-dried for 3 weeks at room-temperature and then filtered using a 2-mm sifter in order to determinate soil properties. And the rest part was stored in a −80°C in order to analyse microbial community and function. Soil physicochemical factors were tested as previously described (Li et al., 2019).

2.3 Illumina sequence and statistical analyses

Total DNA from the six soil samples was extracted by means of PowerSoil-DNA-isolation kit (MoBio, Carlsbad, CA). Moreover, V3-V4 region in 16S rRNA gene was amplifed using primers 338F and 806R. PCR amplification was performed in a total volume of 20 μL (contained 4 μL Buffer, 0.4 μL FastPfu Polymerase, 2 μL dNTP, 5 μM of each primer and 10 ng genome DNA). Thermal cycling conditions were as follows: an initial denaturation at 95°C for 3 min, followed by 35 cycles at 95°C for 30 s, 55°C for 30 s, and 72°C for 45 s, with a final extension at 72°C for 10 min. The PCR products were further performed based on Illumina-MiSeq-platform (Shanghai-Majorbio Bio-pharm Technology Co., Ltd., China). Processing of raw sequences obtained from Illumina sequencing was performed using QIIME software (version 1.9.1). We assembled paired-end reads using FLASH (version 1.2.11, https://ccb.jhu.edu/software/FLASH/index.shtml), where forward and reverse reads had overlapping base lengths ≥10 bp, and base mismatches were prevented. Reads with a quality score <20, ambiguous bases, and improper primers were discarded before clustering. High-quality sequences of 252096 were acquired with 36934–48033 sequences for each soil sample. The obtained sequences were further clustered through USEARCH with 97% similarity as OTUs. And the taxonomy was verified by the Silva databases. To reduce the influence of sequencing depth on treatment effects, the samples were randomly resampled to the same sequence depth based on the least number of sequences. Correlation analysis (CA) was used to uncover the interrelation between crucial phyla, function gene, and soil property. Principal coordinate analysis (PCoA) was utilized to identify microbial community difference. Redundancy analysis was performed to investigate the key factors shaping microbial community and function. Shannon index, functional gene, and metabolic pathway were obtained using Quantitative Insights into Microbial Ecology (QIIME) and Phylogenetic Investigation of Communities by Reconstruction of Unobserved States (PICRUSt) (Chen et al., 2016; Guo et al., 2022).

10.3389/fmicb.2024.1354279

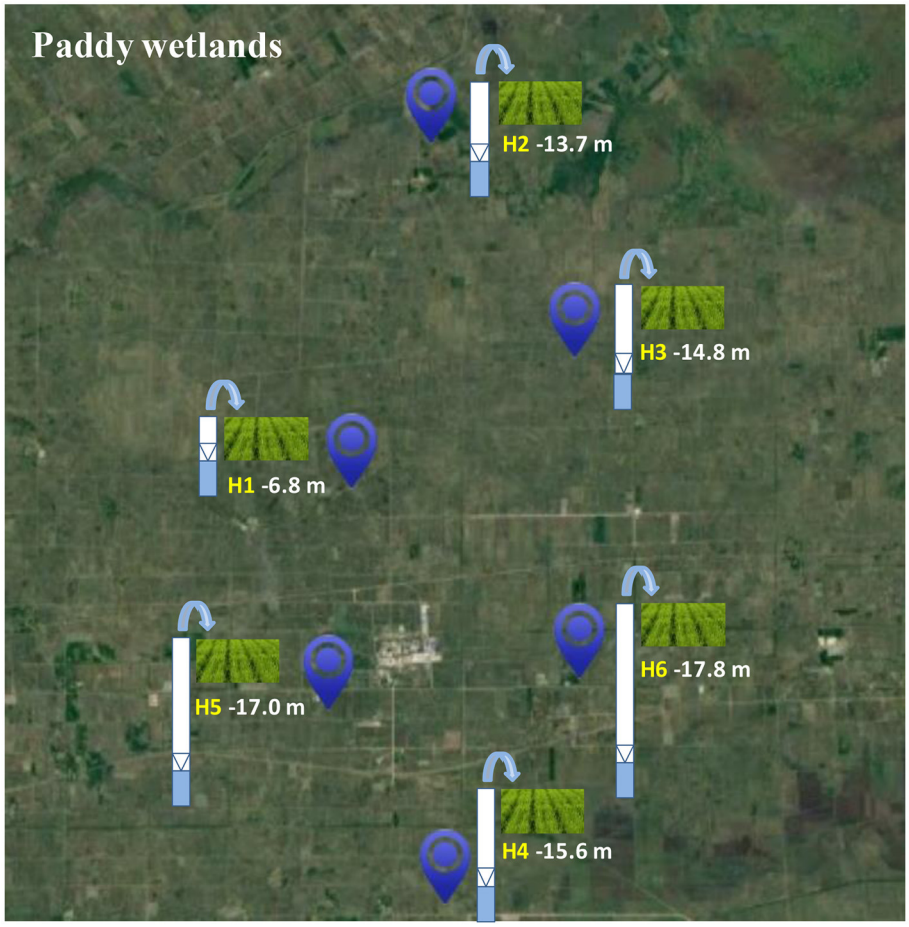

FIGURE 1
Sampling sites of paddy wetlands under groundwater irrigation.

3 Results and discussion

3.1 Soil characteristics

The soil of paddy wetlands was weakly acidic and had low salinity for groundwater's irrigation at various depths, whereas the contents of SOM, TN, and TP were relatively high in the ranges of 2.93–5.90%, 1571.46–3397.90 mg/kg, and 4892.93–6347.79 mg/kg, respectively (Figure 2). The level of NH_4^+-N was high and that of NO_3^--N was low. Fe, Mn and SO_4^{2-} were abundant in paddy soil. In particular, SOM, NH_4^+-N, and TN had high levels in H3 and H5, indicating their good nutrient condition that was conducive to paddy growth and material transformation. Meanwhile, the low levels in H2 and H4 may be related to their soil structure and properties. The low NO_3^--N level was consistent with high SOM amount, suggesting that a high SOM content in paddy soil could promote denitrification (Li et al., 2019). Mn had high levels in H2, H4, and H6; Fe was significantly enriched in H2, H3, and H6; and SO_4^{2-} was high in H6. These findings implied that deep-groundwater's irrigation was beneficial to the enrichment of multiple electron acceptors. CA showed that salinity had a positive correlation with NO_3^--N, and TN levels ($p < 0.05$; Supplementary Table 1), indicating that high salinity had inhibitory effects on denitrification (Wang et al., 2018a). SOM had a positive correlation with TN ($p < 0.01$), suggesting that SOM accumulating was beneficial to TN enriching. Mn was negatively correlated with SOM, NO_3^--N, and TN, indicating that Mn was mainly affected by groundwater irrigation. No significant correlation was found among Fe, SO_4^{2-}, and other soil properties. In summary, SOM, TN, and TP were abundant in paddy soil; some differences were observed among the paddy soil samples for groundwater's irrigation at various depths; and deep-groundwater's irrigation could promote the accumulation of various electron acceptors.

3.2 Microbial community composition and difference

The community of microorganisms under phylum- and genus-levels was shown in Figure 3. Acidobacteriota, Desulfobacterota, Actinobacteriota, Myxococcota, Bacteroidota, Firmicutes, Chloroflexi, Nitrospirota, Planctomycetota, and Proteobacteria were the important phyla with over 97% bacterial abundance (Figure 3A). Among them, Actinobacteriota, Chloroflexi, and Firmicutes had a correlation with organics degradation (He

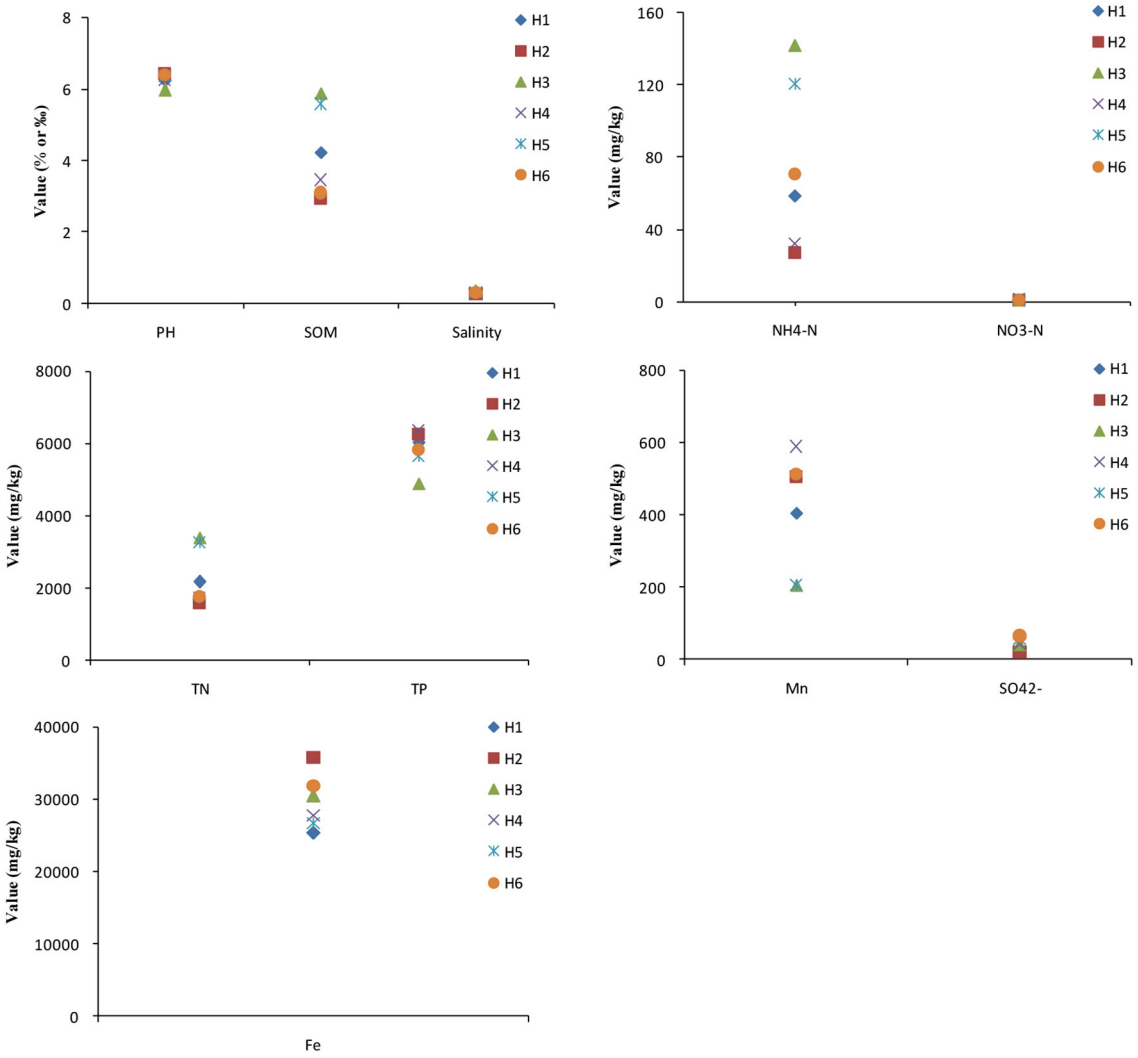

FIGURE 2
Physicochemical parameters of paddy wetland soils at different sampling sites.

et al., 2018; Chi et al., 2021b), and Acidobacteriota, Bacteroidota, Nitrospirota, Planctomycetota, and Proteobacteria were connected with nitrogen cycling (Chi et al., 2021e). Desulfobacterota and Myxococcota were involved in sulfur and iron cycle (Langwig et al., 2022). Bacteroidota and Firmicutes were the most abundant in H1, and Acidobacteriota and Proteobacteria had the highest abundance in H2. The abundance of Acidobacteriota was lower in H1 than in H2-H6; this species played key roles in denitrification (Zhang et al., 2020). In addition, low abundance of Nitrospiota was consistent with the relatively anoxic environment of paddy wetlands. High abundance of Proteobacteria in paddy wetlands was relating to its diverse substrate-utilizing and environmental-adaptability (Bernhard et al., 2005). High abundances of Actinobacteriota and Chloroflexi were consistent with high SOM amount in the soil. Therefore, the phyla related to carbon and nitrogen cycling were widespread and abundant in paddy wetlands, and some phyla had high abundance under deep groundwater irrigation.

The dominant genera were MND1, *Sphingomonas*, *Ellin6067*, *Flavobacterium*, *Pseudolabrys*, *Rhodanobacter*, *Gemmatimonas*, *Anaeromyxobacter*, *Bacillus*, *Geobacter*, *Citrifermentans*, *Methylocystis*, *norank_f_Methyloligellaceae*, *Pseudarthrobacter*, and *Conexibacter* (Figure 3B). The abundances of nitrifying bacteria MND1 and *Sphingomonas* were relatively low, although NH_4^+-N level was high in paddy soil; the discrepancy may be related to the relatively anoxic environment of paddy wetlands (Tolar et al., 2020; Gao et al., 2021). High abundance of nitrifying bacteria *Ellin6067* was related to its diverse metabolic capabilities (such as nitrification and organic matter degradation) (Lezcano et al., 2017; Li et al., 2021b), and *Ellin6067* was abundant in deep groundwater irrigation. In addition, aerobic *Candidatus_Udaeobacter* was widely distributed in paddy soil but had low abundance, further indicating the relatively anoxic environment of paddy wetlands (Li et al., 2021a). The denitrifying bacteria *Flavobacterium* was widely distributed in paddy wetlands, with the highest abundance

10.3389/fmicb.2024.1354279

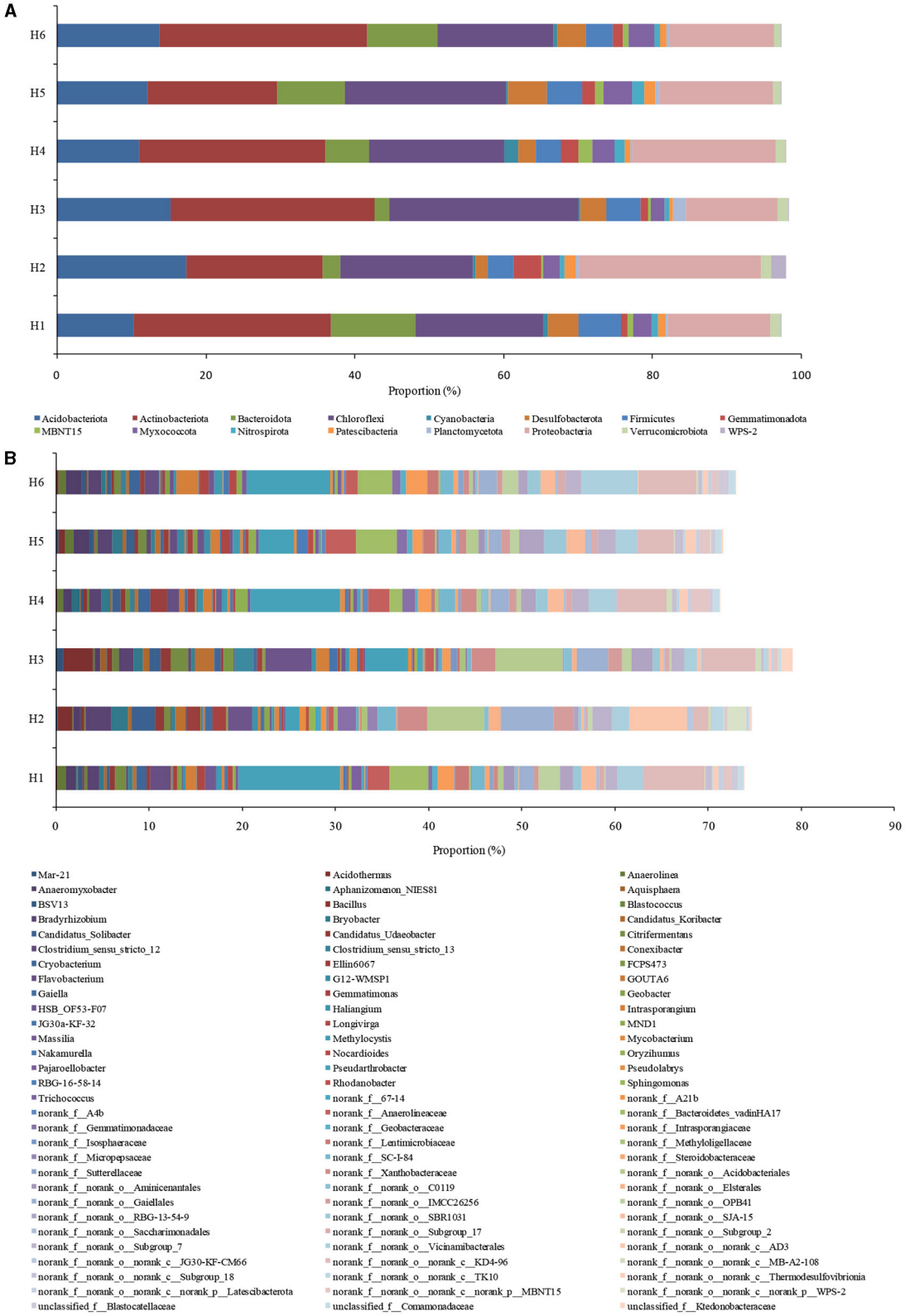

FIGURE 3
Taxonomic classification of bacterial community at **(A)** phylum and **(B)** genus levels. Less than 0.5% was not included.

found under shallow groundwater irrigation (Pishgar et al., 2020). Meanwhile, *Pseudolabrys*, *Rhodanobacter*, and *Gemmatimonas* were abundant under deep groundwater irrigation (Van Den Heuvel et al., 2010; Green et al., 2012; Yan et al., 2019), indicating the diversity of denitrifying bacteria. As an aerobic denitrifier, *Gemmatimonas* could reduce N_2O to N_2 and decrease greenhouse

gas emissions (Park et al., 2017). The high presence of denitrifying bacteria was consistent with the high SOM amount in the soil. The organic-degrading bacteria *Pseudarthrobacter* was abundant in all the samples, with the highest abundance found under shallow groundwater irrigation. *Conexibacter* had high abundance under deep groundwater irrigation. *Pseudarthrobacter* showed the organic matter degradation potential at low temperature (Zhang et al., 2016), and *Conexibacter* could decompose refractory organic matter (Liang et al., 2021). Iron-reducing bacteria *Geobacter* was abundant under shallow groundwater irrigation, and *Anaeromyxobacter*, *Bacillus*, and *Citrifermentans* were dominant under deep groundwater irrigation; all these genera had Fe-anammox potential (Chi et al., 2021a; Ottoni et al., 2022). Studies have shown that *Anaeromyxobacter* and *Geobacter* could participate in Fe-anammox (Zhou et al., 2016). Furthermore, *Geobacter* had dissimilar nitrate reduction potential and could drive dissimilatory nitrate reduction to ammonia (DNRA) using divalent iron, thus providing substrate for anammox (Finneran et al., 2002). Excitedly, *Intrasporangium* had chromium-reducing potential and was widely distributed in paddy wetlands (Yang et al., 2009). *norank_f_Gemmatimonadaceae* was abundant under deep groundwater irrigation and had good nitrate- and vanadium- reduction ability (Jia et al., 2019; Fei et al., 2022). The existence of these species could promote anammox. The methanotrophs *Methylocystis* and *norank_f_Methyloligellaceae* were widely distributed with low abundance, possibly due to the relatively anoxic environment of paddy wetlands. The presence of aerobic methane oxidation was beneficial to *in-situ* reduction of methane in paddy wetlands. Moreover, *HSB_OF53-F07* had nitrogen metabolism ability and diverse metabolic functions under aerobic/anoxic conditions (Wu et al., 2021). *Bradyrhizobium* with high abundance had nitrogen fixation function and could promote rice growth (Kaneko et al., 2002). *Candidatus_Solibacter* had high abundance under deep groundwater irrigation, which was consistent with the results in paddy soils under mine drainage irrigation and long-term fertilization (Wang et al., 2018b; Yu et al., 2019). *Candidatus_Solibacter* could degrade complex pollutants and outperform the competition in environmental filtration (Ward et al., 2009). *Cryobacterium* and *Trichococcus* had low temperature adaptations and may play important roles in material cycling (Pikuta et al., 2006; Teoh et al., 2021). Therefore, groundwater irrigation was beneficial to organics degradation, denitrification, and Fe-anammox. Meanwhile, nitrification and aerobic methane oxidation in paddy wetlands were relatively weak. Shallow groundwater irrigation increased organics degradation, but deep groundwater irrigation promoted the occurrence of Fe-anammox.

PCoA suggested that the microbial communities had minimal differences under shallow and deep groundwater irrigation, but significantly differed with H2 and H3, which was related to high the SOM, NH_4^+-N, TN, and Fe levels (Figure 4A). The abundance of *Pseudarthrobacter* under groundwater irrigation (above 15 m) was higher than that in other irrigation zones (below 15 m) ($p > 0.05$) (Figure 4B). Meanwhile *Bradyrhizobium* and *HSB_OF53-F07* had high abundances in irrigation zones (below 15 m) ($p > 0.05$), which was consistent with high abundance of *Bradyrhizobium* and low count of *HSB_OF53-F07* and *Pseudarthrobacter* in H2 and H3.

3.3 Key variables influencing the community of microorganisms

The Shannon's index was lower in shallow-groundwater's irrigation than in deep-groundwater's irrigation, indicating that deep-groundwater's irrigation with multiple electron acceptors was beneficial to the improvement of microbial diversity (Supplementary Figure 1). CA suggested that Acidobacteria was positively correlated with Fe ($p < 0.01$; Supplementary Table 2), expressing that Fe accumulation could promote Acidobacteria enrichment and facilitate denitrification. Chloroflexi had a positive correlation with SOM, salinity, moisture, NH_4^+-N, and TN, but negative correlation with TP, and Mn ($p<0.05$), suggesting that SOM and TN accumulation was beneficial to Chloroflexi enrichment. Planctomycetes showed a significant positive correlation with salinity ($p < 0.05$). A previous study found that anammox bacteria Scalindua had favorable salinity adaptation (Zheng et al., 2016). RDA showed that moisture, pH, and TP were the major controlling factors at phylum level, and NH_4^+-N and multi-electron acceptors had significant effects at genus level (Figures 5A, B). Similarly, previous studies found that pH and moisture had crucial effects on the microbial community (Banning et al., 2011; Pan et al., 2021), and nutrients also could alter microbial composition (Francioli et al., 2018). Thus, moisture, pH, and TP had crucial effects in shaping microbial community under phylum- and genus-levels.

3.4 Function prediction of microorganisms

Microbial functions were predicted by PICRUSt (Figure 6). Microorganisms were present in different metabolic pathways, such as metabolism, gene information's processing, environmental information's processing, and cellular processes (Li et al., 2018; Chi et al., 2021c); among which, their abundance in metabolism was the highest (Figure 6A). In particular, the genes involved in cell motility and growth/death were abundant, indicating the high microbial activity in paddy wetlands. High abundance of genes encoding carbohydrates, amino acids, and energy metabolism suggested the good material and energy metabolism of microorganisms. The gene encoding energy metabolism were abundant in H4-H6, and this finding was possibly related to the abundant supply of electron acceptors under deep groundwater irrigation. The expression of genes encoding xenobiotic biodegradation and terpenoids/polyketide metabolism was observed, indicating that microorganisms showed potential to metabolize exogenous substances. The genes related to signal transduction and membrane transport were highly abundant possibly due to the high nutrient levels in paddy wetlands. The repair-related gene was more expressed under shallow groundwater irrigation, indicating that microorganisms were alive to environmental variations. This findings were consistent with the low biodiversity in paddy wetlands.

These genes with regard to nitrogen and methane metabolism were analyzed as shown in Figure 6B. The nitrifying-related genes [EC:1.14.99.39 and EC:1.7.2.6] were abundant and highly expressed under deep groundwater irrigation, indicating that nitrification

10.3389/fmicb.2024.1354279

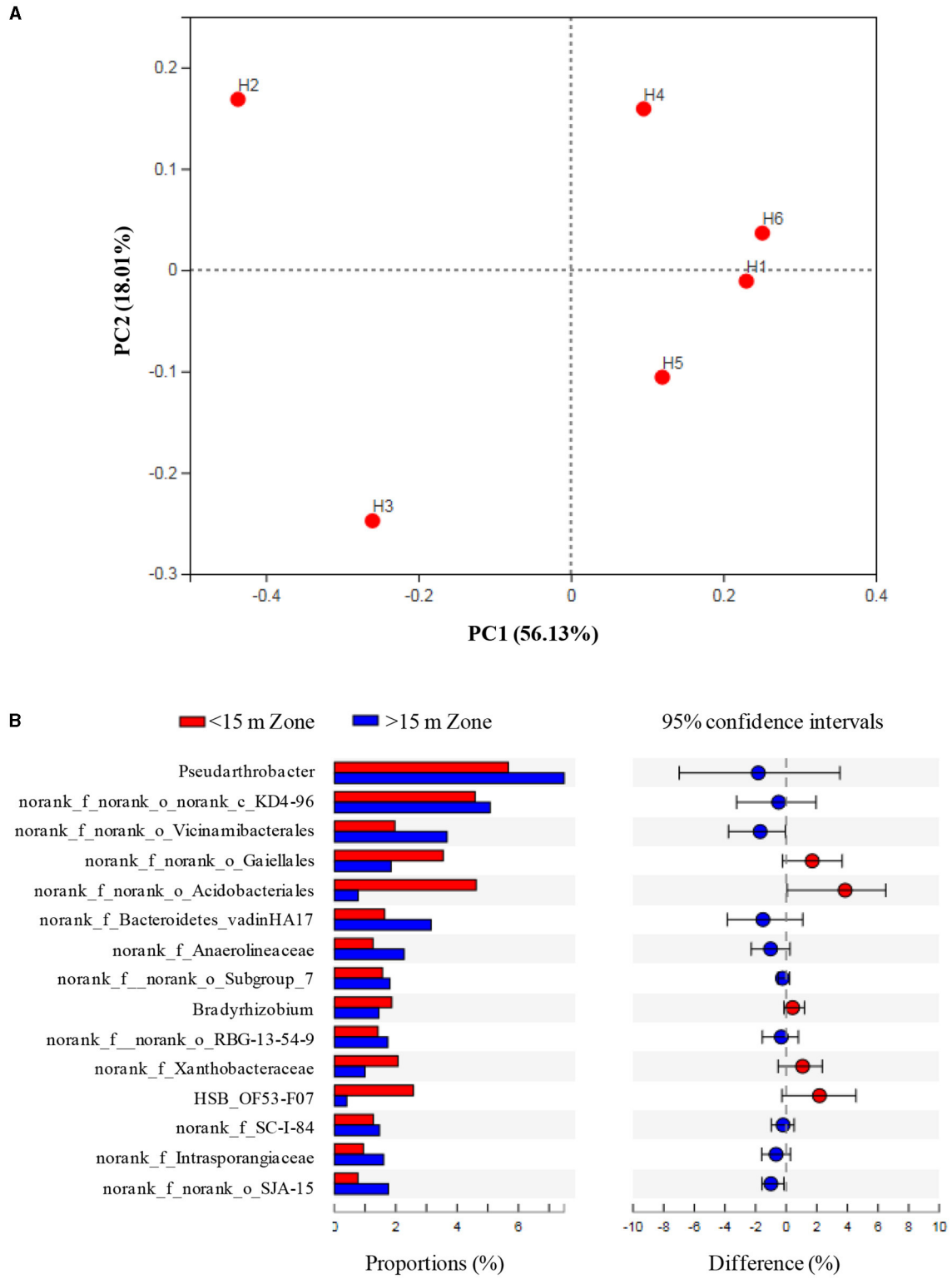

FIGURE 4
Principal coordinate analysis (PCoA) **(A)** and species differences **(B)** at different sampling zones.

occurred in paddy wetlands. The nitrate-reductase gene [EC:1.7.5.1], which could promote denitrification and DNRA, was the most abundant (Chi et al., 2021f). High level of nitrite-reductase gene [EC:1.7.2.1] was beneficial to denitrification and anammox (Chi et al., 2021d). The abundance of denitrifying-related genes coincided with widespread denitrifying bacteria and low NO_3^--N levels. Moreover, the genes related to iron reduction were highly expressed and highly abundant under deep groundwater

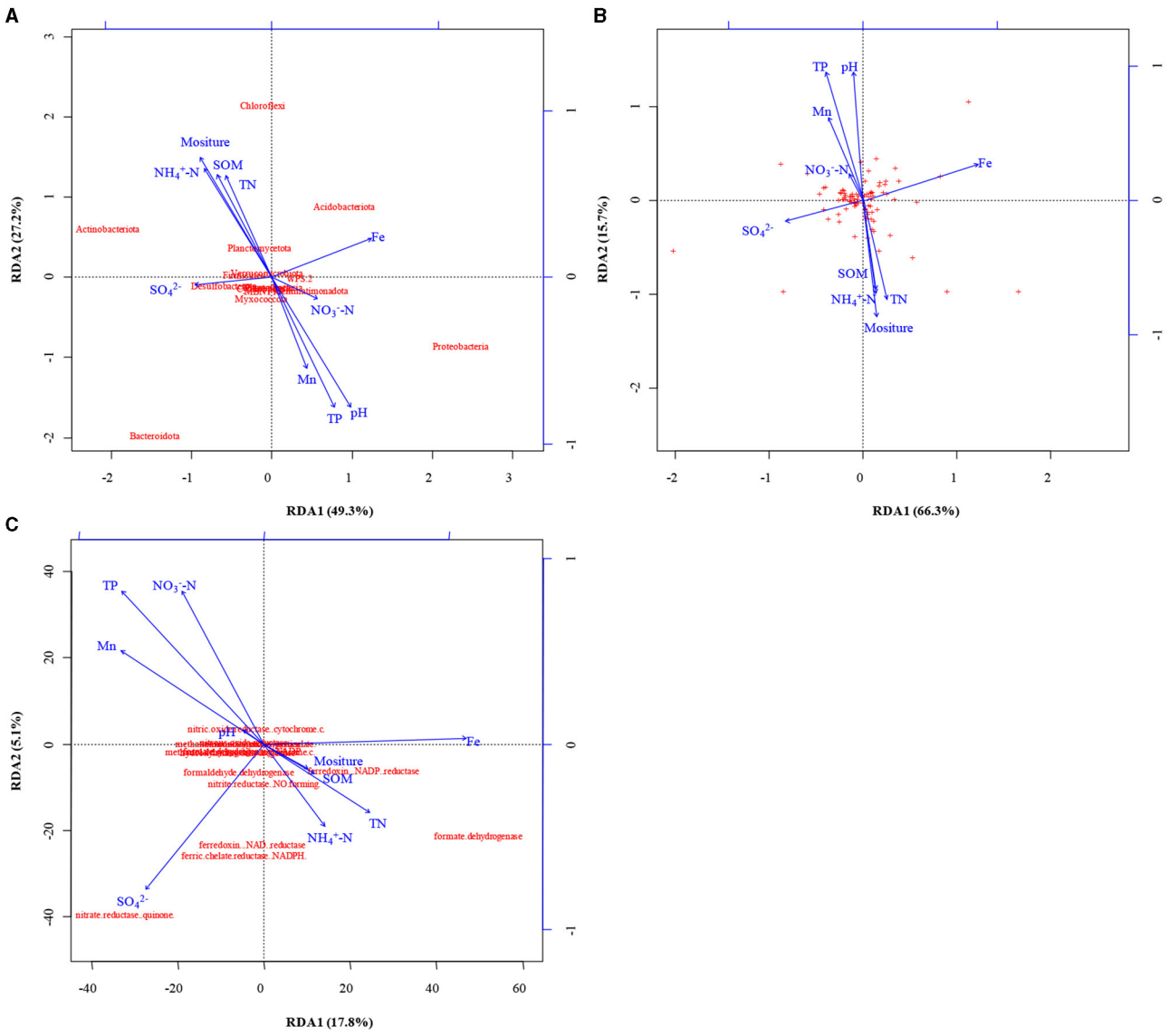

FIGURE 5
The results of redundancy analysis (RDA) between soil properties, microbial community at phyla **(A)** and genus **(B)** level, and functional genes **(C)**.

irrigation. This finding indicated the existence of Fe-anammox in paddy wetlands, which was consistent with the enrichment of Fe-anammox bacteria. The genes encoding methane oxidation were abundant, especially formate dehydrogenase [EC:1.17.1.9], indicating the widespread occurrence of methane oxidation. In particular, the abundance of formate dehydrogenase [EC:1.17.1.9] was more abundant under deep groundwater's irrigation than that under shallow groundwater's irrigation, indicating that deep groundwater's irrigation favored its enrichment. The low level of methane-monooxygenase [EC:1.14.18.3] was consistent with the relatively anoxic environment of paddy wetlands. The complete methane oxidation-related genes was related to the widespread distribution of methanotrophs. Thus, deep groundwater irrigation could promote Fe-anammox, nitrification, and methane oxidation. Meanwhile, denitrification was ubiquitous under groundwater irrigation.

RDA indicated that electron acceptors were the main drivers of functional gene changes, and TN and TP had some effects (Figure 5C). Previous studies reported that nutrients expressed important effects on the functional genes (Chi et al., 2021b), and electron acceptors had a direct role (Li et al., 2022). CA showed that nitrite reductase (NO-forming) had a positive correlation with SOM, salinity, moisture, NH_4^+-N, and TN ($p < 0.01$ or $p < 0.05$) but negative correlation with TP, and Mn ($p < 0.01$ or $p < 0.05$; Table 1), indicating that SOM and TN accumulation was favorable for denitrification. Furthermore, nitrite reductase (NO-forming) showed a positive correlation with NH_4^+-N ($p < 0.01$), suggesting the possibility of anammox (Li et al., 2019). In addition, NH_4^+-N had a positive correlation with ammonia monooxygenase, and hydroxylamine dehydrogenase ($p > 0.05$), implying that NH_4^+-N accumulation could promote nitrification. The genes with respect to iron reduction [ferredoxin–NADP+

10.3389/fmicb.2024.1354279

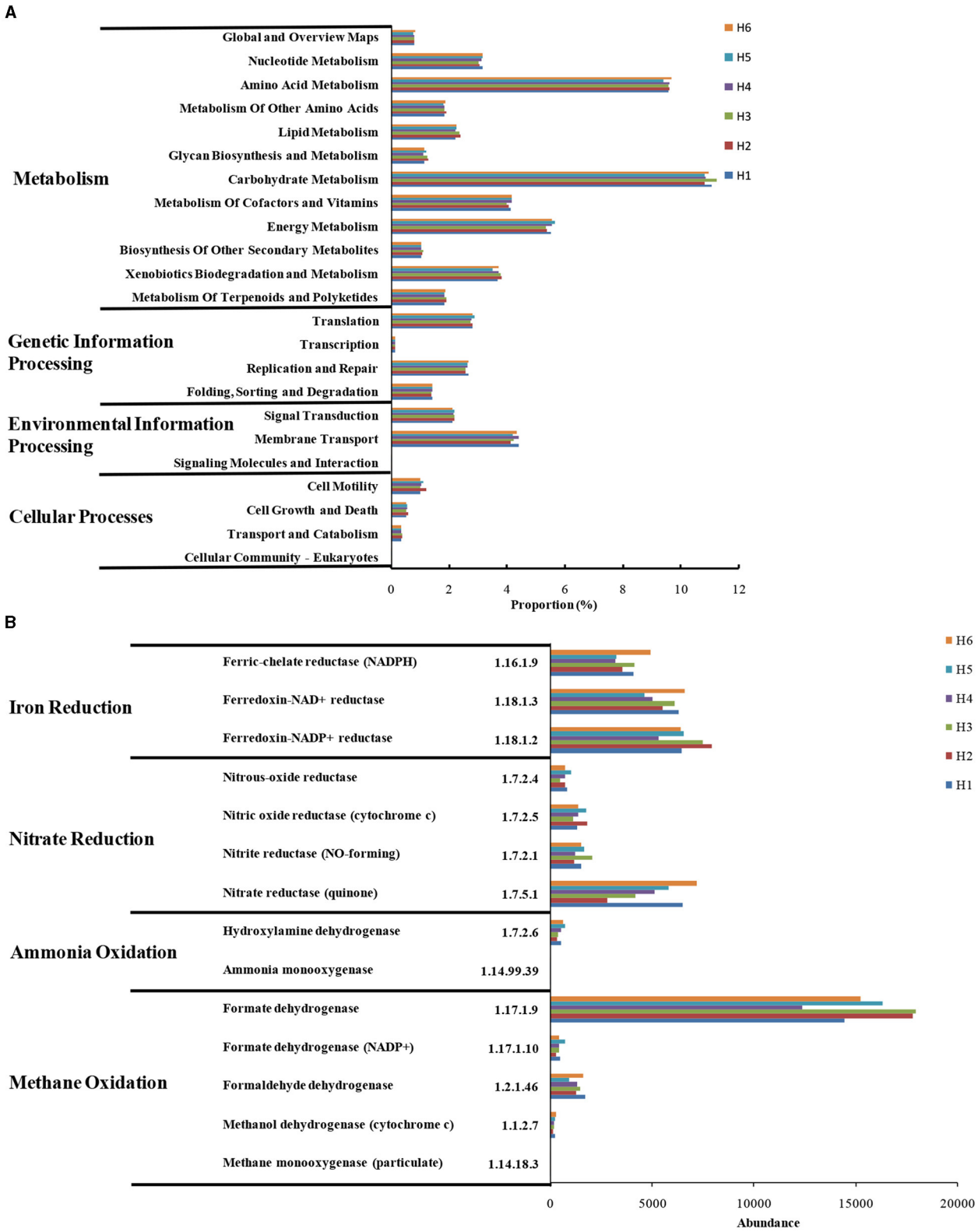

FIGURE 6
KEGG-predicted metabolic pathways **(A)** and functional genes **(B)** at different sampling sites.

reductase, ferredoxin–NAD+ reductase, and ferric-chelate reductase (NADPH)] were positively correlated with NH_4^+-N, and Fe ($p > 0.05$), indicating the existence of Fe-anammox of paddy wetlands.

TABLE 1 Correlation coefficient matrix between functional genes and physicochemical properties.

	pH	SOM	Salinity	Moisture	NH_4^+-N	NO_3^--N	TN	TP	Fe	Mn	SO_4^{2-}
Methane monooxygenase (particulate)	−0.119	0.575	0.215	0.327	0.398	0.251	0.579	−0.218	−0.159	−0.517	0.032
Methanol dehydrogenase (cytochrome c)	0.278	0.083	0.030	−0.150	0.289	−0.491	0.129	−0.119	−0.391	−0.153	0.772
Formaldehyde dehydrogenase	−0.295	−0.291	0.113	0.067	−0.195	−0.197	−0.333	−0.023	−0.020	0.318	−0.133
Formate dehydrogenase (NADP+)	0.016	0.643	0.262	0.310	0.602	−0.311	0.647	−0.304	−0.702	−0.636	0.566
Formate dehydrogenase	−0.104	0.366	0.374	0.276	0.491	−0.657	0.454	−0.593	0.576	−0.587	−0.181
Ammonia monooxygenase	−0.119	0.575	0.215	0.327	0.398	0.251	0.579	−0.218	−0.159	−0.517	0.032
Hydroxylamine dehydrogenase	0.327	0.146	−0.094	−0.162	0.208	−0.116	0.161	0.073	−0.613	−0.124	0.759
Nitrate reductase (quinone)	0.116	0.004	0.014	−0.089	0.128	−0.243	−0.001	0.012	−0.588	0.030	0.668
Nitrite reductase (NO-forming)	−0.719	0.860*	0.958**	0.831*	0.958**	−0.559	0.887*	−0.981**	−0.215	−0.857*	0.353
Nitric oxide reductase (cytochrome c)	0.830*	−0.290	−0.685	−0.597	−0.331	−0.016	−0.237	0.494	0.309	0.109	−0.158
Nitrous-oxide reductase	0.637	0.011	−0.492	−0.333	−0.097	−0.028	0.005	0.420	−0.483	−0.059	0.244
Ferredoxin—NADP+reductase	−0.037	0.156	0.187	0.167	0.232	−0.581	0.221	−0.388	0.657	−0.383	−0.448
Ferredoxin—NAD+reductase	−0.235	−0.209	0.229	0.057	0.012	−0.491	−0.194	−0.248	0.216	0.136	0.007
Ferric-chelate reductase (NADPH)	−0.100	−0.179	0.243	−0.049	0.139	−0.574	−0.124	−0.314	0.228	0.078	0.332

*$p < 0.05$ level significant correlation. **$p < 0.01$ level significant correlation.

4 Conclusions

This study illustrated the potential effects of groundwater's irrigation on the community and function of microorganism in paddy wetlands. Deep-groundwater's irrigation favored the accumulation of multi-electron acceptors. Groundwater irrigation was beneficial to organics degradation, denitrification, and Fe-anammox, but nitrification and aerobic methane oxidation were relatively weak in paddy wetlands. Moisture, pH, and TP played vital roles for microbial communities shaping. Microorganisms were highly sensitive to environmental changes under shallow-groundwater's irrigation, and deep-groundwater's irrigation favored Fe-anammox, nitrification, and methane oxidation. Denitrification was widespread under groundwater's irrigation. The findings offer new ideas for non-point source pollution control and greenhouse gas reduction in paddy wetlands.

Data availability statement

The original contributions presented in the study are included in the article/Supplementary material, further inquiries can be directed to the corresponding author.

Author contributions

HL: Writing—original draft. AS: Writing—review & editing. LQ: Writing—review & editing. SL: Writing—review & editing. ZC: Conceptualization, Funding acquisition, Supervision, Writing—review & editing.

Funding

The author(s) declare financial support was received for the research, authorship, and/or publication of

this article. This work was financially supported by the National Key R&D Program of China (Nos. 2023YFC3207704; 2022YFF1300901), Natural Science Foundation of Jilin Province (No. 20230101100JC), and National Natural Science Foundation of China (No. 42077353).

Conflict of interest

The authors declare that the research was conducted in the absence of any commercial or financial relationships that could be construed as a potential conflict of interest.

Publisher's note

Supplementary material

The Supplementary Material for this article can be found online at: https://www.frontiersin.org/articles/10.3389/fmicb.2024.1354279/full#supplementary-material

References

Banning, N. C., Gleeson, D. B., Grigg, A. H., Grant, C. D., Andersen, G. L., Brodie, E. L., et al. (2011). Soil microbial community successional patterns during forest ecosystem restoration. *Appl. Environ. Microbiol.* 77, 6158–6164. doi: 10.1128/AEM.00764-11

Bernhard, A. E., Colbert, D., McManus, J., and Field, K. G. (2005). Microbial community dynamics based on 16S rRNA gene profiles in a Pacific Northwest estuary and its tributaries. *FEMS Microbiol. Ecol.* 52, 115–128. doi: 10.1016/j.femsec.2004.10.016

Cao, Y., Tang, C., Song, X., Liu, C., and Zhang, Y. (2016). Identifying the hydrochemical characteristics of rivers and groundwater by multivariate statistical analysis in the Sanjiang Plain, China. *Appl. Water Sci.* 6, 169–178. doi: 10.1007/s13201-014-0215-5

Chen, C., Sun, F., Zhang, H., Wang, J., Shen, Y., and Liang, X. (2016). Evaluation of COD effect on anammox process and microbial communities in the anaerobic baffled reactor (ABR). *Bioresource Technol.* 216, 571–578. doi: 10.1016/j.biortech.2016.05.115

Chen, X., Sheng, Y., and Wang, G. (2024). Spatiotemporal successions of N, S, C, Fe, and As cycling genes in groundwater of a wetland ecosystem: enhanced heterogeneity in wet season. *Water Res.* 251, 121105. doi: 10.1016/j.watres.2024.121105

Chi, Z., Hou, L., and Li, H. (2021a). Effects of pollution load and salinity shock on nitrogen removal and bacterial community in two-stage vertical flow constructed wetlands. *Bioresource Technol.* 342, 126031. doi: 10.1016/j.biortech.2021.126031

Chi, Z., Hou, L., Li, H., Li, J., Wu, H., and Yan, B. (2021c). Elucidating the archaeal community and functional potential in two typical coastal wetlands with different stress patterns. *J. Clean. Prod.* 285, 124894. doi: 10.1016/j.jclepro.2020.124894

Chi, Z., Hou, L., Li, H., Wu, H., and Yan, B. (2021b). Indigenous bacterial community and function in phenanthrene-polluted coastal wetlands: potential for phenanthrene degradation and relation with soil properties. *Environ. Res.* 199, 111357. doi: 10.1016/j.envres.2021.111357

Chi, Z., Ju, S., Li, H., Li, J., Wu, H., and Yan, B. (2021d). Deciphering edaphic bacterial community and function potential in a Chinese delta under exogenous nutrient input and salinity stress. *Catena* 201, 105212. doi: 10.1016/j.catena.2021.105212

Chi, Z., Wang, W., Li, H., Wu, H., and Yan, B. (2021e). Soil organic matter and salinity as critical factors affecting the bacterial community and function of *Phragmites australis* dominated riparian and coastal wetlands. *Sci. Total Environ.*762, 143156. doi: 10.1016/j.scitotenv.2020.143156

Chi, Z., Zhu, Y., Li, H., Wu, H., and Yan, B. (2021f). Unraveling bacterial community structure and function and their links with natural salinity gradient in the Yellow River Delta. *Sci. Total Environ.* 773, 145673. doi: 10.1016/j.scitotenv.2021.145673

Chong, L., Liu, H. J., Qiang, F. U., Guan, H. F., Ye, Q., Zhang, X., et al. (2020). Mapping the fallowed area of paddy fields on Sanjiang Plain of Northeast China to assist water security assessments. *J. Integr. Agric.* 19, 1885–1896. doi: 10.1016/S2095-3119(19)62871-6

Ding, B., Zhang, H., Luo, W., Sun, S., Cheng, F., and Li, Z. (2021). Nitrogen loss through denitrification, anammox and Feammox in a paddy soil. *Sci. Total Environ.* 773, 145601. doi: 10.1016/j.scitotenv.2021.145601

Fei, Y., Zhang, B., He, J., Chen, C., and Liu, H. (2022). Dynamics of vertical vanadium migration in soil and interactions with indigenous microorganisms adjacent to tailing reservoir. *J. Hazard. Mater.* 424, 127608. doi: 10.1016/j.jhazmat.2021.127608

Finneran, K. T., Housewright, M. E., and Lovley, D. R. (2002). Multiple influences of nitrate on uranium solubility during bioremediation of uranium-contaminated subsurface sediments. *Environ. Microbiol.* 4, 510–516. doi: 10.1046/j.1462-2920.2002.00317.x

Francioli, D., Schulz, E., Buscot, F., and Reitz, T. (2018). Dynamics of soil bacterial communities over a vegetation season relate to both soil nutrient status and plant growth phenology. *Microb. Ecol.* 75, 216–227. doi: 10.1007/s00248-017-1012-0

Gao, F., Liu, G., She, Z., Ji, J., Gao, M., Zhao, Y., et al. (2021). Effects of salinity on pollutant removal and bacterial community in a partially saturated vertical flow constructed wetland. *Bioresour. Technol.* 329, 124890. doi: 10.1016/j.biortech.2021.124890

Green, S. J., Prakash, O., Jasrotia, P., Overholt, W. A., Cardenas, E., Hubbard, D., et al. (2012). Denitrifying bacteria from the genus Rhodanobacter dominate bacterial communities in the highly contaminated subsurface of a nuclear legacy waste site. *Appl. Environ. Microb.* 78, 1039–1047. doi: 10.1128/AEM.06435-11

Guo, M., Jiang, Y., Xie, J., Cao, Q., Zhang, Q., Mabruk, A., et al. (2022). Bamboo charcoal addition enhanced the nitrogen removal of anammox granular sludge with COD: performance, physicochemical characteristics and microbial community. *J. Environ. Sci.* 115, 55–64. doi: 10.1016/j.jes.2021.07.010

Guo, X., Zhou, X., Hale, L., Yuan, M., Ning D., Feng, J., et al. (2019). Climate warming accelerates temporal scaling of grassland soil microbial biodiversity. *Nat. Ecol. Evol.* 3, 612–619. doi: 10.1038/s41559-019-0848-8

Guo, Z., Wan, S., Hua, K., Yin, Y., Chu, H., Wang, D., et al. (2020). Fertilization regime has a greater effect on soil microbial community structure than crop rotation and growth stage in an agroecosystem. *Appl. Soil Ecol.* 149, 103510. doi: 10.1016/j.apsoil.2020.103510

He, Z. W., Liu, W. Z., Gao, Q., Tang, C., Wang, L., Guo, Z., et al. (2018). Potassium ferrate addition as an alternative pre-treatment to enhance shortchain fatty acids production from waste activated sludge. *Bioresource Technol.* 247,174–181. doi: 10.1016/j.biortech.2017.09.073

Hou, Q., Lin, S., Ni, Y., Huang, S., Zuo, T., Wang, J., et al. (2022). Assembly of functional microbial communities in paddy soil with long-term application of pig manure under rice-rape cropping system. *J. Environ. Manage.* 305, 114374. doi: 10.1016/j.jenvman.2021.114374

Huang, Q., Wang, J., Wang, C., and Wang, Q. (2019). The 19-years inorganic fertilization increased bacterial diversity and altered bacterial community composition and potential functions in a paddy soil. *Appl. Soil Ecol.* 144, 60–67. doi: 10.1016/j.apsoil.2019.07.009

Jia, L., Jiang, B., Huang, F., and Hu, X. (2019). Nitrogen removal mechanism and microbial community changes of bioaugmentation subsurface wastewater infiltration system. *Bioresource Technol.* 294, 122140. doi: 10.1016/j.biortech.2019.122140

Jiang, Z., Yang, S., Pang, Q., Xu, Y., Chen, X., Sun, X., et al. (2021). Biochar improved soil health and mitigated greenhouse gas emission from controlled irrigation paddy field: insights into microbial diversity. *J. Clean. Prod.* 318, 128595. doi: 10.1016/j.jclepro.2021.128595

Jin, W., Cao, W., Liang, F., Wen, Y., Wang, F., Dong, Z., et al. (2020). Water management impact on denitrifier community and denitrification activity in a paddy soil at different growth stages of rice. *Agric. Water Manage.* 241, 106354. doi: 10.1016/j.agwat.2020.106354

Kaneko, T., Nakamura, Y., Sato, S., Minamisawa, K., Uchiumi, T., Sasamoto, S., et al. (2002). Complete genomic sequence of nitrogen-fixing symbiotic bacterium *Bradyrhizobium japonicum* USDA110. *DNA Res.* 9, 189–197. doi: 10.1093/dnares/9.6.189

Langwig, M. V., De Anda, V., Dombrowski, N., Seitz, K. W., Rambo, I. A., Greening, C., et al. (2022). Large-scale protein level comparison of Deltaproteobacteria reveals cohesive metabolic groups. *ISME J.* 16, 307–320. doi: 10.1038/s41396-021-01057-y

Lezcano, M. Á., Velázquez, D., Quesada, A., and El-Shehawy, R. (2017). Diversity and temporal shifts of the bacterial community associated with a toxic cyanobacterial bloom: an interplay between microcystin producers and degraders. *Water Res.* 125, 52–61. doi: 10.1016/j.watres.2017.08.025

Li, H., Chi, Z., Li, J., Wu, H., and Yan, B. (2019). Bacterial community structure and function in soils from tidal freshwater wetlands in a Chinese delta: potential impacts of salinity and nutrient. *Sci. Total Environ.* 696, 134029. doi: 10.1016/j.scitotenv.2019.134029

Li, H., Chi, Z., Lu, W., and Wang, H. (2014). Sensitivity of methanotrophic community structure, abundance, and gene expression to CH_4 and O_2 in simulated landfill biocover soil. *Environ. Pollut.* 184, 347–353. doi: 10.1016/j.envpol.2013.09.002

Li, H., Chi, Z., and Yan, B. (2018). Insight into the impact of Fe_3O_4 nanoparticles on anammox process of subsurface-flow constructed wetlands under long-term exposure. *Environ. Sci. Pollut. R* 25, 29584–29592. doi: 10.1007/s11356-018-2975-1

Li, H., Liang, S., Chi, Z., Wu, H., and Yan, B. (2022). Unveiling microbial community and function involved in anammox in paddy vadose under groundwater irrigation. *Sci. Total Environ.* 849, 157876. doi: 10.1016/j.scitotenv.2022.157876

Li, Q., Song, A., Yang, H., and Muller, W. E. G. (2021a). Impact of rocky desertification control on soil bacterial community in Karst Graben Basin, southwestern China. *Front. Microbiol.* 12, 448. doi: 10.3389/fmicb.2021.636405

Li, X., Lu, Y., Chen, Y., Zhu, G., and Zeng, R. J. (2021b). Constraining nitrification by intermittent aeration to achieve methane-driven ammonia recovery of the mainstream anaerobic effluent. *J. Environ. Manage.* 295, 113103. doi: 10.1016/j.jenvman.2021.113103

Liang, J., Gao, S., Wu, Z., Rijnaarts, H. H. M., and Grotenhuis, T. (2021). DNA-SIP identification of phenanthrene-degrading bacteria undergoing bioaugmentation and natural attenuation in petroleum-contaminated soil. *Chemosphere* 266, 128984. doi: 10.1016/j.chemosphere.2020.128984

Liu, Q., Atere, C. T., Zhu, Z., Shahbaz, M., Wei, X., Pausch, J., et al. (2022). Vertical and horizontal shifts in the microbial community structure of paddy soil under long-term fertilization regimes. *Appl. Soil Ecol.* 169, 104248. doi: 10.1016/j.apsoil.2021.104248

Meng, L., Zuo, R., Wang, J. S., Li, Q., Du, C., Liu, X., et al. (2021). Response of the redox species and indigenous microbial community to seasonal groundwater fluctuation from a typical riverbank filtration site in Northeast China. *Ecol. Eng.* 159, 106099. doi: 10.1016/j.ecoleng.2020.106099

Ottoni, J. R., dos Santos Grignet, R., Barros, M. G. A., Bernal, S. P. F., Panatta, A. A. S., Lacerda-Júnior, G. V., et al. (2022). DNA metabarcoding from microbial communities recovered from stream and its potential for bioremediation processes. *Curr. Microbiol.* 79, 1–10. doi: 10.1007/s00284-021-02752-x

Pan, X., Li, H., Zhao, L., Yang, X., Su, J., Dai, S., et al. (2021). Response of syntrophic bacterial and methanogenic archaeal communities in paddy soil to soil type and phenological period of rice growth. *J. Clean. Prod.* 278, 123418. doi: 10.1016/j.jclepro.2020.123418

Park, D., Kim, H., and Yoon, S. (2017). Nitrous oxide reduction by an obligate aerobic bacterium, Gemmatimonas aurantiaca strain T-27. *Appl. Environ. Microb.* 83, e00502–e00517. doi: 10.1128/AEM.00502-17

Pérez Castro, S., Cleland, E. E., Wagner, R., Al Sawad, R., and Lipson, D. A. (2019). Soil microbial responses to drought and exotic plants shift carbon metabolism. *ISME J.* 13, 1776–1787. doi: 10.1038/s41396-019-0389-9

Pikuta, E. V., Hoover, R. B., Bej, A. K., Marsic, D., Whitman, W. B., Krader, P. E., et al. (2006). *Trichococcus patagoniensis* sp. nov., a facultative anaerobe that grows at−5°C, isolated from penguin guano in Chilean Patagonia. *Int. J. Syst. Evol. Microbiol.* 56, 2055–2062. doi: 10.1099/ijs.0.64225-0

Pishgar, R., Dominic, J. A., Tay, J. H., and Chu, A. (2020). Pilot-scale investigation on nutrient removal characteristics of mineral-rich aerobic granular sludge: identification of uncommon mechanisms. *Water Res.* 168, 115151. doi: 10.1016/j.watres.2019.115151

Su, Z., Dai, T., Tang, Y., Tao, Y., Huang, B., Mu, Q., et al. (2018). Sediment bacterial community structures and their predicted functions implied the impacts from natural processes and anthropogenic activities in coastal area. *Mar. Pollut. Bull.* 131, 481–495. doi: 10.1016/j.marpolbul.2018.04.052

Sun, R., Wang, F., Hu, C., and Liu, B. (2021). Metagenomics reveals taxon-specific responses of the nitrogen-cycling microbial community to long-term nitrogen fertilization. *Soil Biol. Biochem.* 156, 108214. doi: 10.1016/j.soilbio.2021.108214

Sun, X., Ding, J., Jiang, Z., Yang, S., Jiang, Z., Xu, J., et al. (2019). Biochar improved rice yield and mitigated CH_4 and N_2O emissions from paddy field under controlled irrigation in the Taihu Lake Region of China. *Atmos. Environ.* 200, 69–77. doi: 10.1016/j.atmosenv.2018.12.003

Teoh, C. P., Lavin, P., Lee, D. J. H., Gonz}'alez-Aravena, M., Najimudin, N., Lee, P. C., et al. (2021). Genomics and transcriptomics analyses provide insights into the cold adaptation strategies of an Antarctic bacterium, *Cryobacterium* sp. SO1. *Polar Biol.* 44, 1305–1319. doi: 10.1007/s00300-021-02883-8

Tolar, B. B., Boye, K., Bobb, C., Maher, K., Bargar, J. R., and Francis, C. A. (2020). Stability of floodplain subsurface microbial communities through seasonal hydrological and geochemical cycles. *Front. Earth Sci.* 8,338. doi: 10.3389/feart.2020.00338

Torsvik, V., and Øvreås, L. (2002). Microbial diversity and function in soil: from genes to ecosystems. *Curr. Opin. Microbiol.* 5, 240–245. doi: 10.1016/S1369-5274(02)00324-7

Van Den Heuvel, R. N., Van Der Biezen, E., Jetten, M. S. M., Hefting, M. M., and Kartal, B. (2010). Denitrification at pH 4 by a soil-derived Rhodanobacter-dominated community. *Environ. Microbiol.* 12, 3264–3271. doi: 10.1111/j.1462-2920.2010.02301.x

Wang, H., Gilbert, J. A., Zhu, Y., and Yang, X. (2018a). Salinity is a key factor driving the nitrogen cycling in the mangrove sediment. *Sci. Total Environ.* 631, 1342–1349. doi: 10.1016/j.scitotenv.2018.03.102

Wang, H., Zeng, Y., Guo, C., Bao, Y., Lu, G., Dang, Z., et al. (2018b). Bacterial, archaeal, and fungal community responses to acid mine drainage-laden pollution in a rice paddy soil ecosystem. *Sci. Total Environ.* 616, 107–116. doi: 10.1016/j.scitotenv.2017.10.224

Wang, J. L., Liu, K. L., Zhao, X. Q., Zhao, H. Q., Li, D., Li, J. J., et al. (2021). Balanced fertilization over four decades has sustained soil microbial communities and improved soil fertility and rice productivity in red paddy soil. *Sci. Total Environ.* 793, 148664. doi: 10.1016/j.scitotenv.2021.148664

Ward, N. L., Challacombe, J. F., Janssen, P. H., Henrissat, B., Coutinho, P. M., Wu, M., et al. (2009). Three genomes from the phylum Acidobacteria provide insight into the lifestyles of these microorganisms in soils. *Appl. Environ. Microb.* 75, 2046–2056. doi: 10.1128/AEM.02294-08

Wei, G., Andersen, M. N., Qi, X. B., Li, P., Li, Z., Fan, X., et al. (2017). Effects of reclaimed water irrigation and nitrogen fertilization on the chemical properties and microbial community of soil. *J. Integr. Agric.* 16, 679–690. doi: 10.1016/S2095-3119(16)61391-6

Wu, T., Liu, Y., Yang, K., Zhu, L., White, J. C., and Lin, D. (2021). Synergistic remediation of PCB-contaminated soil with nanoparticulate zero-valent iron and alfalfa: targeted changes in the root metabolite-dependent microbial community. *Environ. Sci. Nano* 8, 986–999. doi: 10.1039/D1EN00077B

Yan, Q., Ding, Y., Wen, H., Liu, F., Hu, J., and Cai, R. (2019). Effect of biologicalmatrix on denitrification and microorganisms of SWIS. *Chin. J. Environ. Eng.* 13, 1099–1105.

Yang, J., He, M., and Wang, G. (2009). Removal of toxic chromate using free and immobilized Cr (VI)-reducing bacterial cells of *Intrasporangium* sp. Q5-1. *World J. Microb. Biot.* 25, 1579–1587. doi: 10.1007/s11274-009-0047-x

Yu, Y., Wu, M., Petropoulos, E., Zhang, J., Nie, J., Liao, Y., et al. (2019). Responses of paddy soil bacterial community assembly to different long-term fertilizations in southeast China. *Sci. Total Environ.* 656, 625–633. doi: 10.1016/j.scitotenv.2018.11.359

Zhang, H., Sun, H., Yang, R., Li, S., Zhou, M., Gao, T., et al. (2016). Complete genome sequence of a psychotrophic *Pseudarthrobacter sulfonivorans* strain Ar51 (CGMCC 4.7316), a novel crude oil and multi benzene compounds degradation strain. *J. Biotechnol.* 231, 81–82. doi: 10.1016/j.jbiotec.2016.04.010

Zhang, X., Li, X., Zhao, X., Chen, X., Zhou, B., Weng, L., et al. (2020). Bioelectric field accelerates the conversion of carbon and nitrogen in soil bioelectrochemical systems. *J. Hazard. Mater.* 388, 121790. doi: 10.1016/j.jhazmat.2019.121790

Zheng, Y., Jiang, X., Hou, L., Liu, M., Lin, X., Gao, J., et al. (2016). Shifts in the community structure and activity of anaerobic ammonium oxidation bacteria along an estuarine salinity gradient. *J. Geophys. Res. Biogeosci.* 121, 1632–1645. doi: 10.1002/2015JG003300

Zhou, G. W., Yang, X. R., Li, H., Marshall, C. W., Zheng, B. X., Su, J. Q., et al. (2016). Electron shuttles enhance anaerobic ammonium oxidation coupled to iron (III) reduction. *Environ. Sci. Technol.* 50, 9298–9307. doi: 10.1021/acs.est.6b02077

frontiers | Frontiers in Microbiology

TYPE Original Research
PUBLISHED 18 March 2024
DOI 10.3389/fmicb.2024.1376849

OPEN ACCESS

EDITED BY
Huai Li,
Chinese Academy of Sciences (CAS), China

REVIEWED BY
Jiuling Li,
The University of Queensland, Australia
Yafei Zhang,
Jiangsu University, China

*CORRESPONDENCE
Jiangqi Wu
✉ jiangqiw6236@foxmail.com

RECEIVED 26 January 2024
ACCEPTED 05 March 2024
PUBLISHED 18 March 2024

CITATION
Zhang R, Zhang H, Yang C, Li H and Wu J (2024) Effects of water stress on nutrients and enzyme activity in rhizosphere soils of greenhouse grape.
Front. Microbiol. 15:1376849.
doi: 10.3389/fmicb.2024.1376849

Effects of water stress on nutrients and enzyme activity in rhizosphere soils of greenhouse grape

Rui Zhang[1], Hongjuan Zhang[1], Changyu Yang[1], Hongxia Li[1] and Jiangqi Wu[2]*

[1]College of Water Conservancy and Hydropower Engineering, Gansu Agricultural University, Lanzhou, China, [2]College of Forestry, Gansu Agricultural University, Lanzhou, China

In grape cultivation, incorrect water regulation will lead to significant water wastage, which in turn will change soil structure and disrupt soil nutrient cycling processes. This study aimed to investigate the effects of different water regulation treatments [by setting moderate water stress (W1), mild water stress (W2), and adequate water availability (CK)] on soil physical–chemical properties and enzyme activity in greenhouse grape during the growing season. The result showed that the W2 treatment had a negative impact on the build-up of dissolved organic carbon (DOC), nitrate nitrogen (NO_3-N), and available phosphorus (AP). Throughout the reproductive period, the W1 and W2 treatments decreased the soil's microbial biomass carbon (MBC) and microbial biomass nitrogen (MBN) contents, and MBC was more vulnerable to water stress. During the growth period, the trends of urease, catalase, and sucrase activities in different soil depth were ranked as 10–20 cm > 0–10 cm > 20–40 cm. The urease activity in 0–10 cm soil was suppressed by both W1 and W2 treatments, while the invertase activity in various soil layers under W1 treatment differed substantially. The W1 treatment also reduced the catalase activity in the 20–40 cm soil layer in the grape growth season. These findings suggested that W2 treatment can conserve water and enhance microbial ecology of greenhouse grape soils. Therefore, W2 treatment was the most effective water regulation measure for local greenhouse grape cultivation.

KEYWORDS

water stress, physical–chemical properties, microbial biomass, enzyme activity, greenhouse grape

1 Introduction

Water scarcity is the most main environmental stress for crop growth, and water stress-induced agriculture failure will cause serious ecological and food security issues (Yang et al., 2021; Zhang C. et al., 2023). Water stress not only affected crop growth and microbial structure, limits soil nutrient transport but also leaded to a significant decrease in soil microbial biomass (Manzoni et al., 2012). The rhizosphere is the site of plant–soil-microorganism interaction, and the soil area where plants are highly sensitive to external environmental stress (Zhang et al., 2019). Studies have shown that water stress can impact crop chlorophyll levels (Ru et al., 2020), metabolic processes (Kapoor et al., 2020), root growth (Wang et al., 2019), and soil microbial communities (Bogati and Walczak, 2022). Secretions released during crop growth

period also changed soil enzyme activity (Xiao et al., 2023). Therefore, complex interactions between soil water and crops combine to influence changes of rhizosphere soil microbials.

Physical–chemical property and microbial biomass are important regulators of soil element cycling and crop nutrient supply, and are the most sensitive and potential soil biological indicators (Marschner et al., 2005; Zhang et al., 2016; Yang et al., 2019). Soil organic carbon (SOC), total nitrogen (TN), total phosphorus (TP), nitrate nitrogen (NO_3-N), ammonia nitrogen (NH_4-N), and availability phosphorus (AP) are the main nutrients in soil and are crucial to all biological processes (Wu et al., 2020). Water stress severely disrupted the structure and function of soil, soil microbial biomass reaches 14.3%, and soil moisture is maintained above 10%, which in turn avoided damaging the soil system (Geng et al., 2015). Water stress not only decreases soil chemical fertility but also reduces microbial activity, including the activities of invertase and urease (Wu et al., 2012). The plant root system will firstly experience water stress, mainly as a result of inadequate or excessive water in the soil (Kim et al., 2020). Soil moisture affects the transfer and transportation of soil nutrients, which in turn affects the growth and reproduction of microorganisms (Xue et al., 2017). Therefore, the investigation of the impact of water stress on rhizosphere soil moisture, nutrients, and microorganisms in plants were critical.

Soil enzymes are specialized proteins with biocatalytic activity, known as "active reservoirs of plant nutrients." Enzyme activity is higher in rhizosphere soil than in bulk soil (Marschner et al., 2005). In addition, catalase, urease, and sucrose were the main environmental variables affecting the composition of the soil microbial community in the grape rhizosphere (Song et al., 2024). Soil enzyme activity increased with increasing soil moisture, but decreased with excess soil water, as shown by Chrost (2014). Gramss et al. (1999) also found that adequate water stress (80% field water holding capacity) could stimulate plant roots to produce more enzymes, and this was due to oxygen limiting microbial activity. Soil enzyme activities were related to soil temperature, physical–chemical properties, and pH, respectively, and varied in different planting types and growth stages (Barta et al., 2014; Menichetti et al., 2015; Liu and Zhang, 2019; Jing et al., 2020; Zhao et al., 2020). In addition, some studies have shown that water stress can increase soil peroxidase, phosphatase, dehydrogenase, saccharase, and phosphatase activities (Song et al., 2012; Padhy et al., 2018; Kátai et al., 2020). However, the response of soil enzyme activities to water stress remains highly uncertain. Therefore, the aim of this study was to analyze the changes in rhizosphere soil enzyme activities of greenhouse grapes by different water stresses, which could further characterize the changes in enzyme activities.

In this study, the rhizosphere soil of greenhouse grapes in arid area was the object of study, and different water stress treatments were established. We analyzed the physical–chemical properties, microbial biomass, and enzyme activities of the soil to provide a theoretical basis for the scientific cultivation of greenhouse grapes in the arid region. The objectives of the study were: (1) to analyze the effects of different water stress conditions on physical–chemical properties, microbial biomass, and enzyme activities in rhizosphere soil at different growth stages; and (2) to explore the correlation between soil physical–chemical properties, microbial biomass and enzyme activity.

2 Materials and methods

2.1 Study site

The field experiment was conducted in 2019 at the Yongdeng Irrigation Experiment Station (36°43′34″N; 103°16′24″E; altitude: 2100 m) in Gansu Province, China. The study area is located in a semi-arid region, with a typical continental monsoon climate, and the average annual rainfall, evaporation, and temperature were 290 mm, 1,000 mm, and 5.9°C, respectively. The soil type of the experimental field was mainly loam, the water capacity was 29.2%, the density was 1.42 g cm^{-3}, and the soil pH was 8.15.

2.2 Experimental design and management

Red globe, a 5-year-old Eurasian grape variety, was used as the test material. Grapes were planted in a plastic greenhouse of 8 m × 80 m with an earth wall straw curtain and the cultivation method of a single-arm Y-shaped low single-hedge frame was adopted. The row spacing was 2.0 m, and the plant spacing was 0.8 m. Each row (each treatment) comprised eight grapes, and the row direction was perpendicular to the greenhouse direction (Zhang et al., 2019). The experimental plots were designed in a randomized block group design and there were three replications for each treatment, containing a total of nine plots with a plot size of 8 m × 2 m.

The growth period of grapes was divided into five stages based on local protected-cultivation grape water consumption and irrigation experience (Table 1). The experiment included three treatments: (1) W1 treatment was moderate water stress (lower limit of soil moisture content was 55%); (2) W2 treatment was mild water stress (lower limit of soil moisture content was 65%); (3) CK treatment was the control treatment (sufficient water supply). The field trial of greenhouse grapes was irrigated by drip irrigation with the control mode of "one pipe and one row," and the flow rate of sprinkler head was 3 L H^{-1}. The irrigation was performed when the soil moisture in the field trial reached the lower limit of the experimental design, and the irrigation rate was 270 m^3 hm^{-2}. The valves and the water meters installed in each plot were used to control the amount of irrigation. The irrigation amount and irrigation time were determined by the soil moisture content and measured using a water meter. The soil moisture ratio was 0.5, and the planned depth of the wetting layer was 80 cm.

Local farming management practices were referred to for the use of fertilization, and insecticide and herbicide management. On 24th February, basal fertilizer (chicken manure; 5,000 kg hm^{-2}) was applied along with 2 kg diammonium phosphate and 4 kg ammonium bicarbonate. Each treatment received 1 kg diammonium phosphate, 0.8 kg calcium ammonium nitrate for agriculture, 0.8 kg of organic fertilizer, and 0.5 kg of potassium magnesium sulfate at the 16th June, respectively. On 16th August, 0.8 kg diammonium phosphate, 0.8 kg calcium ammonium nitrate for agriculture, 0.8 kg organic fertilizer, and 0.6 kg potassium and magnesium sulfate were applied.

2.3 Collection of rhizosphere soil sample

Soil samples (0–40 cm) were collected on May 15, June 15, July 20, August 15, and October 15, 2019 at different growth periods. Three

soil cores (3 cm diameter) of grape rhizosphere soil in each plot were taken at a depth of 0–10, 10–20, and 20–40 cm, respectively. Then, the samples in each plot were pooled by depth and transported to the laboratory. In the lab, the samples were sieved through a 2 mm mesh. The soil layer of 10–20 cm was divided into three parts; one part was air-dried at room temperature for determining some basic physical–chemical indices of the soil, and the other part was stored in a refrigerator at 4°C for fresh sample analysis (partial basic physical–chemical indices of soil and enzyme activity). Sterile gloves were worn during the sampling process. The ziplock bag, spatula, and other tools used for sampling were sterilized at high temperature to eliminate test errors. The measurement of each index was completed within 1 month after the completion of the sampling.

2.4 Soil physical–chemical properties

Total nitrogen (TN), nitrate nitrogen (NO_3-N), and ammonia nitrogen (NH_4-N) contents were determined by the Kjeldahl method (Boell and Shen, 1954) (Table 2). The soil total organic carbon (TOC) content was measured using a carbon and nitrogen combined analyzer (Multi N/C 2100 s, Jena, Germany) after removing inorganic carbon with 0.5 mol/L dilute hydrochloric acid. The dissolved organic carbon (DOC) content was determined with a carbon and nitrogen combined analyzer (Multi C/N 2100 s) after leaching with ultrapure water (water: soil = 5: 1). The microbial biomass carbon (MBC) and microbial biomass nitrogen (MBN) content were determined using a carbon and nitrogen combined analyzer after 0.5 mol·L^{-1} K_2SO_4 extraction (Multi C/N 2100 s) (Xu et al., 2016).

To determine the sucrase activity, 5 g of air-dried soils were incubated for 24 h at 37°C with 15 mL of 8% sucrose, 5 mL of phosphate buffer at pH 5.5, and 0.1 mL of toluene. The glucose released by sucrase reacted with 3-5-dinitrosalicylic acid and then was measured based on the absorbance at 508 nm (UV-2450, Shimadzu Corporation, Kyoto, Japan) (Wu et al., 2020). The results were expressed as mg glucose g^{-1}·h^{-1}. Soil urease activity was determined by indophenol blue colorimetry and expressed as mg of NH_3-N in 5 g air-dried soil after incubating for 24 h at 37°C with 20 mL of citrate buffer at pH 6.7, 10 mL of 10% urea, and 0.1 mL of toluene (Xie et al., 2017). Soil catalase activity was determined by the $KMnO_4$ liquid titration method and expressed as the volume of 0.02 mol·L^{-1} $KMnO_4$ consumed of 2 g air-dried soil within 20 min (Li et al., 2014).

2.5 Statistical analysis

The relationships between soil microbial biomass, enzyme activities and soil physical–chemical properties were analyzed using Spearman's correlation method (SPSS 27.0). Correlations among soil physical–chemical properties, enzyme activities, and microbial biomass were assessed using Person correlation analysis. One-way ANOVA was used to investigate the data for the different water stress treatments ($p < 0.05$).

3 Results

3.1 Effect of water stress on basic physical–chemical properties of greenhouse grape rhizosphere soil

Compared with CK treatment, the NO_3-N content of W1 and W2 treatments decreased by 17.99, 16.07, 16.85, and 8.94% at the new shoot elongation and fruit enlargement stage, respectively (Table 3).

TABLE 1 Field experiment design for greenhouse grapes.

Growth stage	Treatment		
	W1	W2	CK
	Lower limit of water content/%	Lower limit of water content/%	Lower limit of water content/%
Budburst stage (May 15–May 24)	55	65	75
New shoot elongation stage (May 25–June 22)	55	65	75
Flowering stage (June 23–July 15)	55	65	75
Fruit enlargement stage (July 16–September 22)	55	65	75
Coloring maturity stage (September 25–October 22)	55	65	75

TABLE 2 Parametric determination of physical–chemical properties of greenhouse grape rhizosphere soils.

Index	Determination method
TN (mg kg^{-1}), NO_3-N (mg kg^{-1}), and NH_4-N (mg kg^{-1})	The Kjeldahl
TOC (g kg^{-1}), DOC (mg kg^{-1}), MBC (mg kg^{-1}), and MBN (mg kg^{-1})	The carbon and nitrogen combined analyzer
Soil sucrase activity (mg g^{-1} $24\,h^{-1}$)	The 3–5 dinitrosalicylic acid method
Soil catalase activity (mg g^{-1} $24\,h^{-1}$)	The $KMnO_4$ liquid titration method
Soil urease activity (mg g^{-1} $24\,h^{-1}$)	The indophenol blue colorimetry method

TN, Total nitrogen; NO_3-N, Nitrate nitrogen; NH_4-N, Ammonia nitrogen; TOC, Total organic carbon; DOC, Dissolved organic carbon; MBC, Microbial biomass carbon; and MBN, Microbial biomass nitrogen.

The soil AP content showed an increasing and then stabilizing trend. In addition, the soil AP content was significantly ($p < 0.05$) higher in the CK treatment than in the W1 treatment during both shoot elongation and fruit enlargement stage. Thus, the AP content in the soil had specific adaptability to water stress. Moreover, there was no significant difference of TOC content between W1 and W2 treatment (Figure 1A). The soil DOC content showed an increasing trend and then decreasing during the growth period under different treatments, and peaked at the fruit enlargement stage (Aug-15) (Figure 1B). At the same time, compared with CK treatment, the DOC content of W1 treatment in maize growth stage was 19.84% ($p < 0.05$), 12.60% ($p < 0.05$) and 8.34% ($p < 0.05$) lower than that of CK treatment,

TABLE 3 Changes in basic physical–chemical properties (mean ± standard deviation, $n = 3$) of soil under different water stresses.

Stage	Treatment	TN (mg kg^{-1})	NO_3-N (mg kg^{-1})	NH_4-N (mg kg^{-1})	TP (mg kg^{-1})	AP (mg kg^{-1})	SOM (mg kg^{-1})
Jun-15	W1	0.83 ± 0.03a	12.06 ± 0.97b	3.65 ± 0.76a	0.82 ± 0.09 a	28.88 ± 1.91b	16.03 ± 1.71a
	W2	0.82 ± 0.03a	12.26 ± 0.56b	3.42 ± 0.29a	0.79 ± 0.06 a	30.88 ± 1.88ab	16.44 ± 1.61a
	CK	0.83 ± 0.03a	14.23 ± 0.74a	3.88 ± 0.34a	0.77 ± 0.21 a	34.68 ± 2.50a	16.49 ± 0.57a
Aug-15	W1	0.83 ± 0.03a	15.85 ± 0.61b	4.50 ± 0.63a	0.83 ± 0.01 a	39.24 ± 1.08b	16.22 ± 0.95a
	W2	0.82 ± 0.03a	17.00 ± 1.18ab	4.47 ± 0.32a	0.84 ± 0.06 a	40.28 ± 1.63ab	17.21 ± 0.62a
	CK	0.81 ± 0.03a	18.52 ± 0.67a	4.88 ± 0.84a	0.79 ± 0.01 a	44.66 ± 3.45a	18.27 ± 1.47a
Oct-15	W1	0.84 ± 0.01a	12.49 ± 1.24a	3.53 ± 0.41a	0.82 ± 0.04 a	41.30 ± 1.63a	15.64 ± 1.68a
	W2	0.83 ± 0.01a	12.29 ± 0.76a	3.83 ± 0.38a	0.85 ± 0.09 a	37.66 ± 8.19a	16.71 ± 1.48a
	CK	0.82 ± 0.01a	13.80 ± 1.21a	3.57 ± 0.28a	0.84 ± 0.06 a	46.81 ± 2.15a	16.42 ± 1.19a

Different lowercase letters indicate significant differences among treatments ($p < 0.05$). W1, Moderate water stress (55% of field capacity); W2, Mild water stress (65% of field capacity); CK, Sufficient water supply (75% of field capacity). TN, Total nitrogen; NO_3-N, Nitrate nitrogen; NH_4-N, Ammonia nitrogen; TP, Total phosphorus; AP, Availability phosphorus; and SOM, Soil organic matter.

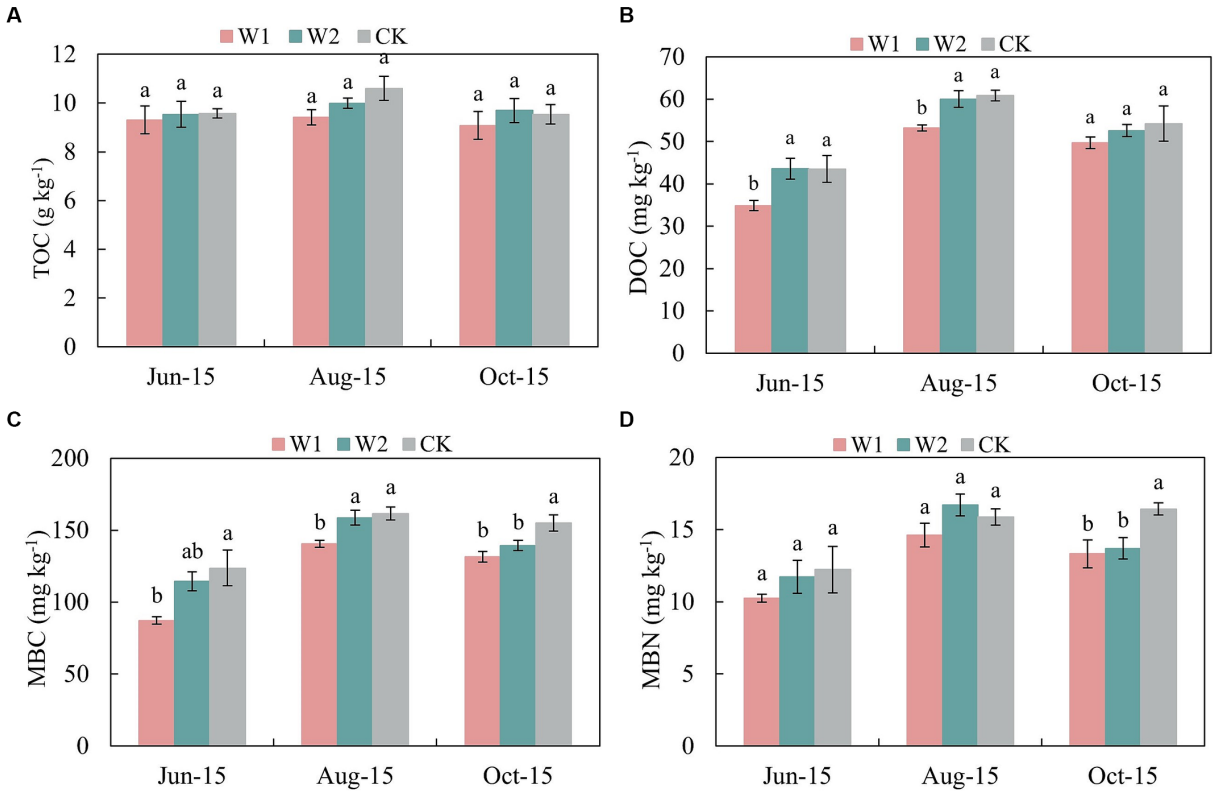

FIGURE 1
Effects of water stress on the TOC, DOC, MBC, and MBN content of greenhouse grape rhizosphere soil. Error bars indicate standard errors of the mean ($n = 3$). Different lowercase letters indicate significant differences among treatments ($p < 0.05$). W1, Moderate water stress (55% of field capacity); W2, Mild water stress (65% of field capacity); CK, Sufficient water supply (75% of field capacity). TOC, Total organic carbon; DOC, Dissolved organic carbon; MBC, Microbial biomass carbon; and MBN, Microbial biomass nitrogen. **(A)** is TOC content; **(B)** is DOC content; **(C)** is MBC content; **(D)** is MBN content.

respectively. Compared with CK treatment, the soil MBC content of W1 and W2 treatments was significantly lower by 5.61% ($p < 0.05$) and 15.63% ($p < 0.05$) at the coloring maturity stage (Oct-15), respectively (Figure 1C). With the increase duration of water stress, MBN was significantly lower in the W1 and W2 treatments than in the CK treatment ($p < 0.05$) when the coloring maturity stage was reached (Figure 1D).

3.2 Effects of water stress on soil enzyme activities in greenhouse grape rhizosphere soil

Throughout the grape growing period, urease, catalase, and sucrase activities in different soil layers were ranked as: 10–20 cm > 0–10 cm > 20–40 cm (Table 4). Compared with the CK treatment, the urease activity in the 0–10 cm soil layer of W2 and W2 treatments was significantly lower by 27.40% ($p < 0.05$), 26.03% ($p < 0.05$), 20.69% ($p < 0.05$), and 44.87% ($p < 0.05$) at the new shoot elongation stage (Jun-15) and flowering stage (Jul-20), respectively. The urease activity in the 10–20 and 20–40 cm soil layers were significantly higher in the CK treatment than in the W1 treatment at the coloring maturity stage (Oct-15) ($p < 0.05$). The peroxidase activity of all soil layers of grapes decreased significantly during the period from budburst stage (May-15) to fruit enlargement (Aug-15). Compared with CK treatment, the peroxidase activity of W1 treatment in different soil layers (0–10, 10–20, and 20–40 cm) was significantly decreased by 3.65% ($p < 0.05$), 1.09% ($p < 0.05$), and 8.89% ($p < 0.05$) at budburst stage (May-15), respectively. With the increase of stress duration, the surface soil invertase activity of W1 treatment was significantly lower than that of CK treatment by 32.07% ($p < 0.05$) and 42.73% ($p < 0.05$) at the fruit enlargement stage (Aug-15) and coloring maturity stage (Oct-15), respectively. Furthermore, the conversion enzyme activity in the 20–40 cm soil layer under the W2 treatment

TABLE 4 Effect of water stress on urease, catalase, and sucrase enzyme activity (mean ± standard deviation, $n = 3$) in the rhizosphere soil of delayed-cultivation greenhouse grapes ($mg \cdot g^{-1} \cdot day^{-1}$).

Enzyme	Soil depth/cm	Treatment	May-15	Jun-15	Jul-20	Aug-15	Oct-15
Urease	0–10	W1	0.64 ± 0.01b	0.53 ± 0.05b	0.46 ± 0.01b	0.52 ± 0.08b	0.39 ± 0.02b
		W2	0.74 ± 0.02a	0.54 ± 0.04b	0.42 ± 0.01b	0.83 ± 0.08a	0.59 ± 0.09a
		CK	0.54 ± 0.03c	0.73 ± 0.04a	0.58 ± 0.05a	0.74 ± 0.08a	0.46 ± 0.04b
	10–20	W1	0.54 ± 0.01a	0.61 ± 0.06a	0.58 ± 0.02a	0.39 ± 0.04b	0.56 ± 0.02b
		W2	0.61 ± 0.01a	0.61 ± 0.03a	0.89 ± 0.09a	0.59 ± 0.04a	0.60 ± 0.02b
		CK	0.58 ± 0.09a	0.56 ± 0.03a	0.69 ± 0.25a	0.42 ± 0.07b	0.75 ± 0.10a
	20–40	W1	0.38 ± 0.01a	0.31 ± 0.03b	0.37 ± 0.02a	0.36 ± 0.05b	0.44 ± 0.04b
		W2	0.40 ± 0.03a	0.44 ± 0.01a	0.39 ± 0.02a	0.46 ± 0.04a	0.65 ± 0.04a
		CK	0.42 ± 0.02a	0.43 ± 0.07a	0.41 ± 0.03a	0.37 ± 0.03b	0.60 ± 0.03a
Catalase	0–10	W1	1.85 ± 0.02b	1.73 ± 0.03b	1.84 ± 0.03a	1.81 ± 0.02a	0.94 ± 0.15a
		W2	1.88 ± 0.02b	1.80 ± 0.00a	1.87 ± 0.02a	1.82 ± 0.01a	0.96 ± 0.09a
		CK	1.92 ± 0.02a	1.73 ± 0.02b	1.87 ± 0.02a	1.82 ± 0.02a	0.96 ± 0.12a
	10–20	W1	1.82 ± 0.00b	1.95 ± 0.02a	1.92 ± 0.02a	1.85 ± 0.01a	0.94 ± 0.05a
		W2	1.84 ± 0.01a	1.96 ± 0.01a	1.93 ± 0.00a	1.87 ± 0.01a	1.04 ± 0.05a
		CK	1.84 ± 0.01a	1.96 ± 0.01a	1.94 ± 0.00a	1.84 ± 0.03a	1.02 ± 0.07a
	20–40	W1	1.64 ± 0.06b	1.65 ± 0.07b	1.50 ± 0.08c	1.60 ± 0.02b	0.44 ± 0.03b
		W2	1.78 ± 0.02a	1.82 ± 0.02a	1.76 ± 0.03b	1.83 ± 0.02a	0.57 ± 0.01a
		CK	1.80 ± 0.02a	1.84 ± 0.03a	1.92 ± 0.07a	1.85 ± 0.05a	0.54 ± 0.02a
Sucrase	0–10	W1	24.83 ± 2.79a	18.67 ± 1.33a	17.54 ± 1.07b	13.28 ± 1.06b	15.14 ± 1.94b
		W2	24.71 ± 2.12a	19.88 ± 3.39a	23.17 ± 1.03a	18.04 ± 1.53a	26.98 ± 1.99a
		CK	23.04 ± 2.51a	17.09 ± 1.79a	17.26 ± 0.00b	19.55 ± 1.41a	28.42 ± 2.47a
	10–20	W1	20.30 ± 1.78a	17.51 ± 1.79b	14.94 ± 0.58b	16.83 ± 0.87b	20.61 ± 1.01b
		W2	18.74 ± 0.27a	18.50 ± 0.59b	19.58 ± 1.70a	22.93 ± 0.86a	26.78 ± 1.57a
		CK	21.53 ± 2.12a	24.48 ± 1.87a	16.21 ± 0.60b	23.32 ± 1.99a	28.27 ± 1.10a
	20–40	W1	10.05 ± 1.88b	11.70 ± 1.34b	10.89 ± 1.18b	10.82 ± 0.62c	14.16 ± 0.85b
		W2	15.45 ± 1.77a	15.81 ± 1.78a	14.37 ± 0.36a	16.45 ± 1.56a	19.45 ± 0.45a
		CK	17.75 ± 2.34a	13.12 ± 0.84ab	13.06 ± 0.42a	14.16 ± 1.04b	18.50 ± 1.16a

Different lowercase letters indicate significant differences among treatments ($p < 0.05$). W1, Moderate water stress (55% of field capacity); W2, Mild water stress (65% of field capacity); and CK, Sufficient water supply (75% of field capacity).

was slightly higher than that in the W1 treatment during the period from the new shoot elongation stage (Jun-15) to coloring maturity stage (Oct-15). This result indicated that both W2 and W1 treatments inhibited soil urease, catalase, and sucrase activity convertase during the greenhouse grape growth.

3.3 Correlation analysis between soil physical–chemical and soil enzymes

The correlations between soil microbial biomass and basic soil physical–chemical indicators differed considerably between different growth periods of greenhouse grape rhizospheres (Figure 2). Among them, MBC and MBN showed significantly negative correlations ($r = -0.67$ and-0.78) with soil TP at the new growth stage (Jun-15) ($p < 0.05$), but significant positive correlations with soil AP and DOC ($p < 0.05$). In contrast, there was a highly significant positive correlation between MBC and DOC in the fruit enlargement stage (Aug-15) and coloring maturity stage (Oct-15). The correlation analysis between soil physical–chemical indicators and soil enzyme activities (Figure 3) showed that there were significant positive correlations between soil urease, catalase, and sucrase to varying degrees during the new growth stage (Jun-15), fruit enlargement stage (Aug-15), and coloring maturity stage (Oct-15). There were significant positive correlations between soil urease (Jun-15) and catalase (Aug-15) and nitrate nitrogen ($r = 0.81$, 0.70) ($p < 0.05$). Meanwhile, catalase showed a significant positive correlation between organic matter and TOC during the fruit enlargement stage (Aug-15). Soil enzyme activity was positively correlated with DOC, MBC, and MBN at different stages.

4 Discussion

The results of this study indicated that TN, NH_4-N, and TP content in grape rhizosphere soil had the similar response to water stress, without the significant difference among three treatments (moderate and mild water stress and adequate water supply). The results were consistent with previous finding that soil TN and TP contents were not sensitive under different water stress (Wu et al., 2012; Bu et al., 2018). In addition, the study also found that the effect of water stress on soil NO_3-N and AP contents were closely related to the degree and time of stress because the soil NO_3-N and AP contents were significantly lower under moderate (W2) and mild (W1) water stress than with sufficient water (CK) in the new shoot elongation stage (Jun-15) and fruit enlargement (Aug-15) stages. Water stress reduced the vitality of the plant's root system, which in turn decreased the secretion of all kinds of organic and inorganic substances by the plant's root system (Draye et al., 2010). On the contrary, in the coloring maturity stage (Oct-15), there was no significant difference in the NO_3-N and AP contents of grape rhizosphere soil under continuous water stress (Li et al., 2021). The cause was due to the decrease of nutrient uptake by the crop's root system as the grapes mature. However, the result showed stronger selective absorption of nitrate nitrogen compared with NH_4-N, as well as the promotion of the absorption of AP content in the soil under water stress.

Another important finding was that there was no significant effect on soil TOC content in the rhizosphere of grapes under water stress during the growth period. A possible explanation may be that the accumulation in soil organic carbon pool storage was a relatively long process, and the change in the amount of grape root exudates caused by water stress was not enough to cause an obvious change in the soil organic carbon content. Additionally, the grape rhizosphere exudates were first supplied to rhizosphere soil microorganisms for utilization and reproduction (Song et al., 2012). Therefore, water stress had no significant effect on the soil TOC content; during the growth period had small fluctuations. Meanwhile the soil DOC content significantly reduced. The soil DOC content under moderate water stress was significantly lower than that under mild water stress and for control treatment with the promoted degree of water stress (W2 and W1 treatments) and the prolonged stress time. This finding was contrary to previous results that suggested DOC could increase with the decline of soil moisture (Wang et al., 2017). The results of the present study showed that moderate water stress reduced the DOC content of grape rhizosphere soil, but mild water stress had no significant effect. This finding was also reported by Li et al. (2016). In summary, soil carbon content may be related to a number of factors such as geographical location, field management, and irrigation practices (Zhang R. et al., 2023). However, water stress reduced the soil MBC and MBN contents of the grape rhizosphere soil, which was contrary to previous findings that drought stress increased the MBC content (Mganga et al., 2019). Previous studies also suggested that excessive water stress (Hueso et al., 2012) and long-term water stress also reduced the soil microbial biomass content (Schimel et al., 1999; Wang et al., 2017). This could be explained by the fact that water stress reduced the vitality of plant roots, which in turn caused the reduction of various organic and inorganic substances secreted by plant roots. This finding was contrary to previous results suggesting that water-soluble compounds and mucilage secreted by plant roots under drought stress promoted the production of microbial biomass (Sanaullah et al., 2011).

Soil moisture was an important factor affecting soil enzyme activity in plant rhizosphere (Geisseler et al., 2011; A'Bear et al., 2014). This experimental study showed that the soil urease activity increased during the initial period of water stress and decreased significantly in the mid-stress stage in soil layers of 0–10 and 10–20 cm, which was probably varied in different plant growth period (Song et al., 2012; Zhang et al., 2018). With the increase of stress duration, moderate water stress reduced the soil urease activity in the soil layer of 0–10 cm, and the moderate and mild water stress reduced the soil urease activity in the soil layer of 40 cm during the coloring mature stage. Adequate water supply and mild water stress helped increase the urease activity in the soil layer of 20–40 cm. Another finding was that in terms of spatial distribution, the activity of urease, catalase, and sucrase in greenhouse grape rhizosphere soil in different soil layers followed the order: 10–20 cm > 0–10 cm > 20–40 cm. This result might be explained by the fact that fertilizers (organic fertilizer, farmyard manure, and chemical fertilizer) were sprayed onto the soil trough 20 cm away from the grape roots and then covered with topsoil (Liu et al., 2024). The urease and sucrase activities in rhizosphere soil were basically stable during the whole growth period of grapes. Hence, further studies should be conducted to investigate the growth, yield, and quality of grapes under different water stresses, and to provide a better description of the influence of water regulation

10.3389/fmicb.2024.1376849

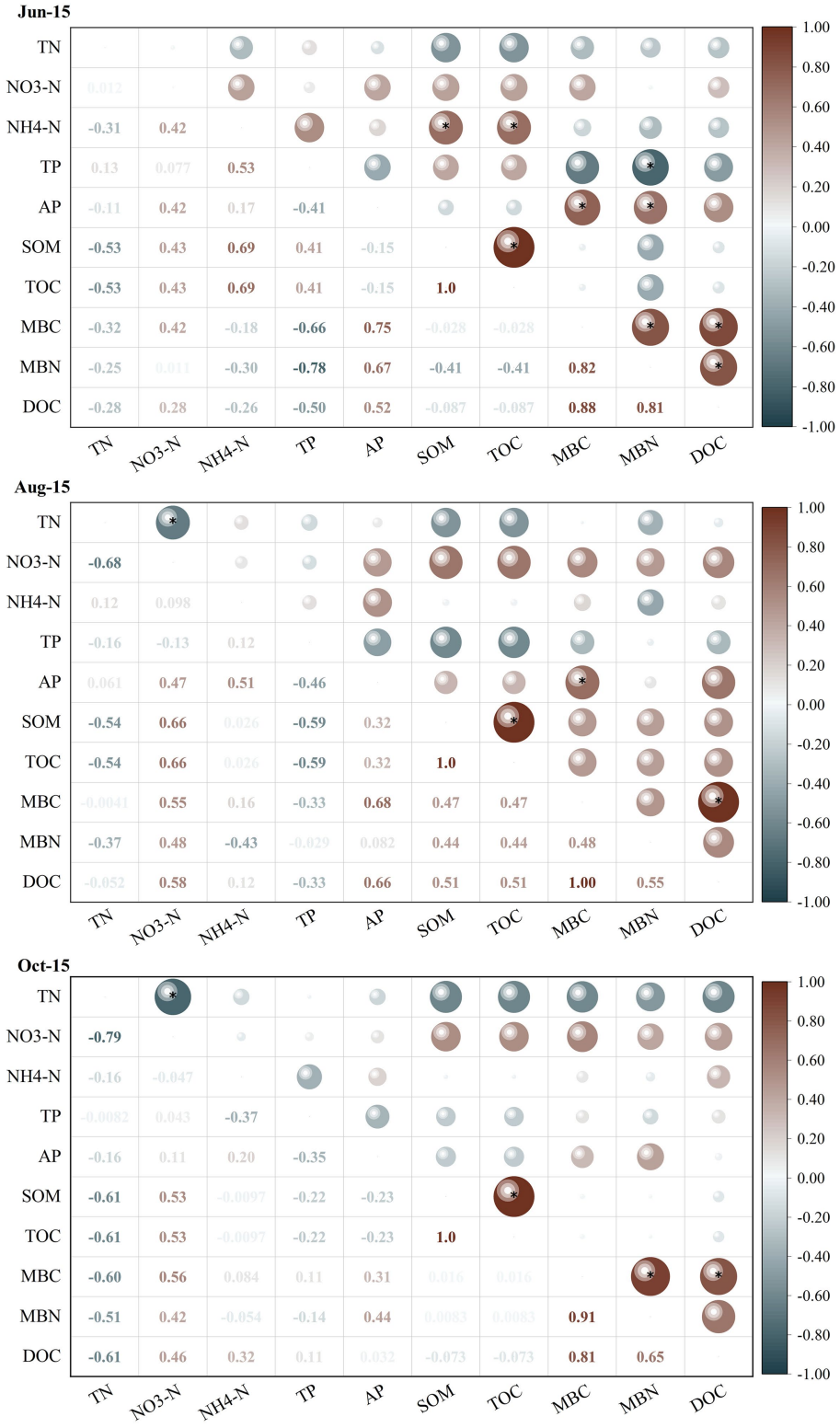

FIGURE 2
Correlation between soil physical–chemical indicators and microbial biomass indicators. *Significantly correlated at the 0.05 level (two sides). TN, Total nitrogen; NO_3-N, Nitrate nitrogen; NH_4-N, Ammonia nitrogen; TP, Total phosphorus; AP, Availability phosphorus; SOM Soil organic matter; TOC, Total organic carbon; MBC, Microbial biomass carbon; MBC, Microbial biomass nitrogen; and DOC, Dissolved organic carbon.

on the water-rhizosphere soil–plant system. In addition, mild water stress helped increase the catalase activity in grape rhizosphere soil in the soil layer of 0–10 cm on Jun-15 (new shoot growth stage) and Aug-15 (fruit expansion stage). On May-15 (budburst stage), the soil catalase activity under moderate water stress was significantly lower than that with an adequate water supply and under mild water stress.

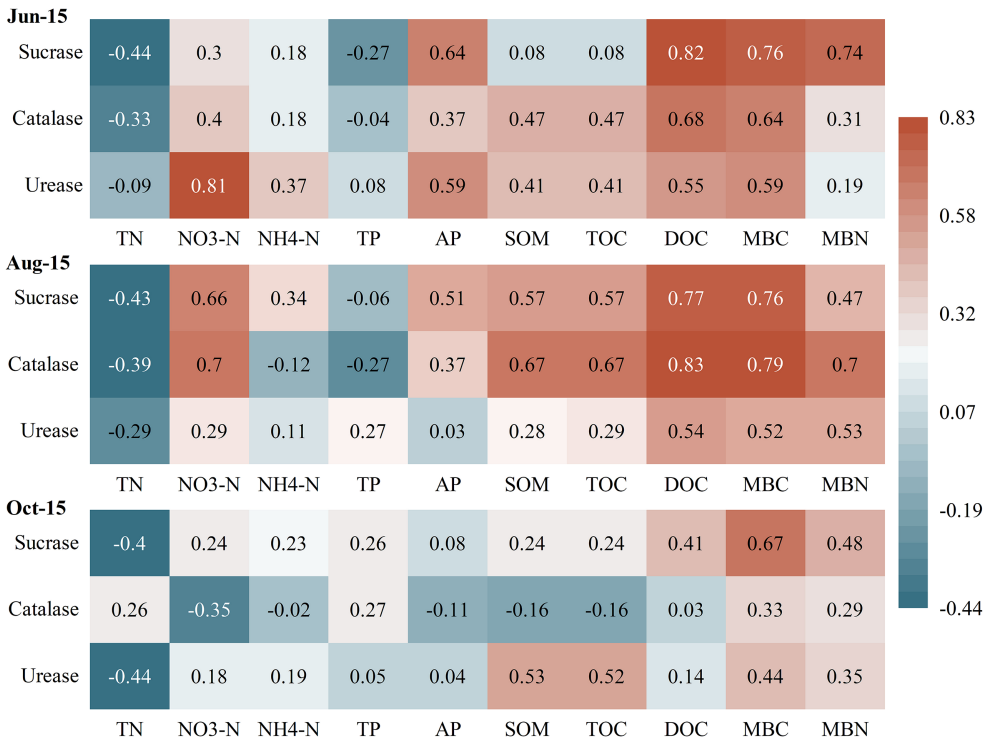

FIGURE 3
Correlation between soil physical–chemical indicators and soil enzymes. *Significantly correlated at the 0.05 level (two sides). TN, Total nitrogen; NO_3-N, Nitrate nitrogen; NH_4-N, Ammonia nitrogen; TP, Total phosphorus; AP, Availability phosphorus; SOM, Soil organic matter; TOC, Total organic carbon; MBC, Microbial biomass carbon; MBC, Microbial biomass nitrogen; and DOC, Dissolved organic carbon.

Soil catalase activity was related to various factors such as soil fertility, texture, pH, aeration, and climatic conditions (Bao et al., 2022). This experimental study found that W2 treatment helped increase the soil sucrase activity in the soil layer of 0–10 cm on July 20 (flowering stage), but it reduced the soil invertase activity from May-15 (budburst stage) to Jun-15 (new shoot growth stage). This was because the soil conditions between the roots may become anaerobic microdomains due to reduced water content, and could lead to the inhibition of sucrase activities because of limited substrate diffusion and oxygen content (Zhang, 2005).

5 Conclusion

This study detected significant differences in rhizosphere soil enzyme activities and microbial biomass of greenhouse grape under water stress ($p < 0.05$). Moreover, water stress had less effect on soil physical–chemical properties. Compared with the adequate water supply conditions, the water stress (mild W2 and moderate W1) effectively reduced the accumulation of soil MBC content throughout the grape growing season and reduced soil MBN content in later growth. Both W2 (mild water stress) and W1 (moderate water stress) treatments inhibited the activities of urease, catalase, and sucrase activities transforming enzymes in the soil during greenhouse grape growth. These results illustrated that water stress altered both soil microbial structure and function in rhizosphere soil enzyme activities. Overall, this study provides a theoretical basis for water-saving greenhouse grape cultivation and soil environment regulation. Considering the effects of successive years of water stress on soil microbial and rhizosphere enzyme activities in greenhouse grapes needs to be further deepened and broadened. We suggest that future studies should focus more on changes in greenhouse grape rhizosphere soil enzyme activities and microorganisms as a result of multi-year water stress, and should incorporate changes in microbial communities, which play a crucial role in the regulation of soil quality and plant acclimatization.

Data availability statement

The original contributions presented in the study are included in the article/supplementary material, further inquiries can be directed to the corresponding author.

Author contributions

RZ: Funding acquisition, Writing – review & editing. HZ: Data curation, Writing – original draft. CY: Data curation, Writing – review & editing. HL: Investigation, Writing – review & editing. JW: Formal Analysis, Methodology, Writing – review & editing.

Funding

The author(s) declare financial support was received for the research, authorship, and/or publication of this article. This study was supported by the National Natural Science Foundation of China (52169007), the Key R&D Plan of Gansu Province (22YF7GA107),

and the Fuxi youth talent training program of Gansu Agricultural University (Gaufx-03Y10) for funding.

Conflict of interest

The authors declare that the research was conducted in the absence of any commercial or financial relationships that could be construed as a potential conflict of interest.

Publisher's note

References

A'Bear, A. D., Jones, T. H., Kandeler, E., and Boddy, L. (2014). Interactive effects of temperature and soil moisture on fungal-mediated wood decomposition and extracellular enzyme activity. *Soil Biol. Biochem.* 70, 151–158. doi: 10.1016/j.soilbio.2013.12.017

Bao, L., Sun, B., Wei, Y., Xu, N., Zhang, S., Gu, L., et al. (2022). Grape cultivar features differentiate the grape rhizosphere microbiota. *Plan. Theory* 11:1111. doi: 10.3390/plants11091111

Barta, J., Slajsova, P., Tahovska, K., Picek, T., and Santruckova, H. (2014). Different temperature sensitivity and kinetics of soil enzymes indicate seasonal shifts in C, N and P nutrient stoichiometry in acid forest soil. *Biogeochemistry* 117, 525–537. doi: 10.1007/s10533-013-9898-1

Boell, E. J., and Shen, S. C. (1954). An improved ultramicro Kjeldahl technique. *Exp. Cell Res.* 7, 147–152. doi: 10.1016/0014-4827(54)90049-X

Bogati, K., and Walczak, M. (2022). The impact of drought stress on soil microbial community, enzyme activities and plants. *Agronomy* 12:189. doi: 10.3390/agronomy12010189

Bu, X., Gu, X., Zhou, X., Zhang, M., Guo, Z., Zhang, J., et al. (2018). Extreme drought slightly decreased soil labile organic C and N contents and altered microbial community structure in a subtropical evergreen forest. *Forest Ecol. Manag.* 429, 18–27. doi: 10.1016/j.foreco.2018.06.036

Chrost, R. J. (2014). Microbial enzymes in aquatic environments. *Freshwater Sci.* 13:978. doi: 10.1007/978-1-4612-3090-8

Draye, X., Kim, Y., Lobet, G., and Javaux, M. (2010). Model-assisted integration of physiological and environmental constraints affecting the dynamic and spatial patterns of root water uptake from soils. *J. Exp. Bot.* 61, 2145–2155. doi: 10.1093/jxb/erq077

Geisseler, D., Horwath, W. R., and Scow, K. M. (2011). Soil moisture and plant residue addition interact in their effect on extracellular enzyme activity. *Pedobiologia* 54, 71–78. doi: 10.1016/j.pedobi.2010.10.001

Geng, S. M., Yan, D. H., Zhang, T. X., Weng, B. S., Zhang, Z. B., and Qin, T. L. (2015). Effects of drought stress on agriculture soil. *Nat. Hazards* 75, 1997–2011. doi: 10.1007/s11069-014-1409-8

Gramss, G., Voigt, K. D., and Kirsche, B. (1999). Oxidoreductase enzymes liberated by plant roots and their effects on soil humic material. *Chemosphere* 38, 1481–1494. doi: 10.1016/S0045-6535(98)00369-5

Hueso, S., Garcia, C., and Hernandez, T. (2012). Severe drought conditions modify the microbial community structure, size and activity in amended and unamended soils. *Soil Biol. Biochem.* 50, 167–173. doi: 10.1016/j.soilbio.2012.03.026

Jing, Y., Zhang, Y., Han, I., Wang, P., Mei, Q., and Huang, Y. (2020). Effects of different straw biochars on soil organic carbon, nitrogen, available phosphorus, and enzyme activity in paddy soil. *Sci. Rep.* 10:8837. doi: 10.1038/s41598-020-65796-2

Kapoor, D., Bhardwaj, S., Landi, M., Sharma, A., Ramakrishnan, M., and Sharma, A. (2020). The impact of drought in plant metabolism: how to exploit tolerance mechanisms to increase crop production. *Appl. Sci.* 10:5692. doi: 10.3390/app10165692

Kátai, J., Zsuposné, Á. O., Tállai, M., and Alshaal, T. (2020). Would fertilization history render the soil microbial communities and their activities more resistant to rainfall fluctuations? *Ecotoxicol. Environ. Saf.* 201:110803. doi: 10.1016/j.ecoenv.2020.110803

Kim, Y., Chung, Y. S., Lee, E., Tripathi, P., Heo, S., and Kim, K. (2020). Root response to drought stress in Rice (*Oryza sativa* L.). *Int. J. Mol. Sci.* 21:1513. doi: 10.3390/ijms21041513

Li, Q., Liang, J. H., He, Y. Y., Hu, Q. J., and Yu, S. (2014). Effect of land use on soil enzyme activities at karst area in Nanchuan, Chongqing, Southwest China. *Plant Soil Environ.* 60, 15–20. doi: 10.17221/599/2013-PSE

Li, S., Tan, D., Wu, X., Degré, A., Long, H., Zhang, S., et al. (2021). Negative pressure irrigation increases vegetable water productivity and nitrogen use efficiency by improving soil water and NO_3–N distributions. *Agric. Water Manag.* 251:106853. doi: 10.1016/j.agwat.2021.106853

Li, Z., Zhao, B., and Zhang, J. (2016). Effects of maize residue quality and soil water content on soil labile organic carbon fractions and microbial properties. *Pedosphere* 26, 829–838. doi: 10.1016/S1002-0160(15)60088-1

Liu, X., and Zhang, S. (2019). Nitrogen addition shapes soil enzyme activity patterns by changing pH rather than the composition of the plant and microbial communities in an alpine meadow soil. *Plant Soil* 440, 11–24. doi: 10.1007/s11104-019-04054-5

Liu, S., Zhang, P., Wang, X., Hakeem, A., Niu, M., Song, S., et al. (2024). Comparative analysis of different bio-organic fertilizers on growth and rhizosphere environment of grapevine seedlings. *Sci. Hortic.* 324:112587. doi: 10.1016/j.scienta.2023.112587

Manzoni, S., Schimel, J. P., and Porporato, A. (2012). Responses of soil microbial communities to water stress: results from a meta-analysis. *Ecology* 93, 930–938. doi: 10.1890/11-0026.1

Marschner, P., Grierson, P. F., and Rengel, Z. (2005). Microbial community composition and functioning in the rhizosphere of three Banksia species in native woodland in Western Australia. *Appl. Soil Ecol.* 28, 191–201. doi: 10.1016/j.apsoil.2004.09.001

Menichetti, L., Reyes Ortigoza, A. L., García, N., Giagnoni, L., Nannipieri, P., and Renella, G. (2015). Thermal sensitivity of enzyme activity in tropical soils assessed by the Q10 and equilibrium model. *Biol. Fertil. Soils* 51, 299–310. doi: 10.1007/s00374-014-0976-x

Mganga, K. Z., Razavi, B. S., Sanaullah, M., and Kuzyakov, Y. (2019). Phenological stage, plant biomass, and drought stress affect microbial biomass and enzyme activities in the rhizosphere of *Enteropogon macrostachyus*. *Pedosphere* 29, 259–265. doi: 10.1016/S1002-0160(18)60799-X

Padhy, S. R., Nayak, S., Dash, P. K., Das, M., Roy, K. S., Nayak, A. K., et al. (2018). Elevated carbon dioxide and temperature imparted intrinsic drought tolerance in aerobic rice system through enhanced exopolysaccharide production and rhizospheric activation. *Agric. Ecosyst. Environ.* 268, 52–60. doi: 10.1016/j.agee.2018.08.009

Ru, C., Hu, X., Wang, W., Ran, H., Song, T., and Guo, Y. (2020). Evaluation of the crop water stress index as an indicator for the diagnosis of grapevine water deficiency in greenhouses. *Horticulturae* 6:86. doi: 10.3390/horticulturae6040086

Schimel, J. P., Gulledge, J. M., Clein-Curley, J. S., Lindstrom, J. E., and Braddock, J. F. (1999). Moisture effects on microbial activity and community structure in decomposing birch litter in the Alaskan taiga. *Soil Biol. Biochem.* 31, 831–838. doi: 10.1016/S0038-0717(98)00182-5

Sanaullah, M., Blagodatskaya, E., Chabbi, A., Rumpel, C., Kuzyakov, Y. (2011). Drought effects on microbial biomass and enzyme activities in the rhizosphere of grasses depend on plant community composition. *Applied Soil Ecology* 48: 38–44. doi: 10.1016/j.apsoil.2011.02.004

Song, F., Han, X., Zhu, X., and Herbert, S. J. (2012). Response to water stress of soil enzymes and root exudates from drought and non-drought tolerant corn hybrids at different growth stages. *Can. J. Soil Sci.* 92, 501–507. doi: 10.4141/cjss2010-057

Song, R., Zhu, W. Z., and Li, H. (2024). Impact of wine-grape continuous cropping on soil enzyme activity and the composition and function of the soil microbial community in arid areas. *Front. Microbiol.* 15:1348259. doi: 10.3389/fmicb.2024.1348259

Wang, Y., Yan, D., Wang, J., Ding, Y., and Song, X. (2017). Effects of elevated CO_2 and drought on plant physiology, soil carbon and soil enzyme activities. *Pedosphere* 27, 846–855. doi: 10.1016/S1002-0160(17)60458-2

Wang, Y., Zhang, X., Chen, J., Chen, A., Wang, L., Guo, X., et al. (2019). Reducing basal nitrogen rate to improve maize seedling growth, water and nitrogen use efficiencies under drought stress by optimizing root morphology and distribution. *Agric. Water Manag.* 212, 328–337. doi: 10.1016/j.agwat.2018.09.010

Wu, F., Bao, W., Zhou, Z., and Li, F. (2012). Appropriate nitrogen supply could improve soil microbial and chemical characteristics with *Sophora davidii* seedlings cultivated in water stress conditions. *Acta Agric. Scand.* 62, 49–58. doi: 10.1080/09064710.2011.568515

Wu, J., Wang, H., Li, G., Ma, W., Wu, J., Gong, Y., et al. (2020). Vegetation degradation impacts soil nutrients and enzyme activities in wet meadow on the Qinghai-Tibet plateau. *Sci. Rep.* 10:21271. doi: 10.1038/s41598-020-78182-9

Xiao, L., Min, X., Liu, G., Li, P., and Xue, S. (2023). Effect of plant–plant interactions and drought stress on the response of soil nutrient contents, enzyme activities and microbial metabolic limitations. *Appl. Soil Ecol.* 181:104666. doi: 10.1016/j.apsoil.2022.104666

Xie, X., Pu, L., Wang, Q., Zhu, M., Xu, Y., and Zhang, M. (2017). Response of soil physicochemical properties and enzyme activities to long-term reclamation of coastal saline soil, Eastern China. *Sci. Total Environ.* 607-608, 1419–1427. doi: 10.1016/j.scitotenv.2017.05.185

Xu, N., Tan, G., Wang, H., and Gai, X. (2016). Effect of biochar additions to soil on nitrogen leaching, microbial biomass and bacterial community structure. *Eur. J. Soil Biol.* 74, 1–8. doi: 10.1016/j.ejsobi.2016.02.004

Xue, R., Shen, Y. Y., and Marschner, P. (2017). Soil water content during and after plant growth influence nutrient availability and microbial biomass. *J. Soil Sci. Plant Nutr.* 17, 702–715. doi: 10.4067/s0718-95162017000300012

Yang, N., Nesme, J., Røder, H. L., Li, X., Zuo, Z., and Petersen, M. (2021). Emergent bacterial community properties induce enhanced drought tolerance in Arabidopsis. *NPJ Biofilms Microbiomes* 7:82. doi: 10.1038/s41522-021-00253-0

Yang, H., Wu, F., Fang, H., Hu, J., and Hou, Z. (2019). Mechanism of soil environmental regulation by aerated drip irrigation. *Acta Phys. Sin.* 68:019201. doi: 10.7498/aps.68.20181357

Zhang, K. (2005). Forest litter decomposition is affected by different sources of soil and plant growth. China Agricultural University, Beijing. Available at: https://kns.cnki.net/kcms2/article/abstract?v=sf24_f5fySZ3gys5wcV9Fejlhr5HYn2N_vIFKizFL3ADTh1MiUN8UL56URf57GMPz3YsiaaW9cY2ln92bEffXcixiLSPa5DVBviS7QvngpFpNPBxC745bRKkPwYGzHhbjIi9MNVPdCV7X4Qhftvbyw=&uniplatform=NZKPT&language=CHS

Zhang, R., Chen, L., Niu, Z., Song, S., and Zhao, Y. (2019). Water stress affects the frequency of Firmicutes, Clostridiales and Lysobacter in rhizosphere soils of greenhouse grape. *Agric. Water Manag.* 226:105776. doi: 10.1016/j.agwat.2019.105776

Zhang, C., Nie, S., Liang, J., Zeng, G., Wu, H., Hua, S., et al. (2016). Effects of heavy metals and soil physicochemical properties on wetland soil microbial biomass and bacterial community structure. *Sci. Total Environ.* 557-558, 785–790. doi: 10.1016/j.scitotenv.2016.01.170

Zhang, C., Wang, F., Wang, R., Wang, Z., Song, P., Guo, L., et al. (2023). Drought stress affects bacterial community structure in the rhizosphere of Paeonia ostii 'Feng Dan'. *J. Hortic. Sci. Biotechnol.* 98, 109–120. doi: 10.1080/14620316.2022.2095311

Zhang, R., Wu, J., Yang, C., Li, H., Lin, B., Gao, Y., et al. (2023). Response of water stress and bacterial fertilizer addition to the structure of microbial flora in the rhizosphere soil of grapes under delayed cultivation. *Commun. Soil Sci. Plant Anal.* 54, 2609–2624. doi: 10.1080/00103624.2023.2234947

Zhang, W., Zhu, J., Zhou, X., and Li, F. (2018). Effects of shallow groundwater table and fertilization level on soil physico-chemical properties, enzyme activities, and winter wheat yield. *Agric. Water Manag.* 208, 307–317. doi: 10.1016/j.agwat.2018.06.039

Zhao, Y., Mao, W., Pang, L., Li, R., and Li, S. (2020). Influence of Phragmites communis and *Zizania aquatica* on rhizosphere soil enzyme activity and bacterial community structure in a surface flow constructed wetland treating secondary domestic effluent in China. *Environ. Sci. Pollut. R.* 27, 26141–26152. doi: 10.1007/s11356-020-08904-z

frontiers | Frontiers in Microbiology

TYPE Original Research
PUBLISHED 03 April 2024
DOI 10.3389/fmicb.2024.1383882

OPEN ACCESS

EDITED BY
Jiuling Li,
The University of Queensland, Australia

REVIEWED BY
Yafei Zhang,
Jiangsu University, China
Zicheng Su,
The University of Queensland, Australia

*CORRESPONDENCE
Zhibin Ren
✉ renzhibin@iga.ac.cn

RECEIVED 08 February 2024
ACCEPTED 08 March 2024
PUBLISHED 03 April 2024

CITATION
Du Y, Ren Z, Zhong Y, Zhang J and Song Q (2024) Spatiotemporal pattern of coastal water pollution and its driving factors: implications for improving water environment along Hainan Island, China.
Front. Microbiol. 15:1383882.
doi: 10.3389/fmicb.2024.1383882

Spatiotemporal pattern of coastal water pollution and its driving factors: implications for improving water environment along Hainan Island, China

Yunxia Du[1,2], Zhibin Ren[2,3]*, Yingping Zhong[1], Jinping Zhang[1,2] and Qin Song[1,2]

[1]School of Geography and Environmental Sciences, Hainan Normal University, Haikou, China, [2]Key Laboratory of Tropical Island Land Surface Processes and Environmental Changes of Hainan Province, Haikou, China, [3]Northeast Institute of Geography and Agroecology, Chinese Academy of Sciences, Changchun, China

In the context of human activities and climate change, the gradual degradation of coastal water quality seriously threatens the balance of coastal and marine ecosystems. However, the spatiotemporal patterns of coastal water quality and its driving factors were still not well understood. Based on 31 water quality parameters from 2015 to 2020, a new approach of optimizing water quality index (WQI) model was proposed to quantitatively assess the spatial and temporal water quality along tropical Hainan Island, China. In addition, pollution sources were further identified by factor analysis and the effects of pollution source on water quality was finally quantitatively in our study. The results showed that the average water quality was moderate. Water quality at 86.36% of the monitoring stations was good while 13.53% of the monitoring stations has bad or very bad water quality. Besides, the coastal water quality had spatial and seasonal variation, along Hainan Island, China. The water quality at "bad" level was mainly appeared in the coastal waters along large cities (Haikou and Sanya) and some aquaculture regions. Seasonally, the average water quality in March, October and November was worse than in other months. Factor analysis revealed that water quality in this region was mostly affected by urbanization, planting and breeding factor, industrial factor, and they played the different role in different coastal zones. Waters at 10.23% of monitoring stations were at the greatest risk of deterioration due to severe pressure from environmental factors. Our study has significant important references for improving water quality and managing coastal water environment.

KEYWORDS

coastal water, water quality, WQI model, pollution source, deterioration risk

1 Introduction

Coastal waters as a complex, sensitive, and highly dynamic ecosystem are strongly influenced by land-sea interactions, natural change and usage characteristics of the adjacent land (Wells et al., 2015; Chen et al., 2019; Román et al., 2023). Coastal waters have ecological importance because they can support 25% of primary production and 80% of carbon

production for global scale (United Nations Environment Programme, 1992). It is confirmed that more than 60% of population and two-thirds of large and medium-sized cities in the world are concentrated along coastal areas (Ma et al., 2010; Lv et al., 2016) and most of the population live within 100 km of the coast (Gunnerson and French, 1996). Therefore, the coastal ecosystems offer important support in sustaining major socioeconomic activities, such as tourism, agriculture, and fisheries (Gai et al., 2022). However, coastal waters are therefore influenced by anthropogenic activities directly and significantly (Howard et al., 2016; Malone and Newton, 2020). In recent decades, eutrophication occurs frequently due to various human activities in the coastal area, such as the discharge of urban and industrial wastewaters, inflow of agricultural and atmospheric pollution (Bužančić et al., 2016; Cheng et al., 2020). Since the late 1980s, the rapid expansion of aquaculture in China's coastal areas has promoted the economic development of coastal areas (Ren et al., 2019). At the same time, coastal waters became subject to intense pressure from aquaculture expansion, which inevitably leads to water quality degradation (Wang et al., 2023; Zhang et al., 2023), thus threatening the survival of aquatic life and damaging marine ecosystems. An overview about the historical variations in water quality and pollutant origins in the coastal seas of China during the 1990s and 2000s by Wang et al. (2011), indicated that water quality had not improved significantly over these two decades. Xin et al. (2023) reviewed long-term variations in pollutant sources and water quality in China's coastal waters over the last three decades and the results showed that a turning point in the water quality appears in the mid-2010s, that is, since 2015, there has been a substantial improvement in water quality in China's coastal waters due to the enforcement of the strictest ever Environmental Protection Law. Zhang et al. (2022) also confirmed that coastal water quality in China is improving. However, the dynamics of sensitive coastal water quality should be vigilant at all times under the pressure of enormous socio-economic activities. Sustainable management of water resource has become a challenge of critical importance.

In many countries, a range of policies and guidelines have been adopted to manage water quality and protect ecosystem in order to reverse water quality degradation. The Water Framework Directive (WFD) adopted by Member states of the European Union in 2000 was an effective instrument for the water quality management (Zotou et al., 2018). The WFD and other similar frameworks for water quality management rely mostly on collected datasets to assess water quality. In recent years, many tools and techniques have been developed to assess water quality, the water quality index (WQI) models are one of the most widely used tools (Sun et al., 2016; Sutadian et al., 2018; Uddin et al., 2020, 2022, 2023a,b; Lukhabi et al., 2023). WQI is a tool that describes the overall water quality by converting available water quality parameter data into a single unitless number by mathematical algorithms (Horton, 1965). The method is relatively easy to apply and its results are easy to interpret by both professionals and nonexperts (Uddin et al., 2021; Lukhabi et al., 2023). WQI allows water quality status to be compared across time and space, thus directly communicating information of water quality to the public and decision makers (Poonam et al., 2013; Lukhabi et al., 2023). However, several studies have indicated that there was significant uncertainty in determining the actual water quality due to the fuzziness of WQI model in structure (Kannel et al., 2007; Uddin et al., 2021; Lukhabi et al., 2023). Most of the WQI models are region-specific because their components have been developed based on expert views and local guidelines (Uddin et al., 2021, 2023c). Therefore, how to optimize water quality index (WQI) model to quantitatively assess the water quality on a large temporal and spatial scales is still not well understood.

Although several WQI models have been used to assess water quality in some lakes, rivers, and coastal waters in China (Liu et al., 2011; Hou et al., 2016; Ma et al., 2020). There is still a lack of understanding of the coastal water quality in tropical Hainan Island, China. Coastal waters are the important coastal ecosystem in Hainan Island and are also of particular interest due to their recreational, economic, and ecological values. Human pressures such as aquaculture expansion, tourism development and urban and industrial pollution could pose great risks to the deterioration of water quality and threaten the ecological security of coastal waters. The aim of this research is (1) to propose a new approach to improve the WQI model; (2) to determine spatiotemporal patterns in water quality along tropical Hainan Island by considering the specific parameters; (3) to quantify the pressures from potential environment factors to reveal the deterioration risk of water quality. This research is essential for coastal waters management and pollution control in tropical coastal areas.

2 Materials and methods

2.1 Study area

Hainan Island (108° 37′E - 111° 03′E, 18° 10'N - 20° 10'N) is the main island of Hainan Province, China. Hainan Island is surrounded by sea and located in the south of China, facing Guangdong Province on the north, adjoining to the Beibu Gulf and facing Vietnam on the west, bordering the South China Sea on the east, adjoining to the South China Sea on the southeast and south and bordering the Philippines, Brunei and Malaysia. Hainan Island is an elliptic island with a long axis of about 290 kilometers from northeast to southwest and a short axis of about 180 kilometers from northwest to southeast. It covers an area of about 33,900 km^2 and is the second largest island of China. The precipitation and temperature in Hainan Island show significant spatiotemporal differences, and the vegetation cover in the coastal land area of Hainan Island is unbalanced between regions. Hainan Island is rich in water resources, with 154 rivers flowing into the sea, the main rivers are Nandu River, Changhua River and Wanquan River. As a result, many estuaries and bays were formed. The coastal land of Hainan Island is an important place for human life, amusement, and production activities. Many aquaculture ponds and agricultural land are also distributed on the coastal land of Hainan Island. The water quality monitoring stations are widely distributed offshore within 20 km distance from the coastline. Therefore, the 20 km of sea along the coastline of Hainan Island was selected as the study area (Figure 1) to analyze the nearshore water environment.

2.2 *In situ* data and processing

In situ data were collected from water quality monitoring stations in offshore waters from 2015 to 2020. The frequency of water quality monitoring was generally 3 times a year, and the sampling time is

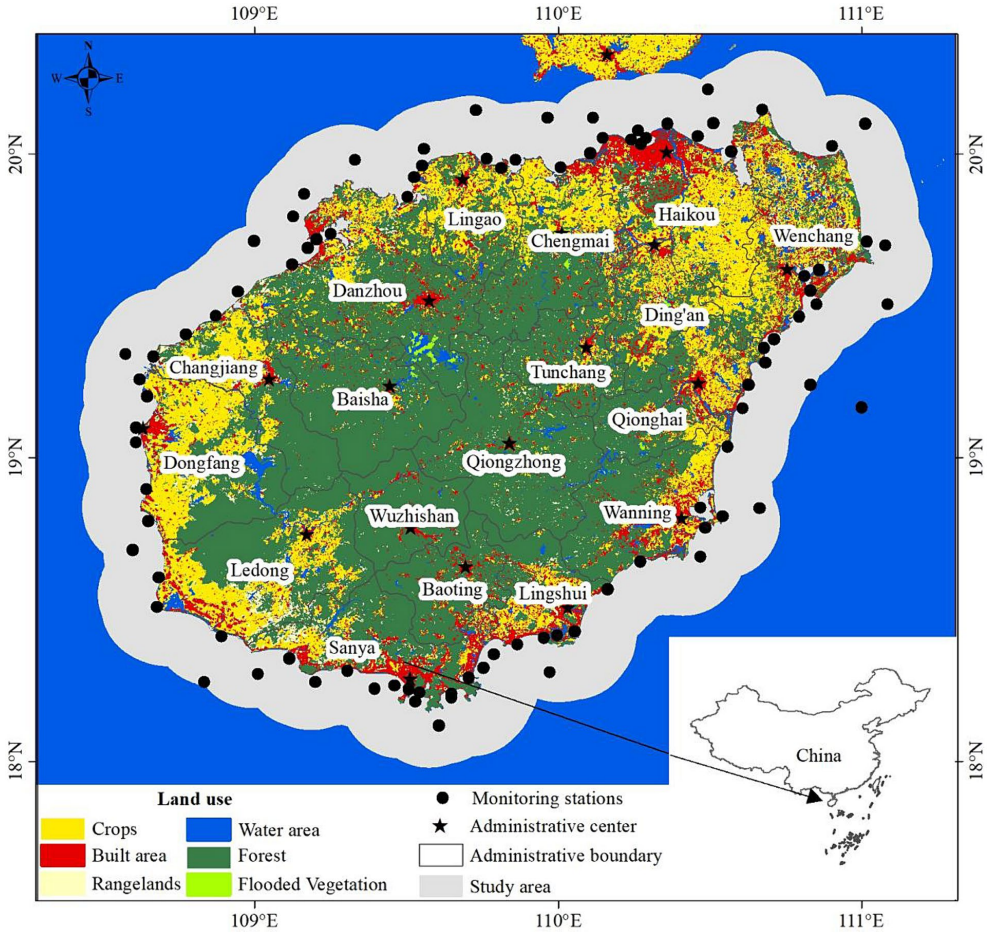

FIGURE 1
The study area and distribution of the monitoring stations for water quality.

arranged in March to May, July to August, and September to November. The interval between two monitoring sessions was more than 2 months. A total of 1,072 *in situ* measurements were collected from a total of 125 different stations distributed in the study area (Figure 1). A total of 39 parameters were collected, including physical, chemical, biological, and toxic substances (Table 1). Chl-a analysis and quality control were carried out in accordance with the relevant requirements of "Technical Specification for Environmental Monitoring of Offshore Waters," Part VI: Biological Monitoring of Offshore Waters (HJ 442. 6). Other parameters were determined in accordance with "Technical Specification for Environmental Monitoring of Offshore Waters," Part III: Water Quality Monitoring of Offshore Waters (HJ 442. 3). The *in situ* data were normalized using min-max normalization, which were then used for the correlation and driving analysis.

2.3 Establishing an optimized WQI model for assessing water quality

The WQI model is a simple method for evaluating water quality and determining pollution levels. The WQI models is summarized into two types according to its sub-index acquisition method. The components of WQI model were determined in four main steps: (1) selecting water quality parameters; (2) computing the sub-index values; (3) assigning a weight for each parameter; (4) aggregating the sub-index value and weight of the water quality parameters (Abbasi and Abbasi, 2012; Sutadian et al., 2018). The WQI model was optimized in these four aspects, establishing an optimized WQI model in this research.

WQI tool transforms several water quality parameters into a single value and epitomized the data in a simple way (Gupta and Gupta, 2021). There were significant differences between the previous WQI models in the type and number of parameters selected and the reasons for selecting them. Parameters were typically selected based on data availability, expert opinion, or the environmental significance of a water quality parameter (Uddin et al., 2021). In our WQI model, the parameter selection ignored the type of water utilization in order to assess the comprehensive status of water quality. Parameters were selected based on the available data from monitoring stations. Total of 31 water quality parameters were applied, including not only commonly used parameters but also hazardous parameters of water quality, such as microbiological contamination, toxic compounds, and trace variables (Table 1).

Purpose of the sub-index process is to convert water quality parameter concentrations into dimensionless values (Abbasi and Abbasi, 2012). Simple linear transform function based on the measured sample range was used to obtain the sub-index. Value of the sub-index was calculated using the below Eqs 1, 2:

10.3389/fmicb.2024.1383882

TABLE 1 Water quality parameters and statistics of multi-annual mean of water quality parameters collected from 2015 to 2020.

Parameter/Pronoun		Min	Mean	Max	Parameter/Pronoun		Min	Mean	Max
Temperature	T	26.	28.112	30.273	Cadmium	Cd	0.00	0.0001	0.0002
Salinity	S	10.991	31.449	34.962	Arsenic	As	0.0003	0.0012	0.003
Total suspended solids	TSS	2.827	7.268	15.136	Zinc	Zn	0.0018	0.0074	0.0136
Dissolved oxygen	DO	6.175	6.701	7.628	Chromium (VI)	Cr	0.00	0.00	0.00
pH	pH	7.893	8.115	8.2	Total chromium	T-Cr	0.00	0.0006	0.0022
Chlorophyll a	Chl-a	0.1	1.997	24.4	Selenium	Se	0.00	0.0001	0.0008
Total nitrogen	TN	0.00	0.233	1.42	Nickel	Ni	0.00	0.0007	0.0016
Total phosphorus	TP	0.00	0.012	0.037	Coliform	CB	0.00	326.17	4999.333
Transparency	SDD	1.25	2.947	8.95	Fecal coliform	FCB	0.00	281.695	4879.167
Active phosphate	AP	0.002	0.007	0.053	Biochemical Oxygen Demand in 5 days	BOD_5	0.00	0.052	2.04
Chemical oxygen demand	COD	0.324	0.826	2.893	Cyanide	$(CN)_2$	0.00	0.00	0.00
Nitrite nitrogen	NO_2-N	0.002	0.01	0.026	Sulphide	MS	0.00	0.002	0.01
Nitrate nitrogen	NO_3-N	0.007	0.045	0.139	Volatile phenol	VP	0.00	0.00	0.00
Ammonia nitrogen	NH_3-N	0.012	0.04	0.172	Hexachlorocyclohexane (total)	$C_6H_6Cl_6$	0.00	0.00	0.00
Inorganic nitrogen	IN	0.021	0.097	0.268	Clofenotane (total)	$C_{14}H_9Cl_5$	0.00	0.00	0.00
Petroleum	Pe	0.0034	0.007	0.022	Malathion	$C_{10}H_{19}O_6PS_2$	0.00	0.00	0.00
Nonionic ammonia	N-NH_3	0.001	0.003	0.022	Parathion-methyl	C_8HNO_5PS	0.00	0.00	0.00
Hydragenum	Hg	0.00	0.000023	0.0007	benzo[a]pyrene	$C_{20}H_{12}$	0.00	0.00	0.00
Cuprum	Cu	0.0008	0.0012	0.002	Anion surfactant	LAS	0.00	0.005	0.029
Plumbum	Pb	0.0002	0.0004	0.0011					

The unit of parameters are shown in Figure 2. Pronouns for these parameters are used in the full text and in the figures.

$$C_i = \left(C_{\max} - C_{\min}\right) \times \frac{\left(X_{\max} - X_j\right)}{\left(X_{\max} - X_{\min}\right)} \quad (1)$$

$$C_i = \left(C_{\max} - C_{\min}\right) \times \frac{\left(X_j - X_{\min}\right)}{\left(X_{\max} - X_{\min}\right)} \quad (2)$$

$$W_i = \left(\frac{1}{N}\sum_{j=1}^{k} C_{ij}\right) / \left(\frac{1}{N}\sum_{i=1}^{n}\sum_{j=1}^{k} C_{ij}\right) \quad (3)$$

$$\sum_{i=1}^{n} W_i = 1 \quad (4)$$

where C_i is the sub-index value of water quality parameter i, which is computed for the sample X_j. C_{max} and C_{min} are the maximum and minimum sub-index values that correspond to the maximum and minimum sample values (X_{max} and X_{min}) or (X_c (threshold) and X_{min}) for parameter i. The threshold X_c is used for these parameters (such as T and DO) which have different effects on water quality depending on the concentration. The scale of the sub-index ranges between 0 and 100 (That is $C_{max} = 100$ and $C_{min} = 0$). Eq. 1 was used when the content of the parameter has a negative effect on the water quality otherwise Eq. 2.

In general, the parameter weight value is determined according to the relative importance of the water quality parameter or the appropriate guidelines of water quality (Sarkar and Abbasi, 2006). In our study, the unequal weighting technique was applied and the sum of weight values was equal to 1. The robustness of WQI model can be improved by using the unequal parameter weighting technology and assigning the most appropriate weighting values (Uddin et al., 2021). In order to avoid the adverse impact of inappropriate weightings on the model evaluation, an objective mathematical method based on sub-index (Eq. 3) is used for calculating weightings.

where W_i is the weight of the ith parameter. C_{ij} is the sub-index value of the jth sample of the ith parameter. N is the number of samples for each parameter. k is the number of samples. n is the number of parameters. The weight values of all parameters must comply with the Eq. 4.

The weighted average function was used to aggregate the final WQI value as follows Eq. 5:

$$WQI = \sum_{i=1}^{n} W_i C_i \quad (5)$$

Where W_i and C_i are the same as above.

2.4 Assessing driving factors affecting water quality

The water quality of a lake, river or ocean depends on environmental factors, including natural and human activities. In this research, water environment quality index (WEQI), which represents

the pressure of natural and human factors, was used to assess water environmental factors quantitatively. The WEQI value was obtained based on an innovation to the optimized WQI model above. After parameter selection, factor analysis based on the selected water quality parameters was need to performed, and sub-index was based on the extracted factor (rather than the selected water quality parameter values). Factor analysis based on water quality parameters can determine the representative of natural and human factors, so it can solve the problem that water environmental factors are complex and variable and difficult to quantify. The calculation of sub-index, factor weighting, aggregation of sub-index and weights were still done using the above Eqs 1, 3, 5, respectively. And the weight values of all parameters still comply with the Eq. 4. The final aggregate value of the sub-index and weights of all factors was the WEQI value. The WEQI values was further classified into several levels (no pressure, slight pressure, significant pressure, extreme pressure, severe pressure) in order to assess the pressure status of water from natural and human factors. According to the pressure state from the environmental driving factors, the tendency of water quality change can be revealed.

2.5 Data statistics and analysis

The maximum difference (R), standard deviation (SD) and coefficient of variation (CV) of the multi-years *in situ* measurements mean between monitoring stations were calculated. The slope of the regression line is a measure of the strength of the relationship between variables, and it can represent the average changing rate of the data set. So with time as the independent variable and water quality parameter measure as the dependent variable, the slope was calculated by regression analysis and used as the changing rate of water quality parameter. A positive slope means that the parameter concentration gradually increases over time, while a negative slope means that it gradually decreases. T test by Ronald Fisher (1925) was used to test the significance. In addition, the value of these statistical indexes was spatialized to analyze their spatial distribution characteristics.

Non-parametric Spearman rank order correlations suitable for the abnormal distribution of variables were used to determine the relationship between two parameters. The correlation analysis was based on the standardized values of *in situ* water quality parameter, and the correlation coefficients (r) and statistical significance tests between parameters were automatically calculated and conducted through the Matlab 2018a software platform. Some sample values that were not tested were ignored as null values. The values of correlation coefficients were in the interval (−1 and 1), where greater than zero indicated positive correlation and less than zero indicated negative correlation.

Factor analysis was used to objectively determine relationships among parameters variables, finding the underlying factors. The KMO (Kaiser-Meyer-Olkin) test and Bartlett's test of sphericity were used to determine whether a variable was suitable for factor analysis. The principal components analysis was used as the extraction method, with the Kaiser criterion (1960) used to guide factor selection. A varimax raw rotation was used to obtain the factor model. Significant factor loading values 0.6 were used to identify the most important variables describing the extracted factors.

The k-means clustering algorithm was used to determine the similarity between the monitoring stations considering the extracted factor scores, and then the study area was divided into different water environment zones. The clustering performance was evaluated by contour coefficient.

3 Results

3.1 Spatiotemporal patterns of water physicochemical properties

The 8 water quality parameters (Cr, $(CN)_2$, VP, $C_6H_6Cl_6$, $C_{14}H_9C_{l5}$, $C_{10}H_{19}O_6PS_2$, C_8HNO_5PS, $C_{20}H_{12}$) were excluded in the following statistics and analysis because their values were 0 (bold in Table 1). Figure 2 showed the spatial distribution of multi-annual mean of water quality parameter from 2015 to 2020. The distribution of some parameters showed significant differences along coastal regions, such as NO_2-N, NO_3-N, IN, Pe, CB and FCB were higher in the northern coastal region (near HaiKou) than in other regions. The lower value of T was mainly distributed in the northern coastal region. TSS showed lower values in the northern, eastern, and southern coastal regions. The higher value of DO was mainly concentrated in the northern coastal area of LinGao and the eastern coastal area of WenChang. BOD_5 was generally low (> 0.001 mg/L at a few stations in the east and west). MS was higher in the north (near Haikou) and the south (near Sanya) and lower in the east and west. Cd, Zn and Se showed higher values in the south, while the low values of As were concentrated in this region. Ni was higher in the east and south than in the north and west. Other water quality parameters showed different spatial variation characteristics of non-significant high-low aggregation (Figure 2).

Statistics based on the multi-annual mean of water quality parameters were listed in Supplementary Figure S1. The maximum difference (R) and standard deviation (SD) of trace element (Cd, Hg, Se, Pb, Cu, Ni, T-Cr and As) among monitoring stations were the lowest (Supplementary Figure S1a), indicating a small dispersion degree relative to the average level. While CB and FCB had the highest R (4879.167 and 4999.333) and SD (787.542 and 738.868) (Supplementary Figure S1b). Coefficient of variation (CV) was used to compare the dispersion degree between different water quality parameters. Water quality parameters with larger spatial variability include Hg, Se, MS, LAS, TN, BOD_5, Chl-a, FCB and CB, whose CV was greater than 100% (Supplementary Figure S1). Compared with these parameters, the spatial variability of other parameters was weak, with a CV less than 100% (Supplementary Figure S1).

Figure 3 shows the changing rate of water quality parameters at the monitoring stations from 2015 to 2020. Overall, the changing rates of CB (−317.69—773.05) and FCB (−149.93—1104.20) had a widest range of values, followed by SDD (−1.4—9.7) (Figure 3A), indicating that the changing rates of these parameters were highly variable among monitoring stations (Supplementary Figure S2). The changing rates of T, S and TSS were significantly different among monitoring stations, and the values of changing rates for TSS at most of stations (3/4) were greater than 0 (Figure 3B), indicating that the TSS at these stations showed an increasing tendency. T generally increased in the north and southwest coastal areas (Supplementary Figure S2). S showed a decreasing tendency in the north, southwest and east (near QiongHai) (Supplementary Figure S2). TSS mainly showed an increasing tendency in the northeast and southwest

10.3389/fmicb.2024.1383882

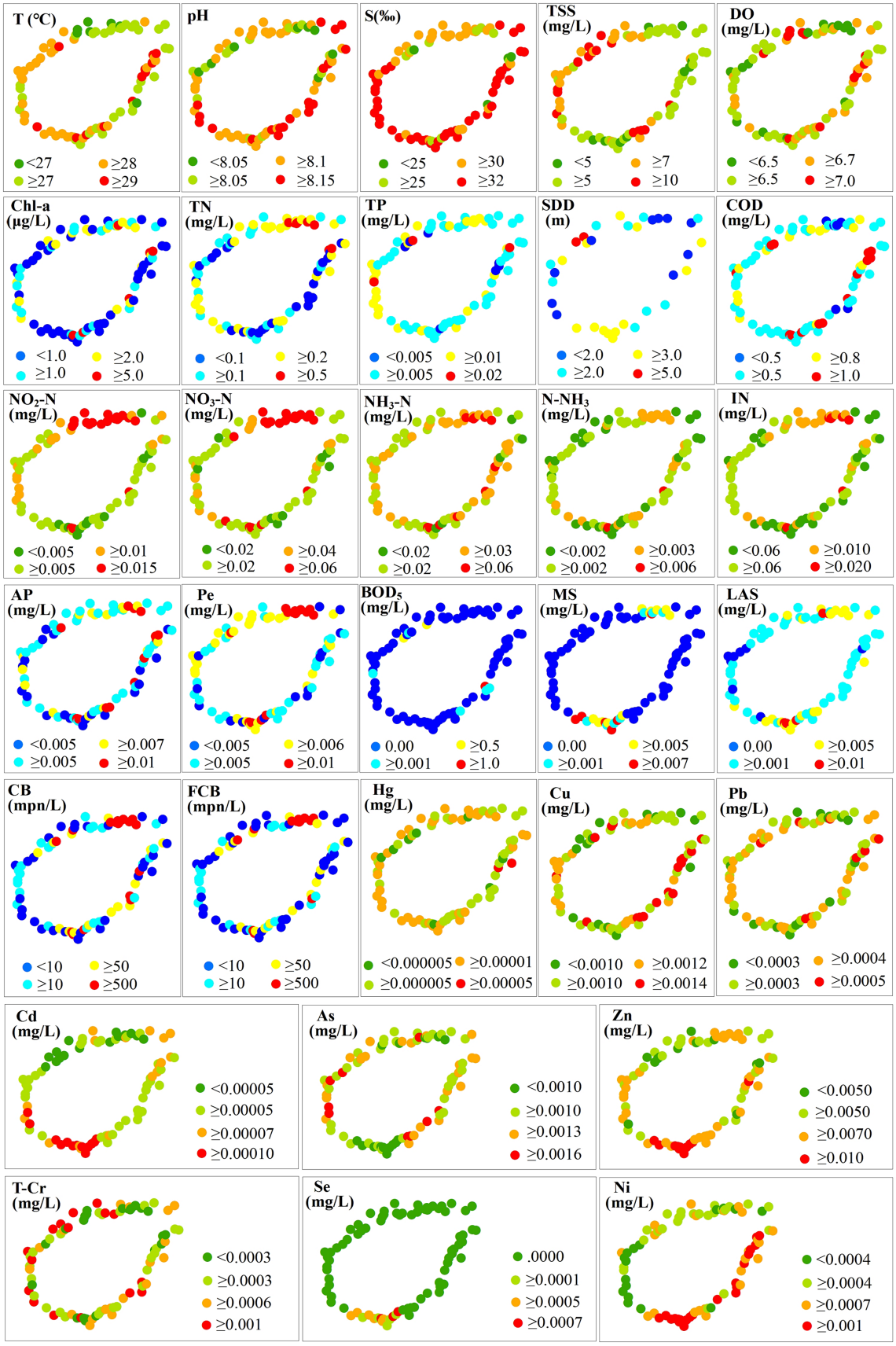

FIGURE 2
Spatial distribution of multi-annual mean of water quality parameter from 2015 to 2020.

(Supplementary Figure S2). The changing rates of DO ranged from −0.16 to 0.31 (more than half of the monitoring stations showed a downward tendency of DO), and DO increase mainly occurred in the north and east (Figure 3B; Supplementary Figure S2). The changing rates of Chl-a were between −1.65 to 0.75 and it decreased at 3/4 monitoring stations (Figures 3B,C; Supplementary Figure S2). The changing rates of TN, TP and BOD_5 were generally lower (−0.09—0.24, −0.03—0.005 and − 0.095—0.32, respectively) and decreased at most monitoring stations (Figures 3B,C; Supplementary Figure S2). The changing rates of COD were between −0.13 to 0.24 (Figures 3B,C; Supplementary Figure S2). The changing rates of other parameters were generally lower and concentrated between −0.04 and 0.04 (Figure 3C).

3.2 Spatiotemporal assessment of water quality along Hainan Island, China

3.2.1 Annual water quality assessment

Based on the annual average value of each water quality parameter collected from 2015 to 2020, the corresponding sub-index value was calculated according to the Eqs 1, 2. The sub-index value determines the size of the final water quality index value and is closely related to water quality. The weight values assigned to each parameter using Eq. 3 were listed in Supplementary Table S1.

Based on the aggregated WQI values by Eq. 5, five water quality levels were recommended to relatively assess the water quality in the study area, including very good ($90 < WQI \leq 100$), good ($80 < WQI \leq 90$), moderate ($70 < WQI \leq 80$), bad ($60 < WQI \leq 70$) and very bad ($0 < WQI \leq 60$). The principle of this classification is to reflect the difference of water quality in the study area. Our results (Figure 4) showed that none of the monitoring stations analyzed showed the level of "Very good." Of these stations analyzed, 40.91% showed as "Good," 45.45% showed as "Moderate," 11.36% showed as "Bad," 2.27% showed as "Very bad" (Figure 4A). The average value of aggregated water quality index for the study area was 77.05, so the water quality of the study area generally showed as a moderate level (Figure 4A). Figure 4B showed the spatial distribution of water quality at each level. The average water quality status at one monitoring station in coastal water of Wanning and one in coastal water of Sanya showed "Very bad" levels. The monitoring stations with "bad" water quality level were mainly located in the coastal water of Haikou and Sanya. Monitoring stations with Moderate water quality were located in coastal waters except the Changjiang. Some coastal waters in the west and east area showed "Good" water quality.

3.2.2 Seasonal water quality assessment

Similarly, the corresponding sub-index value was calculated according to the Eqs 1, 2 based on the average value of each parameter at the monitoring station in each month from 2015 to 2020. The aggregated WQI values by Eq. 5 was still classified as the five water quality levels recommended above. The results showed that none of the monitoring stations and none of the month (March to November)' WQI value was at the level of "Very good"; in any given month, the WQI value at the monitoring stations analyzed was mostly at the levels of "moderate" and "good" (the proportion of monitoring stations at "Moderate" level was greater than that at "Good" level in March and October, it was the

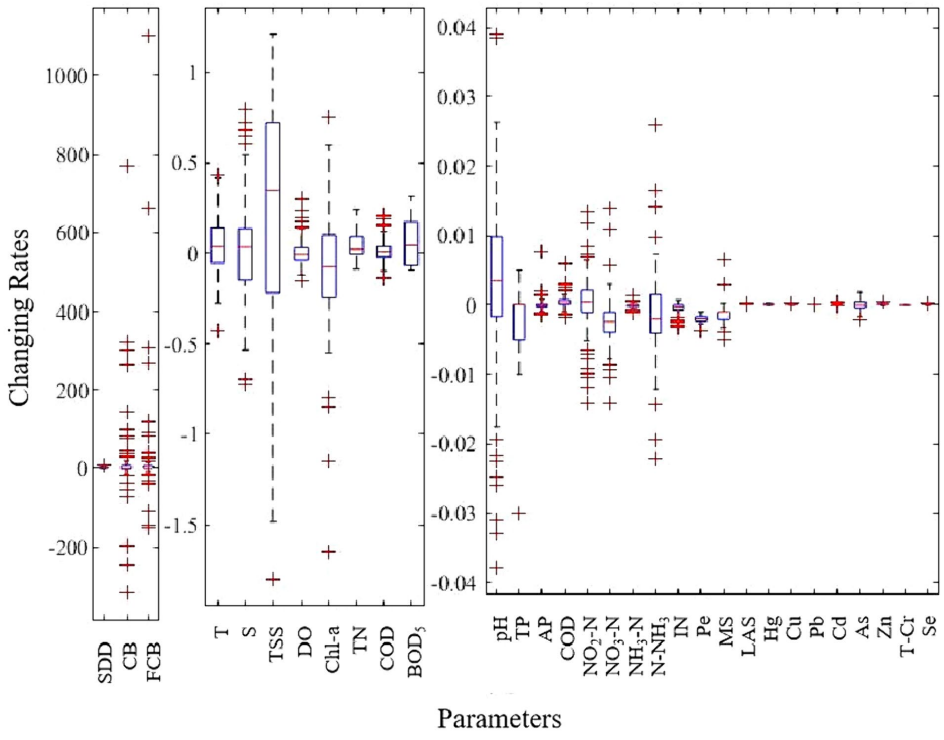

FIGURE 3
Box-plot for the changing rate of each water quality parameter at monitoring stations. Note: the units of y-axis vary depending on the parameter, "m*yr.$^{-1}$" for SDD, "mpn/L*yr.$^{-1}$" for CB and FCB, "°C*yr.$^{-1}$" for T, "μg/L*yr.$^{-1}$" for Chl-a, "yr^{-1}" for pH and "mg/L*yr.$^{-1}$" for all other parameters.

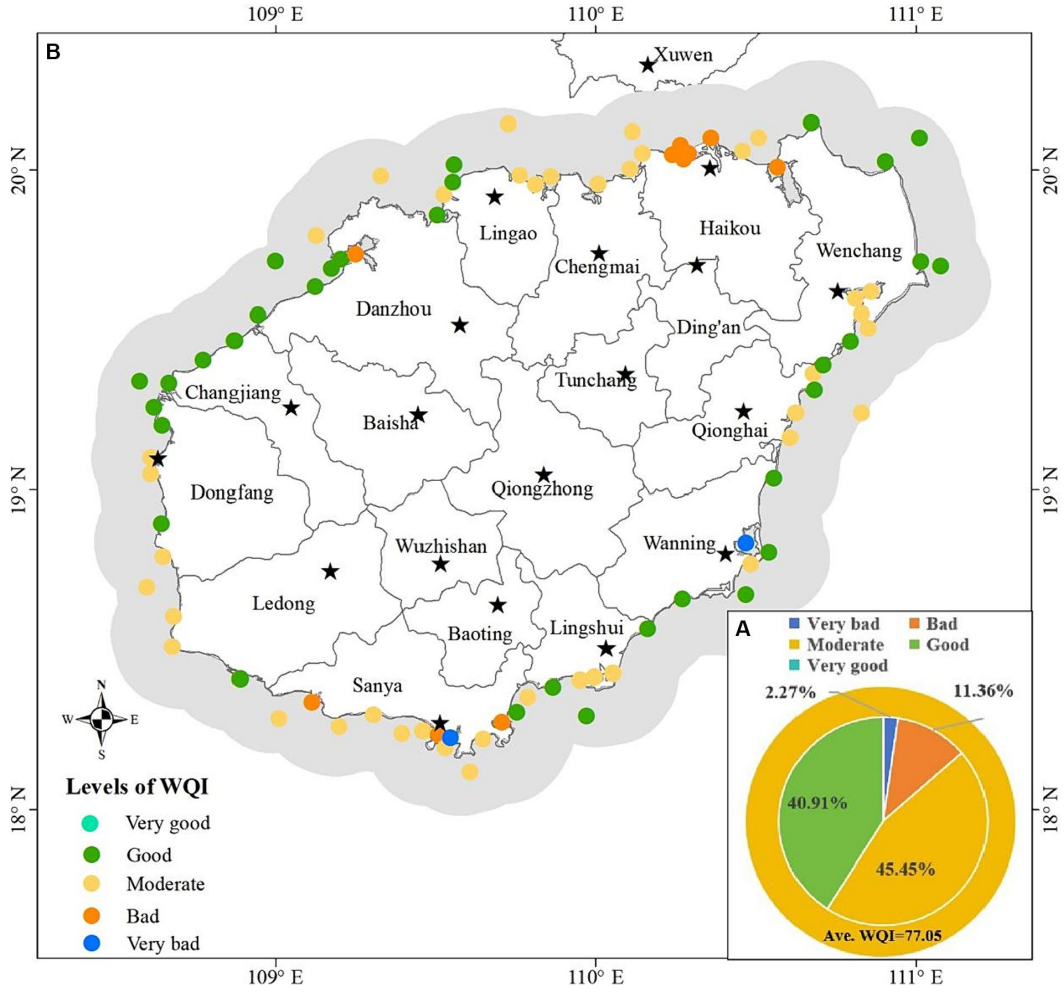

FIGURE 4
Water quality assessment based on the optimized WQI model, **(A)** average water quality and percentage at each level, **(B)** spatial variation of water quality.

opposite in April, May, July, August and September, it was equal in November); the WQI values of a very small number of monitoring stations were at the levels of "Very bad" and "Bad" in April, May, August, October and November (Figure 5). Figure 6 showed the spatial distribution of water quality assessment at each monitoring station for each month. Overall, the averaged water quality of all monitoring stations fluctuated at "Good" level from April to September, and decreased significantly to "Moderate" level in October (Figures 6B–G). From the monitoring stations analyzed, water quality at "Very bad" level occurred in May (Figure 6C), August (Figure 6E) and October (Figure 6G). Water quality at "Bad" level occurred in April (Figure 6B), August (Figure 6E), October (Figure 6G) and November (Figure 6H).

3.3 Assessment of influencing factors for water quality

3.3.1 Correlations between water quality parameters

In addition to the parameters (Cr, (CN)2, VP, $C_6H_6Cl_6$, $C_{14}H_9C_{l5}$, $C_{10}H_{19}O_6PS_2$, C_8HNO_5PS, $C_{20}H_{12}$) that were not found in the 344 samples, the spearman correlation analysis significance test was performed between the simultaneous measurements of other parameters (Figure 7). A total of 259 pairs of parameters were positively correlated, while 206 pairs were negatively correlated. The significance test showed that the significance level (p) of 216 pairs of parameters was less than 0.05, that of 163 pairs was less than 0.01 and that of 117 pairs was less than 0.001. The correlation between the trace element parameters and non-trace element parameters was not universally significant. This indicates that there is no significant interaction between the two types of elements. There were significant correlations between some trace elements parameters (such as between Se, Cd, Ni, Zn). Chemical and processing enterprises are the main external sources of trace element pollution in the Hainan Island region. These trace elements may be abundant in the same material used in industry, resulting in a positive correlation between these elements. There were generally significant positive correlations between Chl-a and nutrient (NO_2-N, NO_3-N, NH_3-N, N-NH_3, IN, AP, TP, TN). This is because nutrients are the main cause of water eutrophication and cyanobacteria reproduction. Phytoplankton containing chl-a can grow rapidly when nutrients are sufficient. These nutrients also had significant positive correlation with each other. In

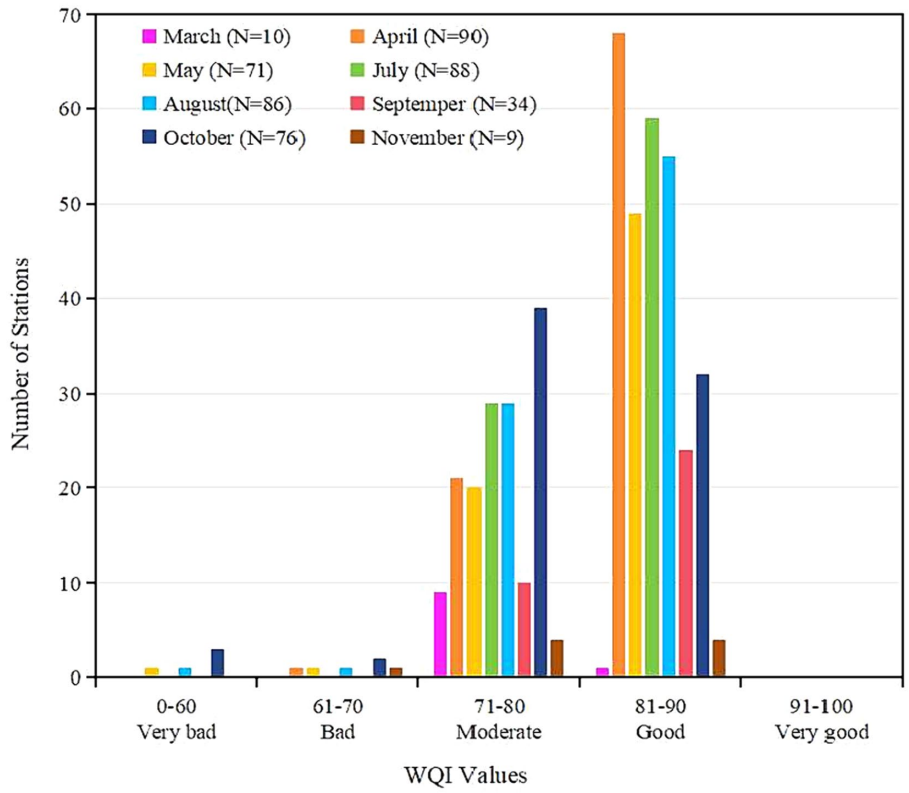

FIGURE 5
Histogram of results of seasonal water quality assessment based on the optimized WQI model. N is the number of monitoring stations analyzed.

general, there are internal and external two sources of nutrients in water. These nutrients can be converted into each other under the action of microorganisms. For example, sufficient NH3-N promotes the enrichment of NO_3-N through digestion, and then increases the content of NO_2-N through oxidation. On the other hand, sufficient NO_2-N is reduced to NH_3-N by denitrification under certain conditions, and the content of NH_3-N is increased. It has been shown that organic matter in water has a strong stimulating effect on the formation of sulfide and organic matter in water is closely related to nutrients. Nutrients in water can promote the growth and reproduction of CB and FCB. Therefore, there was significant positive correlation between nutrients and Pe, MS, LAS, CB and FCB. In addition, these nutrients had significant negative correlation with S and pH. This may be due to the fact that a certain S and pH in the water can promote the absorption of nutrients by phytoplankton. The pH and S can kill CB and FCB, so there was a significant negative correlation between them.

3.3.2 Analysis of the influencing factors for water quality

In order to further objectively reflect the internal relationship between the variables and find the pollution sources of water environment, factor analysis was further carried out based on the water quality parameters. The KMO value was 0.701. In addition, the *p*-value of Bartlett's test of sphericity was 0.00, which was less than 0.05. Therefore, our data was suitable for factor analysis. Based on the initial eigenvalue (greater than 1) obtained by principal component analysis and the eigenroot gravel map (mutation point), four factors were extracted (Supplementary Table S1), which together explained 89.65% of the total variance of the water environment indexes. According to the load values of water quality parameters on the factors, factor 1, factor 2, and factor 3 were interpreted as urban factor, breeding and planting factor, and industrial factor, respectively. Factor 4 may be derived from meteorological conditions, recreational activities, etc., so it was interpreted as other factors (Supplementary Table S1). Spatial distribution of the extracted factors (Figure 8) indicated that there was variability in the influencing factors of water environment in the study area. Spatial distribution of the urban factor (Figure 8A) showed that high and intermediate values occurred in the northern region, which is close to the provincial capital (Haikou). High values of the breeding and planting factor (Figure 8B) were detected in the regions, which is close to Wenchang, Wanning, Lingshui, Sanya and Danzhou. Intermediate values were also found in other regions. According to the spatial distribution of industrial factor (Figure 8C), high values occurred in the southern region, low and intermediate values occurred in the northern region. Intermediate to high values for the other factors were widespread at most stations.

According to the characteristics of extracted factor scores, monitoring stations were classified into five types of water environment zones through clustering of monitoring stations (Figure 9A), indicating that the water environment in the study area had significant spatial heterogeneity. The nearshore sea near the northern Haikou showed type 4 (Figure 9A), which was mainly affected by urban factors and is weakly affected by industrial factors (Figure 9B). The nearshore sea along Sanya in the south showed the

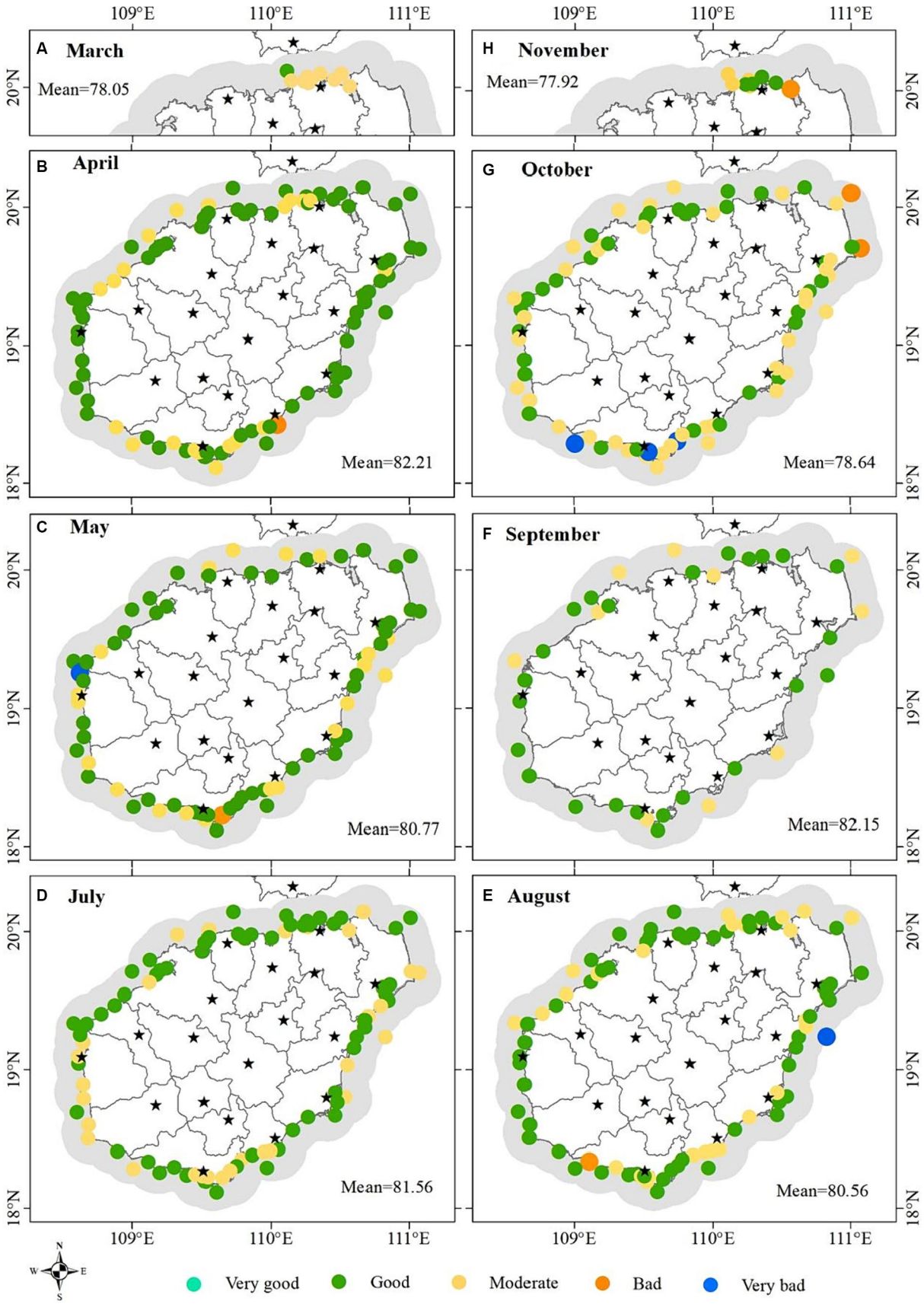

FIGURE 6
(A–H) Spatial distribution of water quality assessment at the analyzed monitoring stations in March, April, May, July, August, September, October, and November, respectively.

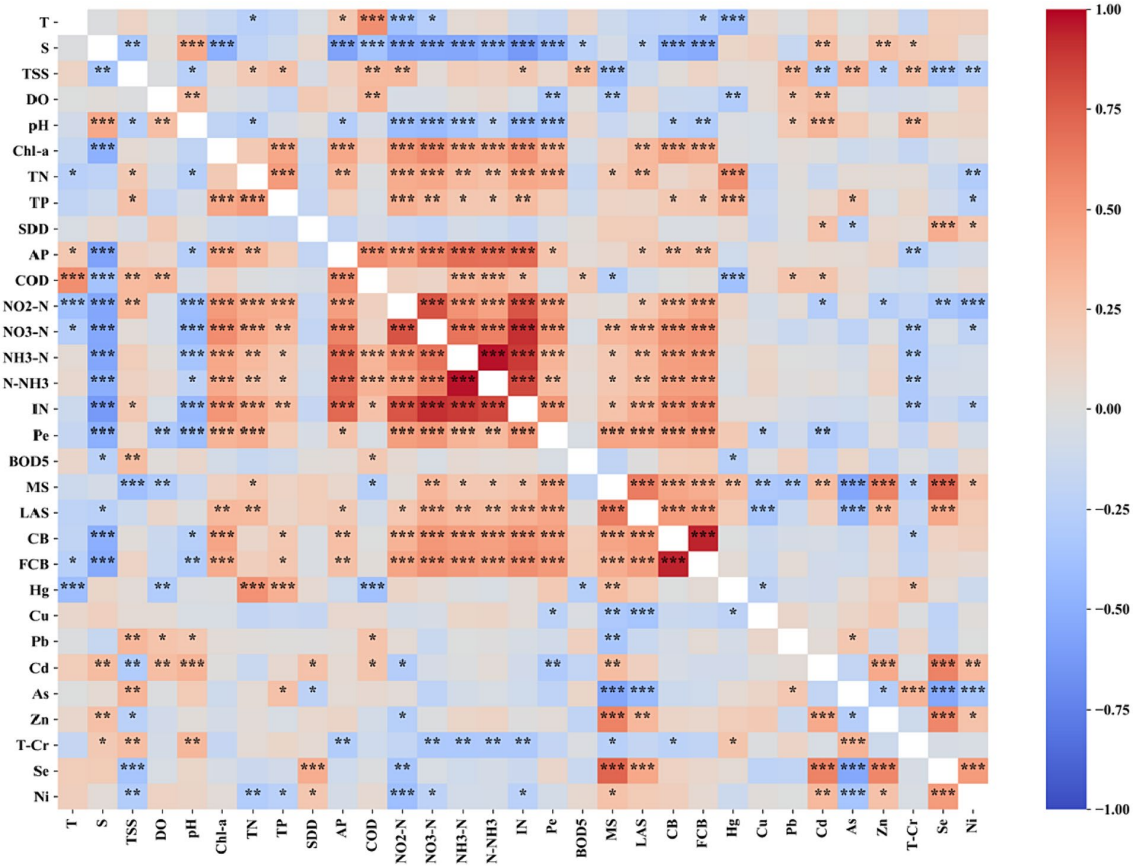

FIGURE 7
Correlation coefficient (r) and significance level (p) between water quality parameters. Note: The white blocks in the matrix represent missing r values due to no synchronized measurements; "***" is the significance level $p < 0.001$, "**" is the significance level $0.001 \leq p < 0.01$ and "*" is the significance level $0.01 \leq p < 0.05$.

type 3 water environment zone (Figure 9A), which was mainly affected by industrial factors (Figure 9B). In the west, the nearshore sea along Wenchang southeast and Qionghai mainly displayed as type 5 (Figure 9A), and this type of water environment zone was mainly affected by breeding and planting factor (Figure 9B). The nearshore sea along Wenchang northeast and WanNing displayed as type 2 (Figure 9A), which was mainly affected by other factors (Figure 9B). Danzhou, Dongfang and Ledong in the east mainly showed as type 2 water environment zone (Figure 9A). Lingshui in the southeast, Chengmai and Lingao in the north, and Changjiang in the west showed two types of water environment zones (type 2 and type 5). Water environment zone type 1 was located at the estuary of Wanning (Figure 9A), which was mainly influenced by breeding and planting factor, and was influenced by other factors weakly (Figure 9B).

Environmental factors were further quantified based on the factor analysis. The WEQI values were calculated by taking the factors extracted from factor analysis as input parameters of the optimized WQI model (all factors were considered to have negative effects on water environmental quality). The weights of each factor were shown in Supplementary Table S1. The aggregated WEQI values were shown in Figure 10. The low WEQI value indicated that the water was under great pressure from environmental factors. It could be seen that 10.23% of the monitoring stations were under the level of "Severe pressure" from environmental factors, 18.18, 54.55 and 17.05% were at the pressure level of "Extreme pressure," "Significant pressure" and "Slight pressure," respectively (Figure 10A). Those monitoring stations at the level of "Severe pressure" were located in the coastal water of Haikou, Sanya and Wanning, and those at the level of "Extreme pressure" were in the coastal waters of Haikou, Sanya and Danzhou (Figure 10B). Some coastal waters in Wenchang, Qionghai, Danzhou and Changjiang were just under "Slight pressure" level from environmental factors (Figure 10B).

4 Discussion

4.1 The reliability of the optimized WQI model

Each of the four main processes involved in a WQI model can contribute to the model uncertainty (Gupta and Gupta, 2021; Uddin et al., 2023a,b,c). In this research, the correlation analysis between water quality parameters showed that there were significant correlations among some parameters (Figure 7). Nevertheless, the 31 available water quality parameters in our study contained different properties, including physical, chemical, biological and trace elements. This avoided the influence of insufficient selection of typical parameters on the reliability of WQI assessment results. Some

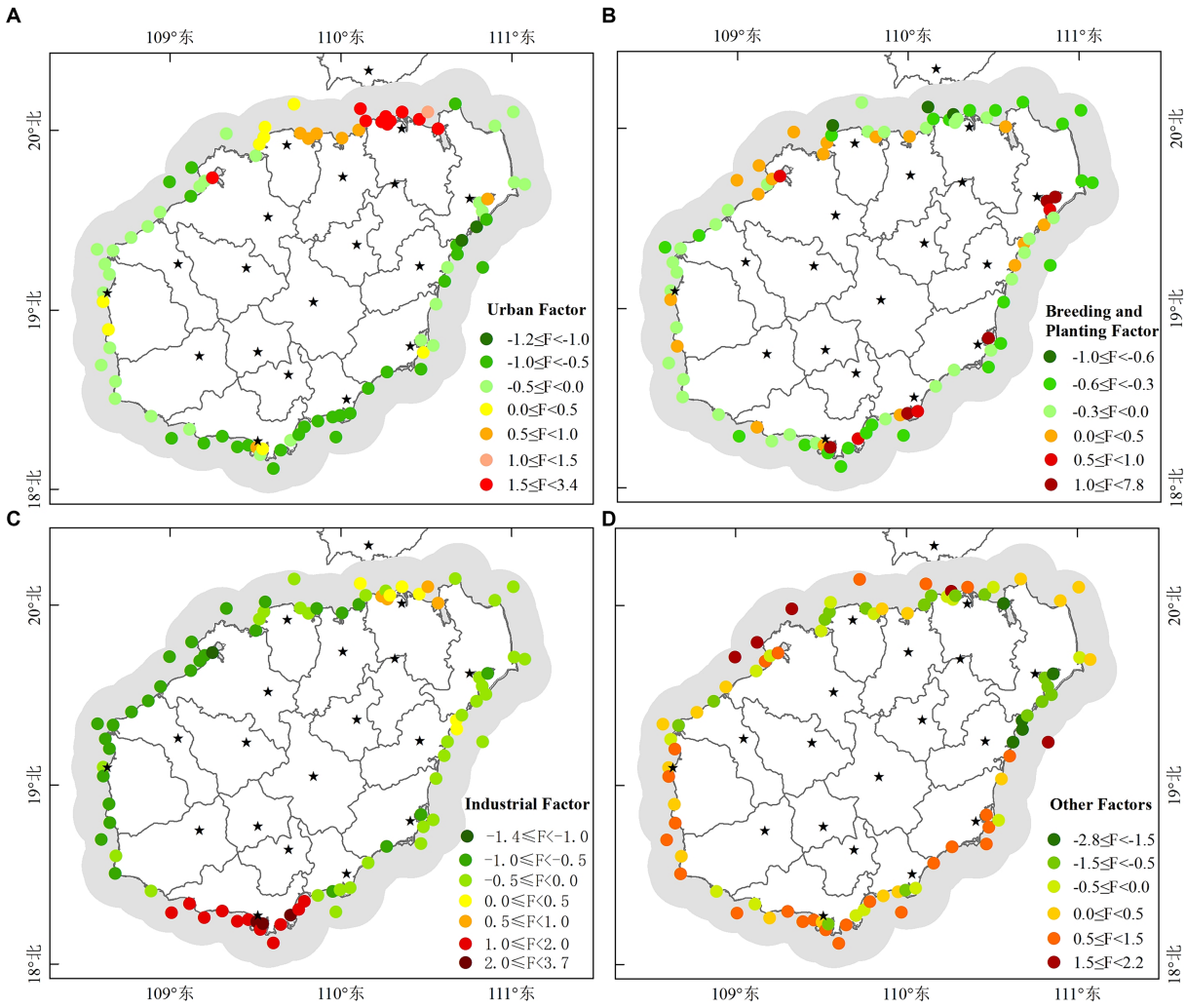

FIGURE 8
Spatial distribution of the factors extracted by factor analysis: **(A)** Urban factor (factor 1), **(B)** breeding and planting factor (factor 2), **(C)** industrial factor (factor 3) and **(D)** other factors (factor 4). The "F" in the legend represents the factor.

parameters such as T, DO, pH should be treated differently when obtaining sub-index due to their influence on water quality is bidirectional (Le et al., 2023). In this research, the bidirectional effects of parameters on water quality were considered through using Eqs 1, 2 in the process of developing the sub-indexes, respectively. Supplementary Figure S3 showed the recommended critical values for each parameter in this research and a simplified depiction of their effects on water quality. It should be noted that the critical value should be determined according to local climatic conditions and geographical environment in practical application. A weighting strategy for parameters based on sub-index was adopted in this research (Eq. 3). Weights of the parameters depends on the values of the sub-index, which could avoid the influence of subjective factors on the reliability of the WQI model. On the premise that water quality parameters are equally important, the WQI model using this weighting strategy is objective and reliable for the evaluation of any specific data set.

Most developed WQI models were region-specific because their components were developed based on expert advice and local guidelines (Gupta et al., 2017). The components of our optimized WQI model were not developed based on expert opinions and local guidelines, and the results from this model are not comparable to those from other WQI models. The approach of optimizing WQI components in this research is applicable to other water quality assessment including lakes and rivers. The assessments obtained by the optimized WQI model can fully reflect the difference of water quality between different regions, so it can provide an effective reference for water environment governance decision makers.

4.2 Environment factors affecting water quality

By performing factor analysis on water quality parameters, representative environmental factors can be determined, which solves the problem that water environmental factors are complex and difficult to quantify (Flo et al., 2011; Le et al., 2023). This research was the first attempt to relate the variability of water quality to

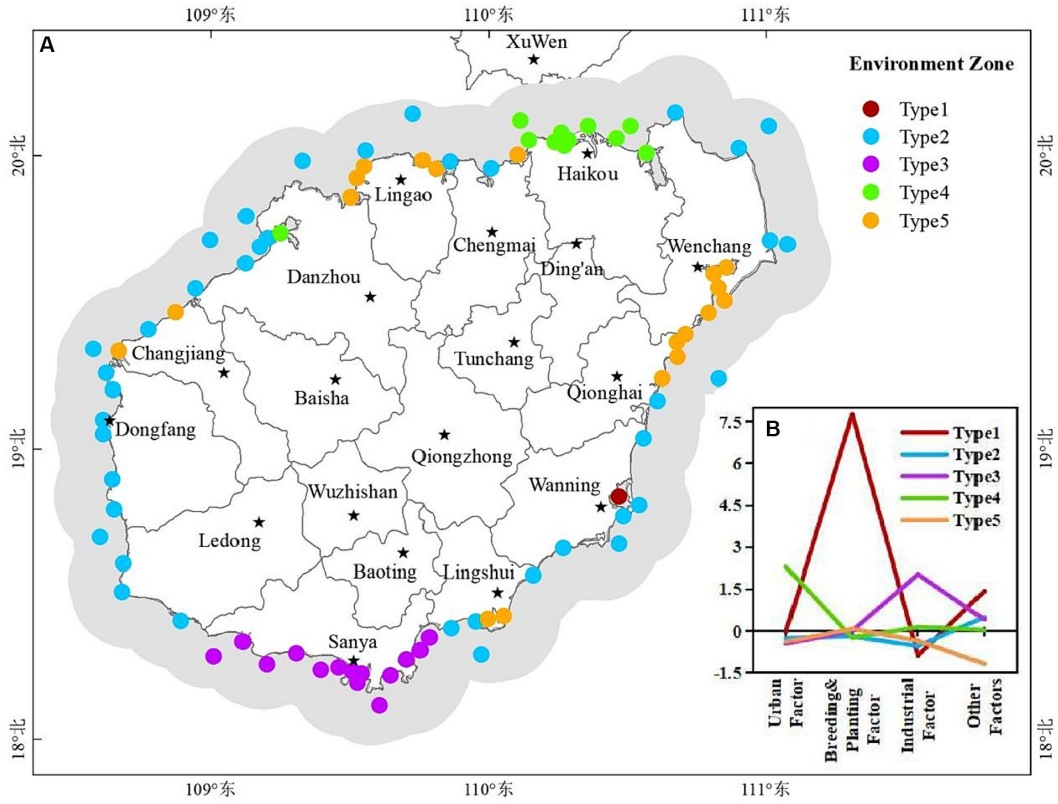

FIGURE 9
(A) Major environment zones for water generated by clustering based on extracted factor features. **(B)** Characteristics of pollution sources for environment zones.

specific factors. We found that there were four major pollution sources which potentially contribute to deteriorating the quality parameters in the study area (Supplementary Table S1; Figure 8). The loading values of factors (Supplementary Table S1) showed that factor 1 was defined by NO_3-N, IN, Pe, NO_2-N, CB, TN, FCB, TP and pH. Domestic sewage from cities entering coastal waters can cause these parameters to increase (Flo et al., 2011; Xiao et al., 2020). The urban pollution source was also strongly supported by results in Figure 2, which showed that the value of these parameters (except the pH) was greater in the coastal waters near city (Haikou). Factor 2 had a higher loading value with AP, N-NH_3, Chl-a, COD, S, BOD_5, NH_3-N and T. They could be affected by runoff carrying agricultural pollutants to coastal waters or by aquaculture effluent discharges carrying pollutants to coastal waters (Le et al., 2023). It was also supported by the characteristics of human activity in the affected areas dominated by factor 2 (Figure 9) that these parameters could be connected to the activities of planting and breeding activities. Factor 3 was defined by Se, MS, Zn, LAS, Cd, As, Ni and TSS. Industrial wastewater discharge and the operation of boats on the water often causes such pollutants in the surface water. The dominant influence area of factor 3 was the coastal waters of Sanya, where industrial facilities are distributed. Therefore, this factor was interpreted as an industrial factor. Factor 4 was defined by T-Cr, Cu, DO and Hg. Specific pollution sources for these parameters were still unclear and may need more research. SDD and Pb were not expressed by any factors. Other potential environmental factors also need to be studied further.

As confirmed in this research, coastal waters are not homogeneous but can be divided into different environment zones based on dominant factors (Figures 9A,B). Urban factors and industrial factors were demonstrated to be the main causes of pollution in coastal water of Haikou and Danzhou (type 4 in Figure 9A), in coastal water of Sanya (type 3 in Figure 9A), respectively. Planting and breeding were demonstrated to be the primary cause of pollution in coastal water of Wanning, Wenchang, Qionghai, Linggao, and Changjiang (type 1 and type 5 in Figure 9A). Therefore, in the practice of environmental management and water pollution treatment, it is necessary to take countermeasures according to the dominant influencing factors in different regions.

4.3 Suggestions for improving water quality

The classified WQI levels could reflect the relative differences of water quality between monitoring stations, which can be the basis for guiding water quality management decisions. This classification method is uncertain because there is no fixed standard. The level threshold needs to be determined based on all the values. Unreasonable classification is not conducive to identifying problematic waters and is not conducive to improving water quality effectively. However, this classification is sufficient to reflect relative differences of water quality between stations and has important significance to guide decisions of water quality management. Water quality near two monitoring stations located in Sanya and Wanning was at "Very bad"

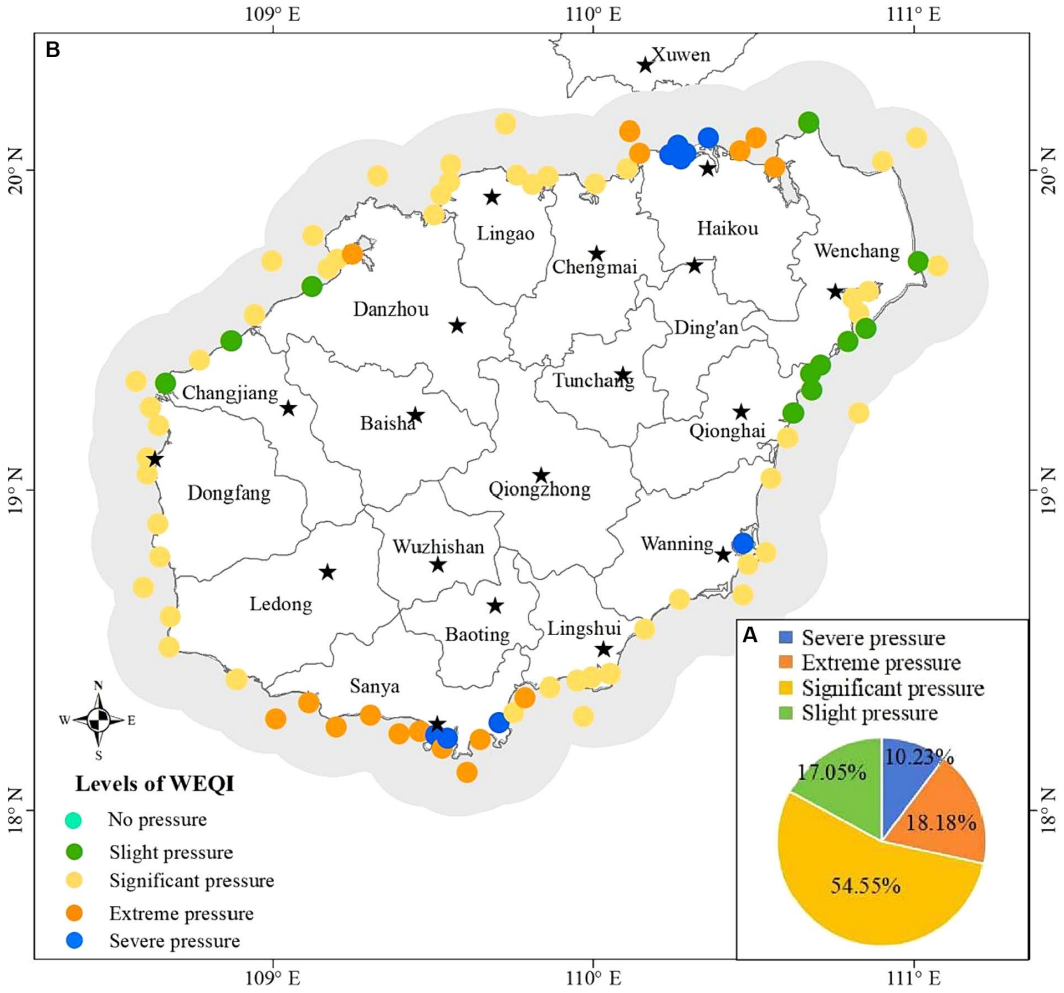

FIGURE 10
Water environmental factors assessment based on extracted factors, **(A)** Percentage of monitoring stations at each pressure level, **(B)** distribution of the pressure levels.

level (Figure 4), so it urgently needs to be improved. These two regions have higher pH, Chl-a, AP, COD, NO_3-N, IN, NO_2-N, CB, FCB, N-NH_3, NH_3-N, T and Ni according to the distribution of water quality parameters (Figure 2). Therefore, improving water quality should focus on the pollution sources of these parameters. The characteristics of environmental areas and pollution sources generated by clustering in this study (Figures 9A,B) can effectively guide the implementation of water quality management measures. According to the Figure 9, the aquaculture factor near the monitoring station in Wanning should be emphasized, that is, we can improve the water quality through reasonable management of the aquaculture industry. And it is recommended to strengthen regulation and control on industrial factors near the monitoring station in Sanya should be strengthened. Similarly, those regions where the water quality at "Bad" level (Figure 4) also need to be improved. According to the distribution of these monitoring stations and their main pollution sources in Figures 4B, 9, measures should be taken in the urban factors for the waters of those monitoring stations along Haikou and Danzhou, while the regulation on industrial factors should be strengthened for those monitoring stations along Sanya. Although the water quality of most stations analyzed in the study area was at "Good" level and "Moderate" level (Figure 4), improvements were still recommended for the parameter that were significantly high (Figure 2). From the seasonal variation of water quality, it could be seen that the water quality of some monitoring stations would be degraded in certain months (Figure 6). For example, the water quality of some monitoring stations along Sanya might deteriorate in October. Therefore, we need to take improvement measures in October for those monitoring stations.

The WEQI value (Figure 10) obtained in this research can showed the pressure status that water is suffer from environmental factors, revealing the risk of water quality deterioration. The statistics of WQI and WEQI (Table 2) showed that waters at 13.64 and 27.27% of the monitoring stations with "Good" level had slight and significant risk of deterioration, respectively; waters at 3.41, 27.27 and 14.77% of the monitoring stations with "Moderate" level showed slight, significant and extreme risk of deterioration, respectively; waters at 3.41 and 7.95% of the monitoring stations with "Bad" level showed extreme and severe risk of deterioration, respectively; waters at 2.27% of the monitoring stations with "Very bad" level showed severe risk of deterioration. Even water at the same WQI level may have different risks of deterioration due to different pressures from environmental factors. Therefore,

TABLE 2 Comparison between the results of water quality assessment and water environmental factors assessment.

WEQI	WQI					Total
	Very good	Good	Moderate	Bad	Very bad	
No pressure	0	0	0	0	0	0
Slight pressure	0	13.64%	3.41%	0	0	17.05%
Significant pressure	0	27.27%	27.27%	0	0	54.55%
Extreme pressure	0	0	14.77%	3.41%	0	18.18%
Severe pressure	0	0	0	7.95%	2.27%	10.23%
Total	0	40.91%	45.45%	11.26%	2.27%	100%

we recommend that in practice, we should not only pay attention to those waters with poor water quality (the lower WQI levels in Figures 4, 6) but also pay attention to those waters with greater risk of deterioration (the Significant, extrem and severe pressure levels in Figure 10).

4.4 Potential hazards from water pollution

Coastal waters are important places for aquatic organisms to reproduce and multiply. Pollutants can cause serious disasters to the ecology and biodiversity of coastal waters, and also endanger human health (Zoppini et al., 2019; Chi et al., 2021). It has been reported that a decrease in DO concentration will result in a decrease in the number of aerobic bacteria (Zhao et al., 2014). DO at several stations in this research was found to be less than 6.5 mg/L (Figure 2), which is not conducive to the growth of aerobic bacteria. Liu et al. (2024) showed that chl-a, pH and phosphate-P in summer, and electric conductivity, nitrate-N and ammonium-N in winter affected the bacterial community variation. And they argued that high nitrate and ammonia nitrogen can promote nitrification and increase the abundance and diversity of bacteria. Significant nutrient pollutions were found at some stations in our research, such as high NO_2-N (≥0.015 mg/L), NO_3-N (≥0.06 mg/L), NH_3-N (≥0.06 mg/L), N-NH_3 (≥0.006 mg/L), IN (≥0.02 mg/L), TP (≥0.02 mg/L) and TN (≥0.5 mg/L) concentrations (Figure 2). These stations are therefore beneficial for nitrogen-oxidizing bacteria and these microorganisms may greatly increase to affect the balance of community structure. High nitrogen and phosphorus nutrients also can lead to eutrophication of water, resulting in cyanobacteria bloom (Bužančić et al., 2016). Several trace elements were detected in our research and several stations have relatively high levels of trace element, such as Cu (≥0.0014 mg/L), Pb (≥0.0005 mg/L), Cd (≥0.0001 mg/L), Zn (≥0.01 mg/L), As (≥0.0016 mg/L), Ni (≥0.001 mg/L), T-Cr (≥0.001 mg/L) (Figure 2). Trace elements like Fe, Cu, Zn, Ni and others are important for the proper functioning of biological systems and their deficiency or excess are detrimental for aquatic microorganisms (Aithani et al., 2023). Trace element in water is thought to be difficult to degrade, bioaccumulative and ecologically toxic (Wu et al., 2016; Saha and Paul, 2019). Aquatic trace element could be absorbed in large quantities by microorganisms and affect terrestrial organisms or humans through biological enrichment, food chain amplification and other pathways (Oropesa et al., 2017). High toxic trace elements in the water may poison some microbes and those heavy metal-resistant (e.g., Acidobacteriota) may increase (Zhang et al., 2024). *Escherichia coli* (CB) and fecal *Escherichia coli* (FCB) in our study are used as microbial indicators of water quality in water quality assessment. CB and FCB in water can seriously harm human health through the food chain (Reynolds et al., 2008; Hu, 2024). Several stations in this research had CB and FCB levels in excess of 500mpn/L, posing a potential risk of outbreak. Outbreaks of these community may result in serious consequences, such as diarrheal disease, which can even lead to death (Reynolds et al., 2008). However, there is still a lack of in-depth research on the relationship between pollution and microbial community and human health, which will be a meaningful content for future research directions.

5 Conclusion

Based on a datasets of 31 water quality parameters collected from 2015 to 2020, an optimized WQI model was developed to assess spatial and temporal water quality. Pollution sources of water quality were also identified by factor analysis and its deterioration risk was further assessed using the index WEQI. The following conclusions can be made:

(1) The uncertainty of water quality assessment can be weakened by the optimization of WQI model process. The approach of optimizing WQI model in our research is applicable to water quality assessment of other regions (including lakes and rivers) or other datasets.
(2) The average water quality was at moderate level. The water quality of this region showed temporal and spatial variability. Water quality at 13.53% of the monitoring stations was relatively poor ("Bad" level or"Very bad" level) and they were mainly appeared in the coastal waters of large cities (Haikou and Sanya) and in some aquaculture waters. Average water quality in March, October and November was worse than in other months.
(3) Water quality of this region was affected by at least four main pollution sources including urban factor, planting and breeding factor, industrial factor and other factors. These factors play a different dominant role in different regions, respectively. Waters at 10.23% of monitoring stations were at the greatest risk of deterioration due to severe pressure from these environmental factors.

Data availability statement

The original contributions presented in the study are included in the article/Supplementary material, further inquiries can be directed to the corresponding author.

Author contributions

YD: Conceptualization, Data curation, Funding acquisition, Methodology, Software, Supervision, Writing – original draft. ZR: Conceptualization, Methodology, Supervision, Validation, Writing – review & editing. YZ: Writing – review & editing, Investigation, Formal analysis. JZ: Writing – review & editing, Formal analysis, Data curation. QS: Formal analysis, Investigation, Validation, Writing – review & editing.

Funding

The author(s) declare that financial support was received for the research, authorship, and/or publication of this article. This work was supported by Hainan Provincial Natural Science Foundation of China (grant number 422QN306, 724MS059, and 423QN233), the National Natural Science Foundation of China (grant number 42261054). Youth Innovation Promotion Association of the Chinese Academy of Sciences (grant number 2020237).

Acknowledgments

We sincerely thank reviewers for their constructive comments and suggestions.

Conflict of interest

The authors declare that the research was conducted in the absence of any commercial or financial relationships that could be construed as a potential conflict of interest.

Publisher's note

Supplementary material

The Supplementary material for this article can be found online at: https://www.frontiersin.org/articles/10.3389/fmicb.2024.1383882/full#supplementary-material

References

Abbasi, T., and Abbasi, S. A. (2012). Water-quality indices: looking back, looking ahead. *Water Quality Indices*. 353–356. doi: 10.1016/B978-0-444-54304-2.00016-6

Aithani, D., Jyethi, D. S., Yadav, A. K., Siddiqui, Z., and Khillare, P. S. (2023). Source apportionment and risk assessment of trace element pollution in Yamuna river water in Delhi: a probability based approach. *Urban Water J.* 20, 1635–1646. doi: 10.1080/1573062X.2022.2086885

Bužančić, M., Gladan, Z. N., Marasović, I., Kušpilić, G., and Grbec, B. (2016). Eutrophication influence on phytoplankton community composition in three bays on the eastern Adriatic coast. *Oceanologia* 58, 302–316. doi: 10.1016/j.oceano.2016.05.003

Chen, L., Liu, J., Xu, G., and Li, F. (2019). Phytoplankton productivity and community structure variations over the last 160 years in the East China Sea coast in response to natural and human–induced environmental changes. *The Holocene* 29, 1145–1154. doi: 10.1177/0959683619838040

Cheng, K. H., Chan, S. N., and Lee, J. H. W. (2020). Remote sensing of coastal algal blooms using unmanned aerial vehicles. *Mar. Pollut. Bull.* 152:110889. doi: 10.1016/j.marpolbul.2020.110889

Chi, Z., Zhu, Y., Li, H., Wu, H., and Yan, B. (2021). Unraveling bacterial community structure and function and their links with natural salinity gradient in the Yellow River Delta. *Sci. Total Environ.* 773:145673. doi: 10.1016/j.scitotenv.2021.145673

Flo, E., Garcés, E., Manzanera, M., and Camp, J. (2011). Coastal inshore waters in the NW Mediterranean: physicochemical and biological characterization and management implications - ScienceDirect. *Estuar. Coast. Shelf Sci.* 93, 279–289. doi: 10.1016/j.ecss.2011.04.002

Gai, Y., Yu, D., Zhou, Y., Yang, L., Chen, C., and Chen, J. (2022). An improved model for chlorophyll-a concentration retrieval in coastal waters based on UAV-borne hyperspectral imagery: a case study in Qingdao, China. *Water* 12:2769. doi: 10.3390/w12102769

Gunnerson, C. G., and French, J. A., (1996). *Wastewater Management for Coastal Cities*. Springer, Germany, p. 345.

Gupta, S., and Gupta, S. K. (2021). A critical review on water quality index tool: genesis, evolution and future directions. *Ecol. Inform.* 63:101299. doi: 10.1016/j.ecoinf.2021.101299

Gupta, N., Pandey, P., and Hussain, J. (2017). Effect of physicochemical and biological parameters on the quality of river water of Narmada, Madhya Pradesh, India. *Water Sci.* 31, 11–23. doi: 10.1016/j.wsj.2017.03.002

Horton, R. K. (1965). An index-number system for rating water quality. *J. Water Pollut. Control Fed.* 37, 300–306.

Hou, W., Sun, S., Wang, M., Li, X., Zhang, N., Xin, X., et al. (2016). Assessing water quality of five typical reservoirs in lower reaches of Yellow River, China: using a water quality index method. *Ecol. Indic.* 61, 309–316. doi: 10.1016/j.ecolind.2015.09.030

Howard, M. D. A., Kudela, R. M., and Mclaughlin, K. (2016). New insights into impacts of anthropogenic nutrients on urban ecosystem processes on the southern California coastal shelf: introduction and synthesis. *Estuar. Coast. Shelf Sci.* 186, 163–170. doi: 10.1016/j.ecss.2016.06.028

Hu, H. (2024). *Experimental study on the distribution and migration of Escherichia coli in multiple media*. Jiaozuo, Henan province, China: Henan Polytechnic University.

Kannel, P. R., Lee, S., Lee, Y.-S., Kanel, S. R., and Khan, S. P. (2007). Application of water quality indices and dissolved oxygen as indicators for river water classification and urban impact assessment. *Environ. Monit. Assess.* 132, 93–110. doi: 10.1007/s10661-006-9505-1

Le, T. V., Nguyen, D. T. P., and Nguyen, B. T. (2023). Spatial and temporal analysis and quantification of pollution sources of the surface water quality in a coastal province in Vietnam. *Environ. Monit. Assess.* 195, 1–14. doi: 10.1007/s10661-023-11026-x

Liu, S., Lou, S., Kuang, C., Huang, W., Chen, W., Zhang, J., et al. (2011). Water quality assessment by pollution-index method in the coastal waters of Hebei Province in western Bohai Sea, China. *Mar. Pollut. Bull.* 62, 2220–2229. doi: 10.1016/j.marpolbul.2011.06.021

Liu, S., Lu, J., Adriaenssens, E. M., Wang, J., McCarthy, A. J., and Sekar, R. (2024). Industrial and agricultural land uses affected the water quality and shaped the bacterial communities in the inflow rivers of Taihu Lake. *Front. Environ. Sci.* 12:1340875. doi: 10.3389/fenvs.2024.1340875

Lukhabi, D. K., Mensah, P. K., Asare, N. K., Pulumuka-Kamanga, T., and Ouma, K. O. (2023). Adapted water quality indices: limitations and potential forWater quality monitoring in Africa. *Water* 15:1736. doi: 10.3390/w15091736

Lv, Y. L., Yuan, J. J., Li, Q. F., Zhang, Y. Q., Lv, X. T., and Su, C. (2016). Impacts of land–based human activities on coastal and offshore marine ecosystems. *Acta Ecol. Sin.* 36, 1183–1191.

Ma, Z., Li, H., Ye, Z., Wen, J., Hu, Y., and Liu, Y. (2020). Application of modified water quality index (WQI) in the assessment of coastal water quality in main aquaculture areas of Dalian, China. *Mar. Pollut. Bull.* 157:111285. doi: 10.1016/j.marpolbul.2020.111285

Ma, L., Ma, W. Q., Velthof, G. L., Wang, F. H., Qin, W., Zhang, F. S., et al. (2010). Modeling nutrient flows in the food chain of China. *J. Environ. Qual.* 39, 1279–1289. doi: 10.2134/jeq2009.0403

Malone, T. C., and Newton, A. (2020). The globalization of cultural eutrophication in the coastal ocean: Causes and consequences. *Front. Mar. Sci.* 7:670. doi: 10.3389/fmars.2020.00670

Oropesa, A. L., Floro, A. M., and Palma, P. (2017). Toxic potential of the emerging contaminant nicotine to the aquatic ecosystem. *Environ. Sci. Pollut. Res.* 24, 16605–16616. doi: 10.1007/s11356-017-9084-4

Poonam, T., Tanushree, P., and Sukalyan, C. (2013). Water quality indices—important tools for water quality assessment. *Int. J. Adv. Chem.* 1, 15–18. doi: 10.5121/ijac.2015.1102

Ren, C. Y., Wang, Z. M., Zhang, Y. Z., Zhang, B., Chen, L., Xi, Y., et al. (2019). Rapid expansion of coastal aquaculture ponds in China from Landsat observations during 1984-2016. *Int. J. Appl. Earth Observ. Geoinform.* 82:101902. doi: 10.1016/j.jag.2019.101902

Reynolds, K. A., Mena, K. D., and Gerba, C. P. (2008). Risk of waterborne illness via drinking water in the United States. *Rev. Environ. Contam. Toxicol.* 192, 117–158. doi: 10.1007/978-0-387-71724-1_4

Román, A., Tovar-Sánchez, A., Gauci, A., Deidun, A., Caballero, I., Colica, E., et al. (2023). Water-quality monitoring with a UAV-mounted multispectral camera in CoastalWaters. *Remote Sens.* 15:237. doi: 10.3390/rs15010237

Saha, P., and Paul, B. (2019). Assessment of heavy metal toxicity related with human health risk in the surface water of an industrialized area by a novel technique. *Hum. Ecol. Risk. Assess.* 25, 966–987. doi: 10.1080/10807039.2018.1458595

Sarkar, C., and Abbasi, S. A. (2006). Qualidex - a new software for generating water quality indice. *Environ. Monit. Assess.* 119, 201–231. doi: 10.1007/s10661-005-9023-6

Sun, W., Xia, C., Xu, M., Guo, J., and Sun, G. (2016). Application of modified water quality indices as indicators to assess the spatial and temporal trends of water quality in the Dongjiang River. *Ecol. Indic.* 66, 306–312. doi: 10.1016/j.ecolind.2016.01.054

Sutadian, A. D., Muttil, N., Yilmaz, A. G., and Perera, B. J. C. (2018). Development of a water quality index for rivers in West Java Province, Indonesia. *Ecol. Indic.* 85, 966–982. doi: 10.1016/j.ecolind.2017.11.049

Uddin, M. G., Jackson, A., Nash, S., Rahman, A., and Olbert, A. I. (2023a). Comparison between the WFD approaches and newly developed water quality model for monitoring transitional and coastal water quality in Northern Ireland. *Sci. Total Environ.* 901:165960. doi: 10.1016/j.scitotenv.2023.165960

Uddin, M. G., Nash, S., and Olbert, A. I. (2021). A review of water quality index models and their use for assessing surface water quality. *Ecol. Indic.* 122:107218. doi: 10.1016/j.ecolind.2020.107218

Uddin, M. G., Nash, S., Rahman, A., and Olbert, A. I. (2022). A comprehensive method for improvement of water quality index (WQI) models for coastal water quality assessment. *Water Res.* 219:118532. doi: 10.1016/j.watres.2022.118532

Uddin, M. G., Nash, S., Rahman, A., and Olbert, A. I. (2023b). A novel approach for estimating and predicting uncertainty in water quality index model using machine learning approaches. *Water Res.* 229:119422. doi: 10.1016/j.watres.2022.119422

Uddin, M. G., Olbert, A. I., and Nash, S. (2020). "Assessment of water quality using water quality index (WQI) models and advanced geostatistical technique" in *Civil engineering research Association of Ireland (CERAI)* (Kieran Ruane and Vesna Jaksic Cork: Civil Engineering Research Association of Ireland (CERAI), Cork Institute of Technology), 594–599.

Uddin, M. G., Rahman, A., Nash, S., Diganta, M. T. M., Sajib, A. M., Moniruzzaman, M., et al. (2023c). Marine waters assessment using improved water quality model incorporating machine learning approaches. *J. Environ. Manag.* 344:118368. doi: 10.1016/j.jenvman.2023.118368

United Nations Environment Programme, (1992). *The world environment 1972–1992: Two decades of challenge*. Chapman & Hall, New York, NY (USA), p. 884.

Wang, H., Bouwman, A. F., Gils, J. V., Vilmin, L., Beusen, A. H. W., Wang, J. J., et al. (2023). Hindcasting harmful algal bloom risk due to land–based nutrient pollution in the eastern Chinese coastal seas. *Water Res.* 231:119669. doi: 10.1016/j.watres.2023.119669

Wang, B. D., Xie, L. P., and Sun, X. (2011). Water quality in marginal seas off China in the last two decades. *Int. J. Oceanogr.* 2011, 1–6. doi: 10.1155/2011/731828

Wells, M. L., Trainer, V. L., Smayda, T. J., Karlson, B., Trick, C. G., Kudela, R. M., et al. (2015). Harmful algal blooms and climate change: learning from the past and present to forecast the future. *Harmful Algae* 49, 68–93. doi: 10.1016/j.hal.2015.07.009

Wu, Y., Zhang, H., Liu, G., Zhang, J., Wang, J., Yu, Y., et al. (2016). Concentrations and health risk assessment of trace elements in animal-derived food in southern China. *Chemosphere* 144, 564–570. doi: 10.1016/j.chemosphere.2015.09.005

Xiao, L., Zhang, Q., Niu, C., and Wang, H. (2020). Spatiotemporal patterns in river water quality and pollution source apportionment in the arid Beichuan River basin of northwestern China using positive matrix factorization receptor modeling techniques. *Int. J. Environ. Res. Public Health* 17:5015. doi: 10.3390/ijerph17145015

Xin, M., Sun, X., Xie, L. P., and Wang, B. D. (2023). A historical overview of water quality in the coastal seas of China. *Front. Mar. Sci.* 10:1203232. doi: 10.3389/fmars.2023.1203232

Zhang, L., Bai, J., Zhai, Y., Zhang, K., Wang, Y., Tang, R., et al. (2024). Pollution levels and potential ecological risks of trace elements in relation to bacterial community in surface water of shallow lakes in northern China before and after ecological water replenishment. *J. Contam. Hydrol.* 262:104318. doi: 10.1016/j.jconhyd.2024.104318

Zhang, Y., Jing, W., Deng, Y., Zhou, W., Yang, J., Li, Y., et al. (2023). Water quality parameters retrieval of coastal mariculture ponds based on UAV multispectral remote sensing. *Front. Environ. Sci.* 11:1079397. doi: 10.3389/fenvs.2023.1079397

Zhang, W., Zhang, D., Han, S., Zhang, C., and Shan, B. (2022). Evidence of improvements in thewater quality of coastal areas around China. *Sci. Total Environ.* 832:155147. doi: 10.1016/j.scitotenv.2022.155147

Zhao, J., Zhao, X., Chao, L., Zhang, W., You, T., and Zhang, J. (2014). Diversity change of microbial communities responding to zinc and arsenic pollution in a river of northeastern China. *J. Zhejiang Univ.Sci. B* 15, 670–680. doi: 10.1631/jzus.B1400003

Zoppini, A., Bongiorni, L., Ademollo, N., Patrolecco, L., Cibic, T., Franzo, A., et al. (2019). Bacterial diversity and microbial functional responses to organic matter composition and persistent organic pollutants in deltaic lagoon sediments. *Estuar. Coast. Shelf Sci.* 233:106508. doi: 10.1016/j.ecss.2019.106508

Zotou, I., Tsihrintzis, V. A., and Gikas, G. D. (2018). Comparative assessment of various water quality indices (WQIs) in Polyphytos Reservoir-Aliakmon River, Greece. *Procees.* 2:611. doi: 10.3390/proceedings2110611

frontiers | Frontiers in Microbiology

TYPE Review
PUBLISHED 08 April 2024
DOI 10.3389/fmicb.2024.1397683

OPEN ACCESS

EDITED BY
Yizhi Sheng,
China University of Geosciences, China

REVIEWED BY
Jia Meng,
Harbin Institute of Technology, China
Zhaorui Chu,
Guangzhou University, China

*CORRESPONDENCE
Huai Li
✉ lihuai@iga.ac.cn

RECEIVED 08 March 2024
ACCEPTED 27 March 2024
PUBLISHED 08 April 2024

CITATION
Song A, Liang S, Li H and Yan B (2024) Effects of biodiversity on functional stability of freshwater wetlands: a systematic review. *Front. Microbiol.* 15:1397683. doi: 10.3389/fmicb.2024.1397683

Effects of biodiversity on functional stability of freshwater wetlands: a systematic review

Aiwen Song[1,2], Shen Liang[1,2], Huai Li[1]* and Baixing Yan[1]

[1]State Key Laboratory of Black Soils Conservation and Utilization, Northeast Institute of Geography and Agroecology, Chinese Academy of Sciences, Changchun, China, [2]University of Chinese Academy of Sciences, Beijing, China

Freshwater wetlands are the wetland ecosystems surrounded by freshwater, which are at the interface of terrestrial and freshwater ecosystems, and are rich in ecological composition and function. Biodiversity in freshwater wetlands plays a key role in maintaining the stability of their habitat functions. Due to anthropogenic interference and global change, the biodiversity of freshwater wetlands decreases, which in turn destroys the habitat function of freshwater wetlands and leads to serious degradation of wetlands. An in-depth understanding of the effects of biodiversity on the stability of habitat function and its regulation in freshwater wetlands is crucial for wetland conservation. Therefore, this paper reviews the environmental drivers of habitat function stability in freshwater wetlands, explores the effects of plant diversity and microbial diversity on habitat function stability, reveals the impacts and mechanisms of habitat changes on biodiversity, and further proposes an outlook for freshwater wetland research. This paper provides an important reference for freshwater wetland conservation and its habitat function enhancement.

KEYWORDS

biodiversity, habitat functional stability, freshwater wetlands, habitat change, impact mechanisms

1 Introduction

Freshwater wetlands (FWs) are ecosystems formed by the interaction between freshwater rivers, lakes and land, mainly including riverine wetlands, lakes, marshes and floodplains. FWs not only provide suitable habitats for many plants and animals (McKown et al., 2021), but also play an important role in nutrient cycling, water purification and biodiversity maintenance (Li C. et al., 2022; Yu et al., 2023; Li et al., 2024). FWs have four the ecological services categories: provisioning, regulating, cultural and supporting services (Keddy et al., 2009). However, FWs have been severely damaged due to the increase in global population and economic development, resulting in a decrease in the global wetland area (Davidson, 2014), and a consequent severe destruction of wetland functions and biodiversity (Herbert et al., 2015; Ndehedehe et al., 2020).

Biodiversity is a complex system formed by the interaction between organisms and the external environment, expressing in genetic diversity, species diversity, and ecosystem diversity (Song, 2017; Liang et al., 2023). Habitat function refers to the specific functions and conditions providing for organisms, and many studies have shown that biodiversity plays a crucial role in habitat function and its stability (Weisser et al., 2017; Yao et al., 2017). FWs are complex ecosystems composed of special environmental conditions and organisms, and their functional

stability is affected by many factors (Rideout et al., 2022). In FWs, high biodiversity can enhance the stability of wetland functions, such as nutrient cycling, water purification, and biodiversity maintenance (Thomaz, 2023). Rich diversity can alleviate competitive pressures among organisms by providing more ecological niches through complementary effects, allowing different species in FWs to fully utilize resources such as water, nutrients and sunlight (Steudel et al., 2011). In addition, biodiversity can also improve the stability and disturbance resistance of food chains, mitigating external disturbances in wetlands by building complex foodweb structures (Peel et al., 2019; Hatton et al., 2024).

Although many studies showed that the biodiversity of FWs has an important impact on the functional stability of the habitats in which they exist, few literatures have been reviewed and summarized. Therefore, the objectives of this study are to (1) analyze the effects of biodiversity on the functional stability of freshwater wetland habitats; (2) illuminate the impacts and mechanisms of habitat change on biodiversity; and (3) propose future research directions and perspectives. This paper synthesizes the environmental drivers of functional stability in FWs, the effects of plant and microbial diversity on the functional stability of FWs, and further discusses the effects and mechanisms of habitat change on biodiversity.

2 Environmental drivers of functional stability in freshwater wetlands

Freshwater wetlands provide numerous functions such as biodiversity maintenance, freshwater supply, carbon storage, etc., and at the same time they are one of the most fragile ecosystems (Zedler and Kercher, 2005). Changes in environmental drivers such as hydrological factors, climatic factors, water quality, and soil physicochemical properties have led to serious functional degradation of some wetlands (Xue et al., 2018; Xiu et al., 2019). Therefore, understanding the effects of these environmental drivers on freshwater wetland ecosystems (Table 1) is important for improving the functional stability of FWs and optimizing wetland management options.

2.1 Hydrology

Water plays a crucial role in the formation, development, succession, and extinction of wetlands, directly affecting their structure, function, and ecosystem stability (Wang et al., 2015). Human activities and climate change cause changes in precipitation, evapotranspiration, and temperature, which lead to changes in hydrological conditions such as water-holding capacity, water level, and inundation duration of wetlands (Karim et al., 2015). Changes in these hydrological characteristics in turn affect the structure, distribution (Todd et al., 2010; Maietta et al., 2020a) and biogeochemical cycling (Chen et al., 2013) of biological communities in FWs, leading to degradation of wetland ecosystem functions.

An increase in water loss from FWs leads to hydrological conditions variation and a decrease in available water resources, which can disrupt their freshwater supply (Zhao and Liu, 2016). Hydrological changes can also affect the structure, distribution and biogeochemical cycling of freshwater wetland biological communities, which in turn can degrade wetland ecosystems (Chen et al., 2013; Maietta et al., 2020a). Large fluctuations in water level can affect the structure and diversity of biological communities (Luo, 2009). During periods of low water levels in the Paraná River delta, the beta diversity and individual biomass of zooplankton decreases, leading to a simplification of the functional diversity (Gutierrez et al., 2022) and a degradation of the wetland environment that sustains aquatic vegetation in Lake Michigan-Lake Huron (DeVries-Zimmerman et al., 2021), whereas high water levels have led to a decrease in vegetation cover in Lake Ontario (Smith et al., 2021), resulting in habitat loss and the frustration of the supply functions of FWs. Overall, water level with too low or high is not conducive to wetland ecosystems. Soil water content, aeration conditions and redox potential also change with fluctuations in wetland water level, affecting the ecological processes and metabolic activities of microbial communities (Ma et al., 2018). Therefore, the relative stability of water level plays an important role in maintaining the functional stability of FWs.

2.2 Water quality and soil properties

Humans production and life discharge heavy metals (Li et al., 2021), pesticides and nutrient salts (Sremacki et al., 2020; Ding et al., 2021) into freshwater wetland ecosystems, directly and indirectly leading to changes in water quality and soil physicochemical properties of wetlands, which in turn cause wetland degradation (Wei et al., 2019). Relevant studies have shown that increased loading of nutrients such as nitrogen and phosphorus in water will deteriorate water quality, and cause eutrophication of the water body, leading to significant changes in the structure and function of wetland ecosystems (Khan and Ansari, 2005; Bano et al., 2022). It has been found that increased loading of nitrogen and phosphorus in FWs may affect the rates of nitrification, denitrification, and methane production, which in turn affects the nutrient cycling (Herbert et al., 2020). Soil physicochemical properties are key factors in shaping microbial community structure, composition, and metabolic activity (Ou et al., 2019). Changes in soil physicochemical properties caused by human disturbances and natural processes likewise have serious impacts on freshwater wetland biological communities (Lai, 2010).

2.3 Temperature

Temperature is recognized as one of the key climatic factors influencing the functional stability of FWs (Bano et al., 2022). Changes in temperature can have pervasive effects on the structure and function of freshwater wetland ecosystems (Hamilton, 2010). Wetland plant growth and photosynthesis efficiency increase with increasing temperatures within a certain range, increasing nutrient uptake and conversion (Zou et al., 2014). However, excessively high temperatures may reduce the germination of plant seeds and incubation of animals, which can have serious effects on wetland plant and microbial communities, disrupting wetland biodiversity (Nielsen et al., 2015). Temperature changes can also have an impact on microbial metabolism, for example, the role of iron-reducing bacteria in inhibiting methane production may diminish as the global average temperature increases, thus affecting greenhouse gas emissions from FWs. In addition, temperature changes may also lead to species migration and range shifts (Chen X. et al., 2023).

TABLE 1 Effects of environmental drivers on freshwater wetland ecosystems.

Environmental drivers	Factor change	Functional changes	References
Wetland hydrology: Lake levels, rainfall, runoff, land use, and groundwater recharge	Extreme water level	Reduced primary productivity of wetlands.	Ojdanič et al. (2023)
	Lowering of wetland levels	Reduced biodiversity and biomass simplifies wetland function.	Gutierrez et al. (2022)
	Excessive high/low groundwater levels	Wetland water levels affect biogeochemical cycles, increasing CO and NO emissions when water is low and CH_4 emissions when water is high.	Yang et al. (2013)
	Lowering of lake and river levels	Wetland habitat suitability declines, negatively affecting wetland functions.	Mu et al. (2022)
Physicochemical indicators: 1. Water quality indicators: pH, DO, nutrient salt content, etc. 2. Soil indicators: soil texture, organic matter content, pH, etc.	Wetland salinization	Water chemistry changes negatively impact biological activity and ecological processes in wetlands.	Herbert et al. (2015)
	Increased nutrient salts in the water column	Eutrophication of water bodies; changes in microbial communities and primary productivity.	Donato et al. (2020)
	Increased quality and availability of soil organic matter	Altered microbial community structure and increased wetland CO_2 and CH_4 production rates.	Morrissey et al. (2014)
	Reduced pH of wetland soils	Changes in the structure of microbial communities negatively impact the functions of wetlands.	Zhao et al. (2022)
Temperature	Increased water temperature	Changes in water balance and chemistry degrade wetland functions in hydrological regulation and water purification.	Jolly et al. (2008)
	Elevated temperatures	Organisms' physiological processes affected, reducing biodiversity and impairing freshwater wetland function.	Epele et al. (2022)
	Warmer temperatures	Climate warming affects plant adaptations, degrading nutrient cycling in FWs.	Lindborg et al. (2021)

The hydrological conditions of wetlands are closely related to temperature changes, and global warming will lead to changes in evaporation and precipitation, which may alter the hydrological cycle of wetlands and thus indirectly affect the functional stability of wetlands (Luo, 2009; You et al., 2015). A previous study showed that a 10% decrease in rainfall will lead to changes in the redox conditions of the soil in the Everglades, thus affecting its biogeochemical processes; whereas the elemental load of the wetland ecosystem may increase when rainfall increases by 10%, which helps to maintain suitable redox conditions and promotes biogeochemical elemental cycling (Orem et al., 2015).

3 Impact of plant diversity on functional stability of freshwater wetlands

Freshwater wetlands are rich in plant species, which play multiple roles in wetland ecosystems (Figure 1A). Different types of wetlands have different dominant vegetation, and diverse plants play an important role in maintaining the stability of wetland habitat functions (e.g., water purification, carbon storage, biodiversity maintenance, etc.) (Zhang et al., 2014).

3.1 Water purification

Removal of pollutants by wetlands plants is one of the main ways of water quality purification, mainly through two main pathways involving in direct pollutants removal and microbial processes mediating (Figure 1B; Stottmeister et al., 2003). The uptake of nutrients and heavy metals varies among different plant species (Adhikari et al., 2011; Abbasi et al., 2018). The study showed that the nitrogen uptake and fixation capacity of *Rhododendron ilfescens Siberianum* was higher, and the remediation of nitrogen pollution in wetlands was more effective (Weragoda et al., 2012). In addition, the dissolved oxygen in the water were affected by the abundance of submerged plant species (Qian, 2019), and different plants had different inter-roots, physiological processes, and growth modes, which might affect the community structure and activity of microorganisms, and further affect water quality purification (Zhang et al., 2010; Pang et al., 2016). Resource complementarity between plant species may also play a positive role in nutrient uptake and water purification (Choudhury et al., 2018). Therefore, maintaining high plant diversity can help to improve pollutants removal from water (Brisson et al., 2020).

3.2 Carbon storage

Freshwater wetlands are one of the valuable carbon storage sites, covering about 6% of the land area, and contain more than 30% of the soil carbon pool (Stewart et al., 2024). Plants play an important role in wetland carbon storage (Sheng et al., 2021). Wetland plants can convert atmospheric carbon dioxide into biomass through photosynthesis, and plant residues and leaves are deposited at wetland after death, which is one of the main mechanisms of carbon storage in wetlands (Adhikari et al., 2009). Previous studies have shown that the plants vary in nutrient and light utilization (Abbasi et al., 2018). Plant diversity has an important effect on freshwater wetland productivity

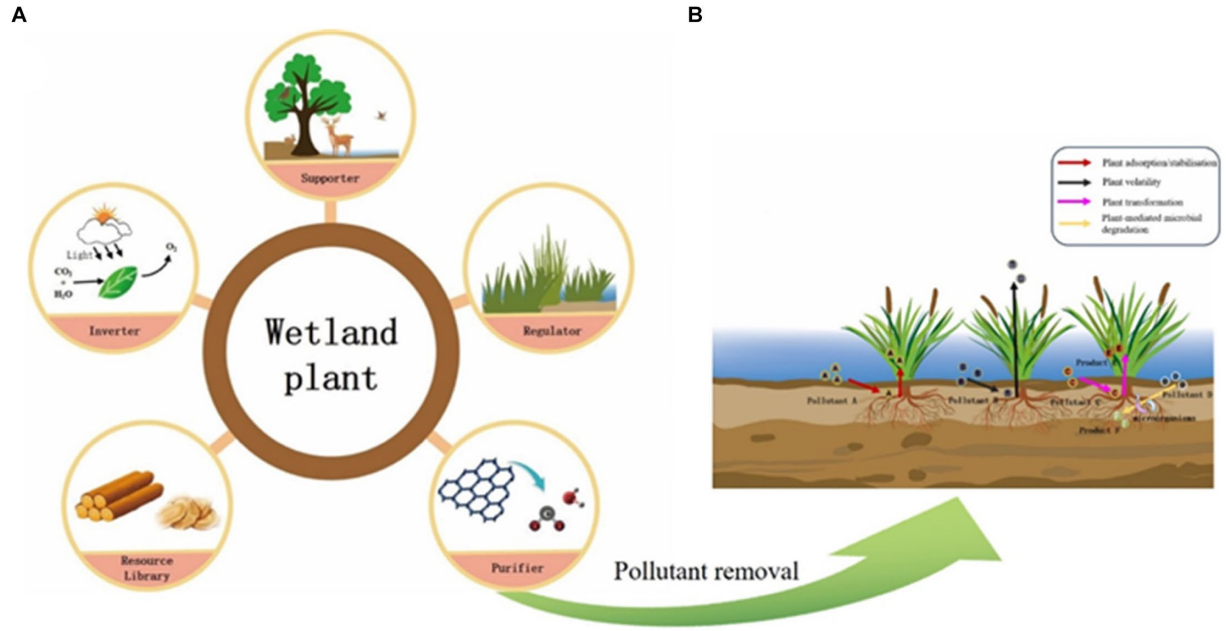

FIGURE 1
Role **(A)** and pollutant removal **(B)** of wetland plants.

(Isbell et al., 2013; Chaturvedi and Raghubanshi, 2015). Means et al. (2016) found a positive correlation between plant diversity and productivity in freshwater artificial wetlands. Cardinale et al. (2011) found that high diversity plant communities can use more ecological niches and increase the efficiency of nutrient utilization, which in turn increases primary productivity. An increase in wetland productivity can increase the capacity and total amount of carbon input from plants to the soil, which in turn increases carbon storage (Zhang et al., 2022).

In addition, the decomposition mode (humification and mineralization) and rate of plant apoplasts are particularly important for wetland carbon storage (Prescott and Vesterdal, 2021). Litter from different types of plants has different chemical compositions (Yan et al., 2018) and decomposition rates (Xi et al., 2023). It has been shown that the litter of freshwater wetland vegetation has the ability to alter the nutrient content of soil nitrogen and carbon, thus leading to the construction of different dominant microorganisms (Bonetti et al., 2021). Some plant litter leads to the production of microbial communities of humification, while others lead to the construction of microbial communities of carbon dioxide or methane production (Lin et al., 2015). Increased plant diversity can provide a wider variety of little, and this little can lead to the construction of more stable and resilient microbial communities, affecting the carbon storage capacity of the wetland (Maietta et al., 2020b).

3.3 Biodiversity maintenance

Plants can create unique microhabitat structures and provide suitable conditions for many animals and microorganisms (Choi et al., 2014; Weilhoefer et al., 2017). Freshwater wetland plants serve as the basis of the food chain in this ecosystem, and rich wetland plant communities provide a more complex and stable food web that supports the nutrient needs of many animals and microorganisms, thus contributing to the maintenance of biodiversity (Peel et al., 2019). In addition, higher plant diversity improves the resistance of wetland ecosystems to invasive alien species and better defends against invasive alien species, thus maintaining the stability of other organisms within the wetland (Peter and Burdick, 2010). Therefore, the protection and maintenance of plant diversity in FWs is essential for maintaining wetland biodiversity.

4 Impact of microbial diversity on functional stability of freshwater wetlands

Microorganisms in FWs are rich and diverse, with some differences in microbial composition among different wetland types, which can be mainly categorized into bacteria, archaea, fungi and protozoa (Cao et al., 2017). Microorganisms play an irreplaceable role in maintaining the stability of freshwater wetland habitat functions (e.g., water purification and biogeochemical cycles, etc.) (De Mandal et al., 2020; Chen M. et al., 2023; Qiao et al., 2023; Chen et al., 2024).

4.1 Water purification

Microorganisms can participate in various water purification processes through a series of metabolic and interaction processes, especially some functional microorganisms play a crucial role in wetland water purification (Wang et al., 2022). For example, some inter-root microorganisms such as *Pseudomonas* and *Flavobacterium* can effectively remove micropollutants (Brunhoferova et al., 2022). *Fusobacterium*, *Rhizobium* and *Erythrobacterium* have significant removal effects on organic pollutants such as petroleum in wetlands,

and their removal rates are positively correlated with the abundance of bacterial species (Xiang et al., 2020). *Burkholderia*, *Hydrophilus*, and *Thiobacillus* play important roles in the remediation of arsenic and antimony pollution in wetlands (Deng et al., 2022).

The areas riched in wetland microbial diversity usually have higher degradation capacity of organic pollutants, and different microbial communities can co-operate together to decompose complex organic matter and convert it into harmless products (Berrier et al., 2022). Studies have shown that hydrocarbon-degrading microorganisms (e.g., *Pseudomonas*, *Rhodococcus*, and *Nocardia*) in FWs can form microbial aggregates, improving the removal efficiency of n-alkanes and polycyclic aromatic hydrocarbons (PAHs) (Liu et al., 2021). Anaerobic ammonia-oxidizing bacteria in wetlands can cooperate with certain archaea (e.g., nitrate archaea and sulfate-dependent archaea) to complete the denitrification process in wetlands (Wang et al., 2019). In addition, some microorganisms can remove multiple pollutants simultaneously. For example, *Flavobacterium* and *Chryseobacterium* can simultaneously degrade nitrogen and organic matter in wetlands (Shen et al., 2018). Sulfate-reducing bacteria, such as *Desulfovibrio*, *Desulfobacter*, and *Desulfobulbus*, also play dual roles in wetland restoration: (1) participating in the sulfate reduction process, producing hydrogen sulfide; (2) hydrogen sulfide reacts with heavy metals to form precipitation, which promotes the passivation of heavy metals (Chen et al., 2021).

4.2 Biogeochemical cycles

Wetland microorganisms are involved in the process of storage, transformation and release of C, N and other elements, and are the dominant driver of the biogeochemical cycle in FWs (Hussain et al., 2023).

The biogeochemical cycle of carbon in FWs has received much attention (Zou et al., 2022; Bao et al., 2023; Qian et al., 2023), and microorganisms are mainly involved in the carbon cycle through the processes of respiration, methane production and conversion, and decomposition of organic matter (Bardgett et al., 2008). Microorganisms play an important role in methane production and transformation of FWs (Figure 2). It is now widely accepted that methanogenic bacteria are distributed in seven orders of the phylum Euryarchaeota (Methanopyrales, Methanococcales, Methanobacteriales, Methanomicrobiales, Methanomassiliicoccales, Methanosarcinales, and Methanocellales) (Dean et al., 2018). Among them, Methanomicrobiales, Methanosarcinales, Methanomassiliicoccales, and Methanobacteriaceae methanogenic bacteria have widely found in wetland ecosystems (Horn Marcus et al., 2003; Zhang et al., 2008; Söllinger et al., 2016). There are three main pathways of freshwater wetland methanogens involved in methanogenesis: acetate fermentation, hydrogenotrophic and methylotrophic methanogenesis (Narrowe et al., 2019), whereas wetland methane oxidation is of two types: aerobic and anaerobic oxidation. The diverse microorganisms can adapt to the different environmental conditions and can better maintain the balance of wetland methane production and conversion. It was found that the microbial community can change the methanogenic pathway by adjusting the composition and activity of the microbial community under the fluctuation of nutrients, and then maintaining the stability of carbon cycle (Holmes et al., 2014). In addition, the richness of microbial diversity in FWs is closely related to the rate of mineralization of organic matter, and an active microbial community can increase organic matter degradation and mineralization (Li et al., 2015).

Microorganisms in FWs are also critical for maintaining the relative stability of the nitrogen cycle, and diverse microorganisms are an important player in driving nitrogen conversion and its cycling processes (Mellado and Vera, 2021; Sheng et al., 2023). Microorganisms such as nitrogen-fixing bacteria and cyanobacteria can convert atmospheric N_2 into bioavailable forms such as ammonia and nitrate, supplying the wetland ecosystem with available nitrogen (Bae et al., 2018). It has been found that the efficiency and rate of

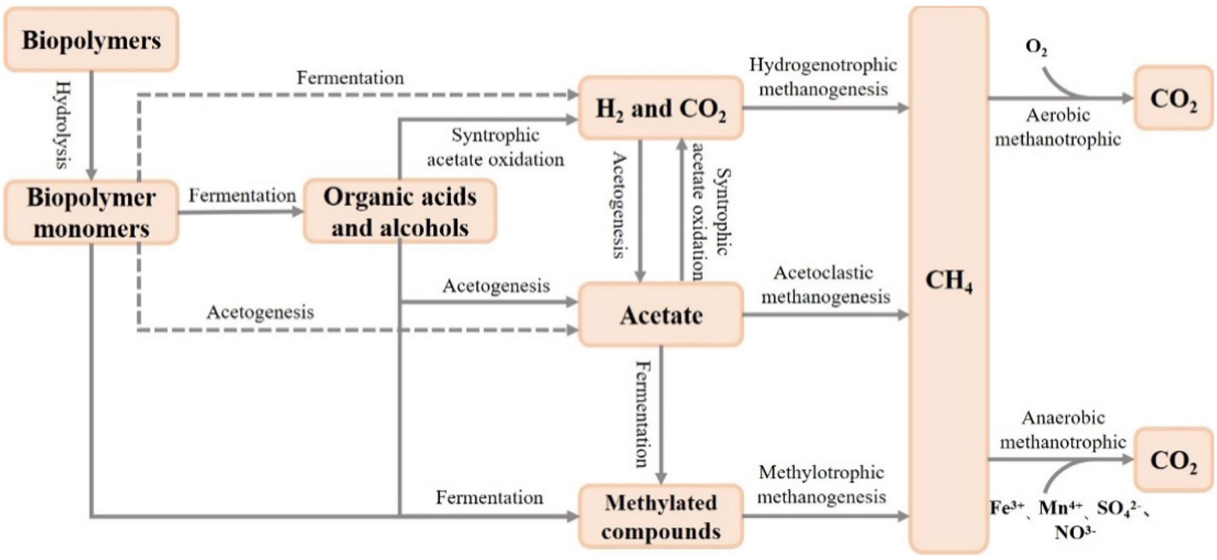

FIGURE 2
Methane production and transformation by wetland microorganisms.

nitrogen fixation are usually positively correlated with the number and diversity of microorganisms such as nitrogen-fixing bacteria (Li H. et al., 2022). On the other hand, some microorganisms (e.g., anaerobic ammonia-oxidizing bacteria, ammonia-oxidizing archaea, and denitrifying anaerobic methane-oxidizing bacteria) are also present in FWs, involved in key nitrogen transformation processes such as ammonia oxidation, nitrification and denitrification (Chen et al., 2020). These microorganisms differ in their tolerance and sensitivity to environmental factors, and a high diversity of microorganisms can provide different kinds of microbial functional groups, improving the adaptability and stability of FWs to environmental changes and maintaining the relative stability of the nitrogen cycle (Hu et al., 2017).

5 Impacts and mechanisms of habitat change on biodiversity

Wetlands provide habitat for nearly 20% of the world's species and are one of the most biodiversity-rich systems, however, they are under great pressure from human activities and climate change (Fang et al., 2006). This is causing a large degree of degradation of FWs and affecting the biodiversity of ecosystems (Al-Obaid et al., 2017). Habitat changes have important effects on wetlands (Figure 3). Among these, habitat changes and alterations in food chains and interspecific relationships are the two main factors (Ohba et al., 2019; Wang et al., 2021).

Habitat loss and fragmentation can result in the reduction and fragmentation of freshwater wetland areas, weakening the available area and connectivity of habitats for species, and these can directly lead to the reduction of the number and distribution range of some species, and consequently the decline of biodiversity (Jamin et al., 2020). For example, the size and connectivity of wetlands in Xin Jiang Wan Town, Shanghai, decreased with the accelerated urbanization of the area, leading to habitat loss and diversity reduction of wetland birds (Xu et al., 2018). Vascular plants in the wetlands of the canton of Zurich in eastern Switzerland became extinct as a result of the reduction of wetland connectivity and patch size under human activities (Jamin et al., 2020). In addition, the movement and migration of amphibians are limited when wetlands are fragmented, which may lead to the delayed extinction of these species (Gimmi et al., 2011).

Habitat change also affects wetland biodiversity by altering wetland food chains and interspecific relationships (Araújo et al., 2014). Previous studies have found that species richness of insectivorous birds in the Lampertheimer Altrhein area has decreased, due to the reducing food resources for insectivorous birds under agricultural intensification (Schrauth and Wink, 2018). The reduction in species richness and cover of plant communities during the degradation of the Ruoerge wetland has led to changes in the trophic structure of omnivores and algae, which in turn had a serious impact on the diversity of nematode communities (Wu et al., 2017). In addition, biological invasions are recognized as one of the main drivers of biodiversity loss (Mazor et al., 2018). Habitat changes can promote the invasion and spread of non-native species (e.g., *Spartina alterniflora*), and these invasive species can disrupt the original food chains and interspecific relationships of ecosystems, thus leading to biodiversity reduction (Wang et al., 2021).

In addition, changes in environmental factors such as wetland water level and pollution have significant impacts on biodiversity. For example, during the degradation of wet marshes to meadows in the Sanjiang Plain, changes in wetland water level alter the living conditions of organisms, which in turn affects the diversity and

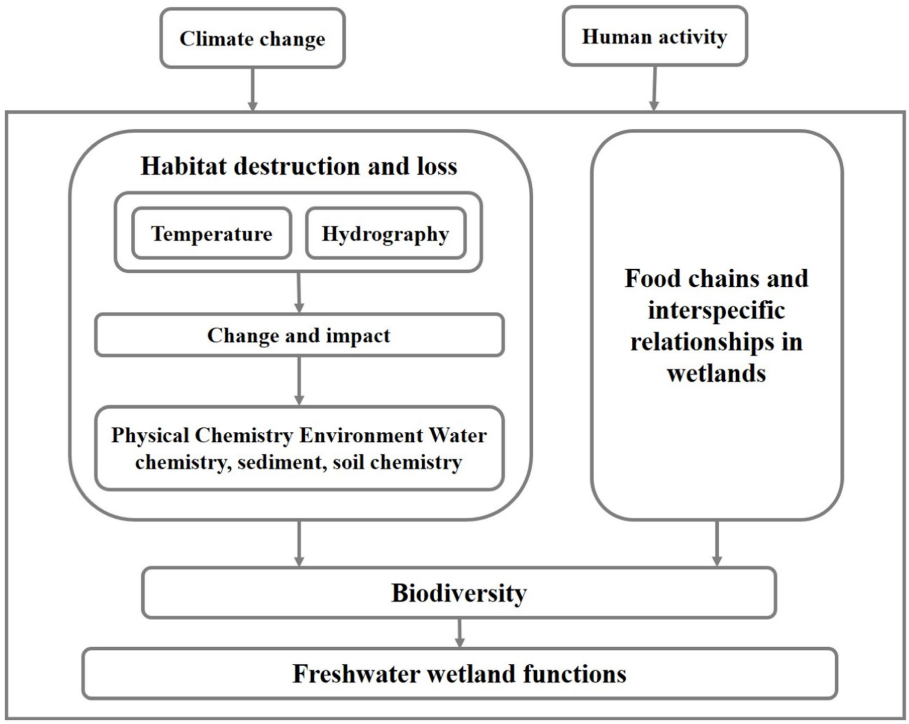

FIGURE 3
Impacts of habitat change on biodiversity in FWs.

community composition of plants and microorganisms (Sui et al., 2017; Liping et al., 2020). The overuse of herbicides and pesticides in agricultural production activities has caused severe pollution of the Infranz wetlands in north-west Ethiopia, adversely affecting their biodiversity (Eneyew and Assefa, 2021).

6 Future prospects

Freshwater wetlands with high biodiversity play an extremely important role in maintaining the functional stability of wetland habitats. Many environmental drivers such as water level, water quality, soil properties, temperature, and biological drivers (e.g., plant/microbial diversity) have important impacts on the functional stability of freshwater wetland ecosystems, but many in-depth studies are needed in the following aspects in the future:

1. Changes in biodiversity can directly or indirectly regulate ecosystem processes, and biodiversity is the main determinant of maintaining ecosystem functional stability. Therefore, it is of great significance to investigate the relationship between biodiversity and functional stability. Nowadays, most studies on the functional stability and biodiversity of freshwater wetland have focused on small-scale scales and homogeneous habitats, ignoring the effects of spatial and temporal scales and environmental heterogeneity. Therefore, the study on the multi-scale integration and relationship between biodiversity and functional stability at different scales is important. This will help maintain the stability of freshwater ecosystems and provide theoretical support for the conservation of FWs.
2. Many studies are about the response of habitat function to environmental and biological elements in the context of global change. Most studies agreed that high levels of biodiversity can better maintain the stability of habitat function. In addition, changes in environmental factors can indirectly affect ecosystem habitat function through biodiversity. Therefore, future research needs to focus on the mechanisms by which environmental and biological factors drive habitat function enhancement through community composition, species diversity, environmental heterogeneity and biological interactions.

7 Conclusion

Freshwater wetlands are one of the most biodiverse ecosystems, and abundant species has a significant impact on the habitat function of FWs. Many environmental factors are changing under global change and human activities, and these changes can either directly affect the stability of wetland habitat functions or indirectly affect habitat functions by altering the biodiversity of FWs. Our study analyzes the roles of environmental drivers maintaining the stability of wetland habitat functions, such as hydrology, temperature, and water quality, discusses the impacts of plant and microbial diversity on the functional stability of FWs, and further reveals the impacts and mechanisms of habitat changes on biodiversity. In general, biodiversity can promote the stability of habitat functions in FWs. However, most studies focus on small-scale scales and homogeneous habitats. Therefore, future studies on biodiversity and stability of habitat functions in FWs at large scales and non-homogeneous habitats still need to be further explored.

Author contributions

AS: Writing – original draft. SL: Data curation, Software, Validation, Writing – review & editing. HL: Conceptualization, Project administration, Supervision, Writing – review & editing. BY: Writing – review & editing.

Funding

The author(s) declare financial support was received for the research, authorship, and/or publication of this article. This work was financially supported by the National Key R&D Program of China (no. 2022YFF1300901), National Natural Science Foundation of China (no. 42077353), and Natural Science Foundation of Jilin Province (no. 20230101100JC).

Conflict of interest

The authors declare that the research was conducted in the absence of any commercial or financial relationships that could be construed as a potential conflict of interest.

Publisher's note

References

Abbasi, H. N., Xie, J., Vymazal, J., and Lu, X. (2018). Kinetics of nutrient uptake by economical vegetable species grown in constructed wetlands. *J. Anim. Plant Sci.* 28:726.

Adhikari, A. R., Acharya, K., Shanahan, S. A., and Zhou, X. (2011). Removal of nutrients and metals by constructed and naturally created wetlands in the Las Vegas Valley, Nevada. *Environ. Monit. Assess.* 180, 97–113. doi: 10.1007/s10661-010-1775-y

Adhikari, S., Bajracharaya, R. M., and Sitaula, B. K. (2009). A review of carbon dynamics and sequestration in wetlands. *J. Wetl. Ecol.* 2, 42–46. doi: 10.3126/jowe.v2i1.1855

Al-Obaid, S., Samraoui, B., Thomas, J., El-Serehy, H. A., Alfarhan, A. H., Schneider, W., et al. (2017). An overview of wetlands of Saudi Arabia: values, threats, and perspectives. *Ambio* 46, 98–108. doi: 10.1007/s13280-016-0807-4

Araújo, M. S., Langerhans, R. B., Giery, S. T., and Layman, C. A. (2014). Ecosystem fragmentation drives increased diet variation in an endemic livebearing fish of the Bahamas. *Ecol. Evol.* 4, 3298–3308. doi: 10.1002/ece3.1140

Bae, H.-S., Morrison, E., Chanton, J. P., and Ogram, A. (2018). Methanogens are major contributors to nitrogen fixation in soils of the Florida Everglades. *Appl. Environ. Microbiol.* 84, e02222–e02217. doi: 10.1128/AEM.02222-17

Bano, H., Rather, R. A., Malik, S., Bhat, M. A., Khan, A. H., Americo-Pinheiro, J. H. P., et al. (2022). Effect of seasonal variation on pollution load of water of Hokersar wetland: a case study of queen wetland of Kashmir, J & K, India. *Water Air Soil Pollut.* 233, 1–25. doi: 10.1007/s11270-022-05988-w

Bao, T., Jia, G., and Xu, X. (2023). Weakening greenhouse gas sink of pristine wetlands under warming. *Nat. Clim. Chang.* 13, 462–469. doi: 10.1038/s41558-023-01637-0

Bardgett, R. D., Freeman, C., and Ostle, N. J. (2008). Microbial contributions to climate change through carbon cycle feedbacks. *ISME J.* 2, 805–814. doi: 10.1038/ismej.2008.58

Berrier, D. J., Neubauer, S. C., and Franklin, R. B. (2022). Cooperative microbial interactions mediate community biogeochemical responses to saltwater intrusion in wetland soils. *FEMS Microbiol. Ecol.* 98, 1–12. doi: 10.1093/femsec/fiac019

Bonetti, G., Trevathan-Tackett, S. M., Carnell, P. E., Treby, S., and Macreadie, P. I. (2021). Local vegetation and hydroperiod influence spatial and temporal patterns of carbon and microbe response to wetland rehabilitation. *Appl. Soil Ecol.* 163:103917. doi: 10.1016/j.apsoil.2021.103917

Brisson, J., Rodriguez, M., Martin, C. A., and Proulx, R. (2020). Plant diversity effect on water quality in wetlands: a meta-analysis based on experimental systems. *Ecol. Appl.* 30:e02074. doi: 10.1002/eap.2074

Brunhoferova, H., Venditti, S., Laczny, C. C., Lebrun, L., and Hansen, J. (2022). Bioremediation of 27 micropollutants by symbiotic microorganisms of wetland Macrophytes. *Sustain. For.* 14:3944. doi: 10.3390/su14073944

Cao, Q., Wang, H., Chen, X., Wang, R., and Liu, J. (2017). Composition and distribution of microbial communities in natural river wetlands and corresponding constructed wetlands. *Ecol. Eng.* 98, 40–48. doi: 10.1016/j.ecoleng.2016.10.063

Cardinale, B. J., Matulich, K. L., Hooper, D. U., Byrnes, J. E., Duffy, E., Gamfeldt, L., et al. (2011). The functional role of producer diversity in ecosystems. *Am. J. Bot.* 98, 572–592. doi: 10.3732/ajb.1000364

Chaturvedi, R. K., and Raghubanshi, A. S. (2015). Assessment of carbon density and accumulation in mono-and multi-specific stands in teak and Sal forests of a tropical dry region in India. *For. Ecol. Manag.* 339, 11–21. doi: 10.1016/j.foreco.2014.12.002

Chen, J., Li, X., Jia, W., Shen, S., Deng, S., Ji, B., et al. (2021). Promotion of bioremediation performance in constructed wetland microcosms for acid mine drainage treatment by using organic substrates and supplementing domestic wastewater and plant litter broth. *J. Hazard. Mater.* 404:124125. doi: 10.1016/j.jhazmat.2020.124125

Chen, X., Sheng, Y., Wang, G., Zhou, P., Liao, F., Mao, H., et al. (2024). Spatiotemporal successions of N, S, C, Fe, and as cycling genes in groundwater of a wetland ecosystem: enhanced heterogeneity in wet season. *Water Res.* 251:121105. doi: 10.1016/j.watres.2024.121105

Chen, X., Wang, G., Sheng, Y., Liao, F., Mao, H., Li, B., et al. (2023). Nitrogen species and microbial community coevolution along groundwater flowpath in the southwest of Poyang Lake area, China. *Chemosphere* 329:138627. doi: 10.1016/j.chemosphere.2023.138627

Chen, H., Wang, H., Wu, M., Yu, G., Chen, J., and Liu, D. (2020). Recent advances in microbe-driven nitrogen transformation in freshwater wetland ecosystems. *J. Hydraul. Eng.* 51, 158–168. doi: 10.13243/j.cnki.slxb.20190592

Chen, M., Zeng, S., Jiang, B., Wen, Z., Wu, J., and Xia, J. (2023). The comprehensive evaluation of how water level fluctuation and temperature change affect vegetation cover variations at a Lake of ecological importance (Poyang Lake), China. *Ecol. Indic.* 148:110041. doi: 10.1016/j.ecolind.2023.110041

Chen, H., Zhu, Q., Peng, C., Wu, N., Wang, Y., Fang, X., et al. (2013). The impacts of climate change and human activities on biogeochemical cycles on the Qinghai-Tibetan plateau. *Glob. Chang. Biol.* 19, 2940–2955. doi: 10.1111/gcb.12277

Choi, J.-Y., Jeong, K.-S., La, G.-H., and Joo, G.-J. (2014). Effect of removal of free-floating macrophytes on zooplankton habitat in shallow wetland. *Knowl. Manag. Aquat. Ecosyst.* 414:11. doi: 10.1051/kmae/2014023

Choudhury, M. I., McKie, B. G., Hallin, S., and Ecke, F. (2018). Mixtures of macrophyte growth forms promote nitrogen cycling in wetlands. *Sci. Total Environ.* 635, 1436–1443. doi: 10.1016/j.scitotenv.2018.04.193

Davidson, N. (2014). How much wetland has the world lost? Long-term and recent trends in global wetland area. *Mar. Freshw. Res.* 65, 934–941. doi: 10.1071/MF14173

De Mandal, S., Laskar, F., Panda, A. K., and Mishra, R. (2020). *Chapter 12—Microbial Diversity and Functional Potential in Wetland Ecosystems, Recent Advancements in Microbial Diversity* Academic Press, 289–314.

Dean, J. F., Middelburg, J. J., Röckmann, T., Aerts, R., Blauw, L. G., Egger, M., et al. (2018). Methane feedbacks to the global climate system in a warmer world. *Rev. Geophys.* 56, 207–250. doi: 10.1002/2017RG000559

Deng, J., Xiao, T., Fan, W., Ning, Z., and Xiao, E. (2022). Relevance of the microbial community to Sb and as biogeochemical cycling in natural wetlands. *Sci. Total Environ.* 818:151826. doi: 10.1016/j.scitotenv.2021.151826

DeVries-Zimmerman, S. J., Yurk, B., Fast, K. M., Donaldson, A., and Hansen, E. C. (2021). Waxing and waning slacks: the changing ecohydrology of interdunal wetlands/slacks in a Lake Michigan coastal dune complex during rising Lake Michigan-Huron levels. *J. Great Lakes Res.* 47, 1565–1580. doi: 10.1016/j.jglr.2021.09.001

Ding, Y. D., Song, C. C., Chen, G. J., Zhang, X. H., and Mao, R. (2021). Effects of long-term nitrogen addition on dissolved organic matter characteristics in a temperate wetland of Northeast China. *Ecotoxicol. Environ. Saf.* 226:112822. doi: 10.1016/j.ecoenv.2021.112822

Donato, M., Johnson, O., Steven, B., and Lawrence, B. A. (2020). Nitrogen enrichment stimulates wetland plant responses whereas salt amendments alter sediment microbial communities and biogeochemical responses. *PLoS One* 15:e0235225. doi: 10.1371/journal.pone.0235225

Eneyew, B. G., and Assefa, W. W. (2021). Anthropogenic effect on wetland biodiversity in Lake Tana region: a case of Infranz wetland, Northwestern Ethiopia. *Environ. Sustain. Indicators* 12:100158. doi: 10.1016/j.indic.2021.100158

Epele, L. B., Grech, M. G., Williams-Subiza, E. A., Stenert, C., McLean, K., Greig, H. S., et al. (2022). Perils of life on the edge: climatic threats to global diversity patterns of wetland macroinvertebrates. *Sci. Total Environ.* 820:153052. doi: 10.1016/j.scitotenv.2022.153052

Fang, J., Wang, Z., Zhao, S., Li, Y., Tang, Z., Yu, D., et al. (2006). Biodiversity changes in the lakes of the Central Yangtze. *Front. Ecol. Environ.* 4, 369–377. doi: 10.1890/1540-9295(2006)004[0369,BCITLO]2.0.CO;2

Gimmi, U., Lachat, T., and Bürgi, M. (2011). Reconstructing the collapse of wetland networks in the Swiss lowlands 1850–2000. *Landsc. Ecol.* 26, 1071–1083. doi: 10.1007/s10980-011-9633-z

Gutierrez, M. F., Epele, L. B., Mayora, G., Aquino, D., Mora, C., Quintana, R., et al. (2022). Hydro-climatic changes promote shifts in zooplankton composition and diversity in wetlands of the lower Paraná River Delta. *Hydrobiologia* 849, 3463–3480. doi: 10.1007/s10750-022-04955-0

Hamilton, S. K. (2010). Biogeochemical implications of climate change for tropical rivers and floodplains. *Hydrobiologia* 657, 19–35. doi: 10.1007/s10750-009-0086-1

Hatton, I. A., Mazzarisi, O., Altieri, A., and Smerlak, M. (2024). Diversity begets stability: sublinear growth and competitive coexistence across ecosystems. *Science* 383:eadg8488. doi: 10.1126/science.adg8488

Herbert, E. R., Boon, P., Burgin, A. J., Neubauer, S. C., Franklin, R. B., Ardon, M., et al. (2015). A global perspective on wetland salinization: ecological consequences of a growing threat to freshwater wetlands. *Ecosphere* 6, 1–43. doi: 10.1890/es14-00534.1

Herbert, E. R., Schubauer-Berigan, J. P., and Craft, C. B. (2020). Effects of 10 yr of nitrogen and phosphorus fertilization on carbon and nutrient cycling in a tidal freshwater marsh. *Limnol. Oceanogr.* 65, 1669–1687. doi: 10.1002/lno.11411

Holmes, M. E., Chanton, J. P., Bae, H.-S., and Ogram, A. (2014). Effect of nutrient enrichment on δ13CH4 and the methane production pathway in the Florida Everglades. *J. Geophys. Res. Biogeosci.* 119, 1267–1280. doi: 10.1002/jgrg.20122

Horn Marcus, A., Matthies, C., Küsel, K., Schramm, A., and Drake Harold, L. (2003). Hydrogenotrophic Methanogenesis by moderately acid-tolerant methanogens of a methane-emitting acidic peat. *Appl. Environ. Microbiol.* 69, 74–83. doi: 10.1128/AEM.69.1.74-83.2003

Hu, Q., Zheng, P., and Kang, D. (2017). Taxonomy, characteristics, and biotechniques used for the analysis of anaerobic ammonium oxidation bacteria. *Chin. J. Appl. Environ. Biol.* 23, 384–391. doi: 10.3724/SP.J.1145.2016.04022

Hussain, S., Chen, M., Liu, Y., Mustafa, G., Wang, X., Liu, J., et al. (2023). Composition and assembly mechanisms of prokaryotic communities in wetlands, and their relationships with different vegetation and reclamation methods. *Sci. Total Environ.* 897:166190. doi: 10.1016/j.scitotenv.2023.166190

Isbell, F., Reich, P. B., Tilman, D., Hobbie, S. E., Polasky, S., and Binder, S. (2013). Nutrient enrichment, biodiversity loss, and consequent declines in ecosystem productivity. *Proc. Natl. Acad. Sci.* 110, 11911–11916. doi: 10.1073/pnas.1310880110

Jamin, A., Peintinger, M., Gimmi, U., Holderegger, R., and Bergamini, A. (2020). Evidence for a possible extinction debt in Swiss wetland specialist plants. *Ecol. Evol.* 10, 1264–1277. doi: 10.1002/ece3.5980

Jolly, I. D., McEwan, K. L., and Holland, K. L. (2008). A review of groundwater-surface water interactions in arid/semi-arid wetlands and the consequences of salinity for wetland ecology. *Ecohydrology* 1, 43–58. doi: 10.1002/eco.6

Karim, F., Dutta, D., Marvanek, S., Petheram, C., Ticehurst, C., Lerat, J., et al. (2015). Assessing the impacts of climate change and dams on floodplain inundation and wetland connectivity in the wet–dry tropics of northern Australia. *J. Hydrol.* 522, 80–94. doi: 10.1016/j.jhydrol.2014.12.005

Keddy, P. A., Fraser, L. H., Solomeshch, A. I., Junk, W. J., Campbell, D. R., Arroyo, M. T. K., et al. (2009). Wet and wonderful: the world's largest wetlands are conservation priorities. *Bioscience* 59, 39–51. doi: 10.1525/bio.2009.59.1.8

Khan, F. A., and Ansari, A. A. (2005). Eutrophication: An ecological vision. *Bot. Rev.* 71, 449–482. doi: 10.1663/0006-8101(2005)071[0449:Eaev]2.0.Co;2

Lai, D. Y. F. (2010). Biogeochemistry of wetlands: science and applications. *Ecol. Eng.* 36, 607–608. doi: 10.1016/j.ecoleng.2010.01.001

Li, X., Hou, L., Liu, M., Lin, X., Li, Y., and Li, S. (2015). Primary effects of extracellular enzyme activity and microbial community on carbon and nitrogen mineralization in estuarine and tidal wetlands. *Appl. Microbiol. Biotechnol.* 99, 2895–2909. doi: 10.1007/s00253-014-6187-4

Li, C., Li, X., Yang, Y., Shi, Y., and Li, H. (2022). Degradation reduces the diversity of nitrogen-fixing bacteria in the alpine wetland on the Qinghai-Tibet plateau. *Front. Plant Sci.* 13:939762. doi: 10.3389/fpls.2022.939762

Li, H., Liang, S., Chi, Z., Wu, H., and Yan, B. (2022). Unveiling microbial community and function involved in anammox in paddy vadose under groundwater irrigation. *Sci. Total Environ.* 849:157876. doi: 10.1016/j.scitotenv.2022.157876

Li, Y., Shi, K. Y., Yuan, J., and Kuang, Q. Y. (2021). Evaluation of heavy metal pollutants from plateau mines in wetland surface deposits. *Front. Environ. Sci.* 8:557302. doi: 10.3389/fenvs.2020.557302

Li, H., Song, A., and Chi, Z. (2024). Deep groundwater irrigation altered microbial community and increased anammox and methane oxidation in paddy wetlands of Sanjiang plain, China. *Front. Microbiol.* 15:1354279. doi: 10.3389/fmicb.2024.1354279

Liang, S., Li, H., and Wu, H. (2023). Microorganisms in coastal wetland sediments: a review on microbial community structure, functional gene, and environmental potential. *Front. Microbiol.* 14:1163896. doi: 10.3389/fmicb.2023.1163896

Lin, Y., Liu, D., Ding, W., Kang, H., Freeman, C., Yuan, J., et al. (2015). Substrate sources regulate spatial variation of metabolically active methanogens from two contrasting freshwater wetlands. *Appl. Microbiol. Biotechnol.* 99, 10779–10791. doi: 10.1007/s00253-015-6912-7

Lindborg, R., Ermold, M., Kuglerová, L., Jansson, R., Larson, K. W., Milbau, A., et al. (2021). How does a wetland plant respond to increasing temperature along a latitudinal gradient? *Ecol. Evol.* 11, 16228–16238. doi: 10.1002/ece3.8303

Liping, S., Song, C., Zhang, X., Wang, X., and Luan, Z. (2020). Responses of above-ground biomass, plant diversity, and dominant species to habitat change in a freshwater wetland of Northeast China. *Russ. J. Ecol.* 51, 57–63. doi: 10.1134/S1067413620010051

Liu, H., Yang, G., Jia, H., and Yao, J. (2021). Impact of long-term cultivation with crude oil on wetland microbial community shifts and the hydrocarbon degradation potential. *Energy Sour. A. Recov. Utilization Environ. Effects* 1-13, 1–13. doi: 10.1080/15567036.2021.1896609

Luo, W. (2009). Growth and morphological responses to water level and nutrient supply in three emergent macrophyte species. *Hydrobiologia* 624, 151–160. doi: 10.1007/s10750-008-9689-1

Ma, Y., Li, J., Wu, J., Kong, Z., Feinstein, L. M., Ding, X., et al. (2018). Bacterial and fungal community composition and functional activity associated with Lake wetland water level gradients. *Sci. Rep.* 8:760. doi: 10.1038/s41598-018-19153-z

Maietta, C. E., Hondula, K. L., Jones, C. N., and Palmer, M. A. (2020a). Hydrological conditions influence soil and methane-cycling microbial populations in seasonally saturated wetlands. *Front. Environ. Sci.* 8:593942. doi: 10.3389/fenvs.2020.593942

Maietta, C. E., Monsaint-Queeney, V., Wood, L., Baldwin, A. H., and Yarwood, S. A. (2020b). Plant litter amendments in restored wetland soils altered microbial communities more than clay additions. *Soil Biol. Biochem.* 147:107846. doi: 10.1016/j.soilbio.2020.107846

Mazor, T., Doropoulos, C., Schwarzmueller, F., Gladish, D. W., Kumaran, N., Merkel, K., et al. (2018). Global mismatch of policy and research on drivers of biodiversity loss. *Nat. Ecol. Evol.* 2, 1071–1074. doi: 10.1038/s41559-018-0563-x

McKown, J. G., Moore, G. E., Payne, A. R., White, N. A., and Gibson, J. L. (2021). Successional dynamics of a 35 year old freshwater mitigation wetland in southeastern New Hampshire. *PLoS One* 16:e0251748. doi: 10.1371/journal.pone.0251748

Means, M. M., Ahn, C., Korol, A. R., and Williams, L. D. (2016). Carbon storage potential by four macrophytes as affected by planting diversity in a created wetland. *J. Environ. Manag.* 165, 133–139. doi: 10.1016/j.jenvman.2015.09.016

Mellado, M., and Vera, J. (2021). Microorganisms that participate in biochemical cycles in wetlands. *Can. J. Microbiol.* 67, 771–788. doi: 10.1139/cjm-2020-0336

Morrissey, E. M., Berrier, D. J., Neubauer, S. C., and Franklin, R. B. (2014). Using microbial communities and extracellular enzymes to link soil organic matter characteristics to greenhouse gas production in a tidal freshwater wetland. *Biogeochemistry* 117, 473–490. doi: 10.1007/s10533-013-9894-5

Mu, S. J., Yang, G. S., Xu, X. B., Wan, R. R., and Li, B. (2022). Assessing the inundation dynamics and its impacts on habitat suitability in Poyang Lake based on integrating Landsat and MODIS observations. *Sci. Total Environ.* 834:154936. doi: 10.1016/j.scitotenv.2022.154936

Narrowe, A. B., Borton, M. A., Hoyt, D. W., Smith, G. J., Daly, R. A., Angle, J. C., et al. (2019). Uncovering the diversity and activity of methylotrophic methanogens in freshwater wetland soils. *mSystems* 4:e00320-19. doi: 10.1128/mSystems.00320-19

Ndehedehe, C. E., Burford, M. A., Stewart-Koster, B., and Bunn, S. E. (2020). Satellite-derived changes in floodplain productivity and freshwater habitats in northern Australia (1991–2019). *Ecol. Indic.* 114:106320. doi: 10.1016/j.ecolind.2020.106320

Nielsen, D. L., Jasper, E. W., Ning, N., and Lawler, S. (2015). High sediment temperatures influence the emergence of dormant aquatic biota. *Mar. Freshw. Res.* 66, 1138–1146. doi: 10.1071/MF14272

Ohba, S.-Y., Suzuki, K., Sakai, Y., Shibata, J.-Y., and Okuda, N. (2019). Effects of irrigation system alterations on the trophic position of a threatened top predator in rice-field ecosystems. *Freshw. Biol.* 64, 1737–1746. doi: 10.1111/fwb.13365

Ojdanič, N., Holcar, M., Golob, A., and Gaberščik, A. (2023). Environmental extremes affect productivity and habitus of common reed in intermittent wetland. *Ecol. Eng.* 189:106911. doi: 10.1016/j.ecoleng.2023.106911

Orem, W., Newman, S., Osborne, T. Z., and Reddy, K. R. (2015). Projecting changes in Everglades soil biogeochemistry for carbon and other key elements, to possible 2060 climate and hydrologic scenarios. *Environ. Manag.* 55, 776–798. doi: 10.1007/s00267-014-0381-0

Ou, Y., Rousseau, A. N., Wang, L., Yan, B., Gumiere, T., and Zhu, H. (2019). Identification of the alteration of riparian wetland on soil properties, enzyme activities and microbial communities following extreme flooding. *Geoderma* 337, 825–833. doi: 10.1016/j.geoderma.2018.10.032

Pang, S., Zhang, S., Lv, X., Han, B., Liu, K., Qiu, C., et al. (2016). Characterization of bacterial community in biofilm and sediments of wetlands dominated by aquatic macrophytes. *Ecol. Eng.* 97, 242–250. doi: 10.1016/j.ecoleng.2016.10.011

Peel, R., Hill, J., Taylor, G., and Weyl, O. (2019). Food web structure and trophic dynamics of a fish Community in an Ephemeral Floodplain Lake. *Front. Environ. Sci.* 7:192. doi: 10.3389/fenvs.2019.00192

Peter, C. R., and Burdick, D. M. (2010). Can plant competition and diversity reduce the growth and survival of exotic *Phragmites australis* invading a tidal marsh? *Estuar. Coasts* 33, 1225–1236. doi: 10.1007/s12237-010-9328-8

Prescott, C. E., and Vesterdal, L. (2021). Decomposition and transformations along the continuum from litter to soil organic matter in forest soils. *For. Ecol. Manag.* 498:119522. doi: 10.1016/j.foreco.2021.119522

Qian, Z. (2019). Does species richness affect the growth and water quality of submerged macrophyte assemblages? *Aquat. Bot.* 153, 51–57. doi: 10.1016/j.aquabot.2018.11.006

Qian, X., Mao, S., Jiang, Y., Ye, C., Lu, B., Shan, N., et al. (2023). Research progress of wetland carbon cycle in China based on bibliometrics. *J. Environ. Eng. Technol.* 13, 742–752. doi: 10.12153/j.issn.1674-991X.20220029

Qiao, Z., Sheng, Y., Wang, G., Chen, X., Liao, F., Mao, H., et al. (2023). Deterministic factors modulating assembly of groundwater microbial community in a nitrogen-contaminated and hydraulically-connected river-lake-floodplain ecosystem. *J. Environ. Manag.* 347:119210. doi: 10.1016/j.jenvman.2023.119210

Rideout, N. K., Compson, Z. G., Monk, W. A., Bruce, M. R., Hajibabaei, M., Porter, T. M., et al. (2022). Environmental filtering of macroinvertebrate traits influences ecosystem functioning in a large river floodplain. *Funct. Ecol.* 36, 2791–2805. doi: 10.1111/1365-2435.14168

Schrauth, F. E., and Wink, M. (2018). Changes in species composition of birds and declining number of breeding territories over 40 years in a nature conservation area in Southwest Germany. *Diversity* 10:97. doi: 10.3390/d10030097

Shen, Y., Zheng, Y., Wang, X., Jia, C., and Zhao, M. (2018). Mechanism of different scales subsurface flow constructed wetlands for purifying polluted river water. *Chin. J. Environ. Eng.* 12, 1667–1675. doi: 10.12030/j.cjee.201711009

Sheng, Y., Baars, O., Guo, D., Whitham, J., Srivastava, S., and Dong, H. (2023). Mineral-bound trace metals as cofactors for anaerobic biological nitrogen fixation. *Environ. Sci. Technol.* 57, 7206–7216. doi: 10.1021/acs.est.3c01371

Sheng, Y., Dong, H., Kukkadapu, R. K., Ni, S., Zeng, Q., Hu, J., et al. (2021). Lignin-enhanced reduction of structural Fe (III) in nontronite: dual roles of lignin as electron shuttle and donor. *Geochim. Cosmochim. Acta* 307, 1–21. doi: 10.1016/j.gca.2021.05.037

Smith, I. M., Fiorino, G. E., Grabas, G. P., and Wilcox, D. A. (2021). Wetland vegetation response to record-high Lake Ontario water levels. *J. Great Lakes Res.* 47, 160–167. doi: 10.1016/j.jglr.2020.10.013

Söllinger, A., Schwab, C., Weinmaier, T., Loy, A., Tveit, A. T., Schleper, C., et al. (2016). Phylogenetic and genomic analysis of Methanomassiliicoccales in wetlands and animal intestinal tracts reveals clade-specific habitat preferences. *FEMS Microbiol. Ecol.* 92:fiv149. doi: 10.1093/femsec/fiv149

Song, G. (2017). What determines species diversity? *Chin. Sci. Bull.* 62, 2033–2041. doi: 10.1360/N972017-00125

Sremacki, M., Obrovski, B., Petrovic, M., Mihajlovic, I., Dragicevic, P., Radic, J., et al. (2020). Comprehensive environmental monitoring and assessment of protected wetland and lake water quality in Croatia and Serbia. *Environ. Monit. Assess.* 192:187. doi: 10.1007/s10661-020-8141-5

Steudel, B., Hautier, Y., Hector, A., and Kessler, M. (2011). Diverse marsh plant communities are more consistently productive across a range of different environmental conditions through functional complementarity. *J. Appl. Ecol.* 48, 1117–1124. doi: 10.1111/j.1365-2664.2011.01986.x

Stewart, A. J., Halabisky, M., Babcock, C., Butman, D. E., D'Amore, D. V., and Moskal, L. M. (2024). Revealing the hidden carbon in forested wetland soils. *Nat. Commun.* 15:726. doi: 10.1038/s41467-024-44888-x

Stottmeister, U., Wiessner, A., Kuschk, P., Kappelmeyer, U., Kästner, M., Bederski, O., et al. (2003). Effects of plants and microorganisms in constructed wetlands for wastewater treatment. *Biotechnol. Adv.* 22, 93–117. doi: 10.1016/j.biotechadv.2003.08.010

Sui, X., Zhang, R., Yang, L., Li, M., Xu, N., Liu, Y., et al. (2017). Differences in the microbial population associated with three wetland types in the Sanjiang plain, Northeast China. *Appl. Ecol. Environ. Res.* 15, 79–92. doi: 10.15666/aeer/1501_079092

Thomaz, S. M. (2023). Ecosystem services provided by freshwater macrophytes. *Hydrobiologia* 850, 2757–2777. doi: 10.1007/s10750-021-04739-y

Todd, M. J., Muneepeerakul, R., Pumo, D., Azaele, S., Miralles-Wilhelm, F., Rinaldo, A., et al. (2010). Hydrological drivers of wetland vegetation community distribution within Everglades National Park, Florida. *Adv. Water Resour.* 33, 1279–1289. doi: 10.1016/j.advwatres.2010.04.003

Wang, Y.-F., Dick, R. P., Lorenz, N., and Lee, N. (2019). Interactions and responses of n-damo archaea, n-damo bacteria and anammox bacteria to various electron acceptors in natural and constructed wetland sediments. *Int. Biodeterior. Biodegradation* 144:104749. doi: 10.1016/j.ibiod.2019.104749

Wang, J., Long, Y., Yu, G., Wang, G., Zhou, Z., Li, P., et al. (2022). A review on microorganisms in constructed wetlands for typical pollutant removal: species, function, and diversity. *Front. Microbiol.* 13:845725. doi: 10.3389/fmicb.2022.845725

Wang, Y., Tan, W., Li, B., Wen, L., and Lei, G. (2021). Habitat alteration facilitates the dominance of invasive species through disrupting niche partitioning in floodplain wetlands. *Divers. Distrib.* 27, 1861–1871. doi: 10.1111/ddi.13376

Wang, C., Zhao, H., and Wang, G. (2015). Vegetation development and water level changes in Shenjiadian peatland in Sanjiang plain, Northeast China. *Chin. Geogr. Sci.* 25, 451–461. doi: 10.1007/s11769-015-0768-8

Wei, J., Gao, J., Wang, N., Liu, Y., Wang, Y., Bai, Z., et al. (2019). Differences in soil microbial response to anthropogenic disturbances in Sanjiang and Momoge wetlands, China. *FEMS Microbiol. Ecol.* 95:fiz110. doi: 10.1093/femsec/fiz110

Weilhoefer, C. L., Williams, D., Nguyen, I., Jakstis, K., and Fischer, C. (2017). The effects of reed canary grass (*Phalaris arundinacea* L.) on wetland habitat and arthropod community composition in an urban freshwater wetland. *Wetl. Ecol. Manag.* 25, 159–175. doi: 10.1007/s11273-016-9507-x

Weisser, W. W., Roscher, C., Meyer, S. T., Ebeling, A., Luo, G., Allan, E., et al. (2017). Biodiversity effects on ecosystem functioning in a 15-year grassland experiment: patterns, mechanisms, and open questions. *Basic Appl. Ecol.* 23, 1–73. doi: 10.1016/j.baae.2017.06.002

Weragoda, S. K., Jinadasa, K. B. S. N., Zhang, D. Q., Gersberg, R. M., Tan, S. K., Tanaka, N., et al. (2012). Tropical application of floating treatment wetlands. *Wetlands* 32, 955–961. doi: 10.1007/s13157-012-0333-5

Wu, P., Zhang, H., Cui, L., Wickings, K., Fu, S., and Wang, C. (2017). Impacts of alpine wetland degradation on the composition, diversity and trophic structure of soil nematodes on the Qinghai-Tibetan plateau. *Sci. Rep.* 7:837. doi: 10.1038/s41598-017-00805-5

Xi, L., Chen, S., Bian, H., Peng, Z., Niu, Y., and Li, Y. (2023). Organic carbon release from litter decomposition of woody and herbaceous plants in the Dongting Lake wetlands: a comparative study. *Ecohydrol. Hydrobiol.* 23, 408–419. doi: 10.1016/j.ecohyd.2023.06.003

Xiang, W., Xiao, X., and Xue, J. (2020). Purification effect and microorganisms diversity in an *Acorus calamus* constructed wetland on petroleum-containing wastewater. *Environ. Pollut. Bioavailab.* 32, 19–25. doi: 10.1080/26395940.2019.1711200

Xiu, L., Yan, C., Li, X., Qian, D., and Feng, K. (2019). Changes in wetlands and surrounding land cover in a desert area under the influences of human and climatic factors: a case study of the Hongjian Nur region. *Ecol. Indic.* 101, 261–273. doi: 10.1016/j.ecolind.2019.01.025

Xu, X., Xie, Y., Qi, K., Luo, Z., and Wang, X. (2018). Detecting the response of bird communities and biodiversity to habitat loss and fragmentation due to urbanization. *Sci. Total Environ.* 624, 1561–1576. doi: 10.1016/j.scitotenv.2017.12.143

Xue, Z., Lyu, X., Chen, Z., Zhang, Z., Jiang, M., Zhang, K., et al. (2018). Spatial and temporal changes of wetlands on the Qinghai-Tibetan plateau from the 1970s to 2010s. *Chin. Geogr. Sci.* 28, 935–945. doi: 10.1007/s11769-018-1003-1

Yan, J., Wang, L., Hu, Y., Tsang, Y. F., Zhang, Y., Wu, J., et al. (2018). Plant litter composition selects different soil microbial structures and in turn drives different litter decomposition pattern and soil carbon sequestration capability. *Geoderma* 319, 194–203. doi: 10.1016/j.geoderma.2018.01.009

Yang, J. S., Liu, J. S., Hu, X. J., Li, X. X., Wang, Y., and Li, H. Y. (2013). Effect of water table level on CO_2, CH_4 and N_2O emissions in a freshwater marsh of Northeast China. *Soil Biol. Biochem.* 61, 52–60. doi: 10.1016/j.soilbio.2013.02.009

Yao, J., Sánchez-Pérez, J. M., Sauvage, S., Teissier, S., Attard, E., Lauga, B., et al. (2017). Biodiversity and ecosystem purification service in an alluvial wetland. *Ecol. Eng.* 103, 359–371. doi: 10.1016/j.ecoleng.2016.02.019

You, H., Xu, L., Liu, G., Wang, X., Wu, Y., and Jiang, J. (2015). Effects of inter-annual water level fluctuations on vegetation evolution in typical wetlands of Poyang Lake, China. *Wetlands* 35, 931–943. doi: 10.1007/s13157-015-0684-9

Yu, Z., Jiang, M., and Chen, F. (2023). Wetland science, ecosystem services and protection actions in China. *Fund. Res.* 3, 831–832. doi: 10.1016/j.fmre.2023.09.001

Zedler, J. B., and Kercher, S. (2005). Wetland resources: status, trends, ecosystem services, and restorability. *Annu. Rev. Environ. Resour.* 30, 39–74. doi: 10.1146/annurev.energy.30.050504.144248

Zhang, G., Tian, J., Jiang, N., Guo, X., Wang, Y., and Dong, X. (2008). Methanogen community in Zoige wetland of Tibetan plateau and phenotypic characterization of a dominant uncultured methanogen cluster ZC-I. *Environ. Microbiol.* 10, 1850–1860. doi: 10.1111/j.1462-2920.2008.01606.x

Zhang, C.-B., Wang, J., Liu, W.-L., Zhu, S.-X., Ge, H.-L., Chang, S. X., et al. (2010). Effects of plant diversity on microbial biomass and community metabolic profiles in a full-scale constructed wetland. *Ecol. Eng.* 36, 62–68. doi: 10.1016/j.ecoleng.2009.09.010

Zhang, Q., Wang, Z., Xia, S., Zhang, G., Li, S., Yu, D., et al. (2022). Hydrologic-induced concentrated soil nutrients and improved plant growth increased carbon storage in a floodplain wetland over wet-dry alternating zones. *Sci. Total Environ.* 822:153512. doi: 10.1016/j.scitotenv.2022.153512

Zhang, Y., Xu, H., Chen, H., Wang, F., and Huai, H. (2014). Diversity of wetland plants used traditionally in China: a literature review. *J. Ethnobiol. Ethnomed.* 10, 1–19. doi: 10.1186/1746-4269-10-72

Zhao, Q. Q., Bai, J. H., Jia, J., Zhang, G. L., Wang, J. N., and Gao, Y. C. (2022). The effects of drainage on the soil fungal Community in Freshwater Wetlands. *Front. Ecol. Evol.* 10:837747. doi: 10.3389/fevo.2022.837747

Zhao, X. S., and Liu, Y. B. (2016). Evapotranspiration partitioning and response to abnormally low water levels in a floodplain wetland in China. *Adv. Meteorol.* 2016, 1–11. doi: 10.1155/2016/3695427

Zou, Y., Wang, G., Grace, M., Lou, X., Yu, X., and Lu, X. (2014). Response of two dominant boreal freshwater wetland plants to manipulated warming and altered precipitation. *PLoS One* 9:e104454. doi: 10.1371/journal.pone.0104454

Zou, J., Ziegler, A. D., Chen, D., McNicol, G., Ciais, P., Jiang, X., et al. (2022). Rewetting global wetlands effectively reduces major greenhouse gas emissions. *Nat. Geosci.* 15, 627–632. doi: 10.1038/s41561-022-00989-0

frontiers | Frontiers in Microbiology

TYPE Original Research
PUBLISHED 22 May 2024
DOI 10.3389/fmicb.2024.1391553

OPEN ACCESS

EDITED BY
Huai Li,
Chinese Academy of Sciences (CAS), China

REVIEWED BY
Chenwei Zheng,
Arizona State University, United States
Shangqi Xu,
Anhui Normal University, China

*CORRESPONDENCE
Na Liu
✉ liuna@jnu.edu.cn

RECEIVED 26 February 2024
ACCEPTED 02 May 2024
PUBLISHED 22 May 2024

CITATION
Li J, Hong M, Lv J, Tang R, Wang R, Yang Y and Liu N (2024) Enhancement on migration and biodegradation of *Diaphorobacter* sp. LW2 mediated by *Pythium ultimum* in soil with different particle sizes. *Front. Microbiol.* 15:1391553. doi: 10.3389/fmicb.2024.1391553

Enhancement on migration and biodegradation of *Diaphorobacter* sp. LW2 mediated by *Pythium ultimum* in soil with different particle sizes

Jialu Li[1,2], Mei Hong[1,2], Jing Lv[1,2], Rui Tang[1,2], Ruofan Wang[1,2], Yadong Yang[3] and Na Liu[4]*

[1]Key Laboratory of Groundwater Resources and Environment, Ministry of Education, College of New Energy and Environment, Jilin University, Changchun, China, [2]National and Local Joint Engineering Laboratory for Petrochemical Contaminated Site Control and Remediation Technology, Jilin University, Changchun, China, [3]School of Environmental Science and Engineering, Jiangsu Engineering Research Center of Biomass Waste Pyrolytic Carbonization & Application, Yancheng Institute of Technology, Yancheng, China, [4]Department of Ecology, College of Life Science and Technology, Jinan University, Guangzhou, Guangdong, China

Introduction: The composition and structure of natural soil are very complex, leading to the difficult contact between hydrophobic organic compounds and degrading-bacteria in contaminated soil, making pollutants hard to be removed from the soil. Several researches have reported the bacterial migration in unsaturated soil mediated by fungal hyphae, but bacterial movement in soil of different particle sizes or in heterogeneous soil was unclear. The remediation of contaminated soil enhanced by hyphae still needs further research.

Methods: In this case, the migration and biodegradation of *Diaphorobacter* sp. LW2 in soil was investigated in presence of *Pythium ultimum*.

Results: Hyphae could promote the growth and migration of LW2 in culture medium. It was also confirmed that LW2 was able to migrate in the growth direction and against the growth direction along hyphae. Mediated by hyphae, motile strain LW2 translocated over 3 cm in soil with different particle size (CS1, 1.0–2.0 mm; CS2, 0.5–1.0mm; MS, 0.25–0.5 mm and FS, <0.25 mm), and it need shorter time in bigger particle soils. In inhomogeneous soil, hyphae participated in the distribution of introduced bacteria, and the total number of bacteria increased. *Pythium ultimum* enhanced the migration and survival of LW2 in soil, improving the bioremediation of polluted soil.

Discussion: The results of this study indicate that the mobilization of degrading bacteria mediated by *Pythium ultimum* in soil has great potential for application in bioremediation of contaminated soil.

KEYWORDS

bacterial migration, growth direction, heterogeneous soil, hyphae, biodegradation of phenanthrene

1 Introduction

Soil is a major environmental sink for hydrophobic organic contaminants (HOCs) (Nam et al., 1998; Collins et al., 2013). HOCs tend to sorb to soil particulates due to their low solubility (Zeng et al., 2010). Wild and Jones (1995) reported that over 90% PAH burden resided in soil in UK, and the complex soil structure causes non-homogeneous distribution

of HOCs (Gu et al., 2017). Biodegradation is often considered as one of the effective methods for contaminated soil remediation. Solids in soil are always arranged in a very complex spatial manner and form tortuous pore spaces. Soil heterogeneity can arise and persist without being mixed well. The bacterial transport in unsaturated soils across macro-scale distance (>10 mm) was primarily driven by water flow and reduced with decreasing water contents and water flow velocities (Or et al., 2007). Griffin and Quail (1968) reported that no movement of *Pseudomonas aeruginosa* was detected at water contents below 28%. Moreover, motile strains only spread 6.4 mm in vertical direction in soil with water content of 13.3% (w/w) after 14 days (Turnbull et al., 2001). Bosma et al. (1996) calculated the average distances between bacterial microcolonies in soil at a range of 50–100 μm. Effective contact between microorganisms and pollutants is a prerequisite for biodegradation. The difficulty of microbial migration in complex soil environments limits the removal of pollutants.

The interactions between fungi and bacteria widely prevail in a variety of habitats, especially in soil (de Menezes et al., 2017; Deveau et al., 2018). Kohlmeier et al. (2005) reported that hydrophilic *Fusarium oxysporum* Fo47 bridged air gaps and provided water channels for the migration of *Achromobacter* sp. SK1. After that, several literature studies reported the bacterial movement mediated by hyphae. Warmink and Elsas (2009) found that the attached soil bacteria moved with growing hyphae and formed biofilms around hyphae. Effects of bacterial type three secretion system and hyphal surface receptors on bacterial migration along hyphae also have been investigated (Vila et al., 2016; Yang et al., 2016). Worrich et al. (2016) proposed that fungal mycelia could maintain the microbial growth and biodegradation even at low osmotic and matric potentials. In addition to microorganisms, soil properties were also important factors affecting bacterial migration. Nazir et al. (2010a) found that *Lyophyllum* sp. strain Karsten alleviated pH pressure in acid soil and enhanced bacterial survival. Higher moisture content and pH in acidic soil are beneficial for hyphal-mediated bacterial migration (Yang et al., 2018).

Except for pH and moisture content, soil particle size was also an important soil characteristic, but the bacterial migration mediated by mycelium in soils with different particle sizes was still unclear. Particle size of natural soil was uneven, and behavior of motile bacteria mediated by mycelium in heterogeneous soil was also unknown. Research on the enhanced biodegradation of phenanthrene in contaminated soil by hyphae is also very limited. In previous study, we have demonstrated that naphthalene- and phenanthrene-degrading *Diaphorobacter* sp. LW2 was able to migrate across air gaps with the hyphae of *Pythium ultimum* (Li et al., 2022). We chose these two microorganisms to investigate the bacterial migration in homogeneous and heterogeneous soil with different particle sizes mediated by mycelium, as well as the biodegradation of phenanthrene-contaminated soil with different particle sizes. First, the effect of *Pythium ultimum* on the biodegradation and growth of LW2 was studied. Next, the migration behavior of LW2 with fresh or old hyphae was studied, and the diffusion and distribution of bacteria introduced at the hyphal tip and end (growth starting point) were investigated. Then, bacterial migration mediated by hyphae in soil with different particle sizes was examined, and the distribution of introduced bacteria in heterogeneous soil in the presence of mycelium was explored. Finally, the effect of additional *Pythium ultimum* on the biodegradation of phenanthrene in soil with different particle sizes by LW2 was studied. We hope that the experimental results provided the theoretical basis for the bioremediation of contaminated soil.

2 Materials and methods

2.1 Experimental materials

2.1.1 Organisms

Fungi, oomycete *Pythium ultimum,* with hydrophilic mycelia (collection number 37386) was purchased from the China Agricultural Culture Collection of China (Beijing, China). *Pythium ultimum* was cultivated at 28°C on solid medium of potato dextrose agar (PDA).

Naphthalene- and phenanthrene-degrading bacteria, *Diaphorobacter* sp. LW2, were isolated from the aged PAH-contaminated soil and had been proven to be able to move via *Pythium ultimum* mycelia. LW2 was cultivated in Luria–Bertani (LB) medium, harvested, and washed three times with 0.01 M PBS. Bacterial suspension used in mobilization experiment contained approximately 1.21×10^8 CFU ml^{-1}. Bacteria were quantified as colony forming units (CFUs) on LB solid medium containing 200 mg L^{-1} actidione to prevent fungal growth.

2.1.2 Soil

Experiment soil was collected from Shandong province, China, and was sieved into four types according to granular sizes: coarse sand-1 (CS1, 1.0–2.0 mm), coarse sand-2 (CS2, 0.5–1.0 mm), medium sand (MS, 0.25–0.5 mm), and fine sand (FS, <0.25 mm). The pH values of CS1, CS2, MS, and FS were found to be 8.05–8.21. The initial water content and organic carbon content of these samples are shown in Supplementary Table S1. All soil samples were sterilized for three times with 30 min each time to ensure sterility. Soil samples were mixed with 5% (w/w) wheat bran to support hyphal growth and were adjusted to be with water content of ~10 wt%.

2.2 Biodegradation and growth of LW2 affected by *Pythium ultimum* hyphae

Pythium ultimum growing on PDA plates was inoculated into 24-well plates. In total, 1.5 mL PDB medium was added in each hole. After 3 days, the mycelium slices with a diameter of approximately 1.6 cm and a dry weight of approximately 2 mg were obtained. The mycelium was washed with PBS buffer three times, and part of it was used as inactivated mycelium after being autoclaved at 121°C for 15 min.

Due to the low solubility of phenanthrene in water, a concentration of 1 mg L^{-1} of phenanthrene was set in this experiment to avoid the interference of undissolved phenanthrene with bacterial growth and mycelium adsorption tests. Overall, 0.5 mL bacterial suspension and two inactivated or non-inactivated mycelium pieces were added to a sterile brown glass bottle containing 9.5 mL phenanthrene-MSM medium and cultured for 72 h at 25°C. Treatments with only the addition of bacteria or mycelium were considered as the controls. Overall, 0.5 mL PBS buffer was added to the groups without LW2 to avoid volume differences. The whole residual content of phenanthrene and OD_{600} of LW2 were tested at 0, 2, 4, 8, 10, 12, 24, 48, and 72 h. The concentration in water and whole residual content of phenanthrene were examined in groups adding only mycelium.

The extraction of phenanthrene is consistent with the report by Gu et al. (2016). The concentration of phenanthrene was measured using high-performance liquid chromatography (HPLC) (Li et al., 2022).

2.3 Influence of fresh or old hyphae on bacterial migration along with hyphae

Fresh (newly grown) or old (grown over 7 days) hyphae were inoculated in Petri dishes containing PDA, and the diameter of mycelium coverage was regarded as an evaluation indicator for the hyphal growth. Bacterial migration along with fresh or old hyphae was tested. In brief, *Pythium ultimum* was introduced on the PDA disk of left side (Figure 1A) and had fully overgrown the system (approximately 4 days), and 10 μL of bacterial suspension was added. For the system that was pre-inoculated before 11 days, hyphae with excessive growth for 7 days were considered as old hyphae. After LW2 inoculation for 3 days, bacterial cells on agar disks at P1 and P2 positions were measured. Fungus-associated bacteria were treated by both vortexing for 60 s and ultrasonication of two times for 30 s, as previously reported (Wick et al., 2007). After appropriately diluted, the bacterial suspension was spread on LB agar containing 200 mg L^{-1} actidione following incubation, and colonies were enumerated. All tests were set up with triplicates.

2.4 Bacterial migration starting from the end or tip of the hyphae

The effect of bacterial inoculation location on the diffusion and distribution of LW2 in *Pythium ultimum* mycelium was investigated. Specifically, *Pythium ultimum* was introduced in the center of PDA plates (diameter: 150 mm), and 100 μL of bacterial suspension was added at center or edge of the plate when the hyphae reached the edge of the plate. The bacteria inoculated at the center of the plate were equivalent to being introduced at the end of the hyphae, while the bacteria inoculated at the edge of the plate corresponded to being introduced from the tip of the hyphae. At set times (2 h and 48 h after bacterial inoculation), small samples were recovered, by punching out, from the marked sites, as shown in Figure 1B. All samples were treated to quantify bacterial cells, as described in *2.3*. The adjacent sampling positions were spaced 10 mm apart, with an angle of 120 ° in the upper, left, and right directions. For each experimental treatment, three replicates were used. Controls received no bacteria or *Pythium ultimum*.

2.5 The bacterial mobilization by *Pythium ultimum* in soil with different particle size

The bacterial mobilization via *Pythium ultimum* mycelia was studied in laboratory systems mimicking air-filled soil environment, as shown in Figure 1C. The ends of the columns (length: 20 cm; diameter: 1.6 cm) were closed with breathable silicone test tube plugs, and 6.0 g glass beads (diameter: 0.4 cm) were placed at the bottom of the columns in purpose of supporting round PDA disks (diameter: 1.6 cm; thickness: 0.2 cm) covered by mycelium. Overall, 100 μL of bacterial suspension was inoculated onto the surface of PDA disks at the bottom simultaneously. The columns were filled with soil of different particle sizes, 1.5 cm or 3 cm thick, and 0.5 g of quartz sand above and below was to separate the PDA disks from the experimental soil. The glass columns were placed at constant temperature and humidity for inoculation, and the bacteria around upper glass beads were quantified. Identical set-ups without fungi or bacteria served as controls. All experiments were at least conducted in triplicates.

2.6 The bacterial distribution mediated by *Pythium ultimum* in heterogeneous soil

To investigate the bacterial distribution with hyphae in soil with different sizes, similar set-up (Figure 1C) has been used. Filled soil in the columns had a little difference; CS1, CS2, MS, and FS were combined in pairs with a 1.5 cm layer of each medium. *Pythium ultimum* was inoculated on the bottom PDA disks. The top PDA disks were removed

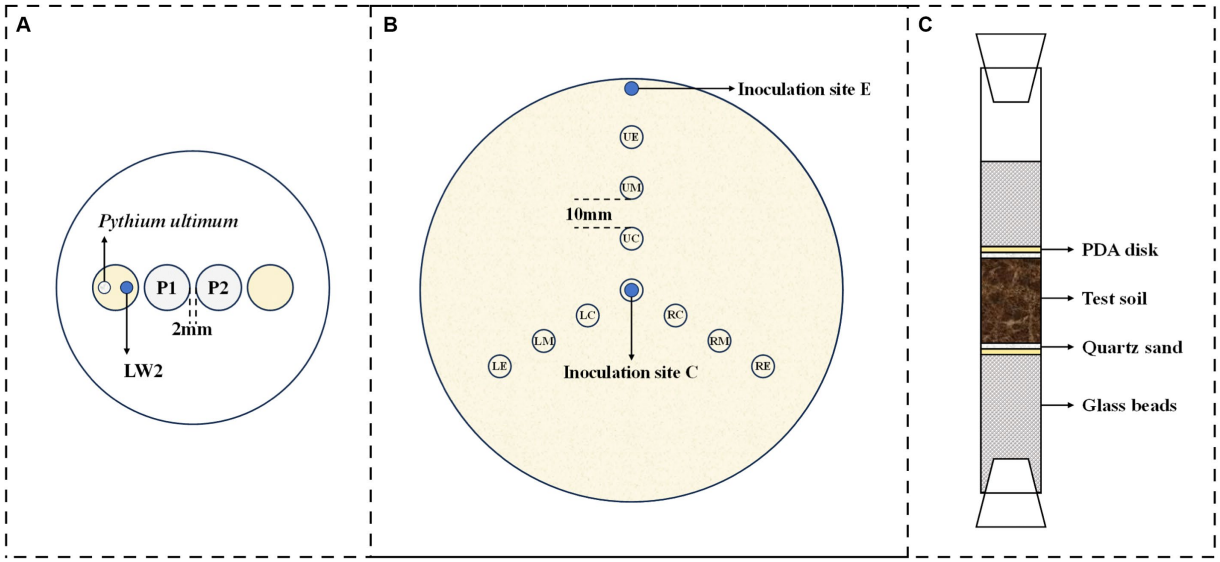

FIGURE 1
Schematic diagrams for microorganism migration experiments (**(A)**, migration of *Diaphorobacter* sp. LW2 affected by fresh or old *Pythium ultimum* hyphae; **(B)**, bacterial distribution in mycelial network; and **(C)**, bacterial migration in soil).

throughout the soil after the growth of hyphae, and 500 μL of bacterial suspension was introduced from above. After 7 days of incubation at room temperature, the number of bacterial cells in soil of upper or lower layers was examined. Samples were suspended in PBS, vortexed (1 min, three times, with 30-s intervals), diluted, and spread on LB agar plates (Yang et al., 2018). Colonies were enumerated and CFU numbers were calculated. Experiments were performed in triplicates. The non-fungal or non-bacterial controls were examined similarly.

2.7 Biodegradation of phenanthrene in soil with different particle sizes by LW2 affected by *Pythium ultimum*

The sterilized soil of different particle sizes with a dry weight of 1 kg was accurately weighed in a sterile beaker, and a small part of it was added with 10 mL of phenanthrene stock solution (5 g L^{-1} dissolved in acetone). The soil was evenly mixed and placed in the fume hood. After the acetone was completely volatilized, it was mixed with the remaining uncontaminated soil and placed in the fume hood for more than 1 week. Due to the loss in the treatment process, the phenanthrene concentration in CS1, CS2, MS, and FS was 47.78, 46, 78, 48, 14, and 48.13 mg kg^{-1}, respectively.

Except that the filled medium was replaced with 5 g contaminated soil, and the set-ups used were consistent with 2.5. *Pythium ultimum* was inoculated on the bottom agar, and a 100-μlL bacterial suspension was added from the top. Columns without inoculating microorganisms and only adding hyphae or bacteria were regarded as the control groups. The columns were cultured in dark at 25°C and destructively sampled on days 7, 14, 21, 28, and 35 to test the residual phenanthrene and bacterial count in the soil. More than three parallel samples were set at each sampling point in all experimental groups. Phenanthrene extracted was from soil according to the description by Chen and Ding (2012). The concentration of phenanthrene in samples was measured using HPLC.

2.8 Statistical analysis of the data

At least three parallel samples were performed for all experiments. All data were subjected to analysis of variance (ANOVA) using SPSS 25. A p-value<0.05 indicated that data were significant.

3 Results

3.1 Biodegradation of phenanthrene in culture medium by LW2 enhance using *Pythium ultimum*

Figure 2 shows the content of residual phenanthrene and the absorbance of solution at a wavelength of 600 nm. Phenanthrene was significantly removed inoculated with LW2 (p<0.05), and the results of additional LW2 with sterilized or unsterilized and without hyphae showed no obvious difference (p>0.05). Over 87% of phenanthrene was removed within 12 h, and the residual phenanthrene was less than 13 μg L^{-1} at 72 h. The unsterilized or sterilized hyphae promoted the growth of LW2, with OD_{600nm} of 0.170 and 0.067 at 72 h, respectively. Groups without LW2, the content of phenanthrene decreased from the initial 941.41 μg L^{-1} (unsterilized hyphae) and 946.26 μg L^{-1} (sterilized hyphae) to 802.57 μg L^{-1} and 800.15 μg L^{-1}. *Pythium ultimum* was unable to degrade phenanthrene. The decrease in phenanthrene was possibly due to photolysis or volatilization.

3.2 Migration of LW2 via fresh or old hyphae

Factors that the inoculum was fresh or old might affect the growth of hyphae. While introducing the growth of old hyphae, the diameter variation of the coverage area of mycelium is shown in Table 1. The younger inoculum had coverage radius of 19 ± 2.24 mm at 24 h, which was larger than that was formed by old hyphae. Moreover, after 3 days of incubation, both mycelia grew over the 90 mm Petri dishes. Fresh hyphae adapted to the environment and grew faster than aged hyphae.

It has been reported that hyphae might release nutrients as its growth may exert positive or negative effects on the bacterial movement at mycelium (Haq et al., 2018). We thus tested the migration of LW2 at newly grown hyphae and hyphae that has grown for more than a week using the set-ups, as shown in Figure 1A. Figure 3 showed the number of bacterial colonies detected on two MSM agar blocks located closer to the bacterial inoculation site (P1) and slightly further away (P2). Fresh or old hyphae showed no significant effect on the number of detected LW2 at P1 and P2 positions (P>0.05). The detected LW2 at P1 was approximately 5–6 × 10^7 CFU ml^{-1} and 4–5 × 10^7 CFU ml^{-1} at P2. The amount of LW2 was all in the same

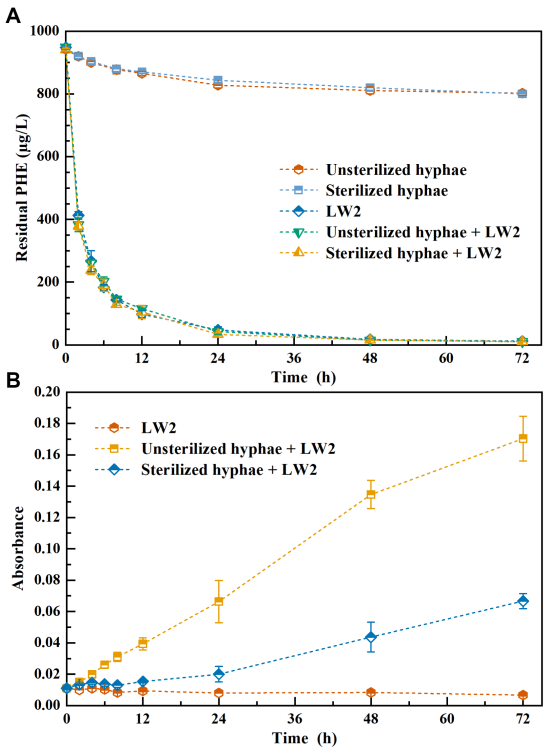

FIGURE 2
The residual phenanthrene **(A)** and the absorbance of solution at a wavelength of 600 nm **(B)** while addition of LW2，sterilized, or unsterilized hyphae and both of them.

order of magnitude. No bacterial migration was detected in the absence of hyphae.

3.3 The diffusion and distribution of LW2 inoculated at the end or tip of *Pythium ultimum* hyphae

After the introduction of hyphae in the center of 150 mm PDA plates for 4 days, the mycelium covered the entire dishes. Following that, bacterial suspensions were inoculated at the end or tip of *Pythium ultimum* hyphae to investigate the diffusion and distribution of LW2 in continuous hyphae. At set times (2 h and 48 h after bacterial inoculation), samples at positions shown in Figure 1B were collected. Colonies were enumerated, and contour maps of lg CFU were drawn to analyze the distribution of LW2 in mycelium (Figure 4). When inoculating LW2 at the center position (Figures 4A,B), there was no significant difference in the detection results in the upper, lower left, and lower right directions at the same distance from the inoculation point ($p > 0.05$), and the bacterial colony numbers were all in the same order of magnitude. There were significant differences in the detection results at different distances from the bacterial inoculation site ($p < 0.001$). The detected colonies in the central position at 2 h was much greater than that in the middle and edge positions, which were 8.32–8.84 and 414–504 times higher, respectively. Over time and bacterial reproduction, CFUs in all positions increased, and the number of bacteria in the center position was approximately 2.2–2.4 and 23.73–25.36 times of that at the middle and edge positions for 48 h.

When LW2 was inoculated at the tip of the mycelium, the number of bacteria detected above was significantly greater than that in the left and right directions ($p < 0.05$), but the results in the left and right directions were not similar ($p > 0.05$). The inoculum diffused from the inoculation point to the surrounding area, but the number of bacteria detected at sites LM and RM was greater than that at positions LC and RC that was closer to the inoculation site ($p < 0.05$). The detection results at 2 h and 48 h were 108–170 and 6.8–9.1 times higher than those at the center of the left and right directions, respectively. With the absence of hyphae, no bacterial migration was detected regardless of where the bacteria were inoculated on the plate.

3.4 Mobilization of LW2 mediated by *Pythium ultimum* throughout soil of different particle sizes

It has been proven that the strain LW2 could migrate along *Pythium ultimum* hyphae across air gaps within a centimeter range. The ability of LW2 to migrate in soil mediated by hyphae would be a favorable factor for its application in contaminated soil remediation, and we reasoned that the migration of LW2 in soil of different particle size also varied. Therefore, the travel of LW2 through coarse sand (CS1 and CS2), medium sand (MS), and fine sand (FS) in the presence of mycelium was studied. Figure 4 shows photos of columns filled with CS1, CS2, and MS cultured for 1 week. The hyphae passed through soil layers with a height of 1.5 cm within 1 week but did not pass through FS of the same height, which finally did it at the third week (Supplementary Figure S2). In the first week, *Pythium ultimum* failed to pass through the soil layers of various particle sizes with a height of 3 cm but crossed the 3 cm soil layers of CS1 and CS2 in the second week. Moreover, the hyphae in the lower soil pores could be observed in CS1 (Figures 5D,E) and MS (Supplementary Figures S1C,D) columns. Over the culturation time, *Pythium ultimum* went throughout MS and FS soil layers of a height of 3 cm at third and fourth weeks (Supplementary Figures S2A,C).

TABLE 1 The coverage range of the hyphal network when the inoculum was fresh and old hyphae.

Time / h	Radius of hyphae /mm	
	Fresh hyphae	Old hyphae
24	19.00 ± 2.24	15.00 ± 1.41
48	35.25 ± 0.56	34.63 ± 1.71

The bacteria that crossed through the filled soil via hyphae were examined. No bacteria were detected around the upper glass beads in controls. The existence of LW2 near the upper glass beads was ensured after inoculation for 2 weeks when hyphae had crossed 3 cm soil layers of CS1 and CS2 and 1.5 cm soil layers of MS. The bacteria crossing 1.5 cm thick soil layers were more than those of 3 cm and differed by approximately one order of magnitude (Table 2). In the columns filled with soil (at a height of 1.5 cm) of different particle sizes, the number of migrating bacteria detected was at a level of 10^{6}. Moreover, in 1.5 cm FS and 3 cm MS columns, hyphae at upper PDA disks were observed, and CFUs ($\times 10^{4}$) were 50.30 ± 4.19 and 18.30 ± 1.20. Mediated by *Pythium ultimum*, LW2 finally migrated over a distance of 3 cm in FS soil (<0.25 mm).

3.5 Distribution of LW2 in soil with different particle sizes

The effect of additional *Pythium ultimum* on the distribution of LW2 in homogeneous and heterogeneous soils was investigated. In soil columns of various sizes without *Pythium ultimum*, the number of bacteria detected in the lower soil layer was lower than that in the upper layer (as shown in Figures 6A,B). Soil particle size and heterogeneity significantly affected the number of LW2 in the upper- and lower-layer soil ($p < 0.05$). When the upper soil was CS1 and FS, the impact on the bacterial count in the upper soil was more significant ($p < 0.05$), and the diffusion of strain LW2 in CS1 and FS was limited. When the upper soil was MS, the influence on the bacterial count in the lower soil was more significant ($p < 0.05$). The CFU of strain LW2 in the lower soil was generally 10^{7}, while in homogeneous MS, the bacterial count in the lower soil is only 1.66×10^{8}. When the lower media were same, except for the case where the upper layer was FS, the larger the particle size difference between the upper and lower media, the more LW2 was intercepted by the upper layer.

With the presence of *Pythium ultimum*, the amount of bacteria significantly increased ($p < 0.05$), especially in the lower soil layer where the bacterial count increases by 2–3 orders of magnitude (Figures 6C,D). In columns filled with CS1 and CS2 in the upper layer, colonies from the upper layers were more than those from the lower layers. When the upper filled media was MS, the numbers of bacteria were similar in both layers, and when it was FS, 10 times bacterial cells in the lower soil layers existed compared with those in upper soils. The

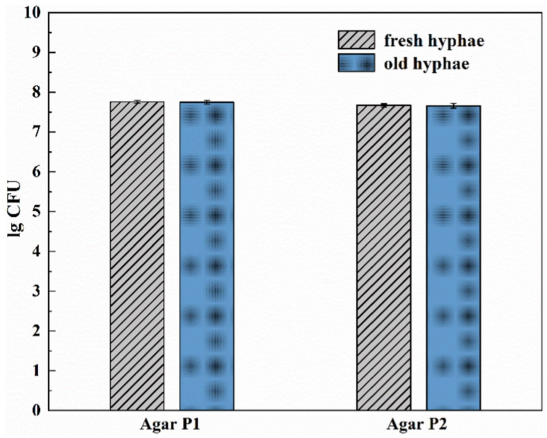

FIGURE 3
Amount of *Diaphorobacter* sp. LW2 migrated to agar P1 and P2 affected by fresh or old *Pythium ultimum* hyphae. Agar P1 and P2 were 2 mm and 12 mm away from the agar block inoculated with bacteria, respectively. Test of inoculation of LW2 when the hyphae just extended to the right PDA agar block was considered as fresh hyphae treatment. Test of inoculation of LW2 after the right agar grew full of hyphae and remained for 7 days was considered as old hyphae treatment.

presence of hyphae promoted the proliferation of LW2 and altered its distribution in soil.

3.6 Biodegradation of phenanthrene in soil with different particle sizes by LW2 enhance by *Pythium ultimum*

The removal of phenanthrene by LW2 in soils of different particle sizes and enhancement of *Pythium ultimum* were investigated. The initial concentrations of phenanthrene in CS1, CS2, MS, and FS-contaminated soil were slightly different ($p > 0.05$), with values of 47.78, 46.78, 48.14, and 48.13 mg kg^{-1}, respectively. The slight decrease ($p > 0.05$) of phenanthrene in soils without microorganisms might be related to the volatilization or photolysis. The addition of hyphae caused a decrease in phenanthrene, and the removal rates in CS1, CS2, MS, and FS were increased by 10.86, 10.57, 4.35, and 2.96%, respectively.

When LW2 was added to the soil, the residual amount of phenanthrene in CS1, CS2, MS, and FS after 21 days was 12.35, 12.74, 9.97, and 2.09 mg kg^{-1}, respectively. The content of phenanthrene in soil with different particle sizes significantly decreased ($p < 0.05$). After 35 days, the remaining phenanthrene in CS1, CS2, MS, and FS were 10.93, 10.81, 7.49, and 2.10 mg kg^{-1}, respectively. In liquid cultivation, LW2 almost completely degraded phenanthrene with the extension of culture time, but there was no significant change in phenanthrene for 21–35 days ($p > 0.05$). In addition, compared with 21 days, the amount of LW2 bacteria detected in soil decreased at 35 days, indicating that the physiological activity of LW2 was restricted. In the columns of *Pythium ultimum* and LW2, the residual phenanthrene in CS1, CS2, MS, and FS after 35 days was 1.35, 2.23, 2.55, and 1.41 mg kg^{-1}, respectively. Compared with treatment with only LW2, the removal rates of phenanthrene were increased by 20.05, 18.36, 10.28, and 1.44%, respectively. The mycelium significantly enhanced the degradation of phenanthrene by LW2 ($p < 0.05$). Compared with columns without hyphae, the content of phenanthrene in the soil treated with hyphae and LW2 continued to decrease for 2–35 days.

4 Discussion

4.1 The effect of *Pythium ultimum* on the growth of LW2

Strain LW2 grew and propagated using phenanthrene as the sole carbon source and energy source in the absence of hyphae. As the concentration of phenanthrene decreases, bacterial reproduction was restricted. In the presence of hyphae, degradation of phenanthrene showed no significant difference (P>0.05), but the biomass increased. Hyphae would secrete some compounds during its growth, and some of them could be utilized for bacterial growth (Boersma et al., 2010; Haq et al., 2018). Gandhi and Weete (1991) have been reported the production of polyunsaturated fatty acids such as arachidonic acid and eicosapentaenoic acid by *Pythium ultimum*, which could serve as nutrients for bacterial growth. The promoting effect of sterilized hyphae is slightly weaker, which is likely due to the high temperature accelerating the release of compounds secreted by hyphae, resulting in a decrease in the amount of nutrients added to the culture medium. *Pythium ultimum* hyphae could enrich and adsorb phenanthrene from solutions (Supplementary Figure S3). Furuno et al. (2012) found that phenanthrene could accumulate in *Pythium ultimum* lipid vesicles and be transported in hyphae. The adsorption of phenanthrene by *Pythium ultimum* hyphae and the promotion of bacterial growth are beneficial to the bioremediation of actual phenanthrene-contaminated soil.

4.2 Transport of LW2 by *Pythium ultimum* on PDA plate

We have demonstrated in previous studies that the strain LW2 could migrate within a centimeter range in Petri dishes through the water channels provided by *Pythium ultimum* (Li et al., 2022). In this study, we compared the migration of LW2 in fresh and old hyphae and found that the difference was very small. Warmink and Elsas (2009) reported that the migration of inoculant strains, *Dyella japonica* BS021 and *Burkholderia terrae* BS001, only occurred at the growing hyphal front of *Lyophyllum* sp. strain Karsten, and no bacterial translocation was observed along hyphae grown over a week at any directions. However, *Achromobacter* sp. SK1 was found to move at old hyphae of *Fusarium oxysporum* Fo47 during their interaction (Kohlmeier et al., 2005). Moreover, Yang et al. (2018) found that the strain BS001 was able to migrate along the old hyphae of *Lyophyllum* sp. strain Karsten while investigating its movement at various acid pH levels. The tropic movement of BS001 was due to its chemotactic response toward oxalic acid that *Lyophyllum* sp. strain Karsten exudated (Haq et al., 2018). In our experiment, the new and old hyphae showed similar impact on the migration of LW2. Meanwhile, no matter inoculum was introduced at the front or end of the hyphae, the bacterial

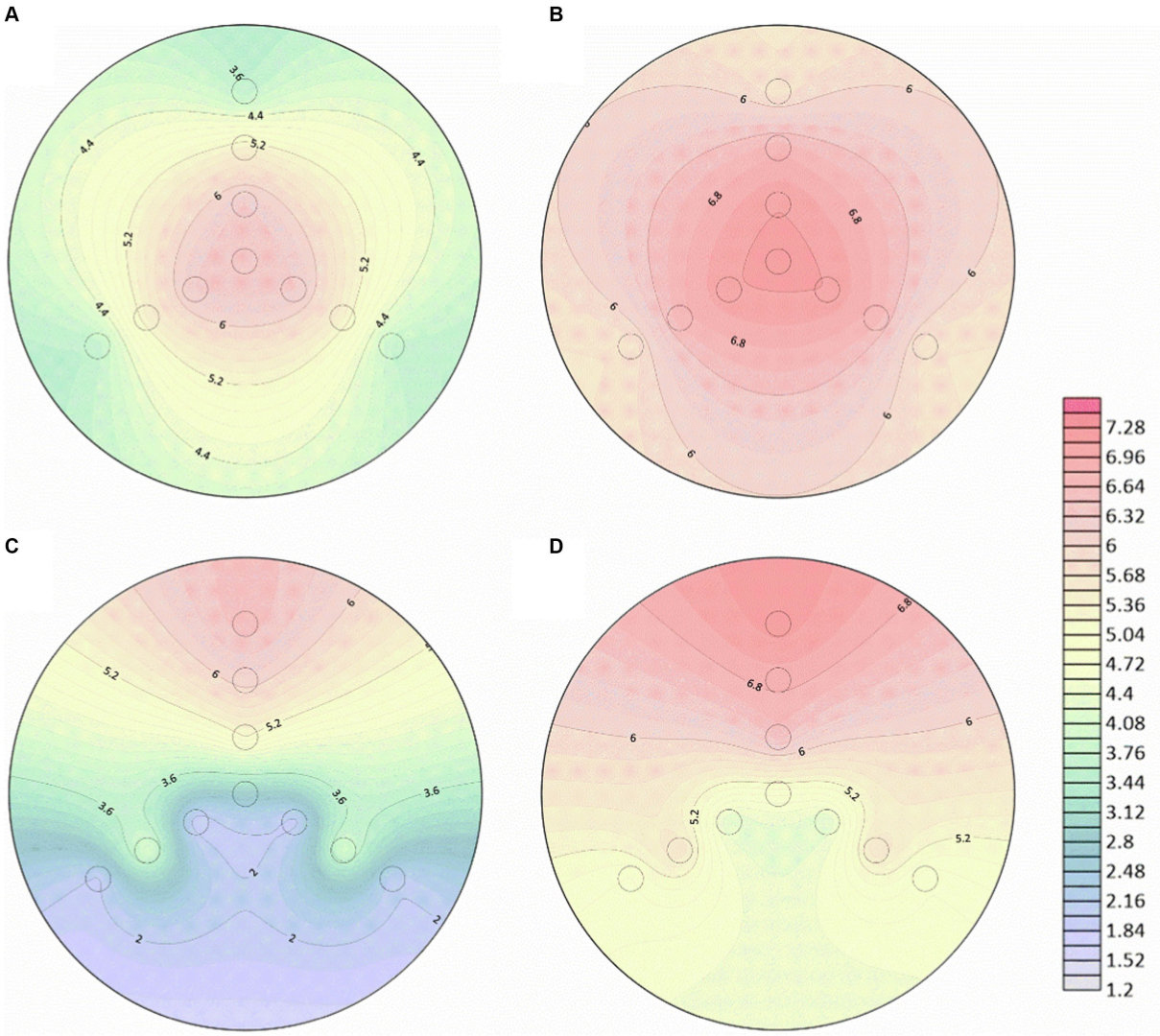

FIGURE 4
Number of bacterial cells at different positions in the mycelial network when *Diaphorobacter* sp. LW2 was inoculated at the starting position of mycelium growth **(A,B)** or hyphal tips **(C,D)**. The bacterial count test was located along the upper (U), left (L), and right (R) directions at an angle of 120 ° each. The edge (E), middle (M), and center (C) detection positions were 10 mm, 28 mm, and 46 mm away from and the hyphal inoculation point, respectively. **(A,C)** were results for 2 h; **(B,D)** were results for 48 h.

distribution in mycelial networks gradually became uniform over time. This was likely due to *Pythium ultimum* secreting different compounds, and LW2 did not receive special signal resulting its isotropic movement. The diffusion of bacterial LW2 along the mycelium in this article was largely related to the diffusion time and bacterial concentration, which was consistent with the research results by Wick et al. (2007).

The detection of bacteria in the opposite direction of mycelial growth proved that LW2 that translocated via the liquid channels provided by hyphae along or against the direction of mycelium growth. The number of bacteria detected at position LM and RM for LW2 was greater than that at position LC and RC closer to the hyphal inoculation location (Figures 4C,D). Overall, hyphae grew radially from the inoculation site to the surrounding area on PDA plates. The intersection of hyphae was relatively less near the inoculation site but increased with hyphal growth, and the water channels formed by the liquid film around the hyphae were interconnected (Heaton et al., 2012). Therefore, fewer bacteria migrated to position LC and RC but increased with time.

Currently, several different mechanisms have been reported by which hyphae enhance the migration of moving bacteria. For hydrophobic hyphae, bacteria anchor on the surface of the hyphae through capillary forces, van der Waals forces, and cross-linking forces and passively migrate as the hyphae grow and elongate (Gu et al., 2017). Bacteria may also attach to the surface of hyphae using the organic matter secreted by the hyphae as a carbon source and energy source for growth and reproduction and form biofilms on hyphae and passively migrate with fungal growth. With this mechanism, bacteria could migrate only when inoculated at the tip of hyphae, and migration occurred along the direction of hyphal growth (Frey-Klett et al., 2007; Warmink and Elsas, 2009; Nazir et al., 2010a,b). For hydrophilic hyphae, a liquid film was wrapped around it, and moving bacteria could actively migrate along the water channel based on their

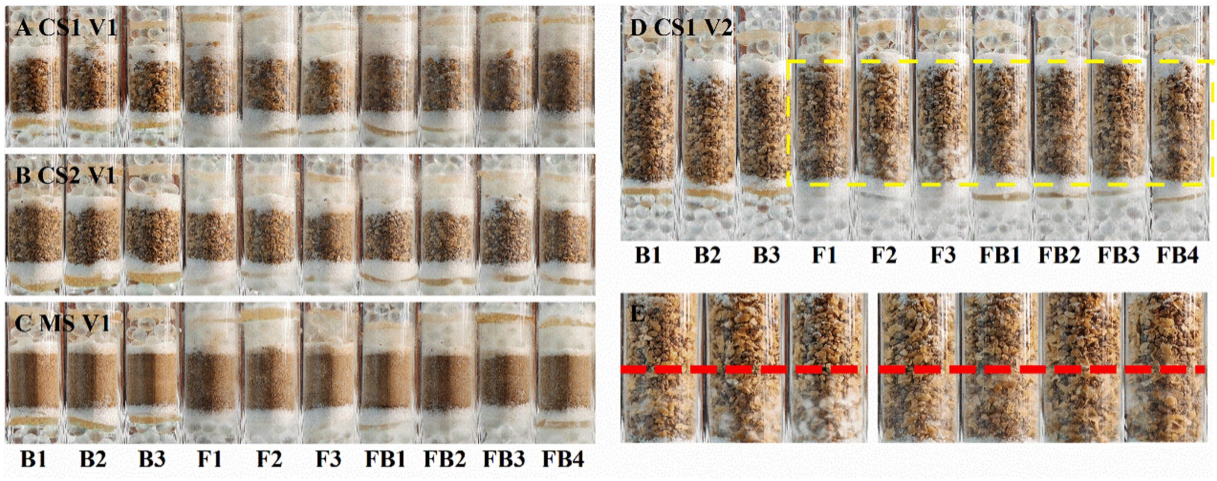

FIGURE 5
Photos of glass columns filled with soil of different particle sizes inoculated with LW2 and *Pythium ultimum* after culturation for 1 week. "FB" represented column inoculated with LW2 and *Pythium ultimum*. "F" and "B" were controls without bacteria or hyphae. **(A,C)** were photos of columns filled with CS1 (coarse sand 1, 1–2 mm), CS2 (coarse sand 2, 0.5–1 mm), and MS (medium sand, 0.25–0.5 mm) with a height of 1.5 cm. **(D)** showed CS1 columns with 3 cm soil layer. **(E)** was an enlarged image of the yellow dashed area in **(D)**. White hyphae could be clearly observed below the red dashed line in **(E)**. *Pythium ultimum* or *Diaphorobacter* sp. LW2 was inoculated onto the agar below the soil layer.

TABLE 2 The number of *Diaphorobacter* sp. LW2 crossing through soil with different particle sizes and thicknesses mediated by *Pythium ultimum*.

Soil thickness	CS1	CS2	MS	FS
1.5 cm	269.33 ± 18.79^{a}	436.67 ± 40.78^{a}	165.67 ± 11.56^{a}	50.30 ± 4.19^{b}
3 cm	41.37 ± 5.77^{a}	56.40 ± 6.89^{a}	18.30 ± 1.20^{b}	7.47 ± 0.95^{c}

a, b, and c were the results measured after 2, 3, or 4 weeks of cultivation, respectively (CFU, ×10 4).

own mobility (Kohlmeier et al., 2005; Wick et al., 2007). *Diaphorobacter* sp. LW2 can be detected along the growth direction or in the opposite direction of *Pythium ultimum* hyphae, indicating that LW2 can migrate in accordance with the "inherent mobility hypothesis."

4.3 Mobilization of LW2 by *Pythium ultimum* mycelium in soil of different particle sizes

The moisture content of experimental soil was appproximately 10%, and the saturation was in range of 15.7 to 20.8%. The discontinuous distribution of water in the soil limits the active migration of bacteria. The diffusion of bacteria in soil usually only occurred when the soil moisture was abundant and the water potential was > −0.05 MPa (Gülez et al., 2010). The water potentials for CS1, CS2, MS, and FS were −2.38, −2.45, −3.07, and −3.07 MPa, which did not meet this limitation. Therefore, LW2 has not been detected at the top in the absence of hyphae.

When crossing soil layers of different particle sizes in hyphae, the amount of mobilized bacteria reduced with the decrease of particle size, with the exception of CS1. Kravchenko et al. found that, when the initial water contents were relatively low, *E. coli* introduced into 4–6 mm soil aggregates and preferred to distribute in pores of 15 μm than pores >100 μm (Kravchenko et al., 2013). The introduced microorganisms tended to inhabit in the liquid habitat maintained by capillary force at the gaps and particle contacts of the medium. LW2 existed not only in the liquid membrane of the hyphae but also in the liquid habitat at the pores of the soil after migrating with the *Pythium ultimum*. It has been reported that microorganisms often colonize at the interface or interior of the aggregates in soil (Xia et al., 2022). Moreover, the bacteria would migrate to other locations via mycelium networks after proliferation. CS1 columns provided less liquid habitat compared with soils with smaller particle size, leading to fewer opportunities for microbial colonization. As a result, the number of bacteria migrating to the top in the CS1 column was less than in CS2. In the columns packed with soils of sizes <1 mm, the positive correlation between the number of migrating bacteria and the particle size was possibly due to mycelial growth. In soils with smaller particle sizes, hyphae need to bypass further paths to reach the same distance, which takes longer.

LW2 succeeded translocation in soil by the mobilization of *Pythium ultimum* and took longer time in soil of smaller particle. The migration of bacteria in unsaturated soil at a macroscopic scale (>10 mm) generally only occurred when the soil was close to saturation (Or et al., 2007), while *Pythium ultimum* hyphae bridged soil pores filled with air, and the liquid film around hydrophilic hyphae provided a continuous water channel for strain LW2, allowing the bacteria to migrate at a macroscopic scale in coarse, medium, and fine sandy soils. As reported by Yang et al. (2018), *paraburkholderia terrae* BS001 also achieved migration in soil under the mediation of mycelium, and the promotion effect of mycelium on bacterial migration was more significant in unsaturated soil with higher water content.

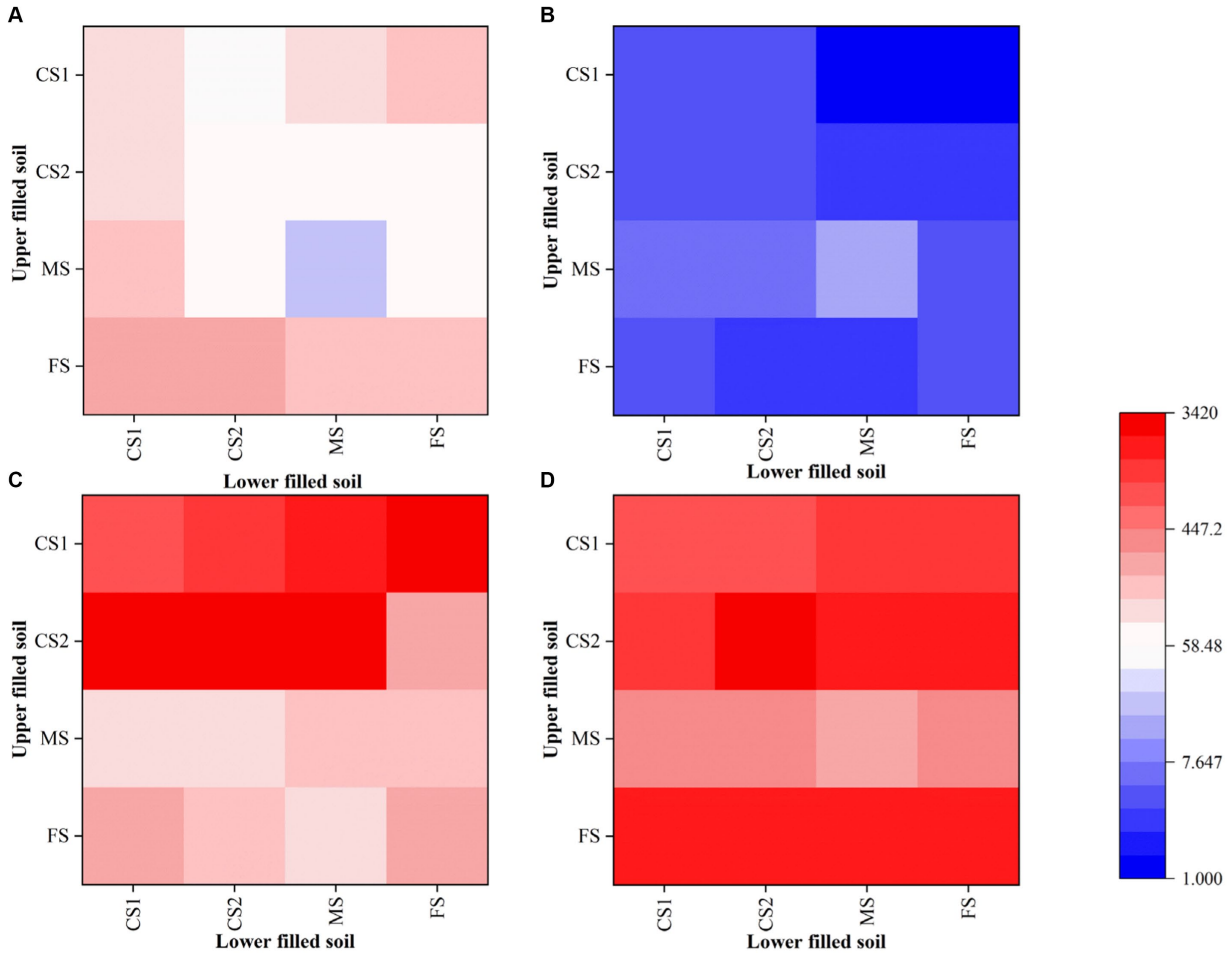

FIGURE 6
Quantity of *Diaphorobacter* sp. LW2 in soil layers with different particle sizes after bacterial inoculation (× 10^{8}). CS1 (coarse sand 1, 1–2 mm), CS2 (coarse sand 2, 0.5–1 mm), MS (medium sand, 0.25–0.5 mm), and FS (fine sand, <0.25 mm) were pairwise combined. The x-axis and y-axis showed the types of the soil in upper and lower layers, respectively. **(A,B)** represented the results in the absence of hyphae. **(C,D)** represented the results in the presence of hyphae. **(A,C)** were number of LW2 cells in the upper soil layer, while **(B,D)** were those in the lower soil layer.

Microorganisms tend to form colonies or biofilms at the corners of soil pores, gathering to form microbial hotspots (Dechesne et al., 2008; Kuzyakov and Blagodatskaya, 2015). Although the number of microorganisms in the soil could reach an average of 10^{7}–10^{12} cells per gram of soil, these microbial environments only account for less than 1% of the total soil volume (Watt et al., 2006). The effective contact between degrading bacteria and toxic compounds was a prerequisite for the bioremediation of polluted soil. The *Pythium ultimum* served as a bridge for the mobile strain LW2, allowing it to diffuse in unsaturated soil, which could increase the frequency of microbial contact with substrates, improve the bio-accessibility of pollutants in soil, and provide feasible methods for improving the remediation effect of polluted soil.

4.4 Redistribution of LW2 in heterogeneous soil by *Pythium ultimum*

The remaining water in unsaturated soils generally formed a liquid habitat in the corners and crevices among particles or thin water films on rough surfaces (Or et al., 2007). The water environment was discontinuous and fragmented, and the intermittent liquid films were not available for free bacterial transporting, resulting in the interception of strain LW2. Bacteria passively transported under the action of water flow in unsaturated environments (Yang and van Elsas, 2018). In the absence of mycelium, the bacterial suspension migrated downward under the action of gravity after entering the soil. The order of soil water potential was CS1 > CS2 > MS > FS, indicating that the water flow in the soil with large particle size was subjected to less resistance, so it was easier to migrate downward. However, the saturation in coarse sandy soil was lower, and microorganisms were easily adsorbed at the air-water interface (Wan et al., 1994; Schafer et al., 1998). Therefore, under multiple effects, the number of bacteria intercepted by coarse and fine sandy soil in homogeneous soil is greater than that in MS. In addition, droplets in pores are also affected by capillary forces. Guber et al. (2009) reported that water flow driven by capillary forces was the main mechanism of *E. coli* entering air-dry aggregates. Supplementary Figures S4, S5 show the longitudinal and transverse sections of soils with different particle sizes, respectively, showing that the pores in soils with larger particle sizes were larger. Kravchenko et al. (2013) found that water had limited entrance into

large biological pores when it reached them from smaller pores and mainly influenced by capillary forces. The size of soil pores changes at the interface of heterogeneous soil. According to the relationship between capillary force and pore radius, water droplets in coarse sandy soil experience less capillary force than in MS and FS. Therefore, when the pores in the lower soil are larger than those in the upper soil, it is difficult for bacteria that introduced in MS and FS to enter the larger sized lower soil and remain in the upper soil.

In the presence of *Pythium ultimum*, the proportion of bacteria in the upper soil decreased from 58.78–99.10% to 0.05–69.50%, promoting the migration of mobile bacteria LW2 in heterogeneous soil. Hydrophilic hyphae penetrated the soil layer, bridging air filled soil pores. The liquid film surrounding the hyphae provided a continuous water channel for the migration of LW2, changing its migration mode from passive transportation to autonomous migration. The energy state of water in soils with smaller particle sizes is lower, and bacterial movement was more restricted. Therefore, when the particle size of the upper layer medium was smaller, the promotion effect of *Pythium ultimum* on bacterial migration was more significant.

Based on the above results, we speculated that in the presence of hyphae, the introduced bacteria migrated from the inoculation position to all directions, possibly all the way down to the lower soil layer along with *Pythium ultimum* hyphae or colonized in suitable habitats in the upper soil layer. The proliferated bacteria then spread to other locations with the hyphae, ultimately making the bacteria to be distributed throughout the soil. The particle size of the soil in the natural environment was often uneven, which caused difficult migration of added bacteria on the basis of greatly varied distribution. The spatial network formed by mycelium could connect different soil pores of different sizes, providing an effective migration pathway for degrading bacteria and improving the uniform distribution of bacteria in heterogeneous soil, offering available assistance for the remediation of contaminated soil.

4.5 The removal of phenanthrene by LW2 in soils and enhancement of *Pythium ultimum*

It was observed that *Pythium ultimum* hyphae penetrated the soil layer in the column and continued to grow outside the soil (Figure 5). *Pythium ultimum* could adsorb and actively transport phenanthrene through mycelium (Furuno et al., 2012). The decrease of phenanthrene in soil can be attributed to the adsorption and transportation of phenanthrene by mycelium. Meanwhile, the concentration of phenanthrene varied more in coarse sand soil, which corresponded to the result that it took shorter time for mycelium to cross the coarse sand soil. LW2 was added to the soil and phenanthrene was degraded. After 21 days, the amount of phenanthrene decreased by more than 70%. However, due to the limited migration of bacteria in unsaturated soil, LW2 cannot sufficiently contact to pollutants in the soil, making it difficult to effectively degrade the pollutants. Phenanthrene was not further degraded for 21–35 days. Compared with the influence of soil environmental factors on the biological activity of degrading bacteria, the poor accessibility of polycyclic aromatic hydrocarbons further limits the microbial bioremediation of polluted soil (Puglisi et al., 2007). Improving accessibility between pollutants and microorganisms is crucial for improving bioremediation efficiency (see Figure 7).

Similar to the extension of plant roots, which can promote the distribution of microorganisms in soil, the mycelial network in pores increases the contact between degrading bacteria and pollutants (Aprill and Sims, 1990). In the soil where hyphae and LW2 coexisted, the removal rate of phenanthrene in soil of different particle sizes was above 94% after 35 days. *Pythium ultimum* promoted the diffusion of LW2 in soil by connecting soil pores and providing effective pathways for bacterial movement, thereby improving the removal of phenanthrene in soil. Meanwhile, due to the fact that *Pythium ultimum* could adsorb phenanthrene and actively transport it, the bioavailability of phenanthrene has also increased (Furuno et al., 2012; Schamfuß et al., 2013). As the cultivation time prolonged, water in the soil evaporated, the suitable microbial environment decreased, and the number of bacteria in the soil gradually decreased. When mycelium was present, the number of LW2 colonies in soil with different particle sizes was always more than that in soils without hyphae (Supplementary Figure S6). The presence of hyphae delayed the decay of bacterial cells in soil and prolonged the biological function of soil, which was consistent with the research results by Nazir et al. (2010a,b). In dry soil, hyphae could transport water from sufficient areas to impoverished areas based on their own growth patterns, which promotes bacterial migration (Heaton et al., 2012). Moreover, the redistribution of soil moisture by hyphae can enhance soil biological activity and metabolic function (Guhr et al., 2015). In soil at various acid pH levels, mycelium *Lyophyllum* sp. strain Karsten promoted bacterial migration and survival, although lower pH levels showed negative effects (Yang et al., 2018).

Bacteria and fungi coexisted in the soil, either not interfering with each other, competing with each other, or cooperating with each other, to jointly maintain the ecological function of the soil (Nazir et al., 2010a,b). The soil matrix was a natural barrier for bacterial migration, and most bacteria did not possess the mycelial growth pattern of filamentous organisms such as actinomycetes and were intercepted in the soil (Schafer et al., 1998). Mycelial organisms, especially fungi, could penetrate air-filled soil pores and transport carbon containing compounds over long distances, providing nutrients for cell growth (Heaton et al., 2012). The participation of mycelial microorganism *Pythium ultimum* enhanced the diffusion and survival of LW2 in soil, which was reflected in soils of different particle sizes. The combination of *Pythium ultimum* and *Diaphoractor* sp. LW2 could improve the bioremediation efficiency of phenanthrene-contaminated soil, which had great potential for application in the remediation of actual contaminated soil.

4.6 The prospect of future research

In this study, we discussed the enhanced migration and biodegradation of LW2 in soil by *Pythium ultimum* in a sterile constant temperature and humidity environment. The actual environment would be more complex. Changes in organic matter, temperature, and moisture in the soil may have unknown effects on the growth, migration, and degradation behavior of mycelium and LW2. More comprehensive research was needed for the practical remediation application of polluted soil. A large number of microorganisms in the soil maintained the ecological function of the soil through mutual interaction. Introducing new microorganisms into the soil might cause changes in the existing biological community.

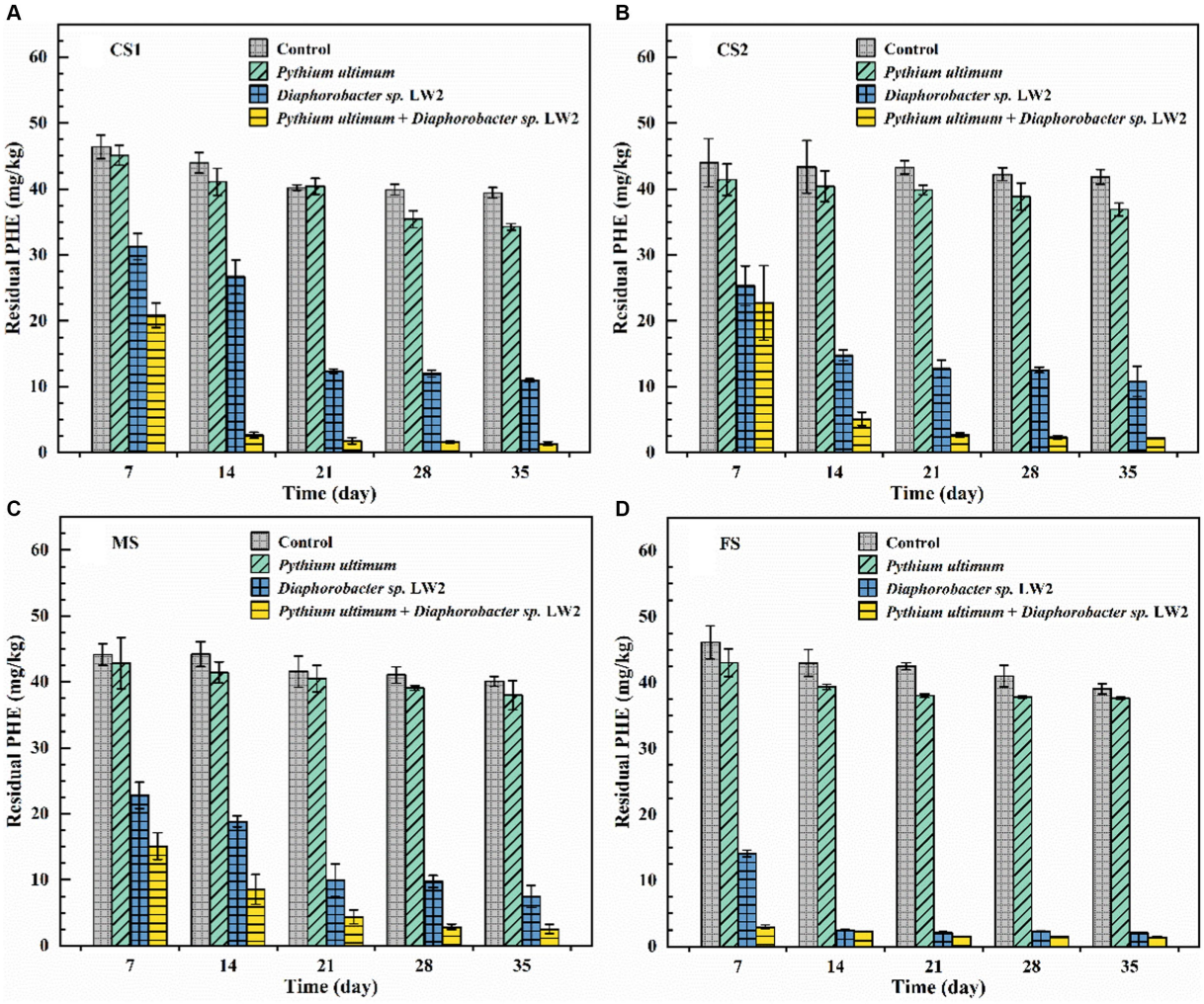

FIGURE 7
The content of phenanthrene in coarse sand (**A**: CS1, **B**: CS2), medium sand (**C**, MS), and fine sand (**D**, FS) with no treatment, only adding *Pythium ultimum* or *Diaphoractor* sp. LW2 or adding both *Pythium ultimum* and *Diaphoractor* sp. LW2.

Studying the interactions and community changes among microorganisms could provide a better understanding of the soil environment and had profound implications for the remediation of contaminated soil.

5 Conclusion

In conclusion, this study confirmed that the movement of *Diaphorobacter* sp. LW2 along with *Pythium ultimum* hyphae was in and against hyphal growth directions, and bacterial cells were gradually distributed evenly in mycelial networks over time. By hyphal transportation, strain LW2 could move in unsaturated soil with different particle sizes in the range of centimeters. The mycelium throughout soil pores reduced the limitation for LW2 of entering larger pore soils from fine soil. In addition, the mobilization of hyphae in uneven soil regulated the distribution of introduced bacteria. The enhancement of mycelium on the growth and migration of LW2 promotes the removal of phenanthrene by LW2 in soils of different particle sizes. Hyphal transportation with pollutant-degrading bacteria may play an important role in the bioremediation of contaminated soil.

Data availability statement

The raw data supporting the conclusions of this article will be made available by the authors without undue reservation.

Author contributions

JLi: Investigation, Writing – original draft. MH: Conceptualization, Supervision, Writing – review & editing. JLv: Validation, Writing – review & editing. RT: Software, Writing – review & editing. RW: Software, Writing – review & editing. YY: Data curation, Writing – review & editing. NL: Conceptualization, Project administration, Supervision, Writing – review & editing.

Funding

The author(s) declare that financial support was received for the research, authorship, and/or publication of this article. This study was supported by the Major Science and Technology Program for Water Pollution Control and Treatment (No. 2018ZX07109-003).

Conflict of interest

The authors declare that the research was conducted in the absence of any commercial or financial relationships that could be construed as a potential conflict of interest.

Publisher's note

Supplementary material

The Supplementary material for this article can be found online at: https://www.frontiersin.org/articles/10.3389/fmicb.2024.1391553/full#supplementary-material

References

Aprill, W., and Sims, R. C. (1990). Evaluation of the use of prairie grasses for stimulating polycyclic aromatic hydrocarbon treatment. *Chemosphere* 20, 253–265. doi: 10.1016/0045-6535(90)90100-8

Boersma, F. G. H., Otten, R., Warmink, J. A., Nazir, R., and van Elsas, J. D. (2010). Selection of *variovorax paradoxus*-like bacteria in the mycosphere and the role of fungal-released compounds. *Soil Biol. Biochem.* 42, 2137–2145. doi: 10.1016/j.soilbio.2010.08.009

Bosma, T. N. P., Middeldorp, P. J. M., Schraa, G., and Zehnder, A. J. B. (1996). Mass transfer limitation of biotransformation quantifying bioavailability. *Environ. Sci. Technol.* 31, 248–252. doi: 10.1021/es960383u

Chen, B., and Ding, J. (2012). Biosorption and biodegradation of phenanthrene and pyrene in sterilized and unsterilized soil slurry systems stimulated by phanerochaete chrysosporium. *J. Hazard. Mater.* 229-230, 159–169. doi: 10.1016/j.jhazmat.2012.05.090

Collins, C. D., Mosquera-Vazquez, M., Gomez-Eyles, J. L., Mayer, P., Gouliarmou, V., and Blum, F. (2013). Is there sufficient 'sink' in current bioaccessibility determinations of organic pollutants in soils? *Environ. Pollut.* 181, 128–132. doi: 10.1016/j.envpol.2013.05.053

de Menezes, A. B., Richardson, A. E., and Thrall, P. H. (2017). Linking fungal–bacterial co-occurrences to soil ecosystem function. *Curr. Opin. Microbiol.* 37, 135–141. doi: 10.1016/j.mib.2017.06.006

Dechesne, A., Or, D., Gülez, G., and Smets, B. F. (2008). The porous surface model, a novel experimental system for online quantitative observation of microbial processes under unsaturated conditions. *Appl. Environ. Microbiol.* 74, 5195–5200. doi: 10.1128/aem.00313-08

Deveau, A., Bonito, G., Uehling, J., Paoletti, M., Becker, M., Bindschedler, S., et al. (2018). Bacterial–fungal interactions: ecology, mechanisms and challenges. *FEMS Microbiol. Rev.* 42, 335–352. doi: 10.1093/femsre/fuy008

Frey-Klett, P., Garbaye, J., and Tarkka, M. (2007). The mycorrhiza helper bacteria revisited. *New Phytol.* 176, 22–36. doi: 10.1111/j.1469-8137.2007.02191.x

Furuno, S., Foss, S., Wild, E., Jones, K. C., Semple, K. T., Harms, H., et al. (2012). Mycelia promote active transport and spatial dispersion of polycyclic aromatic hydrocarbons. *Environ. Sci. Technol.* 46, 5463–5470. doi: 10.1021/es300810b

Gandhi, S. R., and Weete, J. D. (1991). Production of the polyunsaturated fatty acids arachidonic acid and eicosapentaenoic acid by the fungus pythium uftimum. *J. Gen. Microbiol.* 137, 1825–1830. doi: 10.1099/00221287-137-8-1825

Griffin, D. M., and Quail, G. (1968). Movement of bacteria in moist, particulate. *Aust. J. Biol. Sci.* 21, 579–582. doi: 10.1071/bi9680579

Gu, H., Chen, Y., Liu, X., Wang, H., Shen-Tu, J., Wu, L., et al. (2017). The effective migration of massilia sp. Wf1 by phanerochaete chrysosporium and its phenanthrene biodegradation in soil. *Sci. Total Environ.* 593-594, 695–703. doi: 10.1016/j.scitotenv.2017.03.205

Gu, H., Lou, J., Wang, H., Yang, Y., Wu, L., Wu, J., et al. (2016). Biodegradation, biosorption of phenanthrene and its trans-membrane transport by massilia sp. Wf1 and phanerochaete chrysosporium. *Front Microbiol.* 7:38. doi: 10.3389/fmicb.2016.00038

Guber, A. K., Pachepsky, Y. A., Shelton, D. R., and Yu, O. (2009). Association of fecal coliforms with soil aggregates: effect of water content and bovine manure application. *Soil Sci.* 174, 543–548. doi: 10.1097/SS.0b013e3181bccc85

Guhr, A., Borken, W., Spohn, M., and Matzner, E. (2015). Redistribution of soil water by a saprotrophic fungus enhances carbon mineralization. *Proc. Natl. Acad. Sci.* 112, 14647–14651. doi: 10.1073/pnas.1514435112

Gülez, G., Dechesne, A., and Smets, B. F. (2010). The pressurized porous surface model: an improved tool to study bacterial behavior under a wide range of environmentally relevant matric potentials. *J. Microbiol. Methods* 82, 324–326. doi: 10.1016/j.mimet.2010.06.009

Haq, I. U., Zwahlen, R. D., Yang, P., and van Elsas, J. D. (2018). The response of para*burkholderia terrae* strains to two soil fungi and the potential role of oxalate. *Front. Microbiol.* 9:989. doi: 10.3389/fmicb.2018.00989

Heaton, L., Obara, B., Grau, V., Jones, N., Nakagaki, T., Boddy, L., et al. (2012). Analysis of fungal networks. *Fungal Biol. Rev.* 26, 12–29. doi: 10.1016/j.fbr.2012.02.001

Kohlmeier, S., Smits, T. H. M., Ford, R. M., Keel, C., Harms, H., and Wick, L. Y. (2005). Taking the fungal highway mobilization of pollutant-degrading bacteria by fungi. *Environ. Sci. Technol.* 39, 4640–4646. doi: 10.1021/es047979z

Kravchenko, A., Chun, H. C., Mazer, M., Wang, W., Rose, J. B., Smucker, A., et al. (2013). Relationships between intra-aggregate pore structures and distributions of *escherichia coli* within soil macro-aggregates. *Appl. Soil Ecol.* 63, 134–142. doi: 10.1016/j.apsoil.2012.10.001

Kuzyakov, Y., and Blagodatskaya, E. (2015). Microbial hotspots and hot moments in soil: concept & review. *Soil Biol. Biochem.* 83, 184–199. doi: 10.1016/j.soilbio.2015.01.025

Li, J., Hong, M., Tang, R., Cui, T., Yang, Y., Lv, J., et al. (2022). Isolation of diaphorobacter sp. Lw2 capable of degrading phenanthrene and its migration mediated by *pythium ultimum*. *Environ. Technol.* 45, 1497–1507. doi: 10.1080/09593330.2022.2145914

Nam, K., Chung, N., and Alexander, M. (1998). Relationship between organic matter content of soil and the sequestration of phenanthrene. *Environ. Sci. Technol.* 32, 3785–3788. doi: 10.1021/es980428m

Nazir, R., Boersma, F. G. H., Warmink, J. A., and van Elsas, J. D. (2010a). Lyophyllum sp. strain karsten alleviates ph pressure in acid soil and enhances the survival of *variovorax paradoxus* hb44 and other bacteria in the mycosphere. *Soil Biol. Biochem.* 42, 2146–2152. doi: 10.1016/j.soilbio.2010.08.019

Nazir, R., Warmink, J. A., Boersma, H., and van Elsas, J. D. (2010b). Mechanisms that promote bacterial fitness in fungal-affected soil microhabitats. *FEMS Microbiol. Ecol.* 71, 169–185. doi: 10.1111/j.1574-6941.2009.00807.x

Or, D., Smets, B. F., Wraith, J. M., Dechesne, A., and Friedman, S. P. (2007). Physical constraints affecting bacterial habitats and activity in unsaturated porous media – a review. *Adv. Water Resour.* 30, 1505–1527. doi: 10.1016/j.advwatres.2006.05.025

Puglisi, E., Cappa, F., Fragoulis, G., Trevisan, M., and Del Re, A. A. M. (2007). Bioavailability and degradation of phenanthrene in compost amended soils. *Chemosphere* 67, 548–556. doi: 10.1016/j.chemosphere.2006.09.058

Schafer, A., Ustohal, P., Harms, H., Stauffer, F., Dracos, T., and Zehnder, A. J. B. (1998). Transport of bacteria in unsaturated porous media. *J. Contam. Hydrol.* 33, 149–169. doi: 10.1016/S0169-7722(98)00069-2

Schamfuß, S., Neu, T. R., van der Meer, J. R., Tecon, R., Harms, H., and Wick, L. Y. (2013). Impact of mycelia on the accessibility of fluorene to pah-degrading bacteria. *Environ. Sci. Technol.* 47, 6908–6915. doi: 10.1021/es304378d

Turnbull, G. A., Morgan, J. A. W., Whipps, J. M., and Saunders, J. R. (2001). The role of bacterial motility in the survival and spread of *pseudomonas fluorescens* in soil and in the attachment and colonisation of wheat roots. *FEMS Microbiol. Ecol.* 36, 21–31. doi: 10.1111/j.1574-6941.2001.tb00822.x

Vila, T., Nazir, R., Rozental, S., dos Santos, G. M. P., Calixto, R. O. R., Barreto-Bergter, E., et al. (2016). The role of hydrophobicity and surface receptors at hyphae of lyophyllum sp. strain karsten in the interaction with *burkholderia terrae* bs001 – implications for interactions in soil. *Front. Microbiol.* 7:1689. doi: 10.3389/fmicb.2016.01689

Wan, J., Wilson, J. L., and Kieft, T. L. (1994). Influence of the gas-water interface on transport of microorganisms through unsaturated porous media. *Appl. Environ. Microbiol.* 60, 509–516. doi: 10.1128/aem.60.2.509-516.1994

Warmink, J. A., and Elsas, J. D. V. (2009). Migratory response of soil bacteria to lyophyllum sp. strain karsten in soil microcosms. *Appl. Environ. Microbiol.* 75, 2820–2830. doi: 10.1128/aem.02110-08

Watt, M., Hugenholtz, P., White, R., and Vinall, K. (2006). Numbers and locations of native bacteria on field-grown wheat roots quantified by fluorescence in situ hybridization (fish). *Environ. Microbiol.* 8, 871–884. doi: 10.1111/j.1462-2920.2005.00973.x

Wick, L. Y., Remer, R., Würz, B., Reichenbach, J., Braun, S., Schäfer, F., et al. (2007). Effect of fungal hyphae on the access of bacteria to phenanthrene in soil. *Environ. Sci. Technol.* 41, 500–505. doi: 10.1021/es061407s

Wild, S. R., and Jones, K. C. (1995). Polynuclear aromatic hydrocarbons in the United Kingdom environment a preliminary source inventory and budget. *Environ. Pollut.* 88, 91–108. doi: 10.1016/0269-7491(95)91052-M

Worrich, A., König, S., Miltner, A., Banitz, T., Centler, F., Frank, K., et al. (2016). Mycelium-like networks increase bacterial dispersal, growth, and biodegradation in a model ecosystem at various water potentials. *Appl. Environ. Microbiol.* 82, 2902–2908. doi: 10.1128/aem.03901-15

Xia, Q., Zheng, N., Heitman, J. L., and Shi, W. (2022). Soil pore size distribution shaped not only compositions but also networks of the soil microbial community. *Appl. Soil Ecol.* 170:104273. doi: 10.1016/j.apsoil.2021.104273

Yang, P., da Rocha, O., Calixto, R., and van Elsas, J. D. (2018). Migration of para*burkholderia terrae* bs001 along old fungal hyphae in soil at various ph levels. *Microb. Ecol.* 76, 443–452. doi: 10.1007/s00248-017-1137-1

Yang, P., and van Elsas, J. D. (2018). Mechanisms and ecological implications of the movement of bacteria in soil. *Appl. Soil Ecol.* 129, 112–120. doi: 10.1016/j.apsoil.2018.04.014

Yang, P., Zhang, M., Warmink, J. A., Wang, M., and van Elsas, J. D. (2016). The type three secretion system facilitates migration of *burkholderia terrae* bs001 in the mycosphere of two soil-borne fungi. *Biol. Fertil. Soils* 52, 1037–1046. doi: 10.1007/s00374-016-1140-6

Zeng, J., Lin, X., Zhang, J., and Li, X. (2010). Isolation of polycyclic aromatic hydrocarbons (pahs)-degrading mycobacterium spp. and the degradation in soil. *J. Hazard. Mater.* 183, 718–723. doi: 10.1016/j.jhazmat.2010.07.085

frontiers | Frontiers in Microbiology

TYPE Original Research
PUBLISHED 19 July 2024
DOI 10.3389/fmicb.2024.1421094

OPEN ACCESS

EDITED BY
Zifang Chi,
Jilin University, China

REVIEWED BY
Alejandro Rodriguez-Sanchez,
University of Granada, Spain
Lili Wang,
Chinese Academy of Agricultural Sciences, China
Xi Min,
Qingdao University, China

*CORRESPONDENCE
Xiaofei Yu
✉ yuxf888@nenu.edu.cn
Yahya Kooch
✉ yahya.kooch@modares.ac.ir

RECEIVED 21 April 2024
ACCEPTED 02 July 2024
PUBLISHED 19 July 2024

CITATION
Ali H, Min Y, Yu X, Kooch Y, Marnn P and Ahmed S (2024) Composition of the microbial community in surface flow-constructed wetlands for wastewater treatment. *Front. Microbiol.* 15:1421094. doi: 10.3389/fmicb.2024.1421094

Composition of the microbial community in surface flow-constructed wetlands for wastewater treatment

Haider Ali[1,2], Yongen Min[1,2], Xiaofei Yu[1,2,3]*, Yahya Kooch[4]*, Phyoe Marnn[1,2] and Sarfraz Ahmed[5,6]

[1]Engineering Research Center of Low-Carbon Treatment and Green Development of Polluted Water in Northeast China, Ministry of Education and State Environmental Protection Key Laboratory For Wetland Conservation and Vegetation Restoration, School of Environment, Northeast Normal University, Changchun, China, [2]Key Laboratory of Vegetation Ecology of Ministry of Education and Key Laboratory of Geographical Processes and Ecological Security of Changbai Mountains, Ministry of Education, School of Geographical Sciences, Northeast Normal University, Changchun, China, [3]Heilongjiang Xingkai Lake Wetland Ecosystem National Observation and Research Station and Key Laboratory of Wetland Ecology and Environment and Jilin Provincial Joint Key Laboratory of Changbai Mountain Wetland and Ecology, Northeast Institute of Geography and Agroecology, Chinese Academy of Sciences, Changchun, China, [4]Faculty of Natural Resources and Marine Sciences, Tarbiat Modares University, Noor, Iran, [5]School of Life Sciences, Northeast Normal University, Changchun, China, [6]Key Laboratory of Remote Sensing, Northeast Institute of Geography and Agroecology, Chinese Academy of Sciences, Changchun, China

Traditionally constructed wetlands face significant limitations in treating tailwater from wastewater treatment plants, especially those associated with sugar mills. However, the advent of novel modified surface flow constructed wetlands offer a promising solution. This study aimed to assess the microbial community composition and compare the efficiencies of contaminant removal across different treatment wetlands: CW1 (Brick rubble, lignite, and *Lemna minor* L.), CW2 (Brick rubble and lignite), and CW3 (*Lemna minor* L.). The study also examined the impact of substrate and vegetation on the wetland systems. For a hydraulic retention time of 7 days, CW1 successfully removed more pollutants than CW2 and CW3. CW1 demonstrated removal rates of 72.19% for biochemical oxygen demand (BOD), 74.82% for chemical oxygen demand (COD), 79.62% for NH_4^+-N, 77.84% for NO_3^--N, 87.73% for ortho phosphorous (OP), 78% for total dissolved solids (TDS), 74.1% for total nitrogen (TN), 81.07% for total phosphorous (TP), and 72.90% for total suspended solids (TSS). Furthermore, high-throughput sequencing analysis of the 16S rRNA gene revealed that CW1 exhibited elevated Chao1, Shannon, and Simpson indices, with values of 1324.46, 8.8172, and 0.9941, respectively. The most common bacterial species in the wetland system were Proteobacteria, Spirochaetota, Bacteroidota, Desulfobacterota, and Chloroflexi. The denitrifying bacterial class Rhodobacteriaceae also had the highest content ratio within the wetland system. These results confirm that CW1 significantly improves the performance of water filtration. Therefore, this research provides valuable insights for wastewater treatment facilities aiming to incorporate surface flow-constructed wetland tailwater enhancement initiatives.

KEYWORDS

microbial community, constructed wetland, lignite, crushed bricks, pollutant removal

1 Introduction

Rapid urbanization and the continuous growth of industrial production and technology have led to severe water shortages and raised pollution in recent years. Maintaining water quality has become a critical global issue (Kadier et al., 2016; Lu et al., 2016; Qi et al., 2024). Discharging of untreated or partially treated industrial wastewater into local water bodies disrupts ecological sustainability and poses significant human health risks (Jacobson et al., 2013; Hasan and Webley, 2017; Swain et al., 2018). Excessive nitrogen and phosphorus emissions significantly impact the structure and function of river ecosystems, aggravating water eutrophication and disrupting microbial community structures (Huo et al., 2017). Sugar industries are among the most polluting industries (Ingaramo et al., 2009). Molasses, a byproduct of the sugarcane industry, is used as a raw material for ethyl alcohol production, generating 15 liters of spent wash for every liter of the alcohol produced. Inadequate treatment of this spent wash, which has a high organic load, biochemical oxygen demand (BOD) levels between 35,000 and 60,000 mg/L, and chemical oxygen demand (COD) levels between 60,000 and 120,000 mg/L, can have devastating effects on ecosystems (Billore et al., 2001; Zurita and Vymazal, 2023). Anaerobic biological digestion (biomethanation) is a commonly employed traditional treatment technology that effectively mitigates the elevated organic load in wastewater. Distilleries typically use biomethanation to produce methane, which serves as fuel to meet energy requirements. A secondary treatment is implemented, which requires ongoing aeration and substantial energy input. Conventional effluent treatment plants (ETPs) produce high-quality wastewater in the outfalls of the secondary treatment system. This secondary treatment effluent (STE) is usually transported to open earthen lagoons for further natural treatment and is often scattered across open fields for sun drying. This process requires significant land and poses a risk of contaminating groundwater (Billore et al., 2001). In contrast, constructed wetland water treatment technology is recognized for its ability to provide environment friendly solutions with high treatment efficiency at a low cost (Ameso et al., 2023). It is widely used in the treatment of domestic sewage (Lai et al., 2020), agricultural runoff sewage (Vymazal and Březinová, 2015), and industrial and municipal wastewater (Wu et al., 2014; Gupta et al., 2020).

Studies have found that physical structure and operational strategies strongly influence the pollutant removal performance of constructed wetlands (Lu et al., 2016). The efficacy of pollutant removal depends on aerobic, anaerobic, and other active conditions and the type of filler used. Different fillers support the growth of various microorganisms in the substrate layer, which play a vital role in the removal process (Hussain et al., 2019). Removing organic matter and ammonia nitrogen in constructed wetlands mainly depends on their adsorption to substrates and microbial degradation (Kizito et al., 2017). Duckweed-based ponds utilizing *Lemna minor* L. have effectively eliminated nutrients and organic substances (Papadopoulos and Tsihrintzis, 2011), combining proficient wastewater treatment with significant biomass generation (Iatrou et al., 2017). Under natural climatic conditions, duckweed demonstrated superior efficiency in removing chemical oxygen demand, nitrogen (N), and phosphorous (P) from dumpsite leachate (Iqbal et al., 2019). Crushed bricks have a positive impact on the development of plants and microorganisms. Hollow brick crumbs and fly ash are particularly effective in removing total nitrogen (Li H. et al., 2021) and total phosphorous (TP) (Li et al., 2022). Constructed wetlands containing a combination of hollow brick crumbs and fly ash can reduce NH_4^+-N levels by 89% and TP levels by 81% (Ren et al., 2007; Kumar and Dutta, 2019; Nan et al., 2020). Lignite, commonly known as brown coal, is renowned for its adsorptive characteristics. Numerous studies have used lignite as an adsorbent to eliminate heavy metals, organic contaminants, and colorants or dyes from wastewater (Allen et al., 1997; Mohan et al., 2002; Rathi and Puranik, 2002; Kluçáková and Omelka, 2004; Pehlivan and Arslan, 2006; Karaca et al., 2008; Havelcová et al., 2009; Pentari et al., 2009). Numerous comparison studies have examined the treatment performance of various substrates or vegetation in wetlands. Most of these studies have only reviewed the comparison between substrates or vegetation individually, without considering the combined impact of substrates and vegetation (Calheiros et al., 2009; Saeed and Sun, 2011, 2013; Sehar et al., 2015; Toscano et al., 2015; Schierano et al., 2017).

This research addresses the existing knowledge gap by examining the significance of substrate and vegetation in the context of constructed wetland applications. Prior studies have shown that *Lemna minor* L. can absorb pollutants from wastewater and is recognized as a hyperaccumulator for phosphorus. Additionally, porous media such as brick rubble and lignite not only adsorb toxins from wastewater but also create an environment for the growth of microbial communities (Allen et al., 1997; Mohan et al., 2002; Rathi and Puranik, 2002; Kluçáková and Omelka, 2004; Pehlivan and Arslan, 2006; Ren et al., 2007; Karaca et al., 2008; Havelcová et al., 2009; Pentari et al., 2009; Iqbal et al., 2019; Kumar and Dutta, 2019; Nan et al., 2020). Therefore, it is postulated that the implementation of a constructed wetland system that incorporates brick rubble and lignite (as substrates), along with *Lemna minor* L. (as a vegetation plant), may offer a viable, cost-effective, and environmentally sustainable approach to address the issue of wastewater from the effluent treatment plant for secondary treatment. This study was carried out to evaluate the efficiency of a small-scale surface flow-constructed wetland (SFCW) in treating secondary treatment effluent. The primary objectives were to examine the structure of the microbial community and evaluate the efficiency of constructed wetlands in removing organic compounds, specifically COD and BOD, as well as nitrogen and phosphorus. The ultimate goal was to enhance the quality of effluent from sugar industries and mitigate their negative impact on natural water systems, an urgent global problem.

2 Methodology

2.1 Experimental procedure

The whole experiment spans 120 days, from mid-May 2023 to mid-August 2023. The experiment consists of the vegetation period and the treatment phase. The vegetation period lasted for 90 days, during which the constructed wetlands were filled with tap water. The *Lemna minor* L. plants were distributed on the water surface to promote the development of the microbial community within the substrates. During the treatment phase, which started in mid-July, built wetlands were filled with synthetic sugar industrial effluent with hydraulic retention times (HRT) of 3, 6, and 7 days to determine optimal HRT throughout the treatment phase. The study assessed the performance of three different treatment configurations: substrate

alone, vegetation alone, and substrate and vegetation combined. High-throughput sequencing of microbial community 16S rRNA was used to assess the impact and function of the microbial community in the treatment process. Additionally, the individual contributions of *Lemna minor* L. and Substrates (Brick rubble and lignite) to the treatment system were evaluated to determine their impact on the overall performance of the Surface Flow Constructed Wetland (SFCW).

2.2 Synthetic wastewater and wetland reactors

Synthetic wastewater (SWW) provides a controlled environment for thoroughly examining each parameter. With a few adjustments, a synthetic formulation of anaerobically treated distillery wastewater was created based on the specifications in Table 1 (Nacheva et al., 2009).

Synthetic sugarcane industry wastewater was developed in the laboratory by using a locally purchased sugarcane plant bagasse waste. It was then soaked in the water, and the containers were covered with a lid to prevent light penetration for 15 days to produce foul-smelling. This process made a real replicate of the effluent of sugar industry wastewater. Nitrogen (N) and Phosphorus (P) were added as $NaNO_3$ (≥99%), HNO_3 (≥99%), and $NH_4H_2PO_4$ (≥98%), respectively. While NaOH (≥98%) and H_2SO_4 (≥98%) were used to control the pH. KCl (≥98%) was used for optimizing total suspended solids (TSS). The quantity of NaOH and H_2SO_4 was dependent on the buffer capacity of the water. The detailed composition of wastewater effluent is given in Table 1.

Rectangular-shaped wetlands were made of thick polythene plastic with dimensions of 50 cm*50 cm*60 cm. Three holes were drilled into the outer wall of each wetland, and ½ inches of valves were fixed in them, acting as an inlet (at the height of 200 mm), outlet (at 600 mm height), and drain (at 50 mm height) (Supplementary Figure S1).

Common clay bricks were purchased from the local brick industry and crushed to make brick rubble, which was used in combination with Lignite (Brown coal) as substrate. *Lemna Minor* L. was purchased from a local market and quickly transferred to wetlands reactors. The wetlands configuration consisted of T1 (CW1), *Lemna minor* L. (170 g) as vegetation plant, lignite (1,000 g), and Brick rubble (50 kg) as substrates; T2 (CW2), only substrates containing Brick Rubble (50 kg) and Lignite (1,000 g); T3 (CW3) with *Lemna minor* L. (170 g) only. All wetlands T1, T2, and T3 had three replicates and had a free water surface level of 40 cm on the top of the substrates in the tank.

2.3 Sample collection and measuring methods

2.3.1 Influent and effluent water

Samples of influent and effluent water were taken from different systems to assess how well each system had removed the pollutants. Each time, 1 L of water was sampled using different hydraulic retention times to enable the examination of all indicators. The samples were obtained from the effluent valve of each wetland reactor during the treatment phase. They were then kept in a refrigerator at 4°C until all laboratory testing procedures were completed.

TABLE 1 Characteristics of wastewater (concentrations of all parameters are in mg/l.)

Parameter	Concentration
BOD	3,200
COD	7,500
NH_4^+-N	3.85
NO_3^--N	20
OP	2.93
TDS	2,000
TN	35
TP	12
TSS	1,800

The pH and total dissolved solids (TDS) of the water samples were analyzed using a portable water quality meter (METTLER TOLEDO Co. Ltd., based in Switzerland and America). TN, NH_4^+-N, NO_3^--N, COD, ortho phosphorous (OP), and TP concentrations were measured using a fully automated multipara meter and water quality analyzer (SMART CHEN 200, United States). The dissolved oxygen (DO) concentration was measured using a portable DO meter (HACH HQ30d, United States). Total suspended solids were determined using the APHA (American Public Health Association) standard procedure (American Public Health Association, 1926). All experimental data were presented as the mean of three replicates with standard deviation.

The parameters mentioned above were employed for assessing wastewater treatment efficacy, encompassing the quantification of removal efficiency (R, %), as specified by the subsequent equation.

$$R\% = \frac{Ci - Cf}{Ci} \times 100$$

The variable *R* represents the percentage removal efficiency, *Ci* represents the starting concentration of the influent, and *Cf* represents the final concentration of the effluent.

2.3.2 Microbiology

The microbial samples were extracted from the substrate using 0.1 M phosphate buffer solution. Total genome DNA from samples was extracted using the CTAB/SDS method. The DNA concentration and purity were monitored on 1% agarose gel. It was diluted to 1 ng/μL using sterile water. The concentration was determined using the Qubit dsDNA HS Assay Kit and the Qubit 4.0 Fluorometer (Invitrogen, Thermo Fisher Scientific, Oregon, United States). The universal primer sets 341F: 5′-CCTAYGGGRBGCASCAG-3′ and 806R: 5′-GGACTACNNGGGTATCTAAT-3′ were used to amplify the V3-V4 region of the 16S rRNA gene from genomic DNA extracted from each sample. The sequencing was done on the Illumina NovaSeq platform by Biomarker Technologies Co., Ltd. The raw sequences obtained from sequencing were filtered using Trimmomatic (v0.33[1]). Primer sequences were removed using Cutadapt (v1.9.1[2]) to obtain

1 https://github.com/usadellab/Trimmomatic

2 https://cutadapt.readthedocs.org/

clean sequences. The DADA2 (Callahan et al., 2016) method in QIIME2 2020.6 was used for denoising, bipartite sequence splicing, and removal of chimeric sequences to obtain the final valid data 346,434,000 bp. The number of base pairs used to develop the error model was 100,000,000 bp. Amplicon Sequence Variants (ASVs) were identified from high-quality sequences using Vsearch (v2.13.4_linux_x86_64). The effective sequences from sequencing are clustered based on 100% similarity. Using the classify-sklearn algorithm in QIIME2,[3] a pre-trained Naive Bayes classifier was applied to annotate the species for each ASV. The annotation database used was Silva 138.1.[4]

2.4 Analysis

Statistical analyses were conducted using SPSS 27.0 (SPSS, Chicago, United States) to evaluate and compare the performance of various wetland reactor treatments. Prior to analysis, the Shapiro–Wilk test was applied to all data to assess normality, and Bartlett's test was used to examine the homogeneity of variances. Depending on the distribution characteristics of the estimated parameters, either ANOVA or the Kruskal-Wallis test was employed for significant difference analysis among multiple groups. Pairwise data comparisons were conducted using Tukey's HSD test or the Wilcoxon rank-sum test. All experimental data were presented as the mean with standard deviation. Statistical significance was determined at a p-value of less than 0.05.

Microbial community structure was analyzed through Principal Coordinates Analysis (PCoA) based on the Bray-Curtis distance matrix, with significance testing (PERMANOVA test, Adonis tool) performed using 999 permutations, facilitated by the "vegan" package of R (R Core Team, Vienna, Austria). Spearman correlation tests were used to determine the relationships between microbial community and pollution removal using the "psych" package of R (R Core Team, Vienna, Austria).

3 Results

3.1 Total nitrogen, NH_4^+-N and NO_3^--N removal

The analysis of variance (ANOVA) demonstrated statistically significant variations in total nitrogen (TN) levels across the effluent of all SFCW systems ($p < 0.05$). During initial week of the experiment, the wetland treatment CW1 (T1) had the highest rate of TN removal, reaching 74.81% (Figure 1). This rate surpassed the maximum performance of CW3 (51.12%) and CW2 (27.62%). The highest percentage (28.10%) of elimination attained by CW2 was observed during the period spanning from the second to the third week (Table 2).

Table 2 presents statistically significant variations in the concentrations of NH_4^+-N and NO_3^--N in the effluent of the three SFCW systems ($p < 0.05$). During the initial week of the experiment, T1 (79.62%) had the most significant elimination rate for NH_4^+-N, followed by T3 (58.07%) and T2 (19.44%) on the seventh day. During the fourth week, T3 (52.23%) exhibited a rise in NH_4^+-N removal as compared to 51.10% in the third week (Table 2). In the second week of treatment, T2 (19.54%) exhibited a maximum removal rate of NH_4^+-N, which was notably lower than T1 and T3, as depicted in Table 2.

During the second week of the experiment, T2 (38.79%) demonstrated the lowest percentage removal of NO_3^--N. However, T2 exhibited satisfactory NO_3^--N elimination rates compared to NH_4^+-N and TN. In the initial week, T2 had the highest NO_3^--N removal rate, reaching 39.87%. T3 exhibited higher elimination rates for NO_3^--N as compared to T2. On the seventh day of the first week, T3 reduced NO_3^--N by 50.29%, which was 10.42% greater than T2. In the initial 2 weeks of the experiment, the removal percentages for T3 ranged from 50.29 to 49.84%. Subsequently, there was a slight increase, reaching 50.07% in week 3, followed by a decline to 47.71% in the last week (Table 2). T1 exhibited a remarkable NO_3^--N removal efficiency of 77.84%, surpassing the removal rates observed in T2 and T3 (Figure 1).

3.2 Phosphorous removal

The concentrations of phosphorus and ortho-phosphorus in each SFCW effluent varied according to the hydraulic retention time, as depicted in Figure 1. There was also a significant difference in TP content among the wetland systems throughout the same operational period ($p < 0.05$). Treatment T3 (72.08%) demonstrated a significant decrease in TP concentrations within the initial week. In the first week of the experiment, T1 achieved a TP removal rate of 81.07%, surpassing T3 (72.08%) and T2 (36.79%). Conversely, the efficacy of T2 increased from 36.79 to 38.43% from the first to the second week. However, the effectiveness of T2 experienced a slight reduction during the third week, followed by a minor improvement in the fourth week, resulting in a recorded efficiency of 36.61% (Table 2).

3.3 BOD and COD removal

The ANOVA results indicated significant variations in BOD and COD removal among the SFCWs. For BOD, the initial efficacy of the wetland treatment T1 was 71.60% during the first week, followed by a slight decline to 69.24% in the second week. Over 3 weeks, the T2 system experienced a decrease in removal effectiveness, dropping from 51.93% in the first week to 51.56% in the third week and reaching its minimum removal efficiency of 48.54% in the fourth week (Table 2). The efficacy of T3 decreased from 63.33 to 60% over the initial and subsequent weeks, with removal efficiencies of 63.54 and 57.82% in the third and fourth weeks, respectively, indicating a notable decline (Table 2).

T1 showed efficacies of 74.82 and 74.67% for COD elimination during the first 2 weeks, respectively. The performance of T3 exhibited a persistent downward trend, with elimination percentages of 59.34, 55.70, 50.54, and 52.82% during weeks 1, 2, 3, and 4, respectively. Similar to T1, T2 also experienced a decline in performance over the initial 2 weeks, with removal efficiencies of 34.77 and 31.89%, respectively. T3 (59.70%) had the highest

3 https://github.com/QIIME2/q2-feature-classifier

4 http://www.arb-silva.de/

10.3389/fmicb.2024.1421094

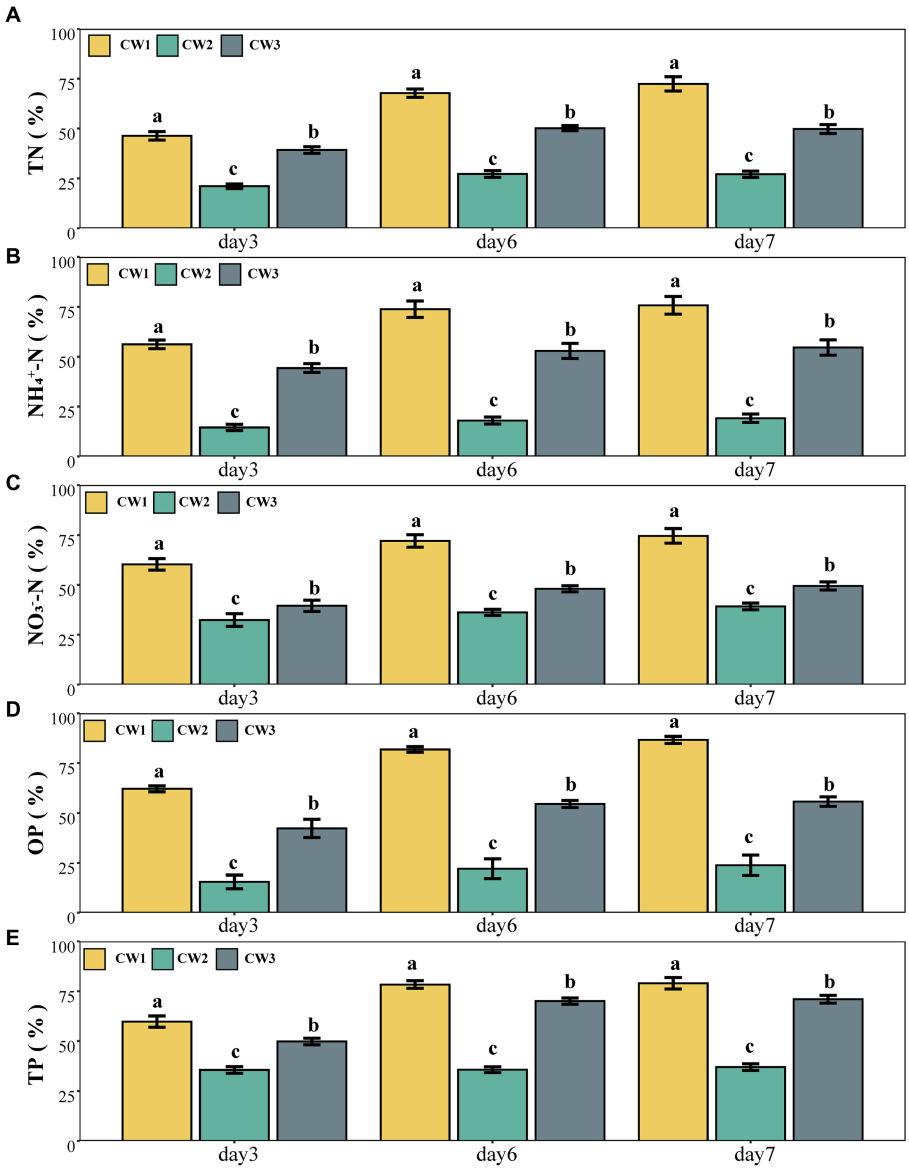

FIGURE 1
Percentage removal of **(A)** TN, **(B)** NH_4^+-N, **(C)** $NO3^-$-N, **(D)** OP, **(E)** TP.

COD removal percentage during the first week, but its effectiveness decreased to a minimum of 50.54% in the third week, representing a decline of 9.16% compared to the first week (Table 2).

3.4 TDS, TSS, and pH

Significant variations in the performance of three types of modified SFCWs were observed with a hydraulic retention time of 7 days ($p < 0.05$). The wetland system T1 (77.16%) exhibited the highest removal efficiency for TDS during the initial week. However, its performance declined to 75.64% by the third week and further to 73.91% by the fourth week (Table 2). T2 achieved a peak TDS removal efficiency of 24.99%, which was 52.17% lower than T1 and 22.66% lower than T3. T3 demonstrated its highest performance in the first week with a removal efficiency of 47.65%, but this decreased to 44.72% by the fourth week (Table 2).

T1 achieved the highest efficiency for TSS removal at 72.65%, outperforming T3 by 26.34% and T2 by 9.96%. T2's peak TSS elimination rate was 62.69% during the fourth week (Table 2). T3 showed improved TSS removal from 44.96% in the first week to 46.31% in the second week, but its performance deteriorated (41.16%) by the fourth week.

Regarding pH levels, T3 recorded a higher pH (7.59) at the end of the experiment. T2 showed a continuous decline in pH, with values of 6.17, 6.14, 6.02, and 5.91 for weeks 1, 2, 3 and 4, respectively. T1 experienced a decline in pH during the first 2 weeks, followed by a consistent upward trend, reaching a peak of 7.66 by the fourth week. All three constructed wetlands exhibited a gradual decrease in pH from day 1 to day seven during the initial phase, but this decline diminished over time (Figure 2).

TABLE 2 The average concentrations of effluent pollutants and their removal efficiency in each treatment wetland reactor.

Time in weeks	Parameter	Unit	Influent	CW 1		CW2		CW3	
				Effluent Conc.	R (%)	Effluent Conc.	R (%)	Effluent Conc.	R (%)
Week 1	BOD	mg/L	3,200	908.89 ± 76.88	71.6 ± 2.40	1538.3 ± 73.53	51.9 ± 2.30	1173.3 ± 50.00	63.3 ± 1.56
	COD	mg/L	7,500	1888.7 ± 240.75	74.8 ± 3.21	4892.4 ± 244.36	34.7 ± 3.26	3049.2 ± 279.39	59.3 ± 3.73
	NH_4^+-N	mg/L	3.85	0.78 ± 0.08	79.6 ± 2.21	3.10 ± 0.06	19.4 ± 1.54	1.61 ± 0.15	58.0 ± 3.84
	NO_3^--N	mg/L	20	4.43 ± 0.66	77.8 ± 3.29	12.03 ± 0.20	39.8 ± 0.99	9.94 ± 0.36	50.2 ± 1.81
	OP	mg/L	2.93	0.36 ± 0.06	87.7 ± 1.93	2.10 ± 0.03	28.2 ± 1.15	1.28 ± 0.06	56.3 ± 2.15
	TDS	mg/L	2.000	456.78 ± 61.16	77.1 ± 3.06	1500.2 ± 23.27	24.9 ± 1.16	1047.0 ± 24.93	47.6 ± 1.25
	TN	mg/L	35	8.81 ± 1.79	74.8 ± 5.13	25.33 ± 0.34	27.6 ± 0.97	17.11 ± 0.51	51.1 ± 1.45
	TP	mg/L	12	2.27 ± 0.23	81.0 ± 1.88	7.59 ± 0.15	36.7 ± 1.29	3.35 ± 0.20	72.0 ± 1.66
	TSS	mg/L	1,800	512.67 ± 51.33	71.5 ± 2.85	676.44 ± 30.34	62.4 ± 1.69	990.67 ± 53.59	44.9 ± 2.98
	pH		7.50	6.99 ± 0.08	–	6.17 ± 0.16	–	7.45 ± 0.27	–
Week 2	BOD	mg/L	3,200	984.44 ± 109.90	69.2 ± 3.43	1556.6 ± 65.72	51.3 ± 2.05	1278.3 ± 55.00	60.0 ± 1.72
	COD	mg/L	7,500	1900.0 ± 217.89	74.6 ± 2.91	5108.6 ± 225.77	31.8 ± 3.01	3322.3 ± 316.08	55.7 ± 4.21
	NH_4^+-N	mg/L	3.85	0.80 ± 0.09	79.1 ± 2.37	3.10 ± 0.09	19.5 ± 2.43	1.65 ± 0.10	57.0 ± 2.67
	NO_3^--N	mg/L	20	4.65 ± 0.27	76.7 ± 1.36	12.24 ± 0.37	38.7 ± 1.86	10.03 ± 0.29	49.8 ± 1.46
	OP	mg/L	2.93	0.40 ± 0.05	86.3 ± 1.65	2.11 ± 0.07	27.8 ± 2.43	1.33 ± 0.04	54.6 ± 1.51
	TDS	mg/L	2,000	503.44 ± 60.14	74.8 ± 3.01	1527.5 ± 39.06	23.6 ± 1.95	1074.6 ± 46.16	46.2 ± 2.31
	TN	mg/L	35	10.13 ± 0.47	71.0 ± 1.35	25.27 ± 0.26	27.8 ± 0.74	17.71 ± 0.32	49.4 ± 0.92
	TP	mg/L	12	2.39 ± 0.26	80.1 ± 2.20	7.39 ± 0.20	38.4 ± 1.66	3.30 ± 0.16	72.4 ± 1.32
	TSS	mg/L	1,800	557.11 ± 70.88	69.0 ± 3.94	683.11 ± 48.98	62.0 ± 2.72	966.44 ± 68.04	46.3 ± 3.78
	pH		7.50	6.87 ± 0.07	–	6.14 ± 0.08	–	7.41 ± 0.10	–
Week 3	BOD	mg/L	3,200	1096.6 ± 109.32	65.7 ± 3.42	1550.0 ± 103.11	51.5 ± 3.22	1166.6 ± 60.83	63.5 ± 1.90
	COD	mg/L	7,500	2309.6 ± 303.38	69.2 ± 4.05	5085.8 ± 362.04	32.1 ± 4.83	3709.1 ± 445.70	50.5 ± 5.94
	NH_4^+-N	mg/L	3.85	1.02 ± 0.10	73.4 ± 2.63	3.11 ± 0.07	19.1 ± 1.76	1.88 ± 0.05	51.1 ± 1.41
	NO_3^--N	mg/L	20	5.31 ± 0.25	73.4 ± 1.23	12.18 ± 0.37	39.0 ± 1.86	9.99 ± 0.42	50.0 ± 2.08
	OP	mg/L	2.93	0.39 ± 0.03	86.7 ± 0.91	2.34 ± 0.07	20.0 ± 2.33	1.29 ± 0.07	56.0 ± 2.36
	TDS	mg/L	2,000	487.11 ± 23.85	75.6 ± 1.19	1552.7 ± 17.56	22.3 ± 0.88	1093.3 ± 51.07	45.3 ± 2.55
	TN	mg/L	35	8.87 ± 0.33	74.6 ± 0.95	25.17 ± 0.27	28.1 ± 0.78	16.93 ± 0.47	51.6 ± 1.33
	TP	mg/L	12	2.50 ± 0.10	79.1 ± 0.83	7.64 ± 0.21	36.3 ± 1.74	3.60 ± 0.12	70.0 ± 1.02
	TSS	mg/L	1,800	492.22 ± 21.99	72.6 ± 1.22	751.33 ± 144.71	58.2 ± 8.04	999.56 ± 92.51	44.4 ± 5.14
	pH		7.50	7.62 ± 0.04	–	6.02 ± 0.05	–	7.54 ± 0.05	–

(Continued)

10.3389/fmicb.2024.1421094

10.3389/fmicb.2024.1421094

TABLE 2 (Continued)

Time in weeks	Parameter	Unit	Influent	CW 1		CW2		CW3	
				Effluent Conc.	R (%)	Effluent Conc.	R (%)	Effluent Conc.	R (%)
Week 4	BOD	mg/L	3,200	1000.0 ± 76.49	68.7 ± 2.39	1646.6 ± 116.14	48.5 ± 3.63	1348.8 ± 151.36	57.8 ± 4.73
	COD	mg/L	7,500	2400.7 ± 251.41	67.9 ± 3.35	4608.0 ± 499.04	33.8 ± 4.78	3538.4 ± 491.39	52.8 ± 6.55
	NH_4^+-N	mg/L	3.85	1.12 ± 0.09	70.8 ± 2.26	3.14 ± 0.11	18.4 ± 2.79	1.84 ± 0.03	52.2 ± 0.89
	NO_3^--N	mg/L	20	5.97 ± 0.29	70.1 ± 1.47	12.20 ± 0.38	39.0 ± 1.89	10.46 ± 0.39	47.7 ± 1.96
	OP	mg/L	2.93	2.57 ± 0.11	85.5 ± 1.94	2.37 ± 0.14	19.1 ± 4.67	1.29 ± 0.09	56.0 ± 3.10
	TDS	mg/L	2,000	521.89 ± 31.93	73.9 ± 1.60	1,510 ± 14.69	24.4 ± 0.73	1105.5 ± 35.13	44.7 ± 1.76
	TN	mg/L	35	10.84 ± 0.17	69.03 ± 0.49	26.32 ± 0.31	24.80 ± 0.89	18.60 ± 0.44	46.87 ± 1.26
	TP	mg/L	12	2.91 ± 0.35	75.71 ± 2.93	7.61 ± 0.15	36.61 ± 1.29	3.68 ± 0.22	69.36 ± 1.86
	TSS	mg/L	1,800	536.22 ± 38.88	70.21 ± 2.16	671.56 ± 42.28	62.69 ± 2.35	1059.11 ± 116.20	41.16 ± 6.46
	pH		7.50	7.66 ± 0.05	–	5.91 ± 0.05	–	7.59 ± 0.02	–

3.5 Effects of substrates and vegetation plant

Tables 3, 4 present a statistical comparison of the adsorption of specific nitrogen and phosphorus between the plants and substrates of CW1 and CW2, as well as CW1 and CW3. This comparison was conducted to assess the individual impact of these factors on the wetland reactors. The paired *t*-test was used for this analysis. A statistically significant difference ($p < 0.05$) was observed in the adsorption of NH_4^+-N and OP between the plants of CW1 and CW3. The adsorption of NH_4^+-N and OP on the substrates of CW1 and CW2 also exhibited a statistically significant difference. In contrast, it is seen that CW1 exhibits superior removal rates for NH_4^+-N and OP in both plants and substrates. This finding suggested that the collective utilization of plants and substrates significantly influences wastewater treatment more than their individual effects.

3.6 Microbial community of different SFCWs

A high-throughput sequencing approach using the Illumina 16S rRNA gene was utilized to investigate the number and diversity of microbial communities in T1 and T2. The operational measures (Chao1, Shannon, and Simpson) used to assess microbial communities' richness and diversity were identified. In July, CW1 exhibited greater richness and microbiological diversity than CW2, as evidenced by its higher Chao1, Shannon, and Simpson values. This pattern remained consistent throughout August, though there was a drop in the Chao1, Shannon, and Simpson values, as indicated in Table 5.

Figure 3A illustrates the phylogenetic diversity of the microbial population at the phylum level across CW1 and CW2. During July and August, Proteobacteria were identified as the dominant taxon in both SFCW microcosms. In CW2, Proteobacteria comprised 67.30 and 54.52% of the microbial population in July and August, respectively. Similarly, in CW1, they accounted for 63.81% in July and 52.91% in August. Additionally, the substrates of both wetland systems contained other phyla such as Spirochaetota (2–18.5%), Firmicutes (0.5–14%), Bacteroidota (4.3–15.55%), Desulfobactota (0.62–10.62%), Actinobacteriota (0.45–4.06%), and Cyanobacteria (0.19–0.6%). According to Miao et al. (2015), Proteobacteria and Firmicutes are essential components in the process of denitrification. Furthermore, Bacteroidetes, Chloroflexi, Patescibacteria, Firmicutes, and Actinobacteria play crucial roles in efficiently eliminating pollutants within wetland systems. Bacteroidetes are widely recognized as polymeric organic degraders (Wang et al., 2009). Firmicutes and Chloroflexi have demonstrated significant efficacy in degrading microbial extracellular polymeric compounds and soluble microbial substances (Liu et al., 2019). Several studies indicate that Patescibacteria is a prominent bacterial phylum following the commencement of ANAMMOX and denitrification (Song et al., 2019). According to Chen et al. (2020), there is a significant correlation between the concentration of TN and gram-negative bacteria. Moreover, the matrix layer strongly correlates with denitrification, elucidating the efficient elimination of chemical oxygen demand (COD), nitrogen, and phosphorus in various wetland systems.

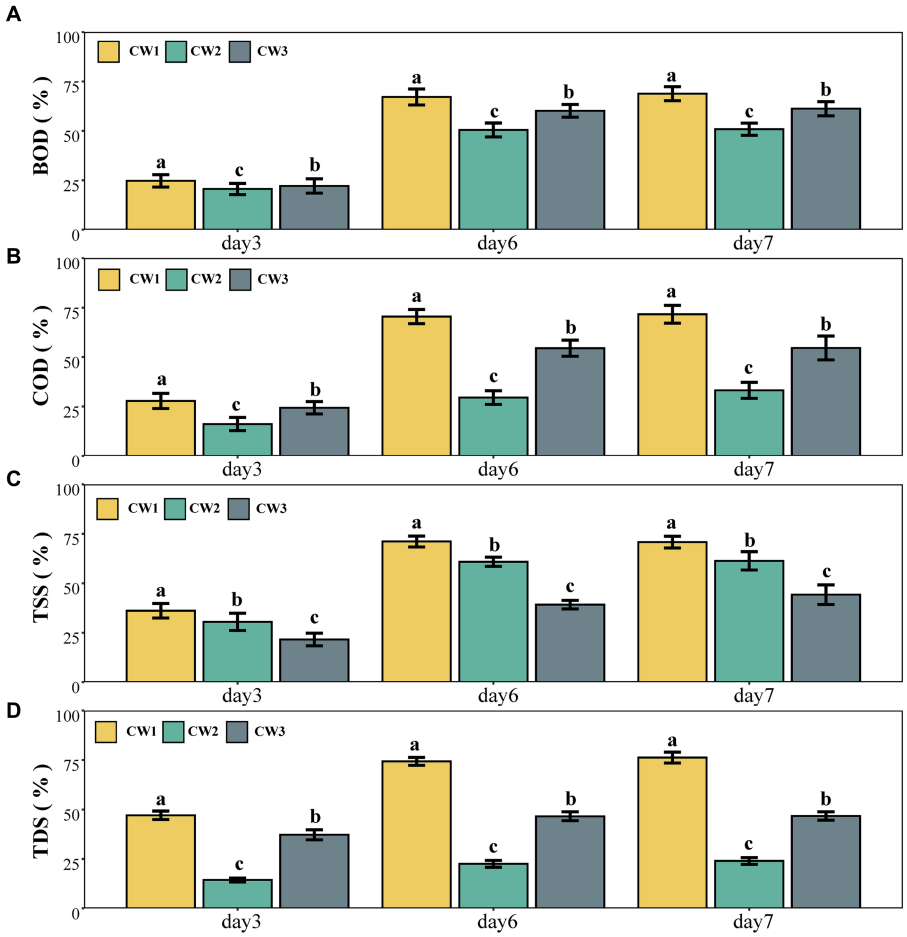

FIGURE 2
Percentage removal of **(A)** BOD, **(B)** COD, **(C)** TSS, **(D)** TDS.

TABLE 3 NH_4^+-N and OP in the plants of CW1 and CW3.

Parameters	Day 0		Day 7		Day 14		Day 28	
	CW1	CW3	CW1	CW3	CW1	CW3	CW1	CW3
NH_4^+-N in plants	62.34 ± 1.17	62.34 ± 0.8	**68.41 ± 0.32**	**64.52 ± 0.31**	64.56 ± 1.14	64.56 ± 1.3	64.52 ± 1.25	64.41 ± 1.33
OP in plants	102.78 ± 1.04	102.78 ± 0.94	104.57 ± 1.42	104.53 ± 1.27	**107.21 ± 0.03**	**104.50 ± 0.05**	104.51 ± 1.10	104.42 ± 1.59

The significant statistical difference ($p < 0.05$) is indicated in bold numbers.

TABLE 4 NH_4^+-N and OP in the substrates of CW1 and CW2.

Parameters	Day 0		Day 7		Day 14		Day 28	
	CW1	CW2	CW1	CW2	CW1	CW2	CW1	CW2
NH_4^+-N in substrate	0	0	0.85 ± 0.02	0.81 ± 0.05	**0.92 ± 0.04**	**0.77 ± 0.05**	0.74 ± 0.10	0.69 ± 0.09
OP in substrate	0	0	0.88 ± 0.17	0.85 ± 0.05	**0.94 ± 0.15**	**0.79 ± 0.06**	**0.79 ± 0.02**	**0.53 ± 0.03**

The significant statistical difference ($p < 0.05$) is indicated in bold numbers.

The microbial phylogenetic diversity at the class level in CW1 and CW2 SFCW systems is depicted in Figure 3B. The dominant groupings included Gammaproteobacteria, Alphaproteobacteria, Leptospirae, Bacteroidia, Clostridia, and Desulfovibrionia. In July, the relative abundances in CW1 were 47.35, 16.47, 11.71, 3.49, 2.47, and 0%, respectively. In CW2, their relative abundances were 48.72, 18.54, 18.59, 5.35, 0.17, and 0%, respectively. In August, the relative abundances in CW1 were 40.89, 12.03, 2.13, 14.89, 8.38, and 5.14%, respectively, while in CW2, they were 35.46, 19.03, 1.59, 13.20, 9.5, and 6.94%, respectively. According to Han et al. (2021), Proteobacteria, Alphaproteobacteria, Betaproteobacteria, and Gammaproteobacteria play significant roles in nitrification and organic matter decomposition,

TABLE 5 Microbial community alpha diversity.

Month	Constructed wetland	Chao1	Shannon	Simpson
July	CW 1	1024.677 ± 266.23	7.111 ± 1.54	0.994197 ± 0.06
	CW 2	537.4286 ± 107.40	5.606602 ± 0.44	0.940525 ± 0.000364
August	CW 1	785.3163 ± 208.00	6.751978 ± 0.80	0.957896 ± 0.04
	CW 2	457.9516 ± 56.40	5.245325 ± 0.78	0.930625 ± 0.02

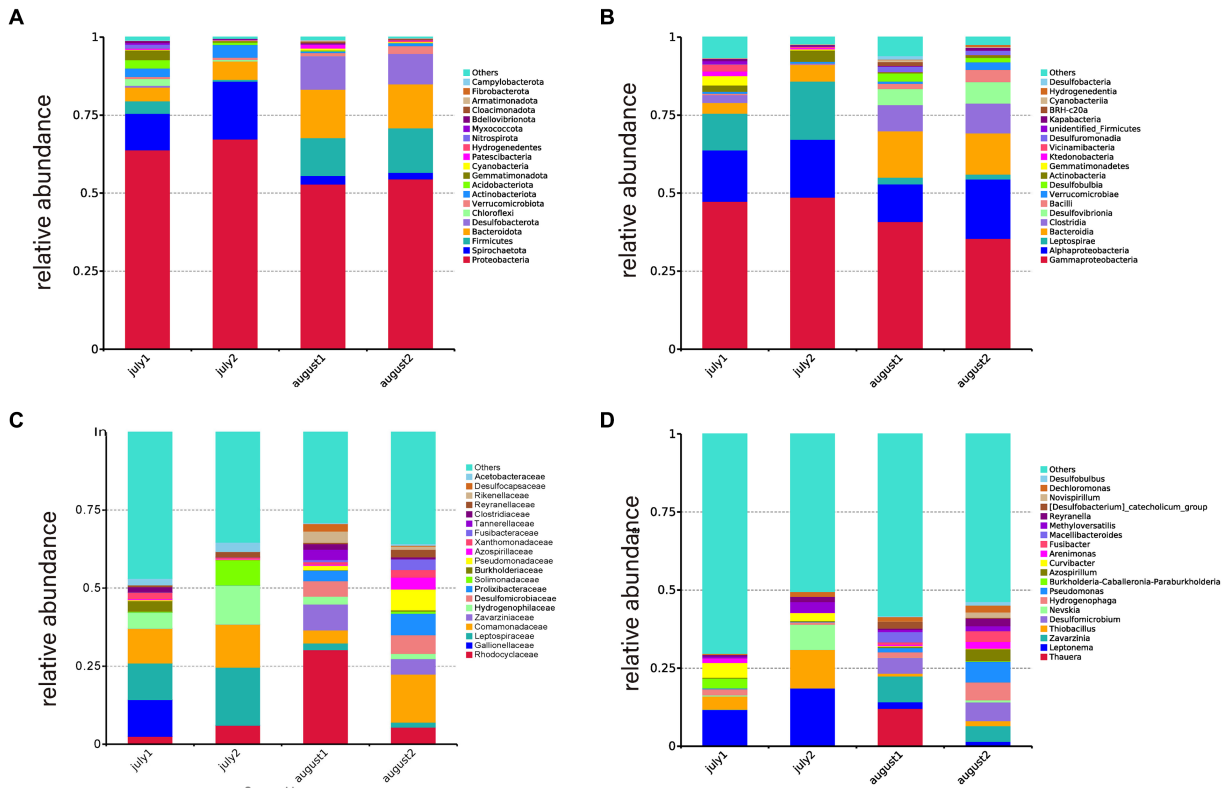

FIGURE 3
Distribution of microorganisms at different taxon levels in the different SFCW (CW1 in July: july 1, CW1 August: august 1, CW2 in July: july 2, CW2 in August: august 2), **(A)** phylum level, **(B)** class level, **(C)** family Level, **(D)** genus level.

including anammox, nitrifying, and nitrite-oxidizing bacteria, which have important ecological roles in reducing nitrate and nitrite (He et al., 2016).

Figure 3C displays the microbial community composition at the family level. The dominant families were Rhodocyclaceae (2.48–30.25%), Gallionellaceae (11.77%), Leptospiraceae (1.59–18.59%), Comamonadaceae (4.18–15.41%), and Zavarziniaceae (0.003–8.22%). Rhodocyclaceae, a significant group of denitrifying bacteria (Lu et al., 2015), was more abundant in CW1, utilizing nitrate or nitrite as the ultimate electron acceptor and playing a role in the denitrification process (Pelissari et al., 2016). Leptospiraceae facilitate biofilm development (Song et al., 2021), while Gallionellaceae promotes nitrogen elimination (Tian et al., 2020).

Figure 3D displays the genus-level microbial community composition. The dominant genera observed were Thauera (12.09%), Leptonema (1.55–18.59%), Zavarzinia (4.96–8.22%), Thiobacillus (0.09–12.27%), and Desulfomicrobium (4.98–5.97%). Thauera, present exclusively in CW1, is recognized as a significant degrader of aromatic compounds in wastewater (Mao et al., 2010) and plays a crucial role in removing nitrogen and phosphorus from low-carbon source sewage (Ren et al., 2021). Leptonema, a member of the Leptospiraceae family, plays a crucial role in the production of lipopolysaccharides and facilitates biofilm development (Song et al., 2021). Zavarzinia, an Alphaproteobacteria, can use carbon monoxide as a source of energy and is primarily responsible for breaking down benzene in oil-sands-contaminated water (Rochman et al., 2017; Lee et al., 2019). Thiobacillus converts NO_3^--N and NO_2^--N into N_2 under facultative anaerobic conditions (Huang et al., 2018) and is categorized as a sulfide-oxidizing bacteria (SOB) in constructed wetlands (Samsó and García, 2013).

Principal Coordinate Analysis (PCoA) is a valuable method for visually representing the dissimilarities or similarities between several groupings. The findings indicate that PC1 and PC2 accounted for 31.38 and 16.28% of the contribution rates, respectively (Figure 4A). In July, the proximity of the bacterial communities in the substrates of CW1 and CW2 suggests a similarity in their community makeup.

Conversely, bacterial communities exhibited more dispersion in August, indicating significant differences in their composition and poor resemblance across the communities. The comparison reveals notable disparities in the distribution distances of communities, suggesting substantial dissimilarities in the makeup of CW1 and CW2.

Figure 4B illustrates the correlation between the microbial community and various pollutants, including BOD, COD, NH_4^+-N, NO_3^--N, OP, TDS, TN, TP, and TSS. Chloroflexi exhibits a strong positive correlation with the removal of BOD and TN, indicating its significant role in eliminating these pollutants. Acidobacteriota is positively associated with BOD and NH_4^+-N and shows a strong correlation with TN. Gemmatimonadota also demonstrates significant positive relationships with various parameters, including TN, OP, and BOD. Additionally, the Chao1 index exhibited a strong positive correlation with several pollutants, such as BOD, COD, NH_4^+-N, NO_3^--N, TDS, and TN, suggesting that greater microbial diversity effectively enhances the removal of these pollutants.

4 Discussion

4.1 Total nitrogen, NH_4^+-N and NO_3^--N removal

Lemna minor L. effectively adsorbed nitrogen from wastewater in the wetland system, yielding better results within a short period of 7 days, especially when substrates such as lignite and brick rubble were present. Nitrification and denitrification are the primary processes influencing the movement and transformation of nitrogen, carried out mainly by nitrifying and denitrifying bacteria (Fan et al., 2013; Sani et al., 2013). However, the denitrification process in constructed wetlands, responsible for removing total nitrogen (TN), may be adversely influenced by several factors (Zhou et al., 2018). To overcome these constraints, lignite can serve as an effective carbon source and exhibit the system's adsorption characteristics while avoiding pollution (Zhou et al., 2017). Brick rubble, with its porous structure, creates anaerobic conditions and provides a large surface area to promote the growth of biofilms rich in denitrifying bacteria, thereby reducing TN (Lima et al., 2018; Li H. et al., 2021). CW1, comprising substrates and plants, demonstrated a significantly higher capacity (74.8%) for total nitrogen removal from wastewater than CW2 and CW3. *Lemna minor* L. has been found to have a high capacity for nitrogen removal (Kern and Idler, 1999; Patel and Kanungo, 2010). Cedergreen and Madsen (2002) reported that *Lemna minor* L. can uptake NH_4^+-N and NO_3^--N from water, with both roots and leaves absorbing nitrogen from wastewater, enhancing nitrogen removal capabilities. Substrates also play a crucial role in eliminating pollutants from wastewater. Findings from the CW2 study (Table 4), which focused exclusively on substrates, indicate that bricks can adsorb nitrogen from wastewater. Ren et al. (2007) demonstrated the effectiveness of using bricks as a substrate in wetlands for removing nitrogen and phosphorus from wastewater. An increase in the hydraulic retention time had improved the efficiency of all wetlands. The duckweed plant significantly contributed to this process, showing that longer hydraulic retention times led to higher removal rates of contaminants (Jing et al., 2002; Adhikari et al., 2015).

4.2 Phosphorous removal

The results from CW3 (Table 3) demonstrate that *Lemna minor* L. can adsorb phosphorus. Furthermore, its adsorption capacities are improved in the presence of substrates, as shown by CW1. CW1 exhibited better phosphorus removal than CW2 and CW3 (Table 2). According to a study by Perniel et al. (1998), *Lemna minor* L. monoculture consistently exhibited the highest phosphorus removal capacity from stormwater within 8 weeks. In the current study, *Lemna minor* L. utilized phosphate as a growth substance, resulting in a substantial decrease of 81% in total phosphorus levels in CW1 over 7 days. This reduction can be attributed to absorption, adsorption, or direct uptake by the plant. Iqbal et al. (2019) examined *Lemna minor* L. (duckweed) growth and nutrient removal efficiency from synthetic

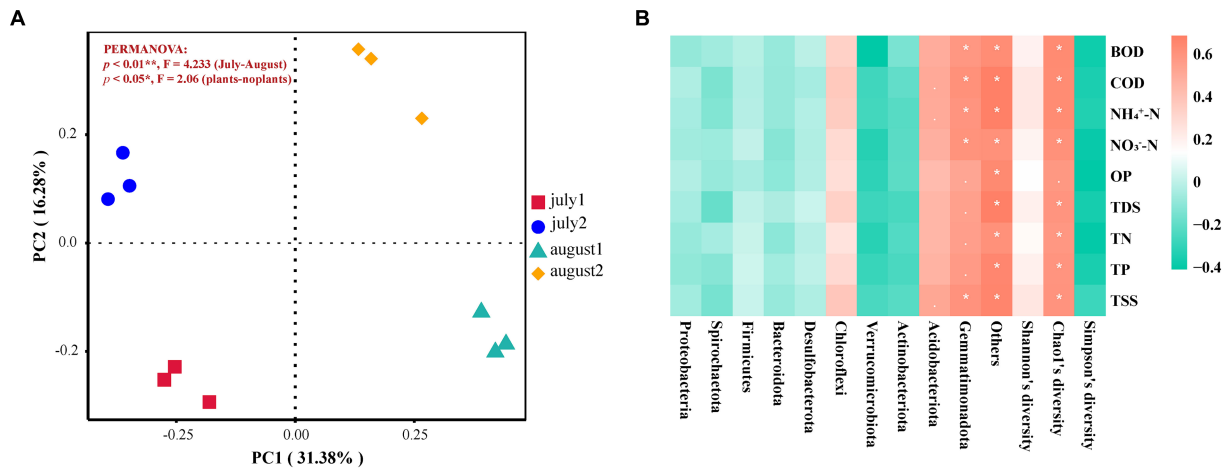

FIGURE 4
(A) PCoA Analysis of microbial community. july 1: at the start of the experiment with plant; july 2: at the start of the experiment without plant; august 1: at the end of the experiment with plant; august 2: at the end of the experiment without plant, **(B)** Correlation Heat Map Between Microbial Community Composition and Pollutant Removal Efficiency.

and dumpsite leachate in both artificial and natural environments, finding that *Lemna minor* L. effectively removes nutrients in both settings. Dinh et al. (2020) employed a laboratory-scale stabilization pond to cultivate duckweed using anaerobically treated wastewater diluted by a factor of 10, achieving 85% TP removal within 5 days. Ceschin et al. (2019) identified duckweed as a viable plant species for wastewater bioremediation due to its ability to withstand and absorb a wide range of contaminants and significant amounts of nutrients. Duckweed exhibits continuous vegetative development throughout the year, achieving high rates by utilizing nutrients from wastewater, which can accumulate within the cells or be used to generate new biomass.

Bojcevska and Tonderski (2007) operated surface flow constructed wetlands planted with *Cyperus papyrus* and *Echinochloa pyramidalis* for 12 months, observing 48–84% TP removal. In the present experiment, comparable TP removal was observed in CW1 within 7 days, indicating effective results in a short time. The substrate media plays a crucial role in phosphorus removal (Vymazal, 2011). In our experiment, CW1 removed more phosphorus than CW3, likely due to the presence of substrates. Bricks, being porous media, have an increased surface area when crushed, aiding in phosphorus adsorption from wastewater (Li J. et al., 2021). Constructed wetlands mainly get oxygen from atmospheric diffusion and plant roots (Zhou et al., 2019). Bricks as substrates may be responsible for the observed phosphorus reduction in CW2. They exhibit qualities to effectively remove phosphorus from wastewater, making them a suitable substrate (Ren et al., 2007).

The substrates in CW2 demonstrated the capacity to remove phosphorus from the influent effectively (Table 4). Additionally, these substrates can facilitate the proliferation of microbial communities and plants. The combined utilization of plants and substrates resulted in a greater phosphorus removal efficiency of 81% for CW1 (Table 2) compared to CW2 and CW3. A study by Wang et al. (2013) assessed the physicochemical characteristics and phosphorus adsorption capabilities of oyster shells, broken bricks, volcanic rock, and zeolite as substrates for treating swine wastewater. All substrates, except volcanic rock, demonstrated suitability for enhancing microorganism and plant development in water treatment systems. Billore et al. (2001) treated distillery effluent in a constructed wetland consisting of four cells. The effluent from cells one and two was directed to cells three and four, which contained plants and brick debris. Following a pretreatment process, the effluent decreased 79% in phosphorus content. Shi et al. (2017) documented a 29.16% reduction in phosphorus using red bricks in a wetland system.

4.3 BOD and COD removal

Lemna minor L. has demonstrated potential for effectively removing BOD. The combined effects of plants and substrates, particularly the porous structure of bricks, enhanced the pollutant removal efficiency. The present experimental findings indicate that plants effectively removed a significant proportion of BOD and COD in CW3 (Table 2). The combined influence of plants and substrates in CW1 significantly impacts the removal of BOD and COD, resulting in notable reductions in these pollutants (Table 2). Körner et al. (2003) conducted a study examining the efficacy of duckweed in treating wastewater. Their findings indicated that duckweed facilitated the breakdown of organic matter, in terms of BOD and COD, by providing increased oxygen and a larger surface area for bacterial proliferation. Duckweed achieved a removal rate of 67.4% for COD and 95.8% for BOD after 20 days in a study by Oron et al. (1987). However, in the current experiment, *Lemna minor* L. removed 63.3% of BOD and 59.3% of COD within 7 days. Mandi (1994) conducted an experiment treating water with the duckweed species *Lemna gibba* at low organic loading, leading to an 82% reduction in wastewater's COD. Adhikari et al. (2015) found similar results when they introduced a mixture of diluted raw dairy manure into a combination of surface flow and subsurface flow wetlands using duckweed as vegetation. The removal of COD in primary duckweed wetlands ranged from 3 to 81%, whereas in secondary duckweed wetlands, it varied from 35 to 38%. These findings are consistent with the results obtained in the current experiment. The BOD of wetland systems CW1 and CW3 abruptly increased on the sixth day due to the generation of gaseous oxygen resulting from the photosynthetic processes of *Lemna minor* L.

The CW2 substrates demonstrated a significant reduction in BOD and COD, indicating their ability to adsorb these pollutants from wastewater, as shown in Tables 2, 4. Saeed et al. (2018) conducted an experiment demonstrating a noteworthy reduction of 83.2% in COD and 87.0% in BOD through the utilization of a hybrid-built wetland system with bricks as the substrate medium. These findings coincide with the outcomes of the present study, which showed that the surface flow-constructed wetland with brick rubble and *Lemna minor* L. has the potential to remove BOD and COD from wastewater.

4.4 TDS, TSS, and pH

Lemna minor L. was primarily responsible for the removal of TDS from the wetland systems. The elimination of TDS was more significant in CW1 than in CW2 and CW3, with CW3 showing a higher reduction than CW2, as indicated in Table 2. The elevated total dissolved solids (TDS) removal can be attributed to the presence of *Lemna minor* L. A study by Amare et al. (2018) demonstrated a 68% reduction in TDS using *Lemna minor* L. in wastewater treatment in tropical semiarid areas of Ethiopia. Ali et al. (2024) constructed a free-water surface flow wetland planted with *Pistia stratiotes* and observed significant removal of TDS and TSS with a hydraulic retention time (HRT) of 30 days. In our experiment, a comparable amount of TDS and TSS removal was observed with an HRT of just 7 days, indicating that CW1 is capable of efficiently removing TDS and TSS in a short period. The substrates were shown to be responsible for the higher clearance rates of TSS seen in CW1. Findings from CW2 validate; bricks (due to their expansive surface area and pores) functioned as filters and effectively absorbed total suspended particles from wastewater. A study by Javani et al. (2016) produced similar results, showing that geotextile sheets and structural brick debris significantly impacted the removal of TSS contaminants in treated municipal wastewater. Saeed et al. (2018) conducted an experiment using recycled bricks to treat industrial wastewater, with findings consistent with our experiment, indicating that bricks are valuable for removing TSS. The present experiment revealed that the elimination of TSS in CW2 was significantly higher than in CW3, attributed to the porous structure of the bricks. Obeng et al. (2023) also found that clay bricks effectively eliminated TSS from wastewater. While bricks are crucial for eliminating TSS, the findings from CW3 suggest that *Lemna minor* L. can also remove TSS from

wastewater. Consistent with our results, Papadopoulos and Tsihrintzis (2011) reported a 63% reduction in TSS using *Lemna minor* L. in wastewater treatment. As indicated in Table 2, a pH decrease was noted at the start of the experiment, particularly in CW2. Throughout the experiment, the continuous pH decrease in CW2 is linked to the presence of lignite, known for its pH-lowering effect due to its limited negative charge, reducing the removal action of H+ ions (Di et al., 2022). The pH value from CW3 provides additional evidence supporting the pH decline observed in CW1 and CW2, attributed to the presence of lignite. However, the pH levels showed a noticeable upward trend during the second week. The observed increase in the ultimate pH values of 7.66 for CW1, 7.37 for CW2, and 7.59 for CW3 can be linked to the photosynthetic process in the plant.

4.5 Microbial community

Brick rubble created an optimal environment for the growth of the microbial community due to its extended surface area and porous structure. Chloroflexi, Acidobacteriota, and Gemmatimonadota were identified as key contributors to the removal of BOD, COD, nitrogen, and phosphorus. In the present experiment, Proteobacteria exhibited the highest abundance at the phylum level. Additionally, at the class level, α-Proteobacteria and γ-Proteobacteria were identified as the most abundant microorganisms (Figure 3). These microorganisms play a crucial role in the degradation of organic matter and nitrification processes and are commonly encountered in sewage treatment systems (Chen et al., 2019; Al Ali et al., 2020). Table 5 demonstrates an increase in the variety and abundance of microbial communities on the substrates of CW1. The increased microbial diversity can be attributed to the presence of brick rubble, which possesses porous qualities that promote microbial development. Shi et al. (2017) reported a comparable microbial composition in a constructed wetland containing diverse construction wastes, such as clay bricks. The predominant phylum identified in their study was Proteobacteria. The purification effects of recycled aggregates derived from construction waste as fillers in created wetlands were investigated by Li et al. (2022). They observed that red bricks exhibited the highest efficiency in terms of microbial community richness. The most prevalent microbial phylum identified was Proteobacteria (Li et al., 2022), which aligns with the findings of the current experiment. Wang et al. (2020) observed that members of the Chloroflexi phylum play a crucial role in nitrogen removal. Similarly, Huber et al. (2022) demonstrated that Acidobacteriota not only remove nitrogen but also phosphorus from wastewater and act as organic carbon degraders. Mujakić et al. (2023) reported that Gemmatimonadota is involved in the removal of various pollutants, including nitrogen and phosphorus. These findings align with our experimental results, where Chloroflexi, Acidobacteriota, and Gemmatimonadota contributed to the removal of nitrogen, phosphorus, biochemical oxygen demand, and chemical oxygen demand (Figure 4B).

The observed variations in microbial communities in the PCoA analysis (Figure 4A) can be associated with the presence of vegetation. The substrates of CW1, planted with *Lemna minor* L., exhibited a higher richness of microbial communities compared to CW2, which did not have any vegetation. Menon et al. (2013) reported similar results, indicating that variations in the bacterial population of the sediment were linked to the specific plant regime employed in their study. Wang et al. (2016) found that the presence of plants positively impacted both the abundance and diversity of microorganisms in a subsurface flow-constructed wetland. These findings align with the results obtained in the current experiment. Therefore, the presence or absence of plant species significantly influenced the composition of the microbial community in the constructed wetland system (Zhang et al., 2010).

Adding brick rubble, lignite, and *Lemna minor* L. to CW1 resulted in distinct bacterial communities at the phylum, class, family, and genus levels. The brick rubble and lignite dissolved organic compounds from wastewater due to their porous structure, promoting microbial growth. The substrates, along with the vegetation plant *Lemna minor* L., supported a rich and diverse microbial community for pollutant degradation. It partially explains the high pollutant removal rates of the SFCW wetland systems.

5 Conclusion

This research examined the composition of the microbial community and the effects of different wetland configurations on the purification of artificial wastewater generated by the sugar industry. *Lemna minor* L. plants assimilated nitrogen, phosphate, and other contaminants. Lignite functioned as a carbon source, promoting the growth of both plants and microbial life in the substrates. These substrates served as efficient filter media, with their porous structure providing adequate space for a thriving microbial population. Plants regulated the diversity of the microbial population. The findings clearly demonstrate that *Lemna minor* L. and brick rubble have significant potential for efficiently removing nutrients from wastewater, particularly sugar mill effluent. Our results support the hypothesis that a constructed wetland system utilizing plants and substrates is effective in treating effluents from sugar industries. This effectiveness is attributed to the rich microbial community fostered by the substrates and plants within the system. This study aims to improve the removal of contaminants from wastewater treatment plants, specifically those connected to sugar mills, by utilizing economical and widely available materials. Additionally, it contributes to the global goal of achieving carbon neutrality and can be easily implemented in underdeveloped nations worldwide.

Data availability statement

The sequencing data that support the findings of this study are available in SRA database at https://www.ncbi.nlm.nih.gov/sra/PRJNA1132581, accession number PRJNA1132581.

Author contributions

HA: Data curation, Visualization, Writing – original draft. YM: Data curation, Formal analysis, Methodology, Writing – review & editing. XY: Funding acquisition, Project administration, Supervision, Writing – review & editing. YK: Writing – review & editing, Conceptualization, Supervision. PM: Data curation, Writing – review & editing. SA: Data curation, Writing – review & editing.

Funding

The author(s) declare that financial support was received for the research, authorship, and/or publication of this article. This work was supported by the National Natural Science Foundation of China (42222102 and 42171107).

Conflict of interest

The authors declare that the research was conducted in the absence of any commercial or financial relationships that could be construed as a potential conflict of interest.

Publisher's note

Supplementary material

The Supplementary material for this article can be found online at: https://www.frontiersin.org/articles/10.3389/fmicb.2024.1421094/full#supplementary-material

References

Adhikari, U., Harrigan, T., and Reinhold, D. M. (2015). Use of duckweed-based constructed wetlands for nutrient recovery and pollutant reduction from dairy wastewater. *Ecol. Eng.* 78, 6–14. doi: 10.1016/j.ecoleng.2014.05.024

Al Ali, A. A., Naddeo, V., Hasan, S. W., and Yousef, A. F. (2020). Correlation between bacterial community structure and performance efficiency of a full-scale wastewater treatment plant. *J. Water Process Eng.* 37:101472. doi: 10.1016/j.jwpe.2020.101472

Ali, M., Aslam, A., Qadeer, A., Javied, S., Nisar, N., Hassan, N., et al. (2024). Domestic wastewater treatment by Pistia stratiotes in constructed wetland. *Sci. Rep.* 14:7553. doi: 10.1038/s41598-024-57329-y

Allen, S. J., Whitten, L. J., Murray, M., Duggan, O., and Brown, P. (1997). The adsorption of pollutants by peat, lignite and activated chars. *J. Chem. Technol. Biotechnol.* 68, 442–452. doi: 10.1002/(SICI)1097-4660(199704)68:4<442::AID-JCTB643>3.0.CO;2-2

Amare, E., Kebede, F., and Mulat, W. (2018). Wastewater treatment by Lemna minor and Azolla filiculoides in tropical semi-arid regions of Ethiopia. *Ecol. Eng.* 120, 464–473. doi: 10.1016/j.ecoleng.2018.07.005

American Public Health Association (1926). Standard methods for the examination of water and wastewater, vol. 6. New York, NY: American Public Health Association.

Ameso, V. C., Essandoh, H. M. K., Donkor, E. A., and Nwude, M. O. (2023). Comparative analysis of greywater pollutant removal efficiency with horizontal free water surface flow wetland with other wetland technologies. *Heliyon* 9:e17637. doi: 10.1016/j.heliyon.2023.e17637

Billore, S., Singh, N., Ram, H., Sharma, J., Singh, V., Nelson, R., et al. (2001). Treatment of a molasses based distillery effluent in a constructed wetland in Central India. *Water Sci. Technol.* 44, 441–448. doi: 10.2166/wst.2001.0864

Bojcevska, H., and Tonderski, K. (2007). Impact of loads, season, and plant species on the performance of a tropical constructed wetland polishing effluent from sugar factory stabilization ponds. *Ecol. Eng.* 29, 66–76. doi: 10.1016/j.ecoleng.2006.07.015

Calheiros, C. S., Rangel, A. O., and Castro, P. M. (2009). Treatment of industrial wastewater with two-stage constructed wetlands planted with Typha latifolia and Phragmites australis. *Bioresour. Technol.* 100, 3205–3213. doi: 10.1016/j.biortech.2009.02.017

Callahan, B. J., McMurdie, P. J., Rosen, M. J., Han, A. W., Johnson, A. J. A., and Holmes, S. P. (2016). DADA2: High-resolution sample inference from Illumina amplicon data. *Nat. Methods.* 13, 581–583. doi: 10.1038/nmeth.3869

Cedergreen, N., and Madsen, T. V. (2002). Nitrogen uptake by the floating macrophyte Lemna minor. *New Phytol.* 155, 285–292. doi: 10.1046/j.1469-8137.2002.00463.x

Ceschin, S., Sgambato, V., Ellwood, N. T. W., and Zuccarello, V. (2019). Phytoremediation performance of Lemna communities in a constructed wetland system for wastewater treatment. *Environ. Exp. Bot.* 162, 67–71. doi: 10.1016/j.envexpbot.2019.02.007

Chen, H., Li, A., Cui, D., Cui, C., and Ma, F. (2019). Evolution of microbial community and key genera in the formation and stability of aerobic granular sludge under a high organic loading rate. *Bioresour. Technol. Rep.* 7:100280. doi: 10.1016/j.biteb.2019.100280

Chen, H., Ma, D., Jiang, X., Liu, M., and Zang, S. (2020). Effects of seasonal freezing and thawing on soil microbial community structure and extracellular enzyme activity in Zhalong wetland. *J. Environ. Sci.* 4, 1443–1451. doi: 10.13671/j.hjkxxb.2019.0435

Di, J., Ma, Y., Wang, M., Gao, Z., Xu, X., Dong, Y., et al. (2022). Dynamic experiments of acid mine drainage with Rhodopseudomonas spheroides activated lignite immobilized sulfate-reducing bacteria particles treatment. *Sci. Rep.* 12:8783. doi: 10.1038/s41598-022-12897-9

Dinh, T. T. U., Soda, S., Nguyen, T. A. H., Nakajima, J., and Cao, T. H. (2020). Nutrient removal by duckweed from anaerobically treated swine wastewater in lab-scale stabilization ponds in Vietnam. *Sci. Total Environ.* 722:137854. doi: 10.1016/j.scitotenv.2020.137854

Fan, J., Wang, W., Zhang, B., Guo, Y., Ngo, H. H., Guo, W., et al. (2013). Nitrogen removal in intermittently aerated vertical flow constructed wetlands: impact of influent COD/N ratios. *Bioresour. Technol.* 143, 461–466. doi: 10.1016/j.biortech.2013.06.038

Gupta, S., Mittal, Y., Tamta, P., Srivastava, P., and Yadav, A. K. (2020). "Textile wastewater treatment using microbial fuel cell and coupled technology: a green approach for detoxification and bioelectricity generation" in Integrated microbial fuel cells for wastewater treatment (Amsterdam, Netherlands: Elsevier), 73–92.

Han, Y., Qian, J., Guo, J., Song, Y., Lu, C., Li, H., et al. (2021). Feasibility of partial denitrification and anammox for removing nitrate and ammonia simultaneously in situ through synergetic interactions. *Bioresour. Technol.* 320:124390. doi: 10.1016/j.biortech.2020.124390

Hasan, F., and Webley, P. A. (2017). "Utilization of CO2 for fuels and chemicals" in Sustainable utilization of natural resources (Boca Raton, Florida, USA: CRC Press), 417–439. eBook ISBN9781315153292

Havelcová, M., Mizera, J., Sýkorová, I., and Pekař, M. (2009). Sorption of metal ions on lignite and the derived humic substances. *J. Hazard. Mater.* 161, 559–564. doi: 10.1016/j.jhazmat.2008.03.136

He, Q., Zhou, J., Wang, H., Zhang, J., and Wei, L. (2016). Microbial population dynamics during sludge granulation in an a/O/a sequencing batch reactor. *Bioresour. Technol.* 214, 1–8. doi: 10.1016/j.biortech.2016.04.088

Huang, J., Cao, C., Yan, C., Guan, W., and Liu, J. (2018). Comparison of Iris pseudacorus wetland systems with unplanted systems on pollutant removal and microbial community under nanosilver exposure. *Sci. Total Environ.* 624, 1336–1347. doi: 10.1016/j.scitotenv.2017.12.222

Huber, K. J., Pester, M., Eichorst, S. A., Navarrete, A. A., and Foesel, B. U. (2022). Acidobacteria–towards unraveling the secrets of a widespread, though enigmatic, phylum. *Front. Microbiol.* 13:960602. doi: 10.3389/fmicb.2022.960602

Huo, Y., Bai, Y., and Qu, J. (2017). Unravelling riverine microbial communities under wastewater treatment plant effluent discharge in large urban areas. *Appl. Microbiol. Biotechnol.* 101, 6755–6764. doi: 10.1007/s00253-017-8384-4

Hussain, Z., Arslan, M., Shabir, G., Malik, M. H., Mohsin, M., Iqbal, S., et al. (2019). Remediation of textile bleaching effluent by bacterial augmented horizontal flow and vertical flow constructed wetlands: a comparison at pilot scale. *Sci. Total Environ.* 685, 370–379. doi: 10.1016/j.scitotenv.2019.05.414

Iatrou, E. I., Gatidou, G., Damalas, D., Thomaidis, N. S., and Stasinakis, A. S. (2017). Fate of antimicrobials in duckweed Lemna minor wastewater treatment systems. *J. Hazard. Mater.* 330, 116–126. doi: 10.1016/j.jhazmat.2017.02.005

Ingaramo, A., Heluane, H., Colombo, M., and Cesca, M. (2009). Water and wastewater eco-efficiency indicators for the sugar cane industry. *J. Clean. Prod.* 17, 487–495. doi: 10.1016/j.jclepro.2008.08.018

Iqbal, J., Javed, A., and Baig, M. A. (2019). Growth and nutrient removal efficiency of duckweed (Lemna minor) from synthetic and dumpsite leachate under artificial and natural conditions. *PLoS One* 14:e0221755. doi: 10.1371/journal.pone.0221755

Jacobson, K., Maheria, K. C., and Dalai, A. K. (2013). Bio-oil valorization: A review. *Renew. Sustain. Energy Rev.* 23, 91–106. doi: 10.1016/j.rser.2013.02.036

Javani, H., Hassanoghli, A., Liaghat, A., and Heidari, A. (2016). A study of columns to reduce mineral and biological pollutants during recharge operation by treated

municipal wastewater. *Desalination Water Treat.* 57, 14919–14928. doi: 10.1080/19443994.2015.1070284

Jing, S. R., Lin, Y. F., Wang, T. W., and Lee, D. Y. (2002). Microcosm wetlands for wastewater treatment with different hydraulic loading rates and macrophytes. *J. Environ. Qual.* 31, 690–696. doi: 10.2134/jeq2002.6900

Kadier, A., Kalil, M. S., Abdeshahian, P., Chandrasekhar, K., Mohamed, A., Azman, N. F., et al. (2016). Recent advances and emerging challenges in microbial electrolysis cells (MECs) for microbial production of hydrogen and value-added chemicals. *Renew. Sustain. Energy Rev.* 61, 501–525. doi: 10.1016/j.rser.2016.04.017

Karaca, S., Gürses, A., Açıkyıldız, M., and Ejder, M. (2008). Adsorption of cationic dye from aqueous solutions by activated carbon. *Microporous Mesoporous Mater.* 115, 376–382. doi: 10.1016/j.micromeso.2008.02.008

Kern, J., and Idler, C. (1999). Treatment of domestic and agricultural wastewater by reed bed systems. *Ecol. Eng.* 12, 13–25. doi: 10.1016/S0925-8574(98)00051-2

Kizito, S., Lv, T., Wu, S., Ajmal, Z., Luo, H., and Dong, R. (2017). Treatment of anaerobic digested effluent in biochar-packed vertical flow constructed wetland columns: role of media and tidal operation. *Sci. Total Environ.* 592, 197–205. doi: 10.1016/j.scitotenv.2017.03.125

Kluçáková, M., and Omelka, L. (2004). Sorption of metal ions on lignite and humic acids. *Chem. Zvesti.* 58:CLA-00:120145.

Körner, S., Vermaat, J. E., and Veenstra, S. (2003). The capacity of duckweed to treat wastewater: ecological considerations for a sound design. *J. Environ. Qual.* 32, 1583–1590. doi: 10.2134/jeq2003.1583

Kumar, S., and Dutta, V. (2019). "Efficiency of constructed wetland microcosms (CWMs) for the treatment of domestic wastewater using aquatic macrophytes" in Environmental biotechnology: For sustainable future (Singapore: Springer), 287–307.

Lai, X., Zhao, Y., Pan, F., Yang, B., Wang, H., Wang, S., et al. (2020). Enhanced optimal removal of nitrogen and organics from intermittently aerated vertical flow constructed wetlands: relative COD/N ratios and microbial responses. *Chemosphere* 244:125556. doi: 10.1016/j.chemosphere.2019.125556

Lee, Y., Park, H. Y., and Jeon, C. O. (2019). Zavarzinia aquatilis sp. nov., isolated from a freshwater river. *Int. J. Syst. Evol. Microbiol.* 69, 727–731. doi: 10.1099/ijsem.0.003214

Li, Y., Wang, J., Lin, X., Wang, H., Li, H., and Li, J. (2022). Purification effects of recycled aggregates from construction waste as constructed wetland filler. *J. Water Process Eng.* 50:103335. doi: 10.1016/j.jwpe.2022.103335

Li, H., Zhang, Y., Wu, L., Jin, Y., Gong, Y., Li, A., et al. (2021). Recycled aggregates from construction and demolition waste as wetland substrates for pollutant removal. *J. Clean. Prod.* 311:127766. doi: 10.1016/j.jclepro.2021.127766

Li, J., Zheng, B., Chen, X., Li, Z., Xia, Q., Wang, H., et al. (2021). The use of constructed wetland for mitigating nitrogen and phosphorus from agricultural runoff: a review. *Water* 13:476. doi: 10.3390/w13040476

Lima, M., Carvalho, K., Passig, F., Borges, A., Filippe, T., Azevedo, J., et al. (2018). Performance of different substrates in constructed wetlands planted with E. crassipes treating low-strength sewage under subtropical conditions. *Sci. Total Environ.* 630, 1365–1373. doi: 10.1016/j.scitotenv.2018.02.342

Liu, J., Liang, X., Yang, C., Yu, S., and Guo, H. (2019). Tracing membrane biofouling to the microbial community structure and its metabolic products: an investigation on the three-stage MBR combined with worm reactor process. *Bioresour. Technol.* 278, 165–174. doi: 10.1016/j.biortech.2019.01.069

Lu, L., Xing, D., and Ren, Z. J. (2015). Microbial community structure accompanied with electricity production in a constructed wetland plant microbial fuel cell. *Bioresour. Technol.* 195, 115–121. doi: 10.1016/j.biortech.2015.05.098

Lu, S., Zhang, X., Wang, J., and Pei, L. (2016). Impacts of different media on constructed wetlands for rural household sewage treatment. *J. Clean. Prod.* 127, 325–330. doi: 10.1016/j.jclepro.2016.03.166

Mandi, L. (1994). Marrakesh wastewater purification experiment using vascular aquatic plants Eichhornia crassipes and Lemna gibba. *Water Sci. Technol.* 29, 283–287. doi: 10.2166/wst.1994.0210

Mao, Y., Zhang, X., Xia, X., Zhong, H., and Zhao, L. (2010). Versatile aromatic compound-degrading capacity and microdiversity of Thauera strains isolated from a coking wastewater treatment bioreactor. *J. Ind. Microbiol. Biotechnol.* 37, 927–934. doi: 10.1007/s10295-010-0740-7

Menon, R., Jackson, C. R., and Holland, M. M. (2013). The influence of vegetation on microbial enzyme activity and bacterial community structure in freshwater constructed wetland sediments. *Wetlands* 33, 365–378. doi: 10.1007/s13157-013-0394-0

Miao, Y., Liao, R., Zhang, X.-X., Wang, Y., Wang, Z., Shi, P., et al. (2015). Metagenomic insights into Cr (VI) effect on microbial communities and functional genes of an expanded granular sludge bed reactor treating high-nitrate wastewater. *Water Res.* 76, 43–52. doi: 10.1016/j.watres.2015.02.042

Mohan, S. V., Rao, N. C., and Karthikeyan, J. (2002). Adsorptive removal of direct azo dye from aqueous phase onto coal based sorbents: a kinetic and mechanistic study. *J. Hazard. Mater.* 90, 189–204. doi: 10.1016/S0304-3894(01)00348-X

Mujakić, I., Cabello-Yeves, P. J., Villena-Alemany, C., Piwosz, K., Rodriguez-Valera, F., Picazo, A., et al. (2023). Multi-environment ecogenomics analysis of the cosmopolitan phylum Gemmatimonadota. *Microbiol. Spectr.* 11, e0111223–e0101123. doi: 10.1128/spectrum.01112-23

Nacheva, P. M., Chávez, G. M., Chacón, J. M., and Chuil, A. C. (2009). Treatment of cane sugar mill wastewater in an upflow anaerobic sludge bed reactor. *Water Sci. Technol.* 60, 1347–1352. doi: 10.2166/wst.2009.402

Nan, X., Lavrnić, S., and Toscano, A. (2020). Potential of constructed wetland treatment systems for agricultural wastewater reuse under the EU framework. *J. Environ. Manag.* 275:111219. doi: 10.1016/j.jenvman.2020.111219

Obeng, E., Essandoh, H. M. K., Akodwaa-Boadi, K., Taylor, T. S., Kusi, I., and Appiah-Effah, E. (2023). Recycled clay bricks and palm kernel shell as constructed wetland substrate for wastewater treatment: an engineered closed circuit circular economy approach. *Environ. Technol. Innovation.* 32:103324. doi: 10.1016/j.eti.2023.103324

Oron, G., Porath, D., and Jansen, H. (1987). Performance of the duckweed species Lemna gibba on municipal wastewater for effluent renovation and protein production. *Biotechnol. Bioeng.* 29, 258–268. doi: 10.1002/bit.260290217

Papadopoulos, F., and Tsihrintzis, V. (2011). Assessment of a full-scale duckweed pond system for septage treatment. *Environ. Technol.* 32, 795–804. doi: 10.1080/09593330.2010.514009

Patel, D., and Kanungo, V. (2010). Phytoremediation potential of duckweed (lemnaminor l:a tiny aquatic plant) in the removal of pollutants from domestic wastewater with special reference to nutrients. *Bioscan* 5, 355–358.

Pehlivan, E., and Arslan, G. (2006). Comparison of adsorption capacity of young brown coals and humic acids prepared from different coal mines in Anatolia. *J. Hazard. Mater.* 138, 401–408. doi: 10.1016/j.jhazmat.2006.05.063

Pelissari, C., dos Santos, M. O., Rousso, B. Z., Bento, A. P., de Armas, R. D., and Sezerino, P. H. (2016). Organic load and hydraulic regime influence over the bacterial community responsible for the nitrogen cycling in bed media of vertical subsurface flow constructed wetland. *Ecol. Eng.* 95, 180–188. doi: 10.1016/j.ecoleng.2016.06.079

Pentari, D., Perdikatsis, V., Katsimicha, D., and Kanaki, A. (2009). Sorption properties of low calorific value Greek lignites: removal of lead, cadmium, zinc and copper ions from aqueous solutions. *J. Hazard. Mater.* 168, 1017–1021. doi: 10.1016/j.jhazmat.2009.02.131

Perniel, M., Ruan, R., and Martinez, B. (1998). Nutrient removal from a stormwater detention pond using duckweed. *Appl. Eng. Agric.* 14, 605–609. doi: 10.13031/2013.19429

Qi, Y., Zhong, Y., Luo, L., He, J., Feng, B., Wei, Q., et al. (2024). Subsurface constructed wetlands with modified biochar added for advanced treatment of tailwater: performance and microbial communities. *Sci. Total Environ.* 906:167533. doi: 10.1016/j.scitotenv.2023.167533

Rathi, A., and Puranik, S. (2002). Chemical industry wastewater treatment using adsorption: NISCAIR-CSIR Available at: http://hdl.handle.net/123456789/17650.

Ren, T., Chi, Y., Wang, Y., Shi, X., Jin, X., and Jin, P. (2021). Diversified metabolism makes novel Thauera strain highly competitive in low carbon wastewater treatment. *Water Res.* 206:117742. doi: 10.1016/j.watres.2021.117742

Ren, Y., Zhang, B., Liu, Z., and Wang, J. (2007). Optimization of four kinds of constructed wetlands substrate combination treating domestic sewage. *Wuhan Univ. J. Nat. Sci.* 12, 1136–1142. doi: 10.1007/s11859-007-0085-x

Rochman, F. F., Sheremet, A., Tamas, I., Saidi-Mehrabad, A., Kim, J.-J., Dong, X., et al. (2017). Benzene and naphthalene degrading bacterial communities in an oil sands tailings pond. *Front. Microbiol.* 8:272817. doi: 10.3389/fmicb.2017.01845

Saeed, T., Muntaha, S., Rashid, M., Sun, G., and Hasnat, A. (2018). Industrial wastewater treatment in constructed wetlands packed with construction materials and agricultural by-products. *J. Clean. Prod.* 189, 442–453. doi: 10.1016/j.jclepro.2018.04.115

Saeed, T., and Sun, G. (2011). A comparative study on the removal of nutrients and organic matter in wetland reactors employing organic media. *Chem. Eng. J. (Amsterdam)* 171, 439–447. doi: 10.1016/j.cej.2011.03.101

Saeed, T., and Sun, G. (2013). A lab-scale study of constructed wetlands with sugarcane bagasse and sand media for the treatment of textile wastewater. *Bioresour. Technol.* 128, 438–447. doi: 10.1016/j.biortech.2012.10.052

Samsó, R., and García, J. (2013). Bacteria distribution and dynamics in constructed wetlands based on modelling results. *Sci. Total Environ.* 461, 430–440. doi: 10.1016/j.scitotenv.2013.04.073

Sani, A., Scholz, M., and Bouillon, L. (2013). Seasonal assessment of experimental vertical-flow constructed wetlands treating domestic wastewater. *Bioresour. Technol.* 147, 585–596. doi: 10.1016/j.biortech.2013.08.076

Schierano, M. C., Maine, M. A., and Panigatti, M. C. (2017). Dairy farm wastewater treatment using horizontal subsurface flow wetlands with Typha domingensis and different substrates. *Environ. Technol.* 38, 192–198. doi: 10.1080/09593330.2016.1231228

Sehar, S., Naeem, S., Perveen, I., Ali, N., and Ahmed, S. (2015). A comparative study of macrophytes influence on wastewater treatment through subsurface flow hybrid constructed wetland. *Ecol. Eng.* 81, 62–69. doi: 10.1016/j.ecoleng.2015.04.009

Shi, X., Fan, J., Zhang, J., and Shen, Y. (2017). Enhanced phosphorus removal in intermittently aerated constructed wetlands filled with various construction wastes. *Environ. Sci. Pollut. Res.* 24, 22524–22534. doi: 10.1007/s11356-017-9870-z

Song, Z.-Z., Lü, S., Liu, Z., Shi, X.-D., Pan, A., and Zhang, Z. (2019). Start-up of simultaneous ANAMMOX and denitrification process and changes in microbial

community characteristics. *Huan Jing Ke Xue* 40, 5057–5065. doi: 10.13227/j.hjkx.201905223

Song, Z., Su, X., Li, P., Sun, F., Dong, W., Zhao, Z., et al. (2021). Facial fabricated biocompatible homogeneous biocarriers involving biochar to enhance denitrification performance in an anoxic moving bed biofilm reactor. *Bioresour. Technol.* 341:125866. doi: 10.1016/j.biortech.2021.125866

Swain, A. K., Sahoo, A., Jena, H. M., and Patra, H. (2018). Industrial wastewater treatment by aerobic inverse fluidized bed biofilm reactors (AIFBBRs): a review. *J. Water Process Eng.* 23, 61–74. doi: 10.1016/j.jwpe.2018.02.017

Tian, T., Zhou, K., Xuan, L., Zhang, J.-X., Li, Y.-S., Liu, D.-F., et al. (2020). Exclusive microbially driven autotrophic iron-dependent denitrification in a reactor inoculated with activated sludge. *Water Res.* 170:115300. doi: 10.1016/j.watres.2019.115300

Toscano, A., Marzo, A., Milani, M., Cirelli, G. L., and Barbagallo, S. (2015). Comparison of removal efficiencies in Mediterranean pilot constructed wetlands vegetated with different plant species. *Ecol. Eng.* 75, 155–160. doi: 10.1016/j.ecoleng.2014.12.005

Vymazal, J. (2011). Constructed wetlands for wastewater treatment: five decades of experience. *Environ. Sci. Technol.* 45, 61–69. doi: 10.1021/es101403q

Vymazal, J., and Březinová, T. (2015). The use of constructed wetlands for removal of pesticides from agricultural runoff and drainage: a review. *Environ. Int.* 75, 11–20. doi: 10.1016/j.envint.2014.10.026

Wang, Z., Dong, J., Liu, L., Zhu, G., and Liu, C. (2013). Screening of phosphate-removing substrates for use in constructed wetlands treating swine wastewater. *Ecol. Eng.* 54, 57–65. doi: 10.1016/j.ecoleng.2013.01.017

Wang, Y., Shen, L., Wu, J., Zhong, F., and Cheng, S. (2020). Step-feeding ratios affect nitrogen removal and related microbial communities in multi-stage vertical flow constructed wetlands. *Sci. Total Environ.* 721:137689. doi: 10.1016/j.scitotenv.2020.137689

Wang, Z., Wu, Z., and Tang, S. (2009). Extracellular polymeric substances (EPS) properties and their effects on membrane fouling in a submerged membrane bioreactor. *Water Res.* 43, 2504–2512. doi: 10.1016/j.watres.2009.02.026

Wang, Q., Xie, H., Ngo, H. H., Guo, W., Zhang, J., Liu, C., et al. (2016). Microbial abundance and community in subsurface flow constructed wetland microcosms: role of plant presence. *Environ. Sci. Pollut. Res.* 23, 4036–4045. doi: 10.1007/s11356-015-4286-0

Wu, S., Kuschk, P., Brix, H., Vymazal, J., and Dong, R. (2014). Development of constructed wetlands in performance intensifications for wastewater treatment: a nitrogen and organic matter targeted review. *Water Res.* 57, 40–55. doi: 10.1016/j.watres.2014.03.020

Zhang, C.-B., Wang, J., Liu, W.-L., Zhu, S.-X., Ge, H.-L., Chang, S. X., et al. (2010). Effects of plant diversity on microbial biomass and community metabolic profiles in a full-scale constructed wetland. *Ecol. Eng.* 36, 62–68. doi: 10.1016/j.ecoleng.2009.09.010

Zhou, X., Jia, L., Liang, C., Feng, L., Wang, R., and Wu, H. (2018). Simultaneous enhancement of nitrogen removal and nitrous oxide reduction by a saturated biochar-based intermittent aeration vertical flow constructed wetland: effects of influent strength. *Chem. Eng. J. (Amsterdam)* 334, 1842–1850. doi: 10.1016/j.cej.2017.11.066

Zhou, X., Wang, X., Zhang, H., and Wu, H. (2017). Enhanced nitrogen removal of low C/N domestic wastewater using a biochar-amended aerated vertical flow constructed wetland. *Bioresour. Technol.* 241, 269–275. doi: 10.1016/j.biortech.2017.05.072

Zhou, X., Wu, S., Wang, R., and Wu, H. (2019). Nitrogen removal in response to the varying C/N ratios in subsurface flow constructed wetland microcosms with biochar addition. *Environ. Sci. Pollut. Res.* 26, 3382–3391. doi: 10.1007/s11356-018-3871-4

Zurita, F., and Vymazal, J. (2023). Oportunities and challenges of using constructed wetlands for the treatment of high-strength distillery effluents: a review. *Ecol. Eng.* 196:107097. doi: 10.1016/j.ecoleng.2023.107097

frontiers | Frontiers in Microbiology

TYPE Original Research
PUBLISHED 16 August 2024
DOI 10.3389/fmicb.2024.1422529

OPEN ACCESS

EDITED BY
Jiuling Li,
The University of Queensland, Australia

REVIEWED BY
Patrick Saccone,
University of Oulu, Finland
Sarvajith,
King Abdullah University of Science and Technology, Saudi Arabia

*CORRESPONDENCE
Lei Wang
✉ wanglei@iga.ac.cn

RECEIVED 24 April 2024
ACCEPTED 02 August 2024
PUBLISHED 16 August 2024

CITATION
Xing S, Wang WJ, Wang L, Du H, Wu Z, Zong S, Cong Y and Ba S (2024) Soil nutrient content dominates short-term vegetation changes in alpine tundra of Changbai Mountains.
Front. Microbiol. 15:1422529.
doi: 10.3389/fmicb.2024.1422529

Soil nutrient content dominates short-term vegetation changes in alpine tundra of Changbai Mountains

Shanfeng Xing[1,2], Wen J. Wang[1], Lei Wang[1]*, Haibo Du[2], Zhengfang Wu[2], Shengwei Zong[2], Yu Cong[1] and Shengjie Ba[1,2]

[1]State Key Laboratory of Black Soils Conservation and Utilization, Northeast Institute of Geography and Agroecology, Chinese Academy of Sciences, Changchun, China, [2]Key Laboratory of Geographical Processes and Ecological Security in Changbai Mountains, Ministry of Education, School of Geographical Sciences, Northeast Normal University, Changchun, China

Alpine tundra, covering 3% of the Earth's land surface, harbors approximately 4% of higher plant species. Changes in this vegetation significantly impact biodiversity and ecosystem services. Recent studies have primarily focused on large-scale and long-term vegetation changes in polar and high-latitude regions. However, the study of short-term vegetation changes and their primary drivers has received insufficient attention in alpine tundra. This study aimed to investigate vegetation changes and their dominant drivers in the alpine tundra of Changbai Mountains-located at the southern edge of the alpine tundra distribution in Eastern Eurasia-over a short period by re-surveying permanent plots in 2019 and comparing them with data from 2014. The results showed that significant changes were observed in alpine tundra vegetation during the study period. The importance values of typical alpine tundra plants such as *Rhododendron chrysanthum*, *Vaccinium uliginosum*, and *Dryas octopetala* decreased noticeably, while those of herbaceous species such as *Deyeuxia angustifolia* and *Sanguisorba sitchensis* increased significantly. Species richness, diversity, and evenness at different altitudinal gradients showed varying degrees of increase. A distinct expansion trend of herbaceous species was observed in the alpine tundra, contributing to a shift in plant community composition toward herbaceous dominance. This shift might result in the meadowization of the dwarf shrub tundra. Our findings further revealed that soil nutrients rather than climate factors, dominated the changes of plant communities over a short period. These findings provide scientific references for the conservation and management of biodiversity, as well as for projecting future vegetation dynamics in alpine tundra.

KEYWORDS

short-term vegetation change, soil nutrient content, herb encroachment, alpine tundra, Changbai Mountains

1 Introduction

Alpine tundra, an integral part of alpine ecosystems, covers 3% of the Earth's land surface and harbors approximately 4% of higher plant species (Körner, 1999). Alpine ecosystems are highly sensitive to climate change because the plant species within these ecosystems are adapted to harsh climate conditions, such as low temperatures and high humidity (Walker et al., 2006; Danby et al., 2011; Alatalo et al., 2017; Czortek et al., 2018; Rantanen et al., 2022). Numerous studies have documented notable shifts in vegetation composition, biomass, and diversity in tundra regions for the past decades, driven by climate change (Lenoir and Svenning, 2014), environmental change (Chu et al., 2016; López-Angulo et al., 2019), and human activities such as land use change (Steinbauer et al., 2018), grazing (Dunwiddie and Research, 1977), and tourism (Walther et al., 2005). These changes could alter biophysical and biogeochemical processes, affecting the exchanges of energy, water, carbon, and nutrients between the soil and the atmosphere (Tarnocai et al., 2009; Myers-Smith et al., 2011). Therefore, understanding the changes in alpine tundra vegetation and their underlying mechanisms is essential for accurately forecasting, alleviating, and adapting to the influences of future environmental shifts on these ecosystems (Rixen et al., 2022).

Recent studies on vegetation changes in alpine tundra have predominantly focused on polar and high-latitude regions (Hallinger et al., 2010; Salminen et al., 2023; Lagergren et al., 2024). Low-elevation vegetation in polar regions and high latitudes was encroaching upon alpine tundra (Sturm et al., 2001; Tape et al., 2006; Formica et al., 2014; Shevtsova et al., 2020), which gradually reduced the area of alpine tundra. Shevtsova et al. (2020) observed vigorous shrub expansion in the northeastern Siberian tundra. Meanwhile, studies focusing on high-mountain vegetation change typically employed large-scale research methods, facilitating the identification and monitoring of spatial and temporal patterns in vegetation changes (Ju and Masek, 2016; Nill et al., 2022). For example, Nill et al. (2022) analyzed Landsat data from 1984 to 2020 and found that shrub cover increased on average by 1.4–4.2% per decade across the entire ecological zone of western Canada. However, these large-scale methods failed to capture subtle vegetation changes and processes, as they were unable to detect changes in the composition, structure, and species diversity within plant communities (Myers-Smith et al., 2019). Establishing permanent monitoring plots could help overcome the limitations associated with large-scale studies by providing a more detailed and accurate representation of actual ecosystem dynamics (Kapfer et al., 2016). By consistently and regularly monitoring these plots, researchers could quantitatively evaluate shifts in the composition and diversity of plant communities (Pauli et al., 2012; Gazol et al., 2017). This approach was particularly effective when permanent plots were established along elevation gradients, as it allowed for a more precise analysis of the dynamics across different vegetation zones (Metcalfe et al., 2018; Walker et al., 2018). Given the high spatial heterogeneity and temporal variability of tundra landscapes (Epstein et al., 2012; Reichle et al., 2018), employing this method is essential to thoroughly investigate changes in the composition, structure, and species diversity of alpine tundra.

Climate warming has long been regarded as the primary driver of vegetation changes (Pickering et al., 2008; Grabherr et al., 2010; Danby et al., 2011; Lenoir and Svenning, 2014). For example, Pickering et al. (2008) demonstrated that climate warming led to shifts in the distribution of thermophilic shrubs, herbs, and invasive weeds towards higher elevations. However, these studies typically analyzed the drivers of long-term vegetation changes (Holzinger et al., 2007), and the impacts of long-term climate change may interact with other environmental changes (Hamid et al., 2020), such as disturbances from typhoons, land use changes, and soil nutrient variations. To avoid biased conclusions that might arise from confounding factors, we focused on investigating the driving factors of plant community changes at short time scales. Short-term studies of changes in plant communities often relied on controlled experiments, such as warming experiments (Klein et al., 2004) and nitrogen fertilization (Britton and Fisher, 2008). However, this approach could only evaluate the impact of controlled environmental factors on plant communities and fails to identify the dominant factors that actually drive changes in these communities (Clark et al., 2007). There is a knowledge gap regarding actual vegetation changes and their dominant drivers over a short period in alpine dwarf-shrub tundra.

The alpine tundra of Changbai Mountains (ATCBM), located at the southern edge of the alpine tundra distribution in Eastern Eurasia, represents one of the most archetypal mountain tundra vegetation ecosystems in China (Huang and Li, 1984). The mean growing season temperature showed a significant increasing trend for the past six decades, with a rate of 0.23°C/decade in the ATCBM, which was higher than the average global surface warming rate over the past 50 years (Wang et al., 2019). Vegetation changes in the ATCBM have increasingly attracted attention in recent years, such as the upward migration of tree line (Du et al., 2017) and the herb encroachment (Jin et al., 2019a). Wang et al. (2019) evaluated changes in the vegetation of the ATCBM for the past three decades by comparing the historical and current vegetation survey results. However, this comparison using non-permanent plot surveys introduced considerable uncertainty into the observed vegetation changes and hindered the attribution analysis of these changes (Kapfer et al., 2016). Therefore, conducting regular field permanent plot surveys is crucial for monitoring changes in alpine tundra vegetation and associated environmental factors, thereby identifying the dominant drivers of vegetation change.

In this study, we established permanent plots in the ATCBM and conducted detailed monitoring in 2014 and 2019. By comparing the results from these two surveys, we systematically analyzed changes in the tundra vegetation over five years and evaluated the underlying mechanisms driving these changes within a short period. We proposed the following hypotheses: (1) the vegetation underwent significant changes over a short period in the ATCBM, characterized by the rising importance of herbaceous plants and increased species diversity; (2) the encroachment of herbaceous species significantly altered the composition and structure of the native plant communities; (3) changes in soil nutrient content, rather than climate factors, were the more significant drivers of alpine vegetation changes over a short period.

2 Materials and methods

2.1 Study area

The alpine tundra is situated on the main peak of Changbai Mountains, at an altitude exceeding 2000 meters (m), spanning from 41° 56'N to 42°04'N and 127°58'E to 128°11'E (Figure 1A). This region experiences a harsh alpine tundra climate, characterized by low temperatures (5.8°C) and abundant precipitation (958 mm) during the growing season (June to September), coupled with a winter that extends over eight months (Hao et al., 2001). The average snow depth reaches about 1 m during winter. The soil in the tundra is notably shallow, typically not exceeding 30 cm in depth, and characterized as coarsely bony, thinly layered, and poorly stratified (Huang and Li, 1984). Vegetation in the area is sparse, primarily composed of a few dwarf shrubs, mosses, and lichens. Prominent plant species include dwarf shrubs such as *Rhododendron chrysanthum*, *Vaccinium uliginosum*, and *Dryas octopetala*, along with herbaceous plants like *Carex pachyneura*, *Sanguisorba sitchensis*, and *Saussurea tomentosa* (Huang and Li, 1984). Recent decades of rapid warming have prompted shifts in alpine tundra vegetation, particularly the upward shift of the tree line (Du et al., 2017) and the increasing prevalence of herbaceous plant encroachment (Wang et al., 2019).

2.2 Vegetation and soil sampling

The field survey utilized a systematic sampling method, establishing permanent quadrats along a transect. At each altitude range within this transect, three replicate 1m x 1m plots were set up, spaced 25 m apart (Figure 1C). These plots were positioned at 100-meter intervals along the slope, extending from the tree line at 2050 m to the upper edge of the tundra at 2560 m. Each set contains 25 quadrats, resulting in a total of 75 quadrats (Figure 1B). To minimize human disturbance and accurately capture changes in plant communities, each set was located at least 50 m away from the nearest highway. The establishment of this transect and permanent quadrats, as well as the initial detailed vegetation survey, occurred in 2014 and 2015 (Wang et al., 2019). We conducted a re-survey of these permanent quadrats in 2019. To accurately capture changes in plant species, we used the same indicators as the previous survey of the quadrats, such as plant name, coverage, number of plants, and plant height. We also used soil auger (3 cm diameter) to collect soil samples from each quadrat to analyze the physicochemical properties of soil, such as particle size (clay, silt, and sand), organic matter (Org), total nitrogen (TN), available nitrogen (AN), available phosphorus (AP), available potassium (AK), and carbon-to-nitrogen ratio (C/N). Specifically, particle size (clay, silt, and sand) was analyzed using the Bouyoucos hydrometer method (Pauwels et al., 1992); Org was determined by using titrimetric methods, and its contents was estimated from the organic carbon content by multiplying by a factor of 1.724 (Walkley and Black, 1934); TN was evaluated using the Kjeldahl distillation method, while AN was assessed through titration (Bremner and Mulvaney, 1982); AP was determined using the Olsen method (Lajtha and Jarrell, 1999); AK was measured using a flame photometer (Olorunfemi et al., 2016). Moreover, the soil microbial community was characterized using Phospholipid Fatty Acid analysis (Bligh and Dyer, 1959; Frostegård et al., 1991).

2.3 Climate data

Since the mid-1980s, herbaceous plants such as *D. angustifolia* have begun encroaching upon the alpine dwarf-shrub tundra from lower altitudes (Zong et al., 2016). Consequently, we utilized historical climate data spanning from 1985 to 2020, acquired from Tianchi Station (42°01'N, 128°05'E), located about 4 kilometers from our research site at an elevation of 2623 m. It should be noted that winter climate data from this station have been unavailable since 1989. These data were subjected to quality control and homogeneity assessments by the National Meteorological Information Center prior to their release.

To accurately monitor soil temperature, we buried a temperature recorder (Tidbit@Tv2) at a depth of 5 cm within each quadrat starting in 2015 (Figure 1E). The soil temperature data used in this study cover five complete growing seasons from June to September, spanning from 2015 to 2020. Additionally, we positioned two automatic weather stations (WeatherHawk 610, Campbell Scientific, Logan, UT, USA) at altitudes of 2135 m and 2246 m to monitor precipitation in the tundra (Figure 1D). Our observations indicated that precipitation increases with altitude in the Changbai Mountains. During the growing seasons from 2014 to 2019, mean precipitation at both elevations were 1270 mm and 1348 mm, respectively. We used the established relationship between precipitation and elevation to interpolate the precipitation value for each plot (Hao et al., 2001; Wang et al., 2019).

2.4 Data analysis

In this study, we applied importance value index (IVI) to assess the structural composition and community dynamics within the tundra vegetation of the Changbai Mountains (Lu et al., 2011; Niu et al., 2017). We calculated the IVI for each species using the following formula (Equation 1):

$$IVI = Rd + Rh + Rc \quad (1)$$

Relative density (Rd) is calculated by dividing the number of individuals of a particular plant species by the total number of individuals across all species and multiplying the result by 100. Relative height (Rh) is determined by dividing the height of a particular plant species by the cumulative height of all species and then multiplying by 100. Similarly, Relative cover (Rc) is calculated by dividing the cover of a single species by the total cover of all species and then multiplying by 100. By calculating these metrics, we systematically analyze the species' IVI in descending order to identify their dominance within the vegetation.

To facilitate the analysis of tundra vegetation changes with altitude, we divided the 75 quadrats into five altitudinal gradients: 2050–2150 m, 2150–2250 m, 2250–2350 m, 2350–2450 m, and 2450–2550 m. This division was established to facilitate a comparative analysis of species diversity across each altitudinal gradient. Specifically, we aimed to compare the species richness,

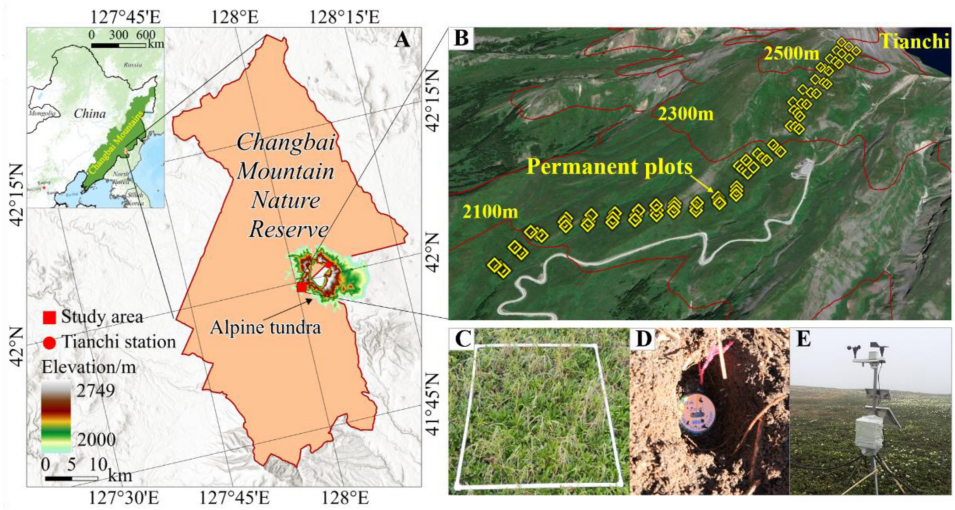

FIGURE 1
Location of the study area in the ATCBM **(A)** and the setup of plots **(B,C)**, automatic weather stations **(D)**, and temperature recorder (Tidbit@Tv2) **(E)**.

diversity and evenness between 2014 and 2019 across each elevation gradient. The calculation formulas for the Patrick index (R), Shannon-Wiener index (H′) and Pielou index (E) of species richness, diversity and evenness were as follows (Equations 2–4; Ma et al., 1995):

Patrick index:

$$R = S \tag{2}$$

Shannon-Wiener index:

$$H' = -\sum_{i=1}^{s} P_i \ln P_i \tag{3}$$

Pielou index:

$$E = H'/\ln S \tag{4}$$

Where: S is the number of species in the sample plots, and P_i is the relative IVI of species i. The Shannon-Wiener index and Pielou index represent α -diversity.

In our study, we used ordination analysis methods to examine the connections between vegetation dynamics and environmental factors in the ATCBM. We first employed detrended correspondence analysis (DCA) to determine the gradient length of the ordination axes and found that the maximum value exceeded 4 for the first four axes. Therefore, we utilized canonical correspondence analysis (CCA). This ordination technique, a key statistical method, was conducted using R software (version 3.0.1, R Foundation for Statistical Computing, Vienna, Austria), which was widely recognized for its robust capabilities in ecological data analysis (Greig-Smith, 1983; Šmilauer and Lepš, 2014). The CCA allowed us to directly correlate changes in plant species with variations in environmental parameters, such as Org, TN, AN, AP, AK, C/N, precipitation (PRE), growing season temperature (TEMP), diurnal temperature range (DTR), growing season length (GSL), and winter snow protection (WSP). A paired t-test was conducted to assess the statistical differences in vegetation and environmental changes between the two surveys, using a significance threshold of $p < 0.05$.

3 Results

3.1 Changes in tundra vegetation

3.1.1 Changes in the importance value of plant species

The IVI of plant species exhibited significant changes ($p < 0.05$) from 2014 to 2019 (Table 1). Native plants, such as *R. chrysanthum*, *V. uliginosum*, and *D. octopetala*, experienced varying degrees of declines in Rd, Rh, and Rc over the 5-year period in the alpine tundra. These declines resulted in a reduction in their IVI, with rates of decrease at 21.36%, 17.71%, and 13.68%, respectively. Despite experiencing the highest rate of decline in IVI, *R. chrysanthum* still ranked first in species importance, significantly surpassing the other species. While encroaching herbaceous plants such as *Deyeuxia angustifolia* and *S. sitchensis* showed different degrees of increase in their Rd, Rh, and Rc over the 5-year period, these changes resulted in a corresponding rise in their IVI, with rates of increase of 22.14% and 7.46%, respectively. In the past 5 years, among the dominant species (with IVI greater than 2), only 30.8% (*R. chrysanthum, S. sitchensis, D. angustifolia*, and *Geranium dahuricum*) maintained the same ranking of IVI, which indicated that the species composition and structure of the tundra vegetation was not stable but rather undergoing continual change.

3.1.2 Changes in species diversity along elevation gradients

The species richness of tundra vegetation exhibited a declining trend with rising altitude on Changbai Mountains (Figure 2). In both 2014 and 2019, species richness in the tundra vegetation

TABLE 1 Changes in Rd, Rh, Rc, IVI, and ranking of different plant species from 2014 to 2019 in the ATCBM.

Plant species	Rd		Rh		Rc		IVI		Rank change
	2014	2019	2014	2019	2014	2019	2014	2019	
Rhododendron chrysanthum	31.76	22.37	6.24	6.12	25.84	21.71	21.28	16.73	0
Sanguisorba sitchensis	7.97	8.02	9.65	9.76	10.32	12.25	9.31	10.01	0
Deyeuxia angustifolia	7.66	6.54	11.09	10.10	5.28	4.47	7.42	9.06	0
Sanguisorba teriuifolia	4.96	7.96	7.49	6.07	6.20	9.12	6.81	5.69	−1
Ligularia jamesii	4.37	4.27	6.23	6.36	3.99	3.67	5.14	5.84	1
Vaccinium uliginosum	4.43	4.82	1.51	1.11	4.75	6.34	3.62	2.98	−3
Trollius japonicus	3.65	2.90	6.50	4.53	5.70	4.93	3.58	2.59	−4
Saussurea tomentosa	4.37	3.81	2.31	2.89	1.94	2.10	3.56	3.61	1
Polygonum viviparum	2.79	1.90	3.25	3.15	4.57	4.41	3.19	3.02	1
Dryas octopetala	2.54	4.13	0.46	0.44	1.69	1.98	2.61	2.25	−2
Rhodiola cretinii	1.90	1.34	3.35	2.56	2.35	1.90	2.53	2.89	1
Carex pachyneura	1.94	2.37	2.99	4.49	1.78	1.46	2.26	3.85	6
Geranium dahuricum	2.65	2.85	2.44	2.29	1.88	1.70	2.05	2.04	0

on Changbai Mountains peaked at a maximum of 47 and 48, respectively, at an altitude range of 2050–2150 m, while the minimum values recorded were 26 in 2014 and 29 in 2019 at an altitude range of 2350–2450 m. Between 2014 and 2019, species richness increased at each elevation gradient. Specifically, the minimal increase was observed in the 2050–2150 m elevation range, with an addition of just one species, whereas the most substantial increase occurred in the 2150–2250 m range, where species richness expanded by six species. In both 2014 and 2019, the Shannon-Wiener index exhibited a consistent decreasing trend with rising altitude, peaking at 2050–2150 m and reaching its lowest value at 2350–2450 m. From 2014 to 2019, the Shannon-Wiener index increased at varying degrees across different altitudinal gradients, with the most significant increase observed at 2150–2250 m. In both 2014 and 2019, the Pielou index displayed consistent trends with increasing altitude, peaking at 2250–2350 m and reaching a minimum at 2350–2450 m. During this period, the Pielou index exhibited varying degrees of increase across the elevation gradients, with the most significant change observed in the 2350–2450 m range.

3.1.3 Changes in species composition and coverage of typical plant communities

Five representative plant communities including three native dwarf shrub communities (*S. sitchensis*, *R. chrysanthum*, and *V. uliginosum*) and two herbaceous communities (*D. angustifolia* and *D. octopetala*) were chosen to examine changes in species composition and cover at the community scale over the period from 2014 to 2019. Species richness decreased in the *D. angustifolia* community and remained essentially unchanged in the *S. sitchensis* community. In contrast, it increased in the *R. chrysanthum*, *V. uliginosum*, and *D. octopetala* communities, with significant increases ($p < 0.05$) observed in the *R. chrysanthum* and *V. uliginosum* communities (Figure 3A). The coverage of dominant species significantly increased ($p < 0.05$) in the *D. angustifolia* community, while these exhibited declining trends in the *S. sitchensis*, *R. chrysanthum*, *V. uliginosum*, and *D. octopetala* communities. Notably, the coverage of dominant species showed a significant decline ($p < 0.05$) in the *R. chrysanthum* community (Figure 3B). Simultaneously, we investigated changes in species cover of *D. angustifolia* in the *S. sitchensis* and *R. chrysanthum* communities, as well as changes in species cover of *S. sitchensis* in the *D. angustifolia* and *R. chrysanthum* communities. We found a significant increase ($p < 0.05$) in the coverage of *D. angustifolia* in both the *S. sitchensis* and *R. chrysanthum* communities (Figure 4A), as well as a significant increase ($p < 0.05$) in the coverage of *S. sitchensis* in both the *D. angustifolia* and *R. chrysanthum* communities (Figure 4B).

3.2 Changes in environmental factors

3.2.1 Changes in climate factors

From 2014 to 2019, various climate factors including TEMP, PRE, DTR, GSL, and WSP showed different variations across five plant communities (Figure 5). TEMP increased across all communities, with significant increases in the *S. sitchensis* and *R. chrysanthum* communities. PRE decreased significantly in all plant communities ($p < 0.05$). DTR increased in the *D. angustifolia*, *R. chrysanthum*, and *V. uliginosum* communities, with a significant increase in the *R. chrysanthum* community ($p < 0.05$); however, it decreased in the *S. sitchensis* and *D. octopetala* communities. In line with the TEMP trend, GSL also increased in all communities, particularly with significant increases in the *S. sitchensis* and *R. chrysanthum* communities. WSP decreased in four of plant communities, except for an increase in the *V. uliginosum* community; a significant decrease was noted in the *R. chrysanthum* community ($p < 0.05$).

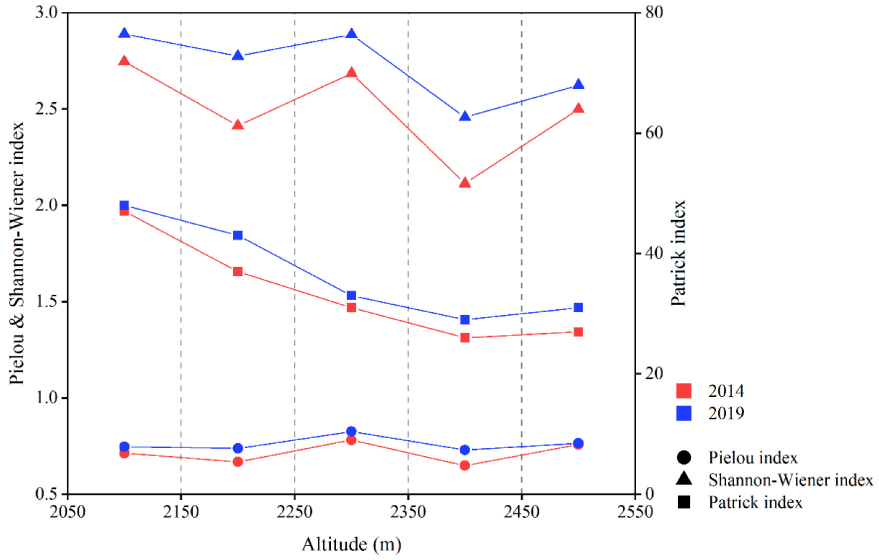

FIGURE 2
The changes in species richness, diversity, and evenness of vegetation along the altitudinal gradient from 2014 to 2019 in the ATCBM.

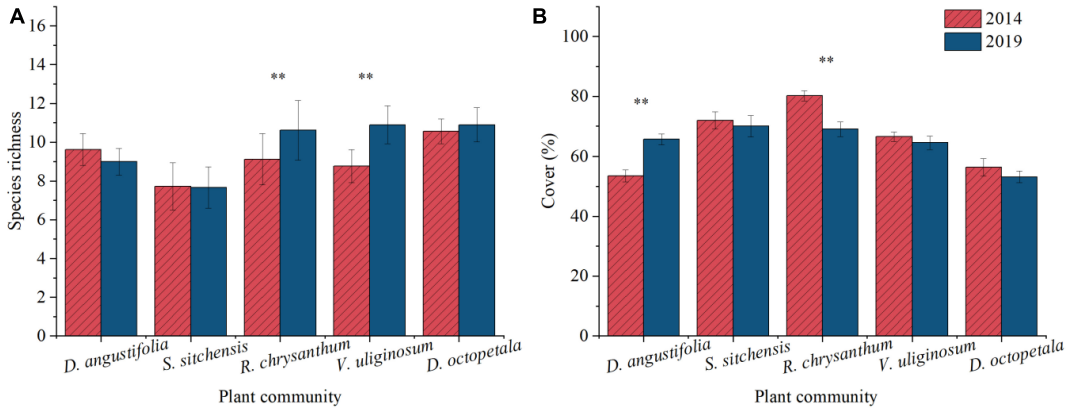

FIGURE 3
Changes in species abundance **(A)** and dominant species cover **(B)** from 2014 to 2019 in typical plant communities. **represents a difference that is significant at the 0.05 level.

3.2.2 Changes in soil nutrient content

Between 2014 and 2019, the distributions of Org, TN, AN, AP and AK exhibited a pattern of initially increasing and then decreasing with increasing elevation (Figure 6). From 2014 to 2019, Org, TN, AN, and AP generally increased across elevation gradients, with the exception of Org in the 2250–2350 m range. Notably, significant increases ($p < 0.05$) were observed in the following elevation ranges: Org within 2350–2450 m; TN within 2050–2150 m and 2450–2550 m; AN within 2050–2150 m and 2450–2550 m; and AP within 2050–2150 m, 2150–2250 m, and 2450–2550 m. AK and C/N decreased across most elevation gradients. However, C/N increased within the 2350–2450 m range. Notably, AK experienced a significant decrease ($p < 0.05$) in the 2150–2250 m range.

Soil nutrient content showed different changes across various plant communities from 2014 to 2019 (Table 2). Specifically, the *D. angustifolia* community exhibited significant increases ($p < 0.05$) in TN, AN, and AP. In contrast, the *S. sitchensis* community experienced a significant decline ($p < 0.05$) in AK. The *R. chrysanthum* community displayed significant increases ($p < 0.05$) in TN, AN, and AP, along with a significant decrease ($p < 0.05$) in AK. Significant increases ($p < 0.05$) were observed in Org, TN, AN, and AP within the *V. uliginosum* community. Finally, in the *D. octopetala* community, Org, TN, AN, and AP all showed significant increases ($p < 0.05$), whereas C/N significantly decreased ($p < 0.05$).

3.3 Driving forces of tundra vegetation changes

Through canonical correspondence analysis, we observed that the explanatory power of environmental factors on plant community distribution remained consistent across both surveys,

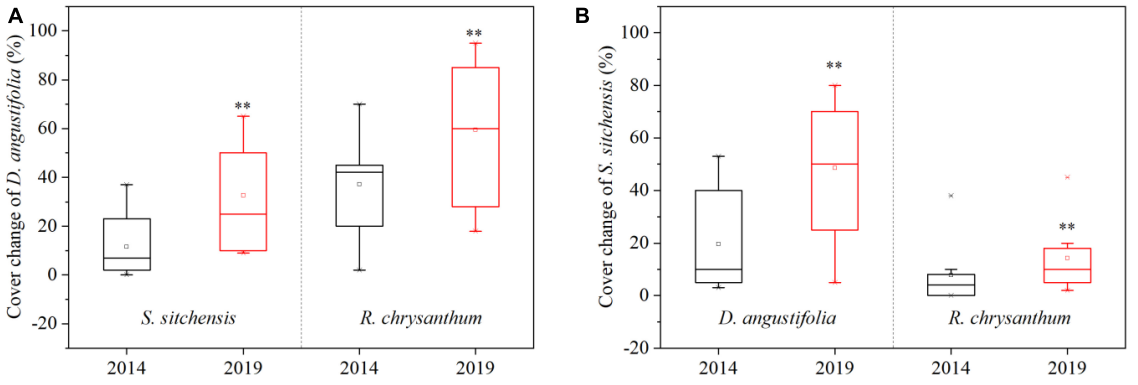

FIGURE 4
Changes in species coverage of *D. angustifolia* from 2014 to 2019 in the *S. sitchensis* and *R. chrysanthum* communities **(A)**; Changes in species coverage of *S. sitchensis* from 2014 to 2019 in the *D. angustifolia* and *R. chrysanthum* communities **(B)**. **represents a difference that is significant at the 0.05 level.

with the dominant factors largely unchanged. In 2014, axes 1 and 2 together explained 49.8% of the variation in plant community distribution (Figure 7A), while in 2019, they explained 48.28% of the variation (Figure 7B). The environmental factors most influential on plant community distribution in 2014 were DTR, PRE, GSL, and C/N. By 2019, the dominant factors shifted slightly to include DTR, TEMP, Org, and PRE. We could find that climate factors, rather than soil nutrients, dominated the distribution of plant communities.

Compared to their explanatory power for plant community distribution, environmental factors demonstrated a lower explanatory power for changes in plant community from 2014 to 2019. Axes 1 and 2 together explained 31.72% of these changes in plant communities (Figure 8). The AN factor, indicated by the longest arrow in the analysis, had the greatest impact on these changes. Among the 11 environmental factors assessed, the impact on changes in the five plant communities, ranked from largest to smallest, were as follows: AK, AN, TEMP, GSL, TN, C/N, PRE, AP, WSP, DTR, and Org. Soil nutrients exhibited a greater impact than climate factors on the short-term changes in plant community.

4 Discussion

4.1 Changes in the importance value of plant species

Permanent plot surveys offer a nuanced examination of shifts in the composition and structure of tundra vegetation, providing a detailed contrast to remote sensing methods, which generally capture only large-scale greening or browning trends in ecosystems with lower precision (Myers-Smith et al., 2019). We observed a significant decrease in the IVI of typical dwarf shrub species in the alpine tundra, including *R. chrysanthum*, *V. uliginosum*, and *D. octopetala*. Conversely, the IVI of herbaceous plants such as *D. angustifolia* and *S. sitchensis* exhibited noticeable increases. This change was primarily attributed to the gradual encroachment of herbaceous plants, such as *D. angustifolia* and *S. sitchensis*, into the traditional growth areas of tundra vegetation (Jin et al., 2019a). This indicated intense competition between the native dwarf shrub species of the tundra and encroaching herbaceous species. It confirmed that the composition and structure of tundra vegetation had undergone significant changes in a short period under the pressure of environmental changes, with a trend towards meadowization (Wang et al., 2019). Moreover, this change further led to the fragmentation of the alpine tundra landscape, contrasting with the trend of tundra shrubification observed in polar and high-latitude regions in the past (Sturm et al., 2001; Cannone et al., 2007; Formica et al., 2014; Schore et al., 2023).

4.2 Changes in plant species diversity along elevation gradients

This study observed a decrease in plant species richness with increasing altitude, consistent with findings from other research (Kazakis et al., 2006; Vanneste et al., 2017; Hamid et al., 2020). This was attributed to temperature directly influencing the ecological niches of plants, affecting their distribution and diversity (Waldock et al., 2018). Additionally, as the terrain's slope increased with altitude, the steeper areas became more susceptible to erosion, thereby reducing the potential growth areas for vegetation (Theurillat et al., 2007). Species diversity and evenness peaked at elevations between 2250 and 2350 m, coinciding with the upper boundary expansion of the encroaching herbaceous species. Although there were signs of encroachment from lower-altitude plant species within this range, the native tundra plat species still dominated. In this region, although the number of species was not the highest, each species had relatively high abundance, and species distribution was relatively even (Han et al., 2023). Consistent with our hypothesis, species diversity increased over time (Steinbauer et al., 2018; Salminen et al., 2023; Zemlianskii et al., 2024), but the degree of change varied across different altitude gradients. Over a five-year period, the greatest changes in species richness and diversity were observed between 2150 m and 2250 m, where six plant species were added and the diversity index increased by 0.36. This was due to the area serving as a mixing zone, where encroaching plant species and native tundra plant species intermingled. Many plants migrated upwards from lower altitudes,

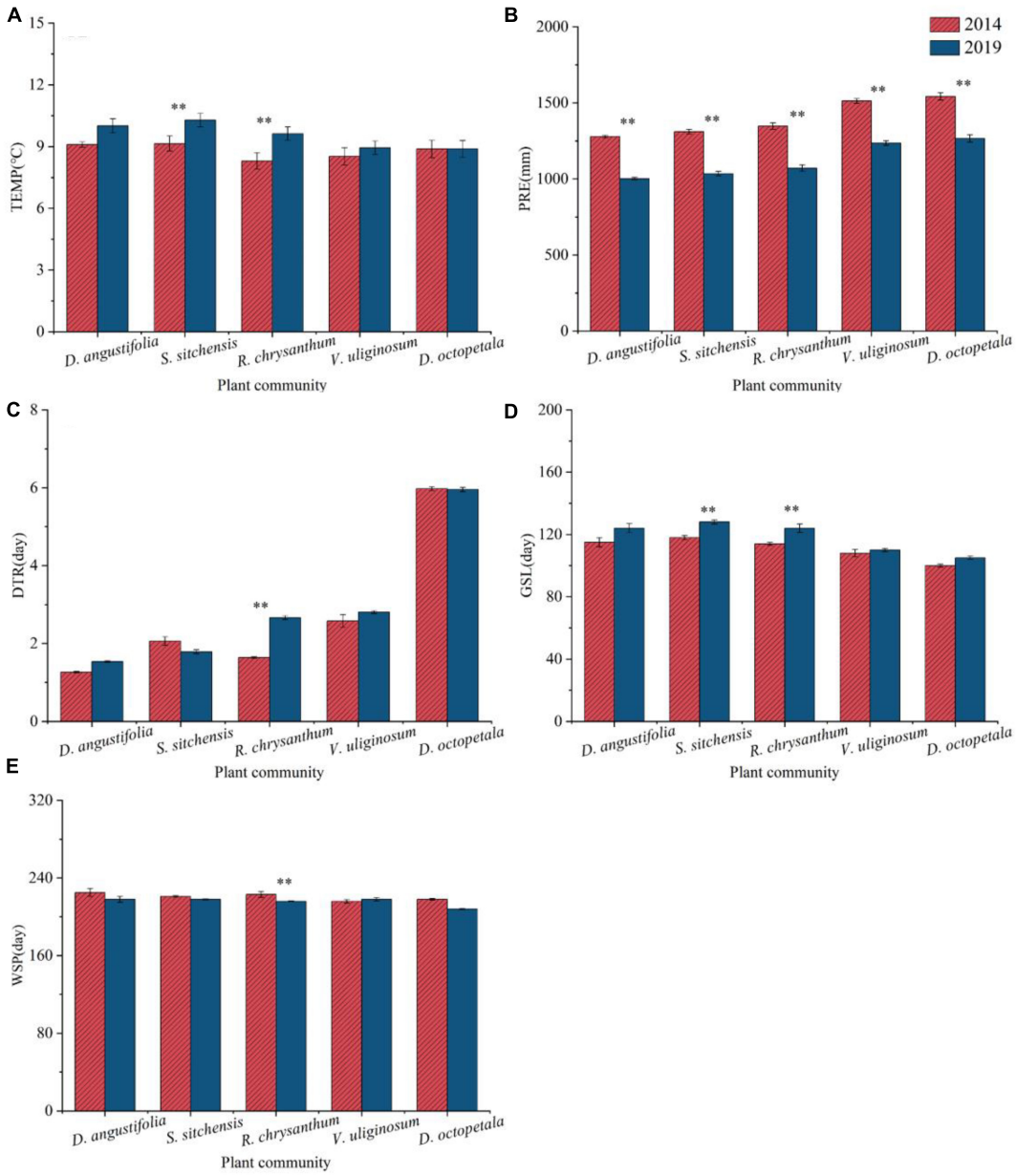

FIGURE 5
Changes in climate factors [TEMP **(A)**, PRE **(B)**, DTR **(C)**, GSL **(D)**, WSP **(E)**] from 2014 to 2019 in different plant communities in the ATCBM. **represents a difference that is significant at the 0.05 level.

intensifying resource competition between encroaching and native species, which ultimately resulted in significant changes in species composition (Dolezal et al., 2016).

4.3 Changes in species composition and coverage of typical plant communities

Plant encroachments significantly influenced the composition and dynamics of communities (Fahey et al., 2020; Livingstone et al., 2020). After encroaching on the alpine tundra, *D. angustifolia* competed with the native dwarf shrub communities, leading to significant changes in the composition and structure of the native tundra plant communities. Species richness increased in these communities of *R. chrysanthum*, *V. uliginosum*, and *D. octopetala*, while it decreased in the communities of *D. angustifolia* and *S. sitchensis*. This may confirm that environment change led to the homogenization of previously heterogeneous tundra plant communities (Stewart et al., 2018). The coverages of dominant species were decreasing to different degrees in the other four plant communities, except for an increase the *D. angustifolia* community. Moreover, the coverage of *D. angustifolia* increased within the *S. sitchensis* and *R. chrysanthum* communities, while *S. sitchensis* coverage also expanded within the *D. angustifolia* and *R. chrysanthum* communities. This indicated that both low-altitude herbaceous plants, such as *D. angustifolia*, and native tundra

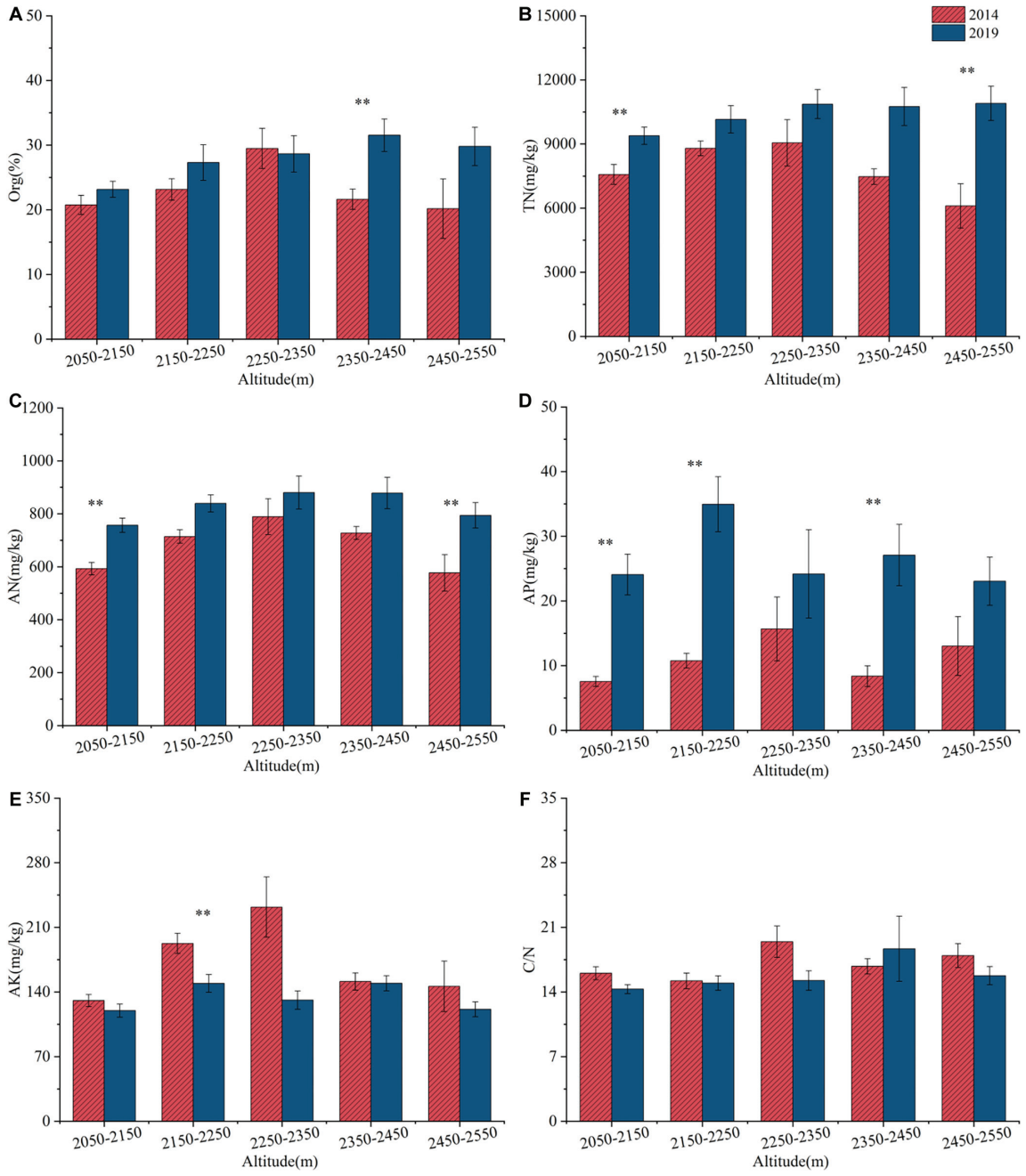

FIGURE 6
Changes in soil nutrient contents [Org **(A)**, TN **(B)**, AN **(C)**, AP **(D)**, AK **(E)**, C/N **(F)**] at different altitudes from 2014 to 2019 in the ATCBM. **represents a difference that is significant at the 0.05 level.

TABLE 2 Changes in soil nutrient content (Org, TN, AN, AP, AK, and C/N) in typical plant communities in the ATCBM.

Plant communities	Org	TN	AN	AP	AK	C/N
D. angustifolia	4.22 ± 2.12	2554.76 ± 933.92**	223.68 ± 93.92**	14.37 ± 5.16**	5.38 ± 14.47	−1.28 ± 1.08
S. sitchensis	0.55 ± 1.77	870.55 ± 602.67	57.33 ± 29.73	8.02 ± 4.18	−70.12 ± 12.74**	−1.28 ± 0.78
R. chrysanthum	4.88 ± 1.76**	2033.64 ± 500.86**	167.11 ± 9.65**	24.51 ± 2.86**	−26.08 ± 11.99**	−0.52 ± 1.03
V. uliginosum	10.14 ± 3.92**	4263.87 ± 723.02**	205.33 ± 55.41**	17.17 ± 4.71**	−8.84 ± 14.55	−1.57 ± 1.76
D. octopetala	7.33 ± 2.96*	4203.83 ± 970.87**	171.17 ± 58.66*	12.18 ± 4.98*	−24.15 ± 25.35	−2.34 ± 0.67**

**Represents a difference that is significant at the 0.05 level.

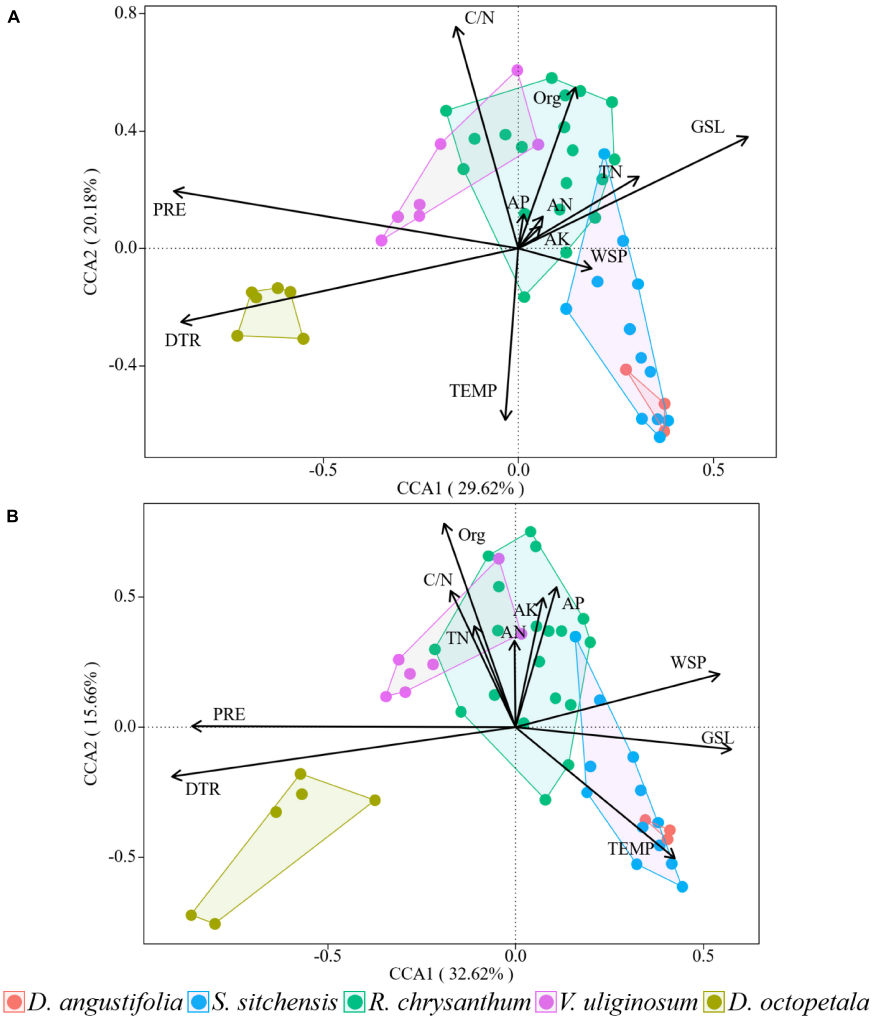

FIGURE 7
Canonical correspondence analysis of the distributions of plant communities and environmental factors in 2014 **(A)** and 2019 **(B)** over the ATCBM.

herbaceous species like *S. sitchensis*, were expanding in the alpine tundra. This expansion contributed to a shift in plant community composition toward herbaceous dominance, ultimately leading to the meadowization of the tundra. In this competitive process, low the dwarf shrubs like *R. chrysanthum* and *V. uliginosum* in lower altitude were at risk of disappearing (Jin et al., 2015; Zong et al., 2016; Wang et al., 2019).

4.4 Analysis of drivers of tundra vegetation change

Vegetation changes were closely related to environmental changes (Dolezal et al., 2016). With climate-induced changes in abiotic mountain environmental factors, the structure and distribution of mountain plants also changed accordingly (López-Angulo et al., 2019; Zu and Wang, 2022). Numerous studies have attributed the distribution of alpine tundra plant communities primarily to global warming (Lenoir and Svenning, 2014), which was confirmed in this study. Both surveys confirmed that climate factors such as PRE, DTR, and TEMP were primary drivers of plant community distribution, surpassing the influence of soil nutrients. However, our findings indicated although climate factors showed some influence on vegetation dynamics, the principal drivers of changes in plant communities during the study period were not climate factors but rather shifts in soil nutrients, particularly AN and AK. Increasing nitrogen levels in alpine tundra areas has been observed to promote the growth of herbaceous plants, while simultaneously leading to a reduction in the population of local dwarf shrubs (Nilsson et al., 2002). Zong et al. (2016) also found that nutrient perturbation had a greater impact than temperature on the expansion of *D. angustifolia* in the ATCBM, which was consistent with our results.

4.5 Potential mechanisms of soil nutrient changes mediated by microbial communities

Changes in soil nutrients were influenced by shifts in the soil microbial communities (Eskelinen et al., 2009; Philippot et al., 2024). Although the temperature change was not significant during

10.3389/fmicb.2024.1422529

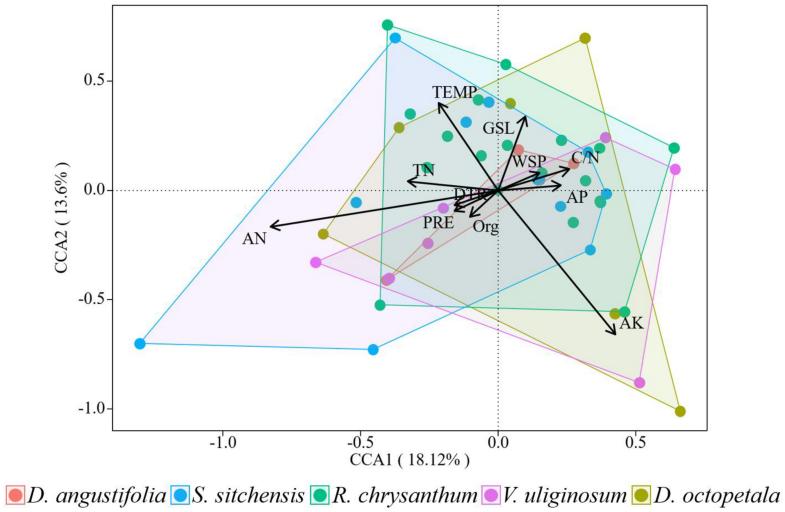

FIGURE 8
Canonical correspondence analysis of the changes of plant communities and environmental factors from 2014 to 2019 over the ATCBM.

the study period, the relatively higher temperatures resulting from decades of warming were stimulating microbial decomposition activity in the ATCBM (Jin et al., 2019b). This heightened microbial activity could accelerate the breakdown of organic matter, thereby affecting soil nutrient levels (Maes et al., 2024). Additionally, the trend towards meadowization of the alpine tundra intensified with the encroachment of *D. angustifolia*, resulting in an increase in herbaceous vegetation. Herbaceous plants contained higher proportions of easily degradable compounds such as monosaccharides and proteins, making their litter more prone to decomposition (Hobbie, 1996; Dorrepaal et al., 2005). At different elevations in our study area, the ratio of Gram-positive to Gram-negative bacteria in the soil microbial communities was significantly lower in areas with *D. angustifolia* encroachment compared to areas without such encroachment (Figure 9). The proportion of Gram-positive bacteria specialized in decomposing recalcitrant substrates, such as the litter of *R. chrysanthum* rich in lignin, cellulose, and other recalcitrant organic compounds, decreased in the microbial community, while the proportion of Gram-negative bacteria specialized in decomposing easily degradable substrates increased (Li et al., 2023). Such microbial changes accelerated the decomposition of herbaceous plant substrates, leading to an increase in nutrient cycling rates, a decrease in soil C/N, and an increase in available nutrients (Li et al., 2017). These changes in soil nutrients further affected vegetation changes (Zhang et al., 2018), promoting the further expansion of herbaceous plants in the alpine tundra. However, due to experimental limitations, this study was unable to separately investigate how changes in soil microorganisms affected changes in soil physicochemical properties.

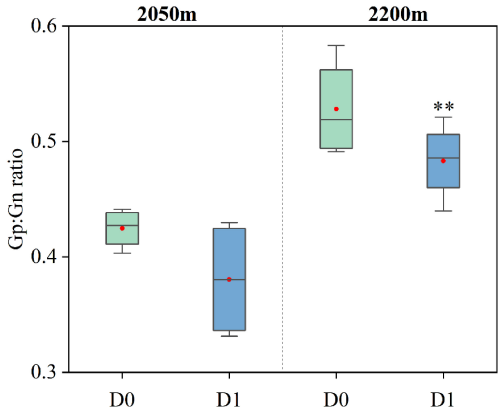

FIGURE 9
Changes in the ratio of Gram-positive to Gram-negative bacteria in soil microbial communities at different elevations in the ATCBM between areas with and without *D. angustifolia* encroachment (D0 = no *D. angustifolia* encroachment, D1 = *D. angustifolia* encroachment). **represents a difference that is significant at the 0.05 level.

4.6 Study implications and limitations

In this study, detailed monitoring of permanent plots in the ATCBM revealed significant short-term changes in tundra plant communities. Soil nutrient changes, rather than climate change, were identified as the main drivers of these vegetation changes. This is particularly notable given that the ATCBM is located in the core area of a national nature reserve, unaffected by agricultural or grazing activities, highlighting the importance of natural factors in influencing alpine tundra vegetation dynamics. Our regular plot surveys effectively pinpointed the actual drivers of vegetation changes, addressing the limitations inherent in controlled experiments (Clark et al., 2007). However, our study faced certain limitations and uncertainties. Although the three plot replicates at each altitude range were spaced only 25 m apart, the variations in elevation, slope, and vegetation types across different sites ensured the independence of the data. Future studies would benefit from expanding the study area and increasing the number of sample plots to enhance data representativeness and reliability. Additionally, due to the complexity of the alpine environment,

we resorted to using interpolation methods to acquire precipitation data. Although these interpolation results were highly correlated with observed data, they still had some uncertainties, necessitating more precise climate data for future analyses (Tapiador et al., 2017). Continuous monitoring of tundra vegetation changes will enable managers to more effectively identify and address ecological challenges, devising robust strategies to respond to future environmental shifts (Reid et al., 2022). This proactive approach is crucial for maintaining the health and stability of the tundra ecosystem, thereby ensuring its long-term sustainability (Rani et al., 2020).

5 Conclusion

This study investigated vegetation changes and their dominant drivers in the ATCBM over a short period by re-surveying permanent plots in 2019 and comparing them with data from 2014. The results revealed significant changes in alpine tundra vegetation during the study period. The importance values of typical alpine tundra plants such as *R. chrysanthum*, *V. uliginosum*, and *D. octopetala* decreased noticeably, while those of herbaceous species such as *D. angustifolia* and *S. sitchensis* increased significantly. Species richness, diversity, and evenness at different altitudinal gradients showed varying degrees of increase. A distinct expansion trend of herbaceous species was observed in the alpine tundra, contributing to a shift in plant community composition toward herbaceous dominance. This shift might result in the meadowization of the dwarf shrub tundra. Soil nutrients rather than climate factors, dominated the changes of plant communities over a short period. These findings provide scientific references for the conservation and management of biodiversity, as well as for projecting future vegetation dynamics in alpine tundra. Furthermore, to accurately simulate vegetation changes and reduce uncertainties in alpine tundra, our findings suggest that vegetation dynamic models should take into account the effect of soil nutrient variation on short-term changes in plant communities.

Data availability statement

The raw data supporting the conclusions of this article will be made available by the authors, without undue reservation.

Author contributions

SX: Writing—original draft, Visualization, Software, Methodology, Investigation, Formal analysis, Conceptualization. WW: Writing—review and editing, Funding acquisition, Conceptualization. LW: Conceptualization, Funding acquisition, Writing—review and editing, Formal analysis, Investigation, Supervision, Methodology. HD: Investigation, Writing—review and editing. ZW: Writing—review and editing, Funding acquisition, Conceptualization. SZ: Writing—review and editing, Investigation. YC: Investigation, Writing—review and editing. SB: Visualization, Writing—review and editing.

Funding

The author(s) declare financial support was received for the research, authorship, and/or publication of the article. The study was jointly supported by the National Natural Science Foundation of China (42271119, 42371075, and 41801081) and Youth Innovation Promotion Association, Chinese Academy of Sciences (2023238).

Conflict of interest

The authors declare that the research was conducted in the absence of any commercial or financial relationships that could be construed as a potential conflict of interest.

Publisher's note

References

Alatalo, J. M., Jagerbrand, A. K., Juhanson, J., Michelsen, A., and Luptacik, P. (2017). Impacts of twenty years of experimental warming on soil carbon, nitrogen, moisture and soil mites across alpine/subarctic tundra communities. *Sci. Rep.* 7:44489. doi: 10.1038/srep44489

Bligh, E. G., and Dyer, W. J. (1959). A rapid method of total lipid extraction and purification. *Can. J. Biochem. Physiol.* 37, 911–917. doi: 10.1139/o59-099

Bremner, J. M., and Mulvaney, C. (1982). "Nitrogen—total," in *Methods of soil analysis. Part 2. Chemical and microbiological properties*, Vol. 9, eds A. L. Page, R. H. Miller, and D. R. Keeney (Madison, WI: American Society of Agronomy, Soil Science Society of America), 595–624.

Britton, A. J., and Fisher, J. M. (2008). Growth responses of low-alpine dwarf-shrub heath species to nitrogen deposition and management. *Environ. Pollut.* 153, 564–573. doi: 10.1016/j.envpol.2007.09.022

Cannone, N., Sgorbati, S., and Guglielmin, M. (2007). Unexpected impacts of climate change on alpine vegetation. *Front. Ecol. Environ.* 5:360–364. doi: 10.1890/1540-929520075[360:Uiocco]2.0.Co;2

Chu, C., Kleinhesselink, A. R., Havstad, K. M., McClaran, M. P., Peters, D. P., Vermeire, L. T., et al. (2016). Direct effects dominate responses to climate perturbations in grassland plant communities. *Nat. Commun.* 7:11766. doi: 10.1038/ncomms11766

Clark, C. M., Cleland, E. E., Collins, S. L., Fargione, J. E., Gough, L., Gross, K. L., et al. (2007). Environmental and plant community determinants of species loss following nitrogen enrichment. *Ecol. Lett.* 10, 596–607. doi: 10.1111/j.1461-0248.2007.01053.x

Czortek, P., Eycott, A. E., Grytnes, J.-A., Delimat, A., Kapfer, J., and Jaroszewicz, B. (2018). Effects of grazing abandonment and climate change on mountain summits flora: A case study in the Tatra Mts. *Plant Ecol.* 219, 261–276. doi: 10.1007/s11258-018-0794-6

Danby, R. K., Koh, S., Hik, D. S., and Price, L. W. (2011). Four decades of plant community change in the Alpine tundra of southwest Yukon, Canada. *Ambio* 40, 660–671. doi: 10.1007/s13280-011-0172-2

Dolezal, J., Dvorsky, M., Kopecky, M., Liancourt, P., Hiiesalu, I., Macek, M., et al. (2016). Vegetation dynamics at the upper elevational limit of vascular plants in Himalaya. *Sci. Rep.* 6:24881. doi: 10.1038/srep24881

Dorrepaal, E., Cornelissen, J. H. C., Aerts, R., WallÉN, B. O., and Van Logtestijn, R. S. P. (2005). Are growth forms consistent predictors of leaf litter quality and decomposability across peatlands along a latitudinal gradient? *J. Ecol.* 93, 817–828. doi: 10.1111/j.1365-2745.2005.01024.x

Du, H., Liu, J., Li, M. H., Büntgen, U., Yang, Y., Wang, L., et al. (2017). Warming-induced upward migration of the alpine treeline in the Changbai Mountains, northeast China. *Glob. Change Biol.* 24, 1256–1266. doi: 10.1111/gcb.13963

Dunwiddie, P. W. J. A., and Research, A. (1977). Recent tree invasion of subalpine meadows in the Wind River Mountains. *Wyoming.* 9, 393–399. doi: 10.1080/00040851.1977.12003932

Epstein, H. E., Raynolds, M. K., Walker, D. A., Bhatt, U. S., Tucker, C. J., and Pinzon, J. E. (2012). Dynamics of aboveground phytomass of the circumpolar Arctic tundra during the past three decades. *Environ. Res. Lett.* 7:5506. doi: 10.1088/1748-9326/7/1/015506

Eskelinen, A., Stark, S., and Mannisto, M. (2009). Links between plant community composition, soil organic matter quality and microbial communities in contrasting tundra habitats. *Oecologia* 161, 113–123. doi: 10.1007/s00442-009-1362-5

Fahey, C., Koyama, A., Antunes, P. M., Dunfield, K., and Flory, S. L. (2020). Plant communities mediate the interactive effects of invasion and drought on soil microbial communities. *ISME J.* 14, 1396–1409. doi: 10.1038/s41396-020-0614-6

Formica, A., Farrer, E. C., Ashton, I. W., and Suding, K. N. (2014). Shrub Expansion over the past 62 years in rocky mountain alpine tundra: Possible causes and consequences. *Arctic Antarctic Alpine Res.* 46, 616–631. doi: 10.1657/1938-4246-46.3.616

Frostegård, Å, Tunlid, A., and Bååth, E. (1991). Microbial biomass measured as total lipid phosphate in soils of different organic content. *J. Microbiol. Methods* 14, 151–163. doi: 10.1016/0167-7012(91)90018-l

Gazol, A., Moiseev, P., and Camarero, J. J. (2017). Changes in plant taxonomic and functional diversity patterns following treeline advances in the South Urals. *Plant Ecol. Divers.* 10, 283–292. doi: 10.1080/17550874.2017.1400126

Grabherr, G., Gottfried, M., and Pauli, H. (2010). Climate change impacts in alpine environments. *Geogr. Compass* 4, 1133–1153. doi: 10.1111/j.1749-8198.2010.00356.x

Greig-Smith, P. (1983). *Quantitative plant ecology*. Berkeley, CA: University of California Press.

Hallinger, M., Manthey, M., and Wilmking, M. (2010). Establishing a missing link: Warm summers and winter snow cover promote shrub expansion into alpine tundra in Scandinavia. *New Phytol.* 186, 890–899. doi: 10.1111/j.1469-8137.2010.03223.x

Hamid, M., Khuroo, A. A., Malik, A. H., Ahmad, R., Singh, C. P., Dolezal, J., et al. (2020). Early evidence of shifts in alpine summit vegetation: A case study from Kashmir Himalaya. *Front. Plant Sci.* 11:421. doi: 10.3389/fpls.2020.00421

Han, J., Yin, H., Xue, J., Zhang, Z., Xing, Z., Wang, S., et al. (2023). Vertical distribution differences of the understory herbs and their driving factors on shady and sunny slopes in high altitude mountainous areas. *Front. Forests Glob. Change* 6:8317. doi: 10.3389/ffgc.2023.1138317

Hao, Z., Dai Limin, H. S. H., David, J. M., and Guofan, S. J. (2001). Potential response of major tree species to climate warming in Changbai Mountain, Northeast China. *Chin. J. Appl. Ecol.* 12:653.

Hobbie, S. E. (1996). temperature and plant species control over litter decomposition in Alaskan Tundra. *Ecol. Monogr.* 66, 503–522. doi: 10.2307/2963492

Holzinger, B., Hülber, K., Camenisch, M., and Grabherr, G. (2007). Changes in plant species richness over the last century in the eastern Swiss Alps: Elevational gradient, bedrock effects and migration rates. *Plant Ecol.* 195, 179–196. doi: 10.1007/s11258-007-9314-9

Huang, X.-C., and Li, C.-H. (1984). An analysis on the ecology of alpine tundra landscape of Changbai Mountains. *Acta Geogr. Sin. Beijing* 39, 285–297.

Jin, Y., Xu, J., He, H., Li, M. H., Tao, Y., Zhang, Y., et al. (2019a). The Changbai alpine shrub tundra will be replaced by herbaceous tundra under global climate change. *Plants (Basel)* 8, 370. doi: 10.3390/plants8100370

Jin, Y., Zhang, Y., Xu, Z., Gu, X., Xu, J., Tao, Y., et al. (2019b). Soil microbial community and enzyme activity responses to herbaceous plant expansion in the Changbai mountains Tundra, China. *Chin. Geogr. Sci.* 29, 985–1000. doi: 10.1007/s11769-019-1067-6

Jin, Y., Xu, J., Wang, Y., Wang, S., Chen, Z., Huang, X., et al. (2015). Effects of nitrogen deposition on tundra vegetation undergoing invasion by *Deyeuxia angustifolia* in Changbai Mountains. *Chin. Geogr. Sci.* 26, 99–108. doi: 10.1007/s11769-015-0746-1

Ju, J., and Masek, J. G. (2016). The vegetation greenness trend in Canada and US Alaska from 1984–2012 Landsat data. *Remote Sens. Environ.* 176, 1–16. doi: 10.1016/j.rse.2016.01.001

Kapfer, J., Hedl, R., Jurasinski, G., Kopecky, M., Schei, F. H., and Grytnes, J. A. (2016). Resurveying historical vegetation data - opportunities and challenges. *Appl. Veg. Sci.* 20, 164–171. doi: 10.1111/avsc.12269

Kazakis, G., Ghosn, D., Vogiatzakis, I. N., and Papanastasis, V. P. (2006). Vascular plant diversity and climate change in the alpine zone of the Lefka Ori, Crete. *Biodivers. Conserv.* 16, 1603–1615. doi: 10.1007/s10531-006-9021-1

Klein, J. A., Harte, J., and Zhao, X. Q. (2004). Experimental warming causes large and rapid species loss, dampened by simulated grazing, on the Tibetan Plateau. *Ecol. Lett.* 7, 1170–1179. doi: 10.1111/j.1461-0248.2004.00677.x

Körner, C. (1999). *Alpine plant life: Functional plant ecology of high mountain ecosystems*. Berlin: Springer, doi: 10.1007/978-3-642-18970-8

Lagergren, F., Björk, R. G., Andersson, C., Belušić, D., Björkman, M. P., Kjellström, E., et al. (2024). Kilometre-scale simulations over Fennoscandia reveal a large loss of tundra due to climate warming. *Biogeosciences* 21, 1093–1116. doi: 10.5194/bg-21-1093-2024

Lajtha, K., and Jarrell, W. (1999). *Soil phosphorus*. Oxford: Oxford University Press, 115–142.

Lenoir, J., and Svenning, J. C. (2014). Climate-related range shifts – a global multidimensional synthesis and new research directions. *Ecography* 38, 15–28. doi: 10.1111/ecog.00967

Li, L., Xing, M., Lv, J., Wang, X., and Chen, X. (2017). Response of rhizosphere soil microbial to Deyeuxia angustifolia encroaching in two different vegetation communities in alpine tundra. *Sci. Rep.* 7:43150. doi: 10.1038/srep43150

Li, N., Du, H., Li, M.-H., Na, R., Dong, R., He, H. S., et al. (2023). *Deyeuxia angustifolia* upward migration and nitrogen deposition change soil microbial community structure in an alpine tundra. *Soil Biol. Biochem.* 180:109009. doi: 10.1016/j.soilbio.2023.109009

Livingstone, S. W., Isaac, M. E., and Cadotte, M. W. (2020). Invasive dominance and resident diversity: Unpacking the impact of plant invasion on biodiversity and ecosystem function. *Ecol. Monogr.* 90:1425. doi: 10.1002/ecm.1425

López-Angulo, J., Pescador, D. S., Sánchez, A. M., Luzuriaga, A. L., Cavieres, L. A., and Escudero, A. (2019). Alpine vegetation dataset from three contrasting mountain ranges differing in climate and evolutionary history. *Data Brief* 27:104816. doi: 10.1016/j.dib.2019.104816

Lu, A., Zhang, X., Wang, S., and Wang, M. J. (2011). Effect of disturbance on the community species diversity in Yunding Mount. subalpine meadow. *Bull. Botan. Res.* 31, 73–78.

Ma, K., Huang, J., Yu, S., and Chen, L. (1995). Plant community diversity in Dongling Mountain, Beijing, China. II. Species richness, evenness and species diversities. *Acta Ecol. Sin.* 15, 268–277.

Maes, S. L., Dietrich, J., Midolo, G., Schwieger, S., Kummu, M., Vandvik, V., et al. (2024). Environmental drivers of increased ecosystem respiration in a warming tundra. *Nature* 629, 105–113. doi: 10.1038/s41586-024-07274-7

Metcalfe, D. B., Hermans, T. D. G., Ahlstrand, J., Becker, M., Berggren, M., Bjork, R. G., et al. (2018). Patchy field sampling biases understanding of climate change impacts across the Arctic. *Nat. Ecol. Evol.* 2, 1443–1448. doi: 10.1038/s41559-018-0612-5

Myers-Smith, I. H., Forbes, B. C., Wilmking, M., Hallinger, M., Lantz, T., Blok, D., et al. (2011). Shrub expansion in tundra ecosystems: Dynamics, impacts and research priorities. *Environ. Res. Lett.* 6:5509. doi: 10.1088/1748-9326/6/4/045509

Myers-Smith, I. H., Grabowski, M. M., Thomas, H. J. D., Angers-Blondin, S., Daskalova, G. N., Bjorkman, A. D., et al. (2019). Eighteen years of ecological monitoring reveals multiple lines of evidence for tundra vegetation change. *Ecol. Monogr.* 89, 106–117. doi: 10.1002/ecm.1351

Nill, L., Grünberg, I., Ullmann, T., Gessner, M., Boike, J., and Hostert, P. (2022). Arctic shrub expansion revealed by Landsat-derived multitemporal vegetation cover fractions in the Western Canadian Arctic. *Remote Sens. Environ.* 281:3228.

Nilsson, M. C., Wardle, D. A., Zackrisson, O., and Jäderlund, A. (2002). Effects of alleviation of ecological stresses on an alpine tundra community over an eight-year period. *Oikos* 97, 3–17. doi: 10.1034/j.1600-0706.2002.970101.x

Niu, Y. J., Yang, S. W., Wang, G. Z., Liu, L., and Hua, L. M. (2017). Evaluation and selection of species diversity index under grazing disturbance in alpine mea-dow. *Ying Yong Sheng Tai Xue Bao* 28, 1824–1832. doi: 10.13287/j.1001-9332.201706.026

Olorunfemi, I., Fasinmirin, J., and Ojo, A. (2016). Modeling cation exchange capacity and soil water holding capacity from basic soil properties. *Eurasian J. Soil Sci.* 5, 266–274. doi: 10.18393/ejss.2016.4.266-274

Pauli, H., Gottfried, M., Dullinger, S., Abdaladze, O., Akhalkatsi, M., Benito Alonso, J. L., et al. (2012). Recent plant diversity changes on Europe's mountain summits. *Science* 336, 353–355. doi: 10.1126/science.1219033

Pauwels, J., Van Ranst, E., Verloo, M., Mvondo, and Ze, A. (1992). *Méthodes d'analyses de sols et de plantes, équipement, gestion de stocks de verrerie et de produits chimiques*. Bruxelles: Publications Agricoles.

Philippot, L., Chenu, C., Kappler, A., Rillig, M. C., and Fierer, N. (2024). The interplay between microbial communities and soil properties. *Nat. Rev. Microbiol.* 22, 226–239. doi: 10.1038/s41579-023-00980-5

Pickering, C., Hill, W., and Green, K. (2008). Vascular plant diversity and climate change in the alpine zone of the Snowy Mountains, Australia. *Biodivers. Conserv.* 17, 1627–1644. doi: 10.1007/s10531-008-9371-y

Rani, G., Kaur, J., Kumar, A., and Yogalakshmi, K. (2020). "Ecosystem health and dynamics: An indicator of global climate change," in *Contemporary environmental issues and challenges in era of climate change*, eds P. Singh, R. Singh, and V. Srivastava (Singapore: Springer), 1–32. doi: 10.1007/978-981-32-9595-7_1

Rantanen, M., Karpechko, A. Y., Lipponen, A., Nordling, K., Hyvärinen, O., Ruosteenoja, K., et al. (2022). The Arctic has warmed nearly four times faster than the globe since 1979. *Commun. Earth Environ.* 3:168. doi: 10.1038/s43247-022-00498-3

Reichle, L. M., Epstein, H. E., Bhatt, U. S., Raynolds, M. K., and Walker, D. A. (2018). Spatial heterogeneity of the temporal dynamics of arctic tundra vegetation. *Geophys. Res. Lett.* 45, 9206–9215. doi: 10.1029/2018gl078820

Reid, K. A., Reid, D. G., and Brown, C. D. (2022). Patterns of vegetation change in Yukon: Recent findings and future research in dynamic subarctic ecosystems. *Environ. Rev.* 30, 380–401. doi: 10.1139/er-2021-0110

Rixen, C., Høye, T. T., Macek, P., Aerts, R., Alatalo, J. M., Anderson, J. T., et al. (2022). Winters are changing: Snow effects on Arctic and alpine tundra ecosystems. *Arctic Sci.* 8, 572–608. doi: 10.1139/as-2020-0058

Salminen, H., Tukiainen, H., Alahuhta, J., Hjort, J., Huusko, K., Grytnes, J.-A., et al. (2023). Assessing the relation between geodiversity and species richness in mountain heaths and tundra landscapes. *Landsc. Ecol.* 38, 2227–2240. doi: 10.1007/s10980-023-01702-1

Schore, A. I. G., Fraterrigo, J. M., Salmon, V. G., Yang, D., and Lara, M. J. (2023). Nitrogen fixing shrubs advance the pace of tall-shrub expansion in low-Arctic tundra. *Commun. Earth Environ.* 4:421. doi: 10.1038/s43247-023-01098-5

Shevtsova, I., Heim, B., Kruse, S., Schröder, J., Troeva, E. I., Pestryakova, L. A., et al. (2020). Strong shrub expansion in tundra-taiga, tree infilling in taiga and stable tundra in central Chukotka (north-eastern Siberia) between 2000 and 2017. *Environ. Res. Lett.* 15:ab9059. doi: 10.1088/1748-9326/ab9059

Šmilauer, P., and Lepš, J. (2014). *Multivariate analysis of ecological data using CANOCO 5*. Cambridge: Cambridge University Press.

Steinbauer, M. J., Grytnes, J. A., Jurasinski, G., Kulonen, A., Lenoir, J., Pauli, H., et al. (2018). Accelerated increase in plant species richness on mountain summits is linked to warming. *Nature* 556, 231–234. doi: 10.1038/s41586-018-0005-6

Stewart, L., Simonsen, C. E., Svenning, J. C., Schmidt, N. M., and Pellissier, L. (2018). Forecasted homogenization of high Arctic vegetation communities under climate change. *J. Biogeogr.* 45, 2576–2587. doi: 10.1111/jbi.13434

Sturm, M., Racine, C., and Tape, K. (2001). Climate change. Increasing shrub abundance in the Arctic. *Nature* 411, 546–547. doi: 10.1038/35079180

Tape, K. E. N., Sturm, M., and Racine, C. (2006). The evidence for shrub expansion in Northern Alaska and the Pan-Arctic. *Glob. Change Biol.* 12, 686–702. doi: 10.1111/j.1365-2486.2006.01128.x

Tapiador, F. J., Navarro, A., Levizzani, V., García-Ortega, E., Huffman, G. J., Kidd, C., et al. (2017). Global precipitation measurements for validating climate models. *Atmosph. Res.* 197, 1–20. doi: 10.1016/j.atmosres.2017.06.021

Tarnocai, C., Canadell, J. G., Schuur, E. A. G., Kuhry, P., Mazhitova, G., and Zimov, S. (2009). Soil organic carbon pools in the northern circumpolar permafrost region. *Glob. Biogeochem. Cycles* 23:3327. doi: 10.1029/2008gb003327

Theurillat, J.-P., Iocchi, M., Cutini, M., and De Marco, G. (2007). Vascular plant richness along an elevation gradient at Monte Velino (Central Apennines, Italy). *Biogeographia* 28:3. doi: 10.21426/b628110003

Vanneste, T., Michelsen, O., Graae, B. J., Kyrkjeeide, M. O., Holien, H., Hassel, K., et al. (2017). Impact of climate change on alpine vegetation of mountain summits in Norway. *Ecol. Res.* 32, 579–593. doi: 10.1007/s11284-017-1472-1

Waldock, C., Dornelas, M., and Bates, A. E. (2018). Temperature-driven biodiversity change: Disentangling space and time. *Bioscience* 68, 873–884. doi: 10.1093/biosci/biy096

Walker, D. A., Daniëls, F. J. A., Matveyeva, N. V., Šibík, J., Walker, M. D., Breen, A. L., et al. (2018). Circumpolar arctic vegetation classification. *Phytocoenologia* 48, 181–201. doi: 10.1127/phyto/2017/0192

Walker, M. D., Wahren, C. H., Hollister, R. D., Henry, G. H., Ahlquist, L. E., Alatalo, J. M., et al. (2006). Plant community responses to experimental warming across the tundra biome. *Proc. Natl. Acad. Sci. U.S.A.* 103, 1342–1346. doi: 10.1073/pnas.0503198103

Walkley, A., and Black, I. A. (1934). An examination of the Degtjareff method for determining soil organic matter, and a proposed modification of the chromic acid titration method. *Soil Sci.* 37, 29–38.

Walther, G. R., Beißner, S., and Burga, C. A. (2005). Trends in the upward shift of alpine plants. *J. Veg. Sci.* 16, 541–548. doi: 10.1111/j.1654-1103.2005.tb02394.x

Wang, L., Wang, W. J., Wu, Z., Du, H., Zong, S., and Ma, S. (2019). Potential distribution shifts of plant species under climate change in Changbai Mountains, China. *Forests* 10:498. doi: 10.3390/f10060498

Zemlianskii, V., Brun, P., Zimmermann, N. E., Ermokhina, K., Khitun, O., Koroleva, N., et al. (2024). Current and past climate co-shape community-level plant species richness in the Western Siberian Arctic. *Ecol. Evol.* 14:e11140. doi: 10.1002/ece3.11140

Zhang, L., Jing, Y., Xiang, Y., Zhang, R., and Lu, H. (2018). Responses of soil microbial community structure changes and activities to biochar addition: A meta-analysis. *Sci. Total Environ.* 643, 926–935. doi: 10.1016/j.scitotenv.2018.06.231

Zong, S., Jin, Y., Xu, J., Wu, Z., He, H., Du, H., et al. (2016). Nitrogen deposition but not climate warming promotes *Deyeuxia angustifolia* encroachment in alpine tundra of the Changbai Mountains, Northeast China. *Sci. Total Environ.* 544, 85–93. doi: 10.1016/j.scitotenv.2015.11.144

Zu, K., and Wang, Z. (2022). Research progress on the elevational distribution of mountain species in response to climate change. *Biodivers. Sci.* 30:21451. doi: 10.17520/biods.2021451

Frontiers in Microbiology

Explores the habitable world and the potential of microbial life

The largest and most cited microbiology journal which advances our understanding of the role microbes play in addressing global challenges such as healthcare, food security, and climate change.

Discover the latest Research Topics

See more →

Frontiers

Avenue du Tribunal-Fédéral 34
1005 Lausanne, Switzerland
frontiersin.org

Contact us

+41 (0)21 510 17 00
frontiersin.org/about/contact